GEOLOGY AND MINERAL RESOURCES OF THE
Buckskin and Rawhide Mountains
WEST-CENTRAL ARIZONA

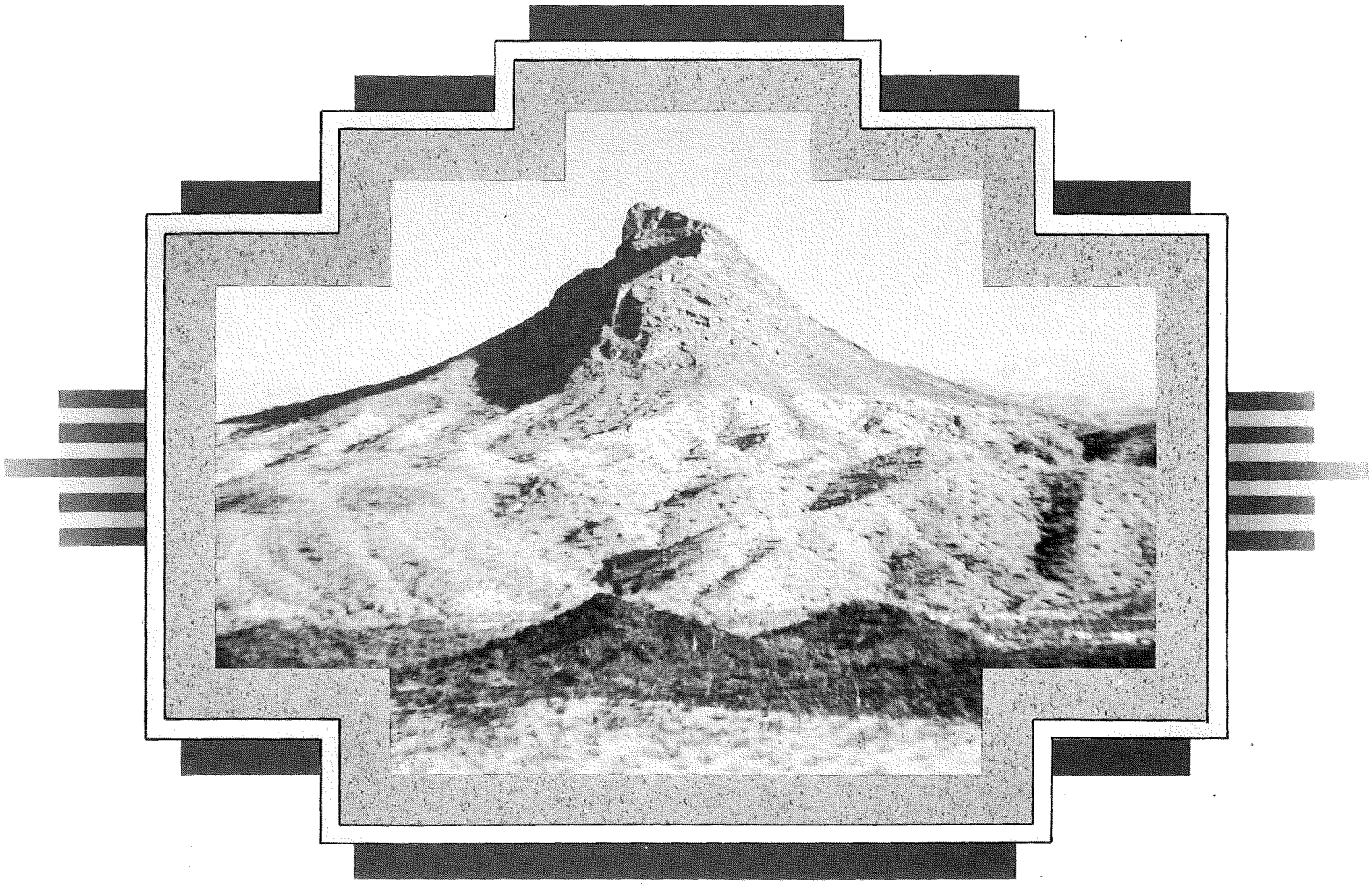

edited by

Jon E. Spencer and Stephen J. Reynolds

ARIZONA GEOLOGICAL SURVEY
BULLETIN 198

(Shackelford Volume)

1989

GEOLOGY AND MINERAL RESOURCES OF THE

Buckskin and Rawhide Mountains

WEST-CENTRAL ARIZONA

edited by

Jon E. Spencer and Stephen J. Reynolds

ARIZONA GEOLOGICAL SURVEY
BULLETIN 198

(Shackelford Volume)

1989

Copyright © 1989, Arizona Geological Survey

Permission is granted for individuals to make single copies for their personal use in research, study, or teaching and to use short quotes, figures, or tables from this bulletin for publication in scientific books and journals, provided that the source of the information is appropriately cited. This consent does not extend to other kinds of copying for general distribution, for advertising or promotional purposes, for creating new collective works, or for resale. The reproduction of multiple copies and the use of articles or extracts for commercial purposes require specific permission from the Arizona Geological Survey.

Published by
Arizona Geological Survey
845 N. Park Ave., #100
Tucson, Arizona 85719

Cover photo: The Clara Peak klippe, composed of Miocene conglomerate and sandstone, as viewed from the northwest. Buckskin-Rawhide detachment fault separates dark upper-plate rocks from light lower-plate rocks. Old mining town of Swansea is partially visible in lower right corner. Dark rocks in foreground are upper-plate rocks in Swansea synform.

Dedicated to the memory of
TERRY JON SHACKELFORD
1946-1983

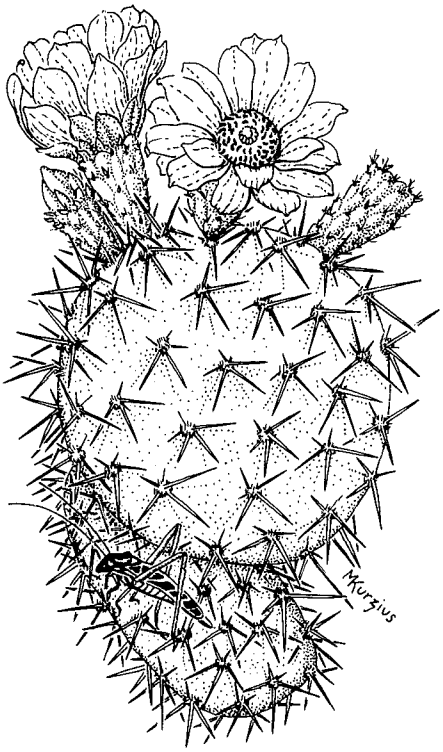
MKurzius

Preface

The text and geologic maps that compose Bulletin 198 represent a major advance in our understanding of the geology and mineral resources of west-central Arizona. The Buckskin and Rawhide Mountains, along with the adjacent Harcuvar and Harquahala Mountains, are one of the approximately 25 metamorphic core complexes in western North America. The geology of the Buckskin and Rawhide Mountains is dominated by the Buckskin-Rawhide detachment fault, a subhorizontal, undulating normal fault. Detachment faults are characteristic features of metamorphic core complexes. Improved understanding of detachment faults is critical in formulating more accurate models of the genesis of mineral deposits in Arizona.

Detachment faults are highly mineralized in the Buckskin and Rawhide Mountains. Mineral deposits associated with the Buckskin-Rawhide detachment fault have yielded more than 50 million lbs of copper and 15,000 oz of gold, which would be worth more than $60 million at 1988 prices. The nearby Copperstone mine, now Arizona's largest gold producer, is also related to a detachment fault.

Detachment-fault-related mineral deposits are a newly recognized type of mineral deposit. Two primary purposes of this report are to describe their characteristics more fully and to clarify their origin. Detachment faults in the Buckskin and Rawhide Mountains are similar in age and origin to those in other metamorphic core complexes in Arizona. Improved understanding of the geology and mineral deposits of the Buckskin and Rawhide Mountains will, therefore, increase the probability of future discoveries of economic mineral deposits both in the study area and in adjacent areas.

Dr. Larry D. Fellows
State Geologist and Director
Arizona Geological Survey

Acknowledgments

The editors of this bulletin gratefully acknowledge Evelyn M. VandenDolder and Karen L. Oden for careful and thorough technical editing and text formatting. Their investment of time and energy in producing this bulletin was large and is greatly appreciated. We also thank Pete Corrao and Sherry Garner for drafting most of the maps and figures in this volume, for designing the cover, and for preparing final camera-ready copy. Joe LaVoie is gratefully acknowledged for drafting Plate 2 and for preparing Plates 1 and 2 for publication. Finally, we thank the many authors for their contributions to this bulletin, and Larry Fellows, State Geologist, for supporting this sizeable project.

Table of Contents

Introduction to the geology and mineral resources of the Buckskin and Rawhide Mountains 1
by Jon E. Spencer and Stephen J. Reynolds

Terry Shackelford and the Rawhide Mountains: A retrospective view 11
by Gregory A. Davis

Structural geology of the Rawhide Mountains, Mohave County, Arizona 15
by Terry J. Shackelford

Lower-plate rocks of the Buckskin Mountains, Arizona: A progress report 47
by Bruce Bryant and J.L. Wooden

Geology of the Battleship Peak area, southern Buckskin Mountains, Arizona: Structural style below the Buckskin detachment fault 51
by Stephen Marshak and Marc Vander Meulen

Pre-Tertiary rocks and structures in the upper plate of the Buckskin detachment fault, west-central Arizona 67
by Stephen J. Reynolds and Jon E. Spencer

Tertiary structure, stratigraphy, and tectonics of the Buckskin Mountains 103
by Jon E. Spencer and Stephen J. Reynolds

Geology and mineral deposits of the central Artillery Mountains 168
by Jon E. Spencer, Michael J. Grubensky, John T. Duncan, Jonathan D. Shenk, John C. Yarnold, and James P. Lombard

K-Ar geochronology of Miocene extension, volcanism, and potassium metasomatism in the Buckskin and Rawhide Mountains 184
by Jon E. Spencer, M. Shafiqullah, Robert J. Miller, and Ledabeth G. Pickthorn

Fluid regimes and geochemical mass transport in the development of mylonites and chloritic breccias at Copper Penny, Buckskin Mountains 190
by R. David Halfkenny, Jr., Robert Kerrich, and William A. Rehrig

Volcanic rocks in the suprastructure of metamorphic core complexes, southwest Arizona: Geochemical and isotopic evidence for primary magma types and secondary hydrothermal regimes 203
by Robert Kerrich, William A. Rehrig, and Elisabeth McLarty

Mineralization in the central part of the Planet mineral district, northwestern Buckskin Mountains 215
by Norman E. Lehman and Jon E. Spencer

Geology of mineral deposits in the Buckskin and Rawhide Mountains 223
by Jon E. Spencer and John W. Welty

Geology of postdetachment, Miocene volcanic rocks in the southwestern Buckskin Mountains 255
by Michael J. Grubensky

Appendix A: Map-unit descriptions and cross sections for Plate 2 (Geologic map of the Planet-Mineral Hill area, northwestern Buckskin Mountains, west-central Arizona) 263
by Jon E. Spencer, Stephen J. Reynolds, and Norman E. Lehman

References Cited 270

Plate 1: Geologic map of the Rawhide Mountains, Mohave County, Arizona (scale 1:42,850) in pocket
by Terry J. Shackelford

Plate 2: Geologic map of the Planet-Mineral Hill area, northwestern Buckskin Mountains, west-central Arizona (scale 1:24,000) in pocket
by Jon E. Spencer, Stephen J. Reynolds, and Norman E. Lehman

Plate 3: Compilation geologic map of the Buckskin and Rawhide Mountains, west-central Arizona (scale 1:100,000) in pocket
by Jon E. Spencer

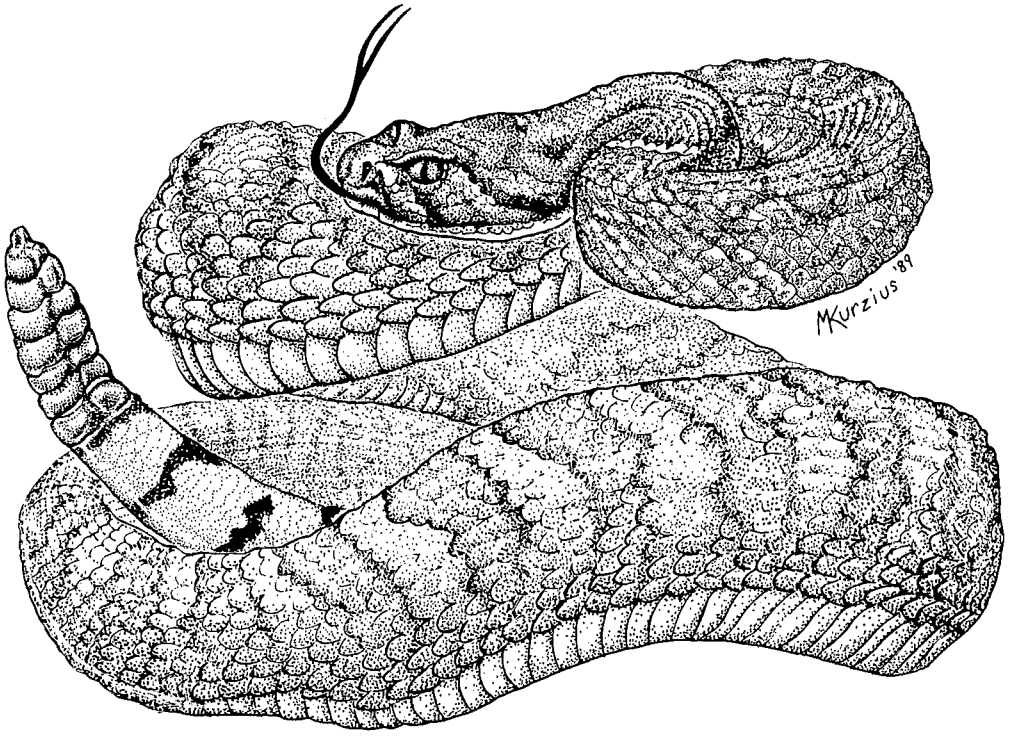

Mohave rattlesnake (*Crotalus scutulatus*), also known as "Mohave green" because of distinctive greenish color (not always present) or "coontail" because of black-and-white banded tail. Unlike the venom of other rattlesnakes, its venom contains a significant proportion of nerve toxin.

Introduction to the geology and mineral resources of the Buckskin and Rawhide Mountains

JON E. SPENCER
STEPHEN J. REYNOLDS
Arizona Geological Survey, 845 N. Park Ave., #100, Tucson, Arizona 85719

INTRODUCTION

Crustal extension and compression are major processes that have shaped the crustal architecture of planet Earth. Crustal compression has long been recognized as the chief architect of most mountain belts and is now moderately well understood. In contrast, the contribution of extensional tectonism to the structure of the crust is less well understood because many extensional structures were only recently recognized and because areas affected by crustal extension are usually buried by sediments.

Cenozoic extension in western North America has left a geologic record that, for areas of extensional tectonism, is unsurpassed in its visibility. Geologic features related to Cenozoic extension are especially amenable to study in the arid southwestern United States where bedrock exposure approaches 100%. Approximately 25 mountain ranges or groups of ranges in western North America are characterized by a distinctive association of geologic features that defied interpretation until the early 1980's. These ranges or groups of ranges are commonly referred to as *metamorphic core complexes*. Distinguishing features include a major low-angle normal fault that separates a brittlely distended and generally highly faulted upper plate from lower-plate crystalline rocks with locally developed, gently to moderately dipping mylonitic fabric. Most geologists now interpret such faults and mylonitic fabrics as products of large-magnitude crustal extension. These distinctive features have been recently recognized in parts of Greece, China, and New Guinea, which indicates that Cordilleran metamorphic core complexes are not idiosyncrasies of western North America geology, but are general products of extensional tectonism.

The Buckskin and Rawhide Mountains, which are part of the Harcuvar metamorphic core complex in west-central Arizona, contain one of North America's most areally extensive exposures of a detachment fault and its mylonitic footwall. In addition, there is abundant evidence of mineralization along the detachment fault, including economic deposits of copper and gold. Detachment-fault-related mineralization is probably nowhere better displayed than in and around the Buckskin and Rawhide Mountains. The largest domestic deposits of manganese, a strategic and critical mineral, are adjacent to the Buckskin and Rawhide Mountains and may have originated by processes associated with extensional tectonism. Because of these various attributes, the Buckskin and Rawhide Mountains have attracted considerable attention from geologists during the past 15 years, beginning with the pioneering Ph.D. study of the geology of the Rawhide Mountains by Terry Shackelford. Most studies presented in this volume focus on aspects of Tertiary extensional tectonism, but several studies pertain to other subjects, such as preextensional structure and stratigraphy or postextensional (late Cenozoic) magmatism. These other studies address important aspects of Cordilleran geologic evolution and suggest that subtle genetic relationships exist between extensional tectonism and younger and older geologic events.

OVERVIEW

The Buckskin and Rawhide Mountains are within the Basin and Range physiographic province of southwestern North America. This province, which includes southern and western Arizona, is characterized by numerous mountain ranges and intervening Cenozoic basins. The physiography of the Basin and Range Province is largely the product of middle and late Cenozoic low- and high-angle normal faulting, volcanism, and erosion. The significance and relative age of each of these processes vary greatly from range to range. Miocene low-angle normal faulting was the dominant process that determined the physiography of the Buckskin and Rawhide Mountains. Younger basaltic volcanism, erosion, and minor, postdetachment high-angle faulting were also important.

Cordilleran metamorphic core complexes are typically characterized by normal-faulted and extended hanging-wall rocks that overlie well-lineated, variably mylonitic footwall rocks along large-displacement, Tertiary low-angle normal faults commonly referred to as *detachment faults* (Fig. 1). The Harcuvar metamorphic core complex, which includes the Buckskin and Rawhide Mountains, is one of the approximately 25 such complexes that are discontinuously exposed in a belt that extends from Sonora, Mexico diagonally across Arizona into southeastern California (Fig. 2) and northward as far as southern British Columbia (Crittenden and others, 1980). Metamorphic core complexes have been intensively studied during the past 15 years (e.g., Davis, G.A., this

in Spencer, J.E., and Reynolds, S.J., eds., 1989, Geology and mineral resources of the Buckskin and Rawhide Mountains, west-central Arizona: Arizona Geological Survey Bulletin 198, p. 1-10.

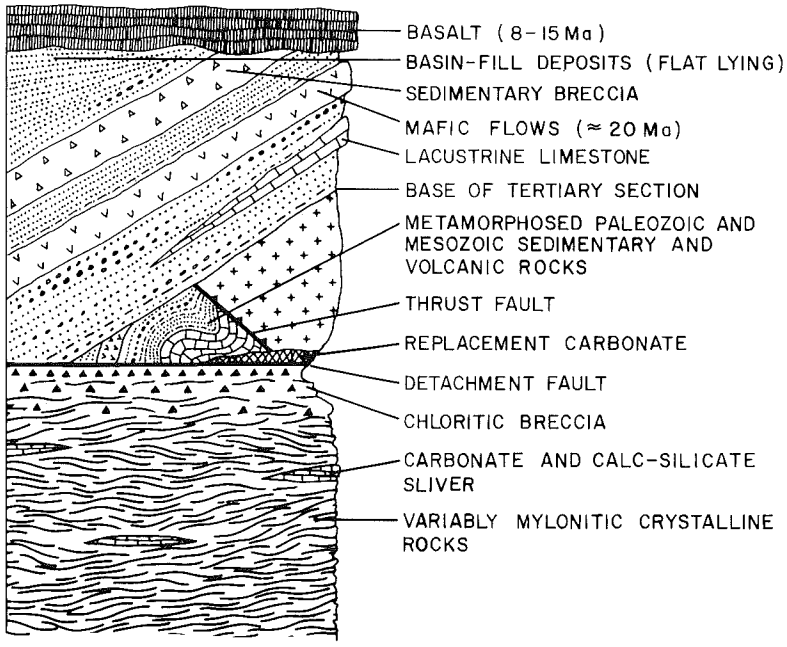

Figure 1. Schematic structure-stratigraphy diagram showing all important pre-Pliocene rock types and some of their contact relationships. Movement on rotational normal faults (not shown) caused tilting of upper-plate rocks.

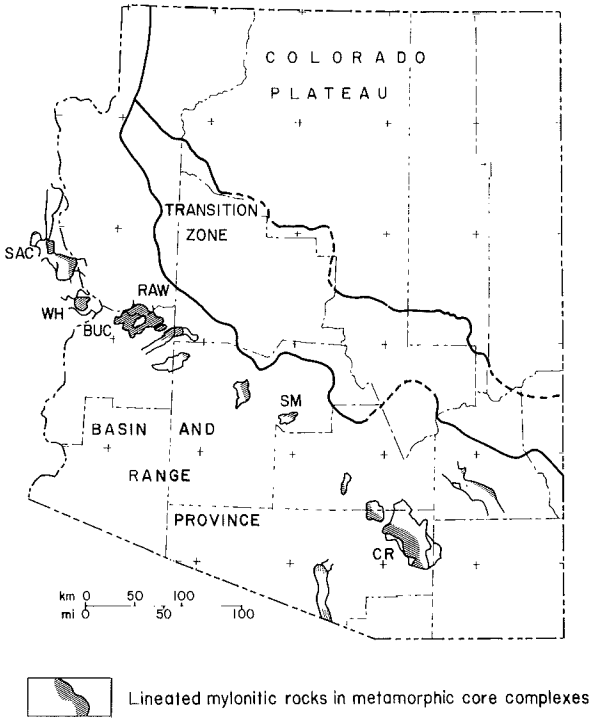

Figure 2. Map of Arizona showing the three physiographic provinces in the State and the locations of lineated mylonitic rocks in metamorphic core complexes. BUC = Buckskin Mountains; CR = Santa Catalina - Rincon Mountains; RAW = Rawhide Mountains; SAC = Sacramento Mountains; SM = South Mountain; WH = Whipple Mountains.

vol.). These once enigmatic associations of rocks and structures are now generally recognized as products of large-magnitude displacement on moderately to gently dipping normal faults and their down-dip continuations as ductile shear zones.

The subhorizontal Buckskin-Rawhide detachment fault is exposed discontinuously throughout the Buckskin and Rawhide Mountains (Fig. 3; Plate 3). Hanging-wall rocks, collectively referred to as the *upper plate*, consist of a variety of complexly normal-faulted and tilted rocks that include syntectonic, mid-Tertiary sedimentary and volcanic rocks (Spencer, Grubensky, and others, this vol.; Spencer and Reynolds, this vol.) and variably deformed and metamorphosed Mesozoic and Paleozoic sedimentary and volcanic rocks (Frost, 1983; Reynolds and others, 1987; Reynolds and Spencer, this vol.; Shackelford, this vol.; Plates 1 and 2). The footwall block, commonly referred to as the *lower plate* (platelike form is not implied), is composed of variably mylonitic crystalline and metasedimentary rocks (Bryant and Wooden, this vol.; Marshak and Vander Muelen, this vol.; Shackelford, this vol.) and is thought to be structurally continuous with similar lower-plate rocks in the nearby Harcuvar and Whipple Mountains (Fig. 4). The mid-Tertiary age of some of the mylonitized rocks in the Whipple, Buckskin, and Rawhide Mountains has recently been established by U-Pb (zircon) geochronologic study (Wright and others, 1986; Bryant and Wooden, this vol.). A northeastward direction of displacement of upper-plate rocks relative to the lower plate is inferred based on a number of criteria (e.g., Davis, G.A., and others, 1980; Reynolds and Spencer, 1985; Howard and John, 1987). The sense of

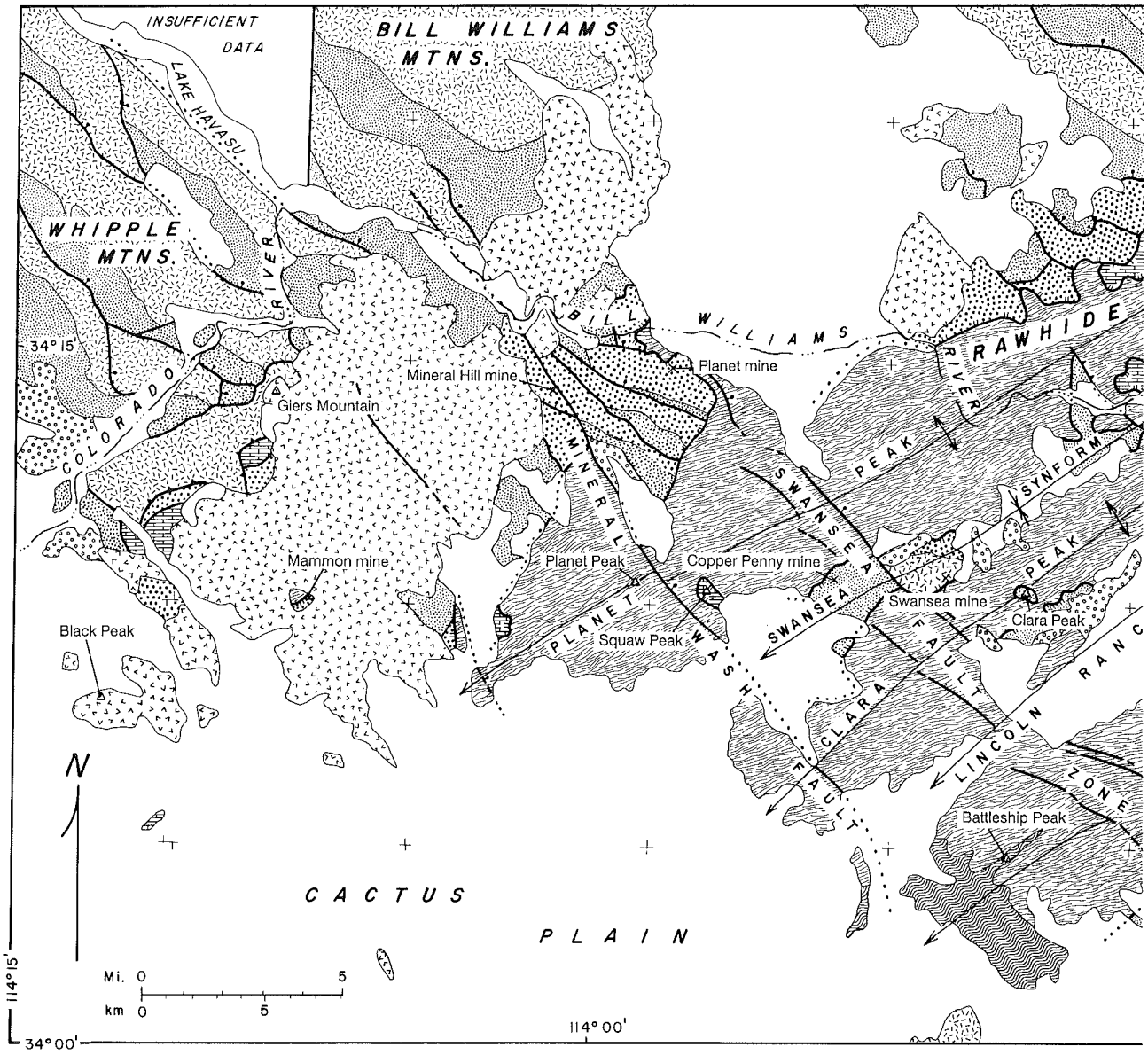

POST-DETACHMENT UNITS

- SURFICIAL DEPOSITS (QUATERNARY TO LATEST TERTIARY)
- BASALT AND LOCAL INTERMEDIATE TO SILICIC VOLCANIC ROCKS AND SEDIMENTARY ROCKS, FLAT LYING TO GENTLY TILTED (MIDDLE TO LATE MIOCENE)
- SEDIMENTARY ROCKS (MIDDLE TO LATE MIOCENE)

UPPER-PLATE UNITS

- SEDIMENTARY AND VOLCANIC ROCKS, GENERALLY MODERATELY TO STEEPLY DIPPING (LATE OLIGOCENE TO MIDDLE MIOCENE)
- METAVOLCANIC AND METASEDIMENTARY ROCKS (MESOZOIC)
- METASEDIMENTARY ROCKS (PALEOZOIC)
- CRYSTALLINE ROCKS (LARGELY PROTEROZOIC, LOCALLY TERTIARY AND MESOZOIC)

LOWER-PLATE UNITS

- MYLONITIC CRYSTALLINE ROCKS (TERTIARY TO PROTEROZOIC)
- MYLONITIC METASEDIMENTARY ROCKS (MESOZOIC AND PALEOZOIC)

displacement on the detachment fault is the same as that indicated for mylonitization by asymmetric petrofabrics in the mylonites (Davis, G.A., and others, 1986; Davis, G.A., and Lister, 1988; Marshak and Vander Muelen, this vol.; Spencer and Reynolds, this vol.).

All of these basic structural features in the Buckskin and Rawhide Mountains, and in metamorphic core complexes in general, are accounted for by the shear-zone model. This model envisions that each metamorphic core complex originated by large displacement on a master low-angle normal fault that extended down dip into a zone of mylonitization. According to the shear-zone model, rocks originally mylonitized at perhaps 8- to 15-km depth rose isostatically and cooled as they were displaced from beneath a wedge of brittlely extending upper-plate rocks, and were overprinted successively by chloritic alteration and brecciation, microbrecciation, and fault-gouge formation along a narrow fault zone (Wernicke, 1981, 1985; Davis, G.H., 1983; Reynolds, 1985; Davis, G.A., and others, 1986). Arching and subareal exposure of the lower plate led to shedding of mylonitic debris into syntectonic sedimentary basins and to the distinctive physiography of many of the complexes (Rehrig and Reynolds, 1980; Howard and others, 1982b; Spencer, 1984b; Pain, 1985; Miller and John, 1988).

Upper-plate rocks in the Buckskin and Rawhide Mountains contain abundant evidence of compressional deformation and metamorphism of Mesozoic and Paleozoic sedimentary rocks. The stratigraphy of the pre-Tertiary rocks is recognizable in spite of variable but typically severe deformation and greenschist-grade metamorphism (Reynolds and others, 1987, 1988; Reynolds and Spencer, this vol.). Deformation occurred in association with generally south-directed, late Mesozoic thrust faulting within the east-west-trending Maria fold-and-thrust belt (Reynolds and others, 1986b).

Mineral deposits are widely distributed in the Buckskin and Rawhide Mountains and, with a few notable exceptions, are along or within a few tens of meters of the detachment fault. Most of the deposits contain massive or fracture-filling specular hematite and younger fracture-filling chrysocolla. Early-formed Cu and Fe sulfides were probably common, but are largely obscured by later oxidation. Hydrothermal-carbonate replacements are also present along the fault and are commonly associated with Cu-Fe mineral deposits. The Cu-Fe deposits have yielded approximately 52 million lbs of Cu and 15,500 oz of Au, with minor amounts of Pb, Zn, and Ag (Keith and others, 1983). All of these deposits formed at the same time that detachment faulting and related structural and sedimentary phenomena occurred, and are interpreted as having formed from aqueous brines that leached metals from strata within extensional sedimentary basins (Wilkins and Heidrick, 1982; Spencer and Welty, 1986, this vol.; Wilkins and others, 1986; Lehman and Spencer, this vol.). The recent discovery of the Copperstone deposit in west-central Arizona, which is estimated to contain more than 500,000 oz of Au and is related to the Moon Mountains detachment fault, has led to renewed interest in detachment-fault-related mineral deposits (Spencer and others, 1988).

Mn deposits hosted in upper-plate, Miocene sedimentary rocks in the Buckskin and Rawhide Mountains have yielded approximately 24 million lbs of Mn. Similar Mn deposits in the nearby Artillery Mountains include the largest of such deposits in the United States (Lasky and Webber, 1949). Some of the deposits in the Artillery Mountains are younger than previously suspected and may postdate detachment faulting and related mid-Tertiary tectonism. These younger deposits formed from low-salinity fluids and thus were not derived directly from the saline aqueous fluids that caused detachment-fault-related mineralization (Spencer, Grubensky, and others, this vol.).

In addition to Mn and detachment-fault-related mineralization, widespread K metasomatism of upper-plate rocks and chloritic alteration of brecciated rocks below the detachment fault attest to the pervasiveness of aqueous geochemical activity during detachment faulting. K metasomatism has been recognized elsewhere in association with detachment faults (Brooks, 1986, 1988) and is known to be older than detachment-fault-related mineralization in the eastern Harcuvar Mountains (Roddy and others, 1988). K metasomatism in the Buckskin Mountains has largely converted mafic volcanic flows, which may have originally been alkalic, to K-feldspar, calcite, and Fe and Mn oxides (Kerrich and others, this vol.). Plagioclase in K-metasomatized upper-plate basalt flows in the Buckskin Mountains has been largely or entirely converted to K-feldspar, and numerous K-Ar dates of feldspar concentrates from these rocks reveal a mid-Miocene age of K metasomatism (Spencer, Shafiqullah, and others, this vol.). Chloritic alteration of lower-plate rocks, involving massive addition of Fe, Mn, and Mg and loss of Si, Na, and K, occurred in a different fluid regime than that associated with later calcite and Fe-Mn-oxide vein emplacement (Reynolds and Lister, 1987; Halfkenny and others, this vol.).

Detachment faulting and related deformation and sedimentation were followed by dominantly basaltic volcanism with local associated felsic volcanism (Suneson and Lucchitta, 1983). Trachyte flows and interbedded pyroclastic rocks in the western Buckskin Mountains are the same age as, and may have evolved from, magmas associated with adjacent postdetachment basalts (Grubensky, this vol.).

Better understanding of the genesis of metamorphic core complexes, their relationship to older tectonic features, and their associated mineral deposits and igneous rocks could elucidate the nature of general processes that occur in extensional tectonic settings, including those related to the genesis of economic mineral deposits. The remarkably well-exposed and well-developed compressional and extensional structures and mineral deposits in the Buckskin and Rawhide Mountains present an exceptional opportunity to improve basic geologic understanding.

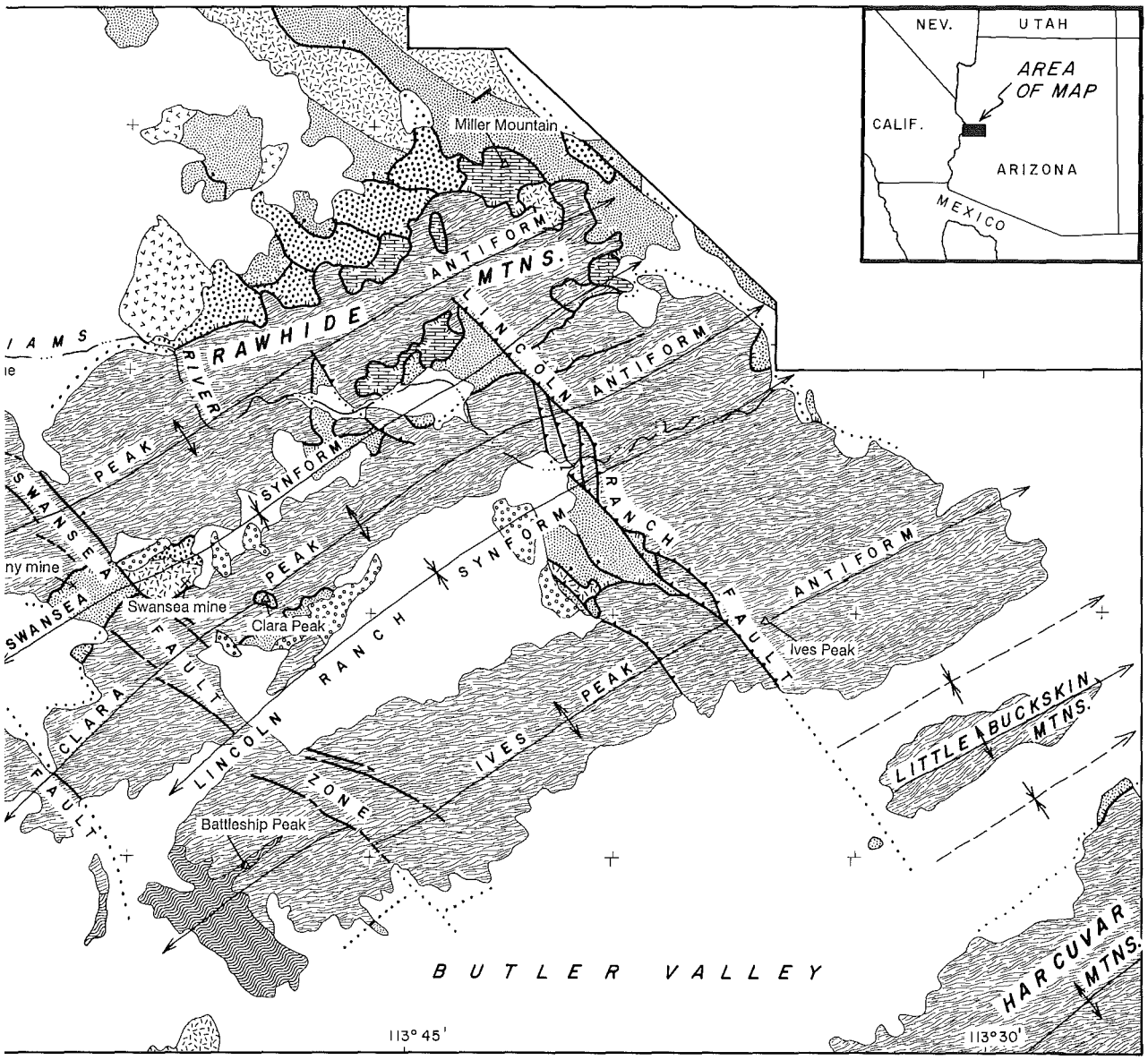

SYMBOLS

BUCKSKIN-RAWHIDE DETACHMENT FAULT

LOW-ANGLE NORMAL FAULT

HIGH-ANGLE NORMAL FAULT

HIGH-ANGLE FAULT

THRUST OR REVERSE FAULT

ALL FAULTS DASHED WHERE APPROXIMATELY LOCATED OR INFERRED, DOTTED WHERE CONCEALED.

Figure 3. Simplified geologic map of the Buckskin and Rawhide Mountains showing the locations of important mines and geographic features. Modified from Plate 3.

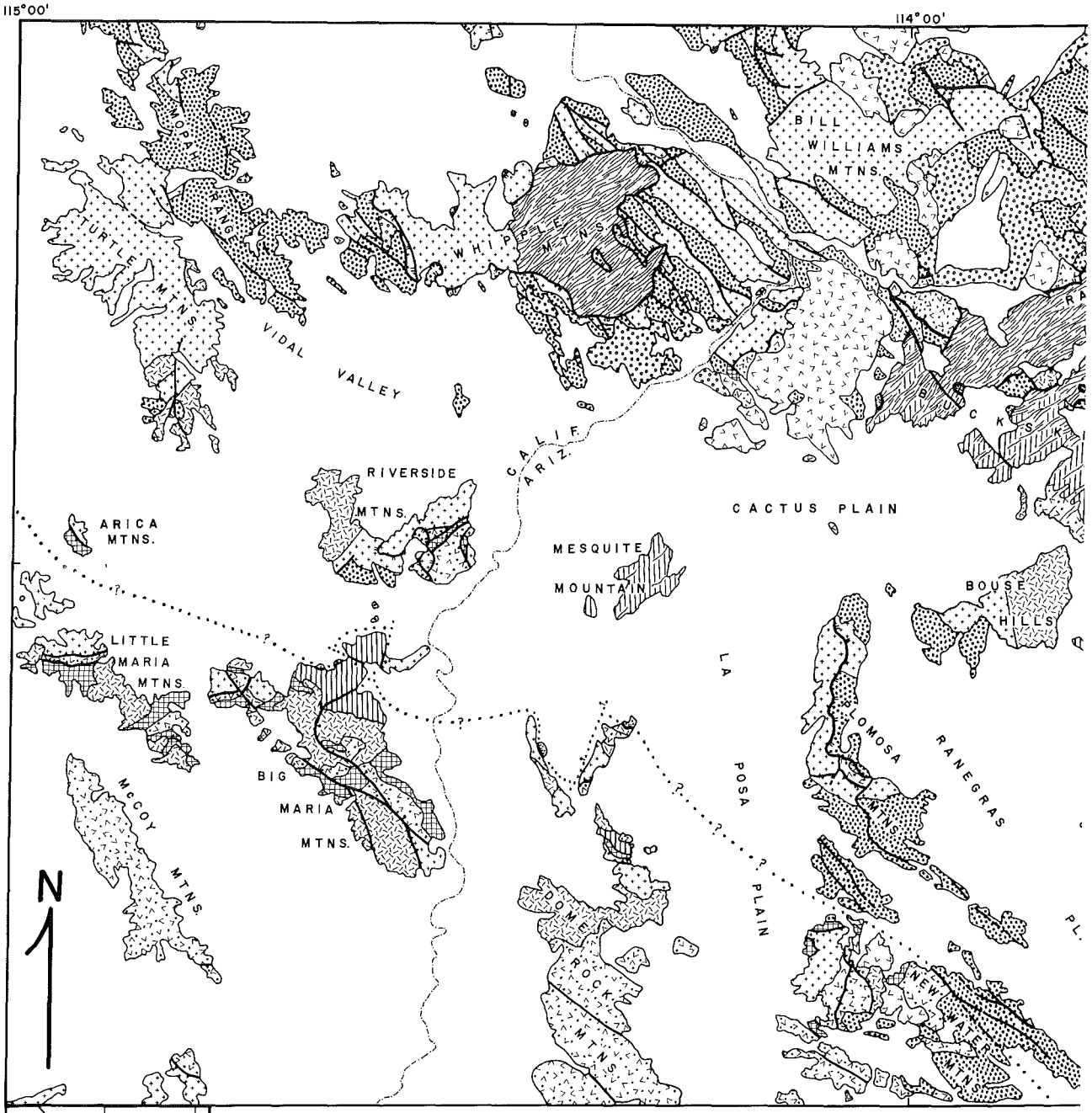

UPPER TERTIARY BASIN FILL

UPPER TERTIARY BASALT, GENERALLY FLAT LYING

MIDDLE TERTIARY VOLCANIC AND SEDIMENTARY ROCKS

TERTIARY-PROTEROZOIC CRYSTALLINE ROCKS WITH MID-TERTIARY MYLONITIC FABRIC

CENOZOIC-MESOZOIC INTRUSIVE ROCKS

MESOZOIC VOLCANIC AND SEDIMENTARY ROCKS

PALEOZOIC SEDIMENTARY ROCKS

MESOZOIC-PROTEROZOIC CRYSTALLINE ROCKS

PROTEROZOIC CRYSTALLINE ROCKS

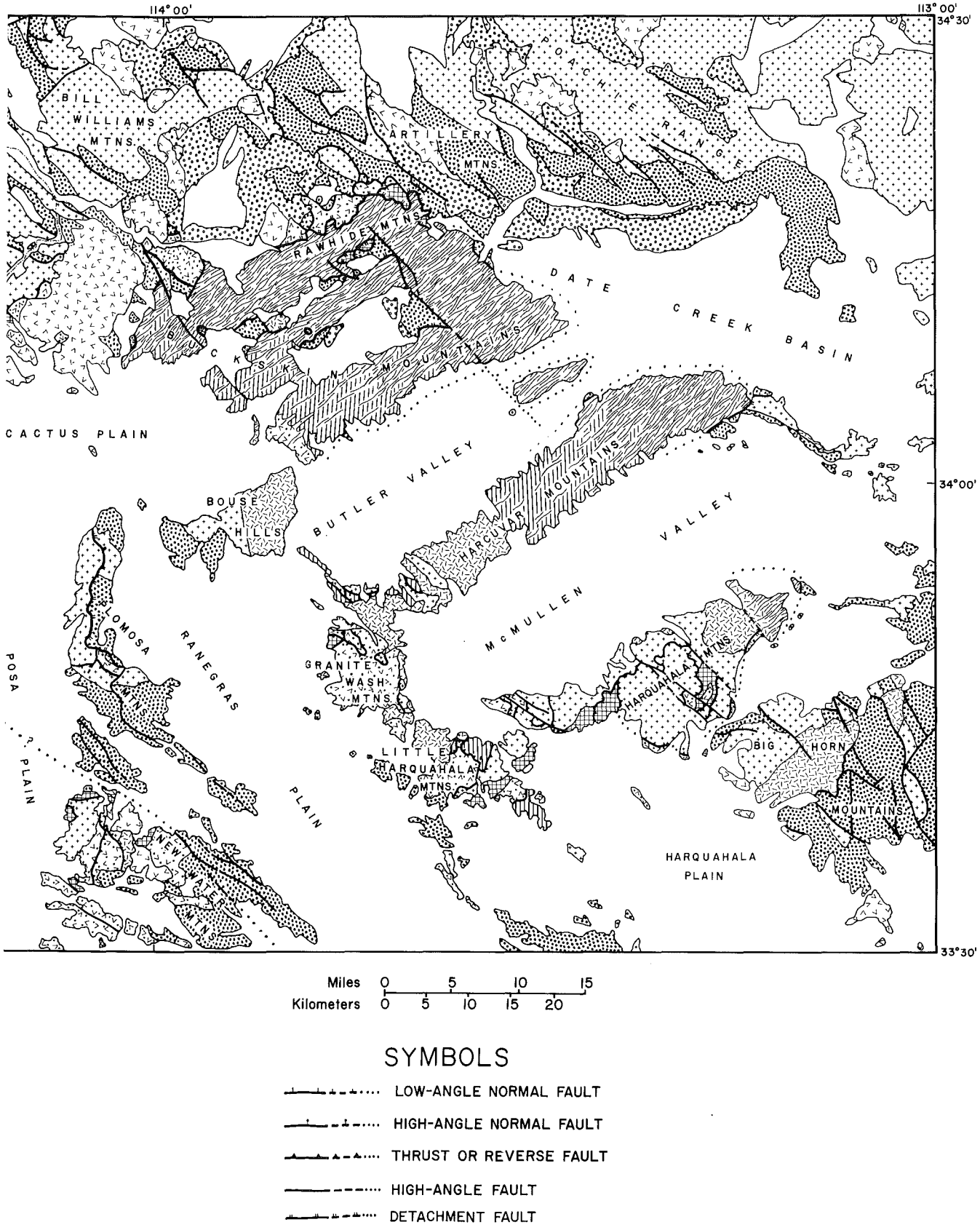

Figure 4. Simplified geologic map of a 1° x 2° area that includes the Buckskin and Rawhide Mountains and adjacent areas.

PREVIOUS WORK

Early studies of the Buckskin and Rawhide Mountains were largely motivated by the presence of economic mineral deposits in these ranges. Bancroft (1911) and Blanchard (1913) recognized the basic mineral assemblages, styles of mineralization, and host-rock lithologies in all of the larger mineral deposits of the central and western Buckskin Mountains, but generally considered the detachment fault to be a depositional contact. Darton (1925) recognized Carboniferous fossils in limestone near the Billy Mack mine in the westernmost Buckskin Mountains and illustrated, in cross section, Precambrian rocks above Paleozoic rocks along a contact that he considered to be an overturned unconformity west of the mine. Lee (1908) and Ross (1922) briefly reported some of the basic rock types and geologic relationships in the Buckskin and Rawhide Mountains.

Lasky and Webber's (1949) detailed study of the Artillery Mountains, just northeast of the Rawhide Mountains (Fig. 4), described the stratigraphy and Mn deposits of a southwest-tilted sequence of mid-Tertiary sedimentary and volcanic rocks. A large, variably brecciated sheet of plutonic and metamorphic rocks in the Tertiary stratigraphic sequence, now referred to as the Artillery megabreccia, was thought by Lasky and Webber to have been thrust over Tertiary sedimentary rocks of the Artillery Formation. Lasky and Webber interpreted the detachment fault along the east flank of the Rawhide Mountains to be a depositional contact.

The Mohave and Yuma county 1:375,000-scale geologic maps (Wilson and Moore, 1959; Wilson, 1960) represent the first moderately accurate geologic maps of the Buckskin and Rawhide Mountains. Many segments of the Buckskin-Rawhide detachment fault were shown as thrust faults on these maps. The contact between crystalline and metasedimentary rocks in the westernmost Buckskin Mountains, previously interpreted by Darton (1925) as an overturned depositional contact, was interpreted by Wilson (1960) as a thrust fault. These interpretations were incorporated into the 1:500,000-scale geologic map of Arizona (Wilson and others, 1969).

An unpublished study by Ransome (1931, as reported by Davis, G.A., and others, 1980) reported a low-angle thrust fault that displaced Tertiary strata in the Whipple Mountains of California. Although Kemnitzer (1937, as reported by Davis, G.A., and others, 1980) recognized the northwest-striking, high-angle normal faults in the range and was aware of Ransome's interpretations of low-angle faults, he considered the gently dipping contacts between Tertiary and pre-Tertiary rocks to be unconformities. Terry (1972) recognized an extensive, gently dipping fault in the Whipple Mountains that juxtaposed crystalline rocks, but also considered the low-angle contacts between Tertiary and pre-Tertiary rocks to be unconformities.

G.A. Davis and J.L. Anderson of the University of Southern California and their numerous students mapped many parts of the Whipple, Buckskin, and Rawhide Mountains and clearly recognized the basic structural and stratigraphic framework of the area. Terry Shackelford's Ph.D. dissertation (1976b; see also 1980, this vol.), which included a geologic map of most of the Rawhide Mountains (reproduced here as Plate 1), represented the first detailed field study of a large part of the Whipple-Buckskin-Rawhide Mountains area and firmly established the existence of the gently dipping Rawhide detachment fault and its mid-Tertiary age (Davis, G.A., this vol.). It was soon recognized that detachment faults in the Whipple, Buckskin, and Rawhide Mountains probably represented segments of a single fault or fault system (Davis, G.A., and others, 1980; see also Carr and Dickey, 1977).

G.A. Davis and others (1980) suggested that the detachment fault was the base of a megalandslide and that the Artillery thrust of Lasky and Webber (1949) was part of the distal telescoped end of the slide. Field studies by Lucchitta and Suneson (1981a,b) and Otton (1982), however, indicated that rocks above the Rawhide detachment fault were structurally continuous with the Colorado Plateau and, therefore, that rocks below the fault must have moved up and out (to the southwest) from beneath structurally overlying rocks. Lucchitta and Suneson's observations require that crustal extension occurred as a consequence of detachment-fault movement (Shackelford, 1981).

A nearly concordant pair of biotite and hornblende K-Ar dates (52.3 and 57.4 Ma, respectively) from mylonitic lower-plate rocks in the Rawhide Mountains (Shackelford, 1980) and other data from the Whipple Mountains (Davis, G.A., and others, 1980, 1982) suggested an early Tertiary or Late Cretaceous age for mylonitization. In contrast, Rehrig and Reynolds (1980) proposed a mid-Tertiary age for the mylonitic fabric in lower-plate rocks based on similarity to mylonitic fabrics of known or suspected mid-Tertiary age in similar tectonic settings elsewhere in Arizona. A mid-Tertiary age was eventually established for at least some of the mylonitic fabric (Wright and others, 1986).

Study of mylonitic petrofabrics in the Whipple Mountains revealed that the sense of shear during mylonitization was the same as the sense of shear along the detachment fault during fault movement (Davis, G.A., and others, 1986; Davis, G.A., and Lister, 1988). This observation supports the now generally accepted model for mylonitization and detachment faulting first proposed by Wernicke (1981, 1985): Mylonitization occurred within ductile shear zones along the down-dip projection of detachment faults; mylonitic fabrics cooled and passed upward through the brittle-ductile transition as they rose isostatically in response to detachment-fault movement and associated tectonic denudation (see also Davis, G.H., 1983; Reynolds, 1985; Davis, G.A., and others, 1986). The existence of a mylonitic front in the Whipple Mountains introduces complexity to models for the origin of the

Figure 5 (next page). Geologic map of the Clara Peak area showing northwest-trending folds of lower-plate mylonitic foliation. Modified from Woodward (1981).

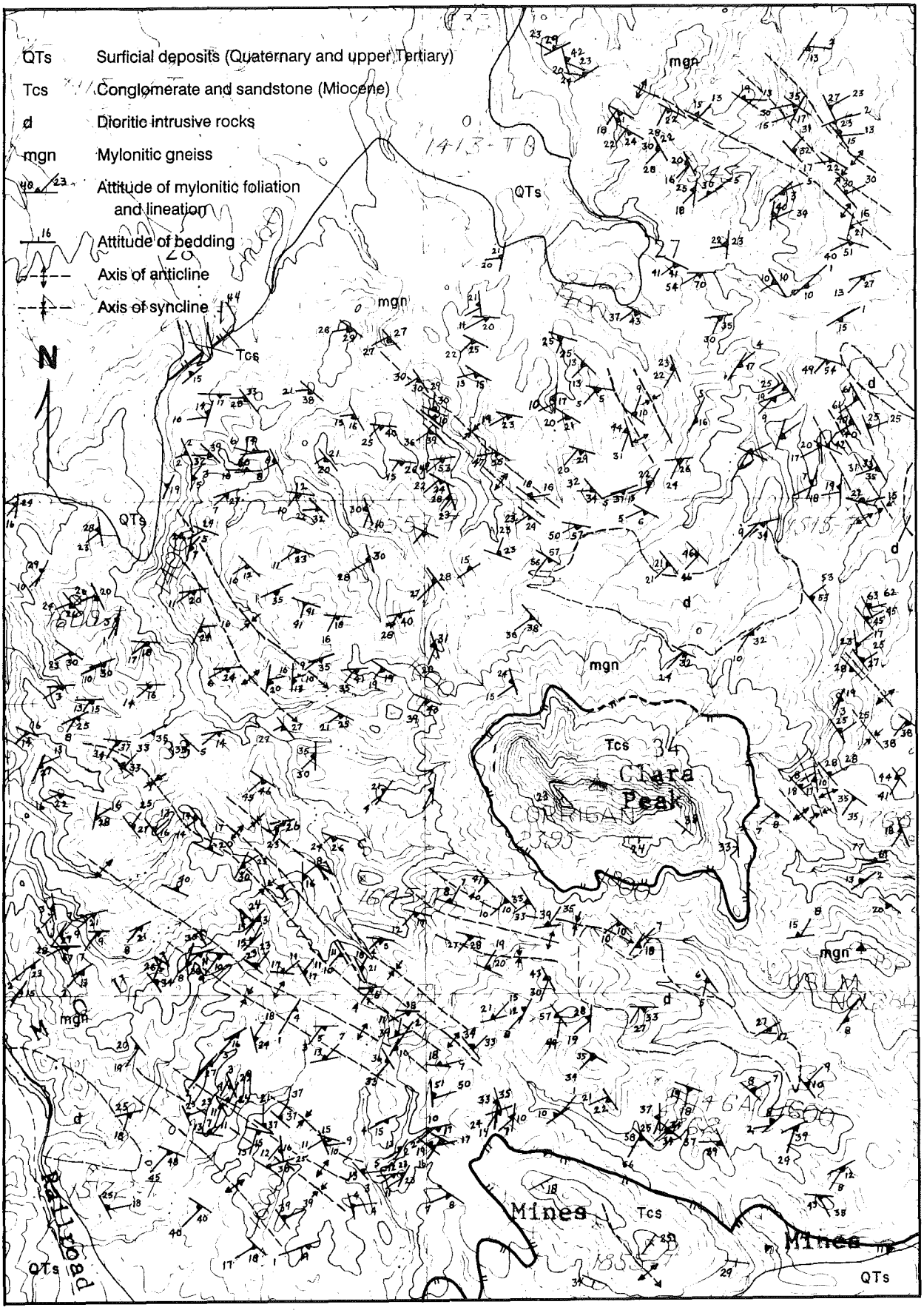
QTs Surficial deposits (Quaternary and upper Tertiary)
Tcs Conglomerate and sandstone (Miocene)
d Dioritic intrusive rocks
mgn Mylonitic gneiss
Attitude of mylonitic foliation and lineation
Attitude of bedding
Axis of anticline
Axis of syncline
N
Clara Peak
Mines
Railroad

mylonites, but there is little doubt that mylonitization reflects mid-Tertiary extensional tectonism (Davis, G.A., 1988; Davis, G.A., and Lister, 1988). Geobarometric and thermochronologic studies confirm the large-magnitude mid-Tertiary uplift, decompression, and cooling predicted by the shear-zone model (Davis, G.A., and others, 1987; Fryxell and others, 1987a; Anderson, J.L., and others, 1988). Laterally varying magnitudes of tectonic denudation and associated isostatic uplift apparently resulted in warping of detachment-fault surfaces (Howard and others, 1982b; Spencer, 1984b).

ENE-trending undulations of the detachment-fault surface in the Buckskin and Rawhide Mountains and nearby ranges were interpreted by Frost (1981a,b) and Cameron and Frost (1981) as folds produced by mid-Tertiary crustal extension parallel to fold axes. In contrast, the undulations in the Buckskin and Rawhide Mountains were interpreted by Osborne and Woodward (1980), Osborne (1981), and Woodward (1981) as primary grooves in the detachment-fault surface and not as folds. This interpretation was based on their recognition of northwest-trending folds in the lower plate (Fig. 5) that were truncated by the detachment fault and not refolded about east-northeast axes. In the nearby Whipple Mountains, folding of lower-plate foliation and of lithologic layering about northeast-trending axes is more pronounced than undulations of the detachment-fault surface, indicating that folding of lower-plate rocks probably occurred before the form of the present detachment fault was established, and that the detachment fault partially mimics the older folds of foliation and lithologic layering (Davis, G.A., and Lister, 1988).

Reynolds (1980a) and Wilkins and Heidrick (1982) first recognized that detachment-fault-related mineral deposits represent a distinct, previously unrecognized deposit type. These deposits were further characterized by Spencer and Welty (1986) and Wilkins and others (1986). Wilkins and others recognized the highly saline character of the aqueous fluids that caused mineralization and proposed that such fluids originated as basin brines. All of these workers considered the detachment-fault zone to be the primary conduit for ascending, mineralizing fluids.

Recent seismic-reflection and seismic-refraction studies of the lithosphere beneath the Buckskin and Rawhide Mountains and adjacent areas indicate that the Moho in this area is fairly flat and is at a depth of between 27 and 30 km (Hauser and others, 1987; McCarthy and others, 1987; McCarthy and Thompson, 1988, Fig. 11). Lithologic layering of lower-plate rocks and a mid-crustal zone of slightly elevated seismic velocities both appear to be broadly uplifted and arched beneath the Buckskin and Rawhide Mountains (Hauser and others, 1987; McCarthy and Thompson, 1988, Fig. 11). Industry seismic-reflection data suggest that the ENE-trending corrugations of lithologic layering are underlain at a depth of several kilometers by rocks that have horizontal reflections (Frost and others, 1987).

THE FUTURE

Although many of the geologic characteristics of the Buckskin and Rawhide Mountains are moderately well understood, some features have defied understanding. Most of the bedrock exposures in these mountains are of lower-plate rocks, yet these are the least understood rocks in the complex. Gneissic lower-plate rocks are suspected to have a largely Proterozoic protolith age and are intruded by sills of Tertiary and probable Cretaceous granitic rocks. It is not known, however, if amphibolite-grade metamorphism and gneissic layering were primarily the product of Proterozoic, Mesozoic, or even Tertiary deformation and metamorphism. Were these rocks affected by deep-seated thrusting related to formation of the Mesozoic Maria fold-and-thrust belt? Detailed geologic mapping, structural and petrographic studies, and sophisticated geochronologic study will be required to unravel the geologic history of the lower plate.

The origin of the ENE-trending sinusoidal folds of lower-plate foliation and lithologic layering is unknown. Approximate parallelism between fold axes and mid-Tertiary mylonitic lineation suggests that folding was mid-Tertiary in age and related to extensional tectonism, but the cause of shortening perpendicular to fold axes remains enigmatic. Possibly the lower plate of the Buckskin and Rawhide Mountains was in a constrictional strain field during mid-Tertiary folding and extension. Reduction of the flexural strength of the upper crust due to slip on low-angle faults and perhaps to slip between gneissic layers may have been necessary for folding to occur (Spencer, 1982, 1987). Some new ideas and more sophisticated numerical simulations will possibly lead to clarification of the origin of the lower-plate folds.

The abundance of evidence for widespread mid-Tertiary mineralization and alteration suggests that complex chemical and physical processes operated on a scale at least as large as the metamorphic core complex itself. Genetic relationships between Cu + Fe $\pm$ Au mineralization and carbonate metasomatism along detachment faults and K metasomatism and Mn mineralization in the upper plate have not been established, yet all were produced approximately synchronously in the same tectonic environment and are remarkably well developed in the Buckskin and Rawhide Mountains. Careful geochemical, isotopic, fluid-inclusion, petrographic, and field studies will probably be required to determine the independence or relatedness of different mineralization and alteration phenomena.

Although this volume represents a major step forward in deciphering the complex geologic evolution of a major Cordilleran metamorphic core complex, it is clear that many questions remain unanswered. One can only hope that future investigators find these problems interesting and tractable and that the momentum established since Terry Shackelford's pivotal dissertation will continue to advance the geologic understanding of this remarkable area.

Terry Shackelford and the Rawhide Mountains: A retrospective view

GREGORY A. DAVIS *Department of Geological Sciences, University of Southern California, Los Angeles, California 90089-0741*

Terry Shackelford camped, that summer of 1973, just inside the portal of an adit at the Rawhide mine. It was simply too hot to camp anywhere else during his first June and July in western Arizona. For 18 consecutive days in the middle of his first field season, the temperature had climbed above 110°, and above 115° for 9 of those days! Those, of course, were shade temperatures, although shade was hard to find in the Rawhide Mountains. In his adit, however, the temperature was a constant 72°, the product of an ever-present stream of cool air that flowed, bewilderingly in those scorching summer months, from the depths of the mine behind him. The adit was just wide enough for one cot, but it was "home." As befitting one of the most temperate microclimates for miles around, it was a home shared with others: an occasional, unwelcome rattlesnake; a tiny, persistently curious lizard; an everchanging number of bees, which fortunately never entered the portal very far; and a frustrated, sulky bat with a wingspan of 8 or 9 inches. Terry's and the bat's lives were very much out of phase: he was a daytime person; it was a nighttime bat. Dusk would fall and the bat, in response to instincts or hunger, would feel the need to escape the mine. From somewhere in the inner workings, it would fly in dramatic Draculian fashion down the long, dimly lit adit toward Terry, who sat on his blockading cot, inking the results of another day's mapping. While I visited Terry, the bat never had the courage to fly by him, but with an almost audible sigh of frustration, it would slow its flight, turn sharply around to reverse its course, and return to the depths of the mine.

That was an exciting summer for Terry and for me as his adviser. He had begun the detailed mapping of cryptic rock assemblages and structures that defied easy geologic categorization, but were so extensively developed on both sides of the Colorado River in western Arizona and southeastern California that they signaled the past operation of unknown tectonic processes on a regional scale. Although we did not know it at the time, we were experiencing the excitements and puzzlements that Peter Misch and his students at the University of Washington must have encountered 15 years earlier in their mapping of the "northeastern Nevada structural province," the domain of the extraordinary Snake Range décollement and its associated rocks and structures (e.g., Misch, 1960). In the early 1970's, the lower Colorado River region was one of the largest geologically unstudied areas of the southern U.S. Cordillera. It was a region too far from the major universities of southern California and southern Arizona and too inhospitable during summer recess to be a favored area for academic geoscientists or their students. At least, that was the case before Ann Terry arrived.

Ann Terry began field studies in the northeastern Whipple Mountains in 1968 for an undergraduate thesis project at San Diego State University and continued them for a master's thesis, which was completed in 1972. Her work was the first in that range since the 1937 Cal Tech Ph.D. dissertation of Luis Kemnitzer. The principal importance of her work was that she rediscovered the low-angle Whipple fault, which H. L. Ransome had described locally in 1931 as the Bowman Wash overthrust separating upper-plate Tertiary strata from lower-plate crystalline rocks. Kemnitzer's later mapping delineated the fault-block geometry of Tertiary and basement rocks in the eastern Whipple Mountains, but he discounted Ransome's observation of a major low-angle fault and did not recognize that the tilted fault blocks he mapped lay in the upper plate of that structure.

In June 1970, Ann Terry invited Clark Burchfiel and me to visit her field area and to see the Whipple Mountain fault, which she interpreted as a Mesozoic thrust fault involving only crystalline rocks. We were impressed by her studies in that remote, rugged area, but failed to convince her that tilted Tertiary rocks above the fault were truncated downward by it, a relationship that requires the fault to be late Tertiary in age. With Ann Terry and her fellow student Judy Gassaway as our guides, we next traveled into western Arizona, where we were introduced to the Whipple-like structures and rock units of the Rawhide and Buckskin Mountains. Gassaway was then engaged in undergraduate thesis mapping (completed in 1972) in the Lincoln Ranch area of the Buckskin Mountains, directly south of the Rawhide Mountains. Burchfiel and I were staggered by the evidence for regional development of a cryptic, lineated, mylonitic, crystalline terrane and an overlying low-angle brittle fault, which we interpreted to be Tertiary in age. Ann Terry's 1972 thesis was the first to discuss the regional extent of that mylonitic lower plate and to define correctly its northeastern and southwestern geographic limits. The "mylonitic zone" that she defined and

in Spencer, J.E., and Reynolds, S.J., eds., 1989, Geology and mineral resources of the Buckskin and Rawhide Mountains, west-central Arizona: Arizona Geological Survey Bulletin 198, p. 11-14.

mapped below the "Whipple Mountain thrust fault" consisted of the highly cataclasized rocks that are now generally referred to as "chloritic breccias." She recognized, however, that these cataclasites had been developed across preexisting laminated and lineated gneisses, the "mylonitic gneisses" of Shackelford (1976b) and later workers in the Whipple Mountains (Davis, G.A., and others, 1980).

Spurred by the desire to know more about this puzzling terrane, I encouraged Terry Shackelford to begin doctoral mapping studies in the Rawhide Mountains in the summer of 1973. Terry had graduated from the University of Wisconsin in 1968 and had entered USC after a 3-year stint as an officer in the U.S. Army. A soft-spoken, deliberate young man, Terry was everything one looked for in prospective students. He was bright, mature, serious about his education, and eager to start a challenging project in structural geology. He further endeared himself to me with three other attributes: a low-key, understated sense of humor, a healthy skepticism about my pontifications and pronouncements, and talents for field cuisine never before, or since, equaled among my students. His Cointreau-accented crepe suzettes made him a culinary legend in his own time. Terry's was the first of 18 USC thesis and dissertation projects in the lower Colorado River region, all supported by National Science Foundation grants to me and my colleague, J. Lawford Anderson.

In the fall of 1973, I joined Terry in mapping the lower Colorado River region when I undertook local field studies in the south-central Whipple Mountains during an investigation of a possible nuclear-power plant site east of Vidal Junction. A year later, W.J. Carr and D.D. Dickey began extensive reconnaissance mapping in the greater Whipple Mountains region as part of the U.S. Geological Survey's evaluation of the Vidal site. It was they who first applied the adjective "detachment" to the Whipple Mountains fault (Carr and Dickey, 1976), an adjective that Shackelford (1976a) later applied to the similar, probably correlative, Rawhide fault.

The product of Terry's labors (and for many days beneath the searing Arizona sun, they were very much "labors") is presented elsewhere in this volume as an abridged version of his dissertation. That dissertation provided the first in-depth look at a lower Colorado River "metamorphic core complex," where both upper and lower plates and the intervening low-angle normal (detachment) fault are exposed. R.E. Anderson (1971) had previously published the results of his mapping in the extended Eldorado Mountains of southern Nevada, but the underlying, subhorizontal basal fault, which he inferred from the geometry of imbricate, listric, upper-plate normal faults in that area, was not exposed. From field studies, Terry correctly recognized the major geometric elements and kinematic characteristics of Cordilleran mylonitic-gneiss/detachment-fault terranes. These included a regionally developed, low-angle fault of noncompressional origin (his "basal dislocation surface"), a lower-plate assemblage of mylonitized rocks formed by penetrative ductile flow, and an upper plate characterized by a complex Cenozoic history of extensional faulting.

He, as had Ann Terry before him, recognized the northeast-southwest parallelism of mineral lineation in lower-plate rocks and slickenside striae on superimposed and higher faults. Both he and Ann Terry concluded that the mineral lineation had formed parallel to the principal direction of tectonic transport during regional deformation (a controversial view in those days), but their interpretations of causative deformations differed. Ann Terry believed that deformation was due to Mesozoic thrust-faulting along the Whipple fault, although her "mylonitic" rocks were the chloritic breccias spatially associated with the fault. Terry Shackelford believed that the breccias in his area were related to displacement along the Miocene Rawhide fault. He thought that the lineation in the underlying mylonitic gneisses had formed within a somewhat cryptic "major zone of Mesozoic low-angle tectonic transport related to the formation of the infrastructural complex," a concept inherited from Armstrong and Hansen (1966), and was unrelated to the Rawhide fault.

Terry puzzled over the statistical parallelism in trend of striae, associated with Miocene faulting, and the older mylonitic lineation. The mylonites, extensively brecciated and altered beneath the fault, clearly predated it. He thought, however, that there might be a logical reason for parallelism of transport in separate events: "Basement structure(s) that resulted from the Mesozoic event may have controlled the nature and shape of the basement uplift from which the cover slid off." In contrast, a number of Arizona geologists, among them Steve Reynolds, Bill Rehrig, George Davis, and Peter Coney, later proposed various genetic relationships between mylonitization and detachment faulting during crustal extension. The debate between "Arizona" and "California" schools of thought regarding the temporal relationships between ductile deformation that results in mylonitic gneisses and brittle deformation that results in detachment faults was not completely resolved, at least from a USC point-of-view, until 1986, when geochronological studies in the Whipple Mountains unequivocally documented mid-Tertiary mylonitization (DeWitt and others, 1986; Wright and others, 1986).

Terry hypothesized in his dissertation that the Rawhide Mountains allochthon, the upper plate of the Rawhide fault, had been emplaced by northeast-directed gravity sliding of major proportions. Although geologists now believe that the Rawhide fault roots northeastward into deeper levels of the crust (as Terry believed before his death), Terry correctly assessed its geometric and kinematic characteristics *within the area* he mapped. Furthermore, he extended his observations about the nature of the Rawhide fault and its relationship to lower-plate mylonitic rocks to other Tertiary "slide complexes," including those of northeastern Nevada and the Death Valley area.

> Studies of many of the areas where low-angle Tertiary faulting has occurred reveal that there is an apparent correlation between the presence of a

> Mesozoic metamorphic terrane and Tertiary low-angle denudation faulting. Invariably, low-angle dislocation surfaces (dêcollement zones) separate the penetratively deformed autochthon from brittlely deformed allochthonous rocks, although interpretation of the timing relationships between metamorphism and dislocation differ (Shackelford, 1976b, p. 185).
>
> Almost all of the Tertiary slide complexes have certain basic characteristics in common: (1) shingling normal faults that merge with a low-angle basal dêcollement or dislocation surface; (2) intense brecciation of upper plate rocks and only moderate deformation of the lower plate; (3) an upper plate that contains steeply dipping strata which are truncated by the low-angle dislocation surface(s); (4) upper plate strata normally dip in a direction opposite to that of tectonic transport; (5) only minor large-scale folding -- deformation is usually characterized by rigid translation of blocks; (6) general displacement of younger rocks over older rocks; and (7) the general presence of a topographic high off of which the blocks could have moved.
>
> Many, but not all of the slide terranes, are associated with Mesozoic metamorphic complexes. It is interesting to note that many of these metamorphic complexes also yield mid-Tertiary cooling ages, 40 to 20 m.y. B.P. ..., which appears to record the final uplift and cooling of the metamorphic terranes (Shackelford, 1976b, p. 192-193).

Much of what Terry wrote above anticipated major aspects of G.H. Davis' and Peter Coney's 1979 paper, "Geologic development of the Cordilleran metamorphic core complexes." The Davis-Coney paper was an extremely important regional synthesis that is generally, and appropriately, credited with focusing attention on the enigmatic association of mylonitic metamorphic complexes and low-angle normal faults.

The concept that the Rawhide Mountains allochthon had moved unidirectionally northeastward by gravity sliding was first proposed by Shackelford in 1975 at a GSA Cordilleran Section meeting. His conclusion was clearly influenced by the writings of Burchfiel and G.A. Davis (1971), Armstrong (1972), Coney (1974), and G.H. Davis (1975), all of whom had proposed various gravity-driven models for low-angle Tertiary faults elsewhere in the Cordillera. In his dissertation, Terry admitted that there were difficulties with a gravity-sliding tectonic model such as the origin of the "slide" and the location of its eastern toe. For example, he had mapped distinctive plutonic bodies in the Rawhide allochthon, but could not locate their *in situ* lower-plate equivalents in areas to the southwest, even as far as the Buckskin Mountains several tens of kilometers away. Because of this, he privately confided to me, total displacement on the Rawhide fault had probably exceeded 30 or 40 km. He also could not find the offset, upper-plate equivalents of the "autochthonous," lower-plate, mylonitic gneisses. To make matters worse, as Terry readily admitted, there was "no direct evidence" that eastern portions of the 250-km^2 Rawhide Mountains slide complex had ever moved across the earth's surface, although the geology of areas to the northeast was imperfectly known.

Because of my understanding of the Whipple Mountains to the southeast, I remained skeptical of the gravity-sliding model for some time; in an abstract, I simply referred to a "thin-skinned, brittle deformation of denudational (extensional) type" (Lingrey and others, 1977). But by 1979, I had endorsed Terry's model (Davis, G.A., and others, 1980), largely because of "older-over-younger" faulting relationships in the Rawhide Mountains that we interpreted as telescoping within the distal portion of a sliding allochthon, but which are probably inherited from Mesozoic thrust faulting that was unrecognized at the time. The sliding model was not to have a long life.

Lucchitta and Suneson (1981a), in reply to a 1980 paper by Shackelford, reported that the upper plate of the Rawhide fault in areas north of Terry's map area "is anchored at its northeast end to autochthonous basement rocks of Colorado Plateau type." Therefore, they suggested, the mylonitic lower plate of the Rawhide fault must have moved southwestward with respect to the Plateau and out from beneath the brittlely extending upper plate by a process of "non-brittle underflow"; the mylonitic gneisses of the Rawhide and Buckskin Mountains were the Tertiary products of such underflow. A broadly compatible theory had just been advanced by Rehrig and Reynolds (1980) for southern and western Arizona metamorphic core complexes, including the Rawhide and Buckskin Mountains. These authors presented isotopic data favoring Tertiary mylonitization in some of the desert ranges.

Although the Lucchitta-Suneson and Rehrig-Reynolds papers had set the gravity-slide theory reeling, in my opinion it was Brian Wernicke (1981) who provided the knock-out blow. Wernicke, in his insightful *Nature* paper, proposed that low-angle normal faults were the products of extreme lithospheric extension, the extensional counterparts of low-angle thrusts formed during crustal compression. His ideas contained philosophical elements of earlier publications, but eliminated the need to relate regional detachment faults to inferred midcrustal boudins (Davis, G.H., and Coney, 1979), to localized magmatic complexes (Rehrig and Reynolds, 1980), or to areas of crustal uplift and subsequent gravity sliding (Davis, G.A., and others, 1980). The enigmatic lower Colorado River extensional terrane suddenly became less enigmatic. Wernicke had been introduced to that terrane during his undergraduate years at USC. It is fair to state that Shackelford's Rawhide Mountains studies, and those of other USC graduate students and faculty in the Buckskin and Whipple Mountains, provided him with fertile intellectual seeds for his historic paper.

Terry, upon completing his doctorate in 1976, took a position with Shell Oil Company in Houston. Five years later he joined Marathon Oil in Littleton, Colorado, where he assumed directorship of Marathon's research program in structural geology. Although he was involved

in various aspects of structural study, he continued to focus his research and lecturing on extensional tectonics. Terry spoke often of his longing to return to the Rawhide Mountains to resolve some nagging geologic problems left from his dissertation work. That was not to be. His wife Sherry had a health problem aggravated by the high elevation of the Denver area. Terry felt that their departure from Colorado was necessary, and he requested transfer to Marathon's headquarters in Findlay, Ohio. In February 1983, one month after his transfer, Terry, Sherry, and their 6-year-old daughter, Shauna, were killed in a head-on car collision on a rural road in Ohio. He was 36.

He is missed by all of us who knew him.

And ... someday ... on a hot summer day in western Arizona, I would like to return to that cool, narrow adit at the Rawhide mine, where important parts of the geologic story told in this volume began to be assembled.

* * * *

An endowment fund to assist graduate students in their structural geology research has been established in Terry's name in the Department of Geological Sciences at the University of Southern California, Los Angeles, California 90089-0741.

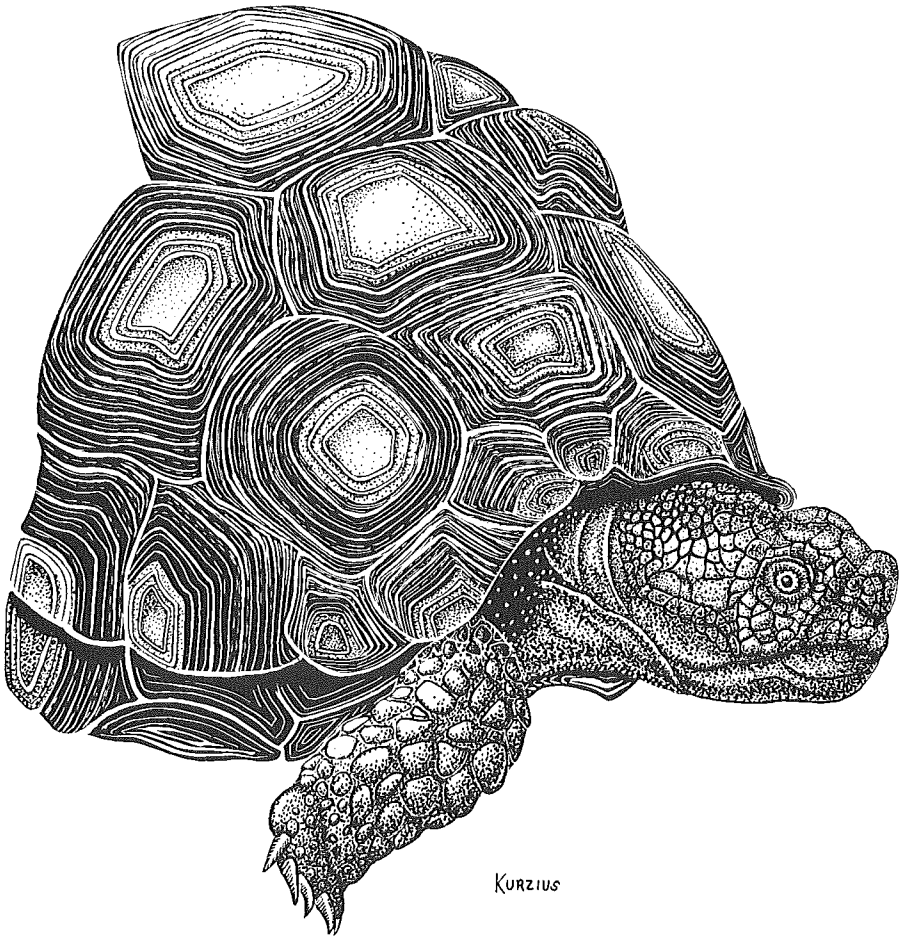

Structural geology of the Rawhide Mountains, Mohave County, Arizona

TERRY J. SHACKELFORD* *Department of Geological Sciences, University of Southern California, Los Angeles, California 90089-0741*

PREFACE BY GREGORY A. DAVIS

The following article, Structural Geology of the Rawhide Mountains, Mohave County, Arizona, *by Terry J. Shackelford, is a condensation of Terry's Ph.D. dissertation at the University of Southern California, which was completed in February 1976. Topics that have been most condensed include those relating to the Precambrian geology of western Arizona; stratigraphic, lithologic, and petrographic descriptions of some rock units; Terry's discussion of microscopic structures and petrofabric analysis; and aspects of regional Cordilleran geology. Much of the deleted material is either too detailed for publication here (e.g., petrography), has undergone major revision in subsequent research by others (e.g., chronology of Tertiary strata), or is outdated and no longer critical to our present understanding of detachment faulting and genetically related mylonitization of lower-plate rocks. The ellipsis mark ". . ." indicates major deletions from the original text. Photographic figures have not been reproduced, but most of the original line figures and plates are included. Footnotes in this abridged version of the dissertation were written by me. I have attempted to condense Terry's original text without seriously disrupting its flow, but some sections might appear disjointed to the reader. If so, I hope that the reader will recognize the disruptions as a consequence of my editorial efforts and not as a negative reflection of Terry's original prose.*

ABSTRACT

The Rawhide Mountains, western Arizona, consist of a complexly deformed assemblage of Precambrian meta-igneous and metasedimentary, Paleozoic sedimentary, Mesozoic(?) igneous plutonic, and Tertiary sedimentary and volcanic rocks. Precambrian rocks include quartzo-feldspathic gneisses of granitic parentage, subordinate impure marbles, and biotite granite. Metavolcanic rocks of Precambrian or Mesozoic age are represented by quartz-sericite and biotite-epidote-quartz schists. Paleozoic sedimentary rocks are quartzites, phyllites, and carbonates. The lowest quartzite and phyllite members are correlated with the Tapeats Sandstone (Bolsa Quartzite) and Bright Angel Shale (Abrigo Formation), respectively. The carbonates are similar to Paleozoic limestones and dolomites in western Arizona, but they are too badly dismembered to make positive correlations. Tertiary rocks include the Artillery (Eocene?) and Chapin Wash (Miocene) Formations. The Artillery Formation is a varicolored sequence of interbedded conglomerates, arkoses, siltstones, limestones, and volcanic rocks. The Chapin Wash Formation consists of red conglomerates, arkoses, siltstones, basalt, and latite. Late Tertiary basalt and Quaternary alluvium comprise the youngest stratigraphic units, which lie unconformably above older rocks.

The structural history of the Rawhide Mountains includes (1) Precambrian intrusion of granitic rocks and the possible extrusion of basaltic to rhyolitic rocks; (2) Mesozoic(?) metamorphism and penetrative deformation of the Precambrian crystalline rocks and overlying Precambrian(?) and Paleozoic rocks; (3) late Tertiary gravity sliding involving Precambrian(?) through Miocene rocks; and (4) latest Cenozoic development of northwest-striking oblique dip-slip and reverse dip-slip faults.

Mesozoic(?) deformation is characterized by the development of a metamorphic infrastructural complex. Precambrian igneous, sedimentary, and metamorphic(?) rocks that form the core of this complex were metamorphosed to amphibolite grade. Penetrative cataclasis (mylonitization) of these rocks occurred synchronously with late(?) stages of metamorphism. Greenschist-facies metamorphism affected some of the overlying Precambrian(?) metavolcanic and Paleozoic rocks. This deformation resulted in the development of a penetrative cataclastic foliation and a strong N50°E mineral lineation. Major northeast-directed tectonic transport is inferred for this terrane.

The dominant structural feature of the range is the late Tertiary gravity-slide complex. This complex appears to cover more than 1,000 km^2 in west-central Arizona. In the Rawhide Mountains the complex is characterized by a chaotic assemblage of Precambrian(?) through Miocene rocks that are separated from underlying mylonitic gneisses by a remarkably sharp basal dislocation surface. Superposition of rock units is primarily younger over older. Almost all of the major rock units are separated from each other by low-angle dislocation surfaces. The chaotic slicing and shuffling of upper-plate rocks has occurred along a complex series of high- and low-angle

* Deceased

in Spencer, J.E., and Reynolds, S.J., eds., 1989, Geology and mineral resources of the Buckskin and Rawhide Mountains, west-central Arizona: Arizona Geological Survey Bulletin 198, p. 15-46.

dislocation surfaces that merge with or are subparallel to the basal dislocation surface. Bedding and foliation in the allochthon typically dip to the southwest at a high angle to the basal dislocation surface. The persistent northwest strike and southwest dip of upper-plate rocks, the geometry of the fault sets, and the orientation of minor structures indicate northeast-directed movement for the slide complex. Gravity sliding occurred between 15.9 m.y. and about 10 m.y. ago.

Latest Cenozoic, high-angle, oblique, normal dip-slip, and reverse dip-slip faulting postdate formation of the gravity-slide complex. The eastern border of the Rawhide Mountains is formed by a major fault with left-lateral dip-slip components. This fault cuts the mylonitic-gneiss terrane and the overlying gravity-slide complex. In the central part of the range, reverse dip-slip faults cut the basal dislocation surface and place mylonitic gneisses on top of isolated slide blocks of Chapin Wash material.

Late Tertiary low-angle deformation is widespread in the Basin and Range Province. Structures in this province previously referred to as late Tertiary thrust faults are here interpreted as gravity slides. The gravity sliding appears to have been the thin-skinned crustal response to the rapid rise of discrete crustal blocks just prior to or contemporaneous with Basin and Range faulting.

INTRODUCTION

Purpose and Background

The Rawhide Mountains, Mohave County, Arizona are an isolated range of low hills in west-central Arizona (Fig. 1), a region of essentially unmapped geology. The purpose of this study was to determine the structural geology of a large portion of the Rawhide Mountains and to relate the structure of this area to the tectonic framework and evolution of the southwestern United States.

The Mesozoic-early Tertiary development of western North America is characterized primarily by igneous plutonic activity, large-scale thrust faulting, and the formation of regional metamorphic terranes. East-directed thrusts extend from Alaska into southeastern California (King, 1969). In Nevada and Utah the thrusts have northeast strikes controlled by Paleozoic paleogeographic elements, including the hinge zone between areas of miogeosynclinal and platform sediments. However, in southeastern California these thrusts depart from the geosynclinal terrain and strike southeastward across platform sedimentary rocks and their cratonal basement (Burchfiel and Davis, 1972, 1975). A logical extension of these thrusts to the southeast appears to be through the

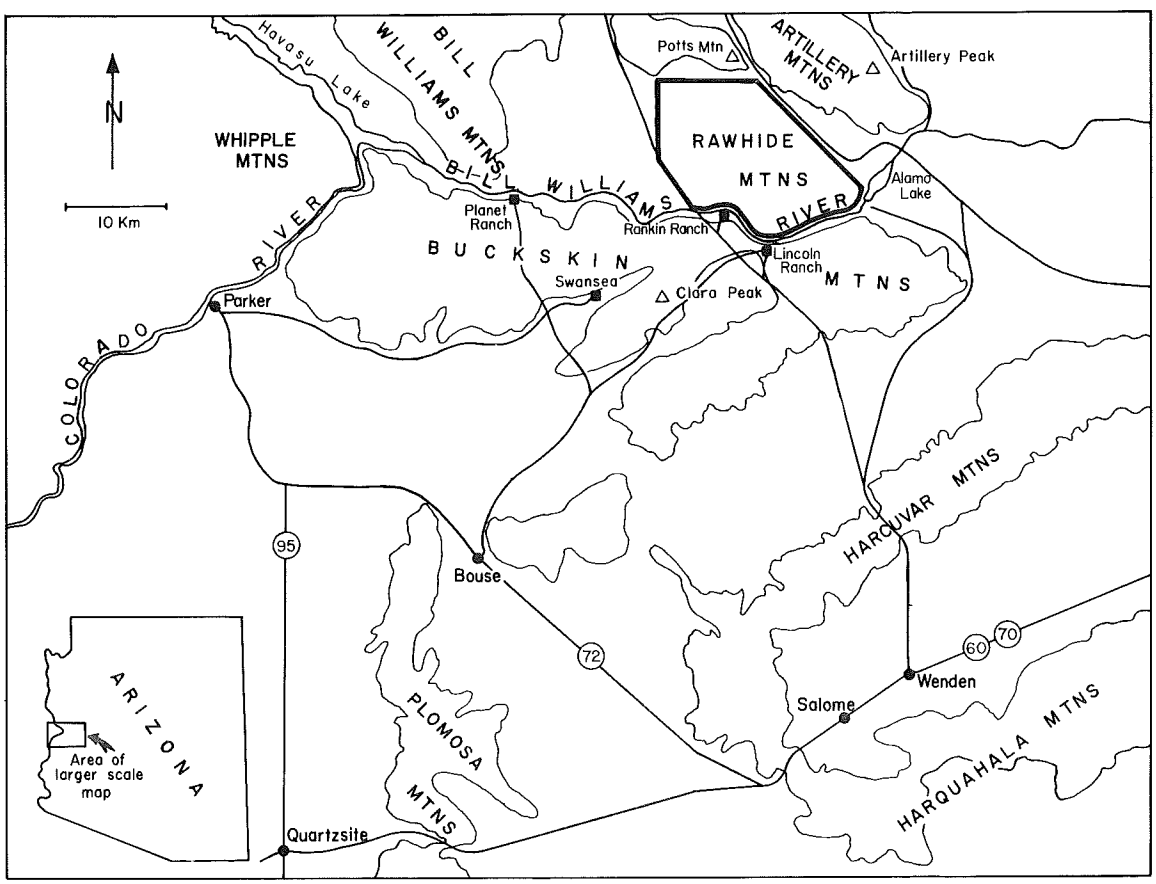

Figure 1. Index map showing location of the Rawhide Mountains and surrounding area. Dark line outlines study area and area of Plate 1.

Rawhide Mountains area of western Arizona and toward thrust faults reported in southeastern Arizona (Cooper and Silver, 1964; Drewes, 1971; Corbitt and Woodward, 1973).

Hamilton (1971) noted that in the Big Maria Mountains, California, thrust faulting appeared to be contemporaneous with and related to the development of a metamorphic infrastructural complex. Similar metamorphic complexes have been reported in the Death Valley area (Lanphere and others, 1964) and in northeastern Nevada, western Utah, and southern Idaho (Armstrong and Hansen, 1966; Armstrong, 1968). The possible existence of an infrastructural complex in western Arizona was noted by the author and Gregory A. Davis during a 1972 reconnaissance of the Rawhide Mountains area. Thus, there appeared to exist in western Arizona an excellent opportunity to study the relationship between southeastward extensions of Cordilleran thrust faulting and the development of regional metamorphic infrastructure.

However, it became apparent very early in this study that probable Mesozoic deformation in the Rawhide Mountains has been greatly modified by late Tertiary deformation of distinctive style. The late Tertiary deformation is characterized primarily by low-angle normal faulting on a scale heretofore unrecognized in the southwestern United States. Therefore, the presence of these late Tertiary low-angle normal faults has provided added significance to the study of the structures in the Rawhide Mountains.

Previous Work

All previous work done in the Rawhide Mountains and most of western Arizona has been of a reconnaissance nature. . . . The only published maps of the study area proper are the geologic maps of Mohave and Yuma Counties (Wilson and Moore, 1959; Wilson, 1960; scale 1:375,000). Thrust faults that variably juxtapose Precambrian, Paleozoic, and Late Cretaceous-early Tertiary(?) rocks are indicated on these maps. This faulting has been suggested (Lasky and Webber, 1949; Wilson, 1962, p. 79) to be contemporaneous with thrust faulting reported in the Artillery Mountains to the east.

Manganese resources in the Artillery Mountains were investigated and mapped by Lasky and Webber (1944, 1949; scale 1:31,680). In their reports, they formally named the Artillery Formation (Eocene?) and the Chapin Wash Formation (lower Pliocene?). Of considerable significance to this study was their recognition (1949, p. 40-42) of the Artillery "thrust," a low-angle fault that places Precambrian(?) gneisses and Paleozoic(?) carbonates over the Artillery Formation.

Tertiary rocks in the Lincoln Ranch basin directly south of the Rawhide Mountains (Fig. 1) were described by Gassaway (1972, 1973). She suggests that sedimentary rocks there may be correlative with the Artillery(?) and Chapin Wash Formations in the Artillery Mountains, but that they are probably Miocene and younger in age. Her age assignments are based on fossil camel and bird tracks. The Tertiary sedimentary rocks of the Lincoln Ranch area are separated from the basement gneisses by a "smooth" and slightly polished . . . "old erosional surface" (Gassaway, 1972, p. 23). A similar surface is present in the Rawhide Mountains, but a much different origin and significance is attributed to it as the result of this study. . . .

Geography

The Rawhide Mountains are a roughly circular range located about 55 km east of Lake Havasu and Parker, Arizona (Fig. 1) and about 150 km northwest of Phoenix. The area consists of a series of low hills, with Fool's Peak (955 m) being the highest feature in the range. The average elevation is about 520 m; the total relief is about 680 m.

The Rawhide Mountains are bounded by distinct physiographic features. On the north, Ester Basin, a northwest-trending, low narrow valley separates the range from the Aubrey Hills to the north. Sandtrap Wash, a large north-northwest-trending valley separates the Rawhide Mountains from the Artillery Mountains 3.5 km to the east. The western border is formed by the wide (7.0-km), alluvium-filled Castaneda Wash, whereas on the south the Bill Williams River delineates the Rawhide Mountains from the Buckskin Mountains. Geologically, the Rawhide and eastern Buckskin Mountains comprise a continuous terrane. . . .

Method of Investigation

Field investigations were carried out during the summers of 1973 and 1974 and for three weeks in the winter of 1974-75. A total of 16 weeks was spent in the field and 250 km^2 were mapped during the course of the study. Mapping was accomplished on topographic base maps enlarged to 1 inch = 1,320 inches (1:15,840) from four U.S. Geological Survey 15-minute quadrangle sheets: Artillery Peak (1966), Castaneda Hills (1966), Ives Peak (1966), and Swansea (1966).

Petrographic analysis of selected rock samples was conducted to determine the mineralogy and texture of the metamorphic and igneous rock. . . . Six oriented samples were collected in the field for petrofabric analysis. Five of these samples were collected from the mylonitic-gneiss complex and one was from a quartzite in the Paleozoic sequence. All the oriented samples were analyzed for the preferred orientation of quartz [0001]-axes.

OUTLINE OF THE MAJOR ROCK UNITS

The Rawhide Mountains consist of a complexly deformed assemblage of Precambrian(?) to late Tertiary rocks. The core of the range consists of Precambrian(?) mylonitic gneisses. A chaotic assemblage of allochthonous rocks is separated from these gneisses by an extremely sharp, low-angle dislocation surface. These allochthonous rocks consist of imbricated slices of Pre-

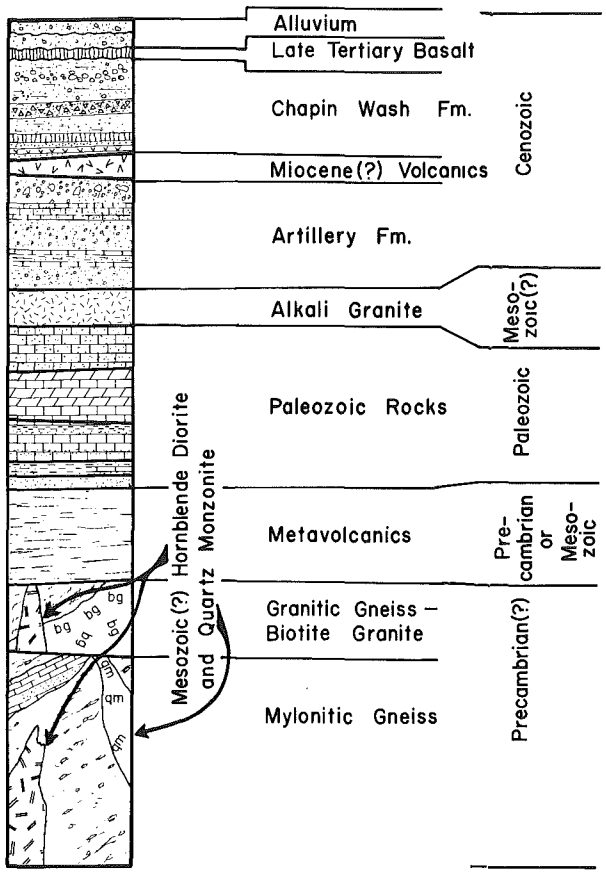

Figure 2. Simplified columnar section of the lithologic units in the Rawhide Mountains, Arizona. Stratigraphic succession is not implied.

cambrian(?) igneous and metamorphic, Paleozoic sedimentary, Mesozoic(?) igneous plutonic, and late Tertiary volcanic and sedimentary rocks. Unconformably overlying this chaotic sequence are late Tertiary basalt and Quaternary alluvium.

Because of structural complexities, the rocks have been divided into 10 basic lithologic units and arranged in an apparent age sequence (Fig. 2). Stratigraphic relationships are very tentative because the majority of the contacts between rock units are dislocational. The extreme disruption of the rock units, coupled with the overall lack of absolute age data and correlative units in nearby areas, has made even relative age assignments tenuous. Despite these difficulties, it is the writer's opinion that the relative age assignments reported herein are reasonably correct.

Mylonitic Gneisses

The mylonitic gneisses are the most extensive rock unit in the Rawhide Mountains. They form a complex that occupies the core of the range (Fig. 3; Plate 1) and is composed of two major assemblages, a quartzo-feldspathic gneiss of probable granitic parentage and a metasedimentary unit of marbles and quartzites. The metasedimentary rocks occur as discontinuous elongate bodies of rock within the more extensive quartzo-feldspathic gneiss terrain.

Texturally the gneisses are highly variable. Although they range from protomylonites and mylonites to uncommon biotite schists, when considered as a single entity they can be classified as mylonitic gneisses. The gneisses are usually light greenish-white in outcrop and compositionally banded. They typically have a distinctive and well-developed foliation, color banding, a pronounced, streaky mineral lineation, and augen of feldspar. Boudinage and recumbent isoclinal folds are common. Near the top of the complex, the rocks are usually highly fractured, deeply weathered, and dark, olive-drab green in color.[1] Wilson and Moore (1959) classified this unit as Precambrian schist. However, the coarse grain size, compositional banding, and overall texture require that these rocks should more correctly be called gneisses. . . .

The gneisses in the Rawhide Mountains are coherent rocks that have undergone intense shearing, show evidence of flowage, have fluxion structure, and have a bimodal grain-size distribution. The finer grained portion shows evidence of some recrystallization or neomineralization, whereas the larger, lensoid feldspar augen are distinctly porphyroclastic. Recrystallization and neomineralization do not appear to have advanced to the point that these rocks may be classified as mylonite gneiss or blastomylonite (Higgins, 1971, p. 11-13). The rocks throughout the complex are characterized by lepidoblastic and granoblastic domains, which impart an overall gneissic texture to the rocks. Following the terminology of Christie (1960) and Higgins (1971), most of the rocks in the gneiss complex may be classified as mylonites. However, the presence of the prevalent gneissic texture and the fact that all the gneisses are not mylonites, *sensu stricto,* suggest that the term *mylonitic gneiss* may be more appropriate to describe these rocks (this term is not to be confused with *mylonite gneiss*; Higgins, 1971, p. 11-13).

Distribution. The mylonitic gneisses cover an area of about 130 km^2 in the heart of the Rawhide Mountains. The gneisses extend to the south and southwest into the Buckskin Mountains and possibly into the Harcuvar Mountains. Thus the gneisses as mapped are part of a much larger terrane in western Arizona. The general outcrop pattern of the gneisses suggests that they may form a large domal structure in this part of Arizona.

The original or stratigraphic top and bottom of the gneisses are not exposed in the study area or in the immediate vicinity. The upper contact of the gneisses, wherever it has been seen in the Rawhide and Buckskin Mountains, is a low-angle dislocation surface that separates the mylonitic gneisses from overlying, at least in part, younger rocks. Limited reconnaissance in the Harcuvar Mountains suggests that at depth gneisses of Rawhide or Buckskin type become anatectic granites. Lit-par-lit injections of granitic material were found interfingering with these gneisses in this range. The

[1] These rocks beneath the Rawhide detachment fault would now be designated as "chloritic breccias."

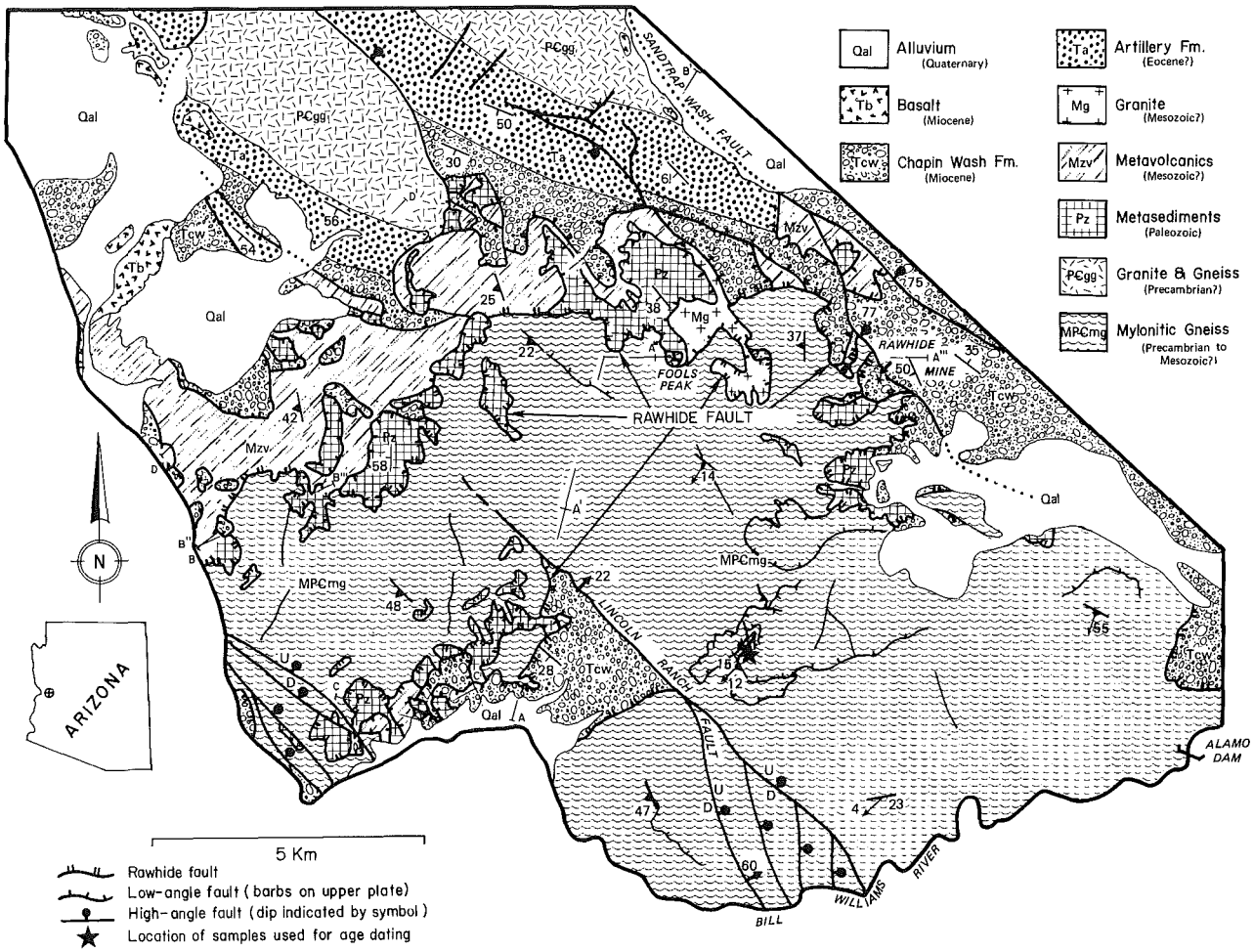

Figure 3. Simplified geologic map of the Rawhide Mountains showing locations of cross sections in Figure 5.

minimum structural thickness of the mylonitic gneiss in the Rawhide Mountains is estimated at about 2,500 m.

Lithologic Description. The mylonitic gneisses are characterized by a well-developed foliation, a streaky mineral lineation, augen of feldspar, and distinct compositional layering and color lamination. They are generally very homogeneous on a large scale and lacking distinctive and/or continuous marker units. Discontinuous lensoidal bodies of metasedimentary rocks, marbles, and quartzites, are the only recognizable units present within the otherwise quartzo-feldspathic gneiss terrane. Generally the gneisses weather to a light greenish-white, although more mafic-rich or highly altered areas often appear dark green.

The foliation in the mylonitic-gneiss terrane is predominantly of metamorphic origin, resulting from the penetrative flattening and elongation of individual mineral components. Foliation is also defined by layering produced by the alternation of compositional and color layers and by layers of varying grain size. Almost all of the rocks show evidence of penetrative ductile deformation: stringers of flattened elongate quartz, patches of mafic minerals, and the dimensional preferred orientation of individual mineral components are common. . . .

Feldspar is the most common mineral in the mylonitic gneisses. Large augen of K-feldspar form about 10 to 30 percent of the rock by volume. The augen range from 0.5 to 5 cm or more in length and are generally flattened in the plane of the foliation and elongated parallel to the lineation. K-feldspar consists of both orthoclase and microcline, with orthoclase being the more abundant. Plagioclase (An_{11-43}) occurs as smaller augen and is distinguishable only in thin section.

All feldspars show evidence of deformation and most are distinctly porphyroclastic. Undulatory extinction, granulated borders, fractures, and bent or offset albite twin lamellae are common features. Finer grained material is deflected around feldspar augen in most cases, although in a few instances, quartz grains appear to be truncated at the sharp border of feldspar grains. . . . There is no evidence that the feldspar augen have been rolled; rather, what one generally sees are tails of fine-grained quartz and feldspar on one or two sides on the feldspar augen. The tails lie in the plane of the foliation and would appear to indicate flattening perpen-

dicular to the foliation and extension in the plane of the foliation.

Quartz is the second most abundant mineral. It generally occurs in quartz-rich bands as elongate, ribbon-like crystals, flattened perpendicular to the foliation and elongated parallel to the lineation. Polygonal, recrystallized quartz is present along many grain boundaries. The individual grains commonly have serrate boundaries. Undulatory extinction, dimensional and crystallographic orientation, serrate grain boundaries, and deformation lamellae all attest to the penetrative deformation that these rocks have undergone. The presence of polygonal, strain-free quartz in some specimens suggests possible posttectonic recrystallization.

Biotite and hornblende are the most important mafic minerals. These minerals are present primarily in the lower parts of the gneiss complex, where they help define conspicuous compositional and color layering. . . . Where hornblende is preserved in the upper portions of the gneiss complex, it shows retrogression to chlorite + epidote + sphene + iron oxides. . . .

The metasedimentary rocks in the gneiss complex include marbles, banded calc-silicate rocks, and quartzites. These rocks usually occur as discontinuous, elongate bodies scattered throughout the quartzo-feldspathic gneiss terrane. Where the metasedimentary rocks show evidence of original sedimentary bedding, this layering is parallel to metamorphic foliation in the surrounding gneisses. Spectacular disharmonic folds and boudinage are well developed in the metasedimentary units. Faint apophyses of granitic material intrude some of the metasedimentary rocks that are exposed near the Little Kimble mine. This relationship suggests that these rocks may, in part, be present as pendants of material in an otherwise predominantly granitic terrain. . . .

Textural and mineralogic associations suggest that deformation and metamorphism were roughly synkinematic. Symmetry requirements for the minor structures (see section titled "Structural Elements") and mineral textures suggest that mylonitization and metamorphism were part of one continuous event. The exact timing of the mylonitization is questionable. It appears to have occurred during the waning stages of metamorphism, but it must have occurred while the rocks were still quite hot and mobile. . . .

The protolith of the mylonitic gneisses is uncertain. A plutonic igneous protolith is favored by the homogeneity of most of the gneisses and by an average mineral percentage (quartz, 28%; K-feldspar, 51%; plagioclase, 10%), which lies within the granite field. . . .

The age of metamorphism and mylonitization of the gneisses is thought to be Mesozoic. A Mesozoic age for the complex is inferred because Paleozoic and possibly Mesozoic rocks contain structural elements of similar style and trend to those in the mylonitic gneisses.

Metamorphism and Deformation. The gneiss complex has undergone progressive metamorphism to amphibolite facies, with subsequent retrograde metamorphism of part of the complex to greenschist facies. Within the complex, index minerals such as hornblende and biotite are found in the quartzo-feldspathic gneisses, and garnet, diopside, and wollastonite occur in the metasedimentary rocks. The occurrence of hornblende and biotite suggests temperatures of metamorphism in excess of 400°C (Turner and Verhoogen, 1960, p. 552-553; Miyashiro, 1972, p. 92). The presence of diopside and wollastonite suggests temperatures greater than 270°C, P_{CO_2} = 1 bar, or temperatures greater than 500°C, P_{CO_2} = 1 kbar (Turner, 1968, p. 144-145).

The dominant mineral assemblage of quartz-orthoclase-plagioclase (microcline-biotite) suggests metamorphism of upper-amphibolite grade (Turner and Verhoogen, 1960, p. 550). However, the assemblage of quartz-orthoclase-plagioclase could have been inherited from preexisting igneous plutonic rocks and thus is not a reliable indicator of metamorphic grade. . . .

An upper age limit for metamorphism is indicated by relationships in the nearby Granite Wash Mountains. The northern part of this range consists of gneisses that appear to be part of the same metamorphic complex as in the Rawhide and Buckskin Mountains.[2] Intruded into these gneisses is a 67-m.y.-old granite (W. Rehrig, 1975, personal commun.). If the metamorphic terranes in these ranges are contiguous, intrusion of the granite postdates metamorphism and deformation of the gneisses.

Granitic Gneiss And Biotite Granite

Outcrops of medium-grained granitic gneiss and coarse-grained biotite granite occur in two separate areas in the northern Rawhide Mountains. The biotite granite is intrusive into the granitic gneiss, but no contact aureole is present. . . . A Mesozoic(?) hornblende diorite intrudes both rock types and these rocks are unconformably overlain by the Artillery Formation. The total areal extent of the two associated rock units is about 17 km^2, of which about 5 km^2 comprise the older granitic gneiss. . . .

The granitic gneiss and biotite granite units appear to be allochthonous with respect to the mylonitic gneisses. Although a contact between these rock units is not exposed, geometric requirements necessitate an allochthonous nature for the gneiss-granite unit. The gneiss-granite unit and unconformably overlying Artillery and Chapin Wash Formations occupy the northern part of the range. The sedimentary units dip steeply to the southwest and into the contact with the mylonitic gneisses. . . .

The presence of macroscopic folds, a mineral lineation, and metamorphic foliation indicate that penetrative metamorphism and deformation occurred prior to intrusion of the biotite granite. This deformation may be Precambrian or Mesozoic. There is no known correlation between this deformational event and the event responsible for the formation of the mylonitic gneisses. It is

[2] According to Rehrig and Reynolds (1980, p. 149, Fig. 7) and Reynolds and others (1986b), the metamorphic rocks of the Granite Wash Mountains are older than and not correlative with the mylonitic gneisses of the Harcuvar, Buckskin, and Rawhide Mountains.

thought that deformation of these granitic gneisses predates deformation of the mylonitic gneisses.

Metavolcanic Rocks

Metavolcanic rocks thought to be of Precambrian or Mesozoic age outcrop over about 25 km^2, primarily in a band that extends across the north-central portion of the map area (Fig. 3; Plate 1). These rocks exist as foliated and highly disrupted allochthonous slices of quartz-mica-feldspar schist. Metasedimentary rocks also appear to be present, but because of strong foliation, similar appearance in outcrop, and lack of original sedimentary or volcanic structures, no attempt was made during mapping to differentiate between volcanic and sedimentary materials. The extent of sedimentary rocks in the sequence does appear to be very limited. Metavolcanic rocks occur as a monotonous sequence of highly deformed quartz-mica-feldspar schists. The lack of identifiable internal marker units and structural complexity within this unit precluded any attempt at an accurate determination of its thickness. An approximate thickness is 1,000 to 1,500 m.

The better outcrops of metavolcanic schists are found in the washes because the fissile nature of these rocks results in the formation of rubble-covered slopes. The best exposures are in sec. 1, T. 11 N., R. 14 W., sec. 8, T. 11 N., R. 14 W., and secs. 13, 14, and 15, T. 11 N., R. 15 W. Similar rocks outcrop in the western Buckskin Mountains along the Bouse-Planet Ranch Road and in the Plomosa Mountains (Miller, 1966, 1970). . . . In all cases, the schists are allochthonous. Wherever the metavolcanic rocks have been seen in these ranges, they are in fault contact with older and younger rocks. In the Rawhide Mountains, the metavolcanics always lie above the autochthonous mylonitic rocks, but are present both above and below Paleozoic and younger rocks.

The metavolcanic rocks predominantly consist of quartz-mica-feldspar schists with subordinate biotite-epidote-quartz schist and quartz-muscovite schists. . . . All of the feldspars are relicts of original igneous phenocrysts. Where feldspars are fresh, both plagioclase and K-feldspar are recognizable. The plagioclase is oligoclase to andesine (An_{27} - An_{39}). Orthoclase is the dominant K-feldspar, although microcline was noted. Epidote, biotite, muscovite, chlorite, and sericite are the dominant metamorphic minerals.

Quartz and feldspar phenocrysts uniformly distributed throughout the sequence are the most characteristic feature of the metavolcanic rocks. The phenocrysts are 1 to 2 mm in size and are surrounded by an aphanitic or schistose groundmass. The feldspars are euhedral, usually with only the cores preserved. Quartz is often euhedral and embayed and shows undulatory extinction. . . .

The metasedimentary rocks in the sequence are distinguished by their higher quartz content and the general lack of feldspar phenocrysts. They appear to exhibit a finer schistosity than the metavolcanics and show greater evidence of small-scale folding. . . . The metasedimentary rocks are present only in limited exposure. They have been recognized on the top of the hill in $S^1/_2$ sec. 5, T. 11 N., R. 14 W., in the valley in $SW^1/_4$ sec. 18, T. 11 N., R. 14 W., and in $NW^1/_4$ sec. 10, T. 11 N., R. 14 W. Their protoliths were probably tuffaceous sandstone and wackes, now quartz-muscovite and quartz-epidote-plagioclase-muscovite schists. . . . The parental volcanic rocks were rhyolitic to andesitic in composition. Dacitic flows appear to be the dominant parental material based on the mineralogy of the samples collected.

The metavolcanic sequence is here assigned a questionable Precambrian age. . . . If one considers the widespread presence of early Mesozoic volcanics in Arizona and California, a Mesozoic age for metavolcanic rocks in the Rawhide Mountains cannot be discounted.[3]

Paleozoic Rocks

Paleozoic rocks are present in the Rawhide Mountains as discontinuous, commonly chaotic assemblages of quartzites, phyllites, and carbonates. These rocks are best exposed in klippen capping the major hills in the range. The recognition of the klippen is easy because the dark color of the Paleozoic rocks contrasts sharply with the underlying light-colored mylonitic gneisses. The rocks have been intensely deformed by both brittle and ductile deformation; they commonly occur as brecciated masses. A myriad of high- and low-angle faults dismember the sequence. Low-angle faults separate all the different lithologies (formations?) within the Paleozoic sequence, making accurate determination of the stratigraphy difficult. Bedding is poorly preserved, and where present, it is often discontinuous or intricately folded. Small isoclinal folds and boudinage are common and a poorly developed mineral lineation is present in the quartz-rich rocks. . . . The most complete and apparently least disrupted exposures of these rocks are at Fool's Peak and Miller Mountain (Plate 1). Other good exposures are near the Cactus Queen mine and Fisher's Camp.

The Paleozoic rocks have undergone very low-grade metamorphism. Sedimentary structures, other than bedding, are rarely preserved in the outcrop. The quartz is often xenoblastic and in some cases elongate. Undulatory extinction is common. A very poorly developed, quartz mineral lineation is present in some of the quartzites. The calcite and dolomite are very fine to coarse grained; occasionally individual rhombohedral faces may be distinguished. In some rocks, the dolomites have a sugary texture. Elsewhere, they are commonly brecciated, whereas the limestones show evidence of flowage. Metamorphic minerals include muscovite, chlorite, epidote, magnetite, and tremolite. Tremolite was noted at only one locality, $S^1/_2$ sec. 32, T. 12 N., R. 14 W., where it occurs along a low-angle shear surface that separates brecciated, white dolomites from the metavolcanic rocks. Even though the dolomitic rocks and the enclosed tremolite are badly brecciated, a weak northeast-southwest alignment of the tremolite crystals is preserved. . . .

[3] A Jurassic (about 160 Ma) age is now accepted for these rocks (Reynolds and others, 1987).

The extremely disrupted nature of the Paleozoic rocks has made the accurate determination of formational units almost impossible. Only where mappable lithologies, hence possible formations, could be identified with a great deal of certainty are separate units shown on the geologic map (Plate 1). In most cases, the rocks are indicated simply as Paleozoic undifferentiated.

Five apparent stratigraphic (lithologic) units were recognized. These units were identified on the basis of distinctive lithologies and similarities with Paleozoic rocks in areas of known geology. The sequence described below was derived by piecing together discontinuous assemblages of rocks at the Cactus Queen mine, Fool's Peak, and Fisher's Camp. By combining these separate assemblages, one can determine that the Paleozoic stratigraphy consists of a lower quartzite, a phyllite, and three higher carbonate units.

Quartzite. The base(?) of the Paleozoic section is a quartzite that varies in color from brown to gray, green, and white. Parallel bedding in this unit ranges from 1 cm to tens of centimeters in thickness. Crossbedding was noted at one locality at the Cactus Queen mine. Grain size is fine to coarse, with the predominant size being about 1 mm. Thin beds of quartzite with grains between 2 and 4 mm were noted near the Cactus Queen mine. Near the top of this unit are thin, up-to-5-cm-thick, interbedded green phyllites and gray limestones. The upper and lower contacts of this unit are faults; thus, its estimated thickness of 40 m is only a minimum.

Phyllite. A green, maroon, and purple phyllitic unit is separated from the underlying quartzite by a low-angle fault. This unit tends to be very heterogeneous, having thin interbeds of maroon, green, and white calcareous quartzite and gray to golden-brown limestone. The lower part of the phyllite is quartz-rich, containing 1- to 2-mm-diameter grains of white quartz in a very fine grained, micaceous matrix. The phyllite unit has a well-developed bedding-plane cleavage. Boudins are common in this unit because the varying competencies of the different lithologies facilitates their formation. The approximate thickness (minimum value) of the phyllite is about 35 m.

Carbonates. Carbonates are the most abundant, but hardest to decipher, of the rocks in the Paleozoic section. These rocks consist of limestones, dolomites, and impure limestones and are often interbedded with thin beds of phyllite and quartzite. The carbonates have been highly disrupted by a system of high- and low-angle faults, which has resulted in intricate slicing and shuffling of these rocks. Each of the three carbonate units described below is separated from the others by faults; what is presented, therefore, is only a rudimentary picture of the overall stratigraphy.

Carbonate Unit 1. The unit structurally above the phyllite is a massive gray limestone with dolomite and interbedded quartzite. The limestone contains irregular patches of pink silty limestone, some nodular chert, and minor interbeds of impure brown limestone. This limestone grades upward into a brown to rusty-brown dolomite with interbedded light-gray limestone. Bedding in the dolomite ranges from a few millimeters to about 1 m. Above the dolomitic layer is a dark-brown limestone with thin, interbedded, green, pink, and white fine-grained quartzite and phyllite.

Carbonate Unit 2. Above(?) carbonate unit 1 is a sequence of white dolomite; pink and gray quartzite, phyllite, and limestone; and white to gray limestone. Dolomitic portions of unit 2 are fine to coarse grained, crystalline, and usually highly brecciated and contain the above-mentioned tremolite. The quartzite, phyllite, and limestone are thin to medium bedded (5 mm to 10 cm), with limestone being the dominant lithology. The uppermost(?) portion of this carbonate unit is a white to gray limestone with bedded and nodular chert horizons. Bedding ranges from a few millimeters to several meters in thickness. . . .

Carbonate Unit 3. The upper(?) unit in the Paleozoic section includes black limestone and dark, reddish-brown sandy limestone that grades into calcareous quartzite. This unit is generally highly brecciated; coherent (continuous) bedding is hard to discern. Where bedding is preserved, it ranges from about 2 mm to 2 cm. The quartzites tend to be fine grained.

Because of the extremely imbricate nature of the Paleozoic rocks, no attempt was made to determine accurately the thickness of the individual carbonate units. However, a reasonable estimate for a minimum total thickness of the Paleozoic section is about 700 m.

Correlation. The extremely disrupted nature of the Paleozoic rocks and the great distances between known Paleozoic formations in western Arizona and southeastern California make reliable correlations difficult. . . . In all cases in western Arizona, the Paleozoic section consists of a basal quartzite or sandstone, a siltstone unit, and an overlying series of carbonates, often with interbedded clastic rocks.

The occurrence of similar lithologies in surrounding areas confirms the Paleozoic age for the quartzite, phyllite, and carbonates. . . . The lower quartzite is considered to be correlative with the Cambrian Tapeats Sandstone (Bolsa Quartzite). The phyllite is correlated with the Bright Angel Shale (Abrigo Formation), also of Cambrian age. The overlying carbonates are not formally subdivided, but lithologic similarities with known Paleozoic carbonates suggest that units 1, 2, and 3 may be dismembered portions of the Martin Formation (Devonian), Escabrosa Limestone (Mississippian), and Supai Group (Pennsylvanian and Permian), respectively. The Coconino Sandstone and Kaibab Limestone were not recognized in the map area.

Quartz Monzonite

A small (3 km^2) pluton of quartz monzonite is located in the southwest corner of the map area near Alamo Reservoir. This medium-grained, light-green intrusive body consists of two parts: an outer, foliated quartz-monzonite sheath and an unfoliated, sheared, equigranular monzonite core. The pluton was apparently intruded into the mylonitic-gneiss complex during waning

metamorphism and deformation of the country rock. No contact aureole is evident; rather, the boundary with the country-rock gneiss is now gradational and the similarity in texture, color, and mineralogy between the gneisses and the monzonite make accurate delineation of the pluton difficult. The quartz monzonite can be distinguished from the mylonitic gneiss only by the lack of a well-developed foliation and a strong mineral lineation. Blocks of foliated and lineated gneiss can be distinguished within the monzonite pluton, a relationship that indicates the monzonite is not simply an unfoliated remnant of an igneous protolith for the mylonitic gneisses. . . .

The mineralogy of the two phases of the pluton is very similar, except for the relative deficiency of quartz in the core of the pluton. In the foliated sheath, quartz shows evidence of cataclasis. It is elongate, has undulatory extinction, and in some cases is recrystallized. In the core of the pluton, quartz occurs as subhedral crystals exhibiting only undulatory extinction. Orthoclase occurs as subhedral fresh crystals in contrast to the plagioclase (oligoclase, An_{30}), which is usually highly altered. . . .

Alkali Granite

An allochthonous alkali granite of probable Mesozoic age is present in the eastern Rawhide Mountains. Isolated exposures of this granite are present at Fool's Peak, at the Rawhide mine, and near the Alamo Reservoir (Plate 1). The largest (2.5-km^2) and best exposures of the alkali granite are at Fool's Peak. Here the granite lies tectonically atop mylonitic gneisses and late Tertiary sedimentary rocks.

The alkali granite is coarse grained, highly sheared, and deeply weathered. Typically the rocks appear light green or reddish brown, depending on the degree of alteration and mineralization. The average grain size is about 5 mm. The texture is typically hypidiomorphic-granular. . . . The major phases and their average percentages are quartz (29%), K-feldspar (59%), and muscovite (6%). Plagioclase was not recognized in any of the thin sections, a relationship that suggests the rock should be classified as an alkali granite, rather than a true granite (Streikeisen, 1967). . . .

In all cases, the alkali granite shows abundant evidence of cataclasis. In outcrop these rocks are crumbly and brecciated. Near the basal dislocation surface, they are often streaked out, altered to clay minerals, or mineralized with iron oxides. In thin section, the quartz shows evidence of granulation into finer grained aggregates; in some cases, grains are elongate in form. The orientation of the elongate grains could not be determined, nor is the time of cataclasis and quartz elongation known with certainty.

The lack of intrusive relationships with other rocks, the absence of a similar intrusive body within the Rawhide Mountains or nearby areas, and the allochthonous nature of the granite make even relative age dating tenuous. . . .

Hornblende Diorite

A medium- to coarse-grained hornblende diorite occurs as small plutons in the northern and southern portions of the map area (Plate 1). The largest pluton (about 2 km^2) is intruded into the granitic-gneiss/biotite-granite terrane in sec. 36, T. 12 N., R. 15 W. Small plugs of hornblende diorite occur along the Bill Williams River, where they intrude the mylonitic gneiss. All the plutons lack contact aureoles and do not appear to have foliated boundaries.

The hornblende diorite weathers dark green because of the high percentage of hornblende. The texture is granitic. Individual grains of hornblende and feldspar can easily be distinguished in hand sample. Although the rock appears fresh in outcrop, in thin section most of the feldspars show the effects of late-stage hydrothermal alteration. Unaltered feldspars are plagioclase (andesine, An_{33} - An_{47}). Altered plagioclase, which makes up more than 25% of the rock, now consists of sericite + epidote + quartz. . . . The hornblende is blue green to green, commonly euhedral, and unaltered.

The age of the hornblende diorite is unknown, but a Mesozoic or Tertiary age is preferred because its emplacement postdates metamorphism of the mylonitic gneisses.[4]

Artillery Formation

The Artillery Formation was named by Lasky and Webber (1944) for the type section exposed in the Artillery Mountains. Exposures of this unit are confined to the northern section of the map area, where they form a disrupted homoclinal sequence resting unconformably on Precambrian(?) biotite granite (Fig. 3; Plate 1). The unit strikes about N50°W, dips about 45° to 50° to the southwest, and is broken into two separate sections by a northwest-striking high-angle fault. The most complete section is located in secs. 33 and 34, T. 11 N., R. 14 W. Here the formation consists of five members: a basal arkosic sandstone, a limestone-sandstone tuff, an arkosic sandstone, a siltstone-limestone, and an uppermost fanglomerate. A basalt dike-and-sill complex and small volcanic pipes(?) of rhyolitic material are intruded into the formation. In secs. 1, 2, and 35, T. 11 N., R. 14 W., the formation consists of the same five members, but the formation is much thinner and more disrupted by high- and low-angle faults and contains lenses of monolithologic breccias of Precambrian(?) metavolcanic rocks and Paleozoic quartzites. The maximum thickness of the Artillery Formation is about 1,400 m. . . . The low hills just south of Ester Basin contain the thickest and best exposed section of the Artillery Formation in the map area. The formation members show great variations in lithology and thickness, but they maintain stratigraphic continuity for at least 10 km. Similar lithologies with

[4] Rocks from a composite, nonfoliated, hornblende diorite-gabbro pluton that discordantly intrudes mylonitic gneisses in the north-central Whipple Mountains yield U-Pb (zircon) and ^{40}Ar-^{39}Ar (hornblende) ages between 19 and 20 Ma.

much greater stratigraphic thickness are present in the type section in the Artillery Mountains.

Member 1. The basal unit in the Artillery Formation is a reddish-brown to green, coarse-grained arkosic sandstone. Feldspar grains up to 2 cm in diameter were noted in a finer grained matrix of quartz, feldspar, and silt. The unit is generally massive, with bedding ranging from about 10 to 50 cm. Bedding is often poorly defined in the lower parts of this unit. Near the top, the arkosic sandstone contains interbeds of limestone and conglomerates. The estimated thickness of this unit is about 160 m.

Member 2. This member consists of gray and brown limestones with interbedded, varicolored clastic sediments. The limestones are thin- to thick-bedded (1 to 20 cm) and commonly sandy and contain sparse chert(?) nodules and red jasper pebbles. The clastic sediments are golden brown, red, and light-green siltstones and sandstones and green tuffaceous shales. These sediments are thin-bedded and often calcareous and show faint crossbedding and ripple marks. Poorly preserved palm roots are present in the gray limestone in NE $^1/_4$ sec. 33, T. 12 N., R. 14 W. and NE $^1/_4$ sec. 30, T. 12 N., R. 14 W. A basalt dike-and-sill complex intrudes the eastern portion of this member. The thickness of member 2 is approximately 120 m.

Member 3. A reddish-brown and green arkosic sandstone and conglomerate conformably overlie member 2. The conglomerate layers are found in the lower part of this member. They contain rounded to subangular clasts of granite, gneiss, metavolcanics, schist, quartzite, red arkosic sandstone, and basalt. The arkosic portion of this member is medium- to thick-bedded (3 to 10 cm) and closely resembles the arkoses in member 1. Grain sizes range from 1 to 7 mm in diameter. Well-developed graded bedding is evident. Member 3 grades upward into the lower sandy limestones of member 4. The approximate thickness of this member ranges from 185 to 280 m.

Member 4. This member of the Artillery Formation consists of a varicolored sequence of calcareous siltstones, sandstones, and limestones. The majority of the member is a golden brown, gray, and pink calcareous siltstone and limestone. The member is well bedded, with bedding thickness ranging from 1 mm to 10 cm. Small stromatolitic structures are present in the gray limestones. The thickness of member 4 ranges from 200 to 400 m. A basalt sill and a volcanic pipe(?) intrude this member in sec. 33, T. 12 N., R. 14 W.

Member 5. The uppermost unit of the Artillery Formation in the Rawhide Mountains is a massive red fanglomerate. The unit is essentially structureless, with only occasional partings of siltstone to define bedding surfaces. The distinctive feature of the fanglomerate is that it is composed almost entirely of debris from the metavolcanic rocks. Boulders up to 60 cm in diameter are present. In places there is so little arkosic matrix material that the rock becomes a monolithologic breccia. Subsidiary clasts of gray Paleozoic quartzite and limestone are also present. The top of member 5 is poorly exposed over most of the map area. It is exposed only in SE $^1/_4$ sec. 1, T. 11 N., R. 15 W. where the Artillery Formation is unconformably overlain by the Chapin Wash Formation. The thickness of this member is highly variable, ranging from 200 to 600 m.

The age of the Artillery Formation is subject to debate. Lasky and Webber (1949) suggested an early Eocene(?) age, but indicated that the formation could be as old as latest Cretaceous or as young as late Eocene. Their age assignment is based on poorly preserved *Chara* fruits and silicified palm roots (Lasky and Webber, 1949, p. 21-22). . . . However, work by J. Gassaway and reconnaissance by the author suggest the need for revision of the stratigraphy of the Artillery Formation. The upper portion of the Artillery Formation (approximately equal to member 5, this report), as mapped by Lasky and Webber, consists of a great thickness of predominantly thin- to thick-bedded siltstones and sandstones, which also contains the basalt member of the formation. It is onto this part of the formation that the Artillery "thrust" plate is emplaced. A basalt flow below the plate, originally interpreted by the writer as a basalt within the upper Artillery Formation, was sampled for radiometric age dating.[5] The rock dated is an olivine-augite basalt flow with well-exposed upper and lower contacts. The Laboratory of Isotope Geochemistry, University of Arizona, determined a K-Ar whole-rock age for this basalt of 15.9 $\pm$ 0.3 m.y. . . . The Miocene age for the upper "Artillery" basalt appears to be valid and its implications for Tertiary stratigraphy are discussed below. . . . The need for major revision of the stratigraphic boundary between the Artillery Formation and the overlying Chapin Wash Formation as defined by Lasky and Webber (1949) is indicated. . . .

Chapin Wash Formation

The Chapin Wash Formation consists of a thick sequence of nonmarine red beds and volcanic rocks. Its type locality is in Chapin Wash, Artillery Mountains (Lasky and Webber, 1949). This unit has an aggregate thickness of at least 1,000 m in the Artillery Mountains and Sandtrap Wash, although only limited exposures of this formation are present in the Rawhide Mountains.

The best exposures of the Chapin Wash Formation in the Rawhide Mountains are near the Rawhide mine and at Rankin (Johnson) Ranch (Plate 1). The formation now consists of a chaotic assemblage of sedimentary and volcanic rocks and monolithologic breccias. Dismembered sections of this formation are also scattered throughout the study area. Low-angle faults highly disrupt the formation and separate it from most other units. Only in the western part of the map area is the Chapin Wash Formation in depositional contact with other rocks. Here this unit appears to lie unconformably on the Artillery Formation, but both units are allochthonous with respect to the underlying mylonitic gneiss.

[5] Sample information and recalculated age (16.2 $\pm$ 0.4 Ma) are presented in Shackelford (1980, p. 192).

The Chapin Wash Formation is distinguished by its pervasive red color and the presence of sedimentary manganese deposits. The major deposits of manganese are in the Artillery Mountains, but minor occurrences of manganese are present in the Rawhide Mountains and serve to aid in identification of this formation.

The formation is composed of pink to red, coarse, clastic sedimentary rocks interlayered with monolithologic breccias and volcanic rocks. The majority of the sedimentary rocks exposed in the study area are thin- to thick-bedded arkosic sandstones, feldspathic sandstones, and conglomerates. Bedding in the sandstones tends to be well developed, with beds ranging in thickness from 2 to 20 cm, whereas the conglomerates are massive, often with no obvious bedding. Siltstones and limestones are present in minor amounts. Crossbedding, graded bedding, ripple marks, rip-up clasts, and soft-sediment deformation structures are common.

The Chapin Wash Formation is relatively well bedded, but individual layers are usually poorly sorted. The clastic beds appear to be composed of similar detrital material and differ from one another chiefly in texture and proportion of clay and rock fragments. The coarser debris consists of subangular to rounded clasts of granite, granitic gneiss, quartz-biotite schist, quartzite, limestone, dolomite, silicified red arkose, latite, and basalt. Scattered clasts of mylonitic gneiss are present, but they appear to be volumetrically insignificant when compared to the other rock types, most of which have no obvious source area. Clast size ranges from 1 to 50 cm. In places the conglomerates are extremely coarse and massive, having the appearance of fanglomerates that form at the base of a steep, actively rising mountain front. Fanglomerates of metavolcanic debris, similar to those in the Artillery Formation, are also present in the Chapin Wash Formation. . . .

The characteristic feature of the Chapin Wash Formation is its pervasive red color and the presence of scattered beds of black sedimentary manganese. The red coloration is due to ferric oxides that coat the grains and assist in cementation. Not only are the sediments coated with iron oxides, but zones of massive hematite, probably the result of supergene enrichment, are also present in scattered exposures. The massive hematite is usually associated with low-angle faults at or near the basal dislocation surface; major occurrences are shown on Plate 1. . . .

Monolithologic breccias in the Chapin Wash Formation are coherent bodies of rock made up of angular debris from a single igneous or metamorphic parent. Breccias consisting of light-pink granitic gneiss, quartz-biotite schist, quartz-orthoclase gneiss, quartz-mica schist, and granite were recognizable. In places the blocks of igneous or metamorphic material are so large (up to tens of square meters) that one gets the impression of an undisturbed unit of igneous or metamorphic rock, except that the unit is interlayered with undeformed sedimentary rocks. The matrix of the breccias is usually composed of the same material as the clasts, although in a few instances a silicified, red feldspathic sand forms a cement around some of the clasts. . . . The material that forms the monolithologic breccias has no obvious source terrane within the Rawhide Mountains, nor does there appear to be a suitable source area within a radius of 20 km of the range. . . .

The origin of the monolithologic breccias is probably similar to that proposed for megabreccias by Longwell (1951) and Burchfiel (1966). Their suggestion that these breccias are the result of landsliding from steep slopes produced by a fault appears to be consistent with evidence of conditions prevalent during deposition of the Chapin Wash Formation. . . .

Volcanic rocks in the Chapin Wash Formation consist of amygdaloidal basalt and latite. Basalt is present at the Rawhide and Deer Trail mines, at Fisher's Camp, and in sec. 15, T. 11 N., R. 15 W. In all cases, the basalt is black weathering, amygdaloidal, sheared, and altered. Phenocrysts of andesine (An_{44}) and olivine are present in a groundmass of plagioclase, magnetite, chlorite, and calcite. A reddish-brown to purple latite occurs structurally below the basalt at the Rawhide mine, and similar latite is present in sec. 28, T. 11 N., R. 14 W. The latite is highly sheared and altered, making accurate identification of all the constituent minerals difficult. Phenocrysts of altered K-feldspar are present in an aphanitic groundmass of altered feldspar. . . .

A middle to upper Miocene age for this unit is indicated by the presence of Miocene rocks beneath or in the lower portions of the Chapin Wash Formation. Deposition of the Chapin Wash Formation definitely postdates extrusion of Lasky and Webber's (1949) basalt member of the Artillery Formation. If the stratigraphic revisions suggested earlier are valid, then this 15.9-m.y.-old basalt is part of the lower(?) Chapin Wash Formation. Even if these revisions are not valid and Lasky and Webber's stratigraphy is maintained, the Chapin Wash Formation is younger than the basalt. . . . In addition, in the Artillery Mountains the Chapin Wash Formation is unconformably overlain by a probable late Tertiary basalt. This basalt may be correlative with 8- to 10-m.y.-old basalts on the southwest edge of the Colorado Plateau (Paul Damon, 1975, personal commun.). . . .

Chapin Wash and equivalent sediments are present over a wide area of western Arizona. Chapin Wash-like sediments are present at Lincoln Ranch and further to the southwest at Clara Peak and Swansea. In these areas, as in the Rawhide Mountains, the red beds of the Chapin Wash Formation are allochthonous. They are separated from the underlying, autochthonous gneisses by a low-angle dislocation surface. . . .

Late Tertiary Basalt

Flat-lying to gently southwest-dipping late Tertiary basalt flows are present in limited areas within the Rawhide Mountains. The flows cap low hills in secs. 27 and 35, T. 12 N., R. 15 W. and secs. 27 and 34, T. 12 N., R. 14 W. and are also found in the low area of secs. 3 and 10, T. 11 N., R. 15 W. The basalt rests with angular unconformity on the Chapin Wash Formation and

older rocks and consists of one or two flows with an aggregate thickness of about 10 to 20 m. A few high-angle faults cut the basalt, but the relatively undeformed nature of this unit suggests that it was emplaced after cessation of gravity sliding.

The flows are vesicular olivine basalt. Phenocrysts of euhedral olivine and plagioclase (An_{48} - An_{54}) occur in an aphanitic groundmass of plagioclase, olivine, augite, and magnetite. Minor alteration of olivine to iddingsite is present. Calcite and analcite line some of the vesicles.

Basalts similar to those in the Rawhide Mountains cap Black Mesa in the Artillery Mountains.[6] Here the basalts are up to 100 m thick. These basalts unconformably overlie the Chapin Wash Formation (Lasky and Webber, 1949). The basalts dip gently to the southwest and can be traced to the southwest into Sandtrap Wash where they are truncated by the Sandtrap Wash fault. The outcrops in the Rawhide Mountains appear to be offset equivalents of this basalt in the Artillery Mountains.

Structural Elements

The Rawhide Mountains consist of two distinctive and contrasting structural-lithologic terranes separated from each other by a low-angle dislocation surface. Precambrian(?) mylonitic gneisses form the lower terrane, the autochthon, whereas the upper terrane, the allochthon, consists of a chaotic assemblage of Precambrian(?) to late Tertiary rocks. The mylonitic gneisses record a period of ductile deformation that resulted in the formation of a metamorphic foliation, well-developed, streaky mineral lineation, boudinage, minor folds, and other structures, and later brittle deformation. The allochthon also shows evidence of both ductile and brittle deformation. Ductile deformation, correlative with the deformation in the autochthon, is confined to the metavolcanic and Paleozoic rocks, whereas late Tertiary brittle deformation has affected all of the rocks. The late Tertiary deformation is characterized by the intricate slicing and shuffling of allochthonous units along high- and low-angle faults. The two terranes are separated by a low-angle dislocation surface of late Tertiary age. This surface cuts indiscriminately across *s* surfaces in both upper- and lower-plate rocks, and yet nowhere are mylonitic gneisses of the allochthon above this surface or rocks of the allochthon below it. The youngest deformation is characterized by high-angle oblique dip-slip, reverse, and normal(?) faults that cut both terranes.

The attitude and style of various structural elements were noted during the course of this study. Large-scale structural elements are described first as they provide a framework for analysis of the many minor structures. Low-angle faults are the dominant structures in the range. Macroscopic folds are present, but not readily obvious. Mesoscopic structures, such as foliation, small folds, lineation, and others, are described in the text. Microscopic structures are briefly considered, along with the quartz [0001]-axis and quartz deformation-lamella orientation data.

Macroscopic Structures

The dominant macroscopic structures in the Rawhide Mountains are faults. All of the rock units are broken by numerous high- and low-angle faults, the majority of which are of late Tertiary age, as discussed below. The most spectacular late Tertiary fault structure in the range is a low-angle dislocation surface that everywhere separates autochthonous mylonitic gneisses from all other overlying, younger(?) rocks. Faults are so numerous in the allochthon that they give it the appearance of a chaotic assemblage of different rock units with little or no obvious geometric arrangement.

To determine the spatial relationships of all the fault surfaces and to aid in unraveling the nature of the deformation, attitudes of fault surfaces were plotted on a stereographic projection. Figure 4A presents the orientation data for fault surfaces in all rock units. The pronounced northeast-trending girdle pattern indicates that there is a preferred northwest-southeast strike to the faults in the range. A plot of the attitudes of fault surfaces present only in the allochthon is shown in Figure 4B. Support for a common origin for all the faults in both autochthon and allochthon is indicated by the similar style of faults in both structural units.

Faults of late Tertiary age comprise the majority of the macroscopic structures studied. Movement on these faults has resulted in the chaotic imbrication of the allochthonous rock units, the formation of the low-angle dislocation surface that separates the two structural terranes, and subsequent modification of the gravity-slide complex. Four generations of late Tertiary faults can be recognized in the field; for ease of presentation these are indicated as F_1 to F_4 in this report. F_1 to F_3 designate faults of the late Tertiary gravity-slide complex, whereas F_4 denotes faults that postdate the gravity-slide complex. Further subdivision of the fault-designation scheme is presented to distinguish between the high- and low-angle portion of curved normal faults, F_2 and F_3 (e.g., F_{2a} and F_{2b}). This fault-designation scheme is based on the apparent time of faulting and the geometric configuration of the faults and is presented only as a means of identifying different ages and configurations of late Tertiary faults. There is no dynamic significance implied in the fault designations, and thus they need not have similar origins, although this possibility cannot be ruled out.

The low-angle dislocation surface that separates the mylonitic gneisses from the overlying rocks is discussed first because it controls the overall structure of the range. This dislocation surface separates two markedly different structural and lithologic terranes. This surface is designated as the basal dislocation surface to distinguish it from similar, but less continuous and less significant, low-angle dislocation surfaces elsewhere within the Rawhide Mountains.

[6] A basalt collected from the top of Manganese Mesa in the western Artillery Mountains yielded a whole-rock K-Ar age of 9.6 $\pm$ 0.3 Ma (Shackelford, 1980, p. 192).

The basal dislocation surface everywhere separates autochthonous mylonitic gneisses from an overlying, chaotic assemblage of younger and questionably younger rocks. The surface is readily identified in the field by the marked color contrast across it. Dark-colored Paleozoic to Tertiary rocks of the allochthon contrast sharply with the light-colored mylonitic gneisses of the autochthon. The basal fault is characterized by a flat, slightly polished surface that appears to have formed by the coalescing of a series of curved(?) normal faults (F_2 faults) along a preferred zone of detachment. Evidence supporting this origin includes the following: (1) F_1 to F_3 faults do not cut the basal dislocation surface; (2) F_2 faults appear to flatten at depth and merge with the basal dislocation surface; (3) along other, higher low-angle dislocation surfaces, curved normal faults merge with a master shear surface in a manner similar to that proposed for the formation of the basal dislocation surface; and (4) almost all of the allochthonous rock units are locally juxtaposed against the autochthonous mylonitic gneiss along this dislocation surface.

The structural features associated with deformation along the basal dislocation surface are spectacular. Upper-plate rocks along the surface are highly brecciated, are commonly chaotically imbricated, and show evidence of extreme extension, whereas lower-plate rocks almost everywhere are massive-looking cataclasites and microbreccias. Numerous small normal faults distend the upper-plate rocks, but do not cut the basal dislocation surface. These small normal faults commonly die out in a shear zone formed by weaker, incompetent rocks that accommodate the brittle extension of the overlying rocks by flowage. Tertiary rocks along the basal dislocation surface are commonly silicified or chloritized.

A similar dislocation surface is present in the Buckskin Mountains at Lincoln Ranch, where it has been mapped by Gassaway (1972) as an "old erosional surface." The author has studied this surface and concluded that it cannot be an erosional surface; rather, it is the same dislocation surface that separates mylonitic gneisses from overlying younger rocks in the Rawhide Mountains. Exposures of a similar, presumably correlative, dislocation surface are also present south of the Bill Williams River at Clara Peak, Swansea, and Butler Well, and perhaps at Planet Ranch in the western Buckskin Mountains. The regional extent of these presumably correlative basal dislocation surfaces may be in excess of 1,000 km^2 in west-central Arizona.

F_1 faults are moderately to steeply dipping faults (maxima I, Fig. 4) that have a general attitude of N50°W, 50°SW. These faults are confined to the allochthon, are most abundant in pre-Cenozoic rocks, and are thought to be the earliest set of faults associated with the late Tertiary deformational events. The fault surfaces are sharp, with only minor brecciation of hanging-wall and footwall rocks, and the fault surfaces are generally parallel or subparallel to *s* surfaces in these rocks. F_1 faults are most conspicuous where they separate the various Paleozoic formations and other units from each other. The present steep southwesterly dip of the F_1 fault surfaces is not original; the present orientation is thought to be the result of later rotation by movement on F_2 faults. Minor structures associated with these

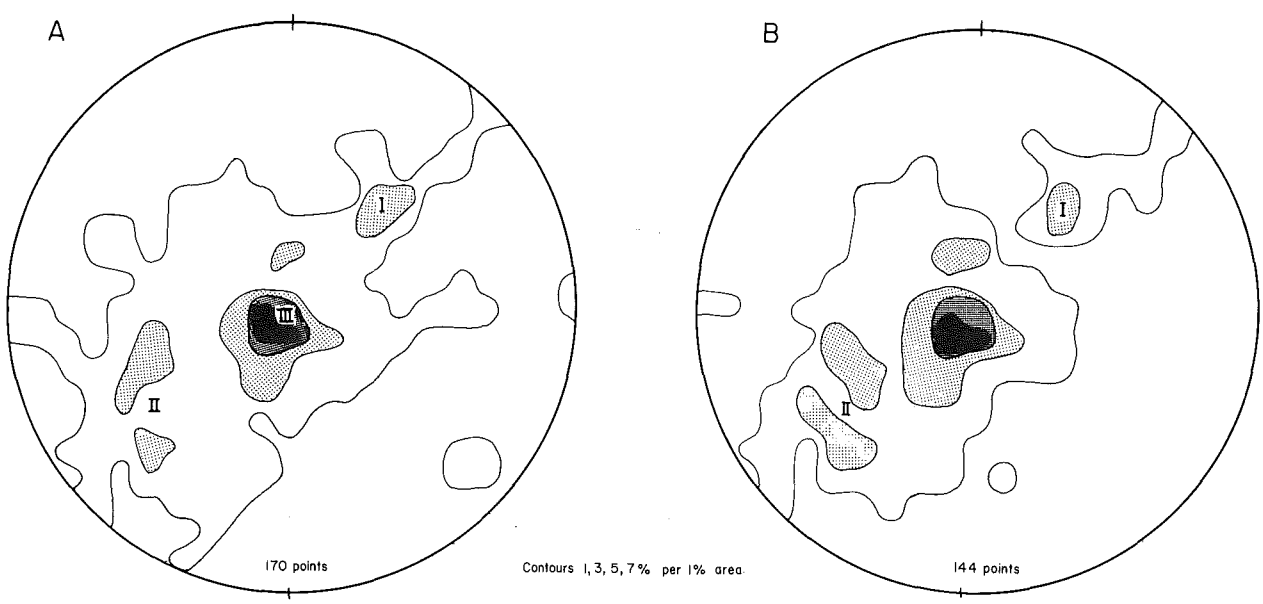

Figure 4. Lower-hemisphere stereographic plots of poles to dislocation surfaces. Figure 4A is a plot of all measured dislocation surfaces. Figure 4B is a plot of dislocation surfaces in allochthon (including basal dislocation surface). Maxima I, II, and III refer to concentrations of dislocation surfaces that are correlated with F_1, F_{2a}, and F_{2b} fault sets, respectively. (Dark area near center is maxima III.)

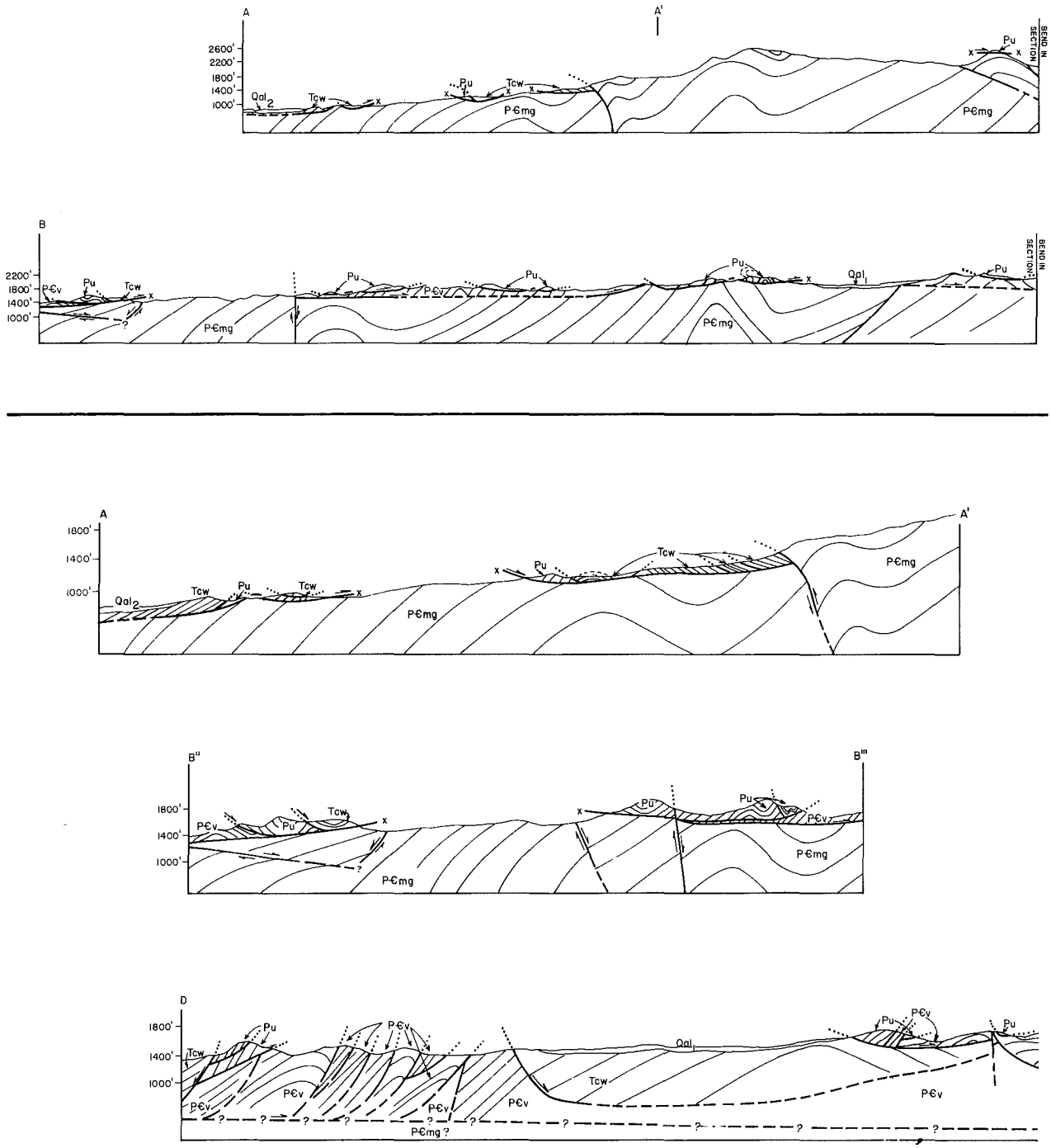

Figure 5. Structural cross sections of the Rawhide Mountains. Locations of cross sections are shown in Figure 3 and on Plate 1.

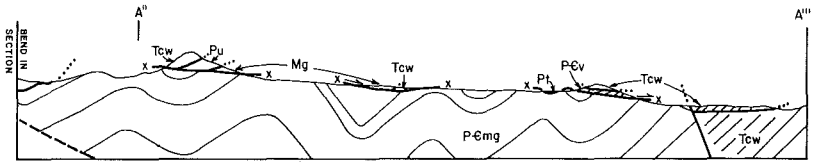

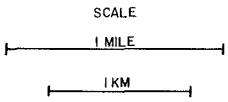

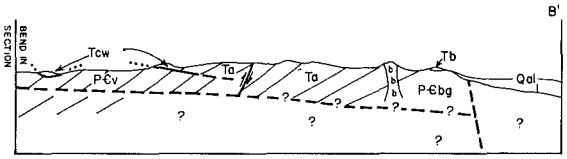

1X

2X (ENLARGED)

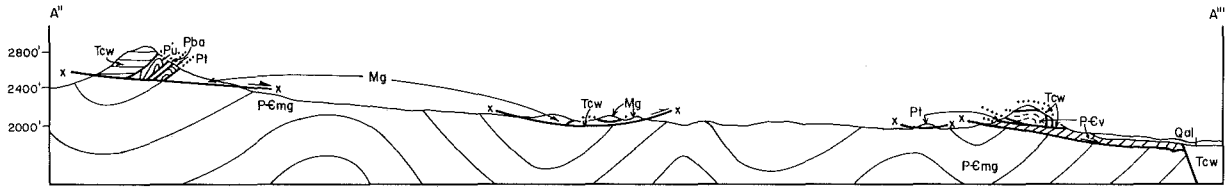

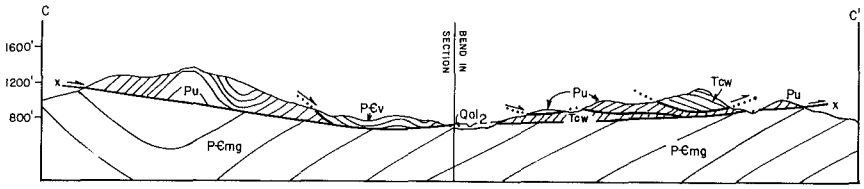

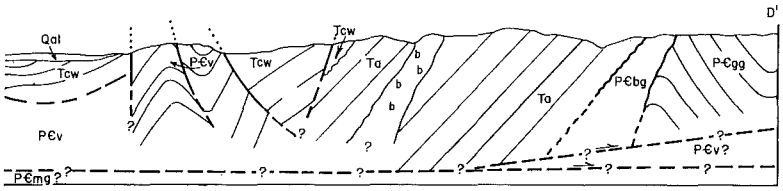

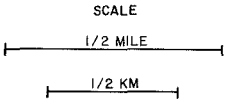

RAWHIDE MOUNTAINS, MOHAVE COUNTY, ARIZONA

faults indicate dip-slip movements in the northeast-southwest quadrants.[7]

In places, secondary copper and iron mineralization is present in the shear zones along these faults; however, even these ore minerals are commonly brecciated, indicating that renewed or continued movement occurred after mineralization.

F_1 faults represent an early stage of the late Tertiary low-angle deformation. A late Tertiary age of origin is preferred because of the following: (1) the lack of large-scale compressional features associated with these faults, (2) the similarity in style and direction of transport of these faults to definite late Tertiary faults, and (3) the presence of Mesozoic(?) alkali granite and Tertiary(?) conglomerates in F_1 fault slices within Paleozoic rocks at the Bonanza mine.

The F_1 faults are locally truncated by F_2 faults, which are the dominant faults of the late Tertiary deformation. In sec. 26, T. 11 N., R. 15 W., a low-angle F_1 surface separates a Paleozoic carbonate and quartzite. Here, the Paleozoic rocks and the F_1 dislocation surface have been folded into a southwest-plunging antiform and truncated by F_2 faults and the basal dislocation surface. The antiform is in a fault slice tectonically overlain by a slice of the Chapin Wash Formation and underlain in the north by metavolcanic rocks and in the south by the mylonitic gneiss (Plate 1). At Rankin (Johnson) Ranch, a highly distorted F_1 dislocation surface separates Paleozoic carbonates from tectonically overlying metavolcanic rocks (Plate 1).

F_2 faults have a bimodal distribution (maxima II & III, Fig. 4): one steep set of faults that dips 50° toward N60°E, here labeled F_{2a} faults, and one shallow set that dips 10° toward N40°E, here designated F_{2b} faults. Both sets appear to be genetically related and may represent different portions of a curved normal-fault set. Exposures of F_{2a} faults are essentially confined to isolated outcrops, where they occur as penetrative sets of mesoscopic normal faults that, in places, merge downward with the lower angle F_{2b} faults. The small size of many of these faults precludes inclusion of them on the geologic map; however, several large F_{2b} faults are indicated on Plate 1. F_{2a} faults are usually oriented at approximately 90° to *s* surfaces in the various rock units.

F_{2b} faults correspond to the low-angle dislocation surfaces that, along with F_1 faults, chaotically imbricate the allochthonous rock units. The F_{2b} faults, which are characterized by thick zones of brecciation, juxtapose younger over older rocks and, less commonly, older over younger rocks (Fig. 5). There is no simple or obvious geometric arrangement of the tectonic slices. Minor structures associated with F_{2b} faults indicate northeast- or southwest-directed movement, parallel with the inferred movement direction on the F_1 faults. The chaotic nature of the F_2 faulting is most visible just north of Rankin (Johnson) Ranch. Here, within an area of less than 1 km^2, fault-bounded slices of Paleozoic rocks are present both above and below Chapin Wash rocks. Metavolcanic rocks that occur tectonically below Paleozoic rocks in other areas are above similar Paleozoic rocks in this area. Faults of F_2 style are also present in the lower-plate (autochthonous) mylonitic gneisses. In Mississippi Wash, just below the McGuffie mine, northwest-striking, northeast-dipping, high-angle normal faults (F_{2a}) merge with a master dislocation surface (F_{2b}). A low-angle dislocation surface near the Little Kimble mine has a similar geometry. Minor structures associated with these faults suggest northeast-directed movement along them.

The F_2 faults may have an origin similar to that proposed for inverse imbricate normal faults and listric normal faults (Armstrong, 1972, Fig. 6). These normal faults have high-angle break-away zones (herein equated with F_{2a} faults) and then flatten at depth, often into a master dislocation surface (F_{2b} faults). The exact structural relationships suggested by Armstrong for this kind of faulting are not readily obvious on a macroscopic scale in the Rawhide Mountains; however, mesoscopic examples of these relationships are present in isolated outcrops. . . .

The structural style of the F_1 and F_2 faults provides a mechanism for the formation of the basal dislocation surface. The structural and lithologic discontinuity formed by the contact between the mylonitic gneisses and overlying rocks would have been a preferential zone for later detachment. F_2 faults that formed in the now allochthonous rocks may have tended to die out in a zone of shear at this structural discontinuity. Thus, chaotic imbrication of units shows dimensional elongation in a N70°E direction. The response of the lower-plate rocks to movement along the basal dislocation surface has been the formation of a thick zone of dark-green, massive-looking cataclasites and microbreccias. As one approaches the basal dislocation surface from below, the fabric in the mylonitic gneisses is gradually obliterated by extreme cataclasis until this older mylonitic texture is no longer identifiable. This zone of intense cataclasis in the upper part of the lower plate is about 20 m thick over most of the range. In a few areas, notably around Rankin (Johnson) Ranch, this zone of coherent cataclasis is absent and the gneisses at the basal dislocation surface are just highly brecciated.

A structure-contour map of the basal dislocation surface was constructed to define the areal geometry of this structure. The contour map (Fig. 6) reveals that its structure is that of a broad, crudely defined, northwest-trending dome modified by northeast-trending arches and troughs. However, the domal nature of this structure is misleading because the present structure defined by the basal dislocation surface is, in part, the result of later faulting. Removal of the reverse dip-slip displacement on the faults that cut the basal dislocation surface in the central part of the range would essentially erase the

[7] This discussion of the origin of F_1 faults lacks clarity. Terry believed that they were originally the subhorizontal downdip portions of northeast-dipping listric normal faults. Their southwestward tilting occurred in the hanging walls of second-generation, northeast-dipping, listric normal faults (Shackelford, 1976b, Fig. 30 [reproduced here as Fig. 12]).

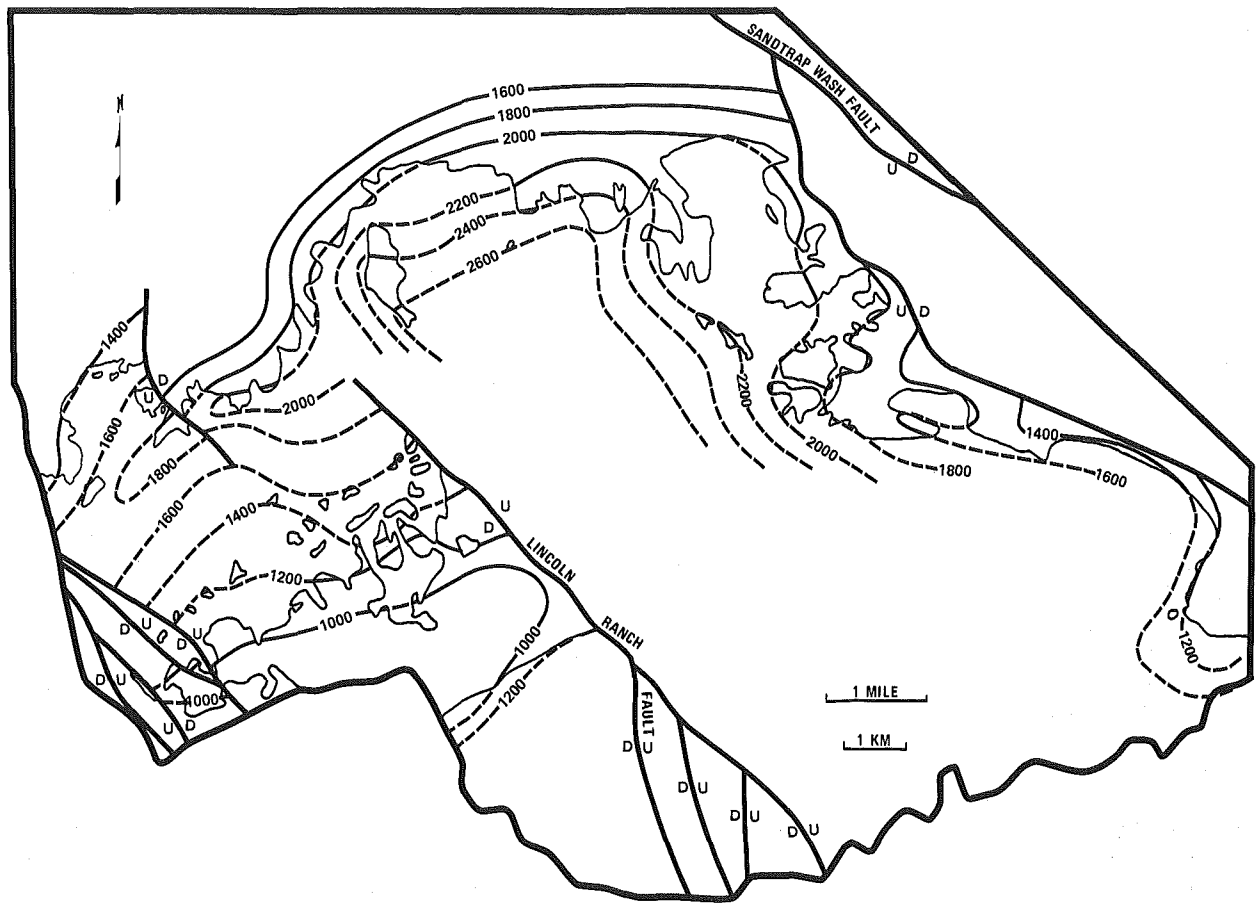

Figure 6. Structure contour map of basal dislocation surface (Rawhide detachment fault).

northwest-trending domal structure, leaving the northeast-trending arches and troughs.

The chaotic shingling of rocks in the Rawhide Mountains is similar to that described by Noble (1941) for the Amargosa chaos, Death Valley, California. . . . Wright and Troxel (1969) suggested that the Amargosa chaos and thrust were formed by the coalescing of a series of listric normal faults at a master dislocation surface. . . . If the above model is correct, then the formation of a "chaos" requires a preferential zone of detachment (decollement?) at some favorable structural or lithologic boundary to accommodate the translation and imbrication of rock units in the allochthon.

F_3 faults consist of high-angle normal(?) faults that cut F_1 and F_2 faults, but do not cut the basal dislocation surface. Two vertical, east-west-striking F_3 faults are present at Miller Mountain where they juxtapose southwest-dipping Paleozoic rocks and Mesozoic(?) alkali granite against other Paleozoic rocks. Another F_3 fault strikes northwest through secs. 30 and 31, T. 12 N., R. 14 W., just west of Potts Landing Strip. This major northwest-striking fault repeats the Artillery Formation and places Precambrian(?) granitic gneiss against the Artillery Formation for much of its length. The fault surface is not exposed, and thus the exact orientation and sense of displacement are not known. The inferred displacement on this fault is dip slip, with the northeast side down.

A few faults postdate formation of the basal dislocation surface and the F_1 through F_3 faults; these faults are considered the F_4 faults. These few faults are the only faults known to displace the basal dislocation surface, and thus must be latest Cenozoic in age. The F_4 faults all strike northwest, dip steeply to the northeast or are vertical, and consist of several varieties of faults that are probably not genetically related. They show both apparent normal and reverse-type displacement. There is not enough data available to determine the interrelationships, if any, among these faults. They are all classified as F_4 because they postdate the major late Tertiary deformation, but do not appear to disturb the older alluvium.

A major fault with both left-lateral and dip-slip components lies along the eastern margin of the Rawhide Mountains. It is herein named the Sandtrap Wash fault for its exposure in Sandtrap Wash near the Rawhide mine (Fig. 3; Plate 1). This fault had not been previously recognized. In most places it is buried by alluvium, although near the Rawhide mine this fault and its subsidiary branches are well exposed. Recognition of the

extent of the Sandtrap Wash fault is complicated because along much of its length it lies within the Chapin Wash Formation. This fault strikes northwest, dips steeply to the northeast, and forms the eastern boundary of the chaotic late Tertiary structural terrane of the Rawhide Mountains. The mylonitic gneisses that form the core of the Rawhide and Buckskin Mountains have not been recognized northeast of this fault. The basement rocks to the northeast are nonmylonitic gneisses and biotite granite.

The amount and sense of displacement on the Sandtrap Wash fault are poorly understood because of the limited exposure of the fault in the Rawhide Mountains, the absence of offset marker units within the range, and the lack of knowledge of adjacent areas. The dip-slip separation on this fault is at least 260 m at Potts Mountain. This is the amount of vertical offset on the base of the late Tertiary basalt. . . . There may be a significant component of left-lateral strike-slip motion on the Sandtrap Wash fault. Slickenside striations on the fault surface plunge gently (0° to 30°) to the north and northwest, indicating that at least the latest movement on the fault was oblique dip slip. Rotation of foliation in metavolcanic rocks near the fault is consistent with inferred left-lateral movement. . . .

The Lincoln Ranch fault, named for its excellent exposure at Lincoln Ranch, is a northwest-striking reverse fault that extends from Fisher's Camp to the southeast (Fig. 3; Plate 1). The fault dips from 20° to 80° to the northeast, with the northeast side up with respect to the southwest side. This fault was first identified by Wilson (1960), who considered it to be a thrust fault. Gassaway (1972) concluded that the Lincoln Ranch fault is a reverse fault with approximately 250 m of dip-slip separation. In the Rawhide Mountains, this fault forms a steep escarpment through the central part of the range. Three hundred meters of vertical separation (throw) is estimated for this fault in the Rawhide Mountains. This offset is based on the estimated maximum amount of offset on the basal dislocation surface. Along the Bill Williams River, the Lincoln Ranch fault bifurcates and is represented by a series of steeply dipping reverse faults. These branches appear to merge with the main branch of the fault in the Lincoln Ranch basin. Similar northwest-striking reverse faults cut the basal dislocation surface near Rankin (Johnson) Ranch (Plate 1). The separation on these faults is minor, ranging from 10 to 30 m. The reverse faulting is thought to have occurred in latest Miocene or Pliocene time. Reverse faults displace the basal dislocation surface and rocks of the gravity-slide complex, which is Miocene in age, but they do not disturb the older alluvium.

A vertical fault cuts the basal dislocation surface near Fisher's Camp. This fault is vertical where exposed and strikes north-south. . . . The maximum separation is about 12 m. . . .

Mesoscopic Structures

Planar Structures. Original sedimentary bedding is confined to the Paleozoic and younger rocks. Foliate structures are primarily confined to the Precambrian(?) gneisses and schists, although a poorly developed "bedding" foliation is present in the mica-rich Paleozoic rocks. The layering in the Paleozoic and Tertiary rocks is primarily of sedimentary origin, although there is a secondary *s* surface in the finer grained Paleozoic rocks. In these rocks, mica flakes and flattened quartz grains define a weak foliation subparallel or parallel to the original sedimentary layering. All of the *s* surfaces in the Paleozoic and Tertiary rocks are represented as bedding.

Foliation in the mylonitic-gneiss complex is shown by a regular compositional layering, by the discontinuous arrangement of lenses of different composition, by a cataclastic flow structure that is penetrative throughout the complex and has resulted in the flattening and smearing of individual mineral components, and by the transposition of other *s* surfaces.

Original sedimentary bedding, S_{1a}, is preserved in the metasedimentary rocks of the mylonitic-gneiss complex as layering formed by alternating layers of marble and/or quartzite and calc-silicates, and possibly by thin bands of quartzo-feldspathic gneiss within a thicker layer of calc-silicate rock.[8] This *s* surface is discontinuous and highly distorted by penetrative ductile flow within these rocks.

A metamorphic foliation, S_{2a}, is defined by mineralogic orientations and by compositional and color layering in all rocks of the gneiss complex. . . . The compositional layering in the mylonitic gneisses is thought to have a complex origin, perhaps resulting from lithologic layering from an older metamorphic terrane and/or from metamorphic differentiation of a preexisting igneous, sedimentary, and metamorphic(?) terrane. Granitic rocks, intrusive into the metasedimentary rocks, indicate that the protolith for part of the mylonitic-gneiss terrane consists of an igneous intrusive complex and that much of the foliation is due to metamorphism and deformation. . . .

The dominant secondary surface in the mylonitic-gneiss complex is a penetrative foliation, S_{3a}, defined by the dimensional preferred orientation and penetrative flattening and smearing of individual mineral components. Flattened quartz, patches of mafic minerals, augen of feldspar, layers of varying degrees of cataclasis, and discontinuous lenses of quartzo-feldspathic material define a layering that is easily visible even in hand specimen. This partly cataclastic foliation exhibits varying degrees of development throughout the mylonitic-gneiss complex, but it is ubiquitous in these rocks. The S_{3a} foliation is subparallel to S_{1a} and S_{2a}.

The parallelism of S_{1a}, S_{2a}, and S_{3a} surfaces suggests that penetrative shear along S_3 surfaces occurred subparallel to, and perhaps synchronously with, formation of the compositional layering (S_{2a}) in these rocks. Evidence for transposition of S_{2a} foliation is best exposed

[8] Shackelford's "a," "b," and "c" subscript notations for surfaces refer to surfaces in the lower-plate mylonitic gneisses, the upper-plate granitic gneisses, and the upper-plate metavolcanic rocks, respectively. No correlation is implied between surfaces with the same subscript number.

in the canyon formed by the Bill Williams River. Exposed in the steep walls of this canyon are many small recumbent isoclinal folds, often rootless, of folded S_{2a} surfaces. S_{3a} is parallel to and equated with the axial surfaces of these isoclinal folds. The parallelism of S_{2a} and S_{3a} surfaces and their relationship to other structural elements (minor folds, mineral lineation, boudinage, and others) suggest that the metamorphic surfaces and associated structures are the result of closely related metamorphic and deformational events and are not the result of two separate events. . . .

Foliate structures are also present in the allochthon. The granitic gneiss and metavolcanic rocks each have a foliation defined by lithologic layering and the preferred orientation of mica flakes. The foliation in the granitic gneiss is primarily the result of metamorphic differentiation and is represented by a distinct compositional banding, herein designated S_{2b}. There does not

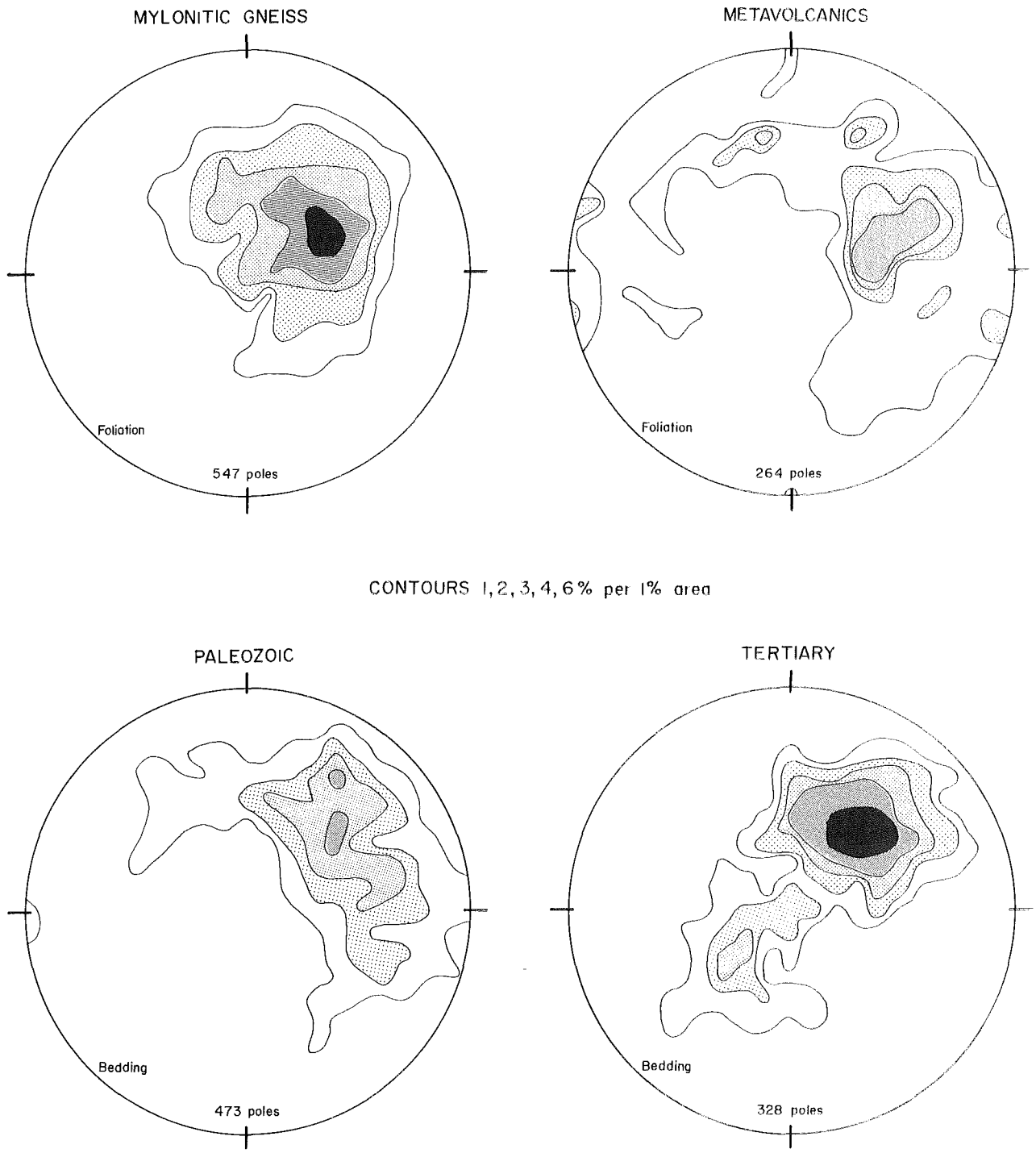

Figure 7. Synoptic Pi diagrams of *s* surfaces in the major rock units in the Rawhide Mountains, Arizona.

appear to be any direct correlation between S_{2b} and S_{2a} or S_{3a}. . . .

The *s* surface in the metavolcanic rocks (S_{2c}) is a metamorphic foliation defined by the orientation of mica flakes and lithologic layering. . . . S_{2c} shows great variation in the degree of development. S_{2c} and thus schistosity are generally best developed adjacent to shear zones within this unit, suggesting that this foliation may in part be cataclastic in origin. It is the author's opinion that S_{2c} and S_{3a} are equivalent *s* surfaces. Both are in large part cataclastic in origin, have subparallel orientations (see below), and can possibly be correlated with a single deformational event.

Pi diagrams of *s* surfaces (Fig. 7) in the various rock units were constructed to determine the spatial preferred orientation, if any, of the various *s* surfaces.

The single maxima represented by *s* surfaces in the mylonitic gneisses indicates that there is a statistical homogeneity to the attitudes of the foliation in these rocks. The data suggest that the *s* surfaces in these gneisses form a homoclinal sequence that strikes about N40°W and dips 26°SW (Fig. 7). A homoclinal structure is only statistically defined, however, because cursory examination of the geologic map reveals marked local variations in foliation attitudes.[9]

The attitudes of *s* surfaces in the metavolcanic rocks define a diffuse girdle pattern with a distinct, but not strong maxima. The foliation attitudes appear to define a statistical *s* surface with an attitude of N36°W, 36°SW (Fig. 7); however, field data indicate that these rocks are extremely deformed and show great variability in attitude within a small area. . . .

Bedding attitudes in Paleozoic rocks define a diffuse girdle pattern with a distinct maxima, indicating that *s* surfaces in these rocks define a statistically planar surface with an attitude of N42°W, 44°SW (Fig. 7). The girdle suggests statistical homogeneity, but as with the older(?) rocks, there is extreme variability in attitudes on a small scale.

Sedimentary bedding in the Tertiary rocks exhibits a strong northwest strike, but shows a bimodal dip distribution (Fig. 7). The dominant bedding attitude is N41°W, 40°SW, with a subsidiary trend of N44°W, 26°NE. This bimodal distribution of bedding attitudes in the Tertiary rocks suggests open concentric folding of these rocks about a N40°W-trending fold axis . . . but the overall outcrop distribution of these rocks and their style of deformation are not compatible with large-scale, concentric folding. . . .

The parallelism between *s* surfaces in the mylonitic gneisses, metavolcanics, and Paleozoic rocks suggests that the attitudes of these rocks may have been subparallel before later Tertiary dislocation and displacement of the latter two rock assemblages. It also suggests that major upright folding of these rocks has not occurred, but isoclinal, recumbent folding of the mylonitic gneisses cannot be ruled out. The statistical parallelism of bedding in Tertiary rocks and *s* surfaces in older rocks implies that all of the rock units were subparallel to each other prior to late Tertiary events.

Linear Structures. Several varieties of linear structures are present in the Rawhide Mountains. These include a streaky mineral lineation, slickenside striations, minor fold axes, boudinage, and a lineation formed by the intersection of two planar surfaces. Two generations of minor fold axes have been recognized. For the purposes of this report they are designated as B_1 and B_2. The dimensional orientation of the linear structures appears to provide valuable information on the kinematic history of the rocks.

Mineral lineation is present in the pre-Cenozoic rocks. This linear structure is defined principally by dimensional preferred orientation of quartz, augen of feldspar, biotite, and rarely, hornblende. Lineated quartz grains are described in more detail in the text section on microscopic structures. A less well developed lineation formed by mica aggregates and streaked out magnetite grains is present in the metavolcanic rocks. Both types of mineral lineation are thought to have formed parallel to the direction of maximum elongation in the rocks. The strong lineation maximum exhibited for the mylonitic gneiss (Fig. 8) has a trend of S48°W, 20°. This is within the plane of, and normal to the strike of, the foliation in these rocks. The mineral lineation in the metavolcanic rocks shows significant scatter because of the highly folded nature of these rocks. Nevertheless, the trend of this mineral lineation is subparallel to the lineation in the mylonitic gneisses (Fig. 8). Quartzites within the Paleozoic sequence also have a poorly developed lineation. Although lineations were identified in only a few localities, the trend of these lineations is approximately parallel to that of the older(?), crystalline rocks (Fig. 8). . . .

The parallelism of the mineral lineation in the mylonitic gneisses, metavolcanics, and Paleozoic rocks appears to indicate that they have undergone a similar penetrative deformation event. Other kinematic data support this conclusion.

Boudinage, though not plentiful, is present in most of the rocks in the Rawhide Mountains. Generally the boudins appear as rounded or lensoid masses of material in a relatively structureless groundmass. Most of the boudins are confined to the plastically deformed pre-Cenozoic rocks, although several boudinage structures are associated with late Tertiary fault zones. The spatial distribution of the boudins (Fig. 8) suggests flattening and extension in at least two directions, northwest-southeast and northeast-southwest. The northwest-southeast preferred orientation of the boudins suggests that the major extension was in a northeast-southwest direction and parallel with the mineral lineation. The northeast-southwest set of boudins is possibly the result of continued penetrative flowage of the rocks and the rotation of early-formed boudins into parallelism with the direction of extension. There is no evidence to support two separate directions of extension.

[9] This paragraph and map data of Plate 1 indicate that the pattern of open folding shown on cross sections of the mylonitic gneisses (Fig. 5) is not valid.

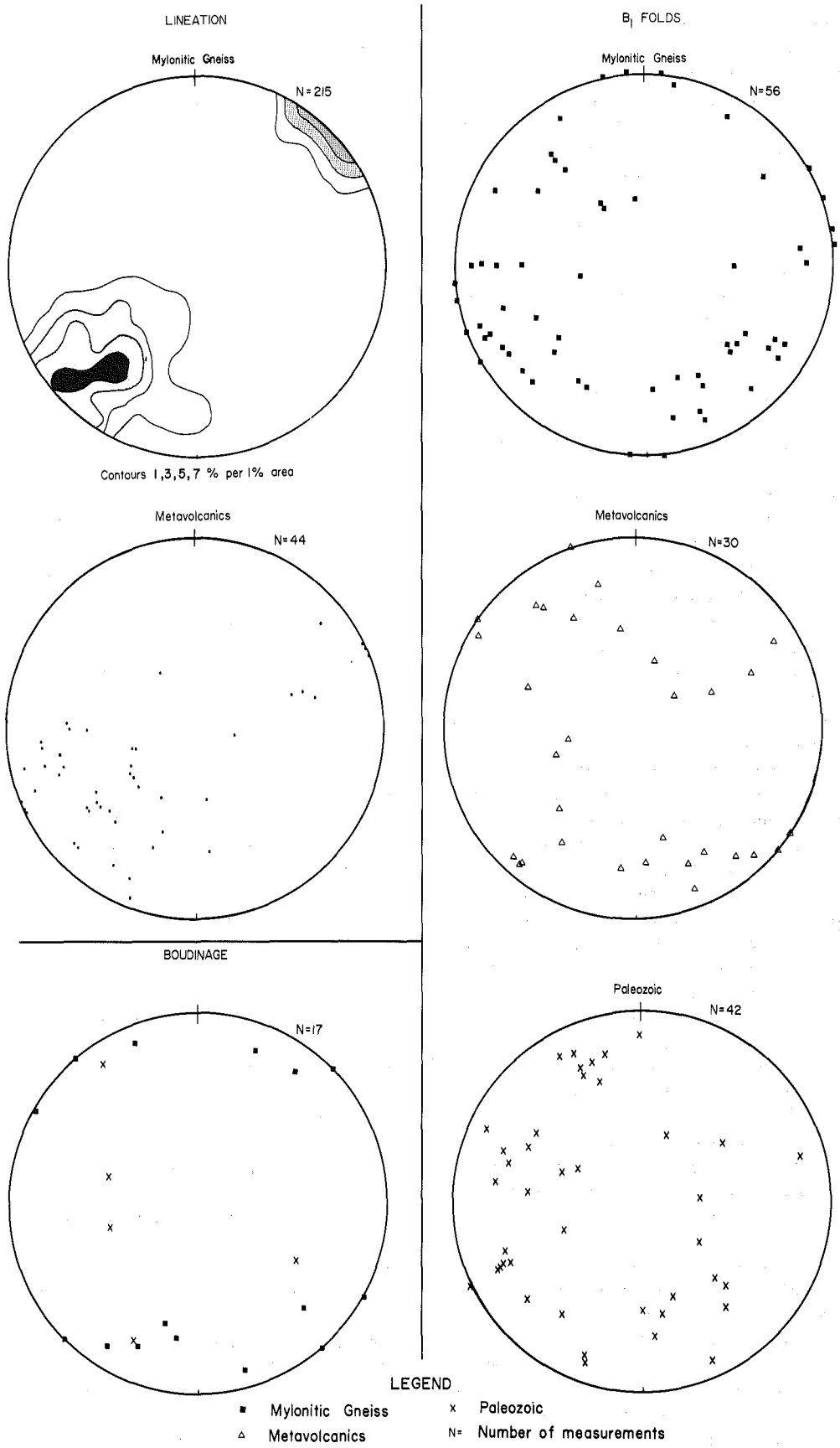

Figure 8. Lower-hemisphere stereographic plots of Mesozoic(?) linear structures.

A distinctive late Tertiary lineation is locally formed by the intersection of bedding or foliation with small, penetrative, shingling normal faults. This lineation has been identified at about a half-dozen localities, where it is always associated with a low-angle dislocation surface. The small faults and the lineation formed by their intersection with an *s* surface are confined to upper-plate rocks at a shear zone and indicate that the upper-plate rocks have undergone penetrative brittle extension adjacent to that shear zone. Thus, the trend of the lineation formed by the intersection of the small normal faults and an *s* surface is normal to the direction of extension. Another lineation of similar origin is formed by the intersection of conjugate normal faults in the highly extended rocks. Both types of lineation are oriented northwest-southeast (Fig. 9), indicating extension in a northwest-southwest direction.

Minor folds are found in all the rock units in the Rawhide Mountains. They exist as two distinct minor fold types: B_1 folds, of similar fold type, are confined to the ductilely deformed Paleozoic and older(?) crystalline rocks; and B_2 folds, concentric folds, are associated with low-angle dislocation surfaces in all the rock units.

B_1 folds are usually recumbent, isoclinal folds with sharp hinges, strongly attenuated limbs, and axial surfaces approximately parallel with bedding or foliation. Many of these folds can be considered as intrafolial folds (Turner and Weiss, 1963, p. 116) because they have tightly appressed limbs and are confined to distortions in a dominantly planar foliation. B_1 folds have wavelengths that range from less than 1 cm to more than 20 cm, but these folds are never large. They appear to have formed through a combination of slippage between layers and flowage within the layers, and thus may be considered to lie between idealized flexural-slip and flexural-flow folds (Donath and Parker, 1964). Examples of B_1 folds are shown in Figure 10. The orientation of B_1 fold axes in the Paleozoic and older(?) crystalline rocks is presented in Figure 8. There is wide variation in trend of the fold axes, though there appears to be a slight concentration of attitudes in the northwest and southeast quadrants of the stereographic projections. These folds do not have a preferred sense of vergence. . . . This deformation is synkinematic with formation of the partially cataclastic S_3 surface in the mylonitic gneisses. The scatter in the B_1 fold-axis orientation suggests that the deformational event responsible for their formation was inhomogeneous or that the early orientation of S_2 surfaces was variable as a result of an earlier deformation.

B_2 folds usually have rounded or angular hinges, limbs of equal thickness measured normal to the bedding or foliation, and axial surfaces at high angles to the bedding or foliation. Wavelengths range from a few centimeters to several meters. B_2 folds may be classified as flexural-slip folds (Donath and Parker, 1964) that evolved through slippage between individual layers. There is a close association of B_2 folds with northwest-striking, low-angle F_1 and F_2 faults. These folds are generally confined to upper-plate rocks at these dislocation surfaces. They are also present in shear zones situated between closely spaced, low-angle F_2 faults. The nature of the B_2 folds suggests that they are "drag folds" formed by the differential slippage of layers along a dislocation surface, and thus the sense of vergence (asymmetry), when present, on these folds may indicate the relative sense of transport of upper-plate rocks with respect to the lower plate.

The axes of B_2 folds are plotted on lower-hemisphere stereographic projections (Fig. 9). The direction of vergence, or sense of relative rotation, is indicated by a curved arrow. Thus, when viewed down the plunge of the fold axis, the sense of rotation around the axis is indicated by a curved arrow around the plot of the axis. It is assumed, following Hansen (1971, p. 27-50), that the slip direction of upper-plate rocks with respect to lower rocks bisects the symmetry of the plot and is in the direction of vergence. Thus, the direction of tectonic transport on the late Tertiary F_1 and F_2 faults may be inferred. . . . The field relationships, coupled with B_2 fold-axis data, support the concept of major northeast-directed tectonic transport; however, the data do not conclusively support pervasive northeast-directed movement. . . .

Slickenside striations are associated with many of the faults in the range and two generations of striations are recognizable. The dominant slickenside trend is associated with F_1 and F_2 faults of the low-angle dislocation complex. These striations trend northeast-southwest (Fig. 9), indicating movement of allochthonous rocks parallel to this direction. Minor discrepancies from the strong northeast trend are noted, but they can be accounted for by irregular movement of individual slices within a larger terrane of relatively homogeneous deformation. A second set of slickenside striations is associated with the latest Cenozoic high-angle, F_4 faults that postdate the low-angle deformation. The northwest-southeast trend of some of these slickenside striations (Fig. 9) is compatible with the inferred sense of oblique, left-lateral with dip-slip displacement on some of the faults, whereas the northeast-southwest trend of the other striations is consistent with the reverse dip-slip displacement of other F_4 faults. . . .

Microscopic Structures

Thin-section analysis was limited to the pre-Cenozoic rocks. These older rocks exhibit abundant microscopic textural evidence of extreme ductility and flowage during one stage of the deformational events in the Rawhide Mountains. The ductile behavior of the rocks during Mesozoic deformation contrasts with the brittle behavior of the rocks during late Tertiary deformation. The following discussion will concentrate on microscopic structures that resulted from the Mesozoic(?) structural event, with special emphasis on the mylonitic gneisses. Deformation textures in the pre-Cenozoic rocks range from simple cataclastic to mylonitic.

The porphyroclastic nature of feldspar augen in the mylonitic gneisses is clearly evident. The margins of the

large grains are granulated and strained, and many grains are bent and fractured. In some cases, individual grains are broken into smaller subgrains. Granulated trails of quartz and finer grained feldspar are present behind some of the larger augen.

The textural relationships of feldspars in the metavolcanic rocks are extremely variable. In the massive little-deformed metavolcanics, the original igneous feldspar phenocrysts are present in a slightly schistose groundmass. However, the majority of these rocks are cataclastic and the feldspars are distinctly porphyroclastic.

Quartz textures are highly variable, reflecting both brittle and ductile deformation. Strain effects are

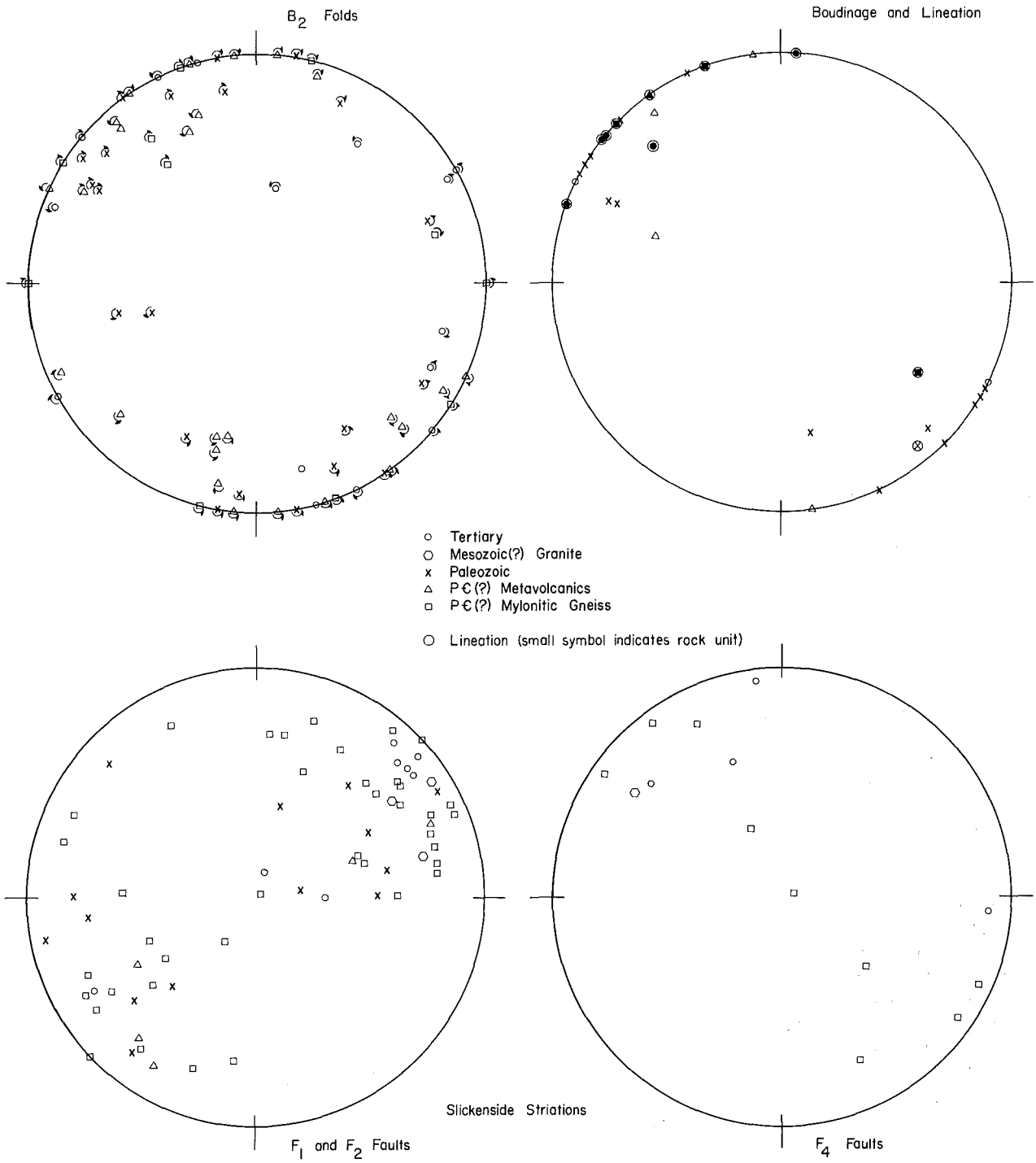

Figure 9. Lower-hemisphere stereographic plots of late Tertiary linear structural elements. Symbols indicate the rock unit in which the linear structure was found. Barbed arrow around B_2 fold axes gives the sense of rotation or vergence, if any, of the fold when viewed down the plunge of the fold.

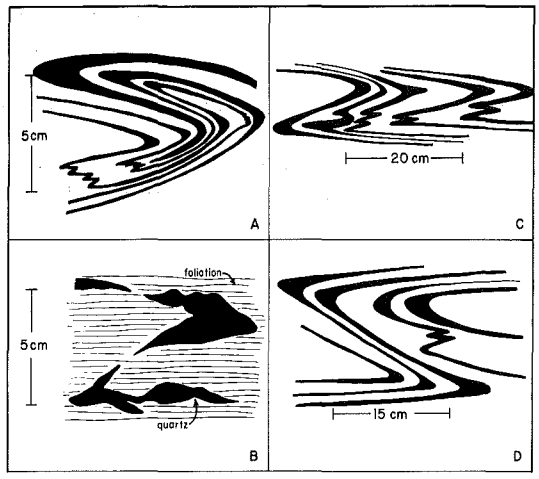

Figure 10. Examples of B_1 folds. (A) Refolded B_1 fold in marble unit in the mylonitic gneiss (fold axes are parallel). (B) B_1 fold formed by a quartz layer in metavolcanic rocks (foliation formed by mica and flattened quartz grains parallels axial surface of fold). (C & D) B_1 fold in Paleozoic rocks.

ubiquitous in thin section. Almost all quartz grains have undulatory extinction. Quartz-deformation lamellae are present in grains in many of the mylonitic rocks. Polygonal grains of recrystallized quartz are associated with larger elongate quartz grains in the higher-grade metamorphic rocks of the mylonitic-gneiss complex. . . . In the mylonitic gneisses, quartz is usually highly elongate and the grains are irregular in outline. Typical triaxial dimensions are 8:2:1, with extreme triaxial ratios of 2:1:1 and 15:2:1. . . .

Petrofabric Diagrams

The mylonitic gneisses are of sufficiently coarse grain size to permit easy microscopic analysis. . . . A study of the quartz [0001]-axis fabric was undertaken to determine if it gave any information regarding this phase of deformation. Five samples of the mylonitic rocks were analyzed. In addition, one sample of Paleozoic quartzite with a recognizable mineral lineation was analyzed to compare the quartz fabric in these nonmylonitic, but highly deformed, allochthonous rocks with that in the autochthonous mylonitic rocks.

The mylonitic rocks vary from pure mylonitic quartzite to foliated and lineated quartzo-feldspathic gneisses that contain only about 25% quartz. The majority of the samples analyzed for quartz [0001]-axis orientation data are quartzo-feldspathic. . . .

All microfabric diagrams are for thin sections cut normal to the mesoscopic lineation.[10] The data are plotted on the lower hemisphere of an equal-area projection. Deformation lamellae are plotted from those samples where they are conspicuously obvious.

All of the quartz-fabric diagrams show a strong maximum of [0001]-axis trends normal to the lineation (Fig. 11). Well-formed *ac* girdles connect the maxima. The crossed girdles are inclined at high angles to the lineation and the maxima are symmetrically grouped with respect to the foliation. All of the samples appear to be statistically orthorhombic, reflecting the suspected orthorhombic symmetry of the overall stress system. The more quartzose samples, 51 and 3031, exhibit stronger maxima than the quartzo-feldspathic samples. This is to be expected because the quartzose rocks are more homogeneous and the orientation of quartz [0001]-axes is affected by inhomogeneities in the rock, such as large augen of feldspar that may distort the quartz grains. The Paleozoic quartzite, sample 1070, shows a moderately strong preferred orientation of the [0001]-axes. The geometry of this rock is similar to that of the mylonitic rocks, which may indicate that a similar stress regime was responsible for the ductile deformation in both rock units.

The quartz [0001]-axis fabric data are consistent with the suggestion that mylonitic rocks are formed in zones of extreme flattening normal to the foliation and of extension parallel to the dominant mineral lineation (Johnson, 1967; Theodore, 1967; Sylvester and Christie, 1968; Ross, 1971). The orthorhombic symmetry of the fabrics is supportive of, but not conclusive evidence for, one episode of penetrative ductile deformation in these rocks.

Quartz-deformation lamellae (Boehm lamellae) are minute discontinuities in deformed quartz grains. Experimental studies of naturally deformed quartz suggest that these structures are planes of high shear stress commonly oriented at low angles to the basal prism in quartz (Carter and others, 1964; Heard and Carter, 1968). The orientation of lamellae noted in the petrofabric studies is presented in Figure 11. The lamellae show symmetrical orientation with respect to the quartz [0001]-axes and generally lie within 30° of the basal prism. This orientation is consistent with the orientation of the maximum compressive stress normal to the foliation, as indicated in experimental studies (Carter and others, 1964; Heard and Carter, 1968).

Interpretation of Structural Elements in the Rawhide Mountains

The structural elements in the rocks of the Rawhide Mountains appear to record at least two major structural events of contrasting style. The pre-Mesozoic rocks have been metamorphosed and have undergone a period of penetrative ductile deformation. This deformation is characterized by the development of a cataclastic foliation, strong northeast-trending mineral lineation, B_1 folds, much of the boudinage, and the fold mullions. This ductile deformation contrasts with the very brittle deformation that accompanied the late Tertiary low-angle faulting. This deformation is characterized by the

[10] This orientation is no longer recommended for quartz petrofabric studies in quartz-rich mylonitic rocks; sections are now generally cut perpendicular to foliation and parallel to the mesoscopic lineation.

extreme brecciation of rock units, major extension of units by penetrative high- and low-angle normal faults, slickenside striations, B_2 folds, and some of the boudinage. Above all, the late Tertiary deformation resulted in the formation of the distinctive basal dislocation surface that everywhere separates the mylonitic gneisses from the younger(?) higher rocks. Structural data from both events indicate movement in a southwest-northeast direction, with the dominant movement direction being to the northeast.

The deformational style recorded by structures in the mylonitic rocks includes the elongation of quartz grains, fracture and elongation of feldspar augen, boudinage, formation of intrafolial similar-type folds and a strong mineral lineation, and refolding of earlier folds by continuous flow. All of the structural evidence indicates that Mesozoic events were of a highly ductile nature.

The orientation of structural elements formed during the Mesozoic event shows a remarkably consistent trend throughout the map area. The mineral lineation trends S48°W, 20° in the mylonitic gneisses and the lineation in the overlying metavolcanic and Paleozoic rocks is approximately parallel to this trend. Boudinage data and the trend of the fold mullions are consistent with the

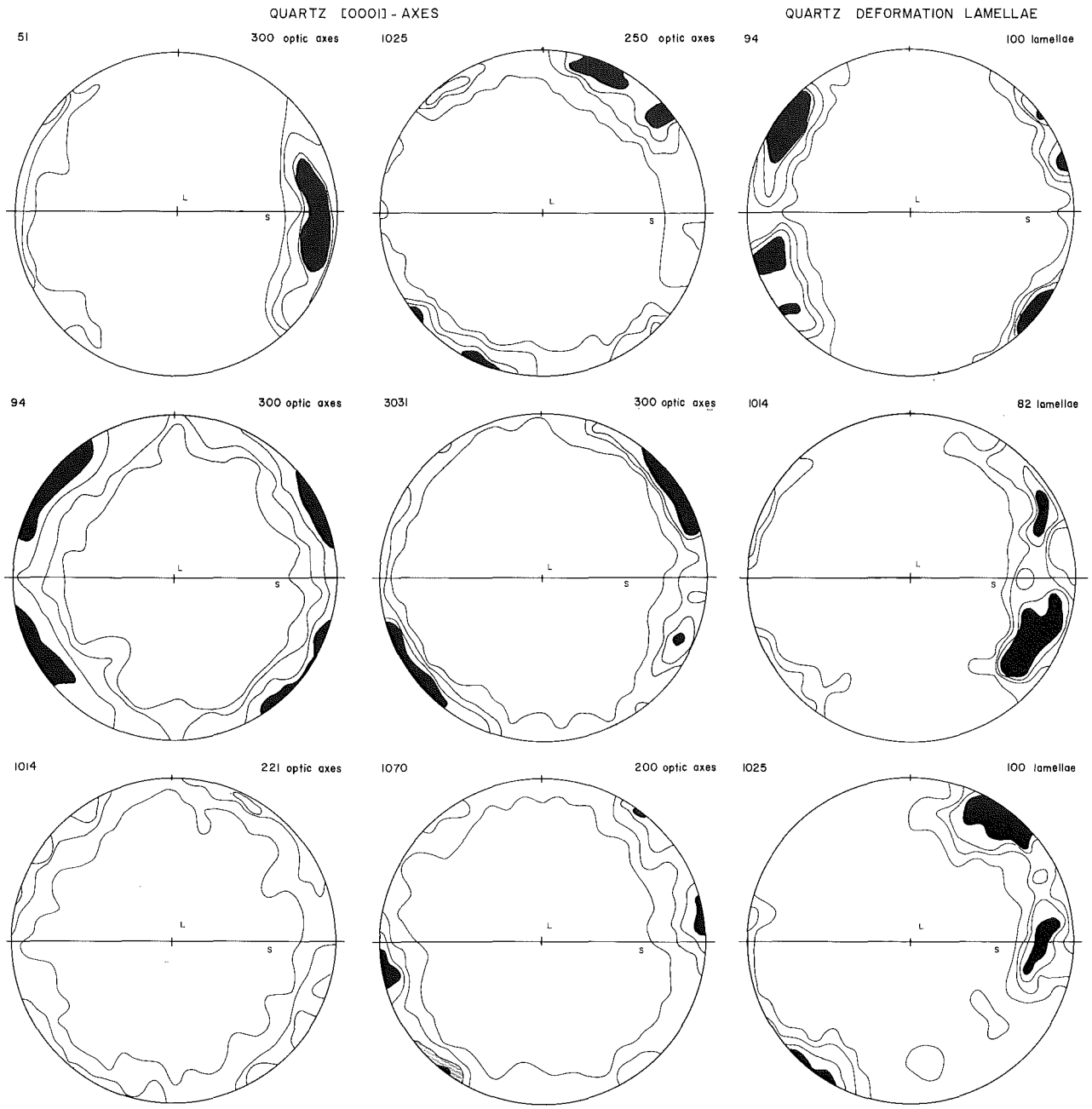

Figure 11. Stereonet plots of quartz [0001]-axis data (left and middle columns) and of quartz deformation-lamella data (right column).

lineation data; together these structures indicate extension in a northeast-southwest direction. B_1-fold orientations are highly variable and provide no information on the direction of tectonic transport for these rocks. The lack of parallelism between the B_1-fold axes and the mineral lineation suggests that the lineation does not correspond to a B-kinematic axis. Rather, it is an "a" lineation and indicates the inferred direction of tectonic transport. The orientation of *s* surfaces in the mylonitic gneisses, metavolcanic rocks, and Paleozoic sedimentary rocks shows a high degree of parallelism (Fig. 7). This similarity in orientation of *s* surfaces in both the autochthon and allochthon indicates that these rocks have undergone a similar post-Paleozoic and pre-Cenozoic deformation event.

The style of deformation and the orientation of minor structures suggest that deformation was characterized by flattening normal to the foliation and by elongation parallel to the mineral lineation. This is consistent with data from other mylonitic terranes.

Late Tertiary deformation has greatly modified the Mesozoic structural terrane. This deformation is characterized by the formation of a distinctive basal dislocation surface that everywhere separates the mylonitic gneisses from an overlying, chaotic assemblage of younger(?) rocks. The chaotic slicing and shuffling of allochthonous Precambrian(?) to late Tertiary rocks occurred along the complex series of F_1 and F_2 dislocation surfaces. These dislocation surfaces merge with or are subparallel to the basal dislocation surface. The primary juxtaposition of rock units is younger over older. Extreme brecciation of rock units, penetrative extension by normal faulting, and the merging of high- and low-angle normal faults attest to the nature of the deformation. The persistent orientation of *s* surfaces in the allochthon, at a high angle to the basal dislocation surface, is indicative of deformation by low-angle normal faulting. Longwell (1945) was the first to recognize low-angle normal faulting in the Basin and Range Province. Longwell noted that high-angle normal faults in the Lake Mead region flatten at depth into what he termed a *low-angle normal fault*. He considered these low-angle faults to be normal faults because the hanging wall was displaced down with respect to the footwall, the opposite of thrust-fault geometry, but in agreement with normal-fault geometry. Longwell also recognized that bedding in the hanging-wall block dips into the curved dislocation surface at a high angle and that the sense of displacement on the hanging-wall block is opposed to the dip direction of the strata.

The tectonic style of the late Tertiary deformation is incompatible with a conventional thrust-fault origin for this deformation in the Rawhide Mountains. The chaotic imbrication of upper-plate rocks by low-angle normal faulting, the marked contrast in lithology and deformational style between the autochthonous mylonitic gneisses and the allochthonous rocks, and the presence of a widespread basal dislocation surface separating the autochthon and allochthon suggest that this late Tertiary terrane was produced by gravity sliding of a relatively unmetamorphosed cover down the slope of the basal dislocation surface. The late Tertiary gravity sliding (denudation faulting) occurred, in large part, along surfaces guided by favorable lithology and/or preexisting structural discontinuities. The destruction of the Mesozoic(?) metamorphic fabric, the presence of the Chapin Wash Formation (Miocene) in fault-bounded slices above the basal dislocation surface, the geometric relationship of *s* surfaces to dislocation surfaces, and the overall brittle and extensional nature of the deformation indicate that this deformation is later than and not related to formation of the Mesozoic(?) infrastructural complex of Late Cretaceous-early Tertiary thrust-fault terranes elsewhere in western Arizona. An idealized model for the geometry of the slide complex and its mode of formation is presented in Figure 12. It is suggested that the slide complex in the Rawhide Mountains formed by the rigid fracturing and translation of discrete crustal blocks along curved normal-fault surfaces. The dominant movement of material occurred down the slope of a basal dislocation surface formed by the merging of the curved low-angle normal faults and a master shear surface. In the case of the Rawhide Mountains, the location of this master shear, herein called the *basal dislocation surface*, is controlled by the "top" of the mylonitic gneisses.

Late Tertiary kinematic data are presented in Figure 9. These data, to be discussed below, and field relationships suggest that the late Tertiary gravity-slide mass moved toward N50°E. The dominant northwest-

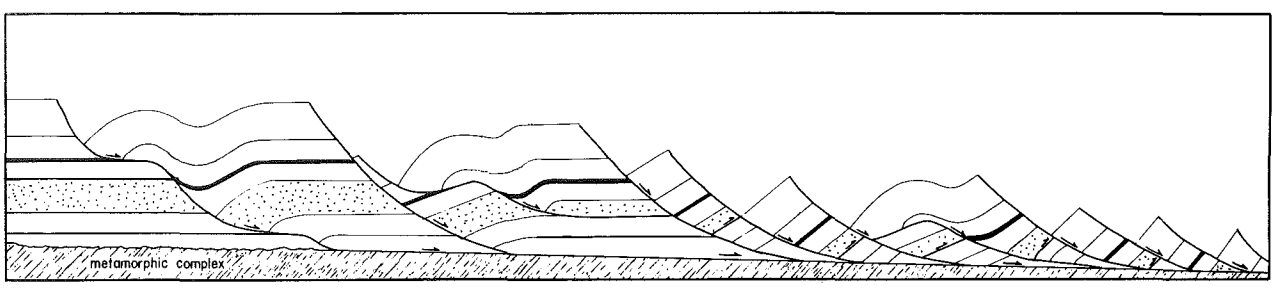

Figure 12. Idealized model for the origin of the gravity-slide complex in the Rawhide Mountains. The combination of listric normal and inverse imbricate faults is required to account for the overall geometry of rock units in the allochthon. The Rawhide Mountains would lie at an unknown distance to the right of this figure.

southeast strike of the "shingling" low-angle normal faults and the consistent displacement of the hanging-wall block down and to the northeast indicate northeast-directed movement. The late Tertiary lineation (formed by the intersection of *s* surfaces and penetrative normal faults), boudinage along F_1 and F_2 fault zones, and slickenside striations on F_1 and F_2 faults indicate northeast- or southwest-directed movement. B_2 folds record the relative direction of transport for individual slices within the gravity-slide terrane. The B_2 fold-axis data (Fig. 9) are concentrated in the northwest and southeast quadrants of the stereographic projection, but the spread in the data and the inconsistent sense of vergence on these folds make the definition of a preferred slip plane and slip-line direction tenuous. However, the bulk of the B_2 fold data suggest transport to N45°E, which is consistent with the rest of the late Tertiary kinematic data.

The *s* surfaces in all of the rock units show a N36°W to N44°W strike and a general, moderately steep (30° to 50°) dip to the southwest (Fig. 7). The units in the allochthon consistently dip 40° to 50° or more into the basal dislocation surface. This persistent orientation of *s* surfaces in the allochthon is supportive of deformation by inverse imbricate or listric normal faulting, whereby the dip of the *s* surfaces in allochthonous rocks will be in the opposite sense from the transport direction. The preferred orientation of *s* surfaces at about N40°W, 40°SW indicates tectonic transport to N50°E, which is consistent with the other structural data and is apparently conclusive evidence for northeast-directed gravity sliding during the late Tertiary.

The macroscopic folds in the allochthon are believed to have formed during the late Tertiary gravity sliding. These folds are confined to individual plates in the allochthon. Only rarely is the dislocation surface folded. Large folds, such as those found in the allochthon, can be generated during extensional deformation only along listric normal faults (Armstrong, 1972). The lack of well-defined macroscopic fold axes supports this mechanism, but is not conclusive.

It is perhaps fortuitous that the direction of tectonic transport for late Tertiary slide blocks is parallel to the inferred direction of tectonic transport for the Mesozoic event. However, this parallelism of movement directions is not unexpected considering the nature of the two deformational events. Basement structure(s) that resulted from the Mesozoic event may have controlled the nature and shape of the basement uplift, from which the cover slid.

The predominantly unidirectional movement of the slide mass in the Rawhide Mountains should not be considered as conclusive evidence against gravity sliding. When viewing a complete gravity-slide terrane, one expects to see radial displacement of material off of a central high. In the Rawhide Mountains, one is viewing but a small part of a much larger gravity-slide terrane in western Arizona. Hence, a single movement direction is not unexpected. As further geologic studies are carried out in this portion of western Arizona, the other flanks of this slide terrane may be recognized.

STRUCTURAL HISTORY

The major geologic events that have affected the rocks of the Rawhide Mountains are listed in apparent chronologic order in Table 1. The relative positions of certain events are tenuous because of sparse knowledge of the geology of nearby areas and the lack of good age criteria for known units. The order of events 1 through 6 is primarily based on speculation, whereas events 10 through 14 are presented in a relative age sequence, even though it appears that some events may have occurred simultaneously. . . . There is only scanty evidence for Precambrian deformation. The data indicate that major Mesozoic events have affected this part of Arizona, although the exact timing of this deformation is

TABLE 1. GEOLOGIC HISTORY OF THE RAWHIDE MOUNTAINS

Cenozoic

16. Deposition of the younger alluvium.
15. Deposition of the older alluvium and minor normal faulting.
14. Extrusion of the late Tertiary basalt, continued movement on the Sandtrap Wash fault, reverse faulting, and minor normal faulting.
13. Initial movement on the Sandtrap Wash fault.
12. Gravity sliding in the Rawhide Mountains.
11. Deposition of the Chapin Wash Formation and extrusion of the Miocene(?) volcanics.
10. Deposition of the Artillery Formation, minor faulting, and landsliding.

Mesozoic

9. Intrusion of hornblende diorite.
8. Regional metamorphism accompanied by mylonitization of the basement gneisses, possible thrust faulting, and intrusion of alkali granite and quartz monzonite.

Paleozoic

7. Deposition of the Paleozoic sedimentary rocks.

Precambrian

6. Intrusion of biotite granite.
5. Granitic intrusions and metamorphism of overlying sedimentary rocks.
4. Deposition of Precambrian sedimentary rocks.
3. Metamorphism of granitic rocks to form granitic gneiss.
2. Intrusion of granitic rocks.
1. Extrusion of intermediate to silicic volcanic rocks (present metavolcanics).

yet unknown. The Cenozoic deformation is the most spectacular and is the easiest to document. It is represented by the chaotic imbrication of most of the rock units in the Rawhide Mountains. The imbricate slicing and shuffling of the rocks by late Tertiary events are the prime reasons for the poor understanding of older events.

Precambrian Deformation

The Precambrian structural history of the Rawhide Mountains appears to contain evidence of events correlative with those elsewhere in Arizona. . . . The granitic gneiss and biotite granite bear no direct relationship to any rocks in western Arizona, although their metamorphism may be correlative with one of the younger Precambrian events. The possible correlation of the granitic gneiss with similar rocks in the Hualpai Mountains suggests that these rocks are older than 1,100 m.y. . . . The metasedimentary rocks must have been deposited on an earlier igneous and/or metamorphic terrane, but the exact nature of this terrane is unknown. Some time after their deposition, the metasedimentary rocks were intruded by granitic rocks. This intrusive activity may be correlative with the Mazatzal Revolution or may be Mesozoic. The former origin is preferred, but there are no data to directly support this conclusion. The knowledge of Precambrian events in the study area is very sketchy and further speculation on the nature of these events in the Rawhide Mountains does not appear to be warranted at this time.

The major problem of Precambrian(?) geology in the Rawhide Mountains is the nature of the metavolcanic rocks. If the metavolcanic rocks are correlative with similar rocks in the Yavapai Series, then they must record part of an older Precambrian orogeny. Moreover, if the metavolcanic rocks are among the oldest rocks in Arizona, why are they not present in the mylonitic-gneiss terrane?. . . If the metavolcanics are part of the Yavapai Series, then their structural position atop younger(?) mylonitized Precambrian(?) rocks must be the result of post-Precambrian thrust(?) faulting. The faulting that juxtaposed these two unlike sequences may have been Mesozoic. Their present structural position does not appear to be readily accounted for solely by late Tertiary gravity sliding.

However, a possible Mesozoic age for the metavolcanic rocks would make some of the structural interpretations more plausible. The lower grade of metamorphism and the nonmylonitic nature of these rocks when compared to the structurally lower mylonitic gneisses suggest that these rocks could have been stratigraphically and structurally above the protolith of the mylonitic gneisses in the Mesozoic. Also, the metavolcanic rocks are not intruded by any major igneous bodies, implying that they may have been extruded and metamorphosed after the major igneous plutonic activity represented by metaigneous rocks in the autochthon. The presence of Mesozoic metavolcanic rocks in south-central Arizona and southern California, in addition to the similar metavolcanic rocks of Mesozoic age in the Dome Rock (Silver, 1975, personal commun.) and Plomosa Mountains(?), gives added credence to a possible Mesozoic age for these rocks in the Rawhide Mountains.

Mesozoic(?) Deformation

A major Mesozoic event is inferred in the Rawhide Mountains because Paleozoic and older rocks have undergone a period of post-Paleozoic, pre-Cenozoic deformation. This deformation is characterized by amphibolite-grade metamorphism of the Precambrian(?) rocks, greenschist-facies metamorphism of presently allochthonous Precambrian(?) and Paleozoic rocks, and penetrative ductile deformation of most of these pre-Cenozoic rocks. The Mesozoic(?) quartz monzonite and alkali granite appear to have been intruded during this event because both show evidence of being partially deformed by it.

The primary feature of this Mesozoic tectonic event was the formation of an extensive mylonitic-gneiss terrane in western Arizona. In the Rawhide Mountains, these gneisses were metamorphosed to amphibolite facies, whereas to the south, in the Harcuvar Mountains, parts of this same metamorphic terrane appear to show evidence of anatectic melting. The mylonitization and accompanying formation of the cataclastic S_3 foliation occurred shortly afterwards, but probably as a result of the same tectonic event that was responsible for the major metamorphism of this terrane. The penetrative ductile deformation of these gneisses resulted in the formation of the strong N50°E lineation in this range, the Buckskin Mountains, and the Whipple Mountains of eastern California.

Metamorphism and mylonitization of the quartzofeldspathic gneisses appear to record the formation of a major metamorphic infrastructural complex. Mylonitization of these rocks is greatest in the upper portion of the complex, whereas metamorphic grade increases with depth. The Rawhide Mountains are interpreted as part of a sheath or upper cover of this infrastructural complex, whereas the Buckskin and Harcuvar Mountains may form the core of this regional complex.

Greenschist-facies metamorphism of the overlying metavolcanic unit and portions of the Paleozoic section must have occurred synchronously with the formation of the infrastructural complex with its mylonitic gneisses. That all of these rock units were subjected to the same event is indicated by the parallelism of the major and minor structural elements within them. Boudinage, B_1 fold axes, and the mineral lineation in the presently allochthonous metavolcanic and Paleozoic rocks are consistently oriented with respect to similar structures in the mylonitic gneisses (Fig. 8). The statistical parallelism of *s* surfaces in the allochthonous rocks and *s* surfaces in the mylonitic rocks further suggests that these metamorphic surfaces formed contemporaneously.

Mylonitic terranes are commonly associated with large-scale thrust faulting. The mylonitic gneisses in the Rawhide Mountains are thought to be associated with a major zone of Mesozoic low-angle tectonic transport

related to the formation of the infrastructural complex. However, the direct presence of Mesozoic thrust faults in the Rawhide Mountains cannot be documented. Older over younger juxtaposition of rock units has not been recognized, unless it is represented by the presence of the metavolcanic rocks structurally above the gneissic terrane. If thrust faults were present in the pre-Cenozoic rocks, any evidence of them has been obliterated by the late Tertiary gravity sliding. This is not unexpected because Mesozoic thrust faults in the metavolcanic and Paleozoic rocks may have been the preferential site for later deformation. The presence of the mylonitic gneisses does indicate that penetrative, presumably deep-seated, low-angle movement of these rocks has occurred. This movement is thought to be northeast-directed.

The exact timing of the Mesozoic deformation is unknown. Metamorphism, mylonitization, and thrust faulting(?) probably occurred during the Late Jurassic or Cretaceous. Events are definitely post-Paleozoic and predate the deposition of the Artillery Formation (Eocene?). If the metavolcanic unit is Triassic or Jurassic, then metamorphism must be Jurassic or Cretaceous. Hamilton (1971) reports a late Mesozoic age for the infrastructural complex in the Big Maria Mountains, California. L. Silver (1974, oral commun.) recently dated this metamorphism and deformation as occurring about 165 m.y. ago. Metamorphism and deformation may have occurred in the Whipple Mountains at about the same time (Terry, 1972). An upper age for the deformation appears to be indicated by a 67-m.y.-old granite body in the Granite Wash Mountains (W. Rehrig, 1975, personal commun.). The granite intrudes gneissic rocks that are similar to those in the Rawhide Mountains, and yet is itself neither metamorphosed nor deformed. . . .

Cenozoic Deformation

The Cenozoic was a time of major structural deformation in the Rawhide Mountains. Widespread faulting is evidenced by the extremely disrupted nature of the late Tertiary and older rocks. The dominant deformation was the late Tertiary gravity sliding, which tectonically denuded a large portion of the range and areas to the south and southwest. Latest Cenozoic left-lateral, oblique dip-slip, and reverse dip-slip faults have subsequently modified the gravity-slide complex.

The oldest known Cenozoic unit is the Artillery Formation. This unit is probably late Eocene to early Miocene in age, but the lack of adequate stratigraphic and structural knowledge on this formation make any more definitive age assignment difficult at this time. The Artillery Formation appears to have been deposited in a northwest-trending structural trough. Deposition was during a time of tectonic unrest, as indicated by the occurrence of monolithologic breccias and coarse clastics within this unit. Monolithologic breccias are not common in the Artillery Formation in the Rawhide Mountains, but Gassaway (1975, personal commun.) reports several thick lenses of these rocks in the Artillery Mountains. In addition, the rapid vertical changes in lithology suggest rapid uplift of the source area for the sedimentary rocks in this unit.

The Chapin Wash Formation (Miocene) locally unconformably overlies the Artillery Formation. The pervasive red color of this unit and the occurrence of sedimentary manganese deposits within it distinguish it from the Artillery Formation. Deposition of this formation also occurred during a time of structural unrest. Monolithologic breccias, coarse clastics, and volcanic material in this unit suggest active faulting and volcanism in this part of Arizona. The nature and extent of the basin of deposition for the Chapin Wash Formation are unknown. . . .

The major late Tertiary gravity sliding occurred shortly after the deposition of the Chapin Wash Formation in the Rawhide Mountains. Everywhere in the Rawhide Mountains the Chapin Wash Formation is highly disrupted and separated from autochthonous rocks by the basal dislocation surface. Chaotic imbrication of rock units during the gravity-slide event resulted in juxtaposition of the Chapin Wash Formation both above and below Precambrian(?) and Paleozoic rocks. The gravity sliding occurred after emplacement of the 15.9-m.y.-old basalt flow in the lower Chapin Wash Formation(?) in the Artillery Mountains and before extrusion of the late Tertiary basalt.[11] The 15.9-m.y.-old basalt lies beneath the Artillery "thrust," herein interpreted as a gravity slide structure formed during the late Tertiary deformation. The Artillery "thrust" is hereafter referred to as the *Artillery Mountains gravity slide*. The age of the basalt places the lower limit on the time of sliding at 15.9 m.y. ago. The low-angle deformation had definitely ceased before extrusion of the late Tertiary basalt. If this basalt is about 10 m.y. old, as is suggested, then the gravity sliding must have occurred sometime between 15.9 and 10 m.y. ago. This is about the same time that similar low-angle deformation occurred elsewhere in the Basin and Range Province (Anderson, R.E., 1971; Armstrong, 1972; Davis, G.A., 1974, personal commun.).

The magnitude and extent of the gravity sliding are as yet unknown because the gravity-slide complex in the Rawhide Mountains is part of a much larger slide terrane with an area in excess of 1,000 km^2 in western Arizona. Such an extensive area of tectonic denudation is suggested by the presence of late Tertiary gravity-slide structures in the Artillery, Rawhide, and Buckskin Mountains (Lincoln Ranch, Clara Peak, Swansea, and Planet Ranch).

The direction of tectonic transport for the slide sheets was to the northeast. Kinematic data from rocks in the Rawhide Mountains indicate transport in a N50°E direction. Minor structures (slickenside striations, small normal faults, and a lineation formed by the intersection of small normal faults and *s* surfaces) associated with the Artillery Mountains gravity slide are parallel to similar structures in the Rawhide Mountains.

A source area has not been recognized for the allochthonous material in the Rawhide or Artillery Moun-

[11] See footnote 5.

tains. It is possible that some of the now allochthonous material was originally deposited in the now denuded areas of the Rawhide and Buckskin Mountains. The apparent absence of a source area for the gravity-slide complex makes any attempt at determining the total displacement on the slide blocks impossible. The best available indicators of the amount of horizontal displacement are thought to be the Precambrian(?) granitic gneiss-biotite granite and the Mesozoic(?) alkali granite, both in the allochthon of the Rawhide Mountains. The *in situ* equivalents of these rocks should be present in the autochthon somewhere in western Arizona. However, correlative igneous and metamorphic bodies have not been recognized in the Rawhide Mountains or in areas to the southwest or northeast. The presence of the granitic gneiss - biotite granite and alkali granite in fault-bounded slices in the allochthon, with no source body within the study area, indicates a minimum displacement of 13 km for this part of the slide complex. This is the distance from the northeasternmost exposure of the alkali granite to the southwesternmost corner of the map area. The apparent absence of correlative in-place rocks in the Buckskin Mountains suggests much greater displacements.

The above discussion does not mean to imply that all of the allochthonous rocks have moved great distances. The Tertiary sedimentary rocks could have been deposited within the confines of the Rawhide Mountains and their present distribution could be due to relatively small-scale sliding and imbrication. At present, there is no evidence for or against large-scale transport for the Tertiary rocks. However, what is significant is that Tertiary sedimentary and volcanic rocks are allochthonous throughout the Rawhide and Buckskin Mountains and in part of the Artillery Mountains.

The major late Tertiary structure in the Rawhide Mountains is the basal dislocation surface. This surface separates the mylonitic gneisses from a chaotic assemblage of younger(?) rocks. The age of the basal dislocation surface is not accurately known. The surface may represent the original "top" of the Mesozoic(?) infrastructural complex, but this is conjecture at this time. The basal dislocation surface now represents the base of the late Tertiary gravity-slide complex in the Rawhide Mountains, and if there is an older structural significance of this surface, it has all but been obliterated by later events. *S* surfaces in both the autochthon and allochthon are truncated, often at high angle, by the basal dislocation surface, and the Mesozoic(?) mylonitic fabric of the lower-plate rocks has been destroyed at this surface. A late Tertiary age for the basal dislocation surface is confirmed by the presence of Chapin Wash rocks in fault-bounded slices at this surface. The basal dislocation surface cannot be an "old erosional surface" as suggested by Gassaway (1972). There is absolutely no evidence of channeling or erosion of this remarkably planar and extensively exposed surface. Also, there is a distinct paucity of mylonitic-gneiss debris in the Tertiary rocks--none in the Artillery Formation and only scattered clasts in the Chapin Wash Formation--a relationship that indicates that the gneisses were not widely exposed to erosion prior to tectonic denudation by sliding.

The thickness of the allochthon and thus the depth at which the basal dislocation surface was formed are poorly understood because of the highly disrupted nature of the upper-plate rocks. The thickness of the Chapin Wash Formation is unknown in the Rawhide Mountains, but it is about 1,200 m thick in the Artillery Mountains and Sandtrap Wash, if no telescoping by low-angle faulting is assumed. The Artillery Formation is about 1,400 m thick in the Rawhide Mountains. If the Paleozoic rocks are about 900 m thick, as suggested here, and the metavolcanics have a minimum thickness of 1,000 m, then the thickness of the allochthon may have approached 3,500 m. If the above thickness for the allochthon is realistic, it indicates that the basal dislocation surface may have been buried at a depth of 3,500 m at the time of its formation. However, there is evidence to suggest that this surface was formed at a shallower depth. The extreme cataclasis of the mylonitic rocks at the basal dislocation surface, the highly polished nature of the basal dislocation surface, and the high degree of brecciation of upper-plate rocks suggest that deformation occurred at levels less than 3 to 4 km in depth. In addition, the presence of isolated clasts of mylonitic-gneiss debris in the Chapin Wash Formation requires that the gneisses were exposed at least locally somewhere in western Arizona prior to sliding.

A major problem with any interpretation of the nature of the Tertiary low-angle faulting involves the room problem. The presence of a major gravity-slide complex requires that upper-plate rocks must have moved out and across a land surface somewhere during the sliding event. Such a geometric requirement is necessary to account for the extensional denudation that has to have occurred at the source area. A problem for the Rawhide Mountains area is that nowhere have late Tertiary slide blocks been found emplaced onto or into sediments that were being deposited contemporaneously with sliding--lower-plate rocks are everywhere those of the mylonitic terrane. Thus, there is no evidence that a portion of the 250 km^2 Rawhide Mountains slide complex moved across a free surface, i.e., the earth's surface. One may avoid the issue by saying that the toe or distal portion of the slide mass was eroded away as fast as it was exposed to the earth's surface. This is suggested for the Amargosa chaos of the Death Valley area (Wright and Troxel, 1969), but there are no data yet available in the Rawhide Mountains area to support or refute this idea. One may also suggest that the toe of the slide mass is buried in some, as yet undefined, sedimentary basin. This possibility holds some promise. If the Sandtrap Wash fault has major left-lateral displacement on it, restoration of this displacement places the Rawhide Mountains slide complex opposite areas now covered by late Tertiary basalt and alluvium. Thus a basin into which the slide mass may have moved could be present in the northern Artillery Mountains, but it will be very difficult to substantiate its presence.

A partial solution to the room problem may be present in the Artillery Mountains. Here the Artillery Mountains gravity slide is emplaced onto Chapin-Wash-like sediments of the upper Artillery Formation. If, as suggested earlier, these sediments are Chapin Wash, then one finds Chapin Wash sediments both above and below the major gravity-slide sheet in this range. If the lower-plate Artillery Formation and the lower Chapin Wash Formation are autochthonous, then the present Artillery Mountains may represent a sedimentary basin into which the Rawhide Mountains slide complex was emplaced. This suggestion may be incorrect, however, because it is not yet possible to directly correlate the slide complexes in the Artillery and Rawhide Mountains. One must also account for apparent large left-lateral displacement on the Sandtrap Wash fault. Removal of the offset on this fault places the Artillery Mountains block opposite the eastern Buckskin Mountains in the Tertiary, not east of the Rawhide Mountains as they are today. The above problems can only be resolved by continued detailed geologic investigation in the Artillery Mountains and adjacent ranges. The current lack of geologic knowledge on this entire section of western Arizona makes any further interpretations highly suspect.

Shortly after cessation of the gravity sliding, movement on the Sandtrap Wash and Lincoln Ranch high-angle faults was initiated. There is no evidence available to indicate that the Sandtrap Wash fault was active prior to the late Tertiary gravity sliding, but this possibility cannot be ruled out. This fault was clearly active during the late Tertiary. It truncates the middle Miocene slide complex in the Rawhide Mountains and vertically displaces the late Tertiary basalt about 260 m. The Sandtrap Wash fault does not appear to cut any postbasalt sediments.

The Lincoln Ranch fault, its branches, and the reverse faults in the western Rawhide Mountains all originated after the gravity sliding. These faults displace the basal dislocation surface and place mylonitic gneisses on top of allochthonous Chapin Wash sedimentary rocks. None of the postsliding, pre-Holocene rock units are spatially associated with these faults; thus, the time of activity on the reverse faults can only be bracketed as postsliding (circa 10 to 15 m.y. ago) and pre-Holocene because these faults do not cut the younger alluvium.

The tectonic styles of the Sandtrap Wash and Lincoln Ranch faults appear to be in marked contrast to the northeast-southwest extension indicated by the late Tertiary gravity sliding. However, the possibility exists that both events, the gravity sliding and later oblique dip-slip and reverse dip-slip faulting, are related. All of these structures may be related to northeast-southwest compressional stresses present in this portion of the Basin and Range Province in the late Tertiary. Regional arching of the basement gneisses and subsequent sliding could have been early responses to these stresses.

Minor normal faulting(?) also occurred after cessation of the gravity sliding. One high-angle dip-slip fault cuts the basal dislocation surface and a normal fault cuts the older alluvium in the western Rawhide Mountains.

THE RELATIONSHIP OF STRUCTURES IN THE RAWHIDE MOUNTAINS TO REGIONAL TECTONICS

. . . The Rawhide, Buckskin, Whipple, and Big Maria Mountains have been metamorphosed to amphibolite grade and exhibit a strong N40°E-N50°E lineation. Northeast-trending mineral lineations of probable Mesozoic age are also present in the Tortolita Mountains, central Arizona (Davis, G.H., and others, 1975).[12] This lineation appears to be an "a" lineation, parallel to the direction of tectonic transport for this Mesozoic deformation. The Mesozoic age for this northeast-trending mineral lineation is significant in that previously this lineation had been considered Precambrian. The regional extent of this lineation and its association with high-grade metamorphic complexes and/or thrust faulting suggest that major penetrative deformation affected a large portion of the southwestern United States during the Mesozoic. . . .

The apparent absence of thrust faults in the Rawhide Mountains is enigmatic. Thrust faults, if present, may have been eroded away, leaving only the core of the infrastructure complex, or may have been remobilized and obscured by the late Tertiary gravity sliding.[13]

Tertiary gravity sliding is a topic poorly understood and much maligned by many geologists working in the western United States. Almost without exception, low-angle faults of Tertiary age have been, until recently, considered thrust faults (Noble, 1941; Hewett, 1956; Hunt and Mabey, 1966). This was in spite of the fact that such "thrust faulting" occurred approximately contemporaneously with extensional tectonics in the Basin and Range Province. This apparent dichotomy may, perhaps, now be resolved with the recognition that a large percentage, if not all, of the middle to late Tertiary low-angle faults can be ascribed to the gravity sliding of material off of structural or topographic highs. The highs, off of which this material slid, are the result of, or are directly related to, the formation of the Basin and Range Province (Armstrong, 1972; Coney, 1974).

Tertiary low-angle faulting has occurred throughout most of the Basin and Range Province. Gravity sliding or structures that can be interpreted as gravity slides are present in many of the ranges of eastern Nevada and western Utah (Willden and others, 1967; Moores, 1968; Armstrong, 1972, Coney, 1974), eastern California (Wright and Troxel, 1969; Burchfiel and Davis, 1971; Reynolds, M.W., 1974), and Arizona (Cooper, 1960; Anderson, R.E., 1971; Blacet, 1972; Krieger, 1974; Davis, G.H., 1975). Studies of many of the areas where low-angle Tertiary

[12] This lineated mylonitic fabric in the Tortolita Mountains is now interpreted to be middle Tertiary in age.

[13] The latter alternative may be correct. Precambrian crystalline rocks are overlain unconformably by Tertiary sediments, but lie above Mesozoic(?) metavolcanic rocks in the northern Rawhide Mountains map area (Figs. 3 and 5DD'). The Tertiary unconformity is cut by northeast-dipping normal faults and rotated to the southwest. These faults may root into a preexisting, now-reactivated, thrust fault between the Precambrian basement rocks and lower-plate metavolcanic rocks. Lineations in the metavolcanic rocks may, therefore, be related to pre-Miocene thrust faulting, not to the episode of regional Tertiary mylonitization.

faulting has occurred reveal that there is an apparent correlation between the presence of a Mesozoic metamorphic terrane and Tertiary low-angle denudation faulting. Invariably low-angle dislocation surfaces (dêcollement zones) separate the penetratively deformed autochthon from brittlely deformed allochthonous rocks, although interpretation of the timing relationships between metamorphism and dislocation differ. In Nevada and eastern Utah, the low-angle dislocation surfaces correspond to the regional dêcollement of Misch and Hazzard (1962), considered by them and others as the detachment zone for Mesozoic thrust faults (Misch and Hazzard, 1962; Nelson, 1966, 1969; Cebull, 1970). However, Armstrong (1972) and Coney (1974) have recently suggested that, in some areas, this dêcollement may in part be the result of late Tertiary gravity sliding off of domal structures cored by Mesozoic metamorphic terranes. The low-angle deformation in Nevada and Utah is thought to have occurred between 25 and 11 m.y. ago (Armstrong, 1972; Todd, 1975).

Similar structures, an autochthon of Mesozoic metamorphic rocks separated by a low-angle dislocation surface from a relatively unmetamorphosed allochthon containing rocks as young as Tertiary, are also present in California and Arizona. In the Death Valley area, the Amargosa "thrust" (Noble, 1941; Hunt and Mabey, 1966) separates a high-grade metamorphic terrane of Mesozoic age from a chaotic assemblage of Precambrian through Tertiary rocks. The Amargosa "thrust" and chaos has recently been interpreted as a massive gravity slide completely formed by the coalescing of a system of listric normal faults (Wright and Troxel, 1969), with the Amargosa "thrust" representing the master dislocation surface. The enigmatic "turtleback" structures have also been interpreted as the result of extension and gravity sliding (Wright and others, 1974). In the Black Mountains, Death Valley, the imbricate structure of the Amargosa chaos includes rocks of the Artist Drive Formation. Volcanic rocks from this unit have yielded K-Ar ages of 6.3 to 8.02 m.y. (Fleck, 1970). The Artist Drive Formation and older rocks are unconformably overlain by the relatively undeformed Greenwater Volcanics, dated at 5.3 to 5.5. m.y. (Fleck, 1970). Thus, the date of gravity sliding and formation of the Amargosa chaos is between 6.3 and 5.4 m.y. (Fleck, 1970).

Gravity-slide blocks that consist of Miocene sedimentary and volcanic rocks appear to surround the Mesozoic(?) metamorphic complex in the Whipple Mountains, California (G.A. Davis, 1973, personal commun.). The gravity sliding in this range occurred between 20 and 14 m.y. ago (G.A. Davis, 1974, personal commun.), roughly contemporaneously with, or perhaps a bit earlier than, sliding in the study area. The structures in the Whipple Mountains are poorly understood and further speculation on their overall natural and deformational history is premature. . . .

From the above presentation, it is obvious that the late Tertiary gravity sliding in the Rawhide Mountains is not an isolated event. Rather, gravity sliding was a common and widespread structural event in the area of the present Basin and Range during the Tertiary. Almost all of the Tertiary slide complexes have certain basic characteristics in common: (1) shingling normal faults that merge with a low-angle basal decollement or dislocation surface; (2) intense brecciation of upper-plate rocks and only moderate deformation of the lower plate; (3) an upper plate that contains steeply dipping strata, which are truncated by the low-angle dislocation surface(s); (4) upper-plate strata that normally dip in a direction opposite to that of tectonic transport; (5) only minor large-scale folding -- deformation is usually characterized by rigid translation of blocks; (6) general displacement of younger rocks over older rocks; and (7) the general presence of a topographic high off of which the blocks could have moved.

Many, but not all of the slide terranes, are associated with Mesozoic metamorphic complexes. It is interesting to note that many of these metamorphic complexes also yield mid-Tertiary cooling ages, 40 to 20 m.y. old (Mauger and others, 1968), which appear to record the final uplift and cooling of the metamorphic terranes. In the Death Valley area and in the Black Mountains, Arizona, uplift may be associated with the intrusion of Tertiary plutons. In either case, there appears to be a common direct correlation between the domal rise of relatively mobile crustal material and gravity sliding, sliding being the thin-skinned crustal response to this doming. The shallow and brittle nature of the deformation, the attenuation of units by faulting, and the often complex and chaotic imbrication of units support a gravitational origin for these structures.

The majority of the gravity sliding occurred between 30 and 10 m.y. ago. This is the time classically reserved for the formation of the Basin and Range Province, a time of crustal extension in the western United States. This is also the time of extensive silicic volcanism and uplift of many of the Mesozoic metamorphic terranes. Thus, it would appear that there was a cause-and-effect relationship between gravity sliding off of isolated highs and the events that accompanied the formation of the Basin and Range. The late Tertiary gravity sliding appears to be the consequence of the rapid rise of discrete crustal blocks and their subsequent denudation by faulting controlled by favorably oriented lithologic or structural discontinuities.

Lower-plate rocks of the Buckskin Mountains, Arizona: A progress report

BRUCE BRYANT *U.S. Geological Survey, M.S. 913, Box 25046, Denver Federal Center, Denver, Colorado 80225*
J.L. WOODEN *U.S. Geological Survey, M.S. 937, 345 Middlefield Rd., Menlo Park, California 94025*

ABSTRACT

Lower-plate rocks in the Buckskin Mountains are composed of layered migmatitic gneiss intruded by gabbro and granodiorite during the Proterozoic and pervasively invaded by leucocratic granite and pegmatite during the Cretaceous. A plutonic suite composed of rocks ranging from gabbro to granite and, at least in part, of early Miocene age forms the central part of the range. Slabs and slices of metamorphosed Mesozoic and Paleozoic supracrustal rocks are present at the top of the lower plate and within migmatite in the lower plate. The slices in the lower plate may mark zones of Mesozoic thrust-related deformation transposed during Tertiary extension. During the middle Tertiary, mylonitization pervasively overprinted rocks in the eastern part of the range and less pervasively affected rocks in the west.

INTRODUCTION

In the Buckskin Mountains, rocks below the Buckskin detachment fault are exposed in three northeast-trending Tertiary arches separated by swales occupied by upper-plate rocks. The arches, from northwest to southeast, are referred to as the Planet Peak, Clara Peak, and Ives Peak arches (Fig. 1).

Lower-plate rocks in the Buckskin Mountains, which are continuous with those in the Rawhide Mountains north of the Bill Williams River, have received little study. Brief descriptions of rocks from a few localities were published in studies of mining districts (Bancroft, 1911; Spencer and others, 1986; Spencer and Reynolds, 1986a) and in a reconnaissance study (Rehrig and Reynolds, 1980). In a pioneering study of detachment faults, Shackelford (1976b) mapped the lower- and upper-plate rocks in the Rawhide Mountains.

The research reported herein is part of the Pacific-Arizona Crustal Experiment (PACE) program of the U.S. Geological Survey (Howard, 1986). This program is a geophysical and geological study of a west-southwest-trending transect from the Colorado Plateau to the Pacific Ocean along the route of deep seismic-reflection profiling by two university consortia: CALCRUST and COCORP. Geologic mapping of the Buckskin Mountains, which lie directly on this transect, is designed for intermediate-scale publication.

This article is a preliminary summary of the geology of lower-plate rocks in the Buckskin Mountains. At this writing, about 90% of the lower plate in the Buckskin and Rawhide Mountains has been mapped in detail suitable for 1:100,000-scale publication.

ROCK TYPES

The lower plate mostly consists of metamorphosed migmatite and plutonic rock. Small areas of metamorphosed sedimentary rock are also present; the largest of these is near Battleship Peak in the Ives Peak arch (Marshak and Vander Meulen, this vol.). The principal rock unit in the Ives Peak and Planet Peak arches and in the eastern Buckskin Mountains is migmatitic gneiss characterized by interlayered dark-gray to black layers and light-gray to white layers. Dark layers consist of amphibolite, biotite-quartz-feldspar schist and gneiss, feldspar-porphyroclast biotite gneiss, and pods of hornblendite and mafic amphibolite. Light-colored layers are granitic gneiss and pegmatite. In intermediate-colored layers, the ratio of mafic to felsic minerals is intermediate between those of dark and light layers. This unit is probably Early Proterozoic in age and represents a deeper crustal level than rocks in the upper plate to the northeast, such as the amphibolite-facies supracrustal sequence near Bagdad, which is not migmatized but is highly intruded by a variety of plutons (Anderson, C.A., and others, 1952; Conway and others, 1986). The protoliths for the migmatite were probably igneous rocks of mafic to intermediate composition, perhaps volcanics intruded by sills and plutons. Very few layers suggest sedimentary protoliths. Locally, however, especially in the far eastern part of the Buckskin Mountains, mica-rich schists are present but are not associated with other rock types that suggest sedimentary parentage. They may represent marine shales or highly altered felsic tuffs.

The layered migmatite is intruded by a variety of plutonic rocks. In the southeastern Buckskin Mountains, a body of gabbro intrudes the layered rocks, and numerous sills and pods of gabbro are present in the migmatite outside the main body. The main body is weakly foliated, whereas the thinner sills tend to have better developed foliation. In the eastern Buckskin Mountains, well-foliated bodies of granodiorite and porphyritic

in Spencer, J.E., and Reynolds, S.J., eds., 1989, Geology and mineral resources of the Buckskin and Rawhide Mountains, west-central Arizona: Arizona Geological Survey Bulletin 198, p. 47-50.

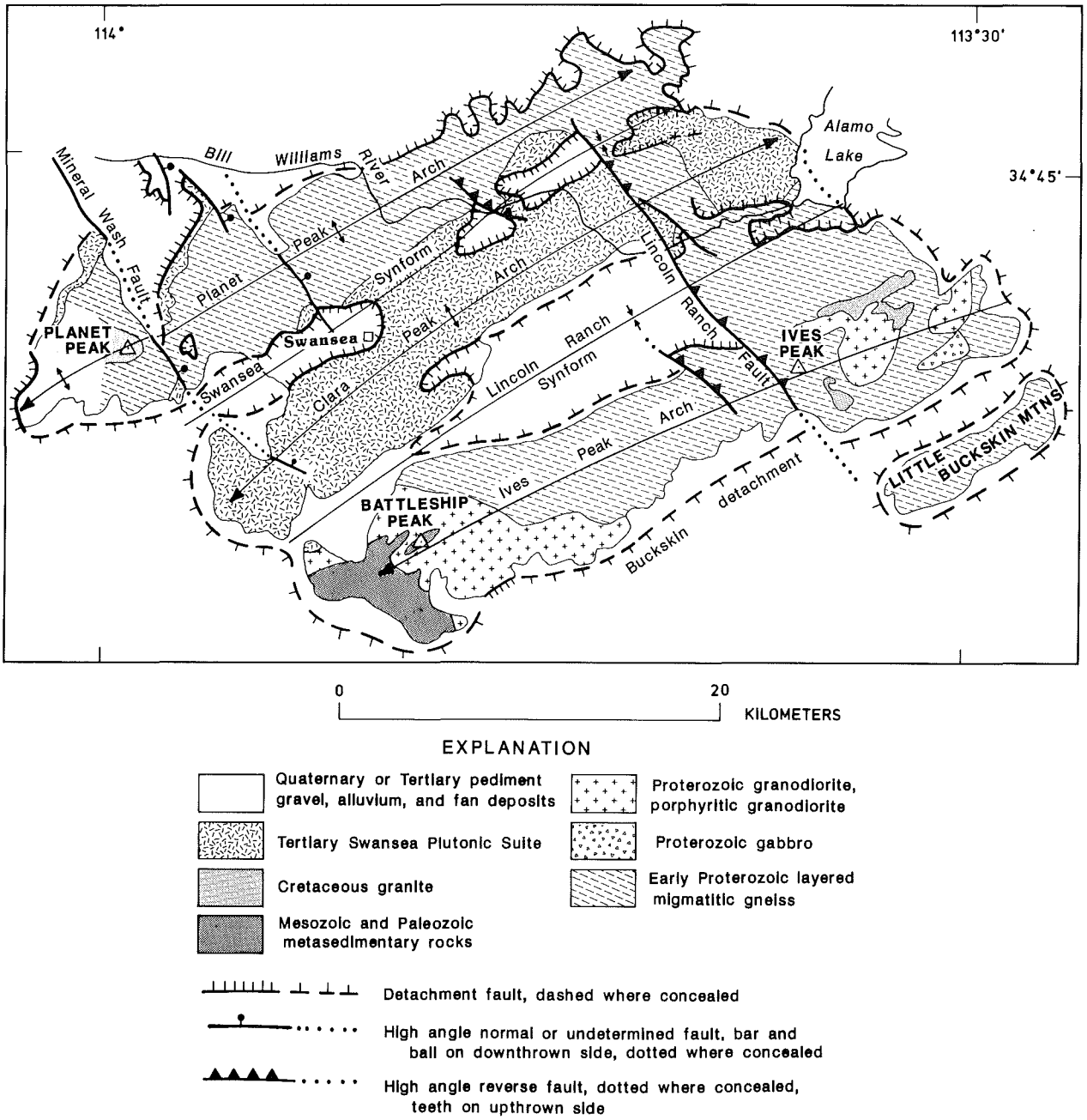

Figure 1. Generalized and preliminary geologic map of lower-plate rocks in the Buckskin and Rawhide Mountains. Upper-plate rocks, postdetachment rocks, and unmapped rocks in the lower plate are unpatterned. Locations of Tertiary sills in the western part of the Planet arch are derived from Spencer and others (1986; Plate 2).

granodiorite intrude the migmatite. In the southwestern Buckskin Mountains in the Ives Peak arch, similar strongly foliated granodiorite and augen gneiss derived from porphyritic granodiorite and quartz monzonite crop out over wide areas. These plutonic rocks are interpreted to be Proterozoic in age.

Light-colored granitic rock and pegmatite intrusions are widespread and may be of more than one age. Some may be Proterozoic, but many are probably Phanerozoic, perhaps broadly correlative with the Cretaceous Tank Pass granite of Reynolds (1980b). Bodies of this rock have been mapped in the eastern Buckskin Mountains and on Planet Peak. Sills of the same rock type are so numerous outside those bodies that it is difficult to decide whether to map granite or migmatite, especially because the granite is more resistant to weathering than the more heterogeneous and mafic migmatite. The abundance of granitic sills varies greatly; they are absent in some migmatitic areas and in the entire Clara Peak arch.

Swansea Plutonic Suite

The Clara Peak arch is composed of a group of igneous rocks, herein named the Swansea Plutonic Suite (Fig. 1). The suite is named after exposures along an unnamed wash in the eastern parts of sec. 33, T. 10 N., R. 15 W. and sec. 4, T. 9 N., R. 15 W., south-southeast of the old mining town of Swansea in NE$^1/_4$ sec. 32, T. 10 N., R. 15 W. The wash contains the abandoned grade of the railroad that served Swansea (Fig. 1). Parts of the suite were mapped as Mesozoic quartz monzonite and diorite in the Rawhide Mountains (Shackelford, 1976b). Rocks of the suite intrude layered migmatitic gneiss near Alamo Dam, on the south flank of the Planet Peak arch north of Swansea, and north of the Bill Williams River west of the Lincoln Ranch fault. Known exposures of the suite are confined to the lower plate in the Buckskin and Rawhide Mountains (Fig. 1).

Rock types in the Swansea Plutonic Suite range from gabbro to granite. In the field, the most abundant types appear to be medium- to coarse-grained gabbro, diorite, porphyritic granodiorite, and leucocratic granodiorite. Petrographic studies indicate that quartz diorites are also widespread and that there is a weak tendency for the rocks of the suite to be bimodal in mafic content, but this tendency is not well reflected by the ratios among quartz, plagioclase, and potassic feldspar. Rocks with few mafic minerals range from quartz diorite to granite. Megascopically visible quartz is lacking in many rocks of the Swansea Plutonic Suite; however, in thin section, quartz is apparent as small matrix grains between larger feldspars. The porphyritic variety contains feldspar porphyroclasts, derived from phenocrysts, as long as 3 cm and superficially resembles augen gneiss derived from Proterozoic plutonic rock. Gabbro and porphyritic diorite are closely associated and have no clear field relations that would indicate contrasting ages. They are intruded by many small and some larger bodies of more felsic rock types. Pegmatites are rare except along the intrusive contact margin of the suite, such as the area north of Swansea. A few dikes of very fine-grained, locally porphyritic, leucocratic rock cut the main part of the suite.

Rocks of the suite are variably deformed. The diorite and gabbro are weakly sheared to well foliated. The felsic rocks everywhere have a well-developed foliation and northeast-trending mineral lineation, although they retain vestiges of igneous texture.

Geologic relations show that the Swansea Plutonic Suite is the youngest major rock unit in the lower plate of the Buckskin Mountains. The intrusive contact north of Swansea cuts marble of probable Mesozoic or Paleozoic age that forms slices along possible Mesozoic thrust faults. The lack of leucocratic granitic intrusions, which are widespread in adjoining rocks, indicates that the suite is younger than those granites. If the leucocratic granite correlates with the Cretaceous Tank Pass granite of Reynolds (1980b), the Swansea Plutonic Suite must be latest Cretaceous or Tertiary in age. The widespread development of mylonitic foliation and northeast-trending stretched-mineral lineation indicates that the suite is older than at least some mylonitization.

A U-Pb date (21.6 $\pm$ 1.5 Ma) of zircon from a granite in the suite 3 km north of Swansea shows that the rock is similar in age to some older volcanic rocks of the upper plate in and near the Buckskin Mountains (Spencer, Shafiqullah, and others, this vol.). A U-Pb date (18.5 $\pm$ 0.5 Ma) of sphene from the same sample is interpreted to be a cooling age. Until ages of zircon are obtained from the older gabbroic phases of the suite, the interval during which the entire suite was emplaced will remain uncertain.

Metasedimentary Rocks

Marble, quartzite, calc-silicate rocks, and other metasedimentary rocks of probable Paleozoic and Mesozoic age are widespread in the Buckskin Mountains. They are present as detached lenses or slabs that form part of the upper plate, as sheets and lenses at the top of the lower plate just below the detachment fault, and as lenses in the migmatitic gneisses of the lower plate. The largest area of metasedimentary rocks in the lower plate is on the southwest end of the Ives Peak arch (Marshak and Vander Meulen, this vol.). Similar metasedimentary rocks are present on the north side of the Ives Peak arch and locally on the south side of the Little Buckskin Mountains. The largest and most complex zone of lenses and sheets of metasedimentary rock crosses the eastern Buckskin Mountains from the Lincoln Ranch fault to south of Alamo Dam (Fig. 1). Similar interleaved metasedimentary rocks and crystalline basement rocks are well exposed in the northern Granite Wash Mountains. There they lack a Tertiary deformational overprint, which is well developed in the Buckskin Mountains, and the presence of the slices is attributed to Mesozoic thrust faulting (Reynolds and others, 1986b).

In the Buckskin Mountains, metasedimentary rocks commonly contain sills and lenses of pegmatite and aplite. Rocks in the southwest corner of the range also contain sills of diorite of the Swansea Plutonic Suite and of biotite-quartz-feldspar porphyry.

STRUCTURE

The structural geology of west-central Arizona indicates that basement rocks of the region have had a long and complex history starting at about 1.7 Ga with deformation, metamorphism, and production of new crust. Cretaceous folding, thrust faulting, and prograde metamorphism were followed by middle Tertiary mylonitization and retrogressive metamorphism. Rather than attempt a comprehensive account of structures in the lower plate of the Buckskin Mountains, we will present only a few general observations.

The most obvious structures in many of the rocks are mylonitic foliation and an accompanying northeast-trending lineation formed by smeared-out mineral grains. In almost all outcrops, mylonitic foliation is parallel with preserved layering, but locally it cuts the layering, especially in the western Buckskin Mountains. The mylonitic foliation and northeast-trending lineation are

most pervasive and well developed in the eastern Buckskin Mountains. Farther west, the rocks are less intensely mylonitized, and northeast-trending lineation is not found on all foliation planes. This lineation is rare on foliation planes in the Battleship Peak area (Marshak and Vander Meulen, this vol.), yet the basement gneisses have a well-developed foliation and a texture that indicate the original plutonic rocks were severely sheared and mylonitized. Mylonitic foliation with a northeast-trending lineation is commonly present along the contact between basement gneisses and overlying supracrustal rocks. This foliation is younger than the well-developed, generally more steeply dipping foliation in the basement gneisses. The older foliation might be Cretaceous or early Tertiary in age.

Minor folds are widespread in the layered migmatitic gneisses and are particularly well developed in the eastern Buckskin Mountains. Axial planes are parallel to mylonitic foliation and most axes trend northeast. These minor folds have well-developed, northeast-trending mineral lineation parallel with their axes, which suggests that they formed during Tertiary extension or were pre-existing folds that were rotated into parallelism with the mylonitic lineation.

Stereonet plots of poles to foliation and the map patterns of foliation indicate the presence of large-scale folds. Large-scale folds with northwest trends are present in the Battleship Peak area (Marshak and Vander Meulen, this vol.). In contrast, other widely separated areas, such as Planet Peak and the Little Buckskin Mountains, have larger folds that trend northeast, parallel with the small-scale folds, the three arches of the Buckskin Mountains, the lineation, and the direction of Tertiary extension.

The lower plate contains a number of low-angle faults marked by breccia or gouge. Many of the faults can only be detected in areas of excellent exposure, such as the canyon of the Bill Williams River west of Alamo Dam (Fig. 1). Some of these features were mapped in the Rawhide Mountains (Shackelford, 1976b, this vol.). In the eastern Buckskin Mountains, one low-angle fault is marked by a zone of brecciated rock several tens of meters thick and a change from uniformly and gently dipping mylonitic foliation below to less regularly and more steeply dipping mylonitic foliation above.

The rocks of the Buckskin Mountains are cut by northwest-trending normal and reverse faults. The Lincoln Ranch fault is a reverse fault that brings mylonites on the east side up and against the upper-plate rocks in the Lincoln Ranch synform between the Clara Peak and Ives Peak arches. The Mineral Wash fault at the west end of the range disrupts the Planet Peak arch (Plate 1). Several northwest-trending faults and fractures cut the rocks; only those with large displacements are shown on Figure 1. Some of the fracture planes have a subhorizontal striation, which suggests that latest movement was strike-slip.

ACKNOWLEDGMENTS

We thank S.J. Reynolds and J.E. Spencer for introducing B. Bryant to, and continuing to educate him on, the geology of west-central Arizona.

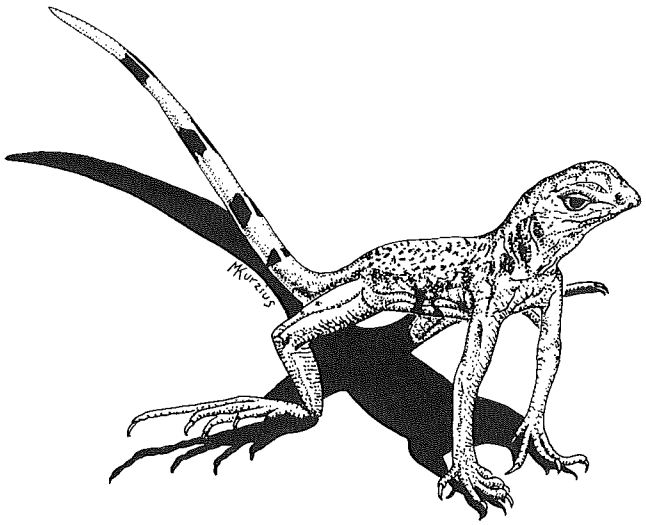

Geology of the Battleship Peak area, southern Buckskin Mountains, Arizona: Structural style below the Buckskin detachment fault

STEPHEN MARSHAK
MARC VANDER MEULEN
Department of Geology, University of Illinois, 1301 Green St., Urbana, Illinois 61801

ABSTRACT

The Battleship Peak area in the southern Buckskin Mountains is underlain by two distinct lithologic terranes: basement and cover. The structurally lower basement terrane is composed of Precambrian augen gneiss and Mesozoic to Cenozoic intrusive rock. The dominant structure in the basement is gneissic foliation, which is locally folded and is cut by discrete nonplanar shear zones; the gneissic foliation is probably Mesozoic or Proterozoic. Basement shear zones contain mylonitic fabric and have gradational boundaries. Basement is juxtaposed along a low-angle, irregular, sheared contact with a cover terrane of metasedimentary and metaigneous rocks, which are derived from Paleozoic and Mesozoic strata and younger intrusive rock. The cover terrane can be divided into several mappable units; however, because of deformation, these units are not in original stratigraphic sequence and vary dramatically in thickness along strike. The cover terrane commonly displays penetrative, low-angle, mylonitic foliation and lineation. Cover foliation varies in attitude, probably because of nonlaminar shear during deformation. The basement-cover contact truncates basement foliation at some localities and is concordant with basement foliation at others. At concordant contacts, the basement has a mylonitic fabric. Structural relationships suggest that the Battleship Peak area lies in a broad, shallow-dipping, internally complex shear zone within the lower plate below the Buckskin detachment fault, which is locally exposed in the study area. Refolding and overprinting relationships suggest that the last ductile deformation event, which overprinted earlier fabrics, occurred under progressively less ductile conditions. Most mylonitic foliation was formed during this event and is associated with top-to-the-northeast shear, whereas late-stage, cross-foliation normal faults resulted in top-to-the-southwest movement. Late-stage structures also include kink folds, brittle fractures, and faults.

in Spencer, J.E., and Reynolds, S.J., eds., 1989, Geology and mineral resources of the Buckskin and Rawhide Mountains, west-central Arizona: Arizona Geological Survey Bulletin 198, p. 51-66.

INTRODUCTION

The Buckskin and adjacent Rawhide Mountains of west-central Arizona (Fig. 1) are divided into three ENE-WSW-trending antiformal ridges separated by synformal troughs. The *Geologic Map of Arizona* (Wilson and others, 1969; henceforth referred to as the *State Map*) indicates that the southeastern antiform of the Buckskin Mountains (known as the Ives Peak arch) is composed of Mesozoic sedimentary rocks in the Battleship Peak area and Precambrian crystalline rocks elsewhere. In nearby ranges, two suites of Phanerozoic structures have been documented (Frost and Martin, 1982; Reynolds and others, 1986b). The first suite developed during multiple phases of Mesozoic contraction (Reynolds and others, 1980; Ellis, 1982; Hamilton, 1982; Laubach, 1986; Reynolds and others, 1986b), and the second developed during Tertiary extension (Davis, G.A., and others, 1980; Rehrig and Reynolds, 1980; Reynolds, 1982b; Davis, G.A., and others, 1986). The research described herein focused on determining the nature of the sedimentary rocks in the Battleship Peak area, considered to be Mesozoic by Wilson and others (1969), and on clarifying the deformational and metamorphic history of the rocks. The Battleship Peak area was mapped (Marshak and others, 1987), outcrop data on deformation fabrics were collected, and fabrics and lithologic characteristics were analyzed using standard methods of optical petrography.

This research delineates two distinct lithologic terranes in the Battleship Peak area: basement, composed of Precambrian gneiss intruded by variably deformed igneous bodies; and cover, composed of mylonitic and nonmylonitic metasedimentary rocks derived from Paleozoic and Mesozoic strata. This study also provides information on basement-cover contact relations and constrains the structural evolution of cover-terrane mylonitic rocks. Structural data indicate that the last episode of deformation and metamorphism affecting the Battleship Peak area occurred within a thick, internally complex shear zone in the footwall below the Tertiary Buckskin detachment fault. This fault is exposed at Redrock hill on the eastern edge of the map area, and breccias associated with the fault are present at the crest of Battleship Peak.

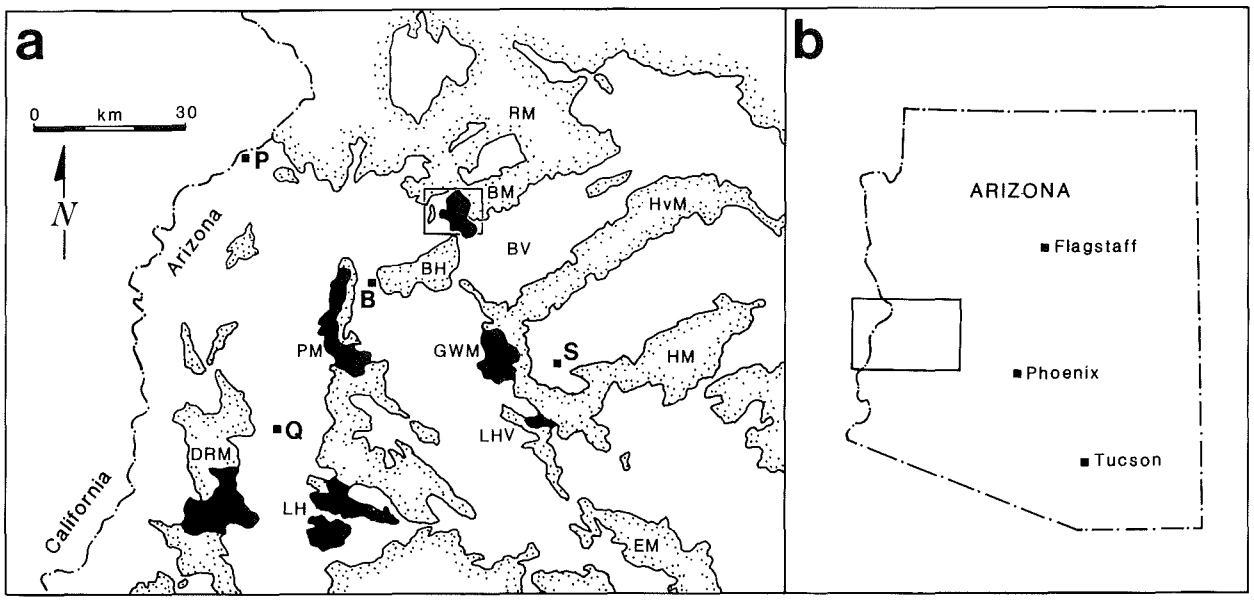

Figure 1. Location map of western Arizona. (a) Study area in Buckskin Mountains is indicated by box. Dot-dash line is Colorado River. Black areas represent regions indicated as "Mesozoic sedimentary rock" (Mzs) on the Geologic Map of Arizona (Wilson and others, 1969). Recent mapping, however, indicates that some of these areas (e.g., the area in the Plomosa Mountains) are not composed of Mesozoic sedimentary rocks. P = Parker; Q = Quartzsite; B = Bouse; S = Salome; GWM = Granite Wash Mts.; BM = Buckskin Mts.; BH = Bouse Hills; HvM = Harcuvar Mts.; HM = Harquahala Mts.; DRM = Dome Rock Mts.; LH = Livingston Hills; RM = Rawhide Mts.; EM = Eagletail Mts.; BV = Butler Valley; LHV = Little Harquahala Mts. (b) Location of map area (a).

Previous Work

The first geologic descriptions of the southern Buckskin Mountains were published in the early 1900's (Bancroft, 1911; Blanchard, 1913; Ross, 1922; Darton, 1925). The area was subsequently mapped in reconnaissance by Eldred Wilson during the 1920's and 1930's for the State Map (Wilson and others, 1969). Although substantial field studies were undertaken elsewhere in the Buckskin Mountains (Wilkins and Heidrick, 1982; Spencer and Reynolds, this vol.), the Battleship Peak area remained essentially unstudied except for brief reconnaissance (Marshak, 1979; Spencer and Welty, 1985).

LITHOLOGIES OF THE BATTLESHIP PEAK AREA

The State Map indicates that the Battleship Peak area contains two distinct units, Precambrian gneiss (p€gn) and Mesozoic sedimentary rocks (Mzs). The contact between p€gn and Mzs separates a terrane composed of gneiss and augen gneiss, widely cut by small igneous bodies, from a terrane of variably mylonitic metasedimentary rocks interlayered with mylonitic metaigneous rocks (Figs. 2 and 3; Marshak and others, 1987). In this article, the outcrop belt of crystalline rocks is referred to as the *basement terrane* and the outcrop belt of predominantly metasedimentary rocks is called the *cover terrane*. Thin erosional outliers of cover rocks lie along the northeast edge of the main outcrop belt; about 35% of the area shown as Mzs on the State Map is actually basement terrane.

Basement Lithologies

Augen gneiss is the most widespread lithology in the basement terrane (Fig. 4a). In general, this rock is composed of 1- to 3-cm-long elongate augen of porphyroclastic alkali feldspar in a medium-grained quartz, feldspar, and mica matrix (Table 1). Most of the quartz forms elongate ribbonlike clusters of small grains; grain boundaries within these clusters are sutured, but boundaries between clusters are smooth. Macroscopically, this rock generally has wavy foliation defined by oriented mica and quartz ribbons that wrap around the augen. Zones of medium- to coarse-grained, augen-free banded gneiss are interlayered with the augen gneiss. Compositional bands in the banded gneiss range in thickness from 0.5 to 10 cm and are defined by variations in abundance of mica. In many places, banded-gneiss and augen-gneiss exposures include concordant layers of tectonized aplite and/or pegmatite. At some localities, the augen gneiss is cut by discrete mylonitic shear zones (Fig. 4b). Mylonitic rocks that lack augen or contain relict augen have a penetrative, smooth planar foliation and a well-developed lineation defined principally by streaks of microcrystalline biotite. No published radiometric dates are available for gneiss outcrops in the Battleship Peak area, but these rocks resemble 1.4 to 1.7 Ga crystalline rocks from nearby areas (S.J. Reynolds and J.E. Spencer, personal commun., 1985). By association, the gneiss of the Battleship Peak area is considered to be Precambrian.

Precambrian gneiss accounts for approximately 60% to 70% of bedrock outcrops in the study area. The remain-

der is composed of silicic, intermediate, and mafic igneous dikes, plugs, and sills (Table 1). Igneous textures characterize these rocks, except where they are cut by shear zones. Igneous rocks of similar composition in nearby ranges are Mesozoic or Cenozoic; therefore, the nongneissic igneous bodies of the basement terrane are also considered to be Mesozoic or Cenozoic.

Cover Lithologies

The cover terrane includes a variety of nonmylonitic to mylonitic, metasedimentary rocks interlayered with mylonitic metaigneous rocks (Table 1). Identification of the protoliths of some cover lithologies is difficult because of deformation. The five most common lithologies include the following:

(1) White Mylonitic Quartzite. This rock is composed almost entirely of fine-grained to microcrystalline quartz and relict ribbon quartz. It is strongly foliated and lineated (stretched-grain mineral lineation) and was probably derived from pure quartz arenite. Grain size varies. In specimens with larger grains, the grains are notably flattened (Fig. 4c).

(2) Micaceous and/or Feldspathic Mylonitic Quartzite. This rock is similar to the white quartzite mylonite except that it contains mica and/or feldspar

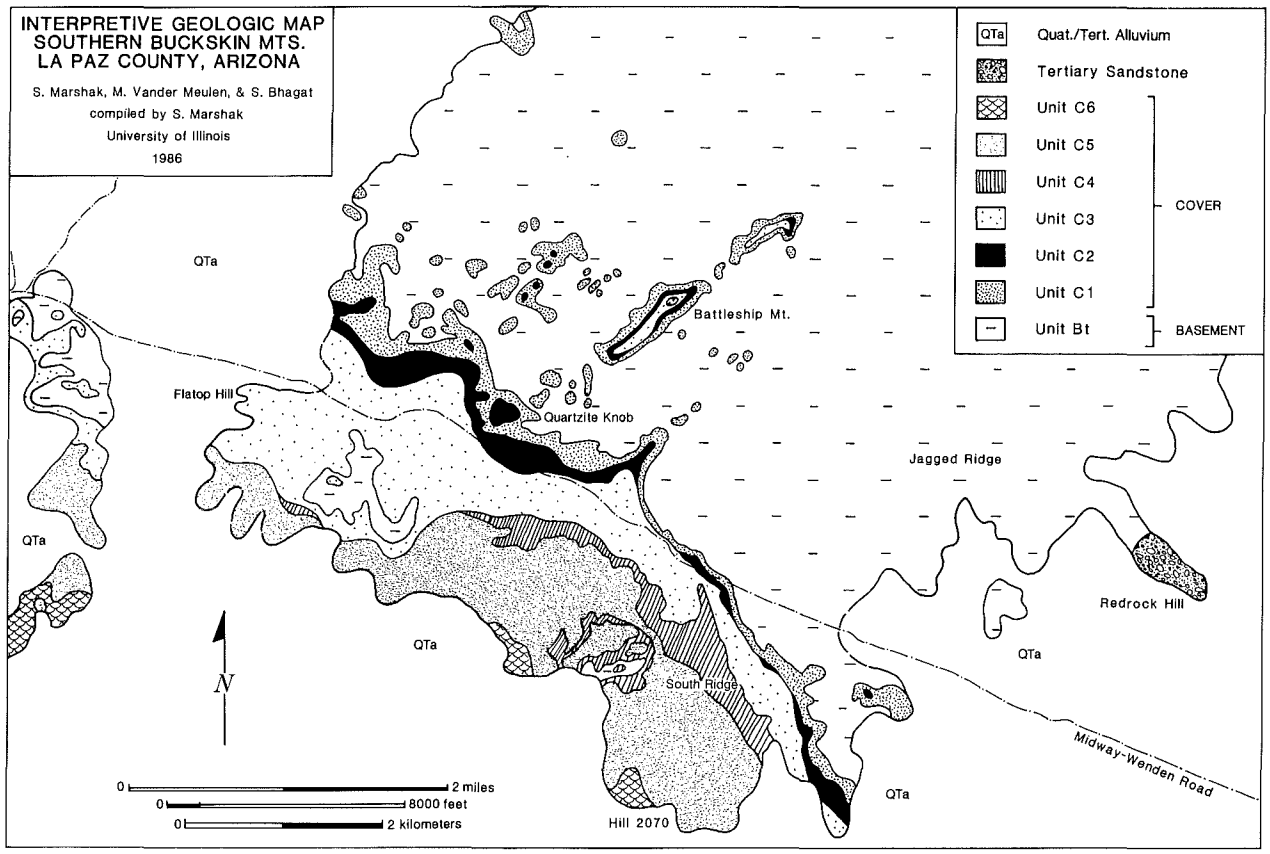

Figure 2. Interpretive geologic map of Battleship Peak area, based on map of Marshak and others (1987). This map emphasizes the lateral continuity of some of the mappable units within the cover sequence. It also shows the variation in unit thicknesses, the thinning and disappearance of some units along strike, and the distribution of erosional outliers of cover-terrane rocks. The circled area at the top of Battleship Peak is the outcrop of breccia and cataclasite.

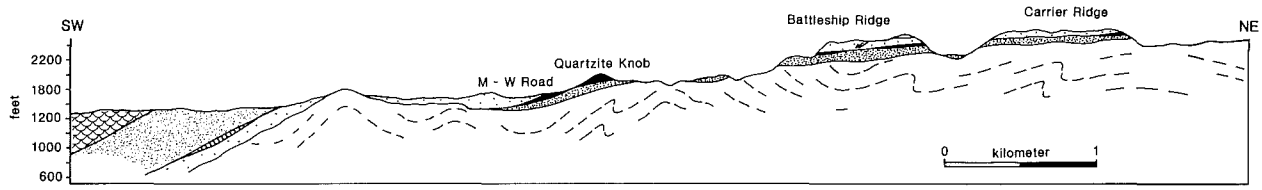

Figure 3. Cross section of Battleship Peak area through Quartzite knob and along crest of Battleship Peak. This section emphasizes the contrast in attitude between the basement and cover sequences. Dashed lines in the basement terrane are merely a schematic representation of foliation. Folds and structural detail in the cover are not shown, nor are shear zones in the basement.

TABLE 1. REPRESENTATIVE LITHOLOGIC DESCRIPTIONS

Lithology: Augen gneiss
Sample Numbers: 15X, 5112, 5113, X176
Description:
Macroscopic. Dark-gray to black, medium- to very coarse-grained gneiss with 0.5- to 4.0-cm white feldspar augen in a micaceous matrix.
Microscopic. Ribbons of sutured quartz and fractured alkali feldspar porphyroclasts set in a foliated groundmass of biotite, muscovite, plagioclase, and opaque minerals. Sericite and granular masses of epidote are present in the matrix. Associated banded gneiss displays similar mineralogical and textural features.
Protolith: Granodiorite or granite.

Lithology: Marble
Sample Numbers: 2139, 5208, 5198, 2184B, 5115, 2104
Description:
Macroscopic. White, gray, blue, buff, yellow, dark-brown, coarse-grained, massive to finely laminated marble.
Microscopic. Equant to slightly flattened calcite grains are typically fine to medium sand sized and display twins; groundmass may be all carbonate or gradational to calc-silicate with quartz-feldspar-epidote-tremolite; tremolite porphyroblasts up to 0.5 cm are confined to specific thin horizons. Muscovite is present in large amounts in the marbles of Unit C4, and fine-grained phyllosilicates are present in the anastomosing shear surfaces in all but one pure marble sample.
Protolith: A variety of pure to siliceous limestones containing some dolostone and chert.

Lithology: Calc-silicate rock
Sample Numbers: 2134, X179B, 2210
Description:
Macroscopic. Dark-brown and pale-green, 0.1- to 10.0-cm-thick, alternating silica- and carbonate-rich layers display convolute folds in base-relief; thin aplite sills are common.
Microscopic. Fine-grained feldspar and quartz porphyroclasts that display sutured boundaries and undulatory extinction are concentrated in the siliceous bands, but individual grains float in the calcite matrix of the carbonate layers; tremolite and epidote are common in some fine-grained phyllosilicates.
Protolith: Cherty limestone and dolostone, and local aplite sills.

Lithology: Quartz-epidote-feldspar schist
Sample Numbers: 2118, 4174, 4175, 5125
Description:
Macroscopic. Brown to reddish-brown, fissile, fine-grained schist with few visible folds.
Microscopic. Foliation defined by quartz-grain elongation, a preferred epidote-grain alignment, and a variety of micas including biotite. Some plagioclase, tremolite, and carbonate present. Fine- to very fine-grained.
Protolith: Siliceous marl or argillaceous calcareous arenite.

Lithology: White mylonitic quartzite
Sample Numbers: 6203, 6107, 6194, 6124, 3149, 3154B, 3156A
Description:
Macroscopic. White, gray, brown, fine- to medium-grained quartzite, locally with distinguishable folds. Pure varieties are vitreous with perfect cleavage and well-developed lineation; other samples display less foliation development.
Microscopic. Elongation of quartz grains defines foliation, which is most pronounced in monomineralic samples. Quartz is sutured with extreme undulatory extinction and subgrain formation. Muscovite, biotite, calcite, and epidote are present in some samples.
Protolith: Quartz arenite with varying clay and carbonate components.

Lithology: Micaceous feldspathic mylonitic quartzite
Sample Numbers: 86-BU-24
Description:
Macroscopic. Gray to grey-green, well-foliated, with foliation slightly wavy. Clusters of microcrystalline mica (dark green-brown) are smeared along foliation planes and define a strong lineation.
Microscopic. Fine-grained quartz-mica (primarily biotite) -feldspar matrix; contains numerous small fractured feldspar porphyroclasts (with recognizable twinning and zoning).
Protolith: Possibly dacite sills and dikes.

Lithology: Intrusive rocks
Sample Numbers: 4173, 2117A, X166, 4190, 4192, 6108, 2103, 5111, 18, 6195, 6196, 5204, 4191
Description:
Macroscopic. White, gray, dark-green sill and dike rocks that display wide variation in intrusive relations and deformational textures.
Microscopic. Composition ranges from quartz-alkali feldspar aplites and pegmatites through intermediate rhyodacitic compositions to actinolite-plagioclase mafic rocks. Textures for each composition range from relict igneous to mylonitic.

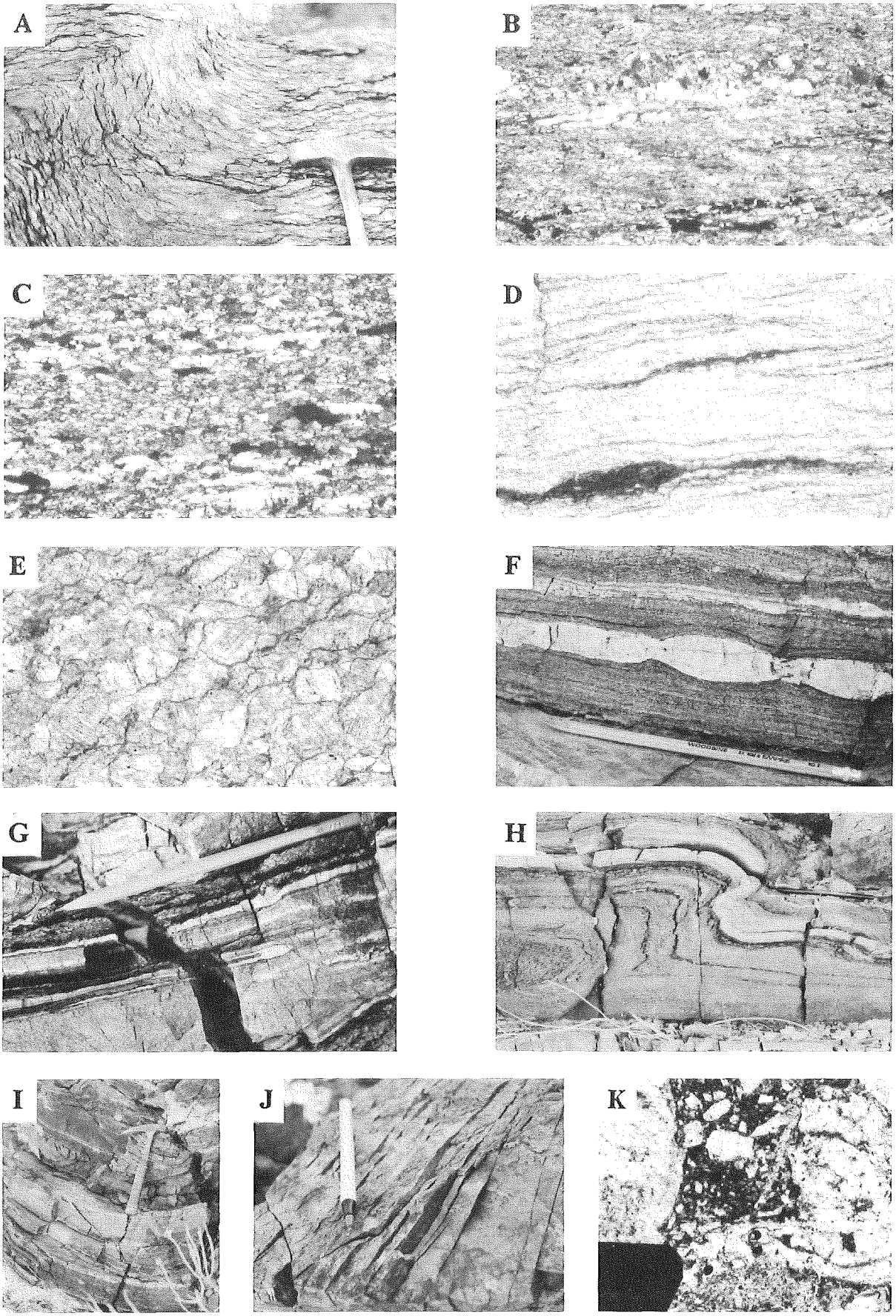

(caption on next page)

Figure 4 (previous page). Photographs of lithologies and structures. Field of view in all photomicrographs is 3 mm; scale in outcrop photos is indicated by standard objects. (a) Outcrop of basement augen gneiss at which gneissic foliation has been folded; (b) Photomicrograph of mylonitic basement augen gneiss; (c) Photomicrograph of quartzite containing flattened quartz grains of Unit C2 (crossed polars); (d) Photomicrograph of micaceous mylonitic quartzite of Unit C2 (uncrossed polars); (e) Equigranular twinned calcite grains in marble of Unit C6; (f) Outcrop of calc-silicate rock from Unit C1, showing color contrast between light-colored, siliceous layer with boudinage and darker carbonate-rich layers; (g) Class-A isoclinal fold in Unit C1; (h) Class-B asymmetric fold involving calc-silicate layer in Unit C2; (i) Class-C synform of foliation in Unit C1; (j) Systematic fractures in Unit C1 showing normal displacement on fracture surface; (k) Photomicrograph of breccia from the crest of Battleship Peak.

(Fig. 4d). The mica fraction is composed of sericite ± biotite(?) and forms smeared-out microcrystalline clusters that define a mineral lineation on foliation planes. Locally, this lithology includes clear euhedral feldspar crystals 1 to 2 mm in diameter. It may have been derived from an intrusive igneous protolith.

(3) Marble. There are several varieties of marble in the study area, including buff-colored sugary-textured marble composed of medium-grained, recrystallized twinned carbonate (Fig. 4e); gray sugary-textured marble; quartz-rich marble (quartz grains are mixed in with calcite grains); and foliated white marble (fine grained with strong foliation).

(4) Calc-Silicate Rock. This rock is typically composed of thin, alternating, light-buff- and dark-brown-weathered layers (Fig. 4f). All layers are a mixture of carbonate and quartz, with minor amounts of tremolite and epidote, but the darker layers contain more quartz. Quartz typically forms ribbonlike clusters of fine sutured grains, but some quartz remains as isolated grains in the carbonate matrix.

(5) Quartz-Epidote-Feldspar Schist. This rock is diverse in appearance (grain size and relative proportions of quartz, epidote, and feldspar vary). Typically, this schist is grainy, well foliated, and fissile and has a well-developed mineral lineation. Locally, it is interlayered with poorly foliated gray quartzite.

DEFINITION OF MAPPABLE COVER UNITS

The cover sequence is subdivided into map Units C1 through C6, of which Unit C1 is structurally lowest and C6 is structurally highest (Fig. 5). Each unit, which is defined by an assemblage of lithologies, varies in thickness and composition along strike (Fig. 2; Marshak and others, 1987). For example, Unit C2 is 35 m thick at Quartzite knob, but is absent 1 km to the north on Battleship ridge. Variation in thickness of the cover terrane is dramatic: the cover sequence is about 800 m thick in the southeast corner of the map area, but is

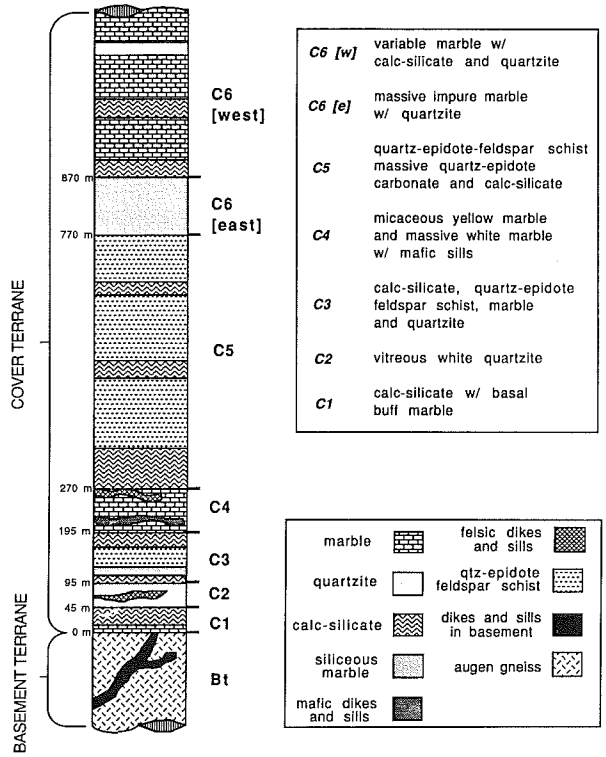

Figure 5. Idealized lithologic column showing mappable units in study area. Maximum observed thicknesses are indicated. Because of tectonism, the complete column is not exposed at any one locality. The sequence of units does not necessarily represent original stratigraphy, and the thicknesses are not stratigraphic thicknesses.

absent 3 km to the northeast (Redrock hill), where Tertiary sedimentary rocks are juxtaposed directly against the basement terrane. Recognition of a mappable sequence of units (Fig. 5) does not imply that there is an undisturbed stratigraphy; original stratigraphy was reordered during one or more deformations.

Unit C1, which is predominantly composed of marble interlayered with calc-silicate and minor quartzite mylonite, ranges in thickness from 8 to 45 m. A distinctive 0.3-m-thick, tan, sugary-textured marble is present at its base. Unit C2, a distinctive marker unit, is composed of white quartzite mylonite (probably from a sedimentary protolith) and quartz-mica-feldspar mylonite (probably from an igneous protolith). Unit C3 varies in composition: north of the Midway-Wenden Road, it is primarily composed of marble and calc-silicate rock with minor quartzite mylonite; south of the road, it includes these lithologies plus quartz-epidote-feldspar schist. Unit C4, also a useful marker unit, is composed of micaceous, yellowish-tan, buff-weathered, tremolite-bearing marble, locally with mafic lit-par-lit intrusions. Unit C5 is a thick interval that is predominantly composed of quartz-epidote-feldspar schist, with local metaconglomerate and gray quartzite. Unit C6 is composed of various types of marble interlayered with calc-silicate and quartzite. The type of marble included in Unit C6 varies across the map

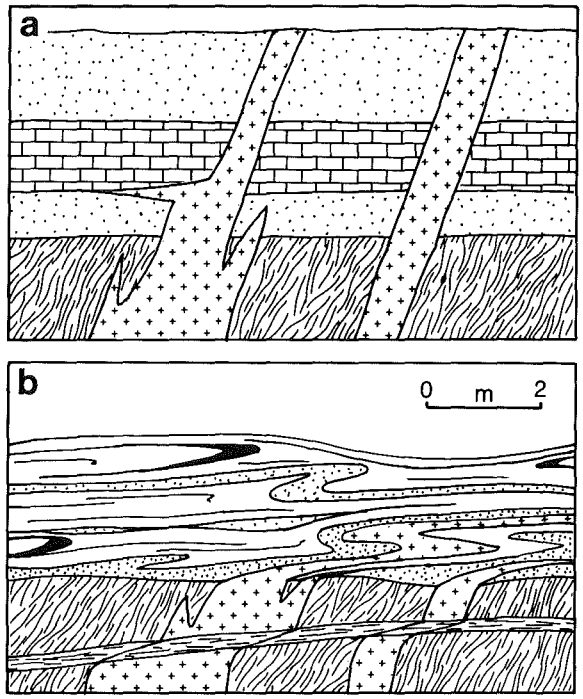

Figure 6. Schematic diagram showing transposition of dikes into cover foliation in cross-section view. This figure also shows that shear zones in the basement terrane are discrete and relatively thin.

area: southwest of Flatop hill, it is virtually pure, but on Hill 2070, it contains a significant proportion of quartz. Because of the lithologic variability of the marble, the structural continuity of Unit C6 over the entire map area (Fig. 2) is speculative.

Intrusions that presently cut the basement terrane probably cut the cover terrane at one time, but they are difficult to identify in the latter. These intrusions may have been transposed into cover foliation (Fig. 6); thus, some lithologies in the cover terrane were derived from pre- and/or synmylonitization intrusions. Intrusions that truncate cover layering, though less common in the basement terrane, are present. A large sill of variably deformed pegmatite is present along South ridge; at its northwest limit, this body cuts across foliation of the enveloping metasedimentary rocks. At several localities, small mafic dikes and sills are present in the cover terrane. Near Quartzite knob, hydrothermally altered breccia cuts the cover terrane. Its matrix is composed of thin plagioclase lathes and hexagonal quartz crystals surrounded by hematite (location shown in Marshak and others, 1987).

METAMORPHISM

Metamorphic grade is difficult to determine from the mineral assemblages in cover rocks. The presence of epidote/clinozoisite, tremolite, biotite, feldspar, and quartz suggests that the rocks are in the middle greenschist or albite-epidote facies. In all metamorphic rocks, most metamorphic minerals lie in the plane of foliation, except in marble, which typically contains coarse equant calcite.

STRUCTURES

Fabrics

The predominant fabric in the basement terrane is foliation in the augen gneiss. This fabric is defined by preferred orientation of phyllosilicates, elongate quartz clusters, and flattened augen (Fig. 4a). Foliation planes are wavy because of the presence of augen and coarse grains of feldspar or quartz. The attitude of this foliation varies (Figs. 7 and 8; Marshak and others, 1987); it commonly strikes WNW-ESE and dips moderately to the NNE, but at many localities it has shallow dips or dips to the SSW. This variability is associated with folding at several scales. Basement gneiss does not usually possess notable lineation.

Locally, grain size of the gneiss is smaller, foliation is more planar and less wavy, and foliation surfaces display strong mineral lineation defined by streaks of microcrystalline mica. It appears that mylonitic outcrops in the basement terrane are part of shear zones that are approximately 1 to 5 m thick. The borders of these shear zones appear gradational and are difficult to recognize. Structural symbols in Figure 7 distinguish between three types of foliation in the basement gneiss: original gneissic foliation, mylonitic foliation, and foliation that is intermediate between these two. The coarse augen-gneiss foliation formed before mylonitization. Most of the mylonitic zones are shallow dipping, but their attitudes vary. Bands of mylonitic augen gneiss are present adjacent to the basement-cover contact at many localities.

Penetrative foliation is obvious in hand specimens of most cover lithologies. On foliation planes of noncarbonate lithologies, a strong lineation is defined by stretched quartz grains and streaks of microcrystalline mica. The character of this foliation varies as a function of lithology: in quartzite, foliation is defined by closely spaced parallel planes; in quartz-epidote-feldspar schist, it imparts a shalelike fissility; and in marble and calc-silicate, it is defined by alteration of silica-rich (dark-brown-weathered) and silica-poor layers.

Thin-section studies clearly indicate that development of foliation in rocks of the cover terrane involved dynamic recrystallization and grain diminution; thus, the rocks of the cover sequence are mylonitic. Some quartzite layers (most notably in Unit C2) are composed almost entirely of slightly flattened, extremely fine quartz grains, whereas others contain larger, highly flattened grains or contain ribbons of quartz composed of sutured grains with undulatory extinction. In feldspathic lithologies, feldspar grains typically contain brittle fractures and offsets and are bounded by elongate aggregates of microcrystalline quartz. Many samples contain porphyroclasts with asymmetric and symmetric tails and streaks of imbricate mica (e.g., Lister and Snoke, 1984). The presence of ubiquitous, rootless isoclinal folds and

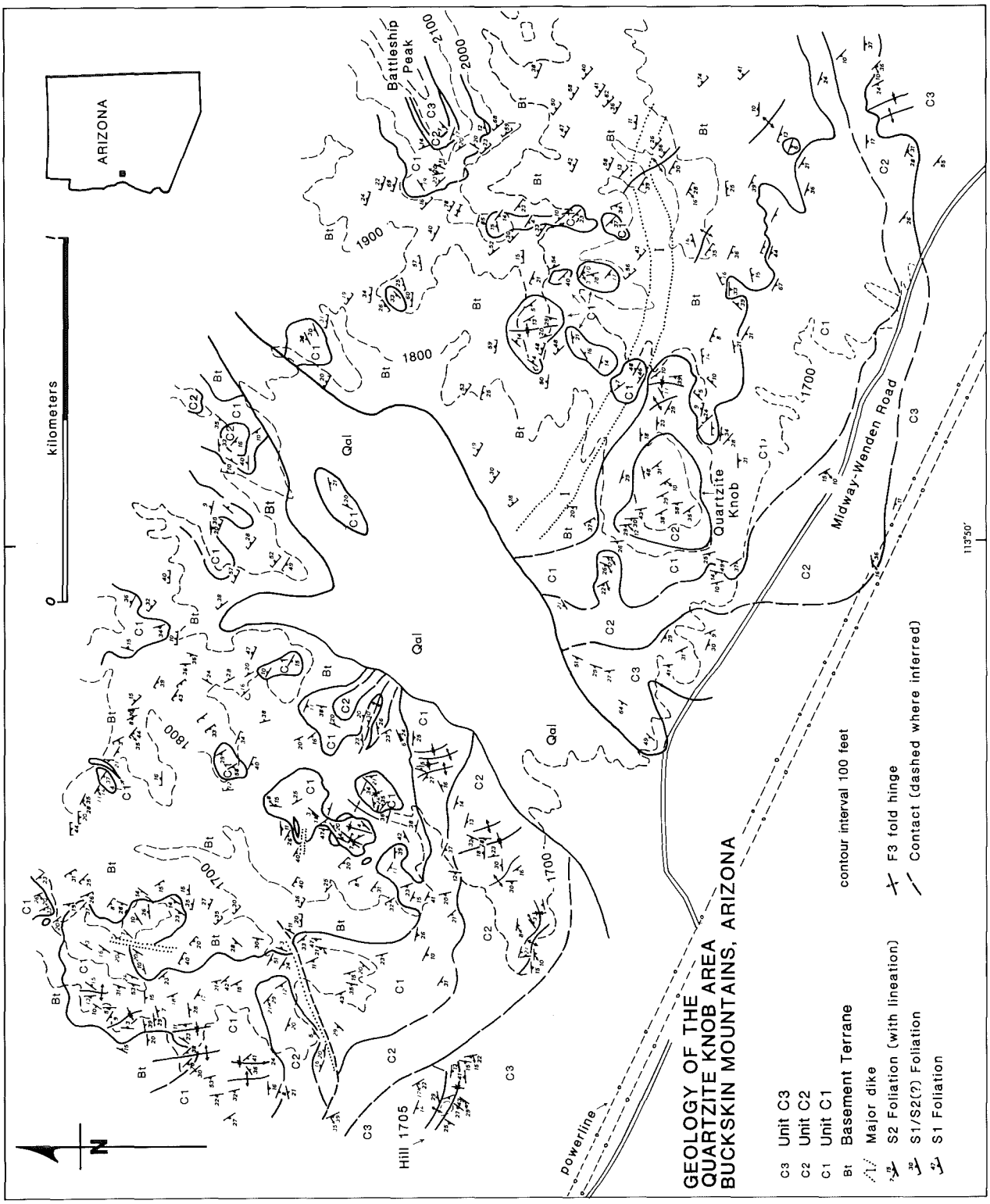

Figure 7. Geologic map of Quartzite knob area near Battleship Peak (modified from Marshak and others, 1987). S1 foliation is the augen-gneiss/banded-gneiss foliation. S2 foliation is the mylonitic foliation in shear zones. Different foliation symbols are used for S1 and S2 foliations. Only Class-C fold hinges are shown. (See text for interpretation of Class-C folds.)

refolded isoclinal folds throughout the cover sequence indicates that original layering was folded, refolded, and sheared. Present compositional banding, though probably inherited from original bedding, no longer represents the original sequence of layers; thus, bedding has been completely transposed into foliation. Overall, microstructural features and structural style suggest that foliation represents development of intense shear strain under dutile conditions and that the entire cover terrane was deformed within a shear zone.

Foliation in the cover terrane (Figs. 7 and 8) generally strikes WNW, dips southwest, and steepens from subhorizontal near the basement-cover contact to 30°SW at Hill 2070 (Fig. 2). At outcrop scale, foliation in the cover terrane varies greatly and is locally quite steep. In some lithologies, foliation surfaces bend around intrafolial folds and boudins (boudins of various sizes are present throughout the study area) and around lenses of apparently less strained rock (e.g., Bell, 1978). Lineation attitudes are fairly constant throughout the map area (Fig. 8), although in some localities, attitudes deviate from the average by as much as 10°.

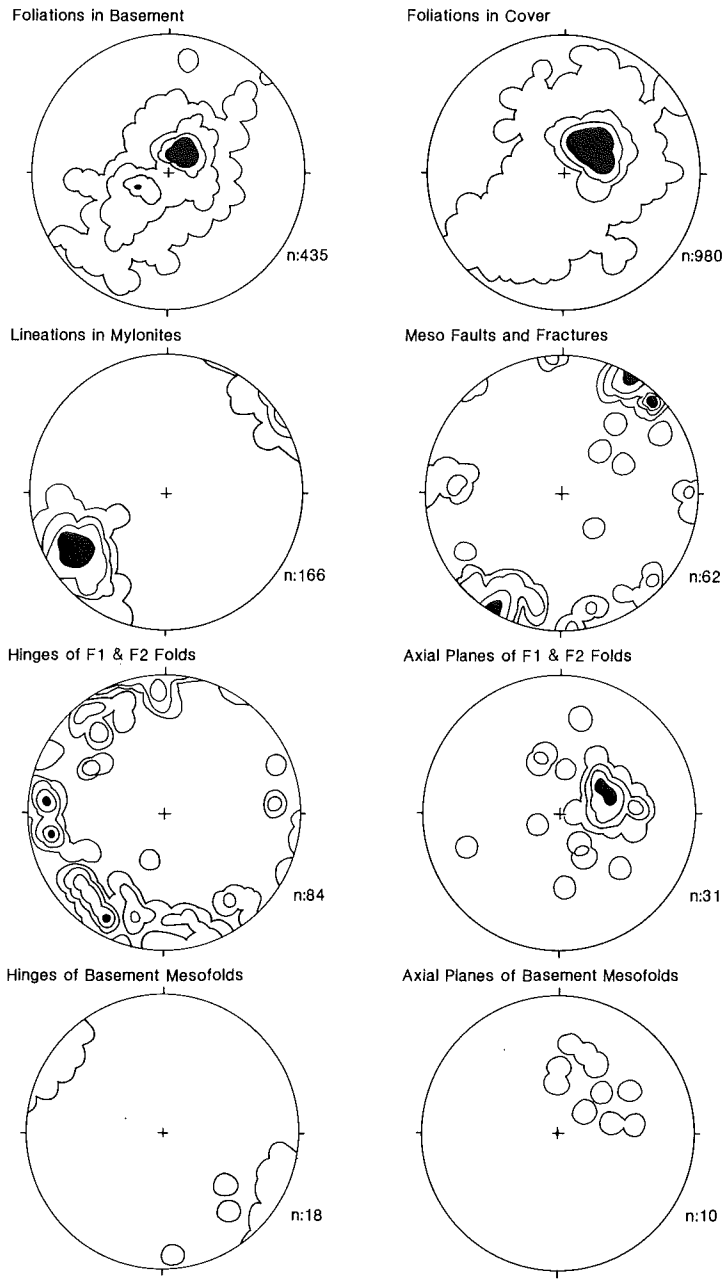

Figure 8. Structural data from Battleship Peak area. The data are contoured and are plotted on lower-hemisphere equal-area projections. The first four contour lines are at 2% intervals. Higher density contours are not shown; they lie within the black-colored area.

Basement Folds

Foliation attitude in the basement terrane is not uniform throughout (Figs. 7 and 8; Marshak and others, 1987). It generally dips steeply to the northeast, but in many places, it has a shallow northeast dip or dips to the southwest. These changes in attitude reflect the presence of large-amplitude folds. The hinge zones of these folds, though difficult to find, are identifiable along some ridge crests, such as Jagged ridge (Fig. 2). Outcrop-scale (1- to 3-m) folds with shallow-dipping axial planes are also present in the basement terrane (Fig. 4a). Most of these folds are north-verging, asymmetric S or Z folds. In the hinge area of outcrop-scale folds, augen-gneiss foliation is strongly crenulated, and on the limbs of the folds, layers are locally thinner and grain size is smaller.

Cover Folds

The cover sequence contains three distinct styles of folds: Class A, Class B, and Class C (Fig. 9). Refolding relationships, described below, indicate that these three styles developed during progressive deformation.

Class-A folds are best displayed by outcrop patterns of thin, dark-weathered siliceous layers in calc-silicate rocks. These folds are rootless and isoclinal and have thick hinges; their axial planes parallel enveloping foliation. Typically, a Class-A fold is defined by a thin (1-cm-thick) siliceous layer bounded by unfolded foliation planes (Fig. 9a). At a few localities, Class-A folds have evolved into sheath folds. The geometry of Class-A folds suggests that they formed in response to intense shear of a foliated sequence under ductile conditions.

Class-B folds (Fig. 4b) are inclined to recumbent,

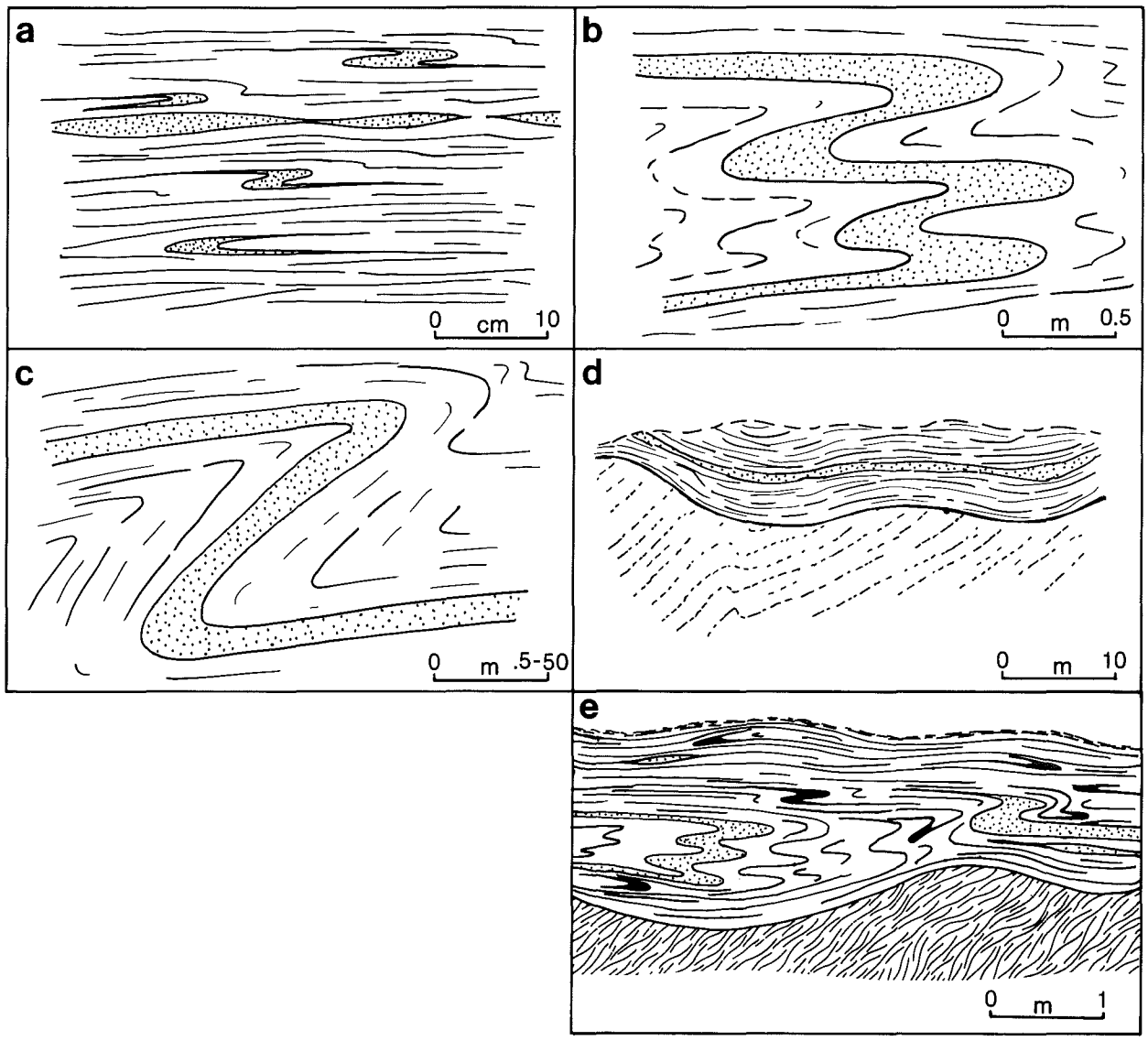

Figure 9. Schematic diagram indicating basic fold styles in study area. The stippled and blackened areas indicate marker layers. (a) Class-A folds; (b) Class-B recumbent fold; (c) Class-B inclined fold; (d) Class-C fold (heavy line is basement-cover contact; dashed lines indicate basement foliation); (e) Outcrop sketch showing relationship among different types of folds (heavy line is basement-cover contact).

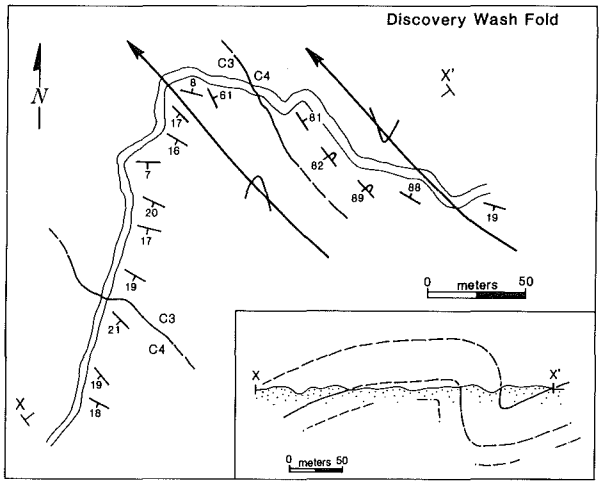

Figure 10. Map and section of Discovery wash fold, 1 km northwest of South ridge. The attitude symbols indicate the orientation of mylonitic foliation in the cover terrane. This fold is the largest example of a Class-B inclined fold in the map area.

affect 10-cm- to 10-m-thick sequences of layers, and refold Class-A folds (there is a gradation between Class-A and Class-B folds). The folds range in amplitude from 0.5 to 50 m. Most are mesoscopic, with amplitudes of 0.5 to 2 m, but in the southeast corner of the map area, such as in Discovery wash, Class-B folds with amplitudes as large as 50 m are present (Fig. 10). Hinge zones of these folds are complex because several second-order folds may be present within the hinge area (Fig. 9b). Layers in hinge zones are thick, but usually not as thick as in Class-A folds. The geometry of Class-B folds suggests that they formed in response to shear of a foliated sequence under less ductile conditions than had prevailed during development of Class-A folds.

Class-C folds (Fig. 4i) are open and upright and have amplitudes of 1 to 4 m and wavelengths of 5 to 50 m. Fold plunges vary in angle but are consistently shallow (Figs. 9c, d). The folds lack symmetry and their hinge traces meander. Class-C folds are responsible for the wide range of local foliation attitudes in the map area (Figs. 7 and 8; Marshak and others, 1987). We suggest that foliation planes in cover-terrane rocks roughly track shear trajectories and that the geometry of Class-C folds reflects nonlaminar shear and a nonuniform distribution of shear strain. It appears that during deformation all cover rocks were sheared, although wavy and anastomosing highly sheared zones bound lenses of less sheared rock (e.g., Bell, 1978); the less sheared pods may preserve earlier fabrics. If this hypothesis is correct, Class-C folds do not represent postfoliation buckling or flexure, but are coeval with foliation and represent the pattern of foliation development. This hypothesis explains the lack of symmetry characteristic of flexural folds, the absence of slip lineations on the surfaces of competent layers, and the uniform orientation of basement-terrane foliation below opposite limbs of folds.

Two folds that do not fit into the above categories are present in the map area. The first fold is the Ives Peak arch, which plunges to the southwest and is responsible for the general southwest dip of the cover-terrane units (Fig. 2). The Ives Peak arch is also defined by the contrast in attitude of the Buckskin detachment fault between Clara Peak (northwest of the map area) and Redrock hill (Spencer and Reynolds, this vol.). The second fold is an outcrop-scale kink band that is present in a uniformly layered interval of quartzite in Unit C2 (Fig. 4h). The kink-band boundaries are oriented 320°, 66°SW, and the vergence of the band is to the southwest. Kink bands were also recognized in thin sections of the quartzite.

Faults

A number of faults are present within the study area. The Buckskin detachment fault is visible at Redrock hill (Fig. 2; Spencer and Reynolds, this vol.). Two shallow, southwest-dipping normal faults are on the crest of Battleship ridge (Marshak and others, 1987) and have displacements of approximately 2 to 3 m. Movement on these faults resulted in the thinning of adjacent marble layers; down-dip slip lineations are visible on the fault surface. Moderately to steeply dipping, cross-foliation, ductile to brittle normal faults, which locally displace the basement-cover contact, are present at many localities. The probable extension of the Mineral Wash fault (Spencer and Reynolds, this vol.) is manifested by the difference in elevation of the basement-cover contact east and west of the swath of alluvium west of Flatop hill (Fig. 2). Evidence of thrust-fault imbrication of basement and cover and of units within the cover has been found in the nearby Granite Wash Mountains and in the upper plate of the Buckskin-Rawhide detachment fault (Reynolds and Spencer, this vol.). Within the study area, however, only equivocal exposures directly above the basement-cover contact, which contain basementlike mylonite interlayered with marble, suggest thrust-fault imbrication. The position of Unit C6 may indicate older over younger faulting. (See section titled "Interpretation of Protoliths.")

Fractures

Nonsystematic fractures are numerous throughout the study area. Abundant fracturing, local brecciation, and minor hydrothermal alteration occurred in a few localities at higher elevations in the cover sequence. Locally, one or two systematic fracture sets are present (Fig. 8); the most common systematic fracture orientation is vertical with a 300° trend. Dip-slip displacement (hanging wall down to the southwest) is evident on some fractures in measurable offsets (1 cm) and by the presence of chlorite-fiber slip lineations (Fig. 4j).

TRANSPORT DIRECTION DURING COVER-FOLIATION DEVELOPMENT

The shear associated with the most prominent mylonitic fabrics and folds in the cover terrane can be

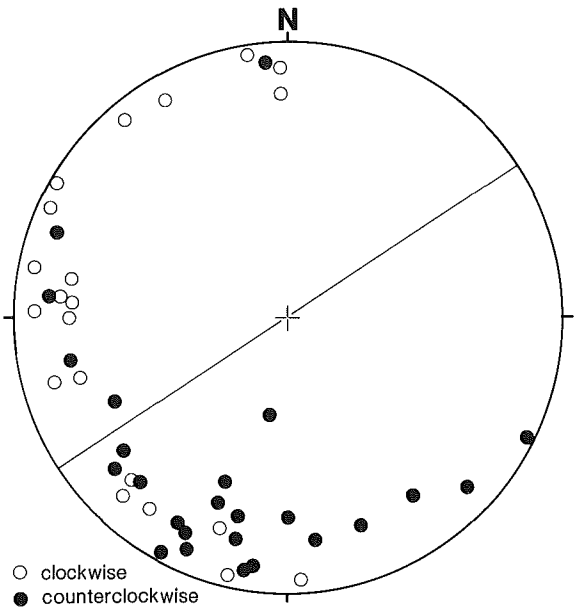

Figure 11. Hansen slip-line calculation of transport direction indicating top-to-the-northeast shear. The points represent the plunge and bearing of mesoscopic Class-A and Class-B fold hinges in the cover terrane, as viewed looking down plunge. Only folds with unambiguous vergence have been plotted. The northeast-southwest-trending line indicates the average mineral-lineation direction in the cover terrane.

interpreted from two types of data: Hanson slip-line calculation and point concentration of mineral-lineation trends. Results of a Hanson slip-line calculation, using asymmetric Class-B mesoscopic folds in Units C1 and C3 (Fig. 11), suggest that structurally higher layers moved toward the northeast with respect to structurally lower layers. The point concentration of mineral-lineation trends (Fig. 8) separates the field of predominantly clockwise folds from that of predominantly counterclockwise folds, which suggests that the lineation represents the transport vector. Not all folds are consistent with this sense of transport; locally, asymmetric folds and kink bands suggest down-to-the-southwest displacement of the hanging wall. In some cases, these folds may be associated with late-stage antithetic normal faults that presently dip toward the southwest (e.g., the faults along Battleship ridge) or they may be relicts of earlier shear episodes.

Microstructures in mylonitic cover-terrane lithologies were not abundant in thin sections and many were ambiguous (e.g., symmetrical tails on porphyroclasts; Simpson and Schmid, 1983). The few unambiguous indicators generally confirmed the hypothesis that the hanging wall moved to the northeast during the main phase of mylonite development. Indicators from the basement-terrane augen gneiss were not used to evaluate shear sense associated with the dominant cover-terrane fabric because the augen-gneiss foliation probably developed during a different deformation event.

BASEMENT-COVER CONTACT RELATIONS

The contact between basement and cover terranes may have been a depositional contact, but subsequent deformation has removed all traces of original depositional relationships. The contact is interpreted as tectonic; therefore, the rocks presently juxtaposed across the contact were not juxtaposed when the cover sequence was deposited. Two characteristics of the basement-cover contact are evident from the map pattern (Fig. 2; Marshak and others, 1987):

(1) The contact is shallow dipping along the northeast edge of the outcrop belt. The map trace of the contact, therefore, is irregular and numerous outliers of cover rock are completely surrounded by basement. The contact steepens toward the southwest; it dips approximately 30°SW at Hill 2070.

(2) The elevation of the contact varies (Fig. 12). The irregularities are interpreted to be the result of three types of structures (Fig. 13): brittle or ductile cross-foliation faults that offset basement blocks, large-scale boudinage of the basement, and variation in trajectory of shear zones that define Class-C folds.

As noted earlier, definable shear zones are present within the basement terrane. At many localities, however, a shear zone is not present in the basement rocks below the contact. In these areas, termed discordant contacts (Fig. 14a), the basement-cover contact truncates the original augen-gneiss foliation; no mylonitic zone is present below the contact. Locally, the basement foliation is vertical and the contact is horizontal. At many localities, however, a shear zone lies directly beneath the basement-cover contact and basement rocks are strongly sheared adjacent to the contact. In these areas, termed concordant contacts (Fig. 14b), the foliation of basement rocks has been rotated parallel to the contact.

CONTACT WITH TERTIARY STRATA

Tertiary volcanic and sedimentary rocks are exposed northwest of the map area (e.g., at Clara Peak; Spencer

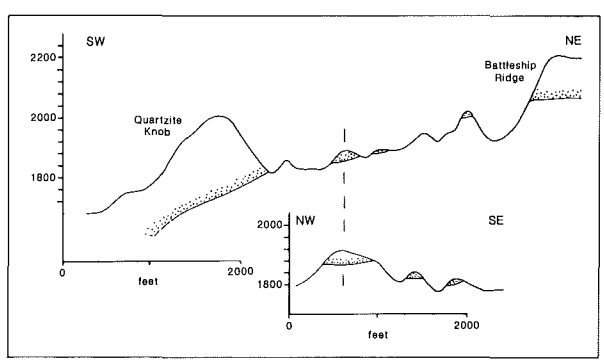

Figure 12. Two cross sections of basement-cover contact in vicinity of Quartzite knob, showing variation in elevation of contact. The two sections are orthogonal to one another and intersect on the hill indicated by the dashed line. The single heavy line is the ground surface; the stippled line is the basement-cover contact.

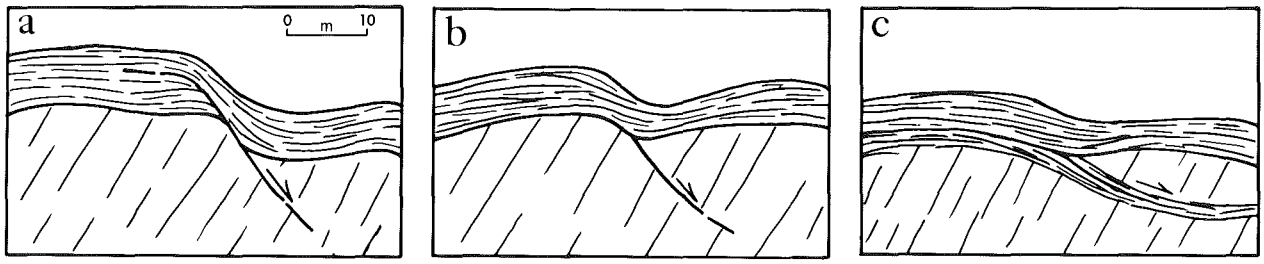

Figure 13. Schematic diagram of three possible origins of variation in elevation of basement-cover contact. (a) Offset on a cross-foliation fault that cuts both basement and cover; (b) Offset on a fault in the basement, perhaps associated with boudinage of the basement; (c) Intersection of a basement shear zone with the basement-cover contact.

and Reynolds, this vol.) and on its eastern edge (e.g., at Redrock hill). At the base of Redrock hill, Tertiary strata are in contact with basement gneiss along the Buckskin detachment fault. Foliation of the augen gneiss is folded within 200 m of the contact and is crenulated in the core of these folds. As one approaches the fault contact, the attitude of foliation varies greatly and is rotated roughly parallel to the contact, and the augens appear to be smaller. Adjacent to the contact, basement rock is brecciated and bleached. The breccia is cut by hematite-rich cataclastic shear zones. At the base of the Tertiary sequence, slip surfaces (030°, 20°SE) are well exposed in a mine adit. The ceiling of the adit is a slip surface marked by 050° slip lineations (Spencer and Reynolds, this vol.). Below this surface, at the entrance to the adit, is another slip plane with dip-slip (plunging 22°, 142°) lineations; this set of lineations is at a high angle to the penetrative lineation in the cover terrane. The presence of dip-slip lineations indicates that not all movement at the basement-Tertiary contact was parallel to the transport vector that is associated with the development of the LS tectonites in the cover terrane.

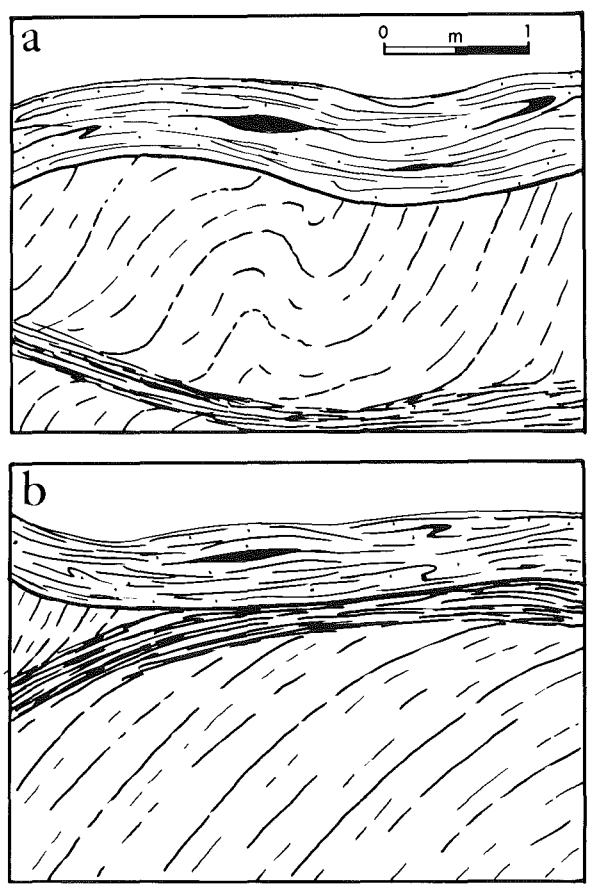

Figure 14. Schematic diagram of the two types of basement-cover contact. (a) Discordant contact (a basement shear zone is not present directly below the contact); (b) Concordant contact (a basement shear zone intersects the contact, so basement rock is mylonitic directly below the contact).

Breccia and cataclasite, probably associated with the Buckskin detachment fault, are exposed at the top of Battleship Peak at the north end of Battleship ridge. About 3 m below the top of Battleship Peak, Unit C3 is in contact along a sharp subhorizontal surface with 0.2 m of green microbreccia, overlain by 0.2 m of coarser breccia (Fig. 4k), in turn, overlain by highly indurated breccias composed of clasts of breccia fragments. The identity of the indurated breccias is enigmatic. In thin section, they are extremely fine grained and appear to be chert sedimentary breccias. The outcrop appearance, however, is very similar to that of an ultra-cataclasite that forms the upper surface of the lower plate beneath Tertiary detachment faults (Appendix 1 in Spencer and Welty, this vol.). Lenses of gray limestone are interlayered with the indurated polystage breccia. In thin section, the limestone resembles caliche; however, the fabric is possibly the result of hydrothermal alteration of sedimentary limestone.

SUMMARY AND DISCUSSION

Interpretation of Protoliths

Two lithologic terranes are distinguishable in the map area: basement terrane composed of augen gneiss, banded gneiss, and variably deformed intrusions; and cover terrane composed of variably mylonitic, metasedimentary rocks interlayered with mylonitic intrusive rocks. Lithologic affinity between the basement gneiss and radiometrically dated gneiss of the southern Cordil-

lera suggests that the basement gneiss is Precambrian (1.4 to 1.7 Ga). Regional relations suggest that the unmetamorphosed intrusions in the basement are probably Mesozoic or Tertiary.

Protoliths of mylonitic rocks in the cover terrane are identified in Table 1. Because of their deformation state, correlation of cover units with Phanerozoic units in Arizona and southeastern California is difficult. Nevertheless, the cover sequence includes several lithologies that are compositionally similar to lithologies of Paleozoic strata (Stone and others, 1983) and Mesozoic strata (Harding and Coney, 1985). The carbonate rocks and pure quartzites were probably derived from Paleozoic protoliths, whereas the quartz-epidote-feldspar schist was derived from a Mesozoic protolith. Some cover lithologies were probably derived from intrusions.

Unit C5, which is predominantly quartz-epidote-feldspar schist, was probably derived from a Mesozoic protolith, whereas Unit C6 was probably derived from a Paleozoic protolith. The presence of Unit C6 above Unit C5 suggests that either the units are separated by a fault or Unit C5 is in the core of a fold. If this fault is related to faults of the Granite Wash Mountains, it would reflect hanging-wall-to-the-southwest movement. The existence of a major fault or fold hinge is suggested by an apparent discordance between Unit-C6 foliation and Unit-C5 foliation just to the northeast of Hill 2070 at the southeast corner of the map (Fig. 15; Marshak and others, 1987).

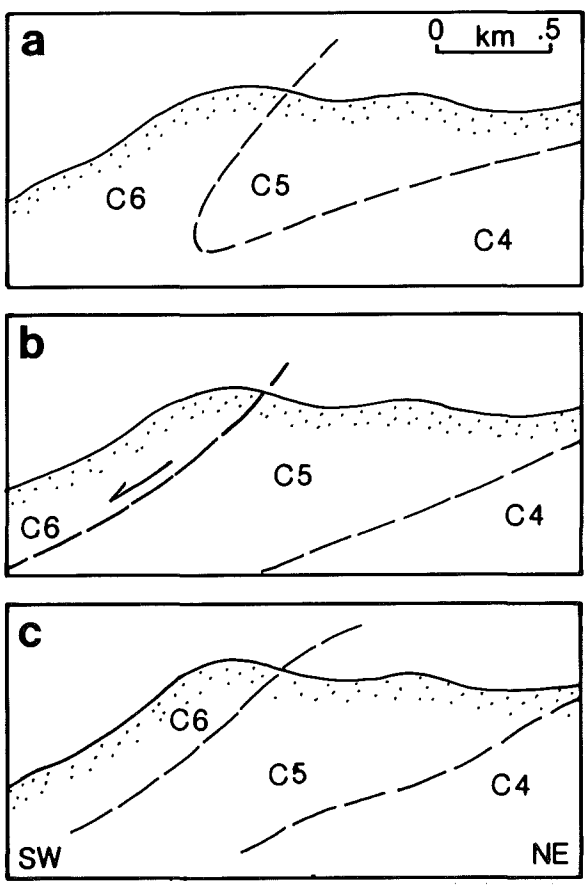

Figure 15. Possible interpretations of structure between South ridge and Hill 2070 to explain position of Unit C6 (possible Paleozoic protolith) above Unit C5 (possible Mesozoic protolith). (a) Large recumbent fold (i.e., Unit C6 = Unit C4); (b) Major thrust fault, hanging wall to southwest; (c) No major structure (i.e., Unit C6 is Mesozoic or Unit C5 is Paleozoic or age calls are altogether wrong).

Interpretation of Structural Data

The contact between the basement and cover terranes is irregular: at some localities, basement foliation is truncated at the contact, but at others the gneiss is mylonitized and foliation merges with the contact. The cover terrane exhibits a penetrative mylonitic foliation and lineation, which suggests that the entire sequence formed part of a thick shear zone. Mylonitic foliation of the basement terrane, however, is confined to relatively narrow shear zones. Variation in the attitude of cover-terrane foliation defines asymmetric noncylindrical folds. It appears that the variation in foliation attitude and some of the irregularity of the basement-cover contact are manifestations of the geometry of the shear zone in the area. (Some of the irregularity of the contact may represent cross-foliation faults or boudinage.) The ductile cover terrane is sheared throughout the study area. Shear trajectories are not laminar and shear strain is not homogeneously distributed; rather, wavy bands of higher shear strain anastomose throughout the cover terrane. Mylonitization of the basement was restricted to relatively narrow shear zones, indicating that in the less ductile basement lithologies, strain softening was confined to narrow bands. The shear zones in the basement are also wavy. Pods between basement shear zones preserve earlier fabrics. Basement foliation is concordant to the basement-cover contact where the contact is within a shear zone and is discordant to the contact where shearing is restricted to cover-terrane rocks (Fig. 16).

The cover sequence, although mylonitized, can be subdivided into mappable units that define outcrop bands trending WNW-ESE. The thickness and lithologic character of cover units vary along strike; marker lithologies delineate unit boundaries. Thickness variations probably reflect variations in the degree of attenuation of the cover terrane. More rigid units, such as Unit C2, are characterized by boudinage, which is common in outcrops (Fig. 4f). Because of shearing and attenuation, the sequence of units is not constant. For example, at the western edge of the map area, Unit C4 is absent, whereas south of South ridge (Fig. 2), Unit C4 rests directly on basement. At Redrock hill, no cover terrane is present and Tertiary strata rest directly on basement. The sequence of lithologies in the cover terrane probably does not reflect original stratigraphy. Transposition has obliterated evidence of structures (faults or isoclinal folds) that could have caused imbrication of units. In addition, intrusive bodies that once crosscut the cover terrane (and still crosscut the basement terrane) were transposed into the plane of foliation.

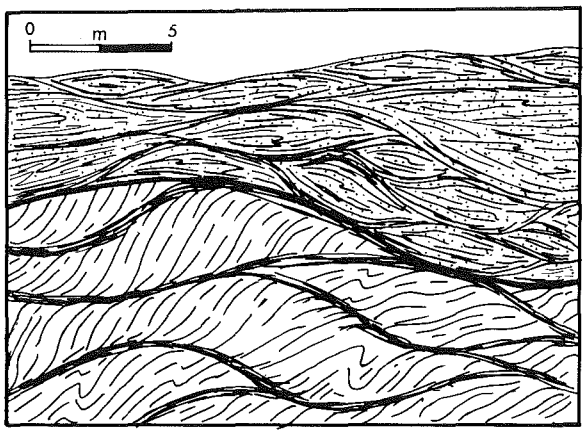

Figure 16. Structural model of distribution of shear in cover and basement terranes. Light stippled unit is cover terrane, line patterns indicate foliation attitudes, and spacing of lines indicates amount of shear strain. In this model, Class-C folds are a consequence of variation in shear trajectories (shear was not laminar), shear strains in the cover terrane are not homogeneous but affected the entire terrane, shear in the basement terrane is concentrated in discrete anastomosing zones, and basement shear zones do not intersect the basement-cover contact at all localities.

Mesoscopic folding is widespread in both cover and basement terranes. The cover terrane contains small, intrafolial, rootless, recumbent isoclinal folds (Class A) and larger recumbent to inclined asymmetric folds (Class B) that contain up to 50-m sequences of rock. Refolding relationships indicate that Class-B folds formed after Class-A folds. Fold style (specifically the degree of hinge thickening and limb attenuation) suggests that Class-B folds formed under less ductile conditions than Class-A folds. Folds in the basement resemble Class-B cover folds. The hinge areas of basement folds commonly contain an axial planar crenulation superimposed on the gneissic layering. A Hansen slip-line calculation indicates that the asymmetric cover folds were formed in a shear couple, with structurally higher layers moving to the northeast with respect to structurally lower layers. There are, however, many exceptions to this pattern; some may be associated with late southwest-dipping normal faults. Some cover foliation may be preserved from earlier hanging-wall-to-the-southwest shear.

The average foliation strike in the basement terrane is subparallel to the average strike of unit contacts in the cover sequence, but the dip of basement foliation is generally steeper. Much of the basement fabric is older than cover fabric; the basement-cover contact crosscuts basement foliation at many localities, and mylonitic shear zones in the basement that parallel cover foliation cut across basement foliation. The parallelism between the strike of cover foliation and the strike of basement foliation (and between basement fold axes and Class-B cover fold axes) could indicate that both fabrics formed during the same progressive deformation. In this model, basement foliation was developed first and was folded and cut by younger shear zones. An alternative model suggests that basement foliation is unrelated to the younger cover foliation, but was rotated into strike parallelism with it during the latter's development.

Mesoscopic faults and fractures are abundant in the study area. They generally strike perpendicular to mineral lineations, dip southward, and have a normal sense of displacement.

Sequence of Deformation

The geometric relationships among many structures in the area suggest a kinematic relationship; most structures in the cover sequence are coaxial and formed during progressive stages of a single deformation event. Refolding and crosscutting relationships suggest that more ductile structures developed first. The sequence of deformation is compatible with regional progressive shear under conditions of changing temperature, pressure, and/or strain rate. As strain continued, temperatures decreased and the rock became more brittle as it cooled. Four stages of deformation can be defined in the cover sequence.

(1) The earliest recognizable deformation event produced the mylonitic foliation. Evidence of pre-foliation deformation events was destroyed by the extreme strain that accompanied foliation development. Thin shear zones in the basement terrane and foliation in the cover terrane are coeval; the shear zones and foliation are roughly parallel and merge locally along the basement-cover contact. During mylonitization, bedding and crosscutting intrusions were transposed into the plane of mylonitic foliation, and Class-A, intrafolial, rootless, recumbent isoclinal folds developed. Shear zones that developed during this time are not planar; curves in the trajectories account for most of the non-planar foliation that defines Class-C folds. Textures of some igneous bodies are intermediate between those of undeformed dikes and completely mylonitized dikes, which suggests that intrusive activity occurred during shearing.

(2) During continued deformation, laterally variable attenuation resulted in lateral changes in the thickness of cover units. Displacement of the basement-cover contact developed because of displacement on discrete shear zones or boudinage of the relatively rigid basement. Continued shear created Class-B folds, which refolded the first-stage Class-A folds. Older Class-B folds are probably recumbent and younger folds, frozen in an intermediate stage of development, are probably inclined. Class-B folds are also found in the basement terrane and are associated with local development of axial-planar crenulation cleavage. This phase of deformation was accompanied by the development of shallow-dipping, ductile normal faults that cut the cover-sequence foliation but were associated with ductile thinning of marbles.

(3) Once mylonitic foliation developed and ductility decreased, kink bands and possibly some Class-C open folds (i.e., folds that formed by flexure of preexisting layering) developed. In addition, cross-foliation brittle-ductile faults developed, which locally displaced the basement-cover contact.

(4) The final structures to form were systematic fracture sets and breccia zones. The nature and orientation of these structures suggest that they formed during the same kinematic regime as the earlier ductile deformation, but after the rocks had cooled through the brittle-ductile transition.

Mesozoic Contraction or Tertiary Extension?

The Battleship Peak area was mapped to determine whether deformation in the area occurred during regional Mesozoic contraction or regional Tertiary extension. The following facts suggest that the dominant cover fabric and the narrow shear zones in the basement formed during the Tertiary event:

(1) Lineation in the map area is parallel to known Tertiary lineations (though it is also parallel to Mesozoic D2 structures in the Granite Wash Mountains; Laubach, 1986).

(2) Shear sense, indicated by many structures in the cover rocks, is hanging-wall-to-the-northeast, unlike shear sense that characterizes Mesozoic deformation in the Granite Wash Mountains (Reynolds and others, 1986b).

(3) Evidence for decreasing temperatures during evolution of the shear zone is compatible with unroofing and removal of the hanging wall.

(4) A detachment fault (Buckskin) that is similar to those above Tertiary mylonitic zones in adjacent ranges is exposed above the mylonite near two localities within the study area.

Within the context of the regionally recognized Tertiary deformation event, the Battleship Peak area represents a thick, internally complex shear zone associated with crustal extension (Wernicke, 1981). Shear strain is concentrated in the cover terrane and is evident in the basement terrane in discrete, wavy shear zones. Tertiary deformation largely overprints earlier structures; however, a relict, Mesozoic southwest-directed thrust might be present on Hill 2070. The entire map area, except for a portion of Redrock hill, lies in the lower plate below the Buckskin detachment fault (Rehrig and Reynolds, 1980). Within the map area, the kinematic indicators suggest top-to-the-northeast movement during formation of the dominant mylonitic foliation. At the time of initial formation, this shear zone dipped to the northeast (i.e., had normal-fault geometry). According to one model (Spencer, 1984b), the present southwest dip of the shear zone, indicated by the general southwest dip of foliations, developed during late stages of movement in response to tectonic denudation. The southwest-dipping normal faults in the area are probably antithetic faults that developed during the latter stages of deformation. Basement augen-gneiss fabric is older than the dominant cover fabric. Basement foliation is probably a relict of Mesozoic shear; although it is coaxial with Tertiary shear zones, it is clearly cut by them. Some basement fabric may be Precambrian in age.

CONCLUSION

Several conclusions can be drawn from this study.

(1) The map pattern of the southern Buckskin Mountains on the State Map distinguishes a basement terrane of Precambrian gneiss from a cover terrane of mylonitized metasedimentary rocks. The metasedimentary rocks were probably derived from both Paleozoic and Mesozoic protoliths, not just Mesozoic protoliths, as indicated on the State Map. The contact between these terranes is more irregular than the State Map indicates.

(2) Structures in the study area are interpreted to have formed during deformation in an internally complex shear zone that may be related to shearing along the downdip projection of the Buckskin detachment fault. Earlier (possibly Mesozoic) fabrics are preserved in the basement terrane. A Mesozoic hanging-wall-to-the-southwest thrust may be preserved at Hill 2070.

(3) The internal geometry of the Tertiary shear zone is complex, with variable foliation attitudes, an irregular basement-cover contact, and discrete shear zones in the basement. Shear trajectories are not laminar. The shear zone, therefore, can be envisioned as a meshwork of anastomosing subzones.

(4) Foliation in the basement and cover is concordant where Tertiary basement shear zones merge with the basement-cover contact; elsewhere, it is discordant.

(5) Several deformation stages were recognized in the cover sequence. Early deformation included development of mylonitic foliation and intrafolial, rootless, recumbent isoclinal folds. Intermediate-stage deformation involved development of asymmetric recumbent to inclined folds. Late deformation included development of cross-foliation ductile faults, kink folds, and brittle fractures and faults. The sequence of deformation events and resultant structures suggests that progressive shear occurred under decreasing temperatures.

ACKNOWLEDGMENTS

We thank J.E. Spencer and S.J. Reynolds for their suggestions about the interpretation of the Battleship Peak area, especially the anastomosing character of shear zones and the identity of cover-terrane units. They also reviewed this manuscript. We also thank S. Bhagat for assistance in the field and D.E. Anderson and R.L. Langenheim for helpful comments. R.S. Marshak's initial reconnaissance of the Buckskin Mountains during 1978 was supported by the Arizona Bureau of Geology and Mineral Technology, of which the Arizona Geological Survey (AZGS) was a part. We thank H.W. Peirce of the AZGS for his encouragement during that time.

Pre-Tertiary rocks and structures in the upper plate of the Buckskin detachment fault, west-central Arizona

STEPHEN J. REYNOLDS
JON E. SPENCER
Arizona Geological Survey, 845 N. Park Ave., #100, Tucson, Arizona 85719

ABSTRACT

The Buckskin detachment fault, a gently dipping normal fault exposed throughout much of the Buckskin Mountains of west-central Arizona, separates a lower plate of mylonitic crystalline rocks from an upper plate of various Tertiary and pre-Tertiary lithologies. Pre-Tertiary upper-plate rocks include Proterozoic crystalline rocks, Paleozoic and Mesozoic supracrustal rocks, and Mesozoic intrusions. These rocks contain a complex assemblage of Mesozoic structures, including thrust faults, large- and small-scale folds, and several generations of cleavage.

Upper-plate Proterozoic metamorphic rocks are most widespread in the western part of the range, where they overlie Paleozoic and Mesozoic supracrustal rocks along a southwest- to northwest-dipping, mylonitic thrust zone. Paleozoic sections beneath the thrust and elsewhere in the mountain range have been ductilely attenuated during Mesozoic thrusting, but represent an originally thin, cratonic section of Devonian Martin Formation, Mississippian Redwall Limestone, Pennsylvanian-Permian Supai Group, Permian Coconino Sandstone, and Permian Kaibab Formation. A thin sequence of Permian Hermit Shale is present in some Paleozoic sections, but is absent in others. Cambrian rocks are absent in all but one Paleozoic section because of thrust-related, structural omission.

The Paleozoic rocks are in both stratigraphic and structural contact with a regionally important sequence of Mesozoic metasedimentary and volcanic rocks. The oldest unit is the Buckskin Formation (new name), which consists primarily of variably calcareous, quartzose clastic rocks and phyllite, with less abundant evaporitic rocks, carbonate rocks, and conglomerate. The Buckskin Formation is correlated with the Triassic Moenkopi Formation of the Colorado Plateau. It is unconformably overlain by conglomerate, quartzite, and immature clastic rocks of the Triassic(?) to Middle(?) Jurassic Vampire Formation (new name). The Vampire Formation reflects an important episode of Early Mesozoic uplift, during which Proterozoic rocks were exposed at the surface. The Vampire Formation is successively overlain by the 160 Ma Planet Volcanics (new name) and a schist unit of uncertain regional correlation.

After deposition of the volcanic rocks and overlying schist unit, the rocks were subjected to several major episodes of Mesozoic deformation. The earliest event was an episode of thrusting that structurally interleaved and attenuated Proterozoic, Paleozoic, and Mesozoic rocks. This episode of thrusting, which was probably southeast directed, formed a penetrative fabric at a low angle to bedding and was localized along structurally weak stratigraphic horizons, including Cambrian shale units, the Hermit Shale, and evaporitic rocks in the lower Buckskin Formation. A ramp-and-flat style of thrusting, with a basal decollement within the Cambrian sequence, explains the structural relations, such as the general absence of Cambrian rocks at the base of Paleozoic thrust slices. During and after this episode of thrusting, the attenuated sections, thrusts, and related fabrics were folded about northeast-trending axes during a major episode of southeast-vergent folding.

A second episode of thrusting, this time in a northeast-southwest direction, emplaced Proterozoic crystalline rocks discordantly over the upturned thrusts, attenuated sections, and southeast-vergent folds. This thrusting produced mylonitic fabrics in crystalline rocks along the thrusts and complex folds within some Paleozoic-Mesozoic rocks. Thrusting was followed by formation of several northwest-trending folds and northwest-, west-, and southwest-trending crenulations and crenulation cleavage. The sequence of deformations is comparable with those documented in the Maria fold-and-thrust belt to the south.

At the end of Mesozoic tectonism, Proterozoic crystalline rocks structurally overlay complexly folded and imbricated Paleozoic and Mesozoic rocks in much of the area. The Proterozoic rocks dominated the middle Tertiary landscape, providing few clues that, at a shallow depth, they overlay Paleozoic and Mesozoic rocks along a major thrust. Middle Tertiary detachment faulting transported the rocks 40 to 50 km to the northeast relative to the lower plate, away from their original site within the Maria fold-and-thrust belt. Detachment faulting was accompanied by the rotation of normal-fault-bounded blocks, thereby helping to exhume the rocks and structures beneath the thrust.

INTRODUCTION

The Buckskin Mountains of west-central Arizona are structurally dominated by the Buckskin detachment fault,

in Spencer, J.E., and Reynolds, S.J., eds., 1989, Geology and mineral resources of the Buckskin and Rawhide Mountains, west-central Arizona: Arizona Geological Survey Bulletin 198, p. 67-102.

a regional low-angle normal fault that is discontinuously exposed over much of the Buckskin Mountains (Spencer and Reynolds, this vol.). The detachment fault has several tens of kilometers of top-to-the-northeast displacement and separates two very different lithologic assemblages. The footwall of the fault is mostly composed of Proterozoic crystalline rocks and Mesozoic and Cenozoic intrusive rocks that are variably overprinted by gently dipping Tertiary mylonitic fabric. Older (premylonitic) metamorphic and structural fabrics are locally preserved in less mylonitic areas.

The upper plate of the detachment fault contains a different and more varied assemblage of pre-Tertiary rock types, including Proterozoic crystalline rocks, variably metamorphosed Paleozoic and Mesozoic supracrustal rocks, and small Mesozoic intrusions. These rocks lack the Tertiary mylonitic fabric, but contain a diverse suite of Mesozoic structures, including mylonitic thrust faults and duplexes, large- and small-scale folds, and several generations of cleavage.

In order to characterize the geology and mineral deposits of the Buckskin Mountains, we mapped almost all exposures of upper-plate rocks at scales of 1:24,000 or 1:12,000. Although our study was addressed primarily at Tertiary rocks and structures (Spencer and Reynolds, this vol.), we made major new discoveries while mapping pre-Tertiary upper-plate rocks and ultimately directed much effort toward unraveling the pre-Tertiary stratigraphy and structure of the area. In this article, we summarize the stratigraphy and structure of pre-Tertiary rocks; present a series of geologic maps, cross sections, and narratives for key areas; and discuss regional implications.

PREVIOUS STUDIES

Previous studies of pre-Tertiary rocks in the Buckskin Mountains were hampered by the lack of a coherent regional structural and stratigraphic framework, which has emerged only within the last decade. Blanchard (1913) produced a generalized geologic map of the western part of the range and described the major rock types and mineralization. Darton (1925) recognized Paleozoic fossils in the Billy Mack area of the western Buckskin Mountains. Zambrano (1965) and Fernandez (1965) studied general geology and mineral deposits in the Cienega and Pride areas, respectively. The entire Buckskin and Rawhide Mountains were mapped in reconnaissance by Wilson (1960; Wilson and others, 1969), who recognized that most Paleozoic and Mesozoic rocks were in low-angle fault contact with underlying crystalline rocks. Wilson also recognized that Proterozoic crystalline rocks in the western Buckskin Mountains were in thrust-fault contact over Paleozoic and Mesozoic rocks to the southeast. Shackelford (1976b; Plate 1) mapped the Rawhide Mountains and recognized (1) the normal-fault character of the regional detachment fault, (2) Cambrian units within the deformed Paleozoic sequence, and (3) that some schist was metavolcanic in origin. Frost (1983, and written commun., 1987) mapped and described Paleozoic and Mesozoic rocks in the westernmost Buckskin Mountains as part of a study that emphasized Tertiary structure and stratigraphy. Because the regional Paleozoic and Mesozoic stratigraphic framework was still not yet worked out, Shackelford and Frost were generally unable to assign their lithologic map units to specific Paleozoic and Mesozoic formations. Subsequently, some important aspects of the Mesozoic stratigraphy of the Planet and Mineral Hill area were recognized by N. Lehman (1985, written commun.). Osborne (1981) and Woodward (1981) mapped and described the Squaw Peak and Swansea areas, concentrating on Tertiary structure and stratigraphy.

Our geologic studies in the Buckskin Mountains have benefited from insights of these previous workers and from recent advances in the Mesozoic stratigraphic and structural framework of the region. We have released preliminary versions of our mapping for some parts of the Buckskin Mountains (Spencer and others, 1986; Spencer and Reynolds, 1986a, 1987) and have incorporated our findings in regional stratigraphic and structural syntheses (Reynolds and others, 1987, 1989; Spencer and Reynolds, 1988). Additional discussion of our results is contained elsewhere in this volume.

REGIONAL SETTING

Rocks in west-central Arizona have savored a complex geologic history that spans approximately 1.8 b.y. The oldest rocks within the region are Proterozoic metamorphic rocks that were deposited, deformed, and metamorphosed between 1.8 and 1.7 Ga. These rocks were intruded by granitoid plutons at about 1.7 Ga and again at 1.4 Ga. The region was uplifted, eroded, and tectonically stabilized before 1.2 Ga.

During Paleozoic time, the region was part of the stable craton of North America and was covered by 1 to 1.5 km of platformal Paleozoic carbonate and clastic rocks. Stable, cratonic conditions continued into the Triassic, when quartzose clastic rocks of the Buckskin Formation were deposited. This stability was interrupted in Late Triassic to Early Jurassic time by a major uplift event that caused at least local erosional removal of the entire Paleozoic section and exposure of the underlying Proterozoic crystalline basement (Reynolds and others, 1989). Uplift was followed by deposition of generally quartzose clastic rocks of the Vampire Formation and by widespread Jurassic silicic volcanism and plutonism at about 160 to 165 Ma (Reynolds and others, 1987; Tosdal and others, 1988; Tosdal, 1988). After volcanism, as much as 7 km of clastic sediments of the Jurassic(?) and Cretaceous McCoy Mountains Formation were deposited in an east-trending basin (Harding and Coney, 1985; Stone and others, 1987).

After deposition of at least the lower part of the McCoy Mountains Formation, the region was widely affected by compressional deformation that formed the Maria fold-and-thrust belt, an east-west-trending zone of mostly Cretaceous large-scale folds and major brittle and ductile thrust faults (Reynolds and others, 1986b). The major folds and thrusts verge southeast, south, and

southwest, but north- and northeast-vergent structures are locally present. Complex overprinting of successive deformations has resulted in exceedingly complex structural geometries, including folded and refolded thrust faults. This deformation was accompanied by widespread metamorphism and largely ended before the emplacement of large Late Cretaceous plutons. The region was subsequently affected by a major episode of early Tertiary uplift and erosion reflected by widespread late Cretaceous and early Tertiary cooling ages on pre-Tertiary rocks of the region (Reynolds and others, 1988).

Renewed tectonism in Late Oligocene to mid-Miocene time was marked by volcanism, plutonism, clastic sedimentation, and a major episode of crustal extension (Spencer and Reynolds, 1988). Crustal extension was largely accommodated by tens of kilometers of normal displacement on regional, gently dipping shear zones, termed detachment zones. Such large-magnitude, normal displacement tectonically exhumed deep-level rocks in the footwalls of detachment zones and brought them to the surface, where they are presently exposed in domal mountain ranges commonly referred to as *metamorphic core complexes* (Crittenden and others, 1980). A detailed discussion of the formation of metamorphic core complexes is given elsewhere (Davis and others, 1986; Spencer and Reynolds, this vol.).

STRUCTURAL FRAMEWORK

Pre-Tertiary rocks in the Buckskin Mountains are structurally complex and record multiple phases of deformation related to the Maria fold-and-thrust belt. Within the main Maria belt, four main phases of deformation have been recognized (Reynolds and others, 1986b). The earliest deformational event (D_1) consisted of section attenuation and repetition during SSE-directed thrusting, followed by the formation of large, southeast-vergent folds. The second phase of deformation (D_2) was dominated by southwest-directed thrusting and associated folding. The third event (D_3) included south- and north-directed thrusting, folding, and development of crenulation. The fourth event (D_4) produced a late-stage, southwest-dipping cleavage with small-scale, northeast-vergent shear zones. An unrelated episode of deformation and metamorphism occurred after development of the Maria fold-and-thrust belt, was most important at deep structural levels, such as those presently exposed in the metamorphic core complexes, and consisted of amphibolite-facies metamorphism that accompanied the emplacement of Late Cretaceous granites (Rehrig and Reynolds, 1980; Reynolds, 1982b; Reynolds and others, 1988). Complex superposition of mostly D_1, D_2, and D_3 structures has resulted in bewildering structural complexity that includes refolded folds and thrusts, overprinted cleavages, and thrusts that truncate upturned sections and preexisting thrusts.

The dominant pre-Tertiary structure in the Buckskin Mountains is the Rio Vista thrust, which places Proterozoic crystalline rocks over strongly deformed Paleozoic and Mesozoic supracrustal rocks in the western Buckskin Mountains (Fig. 1). This thrust and its offset continuations are the main reason why Paleozoic and Mesozoic supracrustal rocks are common in the central and eastern Buckskin Mountains but are absent in a large region to the north and west where Tertiary rocks directly overlie Proterozoic crystalline rocks -- Paleozoic and Mesozoic

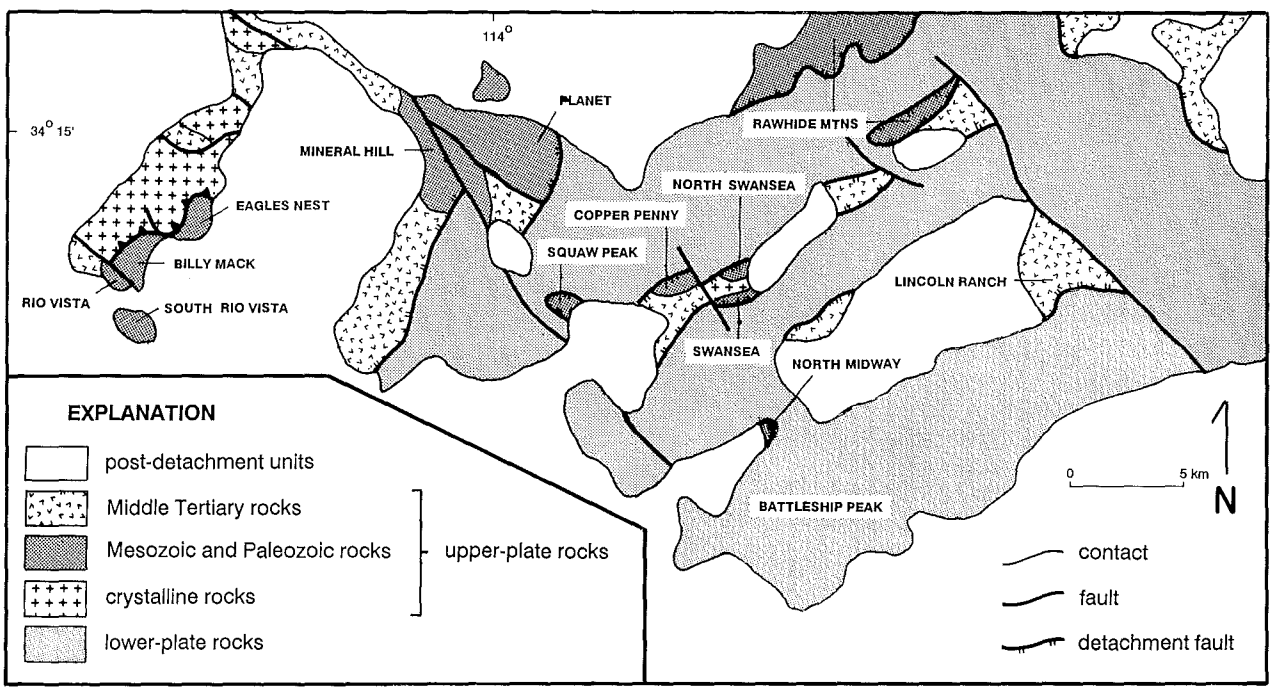

Figure 1. Simplified geologic map of most of the Buckskin and Rawhide Mountains, showing locations discussed in text.

supracrustal rocks are only preserved where they were protected from erosion by the overlying crystalline thrust sheet. In addition to the Rio Vista thrust, Paleozoic and Mesozoic rocks are internally repeated by numerous smaller(?) thrusts and are affected by several generations of large- and small-scale folds and cleavages. These structures are similar to D_1, D_2, and D_3 structures within the main Maria fold-and-thrust belt to the south and would be brought back within the belt by restoring several tens of kilometers of Tertiary displacement on the Buckskin detachment fault (Spencer and Reynolds, this vol.).

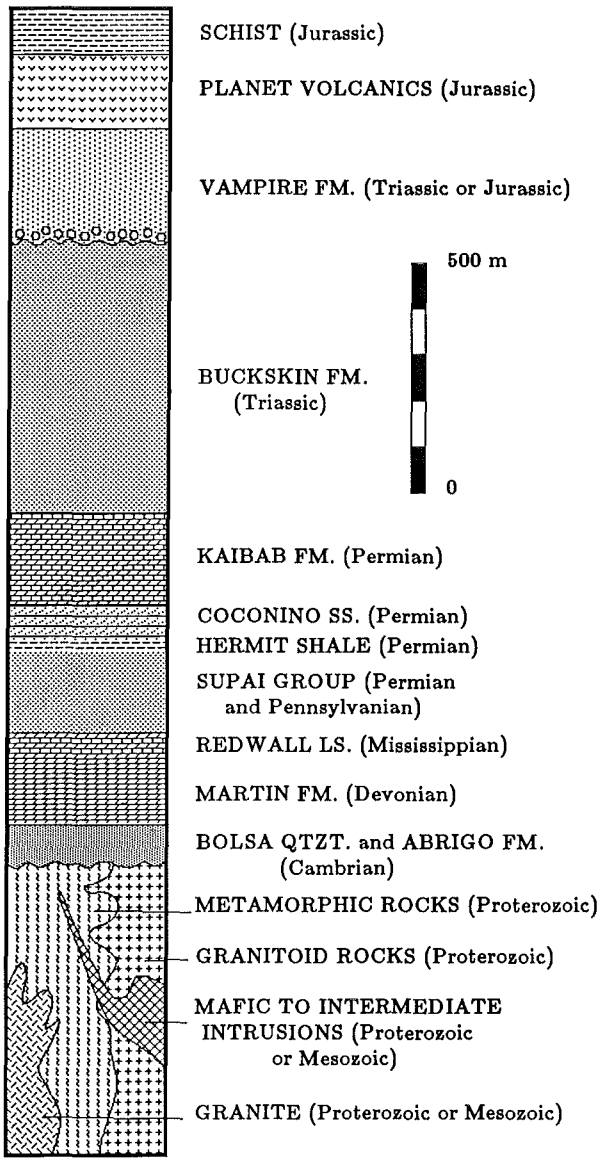

Figure 2. Generalized stratigraphic section for pre-Tertiary rocks in the Buckskin Mountains. Mesozoic units display much variation (not shown) in lithology and thickness between different parts of the range and between adjacent thrust sheets within a single area.

ROCK UNITS

Pre-Tertiary rocks in the upper plate of the Buckskin detachment fault are representative of the region and can be subdivided into the following major rock units (Fig. 2): (1) Proterozoic metamorphic rocks and associated Proterozoic and Mesozoic intrusive rocks; (2) Paleozoic sedimentary rocks; (3) Triassic Buckskin Formation; (4) Upper Triassic(?) to Middle(?) Jurassic Vampire Formation; (5) Middle to Upper Jurassic Planet Volcanics; and (6) Mesozoic rocks of uncertain stratigraphic affinity. We summarize general characteristics of each rock unit below, emphasizing the Mesozoic units, which are regionally the most poorly known and for which we have the most new data to report.

The rocks described in this paper were metamorphosed during Cretaceous and Jurassic(?) regional deformation and thrusting, but their original sedimentary character is still evident and they are described in this paper by their sedimentary names (e.g., conglomerate rather than metaconglomerate). Some metamorphosed quartzose and pelitic sedimentary rocks are referred to as quartzite and phyllite, respectively, because the protoliths are less obvious. Quartzite and sandstone commonly occur together in weakly to moderately metamorphosed terrains, differing only in their type of cementation (quartzose or calcareous, respectively) prior to metamorphism.

Proterozoic Metamorphic Rocks and Associated Proterozoic, Mesozoic, and Cenozoic Intrusive Rocks

Proterozoic crystalline rocks and smaller mafic to granitic intrusions of uncertain age are most widely exposed in the western Buckskin Mountains (Fig. 1), where they overlie Paleozoic and Mesozoic rocks along the northwest- to southwest-dipping Rio Vista thrust zone. Smaller, but structurally important, outcrops are present at Squaw Peak, Copper Penny, Swansea, north Swansea, north Midway, and Lincoln Ranch basin.

The oldest Proterozoic rocks are compositionally diverse, amphibolite-facies gneiss, migmatite, schist, and metaplutonic rocks. These rocks generally have well-developed crystalloblastic foliation and subparallel compositional banding that are interpreted to be relict Proterozoic fabric. In the largest exposures above the Rio Vista thrust, this foliation commonly strikes NNE and dips steeply to moderately (Frost, 1987, written commun.), as is typical of Proterozoic terranes in the region. Because of its general northeast strike, the foliation would not have changed orientation appreciably during middle Tertiary fault-block rotation.

Proterozoic metamorphic rocks are commonly associated with intrusions of unknown age. These intrusions include (1) light-colored, medium-grained granite, such as above the Rio Vista thrust in the western Buckskin Mountains, (2) coarse- to medium-grained biotite granite in the Swansea area, and (3) medium- to fine-grained, mafic to intermediate rocks that form dikes and small plugs within the biotite granite near Swansea. These

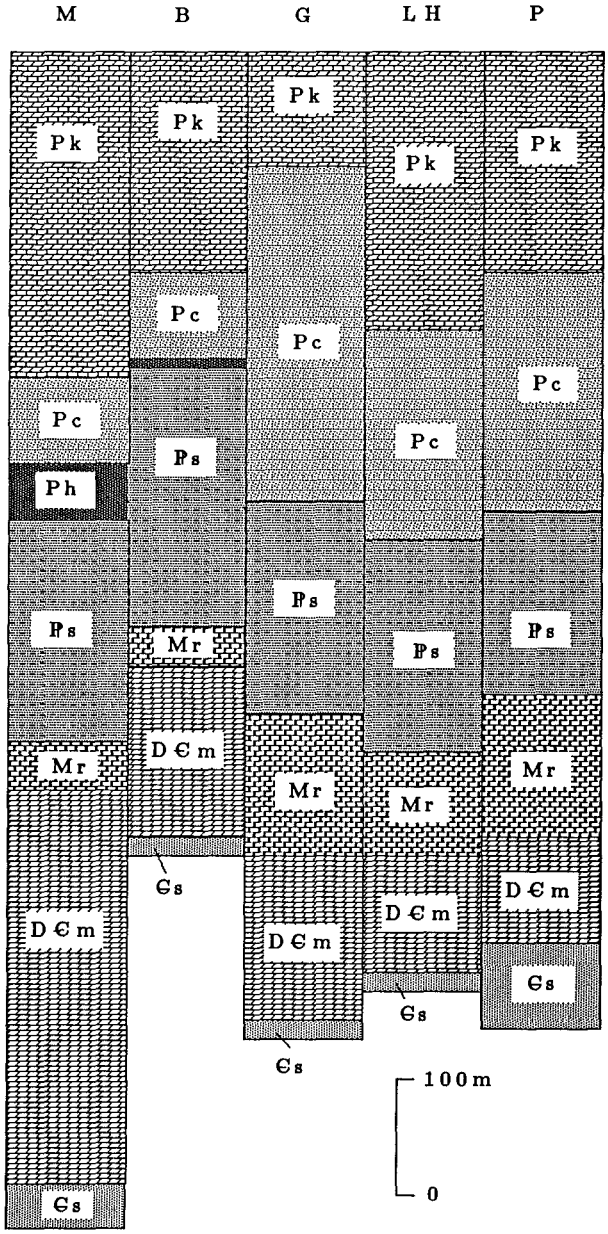

Figure 3 (left). Representative stratigraphic sections of Paleozoic units in west-central Arizona and southeastern California. Sections are arranged geographically from west (left) to southeast (right) and are from the Big Maria Mountains (M - Stone and others, 1983), Buckskin Mountains (B - this study), Granite Wash Mountains (G-Reynolds and others, 1986b and unpublished data), Little Harquahala Mountains (LH - Spencer and others, 1985), and Plomosa Mountains (P - Miller, 1971). Stratigraphic units are Єs - Cambrian rocks, including the Bolsa Quartzite and Abrigo Formation and their respective equivalents the Tapeats Sandstone and Bright Angel Shale, DЄm - Devonian Martin Formation and Cambrian Muav Limestone, Mr - Mississippian Redwall Limestone, Ꝑs - Pennsylvanian and Permian Supai Group, Ph - Hermit Shale, Pc - Permian Coconino Sandstone, and Pk-Permian Kaibab Formation. Thicknesses of units in the Granite Wash Mountains (especially the Kaibab Formation) and the Buckskin Mountains (especially the Devonian Martin Formation) partly reflect tectonic thinning. Note the presence of Hermit Shale in only the westernmost two sections.

intrusions are not dated, but are probably mostly Proterozoic, Jurassic, or Cretaceous based on regional relations and the presence of Cretaceous(?) thrust-related fabric in most bodies. They nowhere intrude Paleozoic or Mesozoic rocks and may, therefore, be Proterozoic.

Paleozoic Rocks

The upper plate of the Buckskin Mountains detachment fault contains numerous exposures of strongly deformed and metamorphosed Paleozoic sedimentary rocks. These rocks lack preserved fossils, except locally (Darton, 1925), but are lithologically distinct and can be correlated with some degree of confidence to less metamorphosed Paleozoic sections elsewhere in the region (Miller, 1970; Richard, 1982; Stone and others, 1983). The stratigraphic succession varies little within the region (Fig. 3) and most variations in unit thicknesses are due to Mesozoic deformation rather than original stratigraphic relations.

Cambrian Rocks. The stratigraphically lowest Paleozoic units in the region (Fig. 3) are an arkosic quartzite and an overlying thin sequence of phyllite and calc-silicate rocks derived from shale and calcareous siltstone. Regionally, the quartzite correlates with the Cambrian Bolsa Quartzite or Tapeats Sandstone and the phyllite correlates with the Cambrian Abrigo Formation or Bright Angle Shale. Surprisingly, both of these units are absent from all Paleozoic sections in the Buckskin Mountains, except for one section in the north Midway area. As discussed later, this absence is due to Mesozoic tectonism, not original nondeposition.

In the north Midway area, the basal quartzite and stratigraphically overlying phyllite are structurally attenuated to less than 7 m thick. The quartzite is vitreous gray on fresh surfaces, gray to maroon weathering, partly arkosic, and a ledge former. The overlying phyllite is thin, poorly exposed, and forms a slope.

Devonian and Mississippian Rocks. The stratigraphically lowest unit exposed in all other Paleozoic sections in the Buckskin Mountains consists of dolomite and dolomitic limestone (now generally marble). This unit is tan, gray, and brown, generally noncherty, and a massively bedded ledge former. The base of the unit is everywhere a fault, except in the north Midway area where it overlies the basal quartzite and phyllite. The dolomite and dolomitic limestone are correlated with Devonian Martin Formation of southeastern Arizona, or perhaps with Cambrian Muav Limestone of the Colorado Plateau.

The dolomite is overlain by a light-gray to white, calcite marble. The calcite marble has been severely attenuated during deformation and is generally less than 10 m thick. The unit is locally cherty, especially near its middle, and has a distinctive pinkish tint in some

outcrops. It is correlated with Mississippian Redwall Limestone.

The Martin Formation and Redwall Limestone have a combined maximum structural thickness of 190 m in the Billy Mack area, but are generally much thinner due to structural attenuation. They are mapped as a single unit in the more attenuated, structurally complex sections.

Pennsylvanian and Permian Rocks. The middle part of the Paleozoic section is occupied by a distinctive, dark-weathering sequence of quartzite and calcareous sandstone with local marble and phyllite. The unit is medium to thick bedded where least deformed, but has a laminated appearance where strongly tectonized. It has a maximum structural thickness of 220 m in the Billy Mack area and is correlated with the Pennsylvanian and Lower Permian Supai Group.

In most areas, the Supai Group is stratigraphically overlain by a distinctive light-gray-, pinkish-tan-, or pinkish-brown-weathering, fine-grained, vitreous quartzite. The unit is generally nonresistant and has a maximum structural thickness of 80 m in the Rio Vista area. It is correlated with the Permian Coconino Sandstone.

In the Eagles Nest area, the Supai Group and Coconino Sandstone are separated by 2 to 5 m of slope-forming, greenish-gray phyllite and metasiltstone. This interval is correlated with the Permian Hermit Shale.

Stratigraphically overlying the Coconino Sandstone are gray, tan, and brown calcite and dolomite marble. Tan and brown dolomite marble are most common in the lower part of the section and gray calcite marble is most abundant in the top half. The unit varies internally from very cherty to noncherty. The top of the unit locally contains thin (less than 1 m) beds of calcareous quartz sandstone. The limestone and dolomite have a maximum structural thickness of 190 m at Squaw Peak, where the base is not exposed, and are correlated with the Permian Kaibab Formation of northern Arizona.

Triassic Buckskin Formation

The stratigraphically lowest Mesozoic unit in the Buckskin Mountains is the Buckskin Formation, which is here named for exposures in the Mineral Hill area where it has a structural thickness of as much as 900 m. The type section, located 400 m west and southwest of the Planet mine, trends SSW from the center of SW $^1/_4$ SW $^1/_4$ sec. 31, T. 11 N., R. 16 W., to the center of NE $^1/_4$ sec. 1, T. 10 N., R. 17 W. A measured reference section (Appendix 1) for the middle of the formation is located 600 m south of the Mineral Hill mine in the center of sec. 10, T.10 N., R. 17 W. In both sections, the formation is faulted at its base and is unconformably overlain by Vampire Formation. The depositional base of the Buckskin Formation is exposed in the Eagles Nest, Billy Mack, Rio Vista, and south Rio Vista areas of the western Buckskin Mountains, where it rests on Permian Kaibab Formation. On the basis of its lithology and stratigraphic position, the Buckskin Formation is considered to be largely correlative with the Lower and Middle(?) Triassic Moenkopi Formation of the Colorado Plateau (Reynolds and others, 1987). The name *Buckskin formation* was first coined by N. Lehman and introduced informally by Spencer and others (1986a).

The Buckskin Formation consists of locally calcareous, quartzose to quartzofeldspathic sandstone and siltstone (now largely quartzite), phyllite, and less abundant conglomerate, impure carbonate rocks, and local gypsiferous zones. In the Mineral Hill and south Rio Vista areas, the formation is composed of four informal members (see Plate 2), which are as follows (from bottom to top): lower member, quartzite member, phyllite member, and upper member. These members are not recognized in sections of Buckskin Formation elsewhere in the range, but are recognized in the Palen Mountains of southeastern California (Reynolds and others, 1987; Stone and Kelly, 1988).

The lower member has a structural thickness of approximately 400 m in the Planet area and 40 m in south Rio Vista. It forms ledges and slopes and is composed of thinly to moderately bedded, quartzose to quartzofeldspathic sandstone and siltstone (now commonly quartzite), sandy metapelite, phyllite, chloritic schist, and rare quartzite- and carbonate-pebble conglomerate. Some sandstone and siltstone was originally calcareous, as indicated by calcareous zones and the presence of metamorphic epidote and calc-silicate minerals. Quartzite is dark gray, weathers medium to chocolate brown, and forms resistant ledges. Sandstone and silty sandstone are generally quartz-rich to slightly feldspathic, medium to fine grained, and well to moderately sorted. They are commonly medium to light brown to orangish brown or tan, are variably calcareous, and form beds 1 to 100 cm thick. Siltstone is generally very quartzose. Phyllite is gray to dark gray or brown weathering, is strongly cleaved and crenulated, and forms slopes. It is locally associated with gypsiferous soil that overlies bedded gypsum or anhydrite at depth.

At least the upper half of the lower member is characterized by coarsening-upward sequences several to several tens of meters thick. Phyllite and phyllitic sandstone grade upward into coarser and less phyllitic sandstone and ultimately into resistant, chocolate-brown quartzite or tan to brown, variably calcareous sandstone. Quartzite and sandstone at the top of each sequence have a sharp upper contact with phyllite or phyllitic sandstone of the overlying coarsening upward sequence.

The overlying quartzite member forms a dark-weathering, resistant ledge and is generally less than 15 m thick in the Planet area and 2 m thick in south Rio Vista. It is composed of massive to poorly bedded quartzite (quartzose sandstone) that is fine grained to very fine grained and well sorted, or less commonly fine to medium grained and moderately sorted. The quartzite member has a greenish-gray to brown color and is locally calcareous. Thin sections show that the rock is now mostly composed of epidote.

The phyllite member is nonresistant and forms a slope that is commonly covered by talus from the overlying, cliff-forming upper member. It is approximately 30

m thick in the Mineral Hill area and 60 m thick at south Rio Vista, and is composed of phyllite, slate, phyllitic siltstone, micaceous sandstone, conglomerate, and rare gypsiferous rocks. Phyllite is thin bedded and medium to light gray, silvery gray, or greenish gray. Sandstone is variably calcareous and contains moderately to well-sorted, medium- to fine-grained quartz sand with minor amounts of white mica. Some poorly sorted, greenish-gray, gritty and micaceous sandstone is also present. The base of the member locally contains 1 to 5 m of conglomerate with rounded pebbles and cobbles of quartzite in a matrix of moderately sorted, medium-grained, micaceous quartz sandstone.

The upper member of the Buckskin Formation forms imposing, dark-colored ridges and cliffs and has a structural thickness of at least 400 m in the Planet area and 40 m at south Rio Vista. It is composed of massive to poorly bedded, fine- to medium-grained, moderately to well-sorted quartzite and quartzose sandstone. Some of the more poorly sorted sandstone is slightly feldspathic. The unit is variably calcareous and includes abundant calc-silicate lithologies. Thin layers of calcareous schist, schistose marble, and quartz-sericite schist are also present near the top of the member northwest of Mineral Hill. Quartz-sericite schist weathers light or medium gray and was presumably derived from slightly impure siltstone and fine-grained sandstone.

Sections of Buckskin Formation in the Eagles Nest, Billy Mack, Rio Vista, and Swansea areas cannot be subdivided into these four members, but can be correlated in a general sense with Buckskin Formation on the basis of lithology and stratigraphic position above Permian Kaibab Formation or below Vampire Formation. As is discussed in the following sections on individual areas, these sequences generally contain more phyllitic rocks and less massive quartzite and calcareous quartzite.

Triassic(?) and Jurassic Vampire Formation

Stratigraphically overlying the Buckskin Formation are quartzite and quartzofeldspathic sandstone with locally interbedded volcaniclastic rocks and conglomerate. The formation has a maximum structural thickness of 300 to 330 m in both the Mineral Hill and south Rio Vista areas. The unit is here named the Vampire Formation for the Vampire mine, which is 1.6 km south of the Mineral Hill mine. The type section of the formation trends SSW from near the center of the western edge of sec. 12 to the east-central part of sec. 11, T. 10 N., R. 17 W. Reference sections are in the center of sec. 2, T. 10 N., R. 17 W., and in the south Rio Vista area. The Vampire Formation is probably correlative with some part of the Upper Triassic Chinle Formation, Lower Jurassic Glen Canyon Group (Moenave and Kayenta Formations and Navajo Sandstone), or Middle Jurassic San Rafael Group (Carmel and Entrada Formations), based on lithologic character and age constraints (Reynolds and others, 1987).

In the Mineral Hill area, the Vampire Formation rests on an unconformity that, from west to east, cuts progressively down through all four members of the Buckskin Formation, so that in eastern exposures Vampire Formation rests on the lower member. The Vampire Formation consists of several to several tens of meters of basal conglomerate overlain by 180 to 300 m of quartzite and sandstone, gritty to conglomeratic sandstone, and volcaniclastic rocks. Quartzite is light gray and derived from well-sorted, fine- to medium-grained sandstone, or less commonly siltstone. The quartzite is locally feldspathic and contains 2 to 5% metamorphic white mica; some fine-grained quartz sandstone is moderately micaceous. Outcrops are commonly stained orange, pink, and red with iron oxides. Small-scale cross bedding is locally preserved. Gritty sandstone and conglomeratic sandstone contain scattered quartzose granules and small pebbles in a poorly sorted, coarse-grained sandy matrix that includes abundant feldspar and metamorphic mica. Quartzite and conglomeratic sandstone are locally interbedded with greenish, poorly sorted, volcanic-lithic sandstone with 5 to 15% quartz grains (1 to 5 mm in diameter) and several percent magnetite. Much of the section is probably fluvial in origin, although some very well sorted quartzite may be eolian. Interlayered volcaniclastic rocks are best exposed in the Mineral Hill area.

The basal conglomerate of the formation is poorly sorted and contains subrounded to angular clasts of quartzite, quartzose sandstone, vein quartz, and less abundant clasts of the following lithologies: (1) poorly to well-sorted sandstone, siltstone, phyllite, and quartz-pebble conglomerate, all probably derived from the underlying Buckskin Formation or equivalent Mesozoic units; (2) fine- to medium-grained, equigranular, leucocratic granite and medium- to coarse-grained biotite granite; (3) light-gray to cream-colored, foliated silicic volcanic, volcaniclastic, and metavolcanic rocks with quartz and feldspar phenocrysts; and (4) fine-grained, quartz- and feldspar-phyric felsite. The conglomerate contains clasts of microcline (up to 2 cm in length) and coarse-grained quartz, probably derived from porphyritic granite. Rb-Sr isotopic analysis indicates that at least one metavolcanic clast is probably Proterozoic (Reynolds and others, 1989).

Jurassic Planet Volcanics

Overlying the Vampire Formation is up to 600 m of generally cleaved and foliated silicic volcanic and metavolcanic rocks, here named the Planet Volcanics for Planet Wash in the Planet and Mineral Hill area. The type locality for the Planet Volcanics is along the west side of Planet Wash in the center of the eastern half of sec. 7, T. 10 N., R. 16. W. Reference localities are along Mineral Wash in the center of sec. 11, T. 10 N., R. 17 W. and in the south Rio Vista area. A sample of Planet Volcanics collected from Planet Wash has been dated at about 160 Ma by U-Th-Pb analyses on zircon (Reynolds and others, 1987). The name *Planet volcanics* was first used informally by Wicklein (1980) for a variety of rocks and was restricted to the presently defined usage by Spencer and others (1986a).

The Planet Volcanics typically consist of quartz-feldspar-muscovite-magnetite schist that is homogeneous in composition over tens to hundreds of meters. Feldspar and quartz phenocrysts typically compose 2 to 20% of the rock. Other local lithologies include the following: (1) volcaniclastic sandstone with quartz and feldspar grains (reworked phenocrysts?); (2) weakly foliated, blocky, reddish-weathering silicic volcanic rocks with quartz and feldspar phenocrysts 1 to 6 mm in diameter; and (3) chloritic schist with quartz and feldspar grains and altered mafic clots 1 to 5 mm in diameter. The entire section represents metamorphosed silicic ash-flow tuff, volcaniclastic rocks, and possible hypabyssal intrusive rocks; the chloritic schist is probably more intermediate in composition, but may locally include hydrothermally altered silicic volcanics.

East of the Mineral Hill mine (center of sec. 2, T. 10 N., R. 17 W.), 1- to 20-m-thick quartzite beds are present within the basal 100 m of Planet Volcanics. Northwest of the Mineral Hill mine, strongly deformed metavolcanic and metavolcaniclastic units are interlayered with light-gray, vitreous quartzite and quartz-muscovite schist; contacts between the quartzite layers and volcanic units are parallel to foliation and not marked by an intensification of fabric. These relations suggest that quartz sandstone, possibly of eolian origin, was originally interbedded with the volcanic rocks.

Mesozoic Rocks of Uncertain Stratigraphic Affinity

Some map units are clearly of Mesozoic age, but are not easily assigned to the Buckskin Formation, Vampire Formation, or Planet Volcanics. These vary considerably in lithology and thickness from place to place and are discussed more fully in the descriptions of individual areas. The most common lithologies include phyllite, phyllitic sandstone, calcareous sandstone, quartz-sericite schist, and quartzite. Some sections are in the proper stratigraphic position to be Buckskin Formation, whereas others overlie the Planet Volcanics and probably represent a higher sequence than is exposed in the Mineral Hill area.

AREA DESCRIPTIONS

Mineral Hill Area

The Mineral Hill area (Fig. 1; Plate 2) contains probably the thickest, most complete stratigraphic sequence of Triassic and Jurassic rocks in western Arizona. This sequence, consisting of Buckskin Formation, Vampire Formation, and Planet Volcanics, is exposed in a series of tilted fault blocks in the upper plate of the Buckskin detachment fault (Fig. 4). The section in each fault block is essentially homoclinal, with cleavage, lithologic layering, and preserved bedding in the Mesozoic rocks all dipping moderately to the southwest, subparallel to bedding in overlying middle Tertiary rocks. The fault blocks provide a series of cross-sectional views for examining structural and stratigraphic relations within the Mesozoic sequence. Some aspects of the geology of the area were recognized by Wicklein (1980), Wilkins and Heidrick (1982), and N. Lehman (see Plate 2).

The area is divided into two domains by the Mineral Wash fault zone, a NNW-trending, generally high-angle fault that exposes the detachment fault and deeper levels of the tilted fault blocks on its uplifted, western side (Fig. 4). The domain east of the Mineral Wash fault zone consists of three large tilted fault blocks. The southern and central fault blocks contain exposures of Planet Volcanics, Vampire Formation, and the upper member of the Buckskin Formation. More complete sections of Buckskin Formation are exposed in the northernmost fault block and in fault blocks west of the Mineral Wash fault zone.

Stratigraphy. Except for Squaw Peak (discussed separately) and one possible exposure of Permian Kaibab Formation east of the Planet mine (Plate 2), the oldest upper-plate unit exposed is the Buckskin Formation. It locally has a structural thickness of more than 900 m and is composed of four members that, for the most part, are laterally continuous across the area. Most of this thickness is from the upper and lower members, which have maximum structural thicknesses of 480 and 400 m, respectively; the phyllite and quartzite members in the middle of the formation have a combined thickness of less than 50 m (Appendix 1).

The lithologic descriptions given previously for each member apply to, and were largely derived from, exposures in the Mineral Hill area. One rare lithology is conglomerate composed of stretched pebbles of carbonate and quartzite that occurs within the upper member north of the Bill Williams River. Layers of marble, also rare in the formation, are present near the top of the section west of the Mineral Wash fault zone (sec. 33, T. 11 S., R. 17 W.).

The most notable stratigraphic feature of the Mesozoic section is an angular unconformity at the base of the Vampire Formation. This unconformity progressively cuts deeper into the underlying Buckskin Formation section from northwest to southeast, as is revealed by variations in the preserved thickness of the upper member of the Buckskin Formation. The upper member is approximately 400 m thick in northwesternmost exposures, but is progressively cut out to the southeast along strike, such that it is only 20 m thick south of the Planet mine. Further to the east, near Planet Wash, the upper member is absent and basal Vampire Formation rests instead directly on the phyllite member or even on the underlying quartzite and lower members. The unconformity cuts most sharply across section southwest of the Planet mine (Plate 2), where it bevels across more than

Figure 4 (next page). Generalized geologic map of the Planet and Mineral Hill area, western Buckskin Mountains. Geology by J. Spencer, S. Reynolds, and N. Lehman (modified from Plate 2). *T* and *R* adjacent to straight lines indicate type and reference sections, respectively. MHM = Mineral Hill mine; PM = Planet mine; VM = Vampire mine.

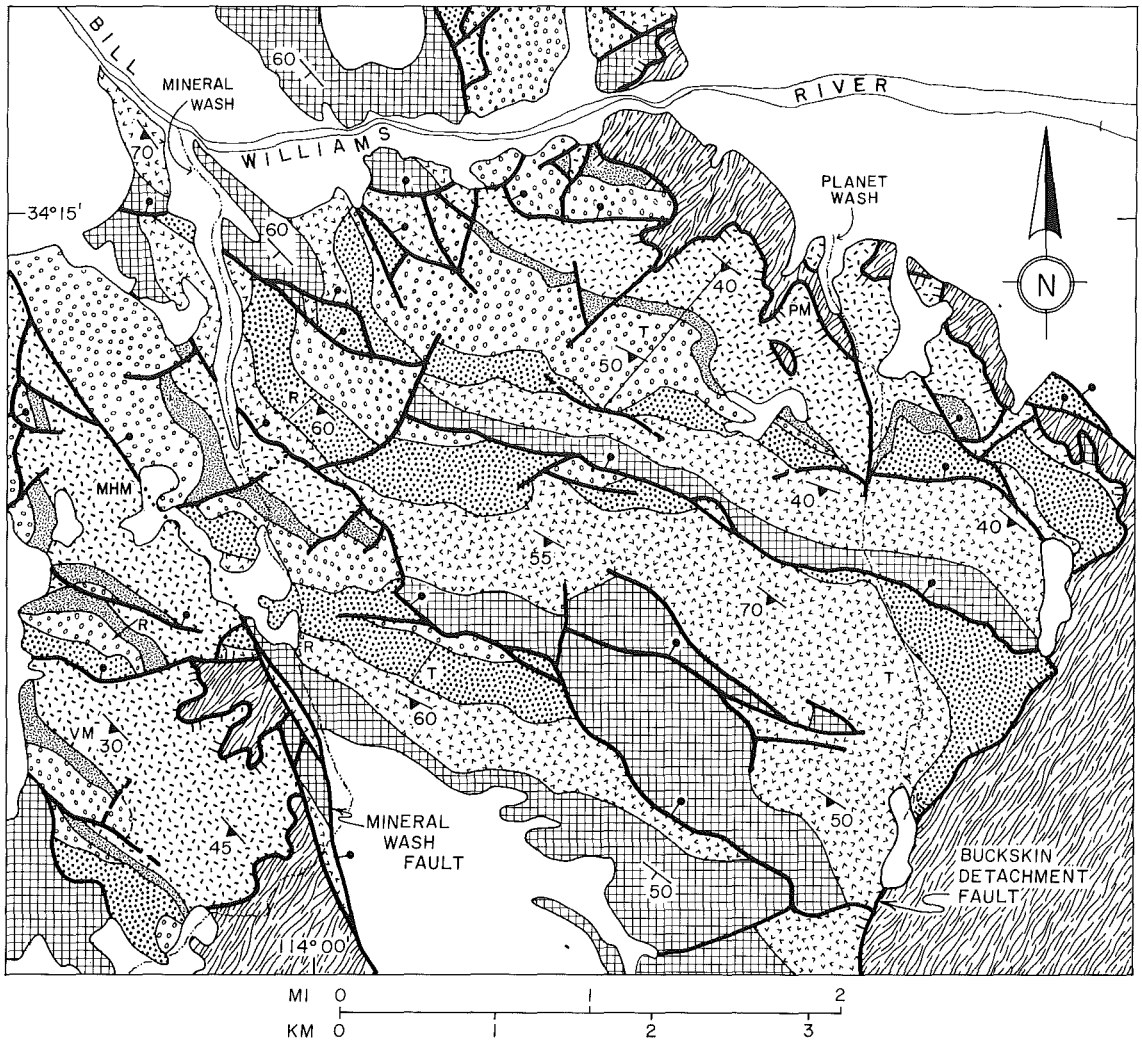

SEDIMENTARY ROCKS AND BASALT (LATE MIOCENE TO HOLOCENE)

SEDIMENTARY ROCKS, BASALT, AND REPLACEMENT CARBONATE (EARLY TO MIDDLE MIOCENE)

PLANET VOLCANICS (JURASSIC)

VAMPIRE FORMATION (JURASSIC ?)

BUCKSKIN FORMATION, UPPER MEMBER (TRIASSIC)

BUCKSKIN FORMATION, PHYLLITE AND QUARTZITE MEMBERS (TRIASSIC)

BUCKSKIN FORMATION, LOWER MEMBER (TRIASSIC)

LOWER PLATE MYLONITIC CRYSTALLINE ROCKS (PROTEROZOIC TO TERTIARY)

50 BEDDING ATTITUDE

30 FOLIATION ATTITUDE

DETACHMENT FAULT, DOUBLE HATCHURES ON UPPER PLATE

HIGH-ANGLE FAULT, BAR AND BALL ON DOWNTHROWN BLOCK

200 m of the upper member within a distance of several hundred meters. In cross section, this relationship suggests that the upper member of the Buckskin Formation formed a southeast-facing slope or erosional escarpment that was sculpted by pre-Vampire erosion and buried during deposition of the Vampire Formation.

The unconformity is well exposed in several areas, especially south of the Vampire mine (near the eastern edge of sec. 15, T. 10 N., R. 17 W.) and east of Planet Wash (near the eastern edge of sec. 5, T. 11 N., R. 16 W.). In both of these areas, the unconformity cuts across the lowermost part of the upper member and onto the underlying phyllite member. The unconformity is overlain by several meters of conglomerate at the base of the Vampire Formation. This conglomerate contains angular clasts of sandstone and siltstone derived from the underlying Buckskin Formation, in addition to granitic and metavolcanic clasts. Thicker, more impressive exposures of the conglomerate are present along Mineral Wash, near the Mineral Hill mine.

Vampire Formation has a structural thickness of 180 to 300 m and is composed of quartzite, micaceous quartz sandstone, phyllitic granule conglomerate, and a locally present, pebble to cobble conglomerate at its base. The unit also locally contains oval, siliceous concretions 4 to 7 mm in diameter. The upper contact of the unit with the overlying Planet Volcanics is generally sharp and is not obviously an unconformity. In exposures east of the mouth of Mineral Wash, and east of the Mineral Hill mine, quartzite at the top of the Vampire Formation is interlayered with volcanic and volcaniclastic rocks that are similar to the overlying Planet Volcanics. This relation implies that the two units at least locally interfinger and are partly contemporaneous in age. This conclusion is further supported by the presence of thin beds of quartzite in tight, layer-parallel contact with Planet Volcanics in the northwesternmost exposures in the Mineral Hill area.

The highest unit, the Planet Volcanics, has a maximum preserved structural thickness of 600 m, but its original top is not exposed in the area. It largely represents metamorphosed and deformed ash-flow tuffs and volcaniclastic rocks. Outcrops vary from well-foliated, quartz-feldspar-muscovite-magnetite schist to massive, weakly deformed, quartz- and feldspar-phyric silicic volcanic rocks. The unit contains some chloritic schist and a distinctive quartz-ribbon metarhyolite tuff at the base of the section.

Granitic rocks, probably of Mesozoic age, occur as several small plugs that have intruded the lower member of the Buckskin Formation west of the Planet mine. These granites are porphyritic, leucocratic, and altered. They have a spaced cleavage parallel to that in the wall rocks and were clearly intruded prior to Mesozoic deformation. Granite is also present in a small, fault-bounded sliver west of the Mineral Hill mine.

Other pre-Tertiary rock units must also have been originally present because they are abundant as clasts and breccia sheets in Tertiary sedimentary units. Clasts and breccia sheets of Permian Kaibab Formation are common adjacent to those of Buckskin Formation, which suggests that the two units were originally in contact, probably in a normal stratigraphic sequence. Breccia sheets of Permian Coconino Sandstone, other Paleozoic units, and Proterozoic crystalline rocks are also locally present. Southwest of Tunnel Peak, Tertiary monolithologic breccia composed of Planet Volcanics is successively overlain by breccia sheets of Buckskin Formation, Paleozoic rocks, and Proterozoic crystalline rocks. The stacking of the breccia sheets implies that a complete sequence of Paleozoic and Proterozoic rocks may have originally underlain the Mineral Hill Mesozoic section in the source area of the breccias.

Structure. The Mineral Hill area is structurally uncomplicated compared to other areas in the Buckskin Mountains, but nevertheless contains some complex Mesozoic structures. Most rocks contain a well-developed cleavage or schistosity that dips moderately to the southwest at a low angle to bedding. Cleavage generally dips somewhat more steeply southwest than bedding, which is consistent with the beds being right side up. Cleavage is penetrative in most phyllitic rocks and in most exposures of Planet Volcanics, but is more widely spaced in thicker bedded units, such as the upper member of the Buckskin Formation. Lineation is rare, even in the most strongly deformed rocks. Clasts within the basal conglomerate of the Vampire Formation are strongly flattened, but only slightly elongated in a down-dip (ESE-trending) direction. In contrast, clasts in the phyllite member near the Mineral Hill mine have a strong northeast-trending elongation. Also, southwest-trending lineation with a top-to-the-southwest sense of shear (based on *S-C* fabrics) was observed in one location within the quartz-ribbon metarhyolite tuff.

Map-scale folds are not common, and most outcrop-scale folds are late crenulations and kinks that fold the main cleavage. These crenulations typically trend west to northwest and range in amplitude from less than 1 mm to several meters. They are locally associated with a late-stage, crenulation cleavage that dips more steeply southwest than the main cleavage. Some of the folds and crenulations have northeast vergence.

Some Mesozoic structural complications are present along the Bill Williams River. Several kilometers west of the Planet mine (SW $^1/_4$ sec. 36), the upper and lower members of the Buckskin Formation are juxtaposed along a fault that is parallel to bedding in the overlying upper member, but is very discordant to bedding and cleavage in the underlying lower member. This fault projects along strike to the southeast into a normal sequence of all four members of the Buckskin Formation, and motion along the fault evidently is transferred into subtle bedding-parallel slip.

Even more complex Mesozoic structures are present northwest of the Mineral Hill mine along both sides of the Mineral Wash fault zone. This area contains large folds that deform bedding and cleavage into atypical north, northeast, and east dips. Along the Bill Williams River (sec. 33), Planet Volcanics and Vampire Formation are locally interleaved via nearly isoclinal folds that fold

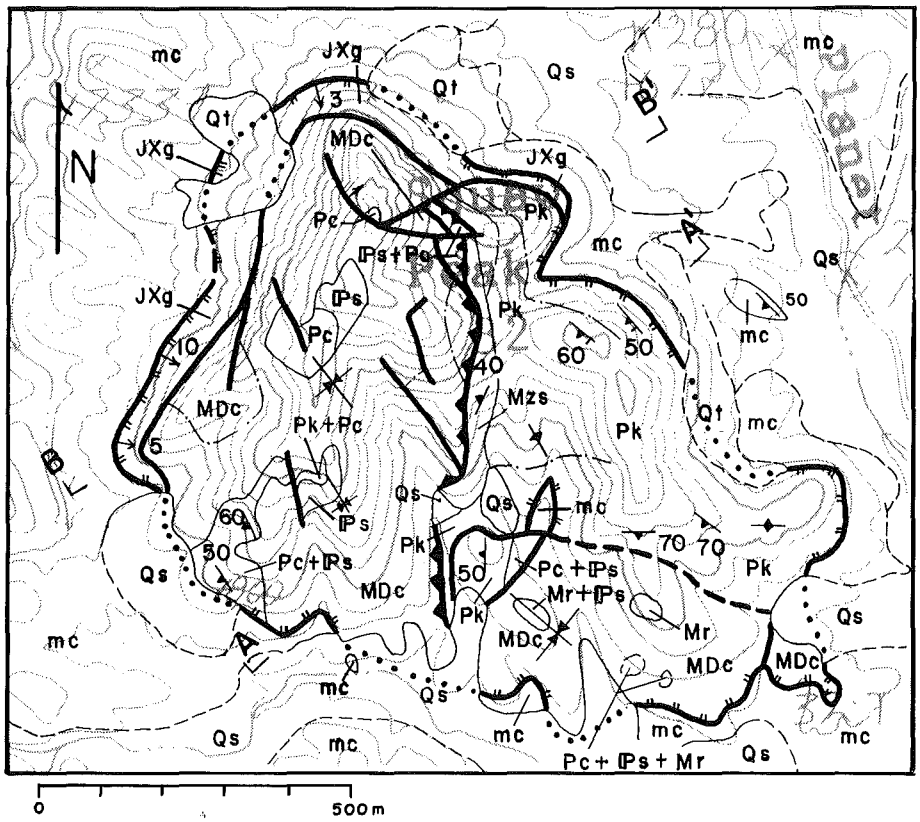

Qs	SURFICIAL DEPOSITS (Quaternary)
Qt	TALUS (Quaternary)
Mzs	SCHIST AND METACONGLOMERATE (Mesozoic)
Pk	KAIBAB FORMATION (Permian)
Pc	COCONINO SANDSTONE (Permian)
Ps	SUPAI GROUP (Pennsylvanian and Permian)
MDc	CARBONATE ROCKS; INCLUDES REDWALL LIMESTONE AND MARTIN FORMATION (Mississippian and Devonian)
JXg	GRANITE (Jurassic or Proterozoic)
mc	MYLONITIC CRYSTALLINE ROCKS BELOW DETACHMENT FAULT (middle Tertiary mylonitic fabric; various protoliths)

CONTACT; dashed where approximately located

10 FAULT, showing dip; dashed where approximately located; dotted where concealed

THRUST FAULT; teeth on upper plate

DETACHMENT FAULT; dotted where concealed; ticks on upper plate

30 FOLIATION

VERTICAL FOLIATION

30 FOLIATION PARALLEL TO BEDDING

MARKER BED

SYNFORM

Figure 5. Geologic map of the Squaw Peak area, western Buckskin Mountains. Boundaries of the map are at 34°9.48', 34°10.16', 113°56.43', and 113°57.4'. Geology by S. Reynolds and J. Spencer.

cleavage in both rock types. In one outcrop, an earlier set of isoclinal folds is discordantly overprinted by two cleavages. Phyllitic zones within the adjacent Buckskin Formation are strongly deformed and probably served as loci of slip during development of the main cleavage and during subsequent folding. One outcrop contains a northwest-trending lineation with *S-C* fabrics that indicate top-to-the-northwest shear.

In summary, the dominant structure within the area is the widely developed cleavage. The tendency for lineation and stretched clasts to trend southwest allies this cleavage with D_2 structures regionally. The dominant sense of transport during this event is uncertain in the Mineral Hill area because some *S-C* fabrics indicate top-to-the-southwest shear, whereas cleavage-bedding relations imply that folds would have a northeast asymmetry. The top-to-the-northwest *S-C* fabrics near the Bill Williams River are of uncertain significance, but could be related to D_1. The superimposed folds and crenulations are similar in style and orientation to those assigned to D_3 elsewhere in the region.

Squaw Peak

Squaw Peak, located southeast of the Mineral Hill area, is an isolated klippe of pre-Tertiary rocks above

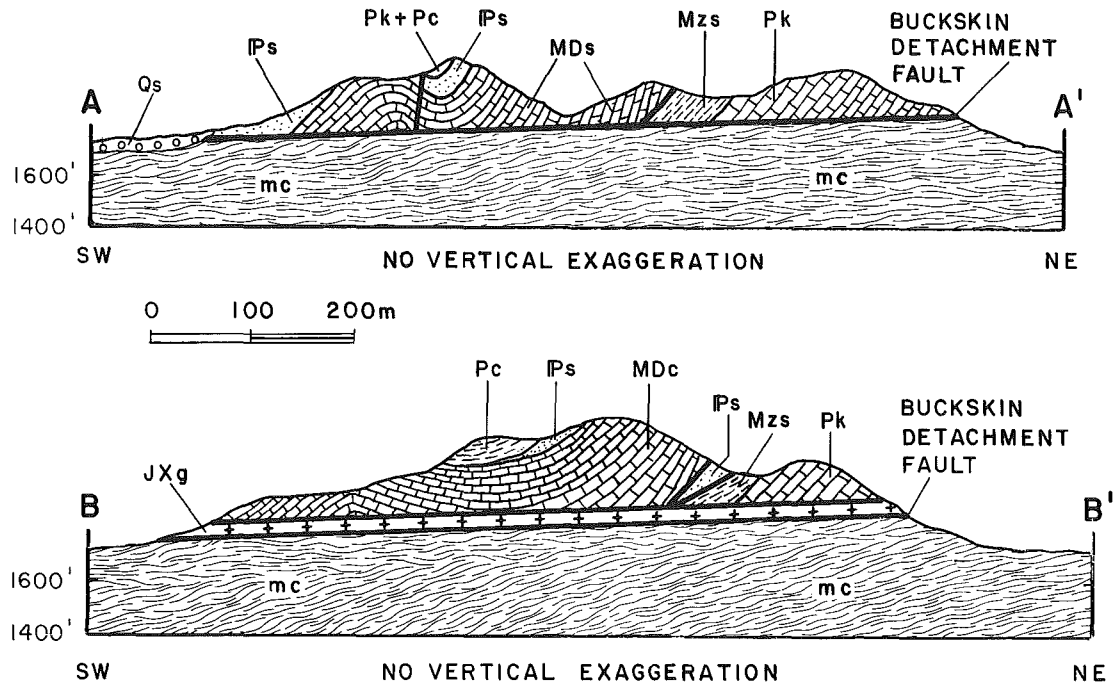

Figure 6. Geologic sections of the Squaw Peak area. See Figure 5 for explanation and location of sections.

the Buckskin detachment fault (Figs. 1, 5, and 6). Rocks within the klippe are separated into three structural plates by two main low-angle faults. The plates consist of, from bottom to top, (1) shattered crystalline rocks, (2) Permian Kaibab Formation overlain by Mesozoic rocks, and (3) an attenuated section from Devonian Martin Formation to Permian Kaibab Formation. The area was first mapped by Osborne (1981), who recognized the detachment fault and the fault between the crystalline rocks and overlying Paleozoic units.

The lowest structural plate is a tabular body of foliated and shattered granite that is bounded by the detachment fault below and by a subparallel low-angle fault above. The granite is coarse grained and porphyritic, with K-feldspar phenocrysts as long as 1.5 cm, and is foliated with local ribbon quartz. It is juxtaposed against overlying Permian Kaibab Formation along a tight, ductile fault that is parallel to foliation in both rock types. The granite is probably either Proterozoic or Jurassic in age.

The granite contains some dikelike bodies of a finer grained, aplitic granite with scattered quartz eyes. It also contains some lenses of strongly foliated, dark-colored, mafic schist that is very fine grained and chloritic. These latter rocks may represent deformed mafic dikes within the granite.

The next higher structural plate contains a thick, southwest-dipping, right-side-up sequence of Permian Kaibab Formation and Mesozoic rocks. The lower part of the Kaibab Formation, exposed on the northeast flank of the peak, consists of tan dolomitic marble and gray to brownish-gray calcite marble with only minor amounts of chert and with weakly expressed foliation and bedding. The upper part of the formation contains these lithologies plus gray to tan, well-foliated and locally very cherty limestone and dolomite marble. Chert occurs in bands as thick as 2 cm and as clots as large as 10 to 20 cm in diameter. Near its top, it contains several-meter-thick beds of quartz sandstone. The entire Kaibab section is 190 m thick, but its base is not exposed.

The Kaibab is depositionally overlain by approximately 50 m of Mesozoic phyllite, schist, sandstone, and conglomerate. Phyllite and schist are strongly foliated and gray to greenish gray, and contain both muscovite and chlorite. Sandstone is gray to greenish gray, fine to coarse grained, moderately sorted, and muscovitic. It is locally gritty and contains moderately to well-rounded, stretched pebbles and cobbles (as much as 20 cm in diameter) of medium- to coarse-grained, moderately to well-sorted quartzite.

The third and highest structural plate overlies the top of the Mesozoic section along a moderately southwest-dipping thrust fault. This sheet consists of an attenuated, but generally upright, southwest-dipping sequence of Paleozoic rocks. The lowest unit in the Paleozoic sequence is correlated with the Devonian Martin Formation and consists of tan, buff, brown, and brownish-gray dolomite and dolomitic calcite marble. This unit generally lacks chert and is massive, unlayered, and only locally foliated. It is overlain by gray to brown, variably cherty calcite marble correlated with Mississippian Redwall Limestone. Some sections of Redwall that are thicker than 10 m consist of a lower well-foliated, variably cherty calcite marble; a middle very cherty, brownish-gray calcite marble; and an upper light-gray to cream-colored, mostly noncherty calcite marble with pink,

purple, and brown tints.

The Redwall Limestone is overlain by several meters to several tens of meters of tan-, brown-, and orange-weathering, light-gray to greenish-gray, calcareous siliciclastic rocks. These rocks, correlated with the Pennsylvanian and Permian Supai Group, have a ledgy aspect due to alternating layers of resistant, well-sorted quartzite and recessive, darker weathering calc-silicate rocks. They are overlain by several to several tens of meters of pinkish-tan-weathering, fine-grained, very well sorted, light-gray to white, vitreous quartzite correlated with the Coconino Sandstone. In two locations, the quartzite is overlain by Permian Kaibab Formation.

Although the Paleozoic rocks have a general dip to the southwest, they are intricately folded on a small scale. Chert layers within the carbonate rocks commonly outline small-scale, rootless isoclines and sets of intrafolial folds. In some outcrops, the overall trace of folded chert beds is markedly discordant to the dominant foliation in the rock; in some cases, they dip northeast, perpendicular to foliation. Larger folds, with amplitudes of several to several tens of meters, are also present, especially within the highest structural plate. Several northwest-trending synclines are marked by downfolded keels of Redwall Limestone, Supai Group, Coconino Sandstone, and Kaibab Formation within the underlying Martin Formation. The most spectacular of these is a nearly isoclinal, synclinal keel on the ridge crest south of Squaw Peak. In this area, Supai Group, Coconino Sandstone, and Kaibab Formation have been attenuated to thicknesses of 3 to 5 m, 1 to 2 m, and 1 m, respectively. The attenuated section is interleaved within Redwall Limestone and folded into very tight, northwest-plunging folds. This relationship shows that structural attenuation of the section preceded the last phases of tight folding. The entire attenuated section is less than 2% of its expected regional thickness.

In numerous places, especially near the detachment fault, the Paleozoic rocks have been overprinted by Tertiary brecciation and carbonate replacement. Some outcrops contain angular fragments of quartzite in an unbrecciated matrix of brown carbonate. Paleozoic carbonate rocks locally have an intricate breccia texture, revealed only by subtle color variations between different generations of carbonate. Replacement carbonate is distinguished from original Paleozoic carbonate by its darker brown color, lack of foliation and folded chert layers, somewhat porous texture, and cross-cutting or matrix-filling habit.

Copper Penny Area

The Copper Penny area is located at the west end of the Swansea synform, between Squaw Peak and Swansea (Fig. 1). Various aspects of the geology of the area were identified by Wicklein (1980), Osborne (1981), Woodward (1981), and Wilkins and Heidrick (1982).

Description. Structurally complex pre-Tertiary rocks are exposed above the detachment fault in the Copper Penny area west of Swansea (Fig. 40 in Spencer and Reynolds, this vol.). At the Copper Penny mine are small, isolated klippen of Paleozoic metasedimentary rocks and Proterozoic(?) granitoid rocks. The Paleozoic rocks have been widely affected by middle Tertiary carbonate metasomatism and replacement (Wicklein, 1980; Spencer and Reynolds, this vol.), but can be differentiated from the replacement carbonate by the presence of tectonite fabrics and local, isoclinally folded chert layers.

Larger, more continuous, and more instructive exposures of pre-Tertiary rocks occur 1 km east of the Copper Penny mine (Figs. 7 and 8). Tertiary faults cut the area into a number of fault blocks, each with a slightly to very different assemblage of pre-Tertiary rocks. The largest block is roughly triangular and is bounded on the north by the detachment fault, which dips gently to the southeast under the block. Tertiary replacement carbonate, characteristically massive and tan to brown, has permeated the pre-Tertiary rocks near the detachment fault. South of the replacement carbonate is an inverted stratigraphic sequence composed of, from bottom to top, Mesozoic schist, Permian Kaibab Formation, and Permian Coconino Sandstone. The Mesozoic schist is silvery gray and greenish gray to purplish gray, consists of quartz, muscovite, and chlorite, and is associated with soft, gypsiferous soil. The overlying Kaibab Formation, in addition to being upside down, is only 5 to 50 m thick (2 to 20% of its normal thickness) because of ductile attenuation. Adjacent units are presumably attenuated equal amounts. The inverted sequence and its layer-parallel tectonite fabric is folded by three northwest-trending, upright to slightly overturned folds. In addition, the sequence is folded by an ENE-trending, overturned synform that is cored by a klippe of mylonitic Proterozoic or Jurassic crystalline rocks, including mylonitic alaskite, granodiorite, and quartzite or vein quartz. The contact between the crystalline rocks and underlying Paleozoic rocks is marked by strongly developed mylonitic or tectonite fabric and is interpreted to be a ductile thrust fault. The thrust and associated fabrics are folded by the synform, such that both are locally overturned along the south flank of the fold. The Paleozoic units along this flank have been folded back into an upright attitude (two successive overturnings have righted the rocks). The major folds are paralleled by small-scale crenulations of the mylonitic and tectonite foliation.

Within the same fault block, but further to the west, is a lens of tectonically interleaved Paleozoic rocks (Supai Group, Coconino Sandstone, and Kaibab Formation), Mesozoic chloritic quartzite, and mylonitic quartz-feldspar-chlorite schist derived from a plutonic rock. This lens either represents a ductile-fault-bounded sliver or an infold, possibly of the overlying thrust sheet.

The next major fault block to the east is also triangular and likewise consists of Paleozoic and Mesozoic metasedimentary rocks that are overlain by a thrust sheet of mylonitic crystalline rocks. The Paleozoic and Mesozoic rocks in this fault block, however, are upright, rather than inverted. Also, the units do not precisely match those in the adjacent fault block. The structurally lowest unit consists of dark-weathering, variably

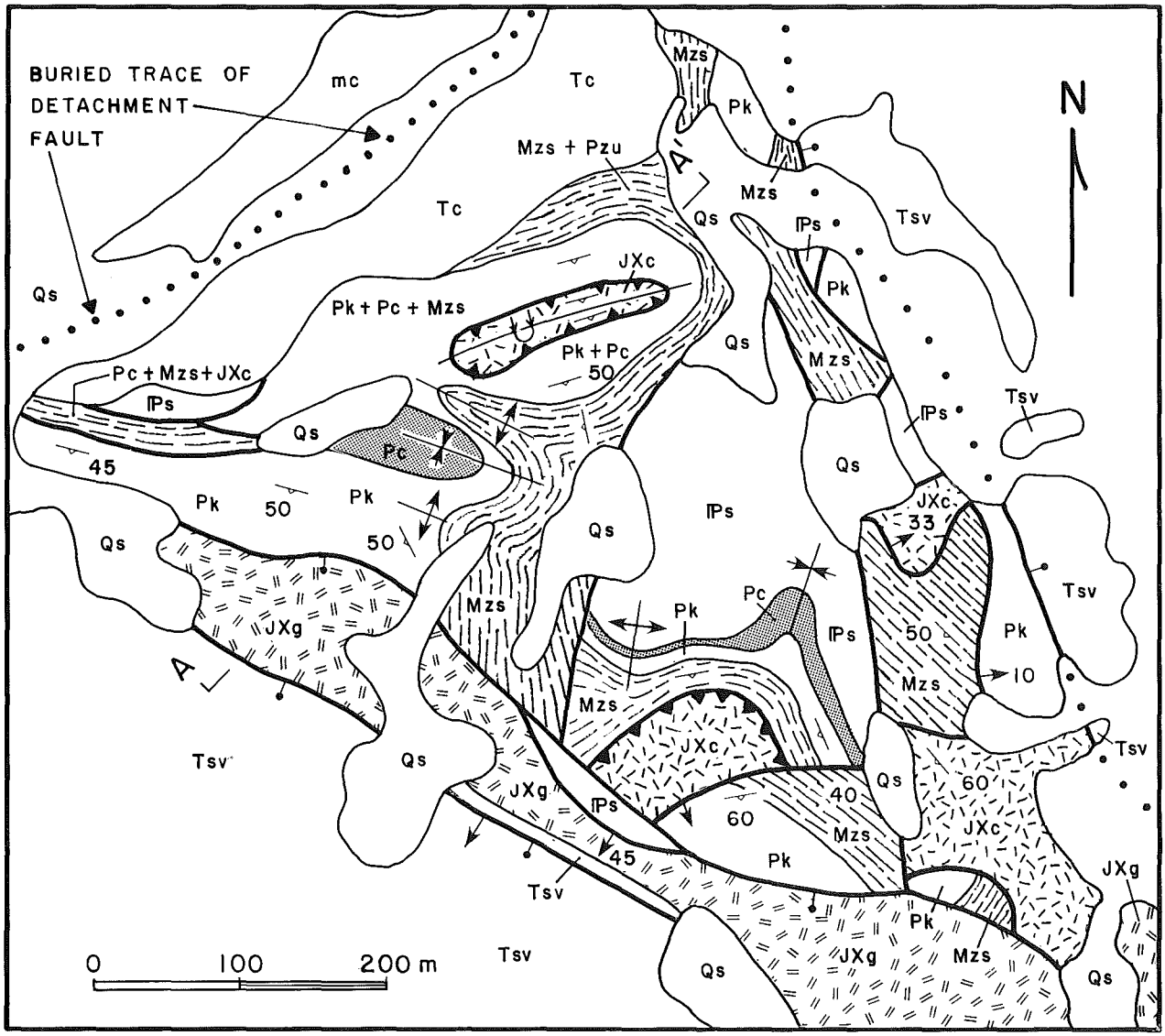

Qs	SURFICIAL DEPOSITS (Quaternary)
Tc	REPLACEMENT CARBONATE ROCKS (middle Tertiary)
Tsv	SEDIMENTARY AND VOLCANIC ROCKS (middle Tertiary)
Mzs	SCHIST AND GYPSIFEROUS ROCKS (Mesozoic)
Ꞧb	BUCKSKIN FORMATION (Triassic)
Ꞧbc	BUCKSKIN FORMATION; CALCAREOUS FACIES (Triassic)
Pk	KAIBAB FORMATION (Permian)
Pc	COCONINO SANDSTONE (Permian)
Ꝑs	SUPAI GROUP (Pennsylvanian and Permian)
Pz	SEDIMENTARY ROCKS (Paleozoic; mostly Permian)
JXg	GRANITE (Jurassic or Proterozoic)
JXc	CRYSTALLINE ROCKS (Jurassic or Proterozoic)
mc	MYLONITIC CRYSTALLINE ROCKS BELOW DETACHMENT FAULT (middle Tertiary mylonitic fabric; various protoliths)

CONTACT; dashed where approximately located

10 FAULT, showing dip; dotted where concealed; bar and ball on downthrown side

THRUST FAULT; teeth on upper plate

30 FOLIATION

SYNFORM

ANTIFORM

OVERTURNED SYNFORM

Figure 7. Generalized geologic map of the eastern Copper Penny area, Swansea synform, central Buckskin Mountains. Boundaries of map area are at 34°10.24', 34°10.63', 113°52.36', and 113°52.89'. Geology by J. Spencer and S. Reynolds.

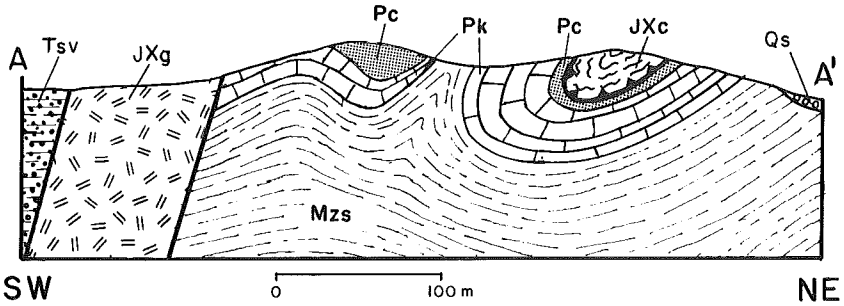

Figure 8. Generalized geologic section of the eastern Copper Penny area. See Figure 7 for explanation and location of section.

calcareous, siliciclastic rocks correlated with the Pennsylvanian and Permian Supai Group. This is overlain by a structurally attenuated, but upright sequence of Coconino Sandstone, Kaibab Formation, and Mesozoic schist. Tectonite fabric in the Paleozoic and Mesozoic rocks parallels lithologic layering and is folded by several NNE-trending upright folds. The Mesozoic schist is overlain by a thrust sheet of mylonitic crystalline rocks derived from granite and less abundant alaskite and compositionally banded gneiss. Mylonitic foliation in the crystalline rocks is concordant to the underlying thrust and dips gently to the south. This assemblage of crystalline rocks is distinct from that described earlier for the fault block to the west.

A third large fault block forms a northwest-trending belt along the southwest edge of the pre-Tertiary outcrop. This block consists mostly of unfoliated, coarse- to medium-grained, Proterozoic or Jurassic biotite granite that is unlike the mylonitic crystalline rocks in either of the other two fault blocks. The granite is depositionally overlain by southwest-dipping middle Tertiary sedimentary rocks.

Other fault blocks in the area contain scraps of upper Paleozoic rocks, Mesozoic schist, and various crystalline rocks. The structural and stratigraphic relations between most of these smaller blocks and the three larger fault blocks described above are uncertain. Mylonitic crystalline rocks in one of these smaller fault blocks contains a southeast-trending stretching lineation.

Interpretation. The field relations indicate that Paleozoic and Mesozoic rocks have been variably metamorphosed, ductilely attenuated, and overridden by sheets of Proterozoic or Jurassic crystalline rocks. The two exposed thrust faults are not obviously correlative because of mismatches in rocks both above and below the thrusts. Paleozoic and Mesozoic rocks beneath the thrusts are inverted in one fault block and upright in another; also, Supai Group is present at the base of the upright sequence, but has been structurally removed from the top of the inverted sequence. The amount of ductile attenuation was equally extreme in both the inverted and upright sequences, and locally thinned the sections to less than 5% of their normal regional thicknesses. In spite of such attenuation, Mesozoic schist units are interpreted to be in depositional contact with Permian Kaibab Formation in both the inverted and upright sections, and are probably facies of the Triassic Buckskin Formation.

Subsequent to thrusting, the inverted and upright sections and overlying thrusts were folded by upright to slightly overturned folds of various trends. This folding was accompanied by crenulation of preexisting mylonitic and tectonite foliations, and was probably the last recorded deformation related to Mesozoic compressional tectonism. The style of folding suggests correlation with D_3, but the earlier thrusting and section attenuation are more similar to either D_1 or D_2.

The coarse-grained granite in the southwestern fault block was the structurally highest rock unit at the beginning of middle Tertiary sedimentation -- it alone is depositionally overlain by middle Tertiary units. The granitic block has been downdropped against the other two fault blocks on a southwest-dipping Tertiary normal fault. Pre-Tertiary rocks in the other two fault blocks are nowhere in depositional contact with Tertiary units and were evidently at a deeper structural level below the middle Tertiary land surface; they may have been structurally beneath the coarse-grained granite, possibly along a major thrust fault. The general lack of Mesozoic fabric in the granite may be attributable to the granite's relatively shallow structural position during Mesozoic deformation and metamorphism.

Swansea and North Swansea

Pre-Tertiary rocks are widespread in the Swansea area, extending in a north-south belt across the entire width of the Swansea synform (Fig. 1 and Fig. 16 in Spencer and Reynolds, this vol.). The most widespread pre-Tertiary unit is an assemblage of igneous rocks, consisting of several types of granite and younger mafic intrusions. Paleozoic and Mesozoic metasedimentary rocks are exposed in two main areas: as a rugged, northeast-trending ridge at Swansea and in an area of low relief 1.5 km to the north, hereafter called north Swansea. The area was previously mapped by Wicklein (1980) and Woodward (1981) and described by Wilkins and Heidrick (1982).

The igneous rocks are widely exposed in a series of low hills between Swansea and north Swansea. The dominant unit is a coarse- to medium-grained, K-feldspar-megacrystic biotite granite that generally lacks a well-

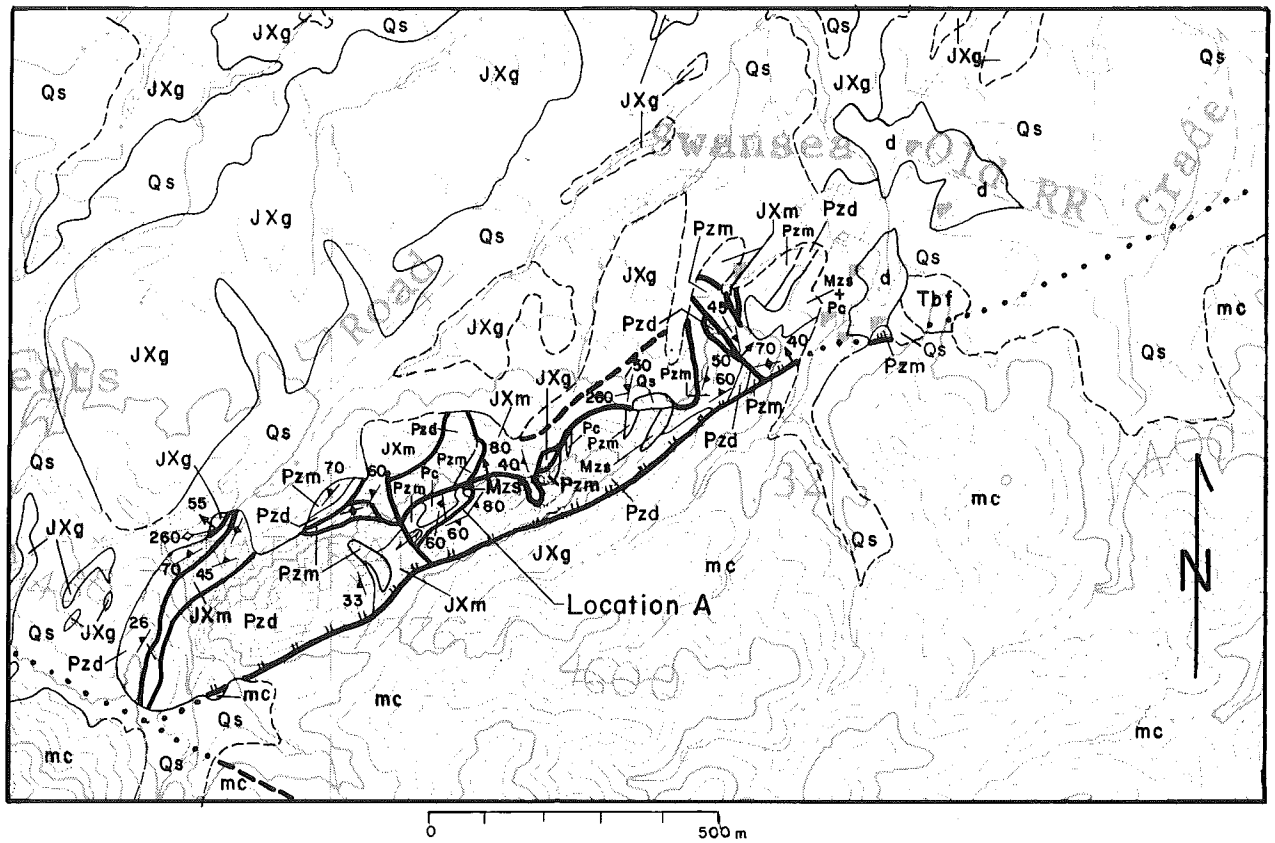

d	MINE DUMP
Qs	SURFICIAL DEPOSITS (Quaternary)
Tbf	BASIN FILL (Late Tertiary)
Mzs	SCHIST; MOSTLY DERIVED FROM SEDIMENTARY ROCKS, BUT INCLUDES SOME MYLONITIC CRYSTALLINE ROCKS (mostly Mesozoic fabric and protolith)
Pc	COCONINO SANDSTONE (Permian)
Pzm	CALCITE MARBLE (Paleozoic; probably Permian)
Pzd	DOLOMITE MARBLE (Paleozoic; probably Permian)
JXm	METAMORPHIC ROCKS, INCLUDING MYLONITIC CRYSTALLINE ROCKS AND METASEDIMENTARY SCHIST (Mesozoic fabric; Mesozoic and probably Proterozoic protoliths)
JXg	GRANITE (Jurassic or Proterozoic)
mc	MYLONITIC CRYSTALLINE ROCKS BELOW DETACHMENT FAULT (middle Tertiary mylonitic fabric; various protoliths)
——--	CONTACT; dashed where approximately located
10	FAULT, showing dip of fault and trend of striae; dashed where approximately located
.....	DETACHMENT FAULT; dotted where covered; ticks on upper plate
30	FOLIATION, showing trend of lineation
—◆—	VERTICAL FOLIATION

Figure 9. Geologic map of the Swansea area, Swansea synform, central Buckskin Mountains. Boundaries of the map area are at 34°9.64', 34°10.37', 113°50.10', and 113°51.54'. Geology by J. Spencer and S. Reynolds.

developed foliation. The granite is locally associated with finer grained, less megacrystic equivalents and with pegmatites. The granite was informally referred to as the *Swansea granite* by Wicklein (1980), who considered it to be Mesozoic based on Rb-Sr whole-rock data on an enclosed pegmatite. Alternatively, the granite could be Proterozoic.

The granite is cut by fine- to medium-grained mafic dikes and irregular intrusions (the Signal diorite of Wicklein, 1980). The intrusions vary from medium-grained diorite to foliated, dark-green aphanitic andesite(?). Several generations of mafic intrusions are probably present because some are strongly affected by fabrics of probable Mesozoic age, whereas others intrude middle Tertiary units.

The crystalline rocks are depositionally overlain to the southwest by the basal sandstone of the Tertiary section. The sandstone dips moderately to the southwest, which indicates that the crystalline rocks have been rotated during Tertiary detachment faulting.

Swansea. The main ridge at Swansea is composed of Paleozoic carbonate rocks with less abundant Mesozoic

schist, Paleozoic quartzite, and Proterozoic or Jurassic crystalline rocks (Fig. 9). These rocks strike northeast, generally dip steeply, and are structurally complex, with most contacts being layer-parallel ductile shear zones. The rocks are bounded to the southeast by the Buckskin detachment fault, which dips moderately to the northwest under the ridge. They are also cut by small, northwest-trending faults that are truncated by the detachment fault.

Swansea Ridge is truncated to the southwest by the northwest-trending Swansea fault, which has approximately 1 km of right slip and several hundred meters of northeast-side-down dip slip (Spencer and Reynolds, this vol.). Offset equivalents of the rocks on Swansea Ridge are present on the southwest side of the Swansea fault.

The ridge crest is dominated by tan dolomitic marble that is generally thick bedded to massive. This unit locally contains isoclinally folded siliceous layers (chert) and is Paleozoic in age, rather than being Tertiary replacement carbonate (Wicklein, 1980). It is probably correlative with either the lower dolomitic part of the Kaibab Formation or the Devonian Martin Formation.

Another common lithology on the ridge crest is gray to brownish-gray calcite marble that contains tectonized chert layers. This unit is locally in tight (tectonized depositional?) contact with Permian Coconino Quartzite and is correlated largely with Kaibab Formation.

Small patches of Mesozoic schist are present on the ridge, especially on the east end of the ridge near the main Swansea mine workings. The schist unit includes gray to greenish-gray quartz-muscovite-chlorite schist, phyllite, micaceous quartzite, and rare quartzofeldspathic schist that may represent mylonitic crystalline (granitoid?) rocks. Some phyllite-dominated outcrops are in tight contact with the calcite marble unit (Permian Kaibab Formation) and may be correlative with Triassic Buckskin Formation. In contrast, other outcrops contain diverse lithologies, including mylonitic crystalline rocks, and probably represent Mesozoic shear zones.

A similar sequence of rocks is shown on Figure 9 as Jurassic to Proterozoic metamorphic rocks, undifferentiated (unit JXm). This unit contains schist similar to that described above, but contains a much larger percentage of crystalline rocks, especially mylonitic granitoid rocks. The lithologies in this unit are strongly deformed and are interleaved on too fine a scale to show separately on Figure 9. This unit probably includes rocks ranging in age from Mesozoic to Proterozoic and represents a tectonic melange formed during Mesozoic thrusting. It is present on the north flank of the ridge, along the contact between the Paleozoic rocks and the Jurassic or Proterozoic granitoids rocks further north.

The structural relationships are complex, but typical for the region. The dominant structural features are foliation, ductile and brittle-ductile shear zones, and small brittle (Tertiary?) faults. Layering, foliation, and layer-parallel shear zones in the rocks all strike ENE and dip steeply. The rocks lack a coherent stratigraphy, so the facing direction is largely unknown. The facing is to the southeast in one area near the center of the ridge where Coconino Sandstone is successively overlain by the calcite marble unit (Kaibab Formation) and several meters of Mesozoic schist. The units are extremely attenuated within this section.

Many contacts between units are layer-parallel shear zones marked by strongly developed tectonite fabric in carbonate rocks, schistosity in micaceous rocks, and mylonitic fabric in crystalline rocks. One such shear zone (location *A* in Fig. 9) is between the Coconino-Kaibab-schist section described above and the main ridge-forming dolomitic marble to the southeast. The shear zone locally cuts out the schist and contains lenses of strongly mylonitic crystalline rocks. The shear zone, related tectonite fabrics in the rocks, and the attenuated section are all strongly folded, both in outcrop and on the scale of the geologic map. Another shear zone separating the Paleozoic rocks from unit JXm is likewise warped into a map-scale folds, including a northwest-opening, steeply plunging fold near the northeast end of the ridge.

The structures at Swansea can be only broadly correlated with those elsewhere in the region (Reynolds and others, 1986b). The northeast strike of lithologic units and layer-parallel shear zones is characteristic of the earliest regional deformation (D_1). Attenuation of the stratigraphic section presumably accompanied formation of the layer-parallel shear zones. The folding of layering and shear zones could be either a continuation of D_1 or a result of later deformations (D_2 or D_3). The rocks were probably rotated during Tertiary detachment faulting, based on the southwest dip of Tertiary rocks that rest on the crystalline rocks to the north. Such rotations are not very apparent on Swansea Ridge, however, because the units strike parallel to the direction of rotation. When restored to their pretilting attitudes, lithologic layering and the shear zones would still strike northeast and be subvertical.

North Swansea. North Swansea, located 1.5 km north of Swansea, likewise contains structurally complex Paleozoic and Mesozoic metasedimentary rocks that are truncated at depth by the detachment fault. Rocks above the detachment fault compose three main structural plates that each contain a distinctive assemblage of rocks (Figs. 10 and 11).

The structurally lowest plate above the detachment fault consists of an isoclinally folded sequence of upper Paleozoic rocks and Triassic rocks. The most extensive unit in this plate is correlated with Triassic Buckskin Formation and forms gentle slopes, punctuated with small ledges. It consists of quartzite, orange-weathering calcareous quartzite, greenish- to purplish-gray phyllite, cream-colored gritty sandstone, and thin lenses of tannish-brown marble. Buckskin Formation is interpreted to be in both upright and overturned depositional contact with tan, brown, and gray, locally cherty marble of the Permian Kaibab Formation. The Kaibab is in continuous sections with Coconino Sandstone and Supai Group. The entire section is very attenuated, with both the Kaibab and Coconino generally being only 1 to 10 m thick. The units define a tight to isoclinal, synformal anticline (the

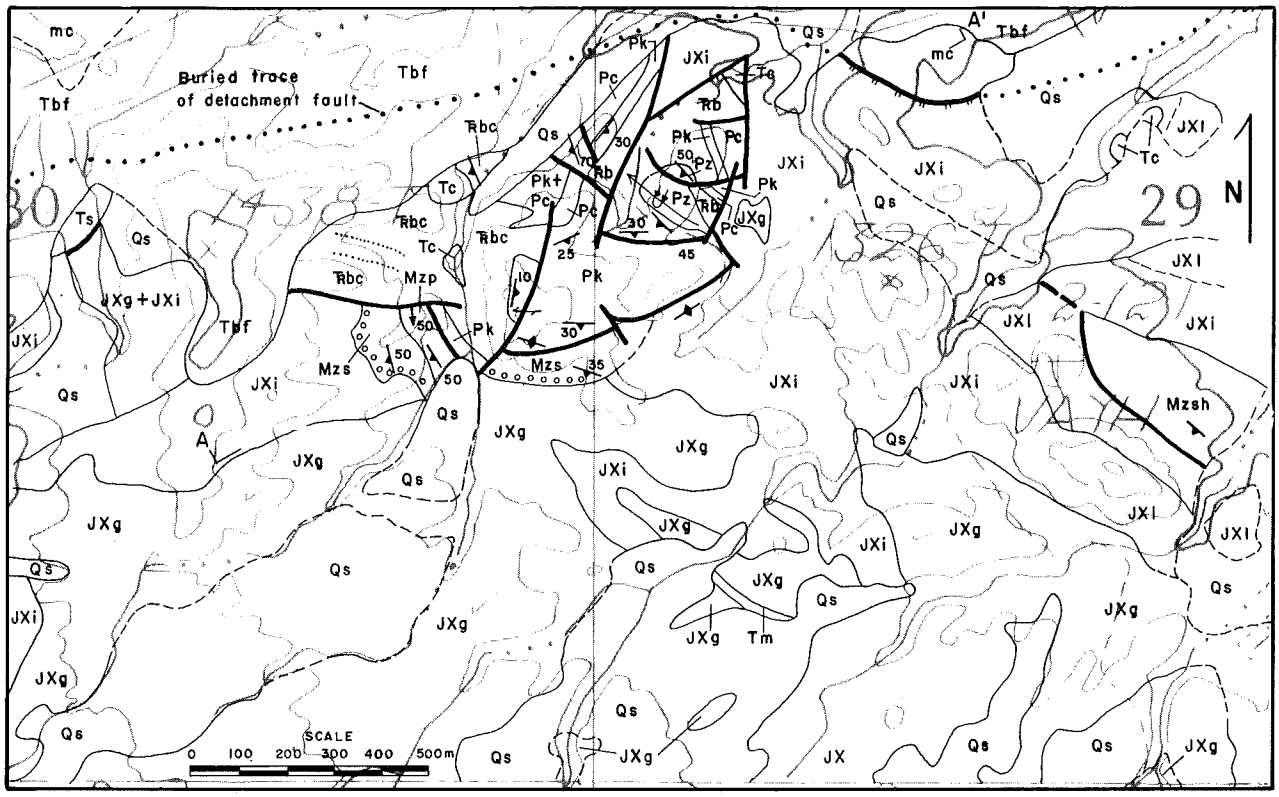

Qs	SURFICIAL DEPOSITS (Quaternary)
Tbf	BASIN FILL (Late Tertiary)
Tc	REPLACEMENT CARBONATE ROCKS (middle Tertiary)
Ts	SEDIMENTARY AND VOLCANIC ROCKS (middle Tertiary)
Tm	MAFIC DIKE (Tertiary?)
Mzp	PHYLLITE (Mesozoic)
Mzs	SCHIST, METASANDSTONE, AND METACONGLOMERATE (Mesozoic)
Mzsh	SCHIST; MOSTLY DERIVED FROM SEDIMENTARY ROCKS, BUT INCLUDES SOME MYLONITIC CRYSTALLINE ROCKS (Mesozoic fabric and dominant protolith)
Rb	BUCKSKIN FORMATION (Triassic)
Rbc	BUCKSKIN FORMATION; CALCAREOUS FACIES (Triassic)
Pk	KAIBAB FORMATION (Permian)
Pc	COCONINO SANDSTONE (Permian)
Pz	SEDIMENTARY ROCKS (Paleozoic; mostly Permian)
JXl	LEUCOCRATIC GRANITE (Mesozoic or Proterozoic)
JXi	MAFIC IGNEOUS ROCKS (Mesozoic or Proterozoic)
JXg	GRANITE (Jurassic or Proterozoic)
mc	MYLONITIC CRYSTALLINE ROCKS BELOW DETACHMENT FAULT (middle Tertiary mylonitic fabric; various protoliths)
——--	CONTACT; dashed where approximately located
10	FAULT, showing dip; dashed where approximately located
.....	DETACHMENT FAULT; dotted where covered; ticks on upper plate
.....	MARKER BED
0000	CONGLOMERATIC ZONE
30	FOLIATION, showing trend of lineation
	VERTICAL FOLIATION
	OVERTURNED SYNCLINE

Figure 10. Geologic map of the north Swansea area, Swansea synform, central Buckskin Mountains. Boundaries of the map area are at 34°10.35', 34°10.95', 113°50.55', and 113°51.73'. Geology by S. Reynolds and J. Spencer.

section would be inverted if the synform were unfolded). To the northeast, the rocks are probably folded around an antiform and into an upright Buckskin-Kaibab-Coconino sequence.

The middle structural plate contains a thicker and somewhat different section of inverted Kaibab Formation and Buckskin Formation. Kaibab Formation is at least 30 m thick and contains tightly infolded keels and irregular masses of Coconino Sandstone, most of which are too small to show on the geologic map or section. The Kai-

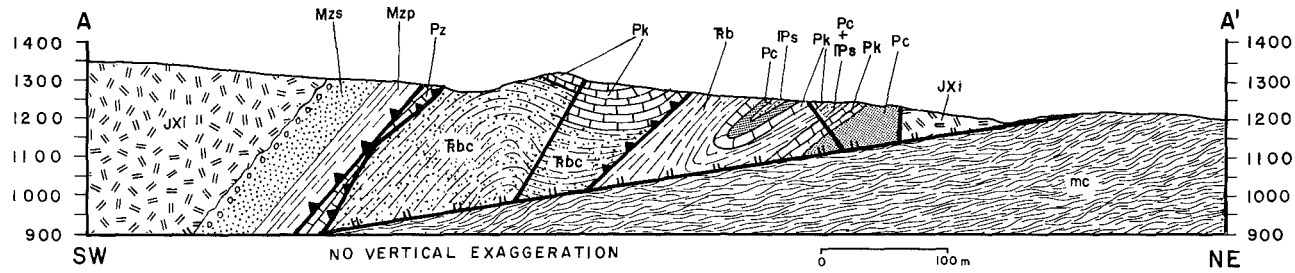

Figure 11. Geologic section of the north Swansea area. Two thrust faults divide the area into three structural plates, each with a different Mesozoic stratigraphy. Note overturned unconformity between units JXi and Mzs. Ps = Supai Group. See Figure 10 for explanation and location of section.

bab overlies a section of Buckskin Formation that consists of dark, cliff-forming, massive calcareous quartzite and greenish calc-silicate rocks -- this Buckskin Formation is very different from that in the underlying structural plate. To the south and southwest, the Kaibab and Buckskin Formations are truncated structurally upward by a shear zone that contains strongly deformed slivers of Paleozoic carbonate rocks and quartzite. The attitude of the shear zone varies from moderately southwest dipping to northeast striking and vertical, and apparently defines a southwest-plunging antiformal nose.

The shear zone is overlain by the highest structural plate, which consists of (1) the granite and mafic intrusions that underlie the area between Swansea and north Swansea; and (2) Mesozoic metasedimentary rocks that are in overturned depositional contact with the overlying mafic intrusions and granite (Fig. 11). The granitic and mafic rocks are locally strongly deformed, with well-developed cleavage and mylonitic fabric, especially near the underlying shear zone. The Mesozoic rocks are moderately deformed, with cleavage that dips moderately to the south and southwest, subparallel to the overlying contact. Along the contact, the Mesozoic rocks consist of poorly sorted grit and sandstone, with lenses of fine-grained, granite-derived conglomerate (paleogrus?). Down away from the contact (up section in the Mesozoic rocks), the grit and sandstone grade into finer grained, calcareous sandstone and quartzite, which in turn grade into greenish- to purplish-gray phyllite. The contact with the igneous rocks is locally well exposed, lacks either strong cleavage or intrusive characteristics, and, in view of the sedimentologic progression described above, is regarded as depositional. Because of their internal stratigraphy and depositional relation to the igneous rocks, the Mesozoic rocks are unlike any other in the Buckskin Mountains. Regionally, the rocks probably correlate with either the Upper Triassic(?) to Middle(?) Jurassic Vampire Formation or some younger unit, such as the Upper Jurassic(?) and Cretaceous McCoy Mountains Formation.

The inverted depositional contact, cleavage, and lithologic units in the Mesozoic rocks mimic the geometry of the underlying shear zone and define a southwest-plunging antiformal nose. In addition, the phyllitic rocks are folded by locally tight, west-trending and northwest-trending, small-scale folds, and cleavage in the rocks is locally overprinted by west-trending crenulations. The rocks are also cut by several small faults that offset contacts and the shear zones.

The igneous rocks in the upper structural plate are depositionally overlain to the southwest by southwest-dipping Tertiary clastic rocks (Spencer and Reynolds, this vol.). Restoring these clastic rocks back to their original subhorizontal attitude rotates the southwest-dipping structures in the north Swansea area into a more gently dipping attitude. Prior to Tertiary tilting, therefore, the depositional contact between the igneous rocks and the underlying Mesozoic rocks would have been gently dipping, but upside down. Likewise, the synformal anticline in the lowest structural plate would have been a southwest-facing, but northeast-opening, recumbent fold. If this fold is paired with the underlying upright Paleozoic-Mesozoic section, then the fold would have an apparent southwest vergence and be correlative with the regional D_2 event.

The overall relations explain how Tertiary sedimentary rocks can be deposited directly on the Proterozoic and Jurassic igneous rocks, whereas Paleozoic and Mesozoic rocks are still present nearby -- the Paleozoic and Mesozoic rocks were preserved during pre-middle Tertiary erosion because they were tectonically buried beneath the igneous rocks. At the start of middle Tertiary sedimentation, the landscape would have been dominated by outcrops of granite that would contain no hints of the structural complications and preserved Mesozoic-Paleozoic sections that lay at depth.

Lincoln Ranch Synform

Pre-Tertiary upper-plate rocks are not abundant in the Lincoln Ranch synform, compared to the Swansea or Planet synforms (Plate 3). Such rocks are exposed only at north Midway and in the southwestern Lincoln Ranch Basin. The Tertiary geology of the Lincoln Ranch Basin was studied by Gassaway(1972, 1973) and Spencer and Reynolds (this vol.).

Exposures at north Midway, located in the southwestern part of the synform, consist of crystalline rocks and less widespread Paleozoic metasedimentary rocks (Fig. 10 in Spencer and Reynolds, this vol.). The crystalline rocks are largely coarse-grained, porphyritic granite with mafic to intermediate dikes, some of which are diabase. The crystalline rocks are overlain by an upright sequence of Paleozoic rocks that dip moderately

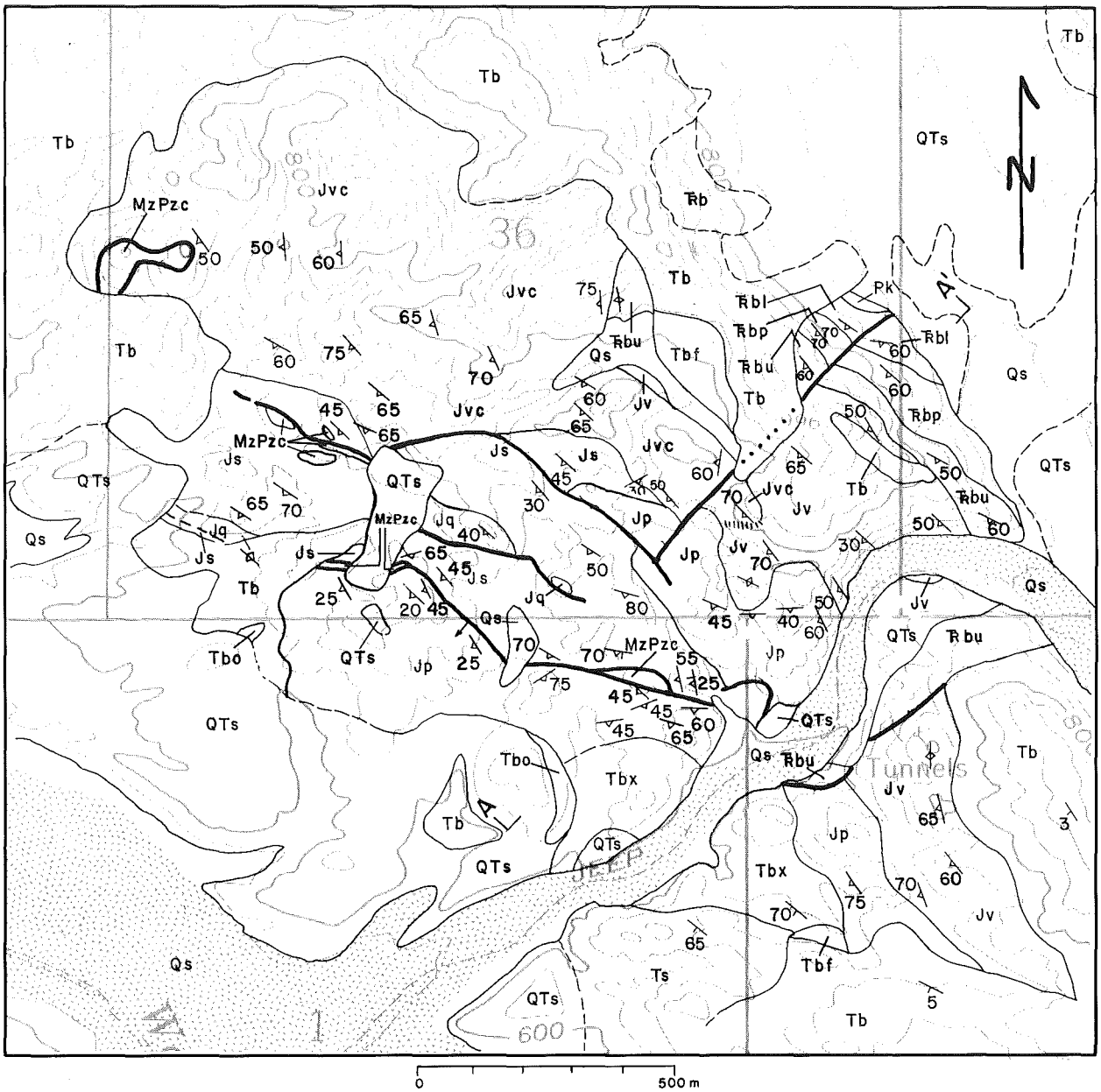

Qs	SURFICIAL DEPOSITS (Quaternary)
QTs	SEDIMENTARY ROCKS (Quaternary and Late Tertiary)
Tb	BASALT (late to middle Miocene)
Tbf	BASIN FILL (late Tertiary)
Tbx	SEDIMENTARY BRECCIA (middle Tertiary)
Ts	SEDIMENTARY ROCKS (middle Tertiary)
Jq	QUARTZITE (Jurassic?)
Js	SCHIST (Jurassic)
Jp	PLANET VOLCANICS (Jurassic; about 160 Ma)
Jv	VAMPIRE FORMATION (Late Triassic to Middle Jurassic)
Ꞧb	BUCKSKIN FORMATION (Triassic)
Ꞧbu	BUCKSKIN FORMATION, UPPER MEMBER (Triassic)
Ꞧbp	BUCKSKIN FORMATION, PHYLLITE MEMBER (Trisssic)
Ꞧbl	BUCKSKIN FORMATION, LOWER MEMBER (Triassic)
Pk	KAIBAB FORMATION (Permian)
MzPzc	CARBONATE ROCKS (Paleozoic or Mesozoic)

CONTACT; dashed where approximately located

GRADATIONAL CONTACT

10 FAULT, showing dip; dashed where approximately located; dotted where concealed

15 BEDDING

30 FOLIATION

VERTICAL FOLIATION

30 FOLIATION PARALLEL TO BEDDING

Figure 12 (previous page). Geologic map of the south Rio Vista area, western Buckskin Mountains. Boundaries of the map area are at 34°9.04', 34°10.18', 114°10.56', and 114°11.96'. Geology by S. Reynolds and J. Spencer.

to steeply to the north. The Paleozoic section is attenuated, but all of the formations are present. The base of the section is composed of about 7 m of quartzite and metasiltstone correlated with Cambrian Bolsa Quartzite and Abrigo Formation -- this is the only exposure of Cambrian rocks in the entire Buckskin Mountains. These rocks are successively overlain by approximately 2 m of Martin Formation, 5 m of Redwall Limestone, 15 m of Supai Group, 20 m of Coconino Sandstone, and 55 m of Kaibab Formation. The entire section is about 100 m thick, or only 10% of its normal regional thickness. Structural attenuation of the section was not uniform, because the Kaibab and Coconino are about 25% of their normal thickness, whereas the Martin-Redwall-Supai section is about 5% of its normal thickness.

Pre-Tertiary rocks are also exposed in the southern Lincoln Ranch Basin (Fig. 38 in Spencer and Reynolds, this vol.). Again, the main pre-Tertiary unit consists of coarse-grained granite cut by mafic to intermediate dikes. The granite locally contains a well-developed, subvertical gneissic foliation. which we interpret to be pre-Tertiary, and probably Proterozoic, in age. Such fabric is best displayed in the canyon in NE $^1/_4$ NE $^1/_4$ sec. 35, T. 10 N., R. 14 W. (see Spencer and Reynolds, this vol.). In this same canyon, the granite contains dikelike bodies of chocolate-brown carbonate that possibly represent carbonate-metasomatized mafic dikes. The entire package of rocks is bounded below by the detachment fault and is depositionally overlain by the basal Tertiary units. The rocks have been widely shattered by Tertiary normal faulting and subsequent reverse faulting, and locally have textures characteristic of a Tertiary sedimentary breccia. A discrete boundary between granite-derived sedimentary breccia and shattered granitic bedrock, if it exists, was not mapped in this area.

Upper Paleozoic rocks are present only within a single klippe above the detachment fault along the south flank of the basin. This klippe contains strongly deformed marble and quartzite that we interpret as an overturned section of Permian Kaibab Formation and Coconino Sandstone. The rocks are strongly foliated parallel to layering and the layering and foliation are folded by tight folds.

South Rio Vista

The south Rio Vista area, located in the westernmost Buckskin Mountains (Fig. 1), contains a southwest-dipping section of mostly Mesozoic rocks, the lower part of which can be correlated with Triassic and Jurassic rocks of the Mineral Hill area (Figs. 12 and 13). Rocks within this section are generally well foliated and cleaved, but are otherwise structurally simple, except for several faults and small-scale folds. The area was first mapped in reconnaissance by Frost (1983, 1987, written commun.).

The lowest unit, exposed on the northeastern edge of outcrop, is a cherty calcite marble correlated with Permian Kaibab Formation. The marble is overlain by 140 m of quartzite, calcareous quartzite, and phyllite of the Triassic Buckskin Formation. This section of Buckskin Formation contains thin equivalents to all four members identified in the Mineral Hill area, including, from bottom to top, the lower, quartzite, phyllite, and upper members. The lower member consists of ledge-forming, variably calcareous sandstone beds that alternate with slope-forming siltstone and phyllite. It is capped by several meters of the ledge-forming, greenish quartzite member, which was not mapped separately. The quartzite is successively overlain by the gray-colored phyllite member and massive, variably calcareous quartzite of the upper member, which forms a dark-weathering cliff.

The Buckskin Formation is overlain by more than 300 m of quartzite, immature quartzite, and quartzose sandstone equivalent to the Triassic(?) and Jurassic Vampire Formation. The contact between the Buckskin and Vampire Formations is apparently conformable. The Vampire Formation comprises two different lithologies that are lateral facies of one another. In the southeastern third of the area, the formation consists of iron-oxide-stained, slightly micaceous quartzite identical to that exposed in the type area near Mineral Hill. The northwestern two-thirds of outcrops of Vampire Formation are slightly micaceous quartzose sandstone that is more friable and darker weathering because of calcareous cement. The two lithologies interdigitate laterally, and beds of one facies can be followed through complete outcrop into their equivalents in the other facies.

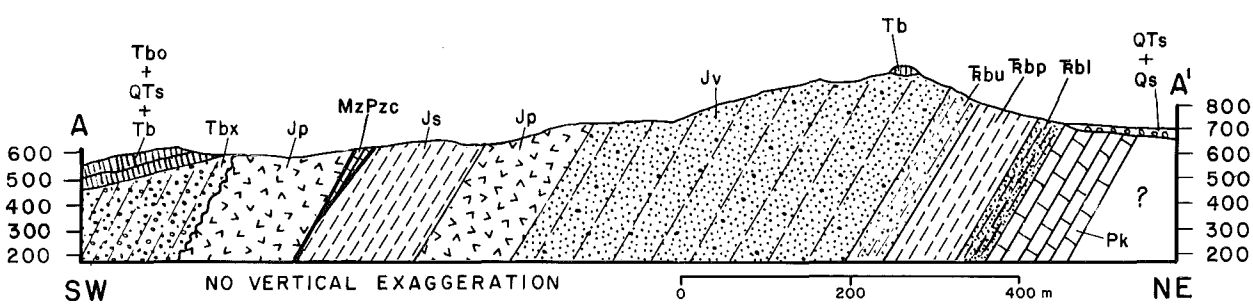

Figure 13. Geologic section of the south Rio Vista area. See Figure 12 for explanation and location of section.

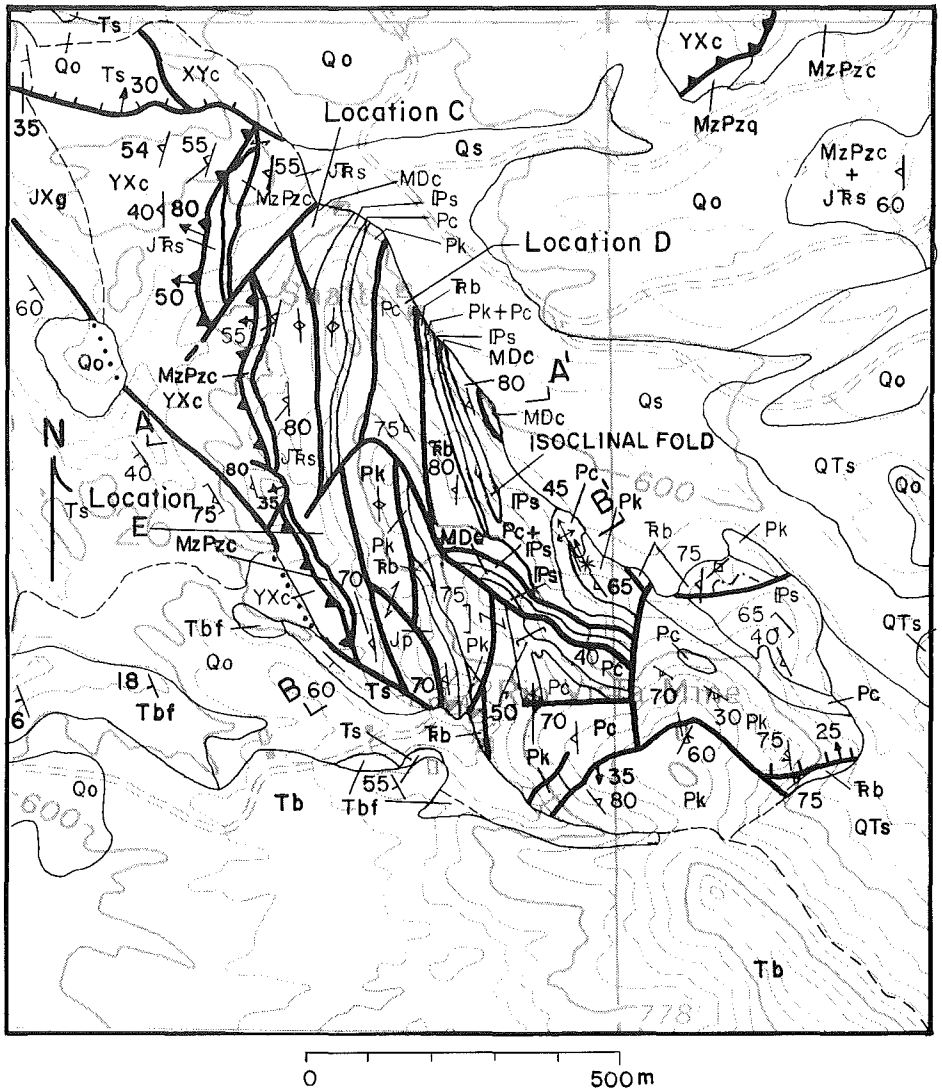

Qs	SURFICIAL DEPOSITS (Quaternary)
Qo	OLDER SURFICIAL DEPOSITS (Quaternary)
QTs	SEDIMENTARY ROCKS; LOCALLY INCLUDES BASIN FILL (Quaternary and Late Tertiary)
Tb	BASALT (late to middle Miocene)
Tbf	BASIN FILL (late Tertiary)
Ts	SEDIMENTARY AND VOLCANIC ROCKS (middle Tertiary)
JTRs	SCHIST; DERIVED FROM SEDIMENTARY AND VOLCANIC ROCKS (Jurassic or Triassic)
Jp	PLANET VOLCANICS (Jurassic; about 160 Ma)
Jv	VAMPIRE FORMATION (Late Triassic to Middle Jurassic)
TRb	BUCKSKIN FORMATION (Triassic)
MzPzc	CARBONATE ROCKS (Mesozoic or Paleozoic)
MzPzq	QUARTZITE (Mesozoic or Paleozoic)
Pk	KAIBAB FORMATION (Permian)
Pc	COCONINO SANDSTONE (Permian)
IPs	SUPAI GROUP (Pennsylvanian and Permian)
MDc	CARBONATE ROCKS; INCLUDES REDWALL LIMESTONE AND MARTIN FORMATION (Mississippian and Devonian)
JXg	GRANITE (Jurassic or Proterozoic)
YXc	CRYSTALLINE ROCKS (Proterozoic)

——— - -	CONTACT; dashed where approximately located
10 ▲ ——— - -	FAULT, showing dip; dashed where approximately located
10 ▲▲▲ - -	THRUST FAULT, showing dip; dashed where approximately located; teeth on upper plate
▙▙▙ . .	LOW-ANGLE NORMAL FAULT; ticks on upper plate
30	FOLIATION, showing trend of lineation
—◇—	VERTICAL FOLIATION
30	FOLIATION PARALLEL TO BEDDING
20	CLEAVAGE
—·—·—	MARKER BED
—✱—	SYNFORM

Figure 14 (previous page). Geologic map of the Rio Vista area, western Buckskin Mountains. Note thrust fault (Rio Vista thrust) that places Proterozoic crystalline rocks over the Paleozoic and Mesozoic rocks. Boundaries of the map area are at 34°10.38', 34°11.25', 114°11.49', and 114°12.48'. Geology by S. Reynolds and J. Spencer.

The Vampire Formation is overlain by metamorphosed quartz-feldspar-phyric volcanic rocks equivalent to the Planet Volcanics. These rocks are gray colored and mostly have a homogenous silicic composition. Where strongly deformed, the metavolcanic rocks are well-foliated, mica-bearing schist. Small blebs of magnetite are conspicuous in most lithologies. The unit includes quartz-sericite-magnetite phyllite and schist derived from volcaniclastic rocks.

Overlying the Vampire Formation is a generally slope-forming sequence of schist and other sedimentary and metasedimentary lithologies. This sequence includes silvery schist, purplish phyllite, and quartz-feldspar-lithic-bearing clastic rocks, with minor amounts of quartzose sandstone and carbonate-rich beds. The rare quartzose sandstone beds are medium to fine grained, variably calcareous, and generally less than 1 m thick; they are very similar to those present in the Vampire Formation. The carbonate beds are less than 2 m thick and are orangish-brown, a color atypical of any Paleozoic unit. Some parts of the section contain quartz-sericite-magnetite phyllite derived from volcaniclastic rocks. This section of rocks represents a higher stratigraphic level than is exposed in the Mineral Hill area.

The schist unit is capped by a shear zone that contains slices of Mesozoic and upper Paleozoic rocks. The shear zone is variably discordant to foliation and is marked by fairly brittle structures along parts of its southern extent, but elsewhere is more ductile appearing and is concordant to foliation in the adjacent rock units. It is considered to be a primarily Mesozoic structure. Above the shear zone is a sequence of Planet Volcanics, which may indicate thrust repetition of the section.

The Mesozoic rocks are depositionally overlain by southwest-dipping Tertiary sedimentary breccia, conglomerate, and sandstone. Removing the tilt of the Tertiary units would restore the Mesozoic units and their foliation to a subhorizontal attitude. The Mesozoic rocks were, therefore, gently dipping and upright prior to tilting that accompanied Tertiary detachment faulting.

Rio Vista

The Rio Vista area to the north (Fig. 1), originally mapped in reconnaissance by Frost(1983, 1987, written commun.), contains a structurally complex assemblage of Paleozoic and Mesozoic metasedimentary rocks that are overlain to the west by a major thrust sheet of crystalline rocks (Figs. 14 and 15). The Paleozoic and Mesozoic rocks generally strike north to NNW and dip steeply to the west, but are elaborately folded and cut by layer-parallel faults and ductile shear zones. The faults and shear zones separate the rocks into tabular or lenticular slices that contain partial stratigraphic sections. Some stratigraphic sections face to the west, others face to the east, and one fault slice contains opposite-facing sections that define a map-scale isoclinal fold.

The Rio Vista area is dominated by a main, north- to NNW-trending ridge. The northern part of the ridge (location *C* in Fig. 14) is composed of a nearly complete, but very attenuated, east-facing Martin-Redwall-Supai-Coconino-Kaibab section. This section is a maximum of 150 m thick, or about 15% of its regional thickness. The next fault slice to the east contains a relatively thick section of Coconino Sandstone. This slice is in fault contact further to the southeast (location *D* in Fig. 14) with Triassic Buckskin Formation that caps a west-facing, attenuated section. The Buckskin Formation is successively underlain by Kaibab Formation, Coconino Sandstone, Supai Group, and marble mostly equivalent to Redwall Limestone. The Redwall Limestone contains a steeply plunging isoclinal fold (see label in Fig. 14) that causes the Kaibab-to-Redwall stratigraphic section to reappear to the east, but with an eastward facing. This east-facing section contains another large tight fold, as defined by the outcrop pattern of the Coconino Sandstone and Kaibab Formation at the eastern limit of their outcrop.

The geologic relations change substantially to the south across a northwest- to NNW-trending fault. The ridge crest in this area is composed of a relatively thick, fault-bounded section of Kaibab Formation. The Kaibab Formation is juxtaposed to the east against a west-facing stratigraphic section that includes, from west to east, Planet Volcanics, Buckskin Formation, Kaibab Formation, and Coconino Sandstone. This section is faulted to the east against a fault block that contains wildly folded Coconino Sandstone and Kaibab Formation. In this block and another one further to the east, the two formations are kneaded together, such that curving keels and infolded sheets of one rock type are common in the other.

The Paleozoic and Mesozoic rocks described above are bounded to the west by a north-trending fault slice of schist (location *E* in Fig. 14) derived from various Jurassic and Triassic protoliths. Lithologic layering, where preserved, and foliation strike parallel to the fault slice and dip steeply. Much of the schist is derived from fine-grained clastic rocks, but metavolcanic rocks are also locally present. The schist belt is overlain to the west by a major thrust fault, here named the *Rio Vista thrust*, which carries Proterozoic crystalline rocks in its hanging wall. The thrust dips steeply to moderately to the west and is marked by thin, discontinuous slices of Paleozoic carbonate rocks, Triassic Buckskin Formation, and brown carbonate rocks of unknown age. Crystalline rocks above the thrust contain a mylonitic foliation that dips westward, parallel to the thrust. The mylonitic fabric dies out upward in the crystalline rocks away from the thrust, generally within several hundred meters. The crystalline terrain includes compositionally banded gneiss, various types of granite, and mafic to intermediate intrusions. Most of these rock types are probably Proterozoic in age, but some of the granitic and mafic

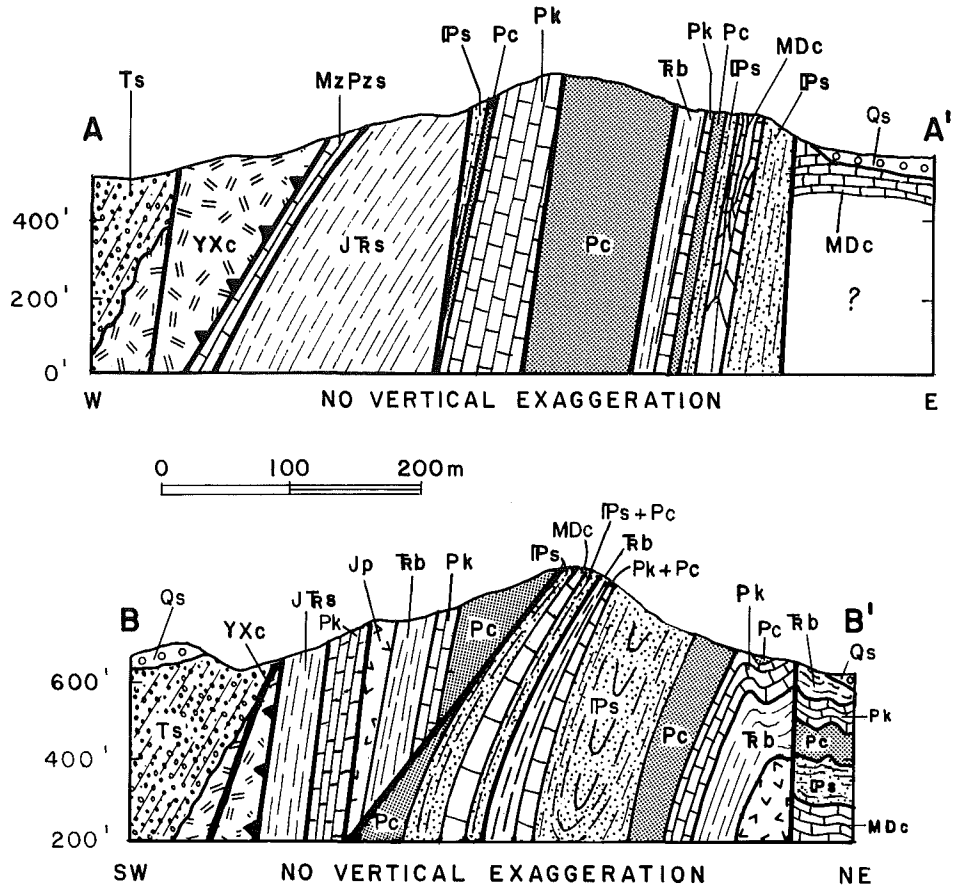

Figure 15. Geologic sections of the Rio Vista area. Note isoclinal fold within units MDc and Ꝑs on right side of sections and also that the basal Tertiary unconformity is approximately parallel to underlying thrust fault (Rio Vista thrust) in A-A'. See Figure 14 for explanation and location of sections.

rocks could be Mesozoic.

The Proterozoic crystalline rocks are depositionally overlain by and faulted against Tertiary sedimentary rocks that dip steeply to moderately to the southwest, approximately parallel to the thrust. Untilting the Tertiary rocks would restore the thrust to a gently dipping pretilting attitude. The geometric relations indicate that, prior to middle Tertiary sedimentation, Proterozoic crystalline rocks were exposed at the surface, but were underlain at a shallow depth by Paleozoic and Mesozoic rocks beneath the Rio Vista thrust.

Billy Mack Area

The Billy Mack area is located directly northeast of Rio Vista; the two are separated only by an alluvium-covered valley and probably by one or two Tertiary normal faults that project into the valley from the west (Spencer and Reynolds, this vol.). The main physiographic feature of the Billy Mack area is a northeast-trending ridge, flanked by smaller ridges to the north and a valley to the south (Figs. 16 and 17). Additional ridges and small hills are present south of the valley. The area was described by Darton (1925) and subsequently mapped and studied in reconnaissance by Zambrano (1965) and Frost (1983, 1987, written commun.).

Description. The geology of the area is dominated by northeast-striking, steeply to moderately dipping, fault-bounded slices of deformed Paleozoic and Mesozoic rocks, with local interleavings of crystalline rocks. The Paleozoic and Mesozoic rocks are overlain to the north by Proterozoic crystalline rocks above a complex thrust zone that is interpreted to be a continuation of the Rio Vista thrust. The rocks units and their bounding faults bend around to the south on the west end of the area, defining a southwest-plunging antiform.

The main ridge, containing Billy Mack Mountain, is underlain by a northeast-striking, southeast-facing section of Mississippian-Devonian carbonate rocks (Martin Formation and Redwall Limestone) and Supai Group. Lithologic layering and concordant foliation in the rocks generally dip 70° to the northwest, so the rocks are overturned. The stratigraphically lowest part of the carbonate rocks is correlated to the Martin Formation and consists of tan, medium-gray, and brownish-gray dolomite and limestone with only minor amounts of chert. The dolomitic rocks are overlain by Redwall Limestone, which consists of, from bottom to top, the following: (1) 2 m of light- to medium-gray limestone with minor amounts of chert; (2) 15 m of variably cherty, tan, tan-

nish-gray, and brown dolomite and limestone; (3) 9 m of brownish-gray limestone with ribbons of orangish-brown-weathering, light- to medium-gray chert; and (4) 4 m of somewhat mottled, medium- to light-gray, noncherty limestone. The Supai Group contains dark-weathering, orangish-brown, fine-grained quartzite with calcareous and calc-silicate beds, and thin layers of gray limestone near the base. It is overlain by Hermit Shale (not mapped) and Coconino Sandstone in two outcrops on the south flank of the ridge. Near the center of the ridge, the Supai-carbonate contact defines several large, map-scale folds. At its southwest end, the strike belt curves around to the south and projects across the main valley and into a small hill to the south. This hill (located west of Lion Hill) contains an overturned and attenuated Devonian through Triassic section.

The Billy Mack strike belt is bounded on the southeast by a northeast-striking fault that dips steeply to the northwest, concordant with lithologic layering and foliation in the strike belt. Southeast of this fault are Proterozoic crystalline rocks that generally have a well-developed mylonitic foliation concordant to the fault. In several mylonitic outcrops, steeply dipping foliation has a southeast-plunging stretching lineation and asymmetric fabrics indicative of a southeast-side-down sense of shear. Along strike to the southwest, the Proterozoic crystalline rocks pinch out and are replaced by Mesozoic schist that contains fault-bounded slices of Paleozoic carbonate rocks.

Further southeast near Lion Hill, the crystalline rocks and Mesozoic schist are in fault contact with another southeast-facing section of Mississippian-Devonian carbonate rocks and Supai Group (location *C* in Fig. 16). The fault and the Supai-carbonate contact curve to the south across the axis of the large, southwest-plunging antiform described earlier. South of Lion Hill, the carbonate rocks are in fault contact with an overturned, southwest-dipping section that includes, from top to bottom, Supai Group, Coconino Sandstone, Kaibab Formation, and Mesozoic schist. The contact between the Coconino Sandstone and Kaibab Formation is a brittle fault that need not have much displacement.

The geologic relations are more complex north of Billy Mack Mountain. The Billy Mack strike belt is bounded on its northwest flank by a fault that is poorly exposed, but probably steeply dipping. North of the fault is a belt of Mesozoic schist that is interleaved with lenticular, fault-bounded masses of Paleozoic or Mesozoic carbonate rocks. The schist includes quartz-sericite schist, silicic schist (metasiltstone), calcareous sandstone, and poorly bedded, quartz-feldspar-lithic sandstone. Some of the intersliced carbonate lenses include Kaibab Formation, but others contain marble of unknown age.

North of the schist-carbonate rocks is a fairly continuous belt composed of an overturned, southeast-facing section of Buckskin and Vampire Formations. This section is overlain to the north by a sheet of carbonate rocks, which are in turn overlain by a thrust sheet of mylonitic crystalline rocks. This thrust zone, interpreted to correlate with the Rio Vista thrust, has several branches that anastomose laterally and that locally contain shear-zone-bounded lenses of various Paleozoic and Mesozoic units.

Similarly complex relations are present to the northeast of Billy Mack Mountain. Near the boundary between sections 24 and 19, the schist belt is interrupted along strike by a southwest-plunging antiform of Kaibab Formation. This antiform is cut off to the east by several northwest-striking faults, one of which offsets the main thrust zone as well. East of the fault is a relatively intact, southeast-facing section of Kaibab, Buckskin, and Vampire Formations. The Buckskin Formation is superficially similar to the Supai Group, but is more dark-weathering (less orange), is more medium-grained, and contains abundant calcareous layers and pods, some of which are a distinctive greenish gray. Small outcrops of Coconino Sandstone are present in the proper stratigraphic position along the north edge of the Kaibab Formation. This strike belt is bounded on the south by complexly interleaved Mesozoic and Paleozoic rocks. It is also truncated to the northeast by a Tertiary normal fault that dips gently to the east and carries middle Tertiary sedimentary rocks and Proterozoic crystalline rocks in its hanging wall (east of map area).

Interpretation. The Billy Mack area contains evidence of several episodes of deformation. The earliest recorded deformation imbricated the sections and formed a well-developed foliation at a low angle to lithologic layering. Shearing during this event probably also formed many small-scale, isoclinal folds and some large-scale folds, such as the one outlined by Kaibab Formation within the Mesozoic schist belt north of Billy Mack Mountain. Subsequent to this deformation, the imbricated sections were upturned so that they strike northeast and face southeast. As is discussed later, this upturning was probably accomplished, in part, by regional, southeast-vergent folding.

The best indication of kinematics during the early episode of imbrication is recorded by mylonitic crystalline rocks southeast of Billy Mack Mountain that have lineation with a steep plunge to the southeast and a southeast-side-down sense of shear. If the upturned, southeast-facing stratigraphic sections adjacent to the mylonitic zone are restored back to a subhorizontal, upright attitude, then the mylonitic rocks would have a subhorizontal foliation, a southeast-trending lineation, and a top-to-the-southeast sense of shear. This relation suggests that the early imbrication event resulted from southeast-directed (D_1) thrusting. It is uncertain whether the thrust that places crystalline rocks over the Paleozoic and Mesozoic rocks is also related to D_1 or is younger.

Sometime after the section-imbrication event, the sections and their bounding faults were folded into an antiform that presently plunges to the southwest. The antiform either is part of a large, southeast-vergent fold or is an upright fold that is unrelated to the southeast-vergent folding event. Outcrop distributions make it impossible to determine whether the main thrust fault is also folded by this antiform, but the geometry of its offset continuation into the Rio Vista area suggests that it

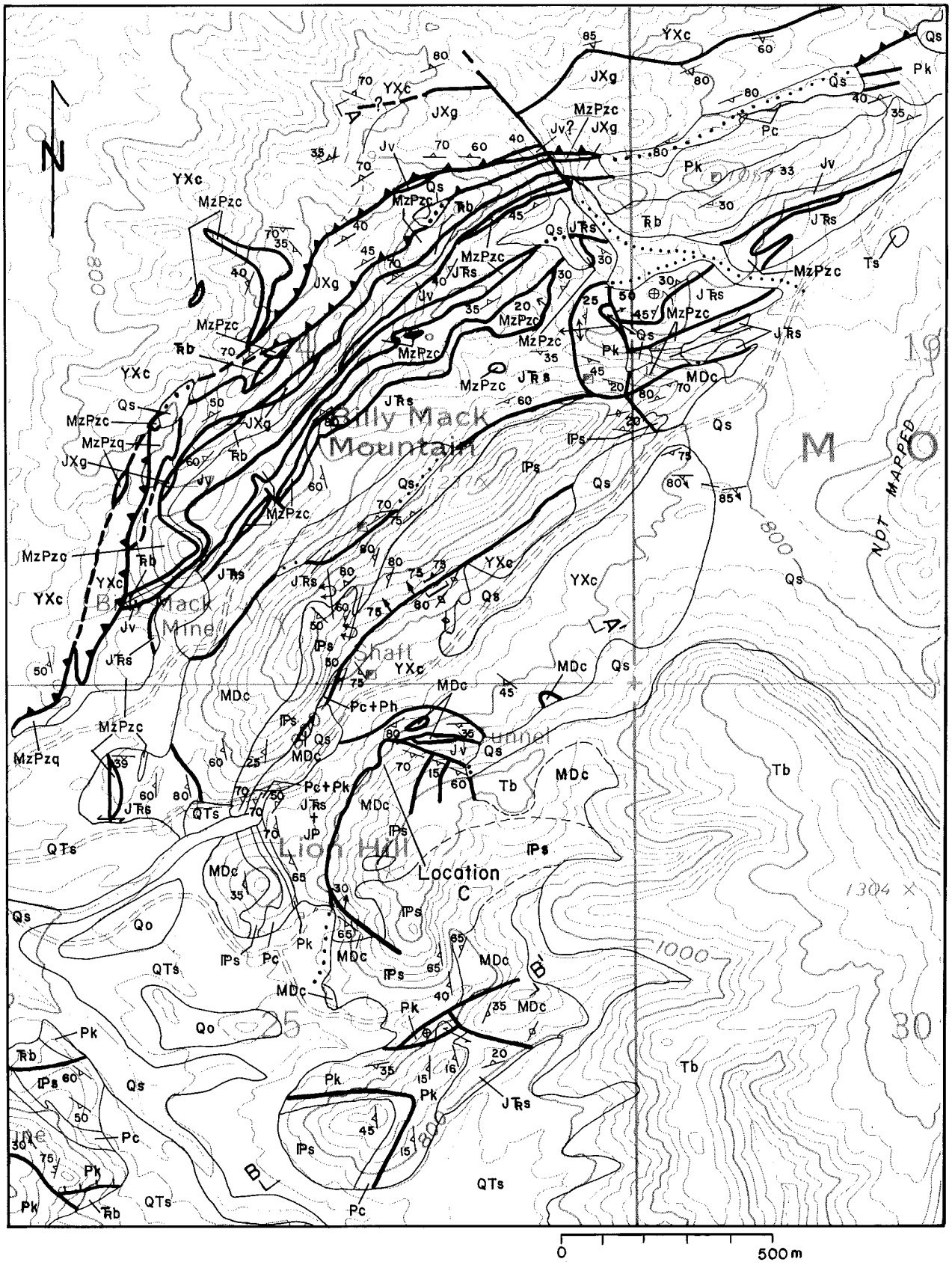

(explanation and caption on next page)

Qs SURFICIAL DEPOSITS (Quaternary)
Qo OLDER SURFICIAL DEPOSITS (Quaternary)
QTs SEDIMENTARY ROCKS; LOCALLY INCLUDES BASIN FILL (Quaternary and Late Tertiary)
Tb BASALT (late to middle Miocene)
Ts SEDIMENTARY ROCKS (middle Tertiary)
JTRs SCHIST; DERIVED FROM SEDIMENTARY AND VOLCANIC ROCKS (Jurassic or Triassic)
Jv VAMPIRE FORMATION (Late Triassic to Middle Jurassic)
TRb BUCKSKIN FORMATION (Triassic)
MzPzc CARBONATE ROCKS (Mesozoic or Paleozoic)
MzPzq QUARTZITE (Mesozoic or Paleozoic)
Pk KAIBAB FORMATION (Permian)
Pc COCONINO SANDSTONE (Permian)
Ph HERMIT FORMATION (Permian)
Ps SUPAI GROUP (Pennsylvanian and Permian)
MDc CARBONATE ROCKS; INCLUDES REDWALL LIMESTONE AND MARTIN FORMATION (Mississippian and Devonian)
JXg GRANITE (Jurassic or Proterozoic)
YXc CRYSTALLINE ROCKS (Proterozoic)

CONTACT; dashed where approximately located
10 FAULT, showing dip; dashed where approximately located; dotted where concealed
10 THRUST FAULT, showing dip; dashed where approximately located; teeth on upper plate
LOW-ANGLE NORMAL FAULT; ticks on upper plate
30 FOLIATION, showing trend of lineation; arrow shows sense of shear
VERTICAL FOLIATION
30 FOLIATION PARALLEL TO BEDDING
SUBHORIZONTAL FOLIATION
20 CLEAVAGE
ANTIFORM
OVERTURNED ANTIFORM

Figure 16. Geologic map of the Billy Mack area, western Buckskin Mountains. Fault that places Proterozoic and Jurassic(?) crystalline rocks over Mesozoic and Paleozoic rocks is shown as a thrust fault (continuation of Rio Vista thrust?), but could alternatively be some other type of fault that was folded into its present attitude. Boundaries of the map area are at 34°10.55', 34°12.12', 114°10.34', and 114°11.83'. Geology by J. Spencer and S. Reynolds.

is. The southwest plunge of the antiform is approximately parallel to the dip direction of Tertiary units in nearby areas, and would have been subhorizontal prior to Tertiary tilting.

Eagles Nest Area

The Eagles Nest area, mapped in reconnaissance by Zambrano (1965) and Frost(1983, 1987, written commun.) is located northeast of Billy Mack (Fig. 1). The area is dominated by a series of northeast-trending ridges and valleys underlain by structurally complex, northeast-striking Paleozoic and Mesozoic rocks (Figs. 18 and 19). These strike belts are overlain to the northeast by Miocene basalt and are truncated on the southwest by a major, southwest-dipping thrust fault. The upper plate of the thrust fault consists of Proterozoic crystalline rocks and Jurassic or Proterozoic granitic rocks. The

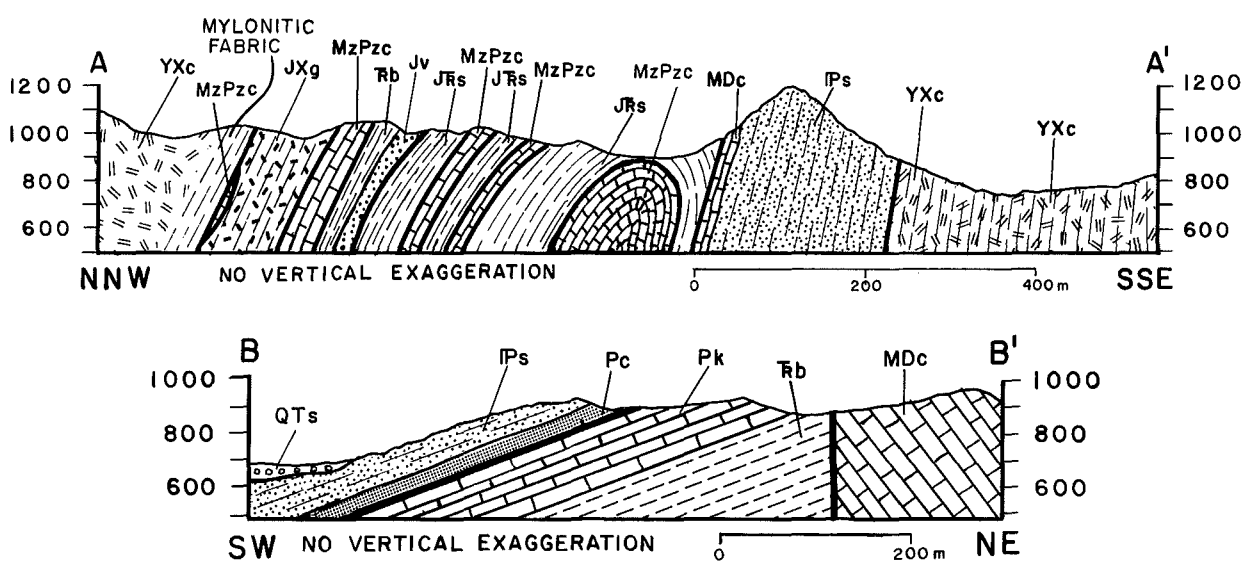

Figure 17. Geologic sections of the Billy Mack area: A-A' Billy Mack Mountain and B-B' south of Lion Hill. See Figure 16 for explanation and location of sections.

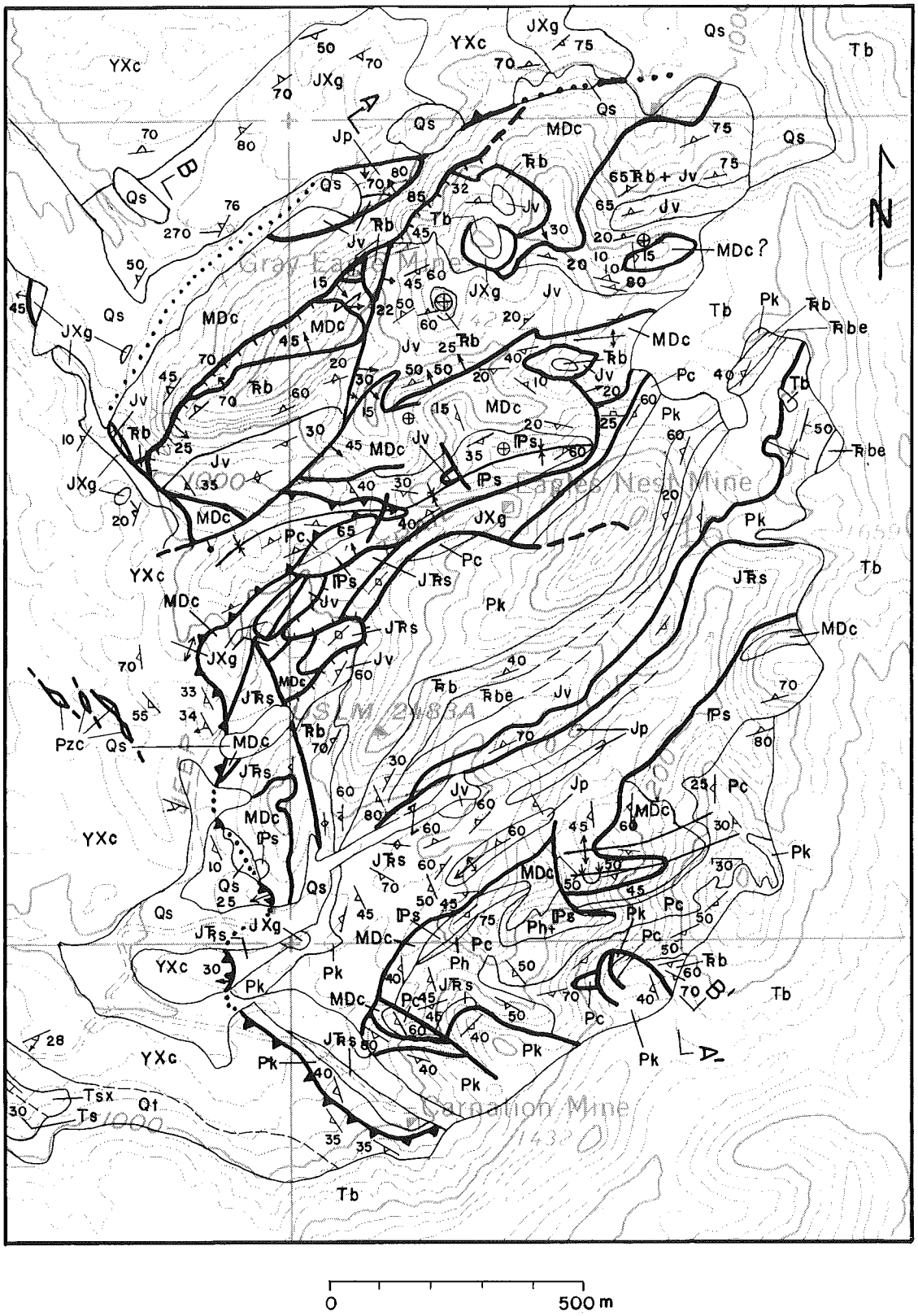

(explanation and caption on next page)

Qs	SURFICIAL DEPOSITS (Quaternary)
Qt	TALUS (Quaternary)
Tb	BASALT; LOCALLY INCLUDES BASIN FILL (late to middle Miocene)
Ts	SEDIMENTARY ROCKS (middle Tertiary)
Tsx	SEDIMENTARY BRECCIA (middle Tertiary)
JTRs	SCHIST; DERIVED FROM SEDIMENTARY AND VOLCANIC ROCKS (Jurassic or Triassic)
Jp	PLANET VOLCANICS (Jurassic; about 160 Ma)
Jv	VAMPIRE FORMATION (Late Triassic to Middle Jurassic)
TRb	BUCKSKIN FORMATION (Triassic)
TRbe	BUCKSKIN FORMATION, GYPSIFEROUS ROCKS (Mesozoic)
MzPzc	CARBONATE ROCKS (Mesozoic or Paleozoic)
Pk	KAIBAB FORMATION (Permian)
Pc	COCONINO SANDSTONE (Permian)
Ph	HERMIT FORMATION (Permian)
Ps	SUPAI GROUP (Pennsylvanian and Permian)
MDc	CARBONATE ROCKS; INCLUDES REDWALL LIMESTONE AND MARTIN FORMATION (Mississippian and Devonian)
JXg	GRANITE (Jurassic or Proterozoic)
YXc	CRYSTALLINE ROCKS (Proterozoic)

CONTACT; dashed where approximately located

10 FAULT, showing dip; dashed where approximately located

10 THRUST FAULT, showing dip; dashed where approximately located; teeth on upper plate

LOW-ANGLE NORMAL FAULT; ticks on upper plate

30 FOLIATION, showing trend of lineation

VERTICAL FOLIATION

30 FOLIATION PARALLEL TO BEDDING

SUBHORIZONTAL FOLIATION

JOINT

SYNFORM

ANTIFORM

OVERTURNED SYNFORM

Figure 18. Geologic map of the Eagles Nest area, western Buckskin Mountains. Boundaries of the map area are at 34°11.80', 34°13.12', 114°8.14', and 114°9.27'. Geology by S. Reynolds and J. Spencer.

Proterozoic rocks are depositionally overlain to the southwest by the southwest-dipping Tertiary sedimentary rocks that continue westward until they are cut off below by the low-angle normal fault in the Billy Mack area (Frost, 1987, written commun.; Spencer and Reynolds, this vol.). The geology of the Eagles Nest area will be described from north to south.

Description. The northern part of the area contains Jurassic or Proterozoic leucocratic granite and Proterozoic crystalline rocks that commonly have a steep, northeast-striking foliation. These rocks are juxtaposed to the southeast against Mississippian and Devonian carbonate rocks along a northeast-striking, steeply dipping fault that is subconcordant to foliation in the crystalline rocks. A sliver of Mesozoic rocks, consisting of a northwest-facing section of Planet Volcanics and Vampire Formation, is locally present along the fault.

The Mississippian and Devonian carbonate rocks strike northeast and generally dip steeply to moderately to the northwest. They consist of massive tan, brown, and gray, noncherty dolomite (Martin Formation) and white to light-gray or pinkish limestone (Redwall Limestone). To the southeast, the carbonate rocks are faulted over Triassic Buckskin Formation along a northwest-dipping ductile shear zone that locally contains small, unmapped slivers of other rock units, including mylonitic Coconino Sandstone and Mesozoic schist. The shear zone has been offset by a southeast-dipping low-angle fault that is interpreted to be Tertiary because it is brittle, is relatively sharp and planar, and contains northeast-trending striae, such as are typical of Tertiary normal faults. The Tertiary fault has an apparent reverse separation in Figure 19 because slip on the fault, based on striae, is perpendicular to the line of section and is more northerly than the strike of the units. The fault is probably a lateral ramp on a northeast-dipping normal fault. Like many Tertiary faults, it is locally mineralized with hematite and chrysocolla.

Triassic Buckskin Formation below the ductile shear zone strikes northeast and is in depositional contact with Vampire Formation to the southeast. The two units are subvertical and face southeast at the lowest structural levels, but become more gently northwest dipping upward, defining an overturned, southeast-facing fold. This fold is also reflected by the geometry of the ductile shear zone that bounds the units to the north, but the shear zone is discordant to the units and locally cuts Vampire Formation in its footwall. The middle of the Buckskin-Vampire strike belt is cut by a northeast-striking, southeast-dipping normal fault that is truncated by the more gently dipping Tertiary normal fault described above.

The Buckskin Formation in this area consists of brown- and tan-weathering, cliffy, medium-grained sandstone that is mostly well sorted and quartzose, but that locally contains several percent muscovite in the matrix and some thin beds of muscovitic phyllite. It is thinly layered to massive and includes thin conglomeratic zones with small (less than 0.5 cm in diameter) quartzite clasts. The section contains greenish-gray calc-silicate rocks and is most calcareous near its base. The Vampire

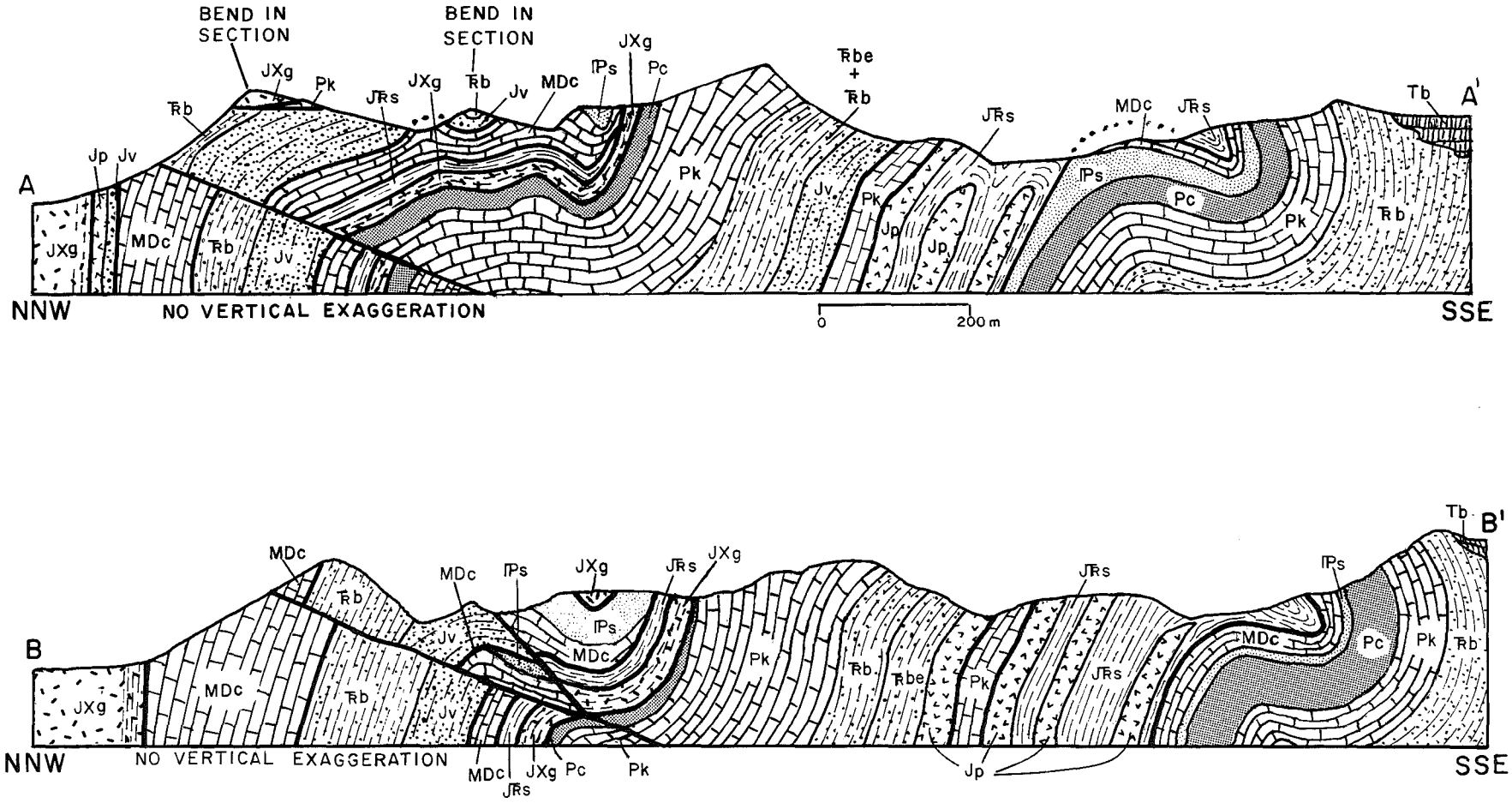

Figure 19. Interpretive geologic sections of the Eagles Nest area. Tertiary normal faults on left side of section have apparent reverse separation on these sections because their displacement direction is perpendicular to the page. See Figure 18 for explanation and location of sections.

Formation is typical, but contains coarser grained sandstone and gritty conglomerate along its basal contact with the Buckskin Formation.

To the south, the Vampire Formation overlies Mississippian and Devonian carbonate rocks along a shear zone that is folded, but that generally dips moderately to the north. The shear zone projects to the south into a synformal klippe (located 300 m NNE of Eagles Nest mine) containing an inverted Vampire-Buckskin section. The carbonate rocks beneath the shear zone contain several large upright and recumbent folds. They are depositionally overlain to the south by a right-side-up section of Supai Group and Coconino Sandstone that define a southwest-plunging syncline.

The Supai Group is in fault contact to the southeast with Jurassic or Proterozoic granite and with Mesozoic schist. This fault is at least locally sharp and quite brittle appearing, but wraps around the hinge of the southwest-plunging syncline as if it was folded.

To the southeast, the granite is in steep fault contact with a northeast-striking, southeast-facing section of Coconino Sandstone and Kaibab, Buckskin, and Vampire Formations. This section generally dips steeply to the northwest and is therefore overturned. The Buckskin Formation in this section is a distinct facies that is largely a slope former containing abundant evaporite rocks. The complete Buckskin section includes the following, from stratigraphic bottom to top: (1) 2 m of cream-colored, fine-grained platy quartzite that is in depositional contact with Kaibab Formation; (2) 12 m of dark-weathering, well-sorted to moderately sorted, fine- to medium-grained, quartzose sandstone that is calcareous, very slightly feldspathic, and locally associated with quartzite-pebble conglomerate; (3) 12 m of cream-colored to pinkish, medium-grained, moderately to well-sorted, quartzose sandstone with a calcareous cement; this sequence contains a 2-m-thick interval of dark-weathering sandstone like that described above; and (4) 9 m of gypsiferous rocks (anhydrite at depth?) interbedded with both cream-colored and dark-weathering sandstones and with greenish mica schist; these rocks are stratigraphically overlain by orange-weathering quartzites typical of the Vampire Formation.

Southeast of the Vampire Formation is a steeply dipping, fault-bounded sliver of Kaibab Formation and evaporitic Buckskin Formation. Further southeast is a belt of Mesozoic schist, calcareous sandstone, and volcanic rocks. Foliation in these rocks generally dips to the northwest or west and is locally folded into southwest-plunging isoclines cored by Planet Volcanics.

The Mesozoic schist is juxtaposed to the southeast against a nearly complete, southeast-facing Paleozoic section, which includes, from north to south, Mississippian-Devonian carbonate rocks, Supai Group, Hermit Shale, Coconino Sandstone, and Kaibab Formation. The Kaibab Formation is depositionally overlain by Triassic Buckskin Formation at the southern limit of pre-Tertiary outcrop. The Paleozoic units vary in attitude from steeply dipping to upside-down and define a southwest-plunging overturned synform and associated antiform that fold the inverted part of the section. The synform and antiform also fold the fault contact with Mesozoic schist to the north; a keel of Mesozoic schist overlies the upside-down Paleozoic section in the core of the synform.

Throughout much of the area, rocks with a well-defined planar fabric (cleavage, schistosity, or foliation) are variably overprinted by crenulations and associated crenulation cleavage. Crenulations typically plunge gently to moderately northwest to southwest and have WNW-striking, subvertical axial surfaces. Crenulation cleavage is parallel to axial surfaces and generally has a spacing of 1 mm to 3 cm. Crenulations are best developed in areas where layering is gently dipping.

In a spectacular relationship, all of the northeast-trending strike belts in the area are truncated discordantly to the southwest by an overlying thrust sheet of crystalline rocks. The thrust zone dips moderately to the southwest and is marked by southwest-dipping mylonitic fabric in the overlying crystalline rocks. As lithologic layering and foliation in the underlying Mesozoic-Paleozoic strike belts approach to within tens of meters of the thrust, they bend into subparallelism with it and are locally detached into fault-bounded slivers along the thrust. The thrust and its associated fabric cut discordantly across the southeast-facing fold in the northernmost strike belt, but are clearly folded by the southwest-plunging synform exposed north of the Eagles Nest mine. Also, the thrust apparently bends around the western end of the northernmost strike belt to merge with or become the fault that juxtaposes the strike belt with crystalline rocks to the north. The key junction is unfortunately buried beneath Quaternary deposits.

Interpretation. The structural framework of the Eagles Nest area is so complex that reconstructing the sequence of deformations is fraught with uncertainties. The earliest structural event imbricated the Mesozoic-Paleozoic rocks along faults that now separate the different strike belts. Shearing associated with the imbrication formed cleavage and foliation at a low angle to lithologic layering in the rocks. Shearing was also accommodated by the formation of some small-scale and perhaps large-scale folds, such as (1) those within the Mississippian-Devonian carbonate rocks north of the Eagles Nest mine and (2) isoclines of Planet Volcanics within Mesozoic schist north of the Carnation mine. The amount of tectonic transport during this event was substantial, as is reflected by the juxtaposition of dissimilar Mesozoic facies in adjacent strike belts. This event would correlate regionally to D_1.

Subsequent to their imbrication, the rocks were upturned, such that they now strike northeast and generally face southeast. This upturning was probably accomplished by folding, based on regional considerations and on the presence of several large, southeast-facing folds. Such large folds are present in the northernmost Buckskin-Vampire strike belt, the central Coconino-Kaibab-Buckskin strike belt south of the Eagles Nest mine, and the southernmost Paleozoic strike belt. In all three areas, faults bounding the strike belts are also warped into southeast-opening folds. The most dramatic example

of this is in the southernmost strike belt, where a synformal keel of Mesozoic schist rests in folded-fault contact on an upside-down Paleozoic section.

If the southeast-facing sections are unfolded and reconstructed back to a subhorizontal, upright attitude, the section-bounding faults would appear as a series of gently dipping thrust faults. Most of the sections between the thrust plates would be upright, except for the central Mississippian-Devonian strike belt -- this section, which is the only one that is presently right-side up, was probably the only one that was originally upside down prior to formation of the southeast-facing folds. The large, tight folds within this strike belt may have formed when the section was originally overturned.

At some point, a thrust plate of Proterozoic and Jurassic(?) crystalline rocks was emplaced discordantly across the upturned sections. This thrust presently dips moderately to the southwest, but would reconstruct to a subhorizontal attitude if the depositionally overlying middle Tertiary rocks are untilted. This thrust cuts discordantly across the large southeast-facing folds, but is folded by the southwest-plunging synform. There is evidence, therefore, for two episodes of folding about northeast-southwest axes: one prior to the thrust and one after it. It is unclear whether the thrust bends around the corner of the northern strike belt because it has been folded or whether the northwest- and northeast-trending thrust segments are actually two different generations of faults. Alternatively, the folding of the thrust reflects a later generation of large-scale, upright folding about northeast-southwest axes.

The timing of the one or more crenulation events within this deformational sequence is somewhat uncertain. The crenulation certainly postdates the section imbrication and southeast-facing folds, because it is overprinted across the folds without regard for orientation of layering; it is best developed where layering was gently dipping -- that is, perpendicular to the direction of shortening during the crenulation-forming event. Some crenulations would have probably been formed during folding that formed the southwest-plunging synform, but others may have formed either earlier or later.

DISCUSSION

The upper plate of the Buckskin detachment fault contains a diverse suite of pre-Tertiary rocks and structures. The rock units include Proterozoic crystalline rocks, middle and upper Paleozoic sedimentary rocks, and a diversity of Mesozoic units. These rocks are structurally very complex because of several intricately superposed episodes of thrusting, folding, and section attenuation. The complex stratigraphic and structural relations, however, are consistent with those of the region, and provide additional constraints on the regional geologic evolution.

Proterozoic and Paleozoic Rocks

The oldest upper-plate units are crystalline rocks, including unfoliated to weakly foliated granitic rocks, mafic intrusions, and compositionally banded gneiss. The gneissic and granitic rocks are inferred to be largely Proterozoic in age because they are (1) lithologic similar to dated Proterozoic rocks, (2) depositionally overlain by Cambrian quartzite in the north Midway area and in other parts of the region, and (3) depositionally overlain by Jurassic(?) rocks in the north Swansea area. For the same reasons, we also regard the high-grade compositional banding in the gneiss to be largely Proterozoic in age, but cannot rule out the possibility that some gneissic fabric is Mesozoic. Arguing against this latter possibility is the absence of comparable high-grade fabric in any Paleozoic or Mesozoic upper-plate rocks. Mesozoic gneissic fabric is probably present, however, in rocks *beneath* the Buckskin detachment fault (Bryant and Wooden, this vol.).

It is remarkable that Proterozoic crystalline rocks are still depositionally attached to the Paleozoic section in only one area in all of the Buckskin Mountains (north Midway). As discussed later, this relation indicates that a regional decollement formed within the Cambrian section during Mesozoic thrusting. This implies that presently adjacent Proterozoic and Paleozoic thrust slices may not have originated in the same part of the region. Further study of the Proterozoic rocks may help identify the regional provenance of such rocks, thereby constraining the magnitudes of tectonic transport during Mesozoic thrusting and Tertiary detachment faulting. At this point, we can state only that Proterozoic rocks above the detachment fault are very different in present appearance and interpreted protolith from those below the fault. This implies that the two assemblages of rocks originated in different parts of the region and (or) different crustal depths. This lithologic mismatch, however, is probably the cumulative effect of large-scale transport during both Mesozoic and Tertiary time.

Paleozoic strata in the Buckskin Mountains have been metamorphosed, ductilely deformed, and slivered into thin fault-bounded slices. Nearly all Paleozoic sequences have been extremely attenuated, some to less than several percent of their original thickness. Individual formations are nevertheless mostly still recognizable because of their distinctive lithologies and position in the stratigraphic sequence. The main difficulty is determining whether some carbonate-siliciclastic-quartzite sequences represent a Martin-Redwall-Supai-Coconino section or a Kaibab-Buckskin-Vampire section. Key distinguishing features include the following: (1) Kaibab Formation is generally more cherty and more gray than Redwall-Martin sequences; also, Redwall Limestone commonly has a pinkish mottling; (2) Supai Group is finer grained, better sorted, and more orangish than Buckskin Formation, which is slightly feldspathic and commonly contains greenish phyllite, evaporitic rocks, and rare conglomerate; and (3) Coconino Sandstone is fine grained, homogeneous, and pinkish-tan weathering, whereas Vampire Formation varies in grain size from fine grained to gritty and weathers to shades of gray, tan, orange, and red. The distinction between Coconino Sandstone and

Vampire Formation is generally the easiest one to recognize. Differentiating Kaibab Formation from Redwall-Martin sequences is especially difficult where Kaibab is dolomitic, rather than being cherty, gray limestone.

There are some lithologic variations among Paleozoic sections, both between neighboring areas and between adjacent fault slices within a single area. For example, Hermit Shale is present in some sections, but not in others. Regionally, Hermit Shale is absent in Paleozoic sections further southeast into Arizona (Reynolds and others, 1986b), but is present as a westward-thickening wedge in areas to the north and west (Fig. 3; Stone and others, 1983). According to the regional trends, the pinch-out of the Hermit Shale should be located near the Buckskin Mountains. The sporadic presence of a thin sequence of Hermit Shale in the Buckskin Mountains is perfectly consistent with these trends, and indicates that (1) the rocks are approximately within their proper regional context, in spite of the extreme Mesozoic deformation, and (2) thrusting has interleaved rocks from both sides of the Hermit pinch-out.

Another possibly important trend is that Kaibab Formation is more gray and cherty where it is overlain by phyllitic and evaporitic Buckskin Formation, but contains more tan, noncherty dolomite where it is overlain by less phyllitic, sandstone-dominated Buckskin Formation. Further study of such variations may help constrain the regional prethrust provenance of individual thrust slices.

From the observed stratigraphy, all Paleozoic sections in the Buckskin Mountains are cratonic in character, as is typical of the region (Stone and others, 1983; Reynolds and others, 1986b). Although extremely attenuated by Mesozoic deformation, most sections were probably originally only about 1 km thick, judging from the thickest preserved sections and from regional relations. The general lack of Cambrian rocks reflects structural omission, not original nondeposition.

Mesozoic Rocks

Mesozoic rocks in the Buckskin Mountains can be largely correlated with those of the surrounding region, but correlation to rocks outside the region (e.g., Colorado Plateau) is made difficult by the lack of fossils and the general lack of reliable geochronologic data. Also, there is much variability within the Mesozoic stratigraphy, because Mesozoic thrusting juxtaposed rocks from different parts of the region and because Mesozoic depositional facies were no doubt complex and laterally variable. On the basis of existing data, all Mesozoic rocks above the Buckskin detachment fault are considered to be Triassic and Jurassic in age. The area evidently lacks Cretaceous units, such as the McCoy Mountains Formation, that are so abundant further south in the region. This implies that the region was structurally high during the Cretaceous and may have been part of the source for clastic detritus in the McCoy Mountains Formation.

The stratigraphically lowest Mesozoic unit is the Buckskin Formation, which in the Buckskin Mountains can be subdivided into two general facies. One facies, represented by the Mineral Hill and south Rio Vista sections, generally contains representatives of the four members, including the distinctive, cliff-forming upper member. This facies is apparently also present in the eastern Rio Vista, northeastern Billy Mack, northern Eagles Nest, and north Swansea areas. The second facies lacks the upper member and is dominated by slope-forming phyllite and sandstone, commonly with evaporitic rocks. This facies is represented in the Copper Penny, central and southern Eagles Nest, western Billy Mack, and northern Rio Vista areas. The two facies have been juxtaposed by Mesozoic thrusting, such as in the Eagles Nest area, where they are present in adjacent strike belts.

The Buckskin Formation depositionally overlies Kaibab Limestone and has been correlated largely with the Lower to Middle(?) Triassic Moenkopi Formation of the Colorado Plateau (Reynolds and others, 1987). The consistent preservation of Permian Kaibab Limestone beneath the Buckskin Formation indicates a lack of significant latest Permian to early Triassic tectonism. Based on analogies with the Moenkopi Formation, the presence of gypsum and rare carbonate beds in the Buckskin Formation implies deposition in a low, marginal marine environment. The lithologic character of the Buckskin Formation in the Buckskin Mountains, including its coarseness compared to sections of Moenkopi Formation farther north and its lack of thick marine carbonate zones, implies that the rocks have more or less remained in their proper paleogeographic setting, in spite of their complex structural history (Reynolds and others, 1987).

The overlying Vampire Formation, because of uncertainties in its age, is more difficult to correlate with units outside of the region. It is equivalent to the upper two members of the Palen Formation of southeastern California (Stone and Kelley, 1988), but the Palen Formation is also essentially undated. The Vampire Formation postdates the Buckskin Formation, predates the 160 Ma Planet Volcanics, and is therefore Late Triassic to Middle Jurassic in age. It could be correlative with the Late Triassic Chinle Formation or some parts of the Jurassic Glen Canyon and San Rafael Groups (Reynolds and others, 1987).

The Vampire Formation records an episode of Late Triassic and Early Jurassic tectonism because it (1) contains an increased feldspathic or volcanic-lithic component; (2) includes a basal conglomerate that contains clasts of crystalline rocks, including some derived from Proterozoic basement; and (3) overlies an unconformity cut on Triassic Buckskin Formation and older rocks (Reynolds and others, 1987, 1989). Regionally, the basal conglomerate of the Vampire Formation reflects the uplift and erosional unroofing of Paleozoic and Proterozoic rocks. Evidence of this uplift is preserved south of the Buckskin Mountains, in the Granite Wash Mountains and southern Plomosa Mountains, where Vampire Formation and Jurassic volcanic rocks unconformably overlie Proterozoic crystalline rocks and Lower Paleozoic strata (Reynolds and others, 1989). This uplift may also be repre-

sented at north Swansea, where Mesozoic rocks are is depositional contact with crystalline rocks. The uplift is a likely source of detritus for Upper Triassic to Middle Jurassic rocks on the Colorado Plateau.

The stratigraphically higher Planet Volcanics are part of a regionally extensive suite of Jurassic volcanic rocks dated at about 160 Ma (Reynolds and others, 1987; Tosdal and others, 1988; Tosdal, 1988). These volcanic rocks were deposited across the eroded remnants of the Late Triassic and Early Jurassic uplift. The volcanic rocks are overlain by or otherwise associated with phyllite and volcaniclastic rocks in the south Rio Vista, Billy Mack, and Eagles Nest areas. These overlying rocks are dissimilar from the Jurassic(?) and Cretaceous McCoy Mountains Formation, which depositionally overlies the Jurassic volcanic sequence further south in the region (Harding and Coney, 1985; Stone and others, 1987; Tosdal and others, 1988). The phyllitic rocks may reflect local sedimentation at about the same time as volcanism, or else may represent a younger, unrelated sequence of rocks that elsewhere in the region was removed by erosion prior to deposition of the McCoy Mountains Formation.

Mesozoic Structures

The complex overprinting of folds, thrust faults, and cleavages in the Buckskin Mountains is typical of the region, especially within the Maria fold-and-thrust belt, an east-west-trending belt of major thrust faults and large-scale folds (Reynolds and others, 1986b). Structures within the Maria belt are interpreted to be the result of four main phases of Mesozoic deformation, referred to (from oldest to youngest) as D_1, D_2, D_3, and D_4.

The first phase (D_1) consisted of southeast-directed thrusting and folding, and has been subdivided into two subphases, termed D_{1a} and D_{1b}. The earliest subphase (D_{1a}) was characterized by southeast-directed thrusting that imbricated and attenuated stratigraphic sections. The second subphase (D_{1b}) consisted of southeast-vergent, recumbent folding of D_{1a} thrusts and associated imbricated and attenuated sections. This folding upturned many attenuated and thrust-repeated sections into a steep, southeast-facing attitudes.

The second main phase of deformation (D_2) was dominated by south- to southwest-directed thrusting (D_{2a} subphase) and subsequent folding about NNW-trending axes (D_{2b}). D_2 thrusts discordantly cut across the upturned D_1 structures and typically carry Proterozoic and Jurassic crystalline rocks in their hanging walls.

The third phase of deformation (D_3) is recorded by west- to northwest-trending folds and crenulations that commonly fold D_2 fabrics and that are associated with localized zones of spaced cleavage, crenulation cleavage, and south- or north-directed brittle-ductile thrusts. D_4 resulted in local folding, northeast-directed shearing, and the development of southwest-dipping cleavage in receptive rocks.

Of these four phases of deformation, only the first three appear to be well represented in the Buckskin Mountains. Structures interpreted to be related to D_1 are nearly ubiquitous, especially in the upturned, southeast-facing sections in the Rio Vista, Billy Mack, Eagles Nest, and Swansea areas. These sections are strongly attenuated, locally contain interfolial, isoclinal folds, and are imbricated by steep, layer-parallel faults that we interpret to be upturned D_{1a} thrusts. D_{1b} southeast-vergent folds locally fold the D_{1a} thrusts and attenuated sections and are interpreted to be responsible for the general southeastward facing of the sections. Steeply plunging lineation in crystalline rocks interslivered with some strike belts is probably originally southeast-trending D_{1a} lineation that has been upturned during D_{1b} folding. Many moderately to steeply dipping thrusts, however, such as those on the north flank of Billy Mack Mountain, are not well lineated and could be either D_1 or D_2 structures.

Some structures are probably related to D_2, including the southwest-dipping thrust that discordantly cuts the strike belts in the Eagles Nest area. Such discordance is typical of D_2 structures. Also, this thrust locally has a southwest-trending stretching lineation similar to that in D_2 thrusts elsewhere in the region. Other structures probably related to D_2 include (1) the Rio Vista thrust, (2) shear zones and fabric in the Mineral Hill and south Rio Vista areas, (3) thrust sheets of crystalline rocks in the Copper Penny area, and (4) a fold with apparent southwest vergence at north Swansea. One common feature of D_2 structures is that they would restore back to subhorizontal attitudes when the effects of Tertiary tilting are removed. This is in contrast to D_1 thrusts, which would retain their steep, northeast-striking attitude.

D_3 is manifest primarily as northwest-, west-, and southwest-trending folds and small-scale crenulations with associated, steep crenulation cleavage. Such structures are well displayed at Copper Penny, where they fold an inverted Paleozoic-Mesozoic section and overlying crystalline thrust sheet. Crenulations are also widespread in the Mineral Hill and Eagle Nest areas. Some larger folds, such as the synform that folds the southwest-dipping thrust in the Eagles Nest area, may also be related to D_3. The large southwest-plunging antiforms at Rio Vista and Billy Mack would be D_3 folds if they fold the Rio Vista thrust and the thrust is a D_2 structure. Alternatively, the antiforms could be related to D_{1b} if the Rio Vista thrust and its probable continuation into the Billy Mack area are D_{1a} structures. The map relations are not diagnostic.

Besides providing evidence for the three main episodes of deformation, structures within the Buckskin Mountains provide insight into the regional controls of deformation. The Eagles Nest, Billy Mack, and Rio Vista areas contain some of the most spectacular examples of D_{1a} thrust sheets in all of the region. An important characteristic of these thrust sheets is the total lack of Cambrian Bolsa Quartzite, the basal Paleozoic unit, in any sheet. Upturned D_{1a} thrust faults are commonly localized within one of three specific stratigraphic intervals: (1) the base of the Devonian Martin Forma-

tion, presumably within the Cambrian Abrigo Formation or its equivalent the Bright Angel Shale; (2) near the base of the Coconino Sandstone (within the Hermit Shale, where present); and (3) the evaporitic section within the lower Buckskin Formation. All three intervals contain structurally weak rocks that would have been ideal zones of décollement during thrusting. We conclude, therefore, that D_{1a} thrusting was characterized by a décollement, ramp-and-flat style, in which the gently dipping segments of thrusts (i.e., the flats) are localized within relatively weak rock units, such as shales. In order for the thrusting to take advantage of sedimentary layering, the layering must have been relatively gently dipping and structurally uncomplicated at the start of thrusting. This implies that D_{1a} was the first major deformation to have affected the Paleozoic and Mesozoic rocks. Extreme attenuation of stratigraphic sections during D_{1a} thrusting also indicates that the rocks were at sufficient depths and temperatures for ductile flow during D_{1a} thrust burial.

In contrast, D_2 thrusts generally were not controlled by preexisting layering in the rocks. The primary explanation of this is that D_1 deformation, especially D_{1b} folding, had placed the rocks into an upturned, northeast-striking attitude that was an extremely unfavorable (one might say impossible) orientation for reactivation during northeast-southwest-directed D_2 thrusting. As a consequence, D_2 thrusts had no choice but to forge new paths discordantly through the upturned sections, D_{1a} thrusts, and D_{1b} folds. D_2 deformation also occurred at deep enough conditions for ductile flow.

The complex Mesozoic structures in the Buckskin Mountains are well north of the main belt of similar structures within the Maria fold-and-thrust belt. Because the structures are above the Buckskin detachment fault, however, they need to be restored several tens of kilometers to the southwest, relative to the lower-plate rocks, to be placed in their proper pre-Tertiary context. Such restoration places the rocks squarely within the main Maria belt, in the vicinity of the Riverside Mountains. The Riverside Mountains contain Mesozoic rocks and structures comparable to those in the Buckskin Mountains (Carr and Dickey, 1980; Lyle, 1982) and are a likely lower-plate source for rocks in the western Buckskin Mountains.

The crystalline rocks above the Rio Vista thrust in the western Buckskin Mountains are part of a large region that extends northward to Lake Mead in which Proterozoic rocks are widely exposed at the surface. Paleozoic and Mesozoic sedimentary rocks were removed by Mesozoic and early Tertiary erosion in this region, but were preserved to the south of the Rio Vista thrust because they were tectonically buried -- and therefore protected from erosion -- by thrust faulting. The Rio Vista thrust, which we consider to be the structurally highest thrust of the Maria fold-and-thrust belt, is therefore a regional feature that helps to account for the widespread preservation of Paleozoic and Mesozoic rocks in west-central Arizona and their absence further north. Note, however, that crystalline rocks in the north Swansea area are depositionally overlain by Mesozoic sedimentary rocks, and therefore are probably in the footwall, rather than the hanging wall, of the Rio Vista or related thrusts.

Finally, it is instructive to point out what the middle Tertiary landscape looked like prior to detachment faulting. Proterozoic crystalline rocks were the most abundant rocks at the surface in middle Tertiary time, because they are the most common substrate for the basal Tertiary units. These crystalline rocks, however, were underlain at a shallow depth by subhorizontal thrusts, beneath which were highly folded and faulted Paleozoic and Mesozoic strata. A primeval geologist walking on the crystalline-dominated landscape may never have surmised that such *terra firma* was actually an allochthonous slice above a regional thrust. We wonder whether other such surprises are lurking in the desert of western Arizona even today.

APPENDIX 1

MEASURED SECTION OF THE MIDDLE PART OF THE BUCKSKIN FORMATION, MINERAL HILL AREA

This measured section is located in the Mineral Hill area, 600 m south of the Mineral Hill mine in the center of sec. 10, T. 10 N., R. 17 W. (location shown on Fig. 4). The units are described below, from top to bottom. Section measured by S. Reynolds, J. Spencer, and R. Nicholson.

UPPER MEMBER

Basal part is poorly bedded to massive quartzose sandstone, light to medium gray with brown tint, fine to medium grained. Generally is heavily desert varnished. This resistant member typically forms dark, precipitous ridges.

PHYLLITE MEMBER, 31.5 M THICK

Interbedded sandstone, phyllitic sandstone, and phyllite, silvery gray and slope forming.

Unit D, 4.5 m thick

Thin-bedded to laminated phyllitic siltstone to quartzose sandstone. Sandstone is moderately sorted, medium to

fine grained, and variably muscovitic. Overall color of unit is light to medium gray and silvery gray with local, greasy greenish clots that could be epidote and quartz. Thin beds and laminations are 1-5 mm thick.

Unit C, 13 m thick

Medium-grained, moderately sorted, variably muscovitic quartzose sandstone with sparse partings on laminations and thin beds of silvery-gray phyllite. Unit is light gray to greenish gray and is slightly more resistant to weathering than underlying units.

Unit B, 10 m thick

Interbedded phyllite and quartz-muscovite phyllitic schist. Phyllite is medium to light gray to medium silvery gray. Quartz-muscovite phyllitic schist is medium to coarse grained, light to medium gray to greenish gray. Unit is slope forming.

Unit A, 4 m thick

Micaceous quartz sandstone, light to medium gray to silvery gray, medium grained, slope forming, with sparse rounded quartzite pebbles and cobbles up to 10 cm in diameter.

QUARTZITE MEMBER, 10-15 M THICK

LOWER MEMBER

Unit 8, 7.5 m thick

Sandstone with sparse siltstone interbeds. Sandstone is fine grained, light gray to locally greenish gray.

Unit 7, 22 m thick

Variably calcareous interbedded siltstone and sandstone. Lower 15 m of unit is dominantly brownish-gray to greenish-gray to light-gray phyllitic siltstone. Sandstone beds are less than 10 cm thick, greenish gray to light gray, fine grained, and variably calcareous. Upper 7 m contains increasingly abundant sandstone beds 10-20 cm thick, but is otherwise similar to lower 15 m.

Unit 6, 7 m thick

Interbedded fine-grained, medium-brown to orange weathering sandstone and irregular (lumpy) weathering, less resistant, silty sandstone and fine- grained sandstone with clotty, calcareous weathering habit. Beds 50-150 cm thick. Tops of sandstone beds have irregular, calcareous weathering habit.

Unit 5, 10 m thick

Quartz-rich greenish-ray calcareous sandstone and siltstone. Mostly fine-grained sandstone and silty sandstone. Distinctive from underlying units because it lacks interbedded phyllitic siltstone and is generally less distinctly bedded. Unit is also of more uniform resistance to weathering, and is not characterized by alternating ledgy and recess-forming beds. Green color is probably due to epidote. Possibly contains chlorite or muscovite as well. This unit is possibly more susceptible to specularite mineralization than underlying units.

Unit 4, 7 m thick

Interbedded sandstone and siltstone. Phyllitic siltstone is less calcareous and less greenish (color is light gray) than similar rocks in underlying unit. Sandstone beds range in thickness from 1 to 100 cm. Tops of thicker sandstone beds have highly irregular weathering habit similar to highly calcareous rocks. Entire unit forms crudely coarsening upward package.

Unit 3, 15 m thick

Interbedded calcareous sandstone and siltstone. Sandstone beds range from less than 1 cm to 30 cm thick. Sandstone is more greenish than sandstone in underlying unit, and contains epidote and small vugs. Basal 5 m is largely covered but appears to be entirely phyllitic siltstone based on float. Entire unit forms coarsening-upward package with 75 cm thick sandstone bed at top.

Unit 2, 4 m thick

Interbedded sandstone and siltstone. Sandstone is medium to fine grained with calcareous cement. Sandstone beds are 10-100 cm thick and have a strong desert varnish. Fine-grained sandstone is gradational into very fine-grained greenish-gray calc-silicate. Approximately 40% of unit is sandstone, rest is siltstone, phyllitic siltstone, and calc-silicate. Alternating ledge and slope former. Top few cm of top sandstone weathers irregularly with holes and pits.

Unit 1, 16 m thick

Thin-bedded phyllitic siltstone and fine grained variably silty and calcareous sandstone. Sandstone beds range from 0.5 to 10 cm thick and weather greenish- brown to tan-brown. Phyllitic siltstone beds form packages 0.5 to 20 cm thick and vary in color from silvery gray to greenish gray to grayish brown. Phyllitic siltstone beds are locally laminated with 1 mm sandy laminations. Epidote, chlorite and white mica are probably present but identification is tentative due to small grain size. Cleavage is approximately parallel to bedding.

Tertiary structure, stratigraphy, and tectonics of the Buckskin Mountains

JON E. SPENCER
STEPHEN J. REYNOLDS
Arizona Geological Survey, 845 N. Park Ave., #100, Tucson, Arizona 85719

ABSTRACT

In the Buckskin Mountains and adjacent ranges, deposition of a lithologically diverse sequence of lower to middle Miocene sedimentary and volcanic rocks occurred in response to extensional faulting associated with large-magnitude displacement on the Buckskin and related detachment faults. The oldest Tertiary sedimentary and volcanic units, representing the lower parts of the Gene Canyon and Artillery Formations, are not obviously correlative and were possibly deposited in separate sedimentary basins. Overlying sedimentary breccias derived from metamorphosed Paleozoic and Mesozoic strata were possibly shed from the same segment of a breakaway fault scarp and may indicate that some degree of integration of the Gene Canyon and Artillery basins had occurred by this time. The basin (or basins) in which these breccias were deposited was dismembered by extensional faulting, and western segments of the basin became tectonically inactive before eastern segments.

Wholesale displacement of a wedge-shaped upper plate resulted in widespread subareal exposure of lower-plate rocks. Slivers of the upper plate were left scattered across the denuded lower plate. Abundant clasts derived from mylonitic lower-plate rocks were shed eastward from a northeast-migrating monoclinal flexure of the detachment fault and lower plate and were deposited in a sedimentary basin that underwent continued dismemberment and tilting. Widespread, tilted, mylonite-clast-bearing sandstone and conglomerate in the eastern Buckskin Mountains are correlated with the Chapin Wash Formation and Sandtrap Conglomerate, respectively, in the Artillery Mountains.

Mylonitic lineation in lower-plate rocks trends N40°E to N50°E and sense-of-shear indicators generally indicate top-to-the-northeast shear during mylonitization. Mylonitization is interpreted as a product of ductile shearing along the downdip continuation of a precursor of the Buckskin-Rawhide detachment fault. The trend of mylonitic lineation is considered to be the best indicator of extension direction in the Buckskin and Rawhide Mountains. Gneissic fabric and lithologic layering in lower-plate rocks are broadly folded about axes that trend N55°E to N60°E. The discordance between trends of mylonitic lineation and fold axes suggests that the two were not synchronously produced.

A minimum of approximately 55 km of displacement on the eastern part of the Buckskin-Rawhide detachment fault must be restored to cover the lower plate with enough bedrock to be at depths and temperatures necessary for mylonitization. Actual displacement could be several tens of kilometers greater, but is probably in the range of 60 to 75 km based on comparison with estimates of net extension in areas to the north and south.

Upper-plate fault blocks become thinner southeastward along strike toward the north flank of the Buckskin and Rawhide Mountains. In the southern Buckskin Mountains and Butler Valley, Miocene sedimentary and volcanic rocks form most of the upper plate. Southeastward tapering of fault blocks is interpreted as reflecting the geometry of an oblique, roughly east-west-trending segment of the breakaway fault. Southward tilting of an east-west-trending belt of Miocene strata on the southern flank of the Artillery and Poachie Mountains is interpreted as a product of reverse drag during displacement from this oblique breakaway fault.

The approximately east-west-trending belt of Tertiary mylonitic fabrics exposed in the lower plates of detachment faults in the Whipple, Buckskin, Rawhide, Harcuvar, and eastern Harquahala Mountains is subparallel to a more southerly belt of generally south-vergent folds and thrusts that form the Maria fold-and-thrust belt. The Tertiary mylonitic rocks thus lie above or within the root zone of the Cordilleran fold-and-thrust belt. The roughly east-west trend of the belt of Tertiary mylonitic fabrics and of the breakaway fault or faults of the associated detachment-fault system is regionally anomalous and is inferred to reflect the geometry of earlier formed Mesozoic tectonic features.

INTRODUCTION

The Tertiary geologic history of the Buckskin and Rawhide Mountains and nearby ranges was fairly uneventful except for an Oligocene(?) to middle Miocene pulse of brittle and ductile extensional deformation, magmatism, and sedimentation that was extreme in its pervasiveness and in the degree to which it affected the geology of the ranges. The dominant Tertiary structural feature in the Buckskin Mountains is the subhorizontal Buckskin-Rawhide detachment fault, an undulating surface that separates a brittlely distended and highly faulted

in Spencer, J.E., and Reynolds, S.J., eds., 1989, Geology and mineral resources of the Buckskin and Rawhide Mountains, west-central Arizona: Arizona Geological Survey Bulletin 198, p. 103-167.

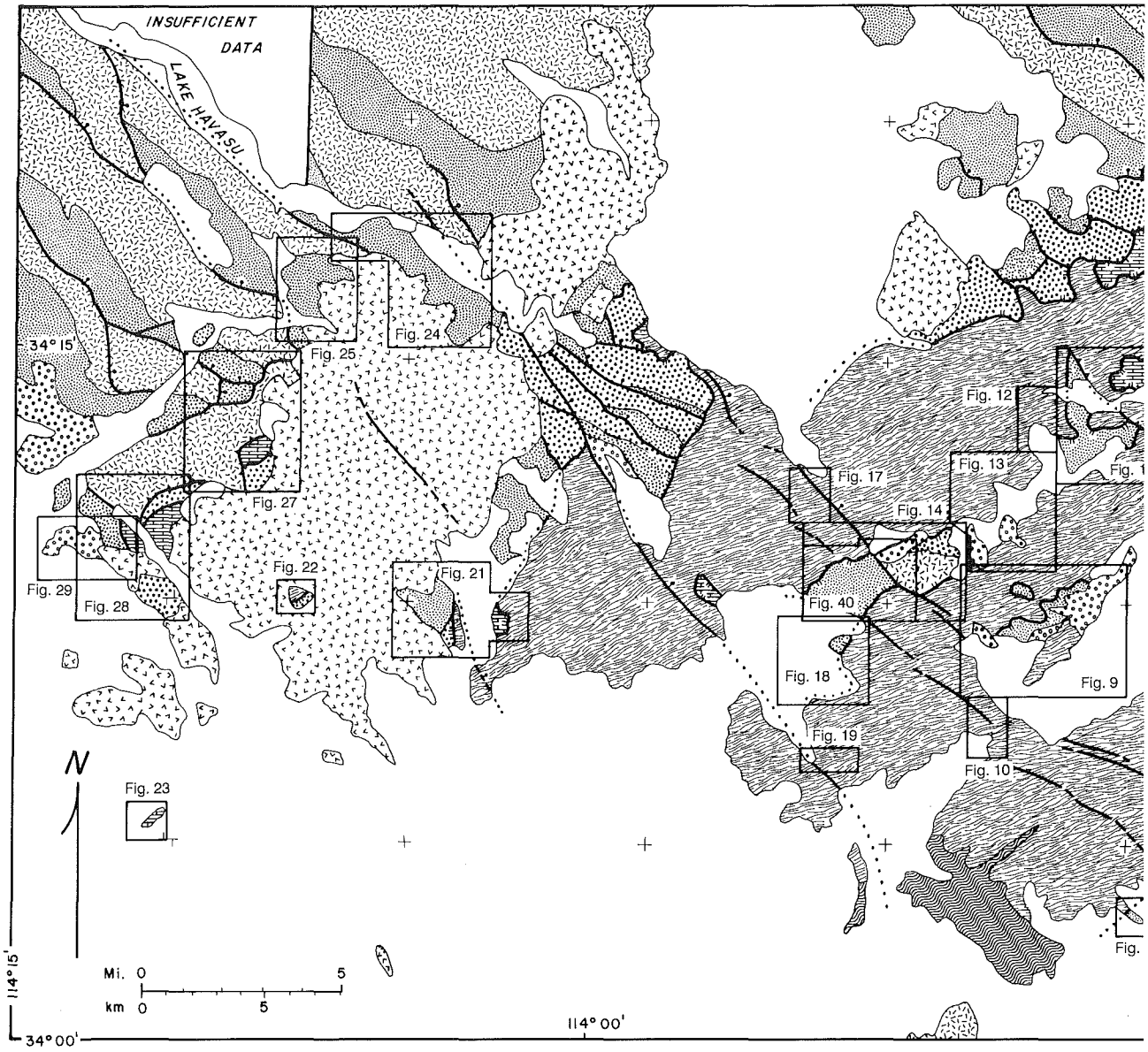

POST-DETACHMENT UNITS

- SURFICIAL DEPOSITS (QUATERNARY TO LATEST TERTIARY)
- BASALT AND LOCAL INTERMEDIATE TO SILICIC VOLCANIC ROCKS AND SEDIMENTARY ROCKS, FLAT LYING TO GENTLY TILTED (MIDDLE TO LATE MIOCENE)
- SEDIMENTARY ROCKS (MIDDLE TO LATE MIOCENE)

UPPER-PLATE UNITS

- SEDIMENTARY AND VOLCANIC ROCKS, GENERALLY MODERATELY TO STEEPLY DIPPING (LATE OLIGOCENE TO MIDDLE MIOCENE)
- METAVOLCANIC AND METASEDIMENTARY ROCKS (MESOZOIC)
- METASEDIMENTARY ROCKS (PALEOZOIC)
- CRYSTALLINE ROCKS (LARGELY PROTEROZOIC, LOCALLY TERTIARY AND MESOZOIC)

LOWER-PLATE UNITS

- MYLONITIC CRYSTALLINE ROCKS (TERTIARY TO PROTEROZOIC)
- MYLONITIC METASEDIMENTARY ROCKS (MESOZOIC AND PALEOZOIC)

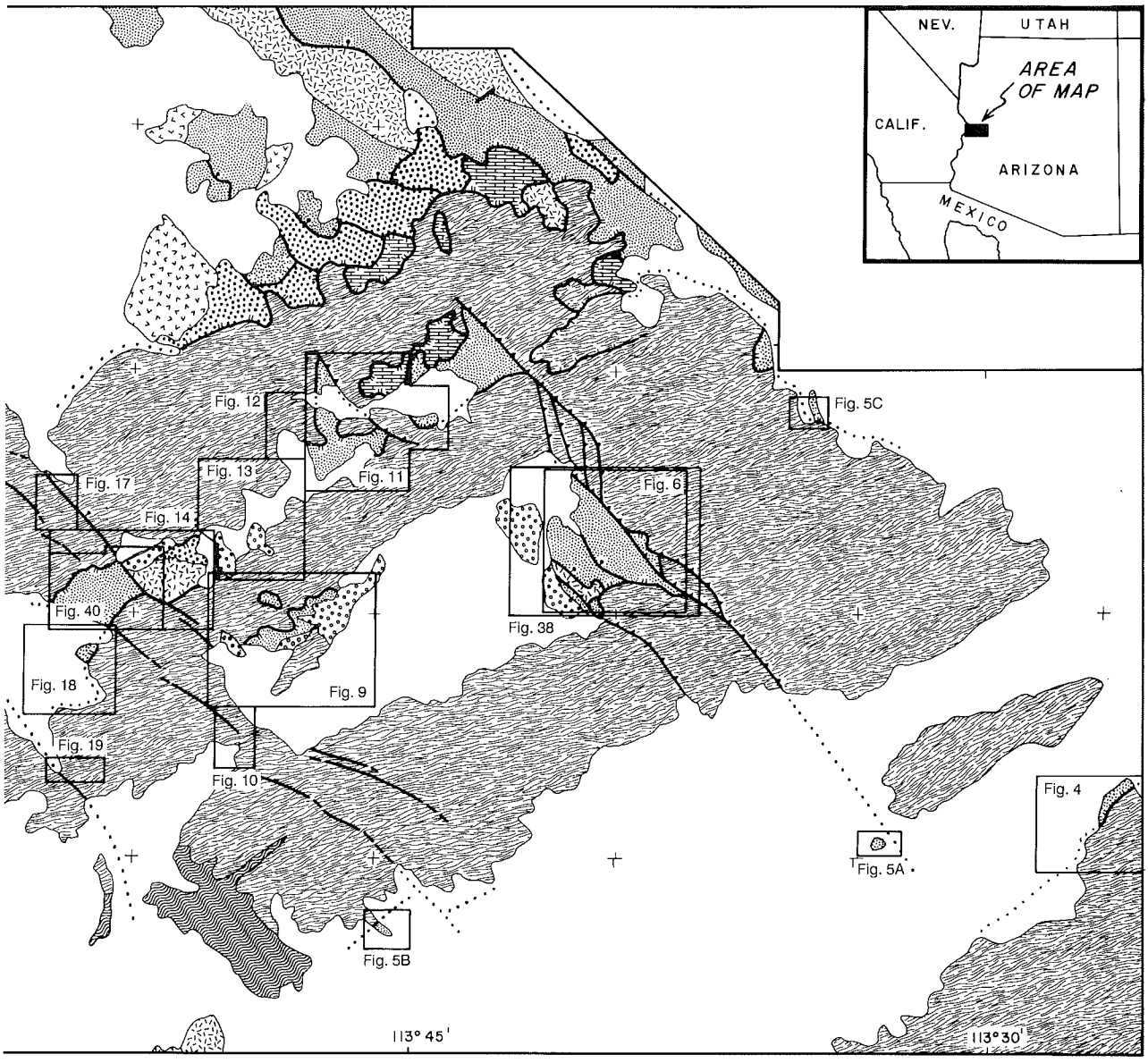

SYMBOLS

BUCKSKIN-RAWHIDE DETACHMENT FAULT

LOW-ANGLE NORMAL FAULT

HIGH-ANGLE NORMAL FAULT

HIGH-ANGLE FAULT

THRUST OR REVERSE FAULT

ALL FAULTS DASHED WHERE APPROXIMATELY LOCATED OR INFERRED, DOTTED WHERE CONCEALED.

Figure 1. Geologic map of the Buckskin and Rawhide Mountains and some adjacent areas showing location of geologic-map figures. Simplified from Plate 3.

upper plate from variably mylonitic crystalline rocks of the lower plate (Fig. 1). Rocks above and below the detachment fault have completely different characteristics and nowhere resemble each other. Upper-plate rocks of diverse ages and lithologies are commonly reddish or reddish brown because of oxidation and are moderately to highly faulted and fractured. They include numerous sequences of generally southwest-tilted sedimentary and local volcanic rocks that were deposited during extensional faulting and that record basin initiation and changing basin geometries. In contrast, lower-plate rocks are commonly greenish because of mid-Tertiary chloritic alteration and consist primarily of variably mylonitized, granitic and amphibolite-grade metamorphic rocks. Mylonitic lineation is approximately parallel to inferred direction of detachment-fault displacement, and the top-to-the-northeast sense of shear is the same for both detachment faulting and mylonitization. The distinctive suite of rocks and structures in the Buckskin and Rawhide Mountains is generally characteristic of Cordilleran metamorphic core complexes (Crittenden and others, 1980).

In this article we present results of geologic mapping, mostly at 1:24,000 scale, of all known upper-plate rocks in the Buckskin Mountains, except those in the area covered by Plate 2 and in part of the westernmost Buckskin Mountains along the Colorado River and Lake Havasu (Fig. 1). Our focus is on the structure and stratigraphy of upper-plate rocks and on inferences that can be made regarding Tertiary tectonic evolution. Lateral and vertical changes in clast composition in Tertiary conglomeratic strata are especially revealing of the unroofing history of the mylonitic lower plate. Consideration of structures and of the distribution of rock types in surrounding ranges indicates that the Buckskin Mountains are within a major lateral ramp of the Whipple-Buckskin-Rawhide-Bullard detachment system. This lateral ramp appears to reflect the influence of Mesozoic thrust-related structures, although the nature of this influence is unclear.

THE BUCKSKIN-RAWHIDE DETACHMENT FAULT

Mylonitic crystalline rocks in the Buckskin, Rawhide, eastern Harcuvar, and eastern Harquahala Mountains are bounded above by an undulating detachment fault known as the Buckskin fault in the Buckskin Mountains, the Rawhide fault in the Rawhide Mountains, and the Bullard fault in the eastern Harcuvar and eastern Harquahala Mountains (see Fig. 4 in Introduction, this vol.). The Buckskin and Rawhide detachment faults are clearly the same fault, although displacement on both faults increases from west to east and is therefore variable. Correlation with the Bullard fault is more difficult to establish, but both faults form the upward-bounding surface of what is almost certainly a single, areally extensive, variably mylonitic footwall block.

The Buckskin detachment fault is also probably correlative with the Whipple detachment fault. A previous suggestion that the Whipple detachment fault continues beneath lower-plate rocks in the Buckskin Mountains (Dokka and others, 1988, Fig. 20) seems unlikely because there is no evidence of mid-Tertiary normal faulting within the lower plate in the Buckskin and Rawhide Mountains, as would be expected if it were above a shallow, gently to moderately dipping detachment fault. In addition, we are aware of no evidence that the southwestern continuation of the Buckskin detachment fault is within the upper plate of the Whipple detachment fault in the Whipple or westernmost Buckskin Mountains, or that it is within the lower plate of, and truncated by, the Whipple Mountains detachment fault (Davis, G.A., and others, 1980, 1982).

TERTIARY GEOLOGY OF LOWER-PLATE ROCKS

Our observations of lower-plate rocks in the Buckskin Mountains are primarily of a reconnaissance nature, with local detailed study in areas of lower-plate mineral deposits (Spencer and Welty, this vol.) and in the area of a Tertiary sill (Plate 2). Lithologically diverse, lower-plate crystalline rocks include variably pegmatitic, quartzofeldspathic, and amphibolitic gneiss; medium-grained, leucocratic granitoid rocks that typically form sills; and local, intermediate to mafic intrusive rocks that also locally form sills. The granitoid rocks are probably of Cretaceous age. Bryant and Wooden (this vol.) recognize an extensive area of commonly mafic, Miocene intrusive rock within the lower plate.

Mylonitic fabric is generally penetrative at high structural levels in the eastern Rawhide and Buckskin Mountains and is progressively weaker or more concentrated within quartz-rich or micaceous layers toward the southwest. Asymmetric tails on feldspar porphyroclasts and S-C fabrics (e.g., Simpson and Schmid, 1983), observed in outcrop at dozens of localities, indicate top-to-the-northeast shear during mylonitic deformation.

Subhorizontal lithologic layering and crystalloblastic foliation in lower-plate rocks are folded into broad ENE-trending antiforms and synforms with wavelengths of 8 to 12 km and amplitudes of approximately 200 m to more than 1 km. The form of the detachment fault mimics the overall form of the folds (Fig. 2). Northwest-trending mesoscopic folds in lower-plate crystalline rocks in the central Buckskin Mountains, which almost certainly formed in response to stresses associated with shearing along a detachment fault or its downdip continuation as a ductile shear zone, do not appear to be refolded by the ENE-trending antiforms and are truncated by the detachment fault. This relationship strongly suggests that the presently exposed, undulating surface that represents the top of the footwall block formed after mesoscopic folding about northwest-trending axes, which, in turn, occurred after folding of the lower plate about ENE-trending axes (Osborne, 1981; Woodward, 1981). Field relationships in the Whipple Mountains suggest that similar ENE-trending undulations of the detachment fault formed after, and were somewhat discordantly superimposed upon, the arch-like form of lower-plate foliation and lithologic layering (Davis, G.A., and Lister, 1988).

Table 1. Cobble counts from Tertiary conglomerates from selected localities in the Buckskin and Rawhide Mountains. (Columns 1 through 12 are percentages.) Cobble-count localities in the Buckskin Mountains are plotted in Figures 9, 11, 13, 24, 38, and 40 and Plate 2. Localities in the eastern Rawhide Mountains are from Rawhide Wash at approximately 1,720-ft elevation (CC-16) and 1,525-ft elevation (CC-17).

SAMPLE NUMBER	1 PLUTONIC UNDIVIDED	2 PALEOZOIC UNDIVIDED	3 MESOZOIC UNDIVIDED	4 METAMORPHIC UNDIVIDED	5 TOTAL A(1-4)	6 TERTIARY VOLCANIC	7 TERTIARY SEDIMENTARY	8 TOTAL B(6-7)	9 TERTIARY MYLONITE	10 CHLORITIC BRECCIA	11 CALC-SILICATE TECTONITE	12 TOTAL C(9-12)	TOTAL COUNTS
Lincoln Ranch Basin													
23-1	51	3.0	-	2.2	56.2	41.5	0	41.5	1.5	0.7	0	2.2	135
23-2	45	2.5	-	5.1	52.6	44	1.3	45.3	1.3	0	0.6	1.9	157
23-2A	55	4.3	-	4.3	63.6	34	1.7	35.7	0.9	0	0	0.9	115
23-3	34	7.6	-	6.1	47.7	9.2	8.4	17.6	28	3.8	2.3	34.1	131
23-4	69	1.8	-	9.2	80.0	17.4	0	17.4	2.8	0	0	2.8	109
23-5	31	4.5	-	4.5	40.0	15	10	25	32	1.8	0.9	34.7	112
23-6	74	0.0	-	2.9	76.9	23	0	23	0	0	0	0	105
23-7	50	4.7	-	8.2	62.9	35	0	35	2.0	0.7	0	2.7	147
23-8	24	4.0	-	7.0	35.0	57	0	57	3.0	2.0	3.0	8.0	99
23-9	30	0.0	-	3.7	33.7	15	13	28	31.8	6.5	0	38.3	107
Clara Peak Area													
CC-9	43.3	5.2	0.0	7.2	55.7	20.6	11.3	31.9	10.3	2.1	-	12.4	97
CC-10	40.5	2.7	1.8	6.3	51.3	34.2	9.0	43.2	2.7	2.7	-	5.4	111
Swansea Synform													
CC-1	28.4	0.0	67.0	2.8	98.2	0.0	1.8	1.8	0.0	0.0	-	0.0	109
CC-2	25.2	1.7	0.0	3.4	30.3	64.7	5.0	69.7	0.0	0.0	-	0.0	119
CC-3	19.4	3.0	28.4	0.0	50.8	26.1	16.4	42.5	6.0	0.7	-	6.7	134
CC-4	22.3	2.9	3.6	3.6	32.4	33.1	15.1	48.2	13.7	5.8	-	19.5	139
Planet-Mineral Hill Area													
CC-5	97.3	0.0	0.0	1.8	99.1	0.9	0.0	0.9	0.0	0.0	-	0.0	112
CC-6	46.4	1.8	17.0	8.0	73.2	9.8	13.4	23.2	3.6	0.0	-	3.6	112
CC-7	45.1	5.3	15.8	2.3	68.5	7.5	20.3	27.8	3.0	0.8	-	3.8	133
CC-8	55.6	0.0	28.7	14.8	99.1	0.9	0.0	0.9	0.0	0.0	-	0.0	115
Lower Bill Williams River													
CC-11	30.8	0.8	13.5	4.5	49.6	18.0	28.6	46.6	3.9	0.0	-	3.9	133
CC-12	40.0	1.7	23.9	3.4	69.0	18.8	7.7	26.5	4.2	0.0	-	4.2	117
CC-13	45.2	3.5	11.3	19.1	79.1	7.8	7.0	14.8	4.3	1.7	-	6.0	115
CC-14	53.5	2.6	11.4	11.4	78.9	7.9	6.1	14.0	5.3	1.8	-	7.1	114
CC-15	79.4	0.9	0.9	2.8	84.0	5.6	3.7	9.3	5.6	0.9	-	6.5	107
Eastern Rawhide Mountains													
CC-16	22.9	0.0	13.2	0.6	36.7	24.7	20.5	45.2	16.9	1.2	-	18.1	166
CC-17	13.9	0.0	1.2	0.0	15.1	23.1	52.2	75.3	7.6	2.0	-	9.6	251

most Tertiary faults have accommodated extension in a northeast or ENE direction. Abundant lower-plate-derived clasts in the upper part of mid-Tertiary stratigraphic sequences in the eastern Buckskin Mountains record tectonic denudation and subareal exposure of the lower plate (Fig. 3; Table 1). In general, faulting accommodated northeast to ENE extension and relative displacement of the upper plate and was associated with sedimentary-basin formation and deposition of thick sequences of mid-Tertiary clastic and volcanic rock.

Butler Valley and Alamo Dam

Butler Valley is underlain almost entirely by upper Cenozoic alluvium and is flanked by variably mylonitic to nonmylonitic lower-plate crystalline rocks in adjacent mountain ranges. The intensity and pervasiveness of mylonitic fabrics decrease westward from strongly mylonitic in the Little Buckskin, eastern Buckskin, and eastern Harcuvar Mountains, to weakly mylonitic in the southwestern Buckskin Mountains, and to nonmylonitic in the westernmost Harcuvar Mountains, northern Granite Wash Mountains, and Bouse Hills. These ranges (except possibly the Bouse Hills) form the footwall block to three small exposures of upper-plate rocks within Butler Valley.

Burnt Well Area. The largest area of exposures of upper-plate rocks in Butler Valley is in the Burnt Well area on the north flank of the eastern Harcuvar Mountains (Fig. 4; Table 2). Conglomerate is the most widely exposed sedimentary rock type in this area and contains pebbles and cobbles up to 30 cm in diameter of well-lineated mylonitic gneiss, chloritic breccia, foliated and unfoliated granitic rocks, Paleozoic(?) quartzite and limestone, Tertiary intermediate volcanic rocks, and reworked Tertiary sandstone and conglomerate. Relative abundances of different clast types vary from outcrop to outcrop, which probably reflects variations in stratigraphic level. Mylonitic gneiss and chloritic breccia, almost certainly derived from the footwall block, typically compose less than 10% of the clasts. Paleozoic(?) quartzite and limestone also compose less than 10% of the clasts. The conglomerate stratigraphically overlies a sandstone unit.

A moderately to steeply northwest-dipping, northeast-trending fault within mylonitic crystalline rocks is

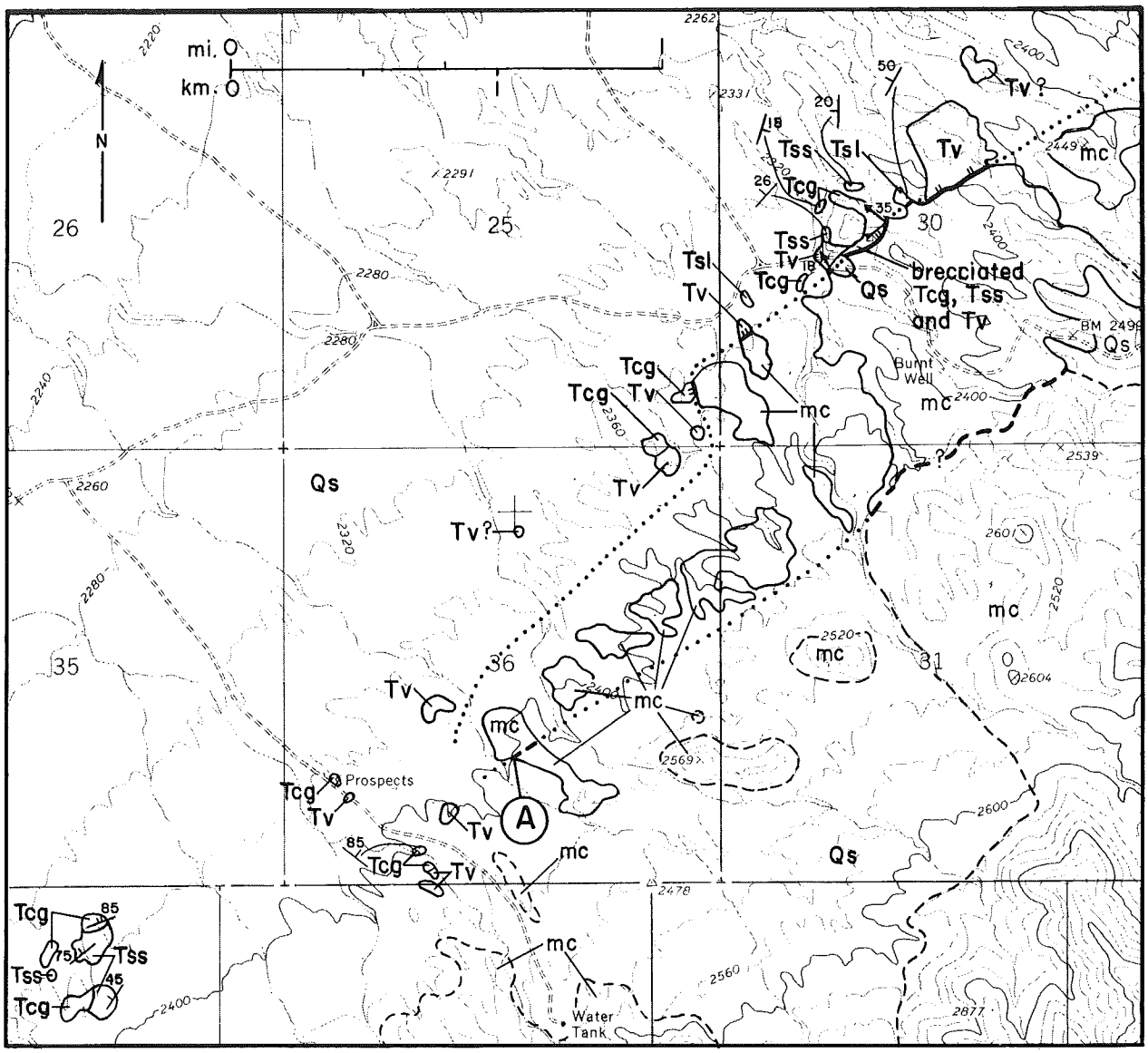

Qs Alluvium (Quaternary)

Tcg Conglomerate, medium brown to medium or dark reddish brown (Miocene)

Tss Sandstone, light tan, light brown, or reddish brown, locally tuffaceous or calcareous, with locally interbedded siltstone (Miocene)

Tsl Siltstone, maroon, locally includes dark-brown sandstone and thin limestone layers (Miocene)

Tv Volcanic flows and flow breccias of mafic to intermediate composition (Miocene)

mc Mylonitic crystalline rocks

Figure 4. Geologic map of the Burnt Well area on the northern flank of the Harcuvar Mountains. Location *A* is described in text. See Figure 1 for location and Table 2 for map-symbol descriptions.

marked by a gouge zone with steeply dipping shears at location *A* on Figure 4. Tertiary(?) volcanic rocks are present within this gouge zone. This fault projects northeastward toward a linear color contrast, clearly visible on aerial photographs, that is parallel to the range margin and is inferred to be a high-angle Tertiary fault based on the exposure at location *A*.

Black Butte. Black Butte, located southwest of the western end of the Little Buckskin Mountains (Fig. 5A), is composed of southwest-dipping, dark reddish-brown conglomerate with sparse sandstone beds. Subrounded to subangular clasts, typically 2 to 20 cm in diameter, are primarily composed of foliated and unfoliated granitoids with sparse clasts of gray limestone. Very sparse clasts of well-lineated mylonitic crystalline rocks were almost certainly derived from rocks below the Buckskin-Rawhide-Bullard detachment fault.

Western Butler Valley. A northwest-striking ridge of Tertiary conglomerate, conglomeratic sandstone, and sandstone is exposed along the southern flank of the

Table 2. Geologic-map symbols used in figures in this paper.

MAP SYMBOLS	
27	Attitude of bedding
45	Attitude of bedding, top direction known
⊕	Horizontal bedding
	Strike of vertical bedding
21 045	Attitude of mylonitic foliation showing trend of mylonitic lineation within foliation plane
	Strike of vertical mylonitic foliation
71 031	Attitude of parallel crystalloblastic foliation and spaced cleavage, showing trend of lineation within foliation plane
	Strike of vertical crystalloblastic foliation and spaced cleavage
	Anticline axis, showing plunge
	Syncline axis, showing plunge
	Crushed or highly sheared rocks
	Leader connecting areas of same map unit
Mn	Manganese deposit
CC-9	Sample location for cobble count
12-21-87-1	Sample location for K-Ar date
FAULTS	
	(All faults dashed where approximately located, dotted where concealed and inferred. Arrow indicates dip of fault. Fault symbols, such as hatchures, teeth, etc., are on hanging-wall block)
8	Buckskin-Rawhide detachment fault
15	Low-angle normal fault
25	Reverse or thrust fault
51	High-angle normal fualt
65	High-angle fault
041	Trend of slickenside striations

western Buckskin Mountains (Fig. 5B). Conglomerate, the dominant rock type, is massive to poorly bedded and contains sparse sandy layers. Sandstone beds are locally amalgamated in zones 1 to 4 m thick that contain sparse silty layers that form parting surfaces. Conglomerate clasts are exclusively composed of medium-grained equigranular granodiorite(?) that contains about 2% to 4% biotite and, in some clasts, sparse hornblende. Clasts are subangular and typically range in size from 1 to 10 cm, locally reaching 30 cm in diameter. A few clasts have a weak spaced cleavage.

The detachment fault that separates the Tertiary strata from the structurally underlying mylonitic crystalline rocks is well exposed in a decline that extends for 105 m down the dip of the fault. The roof of the decline is a smooth polished surface that forms the base of the hanging wall and strikes approximately N50°E. This surface is gently undulating; dips are primarily between 17° and 24°, but locally are as small as 9°. Faint striations on the surface trend N44°E and are approximately parallel to the strike of the fault surface.

Alamo Dam Area. Exposures of Tertiary sedimentary and volcanic rocks, directly adjacent to mylonitic footwall rocks of the Buckskin Mountains in the area southeast of Alamo Dam, were mapped and correlated with the Artillery Formation (Lasky and Webber, 1949). The detachment fault is exposed at two locations in this area. At location *A* in Figure 5C, the detachment fault strikes N60°W and dips 16°NE and red upper-plate sandstone and siltstone strike N75°W and dip 22°NE. Bedding is thus approximately parallel to the detachment-fault surface, which possibly accounts for Lasky and Webber's interpretation of this contact as depositional. At location *B* in Figure 5C, the detachment fault, exposed in a road cut, juxtaposes Tertiary sandstone with structurally underlying chloritic breccia along a contact that strikes N65°W and dips 18°NE.

Lincoln Ranch Basin

Upper-plate rocks are well exposed over approximately 20 km^2 in the Lincoln Ranch basin in the eastern Buckskin Mountains (Fig. 6). Exposures of upper-plate rocks are bounded to the southeast by the underlying detachment fault and to the northeast by the postdetachment, high-angle Lincoln Ranch fault. A previous study (Gassaway, 1972) identified the most common lithologies and the Lincoln Ranch fault, but the detachment fault was considered to be a depositional contact. A detailed geologic map and unit descriptions of the area are presented in Appendix 1 of this article; Figure 6 is a simplified geologic map.

Lower-plate rocks consist largely of mylonitic gneissic and granitic rocks and metasedimentary tecto-

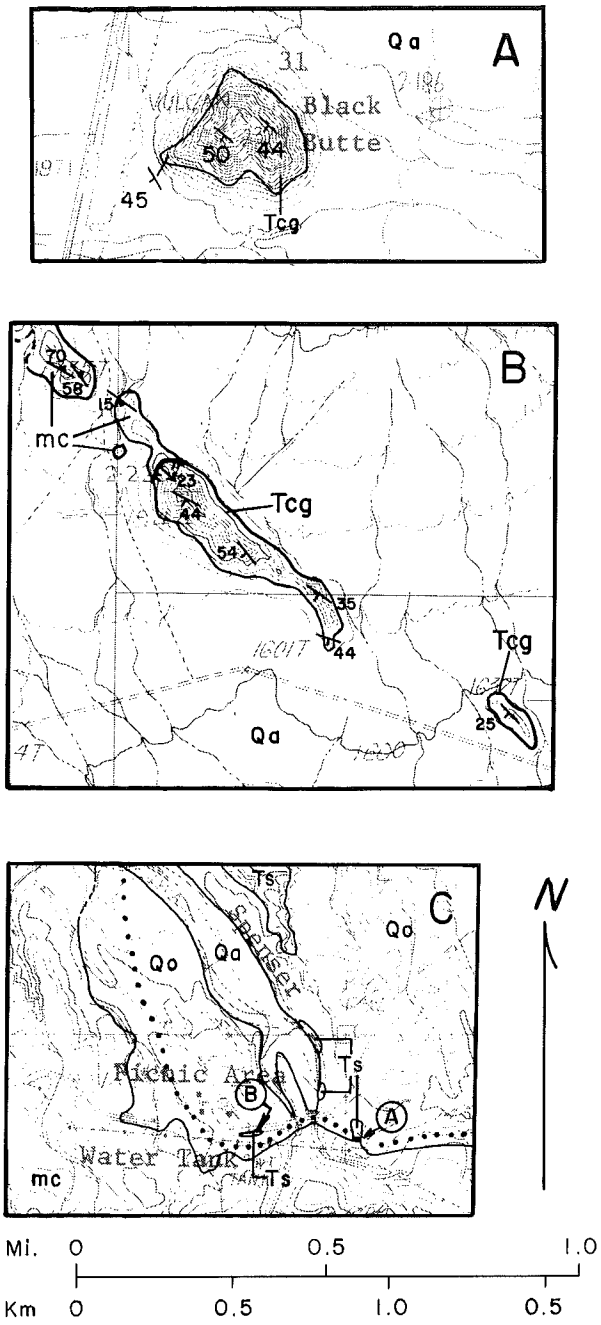

Figure 5. Geologic maps of upper-plate rocks in central (5A) and western (5B) Butler Valley and south of Alamo Dam in the eastern Buckskin Mountains (5C). The detachment fault is described at the dip arrow on the fault in Figure 5B (location of decline), and at locations *A* and *B* in Figure 5C (see text). See Figure 1 for location and Table 2 for map-symbol descriptions.

nites. A zone several tens of meters thick of mylonitic metasedimentary tectonite underlies the detachment fault along the southeast flank of Lincoln Ranch basin (Fig. 38 in Appendix 1). Metasedimentary tectonites are also exposed as slivers and sheets within mylonitic gneissic and granitic rocks northeast of the Lincoln Ranch fault (Bryant and Wooden, this vol.; Spencer and Welty, this vol.). The metasedimentary tectonites strongly resemble rocks exposed in the Battleship Peak area in the southwestern Buckskin Mountains (Marshak and Vander Muelen, this vol.), and we infer that they are correlative.

Exposures of pre-Tertiary upper-plate rocks are restricted to the south flank of the Lincoln Ranch basin in areas adjacent to the underlying detachment fault. Typically shattered granitoids are exposed over an approximately 2-km^2 area in the southwest part of the map area. Paleozoic carbonate rocks exposed in the southeast are metamorphosed and foliated, unlike nearby Tertiary limestone. A klippe above the detachment fault in the south-central part of the map area is composed of an overturned sequence of metamorphosed Permian Kaibab Limestone and Permian Coconino Sandstone that is overlain by an upright sequence of Tertiary sedimentary and volcanic rocks. All fault blocks of pre-Tertiary rock rest directly on the detachment fault.

Stratigraphy of Tertiary Rocks. A lithologically diverse sequence of Tertiary sedimentary and minor volcanic rocks forms most of the upper plate in Lincoln Ranch basin (Figs. 6 and 7; Appendix 1). Rocks of the lower part of this stratigraphic sequence (all Tertiary units below the lacustrine rocks of map-units Tl and Tll) are exposed only in the southwestern part of the map area and along the Lincoln Ranch fault. At the base of this sequence, an arkosic sandstone is probably in local depositional contact with the underlying granitoids (location *B* in Fig. 6), although shearing has variably modified the contact. Tertiary sedimentary breccia derived from Proterozoic granite and high-grade metamorphic rocks forms the stratigraphically lowest exposed rock unit near the east end of cross-section line A-A' in Figure 6 and is overlain depositionally by sandstone in one area and Tertiary volcanic rocks in another. Thin, purplish to maroon ash-flow tuffs are locally present in the arkosic sandstone. Volcanic rocks are exposed near both the east and west ends of cross-section A-A' and are overlain by locally manganiferous, interbedded sandstone and conglomerate.

The volcanic rocks in the lower part of the stratigraphic section consist of flows, flow breccias and, near the Lincoln Ranch fault, possibly ash-flow tuffs. K con-

Figure 6 (next page). Simplified geologic map of the Lincoln Ranch basin area. Base of Miocene stratigraphic sequence is in depositional contact with upper-plate crystalline rocks at location *B*. A moderate-angle upper-plate normal fault at location *C* projects into, and is almost certainly truncated downward by, the detachment fault. See Figure 1 for location, Table 2 for map-symbol descriptions, Figure 8 for cross-section A-A', and Appendix 1 for detailed geologic map and unit descriptions of area.

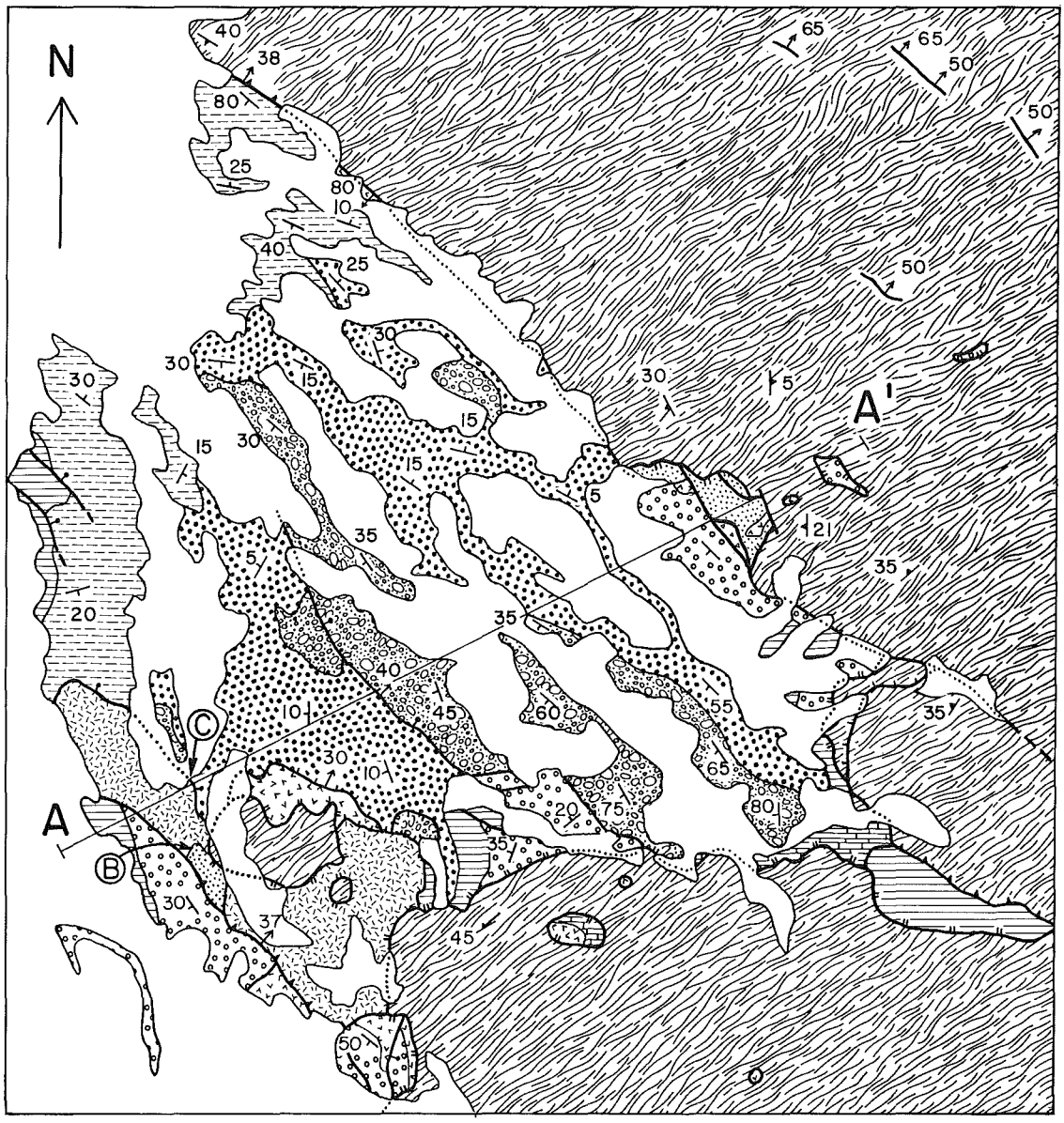

UPPER PLATE

- UPPER CONGLOMERATE (Tuc)
- UPPER SANDSTONE (Tus)
- SILTSTONE (Tslt)
- SILTSTONE (Tl) AND LIMESTONE (Tll)
- LOWER SANDSTONE AND CONGLOMERATE (Tls, Tlc, Tlsc)
- MAFIC VOLCANIC FLOWS (Tv)
- BASAL SANDSTONE, SILTSTONE (Tbs) AND SEDIMENTARY BRECCIA (Tbx)

LOWER PLATE

- MYLONITIC GNEISSIC AND GRANITIC ROCKS (mc, ms)

- TECTONIC BRECCIA
- GRANITIC ROCKS (MzXc)
- PALEOZOIC SEDIMENTARY ROCKS

mi 0 1

km 0 1

tent and K/Na ratios of volcanic flows and flow breccias indicate that they have been variably affected by K metasomatism (Table 3; sample locations given in Figure 38 in Appendix 1), as is typical of syntectonic volcanic rocks in the Buckskin Mountains (Kerrich and others, this vol.; Spencer, Shafiqullah, and others, this vol.). K/Na ratio is an especially good indicator of K metasomatism (Brooks, 1988). The two strongly K-metasomatized samples have K/Na ratios of 78.8 and 127.8, whereas the largely non-K-metasomatized sample has a K/Na ratio of 0.8. Although the three sampled volcanic outcrops are at the same stratigraphic position within the Tertiary sequence and are similar in appearance, it is not known if they are cogenetic and had the same original chemical composition. If their original compositions were similar, chemical analyses indicate that K metasomatism caused loss of Ca, Mg, Na, Mn, Sr, and Cu and enrichment in K, Fe, P, Rb, and Ba. A plagioclase concentrate from the largely non-K- metasomatized sample yielded a K-Ar date of 20.2 ± 0.9 Ma, which is interpreted as the approximate crystallization age of the rock (Spencer, Shafiqullah, and others, this vol.).

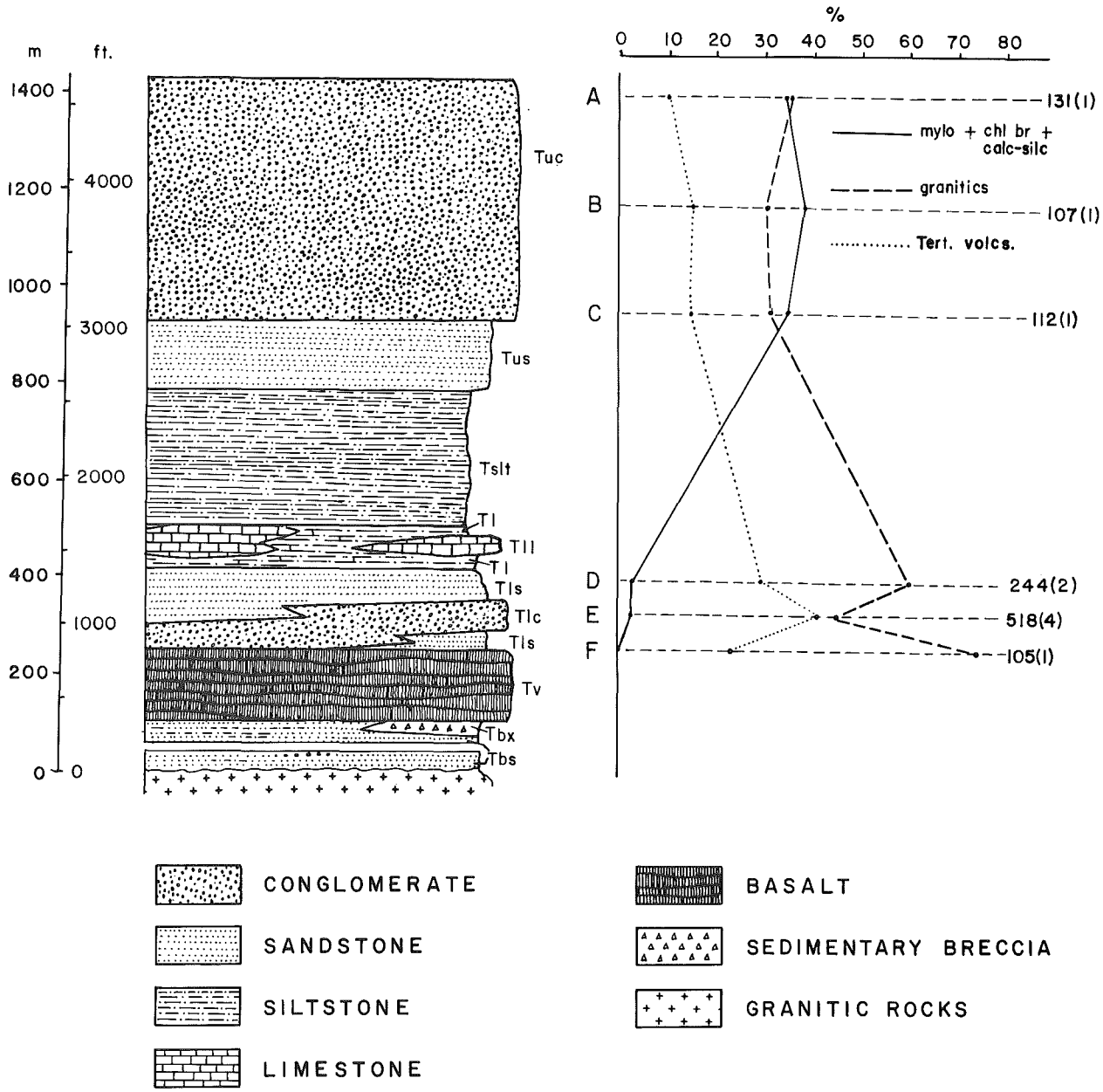

Figure 7. Schematic stratigraphic column of Tertiary strata in Lincoln Ranch basin showing cobble-population data correlated with stratigraphic position. Number of cobbles counted, and in parentheses, number of locations where cobbles were counted at one stratigraphic level, are given at right edge of figure. Solid line represents clasts (mylonitic rocks, chloritic breccia, and calc-silicate tectonite) derived from the lower plate.

Table 3. Major- and trace-element analyses of basalt flows (map-unit Tv in Fig. 38) in Lincoln Ranch basin. K/Na ratios indicate that samples 12- 15-85-1 and 12-19-86-3 are K metasomatized, but sample 12-15-85-2 is not.

MAJOR ELEMENT ANALYSES (%)

SAMPLE	SiO_2	Al_2O_3	CaO	MgO	Na_2O	K_2O	Fe_2O_3	MnO	TiO_2	P_2O_5	Cr_2O_3	LOI	SUM
12-15-85-1	50.8	15.4	6.00	0.18	0.16	12.60	6.98	0.21	0.88	0.30	0.01	5.54	99.4
12-15-85-2	51.8	16.8	10.10	1.36	3.31	2.65	5.74	0.32	0.98	0.21	0.02	6.70	100.2
12-19-86-3	48.6	15.3	5.16	1.12	0.09	11.50	10.20	0.24	1.34	0.38	0.02	5.23	99.5

TRACE ELEMENT ANALYSES (PPM)

SAMPLE	Rb	Sr	Y	Zr	Nb	Ba	Cu	Th	U
12-15-85-1	340	140	30	100	<10	2560	33	<10	22
12-15-85-2	80	480	20	150	20	780	77	<10	<10
12-19-86-3	280	100	10	160	20	1790	62	<10	14

The upper part of the upper-plate Tertiary stratigraphic sequence in Lincoln Ranch basin, encompassing map-units Tl, Tll, and overlying units up to the upper conglomerate (map-unit Tuc), compose a broadly coarsening-upward sequence (Fig. 7). Lacustrine limestone and calcareous siltstone are overlain by a siltstone unit that is in turn overlain by a red sandstone unit. The sandstone is overlain by a thick, generally massive cobble to locally boulder conglomerate that forms the top of the upper-plate stratigraphic sequence.

The relative proportions of different cobble types in map-units Tuc, Tlc, and Tls were determined at several locations, which are identified in Figure 38 in Appendix 1. Virtually all cobble types fall into one of three groups: (1) mylonitic crystalline rocks, chloritic breccia, and variably calcareous siliceous tectonites, all of probable lower-plate origin; (2) nonmylonitic granitoid and metamorphic rocks; and (3) Tertiary sedimentary and volcanic rocks. The relative proportion of each group is graphically represented and correlated with stratigraphic position in Figure 7. Clasts derived from the lower plate of the detachment fault compose a very small percentage of the cobbles in the lower conglomerate and sandstone units, but represent between 34% and 39% of the cobbles in the upper conglomerate unit. The influx of clasts derived from the lower plate is interpreted as a consequence of detachment-fault movement and associated tectonic denudation, isostatic uplift, and subareal exposure of the lower plate.

Tertiary Structures. Four types of Tertiary structures are well developed within the Lincoln Ranch basin: (1) moderate-angle normal faults within the upper plate; (2) moderate- to low-angle faults above, below, and adjacent to the detachment fault; (3) high-angle reverse faults that warp or cut the detachment fault; and (4) northwest-trending folds within the upper plate (Fig. 6; Appendix 1).

Most of the moderate-angle normal faults are northwest-trending and have northeast-side-down displacement. Movement on the major northwest-trending normal fault near the middle of cross-section A-A' has resulted in southwest-side-down tilting of hanging-wall rocks without corresponding tilting of footwall rocks (Figs. 6 and 8). The resultant contrast in bedding dips, plus the curved southern trace of this fault that represents a slightly down-plunge (to the northwest) view, suggests that the fault is listric in cross section (concave-upward curvature) and that fault movement has accommodated tilting of the hanging wall. Movement on a moderate-angle normal fault that places hanging-wall sandstone against footwall granitoid rocks, near the southwestern end of cross section A-A', has apparently

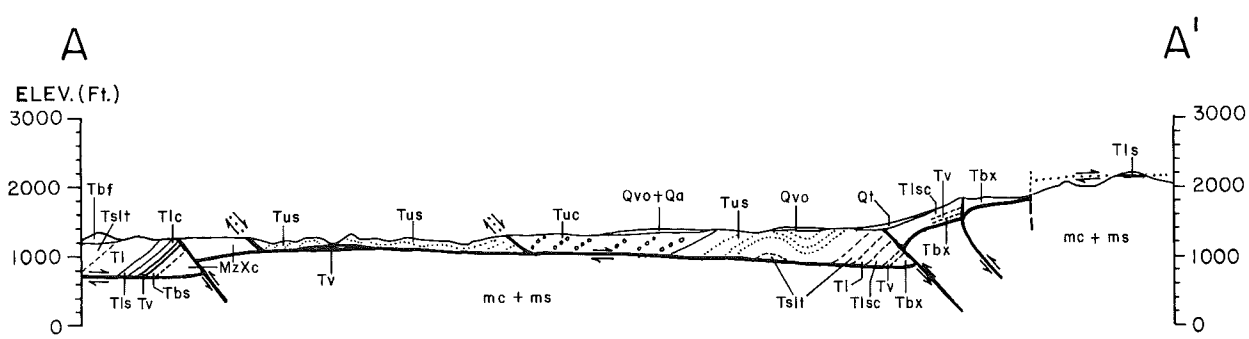

Figure 8. Cross-section A-A' located on Figures 6 and 38. See Figure 7 and Appendix 1 for unit descriptions.

caused reverse-drag folding of the hanging wall and the formation of an anticline (Fig. 38 in Appendix 1). Such anticlines form where the radius of curvature of a listric normal fault increases down the dip of the normal fault (Hamblin, 1965), and indicate a listric geometry for the underlying normal fault.

Slivering along moderate- and low-angle normal faults has produced complex fault patterns in upper-plate rocks in the southwestern part of the map area near the underlying detachment fault. All of these faults place stratigraphically higher rock types against stratigraphically lower rock types and thus are interpreted as normal faults. In the southeastern part of the map area, a low- to moderate-angle fault is present within the lower plate directly below the detachment fault. Slivering along the detachment fault thus appears to have affected both upper- and lower-plate rocks adjacent to the detachment fault.

The Lincoln Ranch fault is a major structure that continues southeastward across the Buckskin Mountains and into Butler Valley, where its buried continuation probably separates Black Butte from the Little Buckskin Mountains, as first suggested by Gassaway (1972). It apparently dies out before reaching the Harcuvar Mountains. It continues to the northwest from the Lincoln Ranch basin and passes through the central Rawhide Mountains before dying out in the northern part of the range (Plate 1). The dip of the fault varies considerably

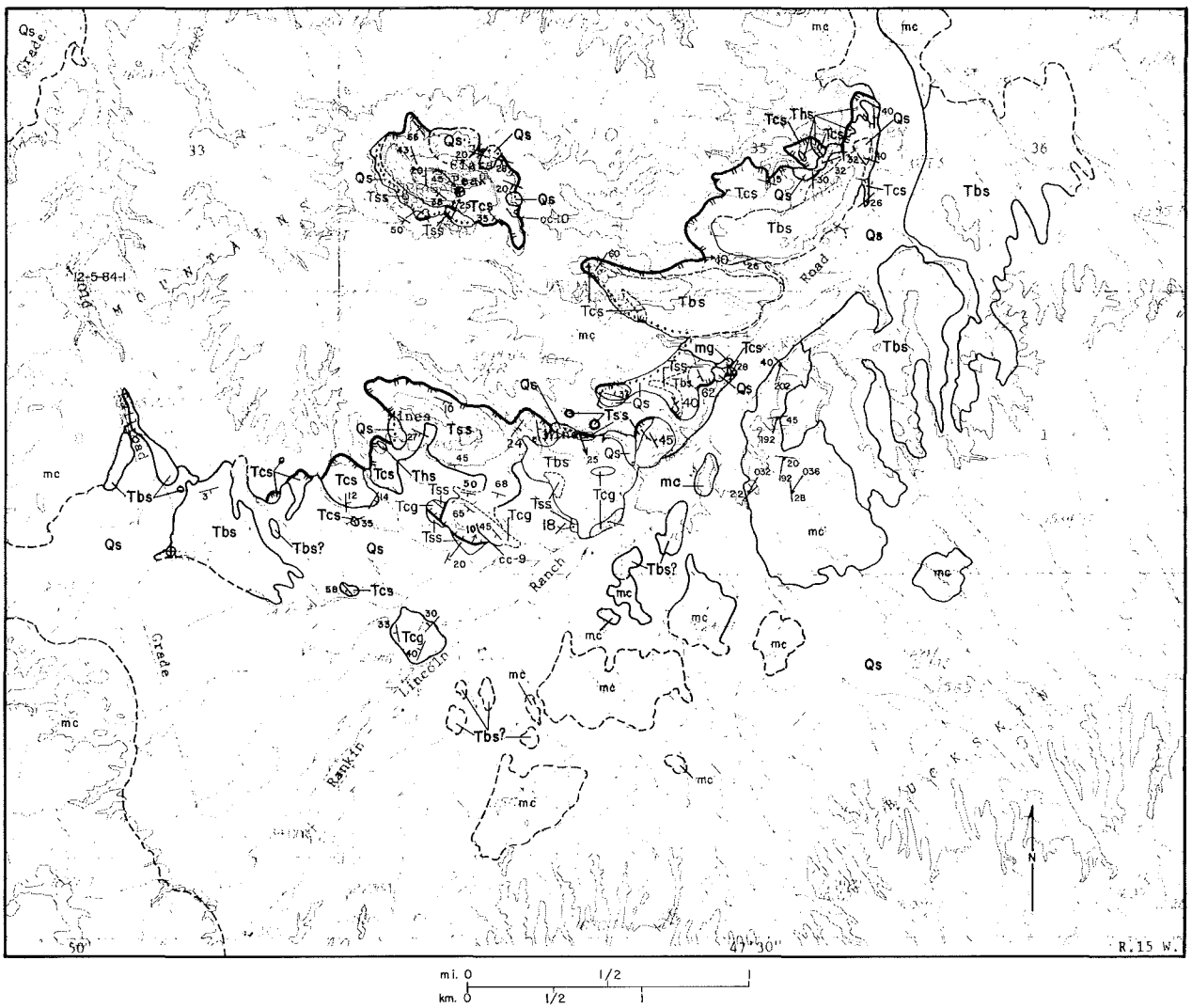

Qs	Surficial deposits (Quaternary)	Tcg	Conglomerate (Miocene)
Tbs	Sedimentary breccia with minor conglomerate and sandstone (Miocene and/or Pliocene)	Tcs	Conglomerate and sandstone, undivided (Miocene)
Ths	Silicic hypabyssal intrusive rock (Miocene)	mc	Mylonitic crystalline rock (Miocene to Proterozoic)
Tss	Sandstone (Miocene)		

Figure 9. Geologic map of the Clara Peak area, central Buckskin Mountains. See Figure 1 for location and Table 2 for map-symbol descriptions.

along strike. In most areas it is a moderately to steeply dipping reverse fault, but at two locations in the Lincoln Ranch basin it dips steeply to the west. The dips of mylonitic fabrics increase progressively southwestward toward the fault and indicate that drag folding of the footwall rocks accompanied reverse faulting. In addition, the detachment fault and underlying microbreccia are locally dragged into moderate to steep southwest dips adjacent to the fault. The Lincoln Ranch fault bifurcates southeastward into two major faults that bound a fault block containing both upper- and lower-plate rocks. The detachment fault in this fault block, and a subparallel fault below the detachment fault, are folded into a southwest-facing monocline (Figs. 6 and 8; Fig. 38 in Appendix 1). Slickenside striations at two exposures of the Lincoln Ranch fault are generally subhorizontal, indicating that the latest movement on the fault was strike slip. The Lincoln Ranch fault has thus had a complex movement history that includes two types of fault movement.

Another, smaller reverse fault in the southwestern part of Figures 6 and 38 juxtaposes various types of upper-plate rocks. Its contact with the detachment fault is concealed, but the detachment fault is warped near the reverse fault and dips to the west in these areas instead of to the north or northwest. The reverse fault is also exposed along the pipeline road south of the area of Figures 6 and 38, where it juxtaposes lower-plate crystalline rocks (Plate 3) and affects the physiography of the range (Fig. 2). Similarity in orientation and structural style between this fault and the Lincoln Ranch fault suggests that the two are related to the same period of deformation.

Several northwest-trending folds on the northeast side of the Lincoln Ranch basin parallel the adjacent Lincoln Ranch fault (Fig. 38 in Appendix 1). It is not known if these folds are truncated downward by the detachment fault (as shown in Fig. 8). Three possibilities for the origin of the folds are as follows: (1) Reverse movement on the Lincoln Ranch fault, entirely postdating detachment faulting, caused folding in the footwall block of the reverse fault. If this occurred, the folds possibly die out structurally downward into reverse faults that emanate from the Lincoln Ranch fault or related faults. The detachment fault itself could have served as a slip surface for top-to-the-southwest displacement during reverse faulting and folding. (2) Folding occurred as upper-plate rocks were impeded in their northeastward transport by an incipient southwest-facing monocline, reverse fault, or reverse-fault zone that is now represented by the Lincoln Ranch fault and related structures. (3) Folding occurred during displacement of upper-plate rocks across irregularities, such as flat-ramp-flat structures, in the detachment-fault surface (Knipe, 1982; Gibbs, 1987).

Clara Peak Area

Upper-plate rocks in the Clara Peak area consist almost entirely of red, reddish-brown, and brown sandstone, conglomeratic sandstone, and conglomerate (Fig. 9). These rocks are typically indurated, probably contain secondary silica and/or calcite, and are possibly K metasomatized. Conglomerate depositionally overlies sandstone in one area approximately 1.5 km south of Clara Peak, and conglomeratic rocks, in hanging-wall blocks of upper-plate normal faults, structurally overlie sandstone in adjacent footwall blocks at two locations. Conglomerate clasts of rocks derived from below the Buckskin-Rawhide detachment fault are intermediate in abundance (5.4% to 12.4%) between those of the lower and upper conglomerate units in the Lincoln Ranch basin (Table 1). These sandstone and overlying conglomeratic rocks are probably correlative with the lithologically similar upper sandstone and conglomerate units in Lincoln Ranch basin.

Postdetachment, pre-Quaternary rocks (map-unit Tbs in Fig. 9) consist of unconsolidated rubble of cobbles and boulders up to several meters across, and stratified, poorly to moderately sorted cobble conglomerate and sandstone. All of the large clasts and many of the smaller clasts in this unit were derived from the faulted and tilted sandstone, conglomeratic sandstone, and conglomerate described above. The unconsolidated boulder rubble was deposited on both upper- and lower-plate rocks. So little erosion of the footwall block had occurred before deposition of the rubble that chloritic breccia and microbreccia are locally preserved beneath it. This deceptive geologic relationship was originally and correctly interpreted by Woodward (1981) as a depositional contact.

Several small exposures of upper-plate rocks approximately 6.5 km south of Clara Peak include a moderately to steeply northwest-dipping, highly attenuated, Paleozoic stratigraphic section that extends upward from the depositional contact at the base of the Cambrian Bolsa Quartzite to the Permian Kaibab Limestone (Fig. 10). The Paleozoic sequence is approximately 10% of its original stratigraphic thickness. Proterozoic crystalline rocks that form the depositional basement to the Paleozoic section are the most widely exposed upper-plate rock type in this area and include coarse porphyritic granite; pegmatite; dark-gray, compositionally banded, quartz-rich metasedimentary(?) rocks; and dikes of mafic to intermediate intrusive rocks that include diabase. A single small exposure of Tertiary conglomerate contains clasts of granitoids, Tertiary volcanics, and less than 5% lineated mylonitic rocks that were probably derived from the lower plate of the detachment fault.

A linear, northwest-trending high-angle fault that offsets the detachment fault is visible on aerial photographs and extends to the northwest out of the area of Figure 10 to an area where it is exposed as a zone of crushed, lower-plate crystalline rock. Another high- to moderate-angle fault in the south-central part of the map area offsets the detachment fault and dips 30° to 70° to the southwest. Both faults have southwest-side-down displacement.

Rankin Ranch Area

Upper-plate rocks exposed in the Rankin Ranch area along the Bill Williams River and within the Swansea synform are primarily composed of red to reddish-brown sandstone and conglomerate (Fig. 11). The sandstone and overlying conglomerate are virtually identical in appearance to, and almost certainly correlative with, the two stratigraphically highest upper-plate units in Lincoln Ranch basin. The abundance of mylonitic clasts

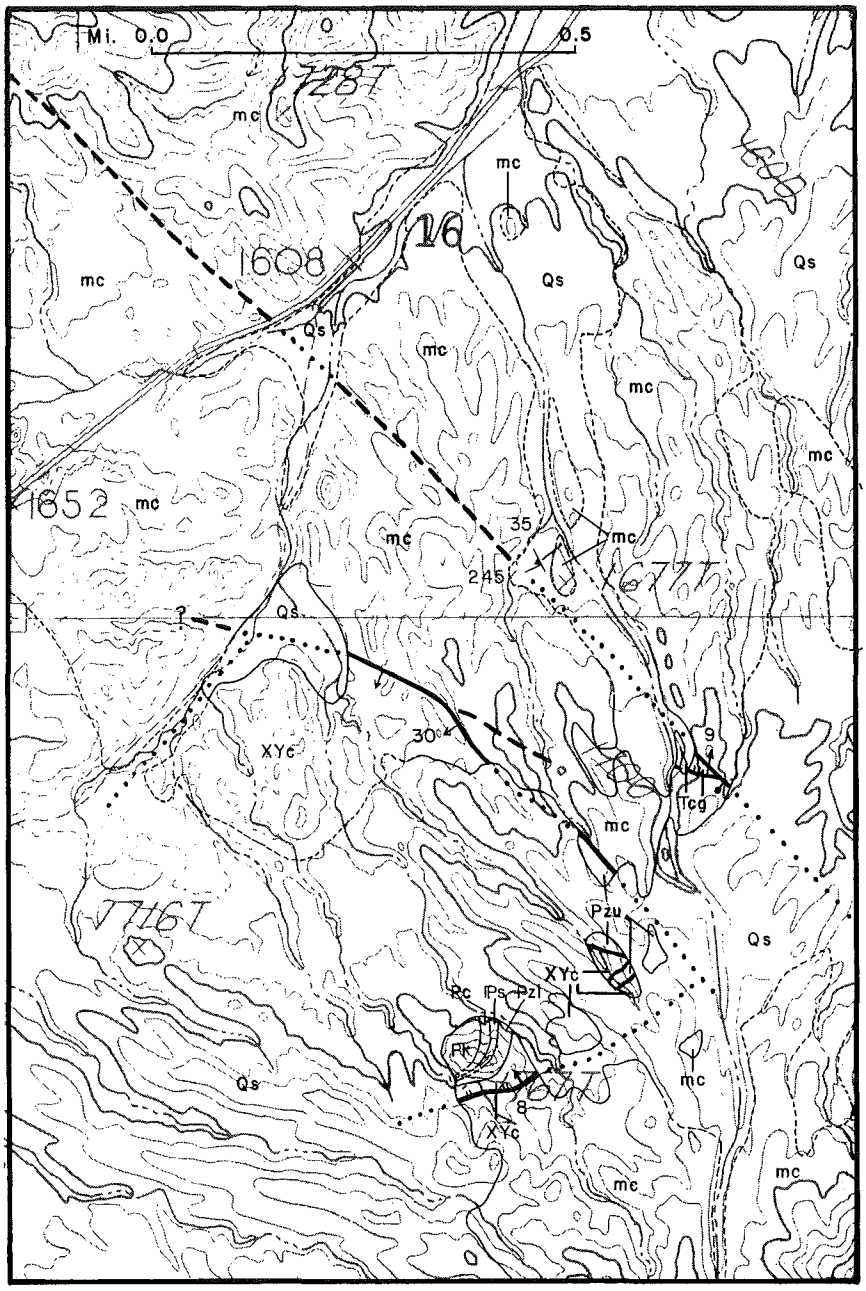

Qs	Surficial deposits (Quaternary)
Tcg	Conglomerate (Miocene)
Pk	Kaibab Limestone (Permian)
Pc	Coconino Sandstone (Permian)
IPs	Supai Formation (Permian and Pennsylvanian)
Pzl	Redwall Limestone, Martin Formation, Abrigo Formation, and Bolsa Quartzite (lower Paleozoic)
Pzu	Carbonate and quartzite, undivided (Paleozoic)
XYc	Crystalline rocks (Proterozoic)
mc	Mylonitic crystalline rocks (Proterozoic to Tertiary)

Figure 10. Geologic map of an area south of Clara Peak and north of Battleship Peak where upper-plate rocks are exposed. See Figure 1 for location and Table 2 for map-symbol descriptions.

in the conglomerate unit (approximately 20%) supports correlation with the upper conglomerate unit in Lincoln Ranch basin (Fig. 3; Table 1). North of the Bill Williams River, a transitional conglomeratic sandstone unit lies stratigraphically between the sandstone and conglomerate. Highly brecciated carbonate and quartzite, probably derived from Paleozoic sedimentary rocks, rest directly on the detachment fault in the western Rankin Ranch area (eastern edge of Fig. 11; Fig. 12).

The detachment fault in the Rankin Ranch area has a complex form that is in part due to movement on postdetachment reverse faults (Fig. 11). These reverse faults and several other faults to the northeast that have possible reverse displacement form a northwest-trending zone of branching subparallel faults (Plate 1; Fig. 11). Complex undulations of the detachment fault, not associated with reverse faults, possibly formed by folding in response to the same stresses that caused reverse faulting. Structural styles are similar to those in the Lincoln Ranch basin. Reverse faulting and warping of the detachment fault in the two areas are probably related to the same period of deformation.

A gently east-dipping, upper-plate normal fault in the western part of the map area (NE1/4 sec. 11) places steeply to moderately southwest-tilted conglomerate over moderately to gently tilted sandstone. The contrast in dips between these two units indicates that the stratigraphically higher conglomerate was tilted during movement above a listric normal fault. The upper-plate normal fault cannot be a rotated planar fault because domino-style fault and fault-block rotation would have caused comparable amounts of tilting of rocks above and below the fault.

Swansea Mine Area - East

Upper-plate rocks northeast of Swansea mine (Fig. 13) consist largely of the same sandstone and conglomerate units that are widely exposed in the Rankin Ranch area. Nonwelded ash-flow or air-fall tuffs, locally exposed within the sandstone unit at the western edge of the map area of Figure 13, are possibly correlative with tuff just south of Rankin Ranch (Fig. 11). The sandstone and conglomerate units, as well as the contact between them, are well exposed along a north-trending ridge in the southwestern part of the map area. Approximately 7% of the conglomerate clasts in this area were derived from the lower plate of the detachment fault, which is similar to abundances of lower-plate-derived clasts from the nearby Clara Peak area (Table 1). Animal tracks, identified as camel, ursine dog, cat, and bird tracks by Gassaway (1972, with photographs), are present along the contact zone between the sandstone and conglomerate.

Postdetachment breccia and conglomerate, similar to those south of Clara Peak, are widespread in the area of Figure 13. A hilltop outcrop of this unit near the eastern edge of sec. 22 in the eastern part of the area of Figure 13 is composed of especially coarse rubble of boulders up to 3 m in diameter; clasts are composed of brown Tertiary sandstone and conglomerate with less abundant, smaller clasts of green chloritic breccia derived from the lower plate.

Swansea Mine Area - West

A lithologically diverse and structurally complex group of rocks form a synformal upper-plate keel in the Swansea mine area (Fig. 14; see also Osborne, 1981; Woodward, 1981; Wilkins and Heidrick, 1982). Right-lateral and northeast-side-down displacement on the northwest-trending, postdetachment Swansea fault has broken the synformal keel into two fault blocks (Fig. 14). Pre-Tertiary rocks compose approximately half of the upper plate in this area and are composed of Proterozoic granite, metamorphosed Paleozoic and Mesozoic sedimentary rocks, and intrusive rocks of probable Mesozoic age (Appendix 2; Reynolds and Spencer, this vol.). The pre-Tertiary rocks are overlain (locally along a depositional contact) by an approximately 1-km-thick sequence of Miocene sedimentary and volcanic rocks. A detailed map and unit descriptions of these rocks are given in Appendix 2; details of the pre-Tertiary rocks are discussed in Reynolds and Spencer (this vol.).

Stratigraphy of Tertiary Rocks. The thickest and most complete Tertiary stratigraphic sequence, forming most of the upper plate west of the Swansea fault, is divided into 24 map units (Appendix 2), which have been lumped into 7 units in Figure 14 and on the left stratigraphic column in Figure 15. In ascending order, these seven units are as follows:

(1) The stratigraphically lowest unit (map-unit Tbs) consists of arkosic sandstone that is locally silty and calcareous and a basal conglomerate. Subrounded to rounded pebbles and cobbles in the conglomerate are composed of a variety of igneous and metamorphic rock types, many of which are present in the vicinity. Depositional contacts at the base of this unit are exposed on both sides of the Swansea fault (Fig. 40 in Appendix 2).

(2) Map-unit Tts consists of a sequence of interbedded tuff, limestone, siltstone, and sandstone. A welded tuff at the top of this sequence yielded K-Ar dates of 20.3 $\pm$ 0.4 Ma (feldspar) and 21.8 $\pm$ 0.8 Ma (biotite; Spencer, Shafiqullah, and others, this vol.). The biotite date is interpreted as the approximate age of the tuff, but it is significantly different from a 27.3 $\pm$ 1.1 Ma biotite K-Ar date reported for the same unit by Wilkins and Heidrick (1982).

(3) Map-unit Txs is primarily composed of massive, monolithologic sedimentary breccia exclusively derived from metamorphosed Jurassic volcanic and volcaniclastic rocks, such as those in the Planet mine area of the northwestern Buckskin Mountains (Plate 2; Reynolds and Spencer, this vol.). Thin layers of limestone and tuff are interbedded with the sedimentary breccia.

(4) Map-unit Ta is primarily composed of dark, mafic to intermediate volcanic flows and flow breccias. Less abundant interbedded conglomerate contains clasts primarily composed of metamorphosed Jurassic volcanic rocks. Hornblende from a drill-core sample of this unit yielded a K-Ar date of 18.6 $\pm$ 1.5 Ma (Wilkins and Heidrick, 1982).

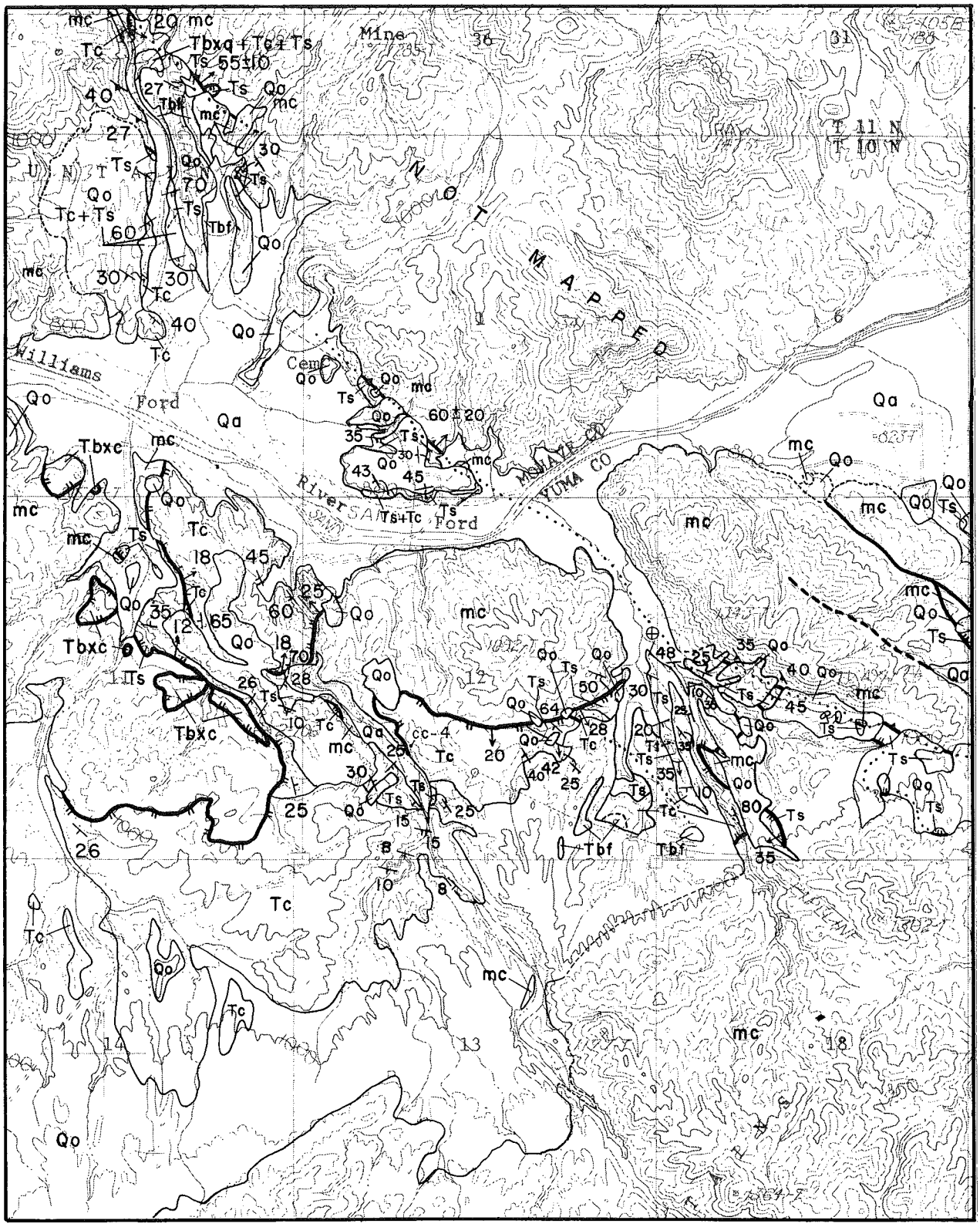

(explanation and caption on next page)

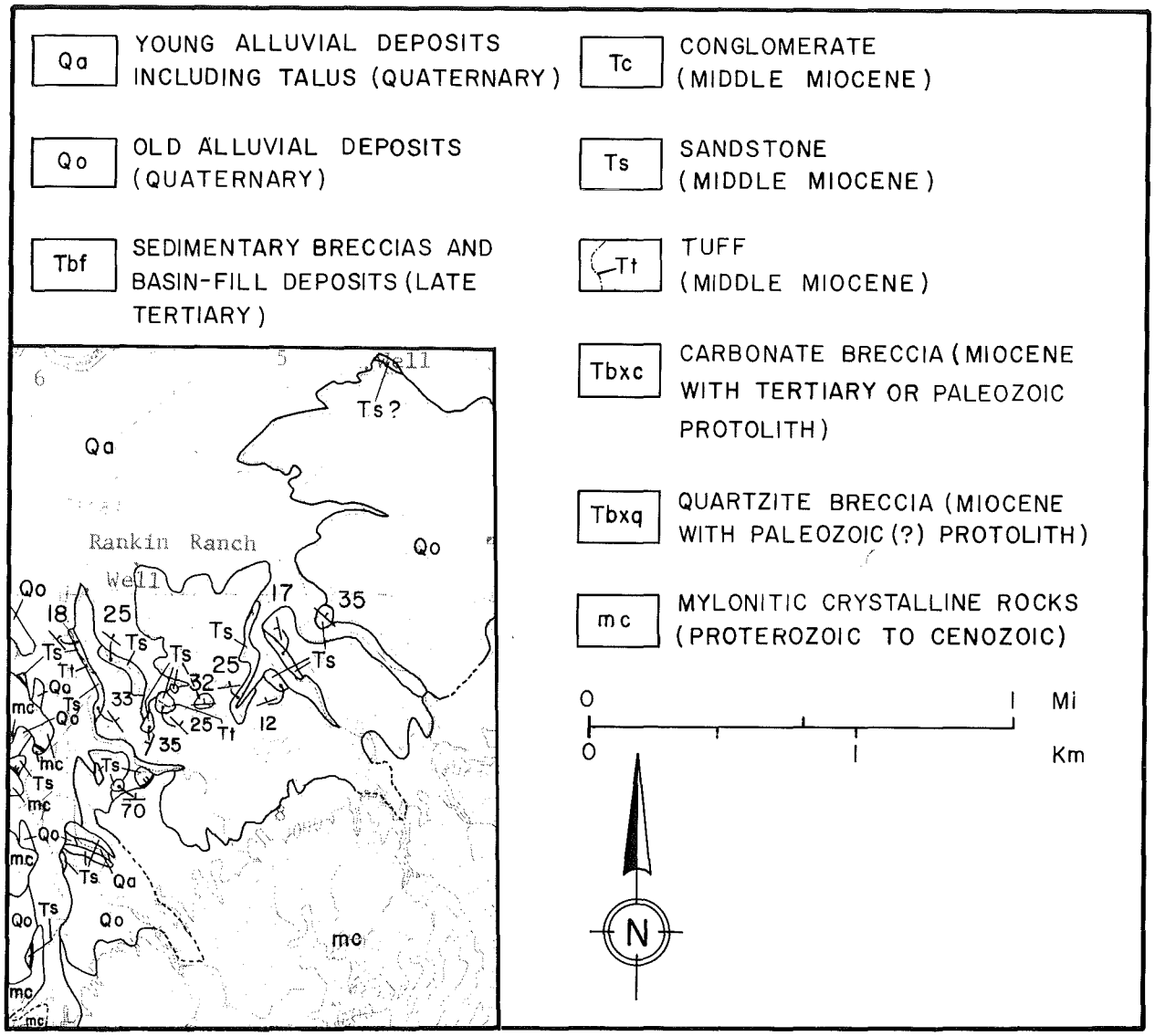

Figure 11. Geologic map of the Rankin Ranch area along the Bill Williams River. See Figure 1 for location and Table 2 for map-symbol descriptions.

(5) Map-unit Tx is composed of heterolithologic sedimentary breccia that contains clasts of metamorphosed Jurassic volcanic rocks, coarse-grained porphyritic granite, and metamorphosed Paleozoic(?) carbonate rocks.

(6) Map-unit Tsv is composed of interbedded, intermediate volcanic flows and flow breccias, limestone, and calcareous sandstone. The volcanic rocks are K metasomatized and have yielded a feldspar-concentrate K-Ar date of 20.1 $\pm$ 0.5 Ma that is interpreted as the age of K metasomatism and as the minimum age of the volcanic rock (Spencer, Shafiqullah, and others, this vol.).

(7) Map-unit Tsc is composed of sandstone and minor conglomeratic sandstone and rests unconformably across several underlying units. Conglomerate clasts up to 10 cm in diameter are composed of carbonate rock and Tertiary sandstone and volcanic rocks.

The Tertiary sequence east of the Swansea fault forms a fault-bounded block that is divided into three units in Figure 14 and the right-hand stratigraphic column in Figure 15. The lowest of the three (map-unit Ta) consists of the same interbedded Jurassic-volcanic-clast conglomerate and mafic to intermediate volcanic flows and flow breccias that compose map-unit Ta west of the Swansea fault; the two are considered to be correlative. East of the Swansea fault, map-unit Ta is overlain by a thick sequence of sedimentary breccias and debris flows that contain a great variety of clast types, including Jurassic volcanic rocks, Mesozoic phyllite, Paleozoic quartzite and carbonate rocks, foliated and unfoliated granite, and Tertiary volcanic and sedimentary rocks. This unit is correlated with the heterolithologic sedimentary breccia (map-unit Tx) west of the Swansea fault. Overlying intermediate volcanic flows, flow breccias, sandstone, calcareous sandstone, and limestone (map-unit Tsv east of the Swansea fault) are correlated with virtually identical rocks that compose map-unit Tsv west of

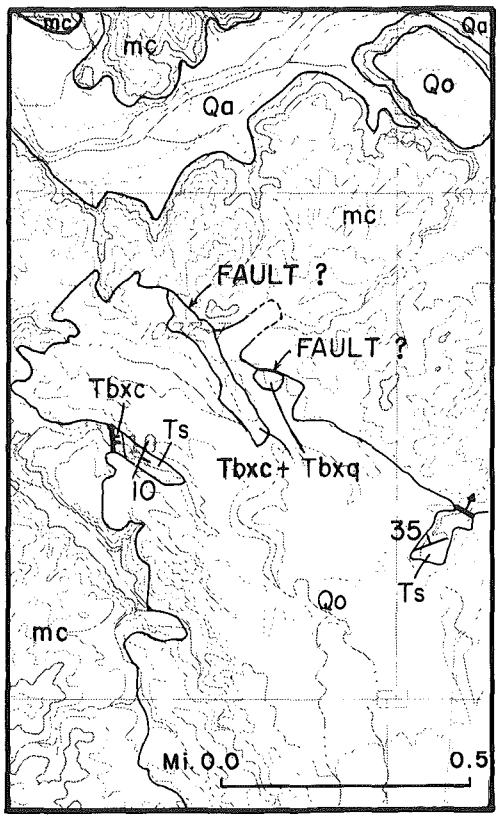

Figure 12. Geologic map of a small area west of the area of Figure 11 on the south flank of the Bill Williams River. See Figure 1 for location, Table 2 for map-symbol descriptions, and Figure 11 for map units.

the Swansea fault. Lateral facies and thickness changes across the Swansea fault are most significant for the sedimentary breccia unit, which is thin or absent west of the fault but is much thicker and contains a greater proportion of debris flows east of the fault (Fig. 15).

Tertiary Structures. Metamorphosed and deformed Mesozoic and Paleozoic sedimentary and volcanic rocks form numerous fault slivers directly above the detachment fault. These metamorphosed rocks are faulted against Proterozoic granite that is depositionally overlain at two localities by the basal Tertiary arkose. We saw no evidence of a fault-bounded sheet of metamorphosed, primarily Tertiary sedimentary and volcanic rocks (the *middle plate* of Wilkins and Heidrick, 1982) above the detachment fault and below the widely exposed, weakly metamorphosed to unmetamorphosed Tertiary rocks. The only contrast in metamorphic grade that we recognized was between metamorphosed pre-Tertiary rocks and altered, but largely unmetamorphosed, Tertiary rocks that are locally in depositional contact with the pre-Tertiary rocks.

Moderately southwest-dipping faults (locations *B* in Fig. 14) on both sides of the Swansea fault juxtapose Tertiary sedimentary and volcanic rocks with underlying Proterozoic granite and its depositionally overlying basal arkose (Fig. 16). These two faults are possibly segments of an originally continuous fault that has been cut and broken into two fault segments by the Swansea fault. There is some difficulty, however, with this interpretation; simple reconstruction of a continuous, moderately southwest-dipping normal fault, by restoration of displacement on the Swansea fault, appears to be precluded by the steepness of fault segments and by insufficient displacement on the Swansea fault (Fig. 16). Based on similarity in fault geometry and in lithology of hanging-wall and footwall rocks, it seems likely that these fault segments are related to the same period of southwest-side-down normal faulting, but are probably not correlative. Unrecognized structural complexities are required for correlation.

The Tertiary sequence west of the Swansea fault is folded into two southeast-plunging anticlines that are separated from each other by a fault (Osborne, 1981; Figs. 14 and 16; Fig. 40 in Appendix 2). The stratigraphic units in the fold are truncated by the detachment fault along the southwest side of the Swansea synform and are interpreted to be truncated downward at a high angle by the detachment fault. These folds were thus truncated by faulting before final juxtaposition of upper- and lower-plate rocks in the Swansea area. A sequence of four events is indicated: (1) deposition of all of the Swansea Tertiary stratigraphic sequence, (2) folding of the sequence, (3) fault dismemberment of the folded sequence, and (4) displacement of the folded, upper-plate rocks to their present position. Deposition of the Swansea Tertiary sequence is interpreted as broadly contemporaneous with detachment faulting; thus, all of these events occurred during the period of detachment faulting. As with the folds in the Lincoln Ranch basin, folding possibly occurred in response to displacement across irregularities in the footwall.

Although complicated by folding and displacement on southwest-dipping normal faults, the general form of the upper-plate rocks in the Swansea area is that of a northwest- to WNW-striking, southwest- to SSW-dipping sequence of Tertiary strata depositionally overlying variably deformed granitic and metamorphic rocks. An approximately 1-km-thick sequence of Tertiary strata and about 2 km of its depositional basement (structural thickness perpendicular to the depositional contact) are exposed in the southwest-tilted synformal keel of upper-plate rocks in the Swansea area.

Several small exposures of upper-plate Paleozoic rocks on the crest of the Planet Peak antiform have probably been preserved because they are on the downthrown block of the adjacent Swansea fault (Fig. 17). Unusually thick (up to several meters) microbreccia forms the flat top of a nearby peak on the upthrown block (Fig. 17). Upper-plate rocks are also preserved southwest of the Swansea area, where their distribution reveals some of the complex, undulatory form of the detachment fault (Fig. 18). This form may be partially the result of displacement on one or more, presently unmapped, northwest-trending, high-angle normal faults. South of this area, the detachment fault is offset by a high-angle fault that is correlated with the Mineral Wash fault, and upper-plate Tertiary volcanic rocks are pre-

served on the downthrown block of the high-angle fault (Fig. 19).

Planet and Mineral Hill Area

Metamorphosed Mesozoic sedimentary and volcanic rocks that compose most of the upper plate in the Planet and Mineral Hill area are locally overlain by Tertiary volcanic and sedimentary rocks (Plate 2). The Tertiary and pre-Tertiary rocks dip steeply to the southwest; there is no significant angular discordance between the two. The basal Tertiary unit, in most areas a sedimentary breccia (unit Tbx in Fig. 20 and Plate 2), was deposited on Jurassic metavolcanic rocks that are the youngest preserved unit of the pre-Tertiary stratigraphic sequence. It therefore appears that the pre-Tertiary

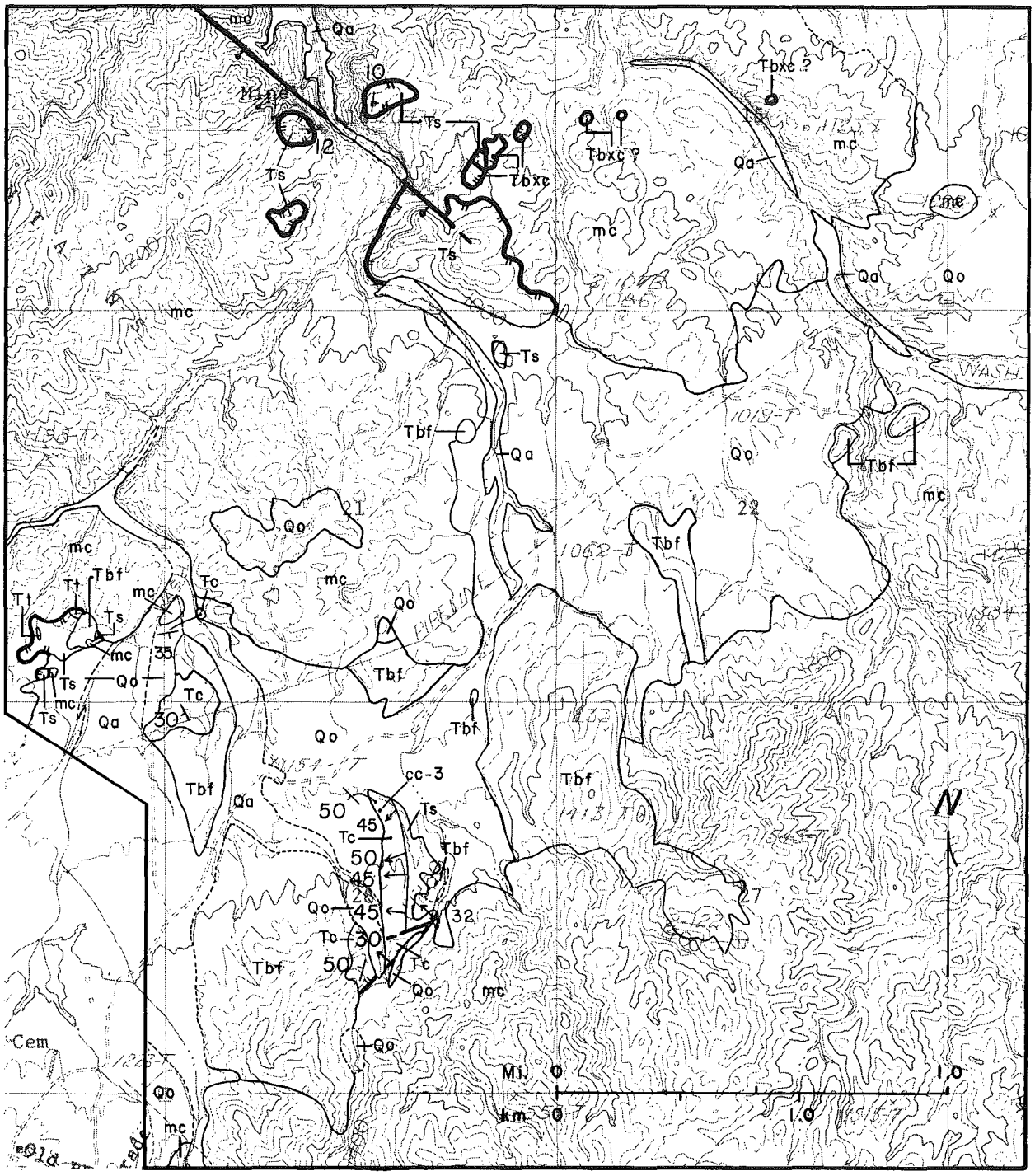

Figure 13. Geologic map of the area northeast of Swansea mine. See Figure 1 for location, Table 2 for map-symbol descriptions, and Figure 11 for map units.

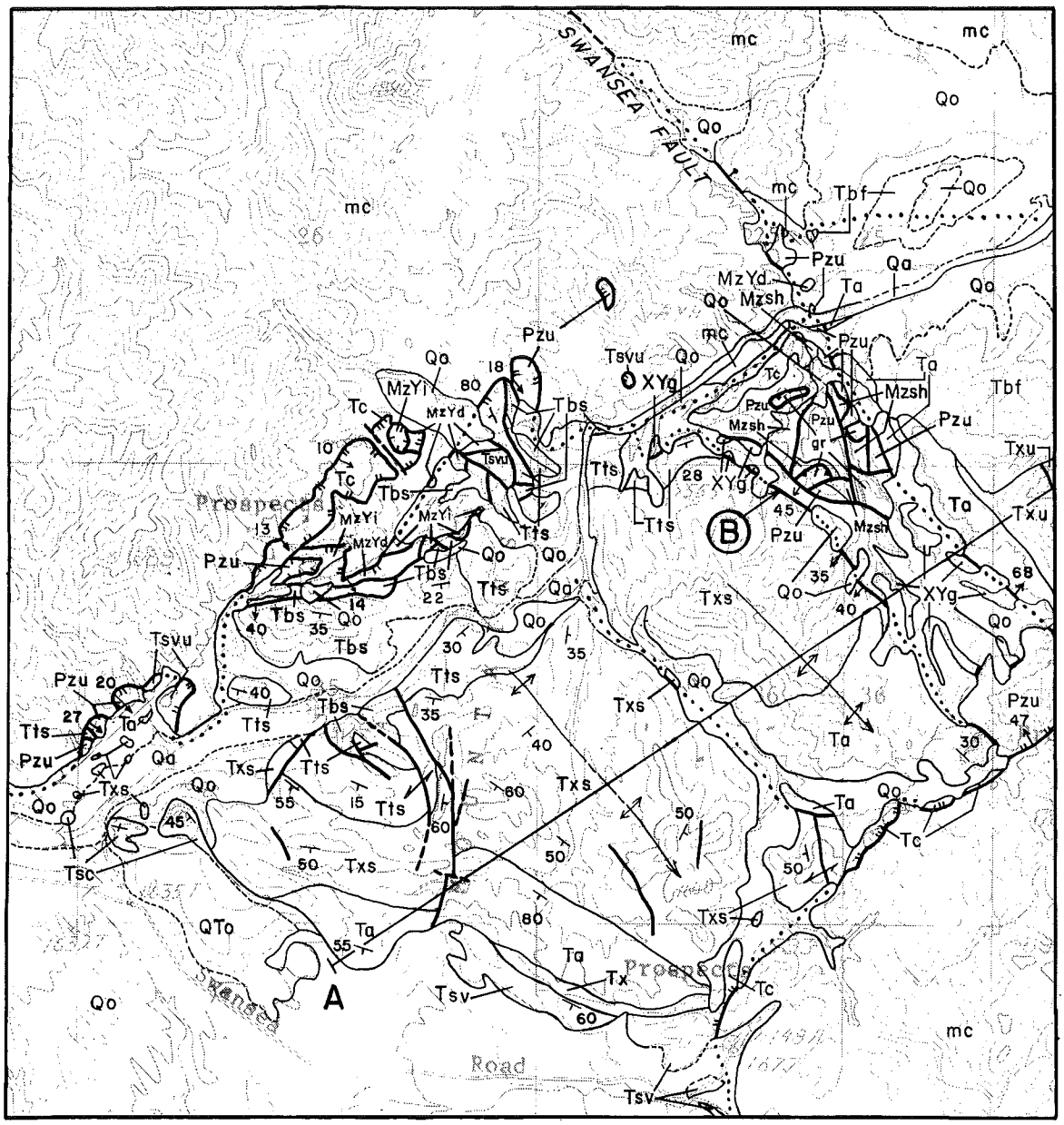

Qa	Alluvium (Quaternary)	
Qo	Older alluvium (Quaternary)	
QTo	Alluvium (Quaternary and Late Tertiary)	
Tbf	Basin fill (Upper Miocene and Pliocene)	
Tc	Hydrothermal replacement carbonate	Miocene
Tsc	Sandstone and conglomeratic sandstone	Miocene
Tsv	Sandstone, limestone, and intermediate volcanic flows	Miocene
Tx	Sedimentary breccia	Miocene
Txu	Sedimentary breccia and debris flows	Miocene
Ta	Andesitic to basaltic volcanic flows and conglomerate	Miocene
Txs	Sedimentary breccea, limestone, and tuff	Miocene
Tts	Welded tuff, limestone, sandstone, and siltstone	Miocene
Tbs	Sandstone, conglomerate, siltstone, and limestone	Miocene
Tsvu	Sedimentary and volcanic rocks, undivided	Miocene

Figure 14. Simplified geologic map of the Swansea - Copper Penny area. In part, modified from Figure 40 in Appendix 2. See Figure 1 for location and Table 2 for map-symbol descriptions.

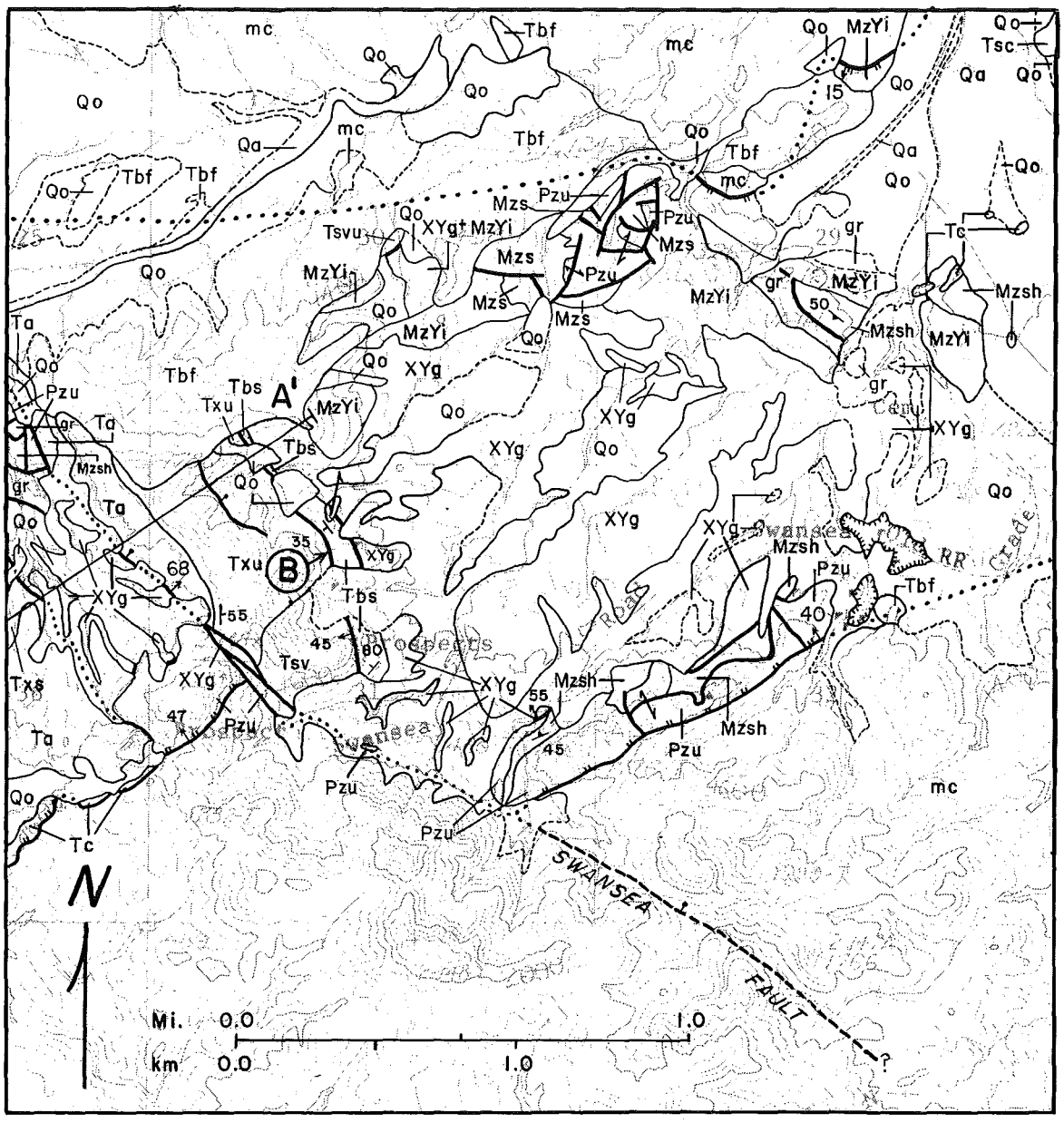

Mzs	Quartzose to quartzofeldspathic sandstone, pebble conglomerate, calc-silicate, and phyllite (Mesozoic)
Mzsh	Quartz-sericite-chlorite schist, locally feldspathic (Mesozoic)
MzYi	Volcanic and hypabyssal intrusive rocks (Mesozoic or Proterozoic)
MzYd	Dioritic rocks (Mesozoic or Proterozoic)
Pzu	Quartzite and carbonate metasedimentary rocks (Paleozoic)
XYg	Granitic rocks (Proterozoic)
gr	Leucocratic granitic rocks (age unknown)
mc	Mylonitic crystalline rocks (Proterozoic to Tertiary)

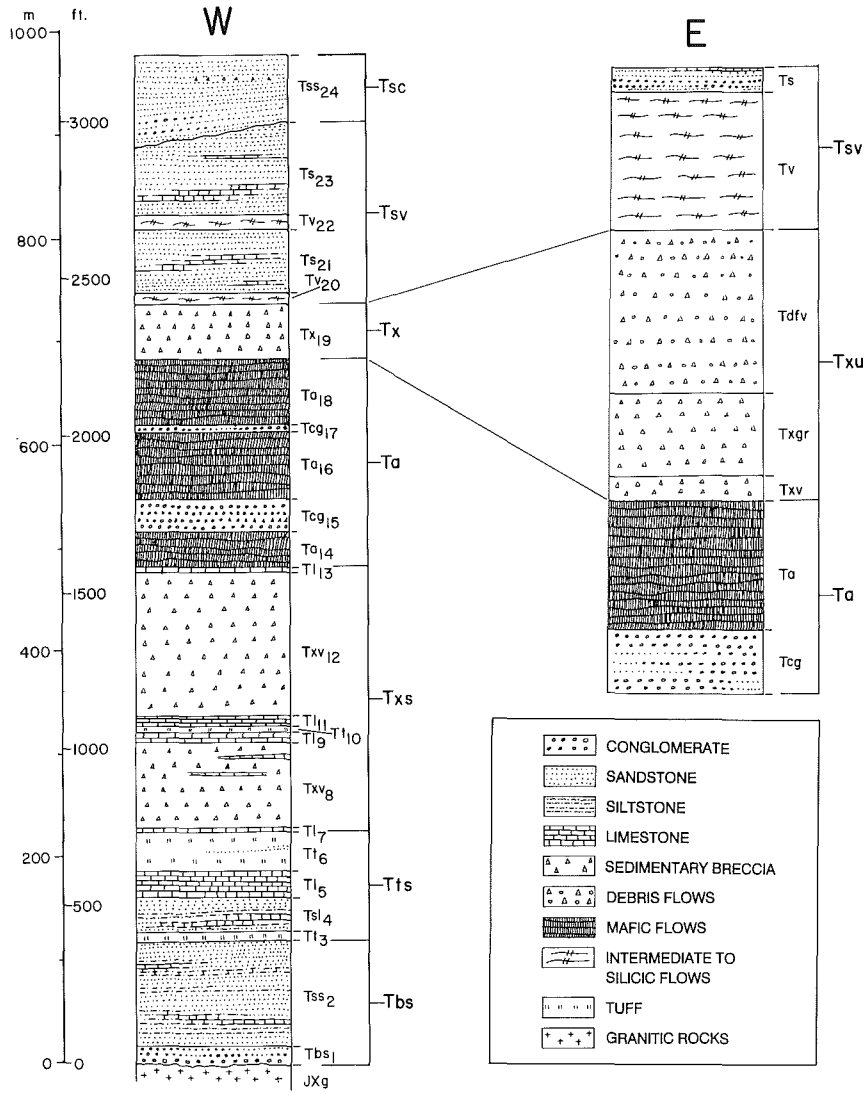

Figure 15. Stratigraphic columns and correlations for upper-plate Tertiary strata in the central and western part of the Swansea - Copper Penny area. Left column is for area west of the Swansea fault; right column is for area east of the fault. Map units used in Figures 14 and 40 are both shown.

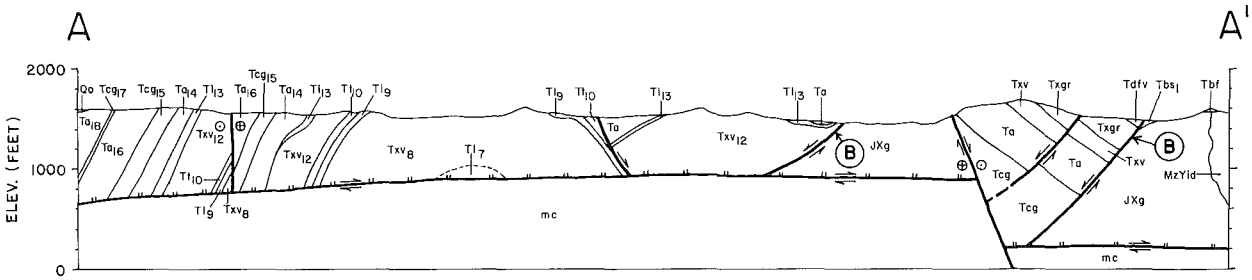

Figure 16. Geologic cross section of the central and western part of the Swansea - Copper Penny area. Map units are those used in Figure 40 of Appendix 2 (see also Figure 14). Cross section is located on Figures 14 and 40. See text for discussion of faults at location *B*.

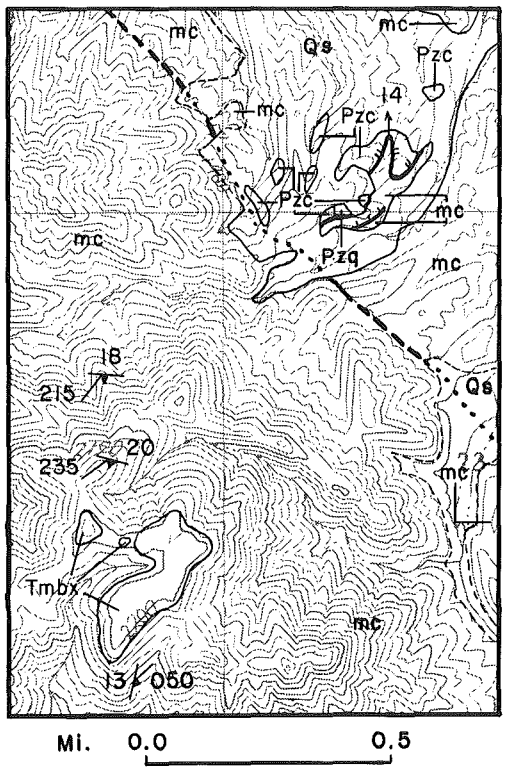

Qs Surficial deposits (Quaternary)
Tmbx Microbreccia and cataclasite (Miocene)
Pzc Carbonate rocks (Paleozoic)
Pzq Quartzite (Paleozoic)
mc Mylonitic crystalline rocks (Proterozoic to Tertiary)

Figure 17. Geologic map of an area along the Swansea fault north of the area of Figure 14. See Figure 1 for location and Table 2 for map-symbol descriptions.

stratigraphic sequence was largely flat lying and lacked significant folds and high- to moderate-angle faults at the time the basal Tertiary unit was deposited. Furthermore, the entire Tertiary sequence below the basin-fill unit (unit Tbf in Fig. 20 and Plate 2) was steeply tilted after it was deposited, with little or no evidence of fanning dips that would indicate tilting during sedimentation.

Stratigraphy of Tertiary Rocks. The basal Tertiary unit is a thick sequence of sedimentary breccia (Fig. 20) primarily derived from Jurassic metavolcanic rocks, such as those that underlie the breccia. Other protolith rock types are older Mesozoic metasedimentary rocks, Paleozoic marble and quartzite, and granitic and gneissic rocks of probable Proterozoic age. Where several lithologies are present in a single stratigraphic sequence, the youngest protolith rock types are generally at the base of the sequence and the oldest are at the top. This upside-down age relationship, combined with the consistently right-side-up (and flat-lying prior to tilting) character of the underlying pre-Tertiary rocks, suggests that the breccias were derived from fault scarps during fault movement and that progressively older rocks were exposed by faulting and became sources for the breccias.

In the Tunnel Peak area (south-central part of Plate 2), the basal sedimentary breccias are overlain by a three-part sequence (Fig. 20): (1) A lower sedimentary unit (unit Tsl in Fig. 20) of conglomerate and local conglomeratic sandstone that varies from massive to moderately well bedded. Cobbles and local boulders consist of a great variety of clast types, but do not include clasts derived from the lower plate of the detachment fault (Table 1, samples CC-5 and CC-8); (2) A middle unit of strongly K-metasomatized mafic to intermediate volcanic flows and flow breccias (unit Tv in Fig. 20) (Spencer, Shafiqullah, and others, this vol.); and (3) An upper sedimentary unit (unit Tsu in Fig. 20) of conglomerate and conglomeratic sandstone that is poorly sorted and poorly to moderately bedded. This upper unit contains fewer plutonic rock clasts and more clasts derived from Tertiary volcanic and sedimentary rocks than does the lower sedimentary unit, and also contains a small percentage of clasts that were probably derived from the lower plate of the detachment fault (Table 1, samples CC-6 and CC-7).

A correlative three-part sequence overlies sedimentary breccia on both sides of the Bill Williams River near the mouth of Mineral Wash. In this area, the lower and upper sedimentary units are primarily composed of sandstone and minor siltstone. It is not known if the sandstone unit that is widely exposed in the southwestern part the area of Plate 2 is correlative with the lower or upper sedimentary units. It may be correlative with both, but a division cannot be made because volcanic rocks were not deposited in the area.

On the north side of the Bill Williams River, the conglomerate of Cave Wash and interbedded basalt is juxtaposed with sandstone of the lower sedimentary unit along a contact that is probably a fault. The conglomerate is massive to moderately bedded and contains unusually well-rounded cobbles and boulders (up to 1 m in diameter) exclusively composed of Proterozoic(?) crystalline rocks. The regional distribution of pre-Tertiary rock units (Plate 3) suggests that the conglomerate of Cave Wash was derived from areas farther north, whereas clasts in adjacent units were derived locally or from areas farther south. Interbedded basalt yielded plagioclase K-Ar dates of 16.2 $\pm$ 0.5 Ma and 15.5 $\pm$ 0.7 Ma (Spencer, Shafiqullah, and others, this vol.). Sediment-dispersal patterns thus changed dramatically before about 16 Ma. The moderate, generally southwest dip of bedding in this unit indicates that tilting, and presumably detachment faulting, continued until after about 16 Ma in this area.

Tertiary Structures. The large sheet of upper-plate rocks in the Planet and Mineral Wash area is cut by the northwest-trending, postdetachment Mineral Wash fault. Upper-plate rocks east of the Mineral Wash fault and south of the Bill Williams River are divided into three major northwest-striking, moderately to steeply southwest-tilted fault blocks. The structure of the upper-plate rocks in areas north of the Bill Williams River and west of the Mineral Wash fault is more complicated, but is also characterized by northeast-dipping normal faults and

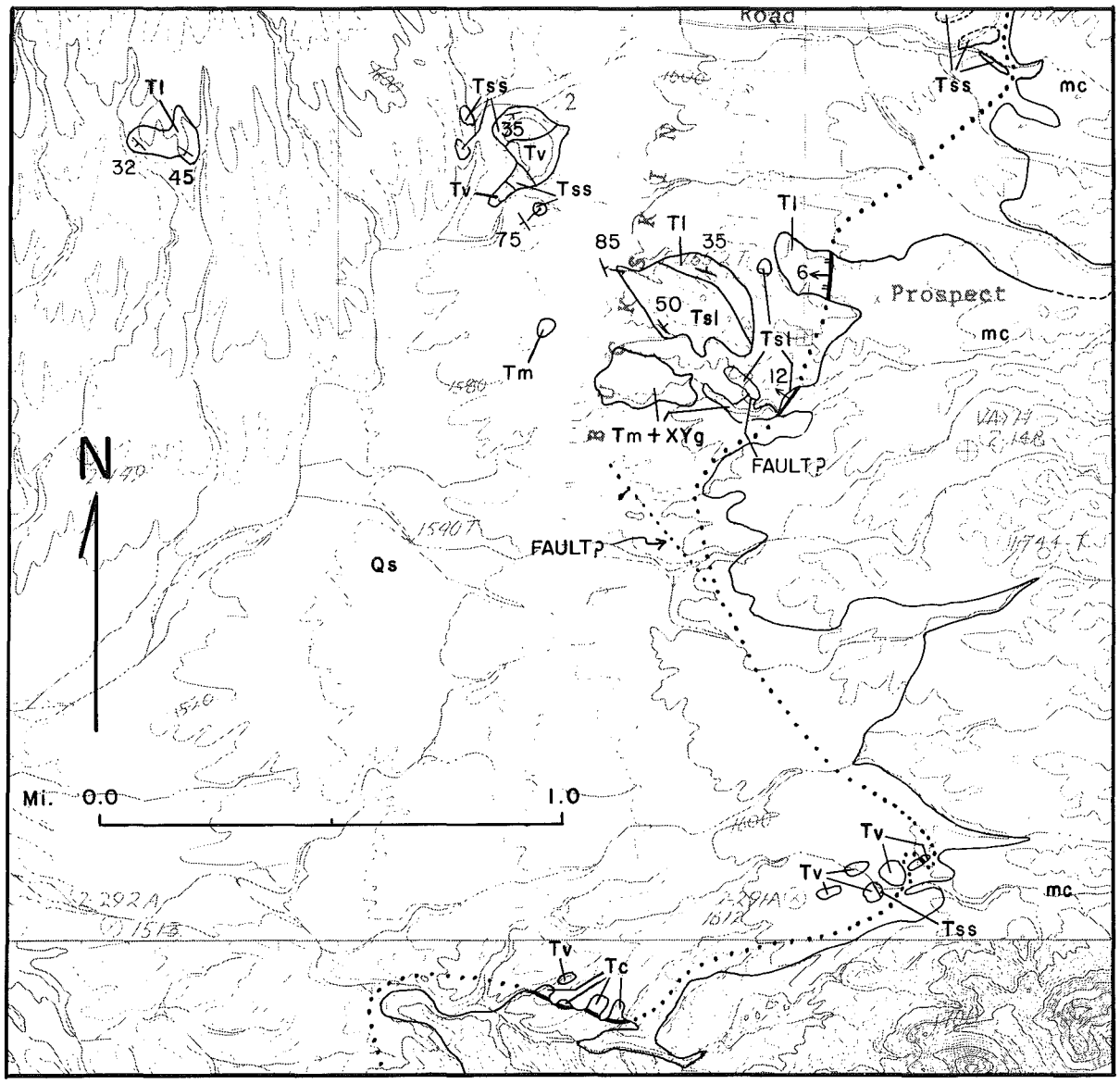

Qs	Surficial deposits (Quaternary)	Tc	Hydrothermal replacement carbonate (Miocene)
Tbf	Basin-fill deposits (Upper Miocene to Pliocene)	Tm	Mafic hypabyssal intrusions (Miocene)
Tss	Sandstone (Miocene)	XYg	Granitic rocks (Proterozoic)
Tv	Intermediate to mafic volcanic flows (Miocene)	mc	mylonitic crystalline rocks (Proterozoic to Tertiary)
Tl	Limestone (Miocene)		
Tsl	Sandstone and limestone (Miocene)		

Figure 18. Geologic map of an area south of the Swansea road. See Figure 1 for location and Table 2 for map-symbol descriptions.

southwest-tilted Mesozoic and Tertiary strata. Upper-plate normal faulting and southwest tilting of fault blocks accommodated major northeast-southwest extension. It is difficult to determine the percentage of extension of the upper-plate because of the high degree of structural complexity, but it is probably in the range of 60% to 140%.

Where exposed, the detachment fault juxtaposes the two stratigraphically highest Mesozoic units against the lower plate along most of the eastern part of the area of Plate 2. Stratigraphically lower Mesozoic units are exposed farther west, especially west of the Mineral Wash fault and near Planet mine. The detachment fault, therefore, cuts downsection to the north or northwest, directions that are at a high angle to the ENE direction of regional extension. This geometry suggests that the

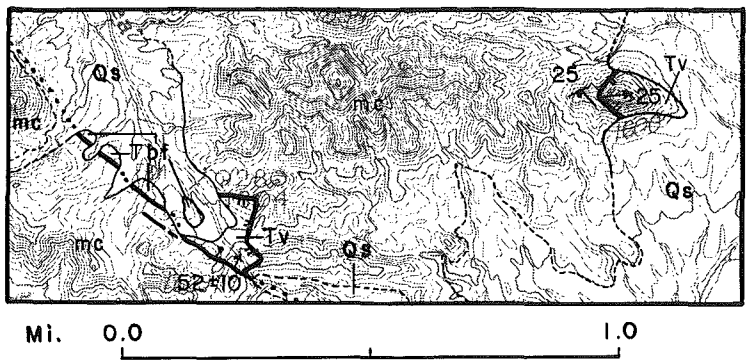

Figure 19. Geologic map of part of the west end of the Clara Peak antiform. The northwest-trending, postdetachment, high-angle fault is interpreted as the southeastward continuation of the Mineral Wash fault. See Figure 1 for location, Table 2 for map-symbol descriptions, and Figure 18 for map units.

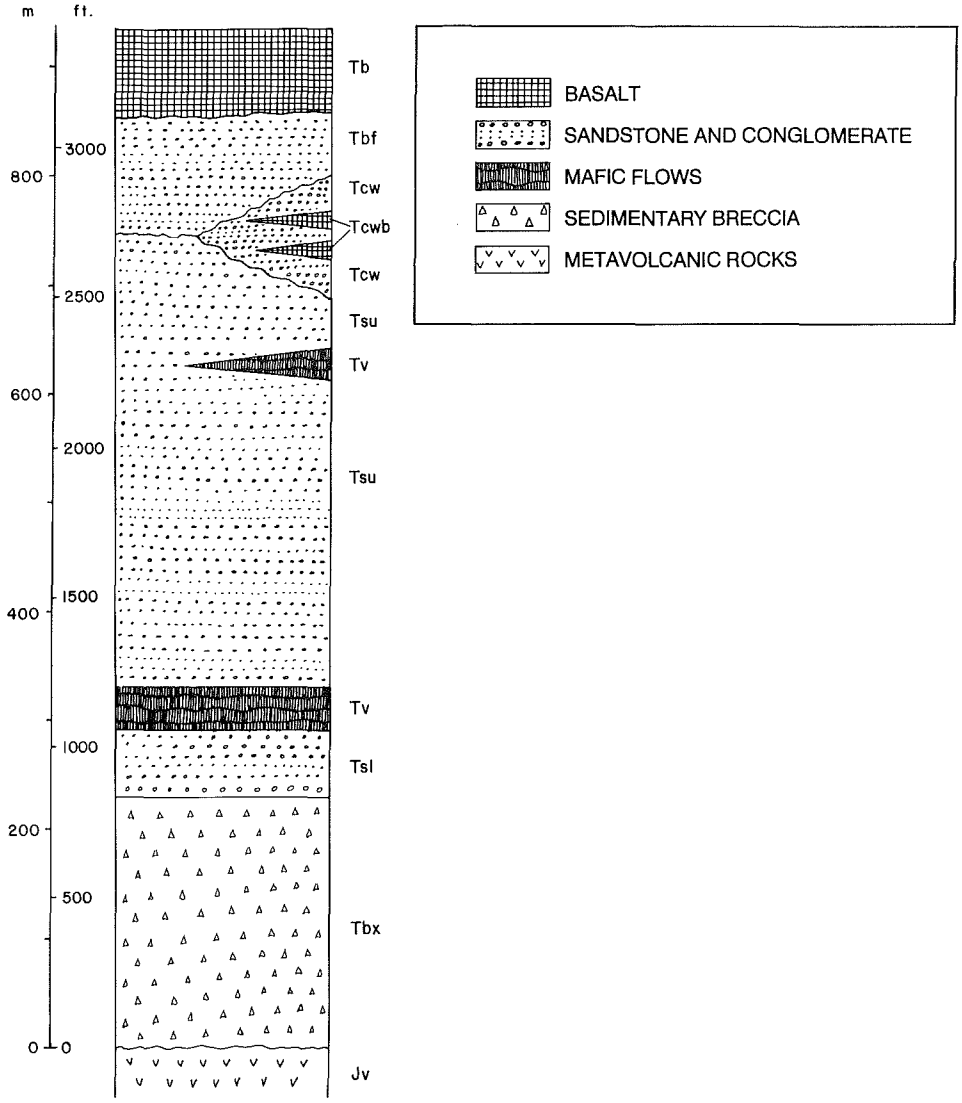

Figure 20. Stratigraphic column for Miocene strata in the Planet - Mineral Hill area (area of Plate 2). See Appendix A for unit descriptions.

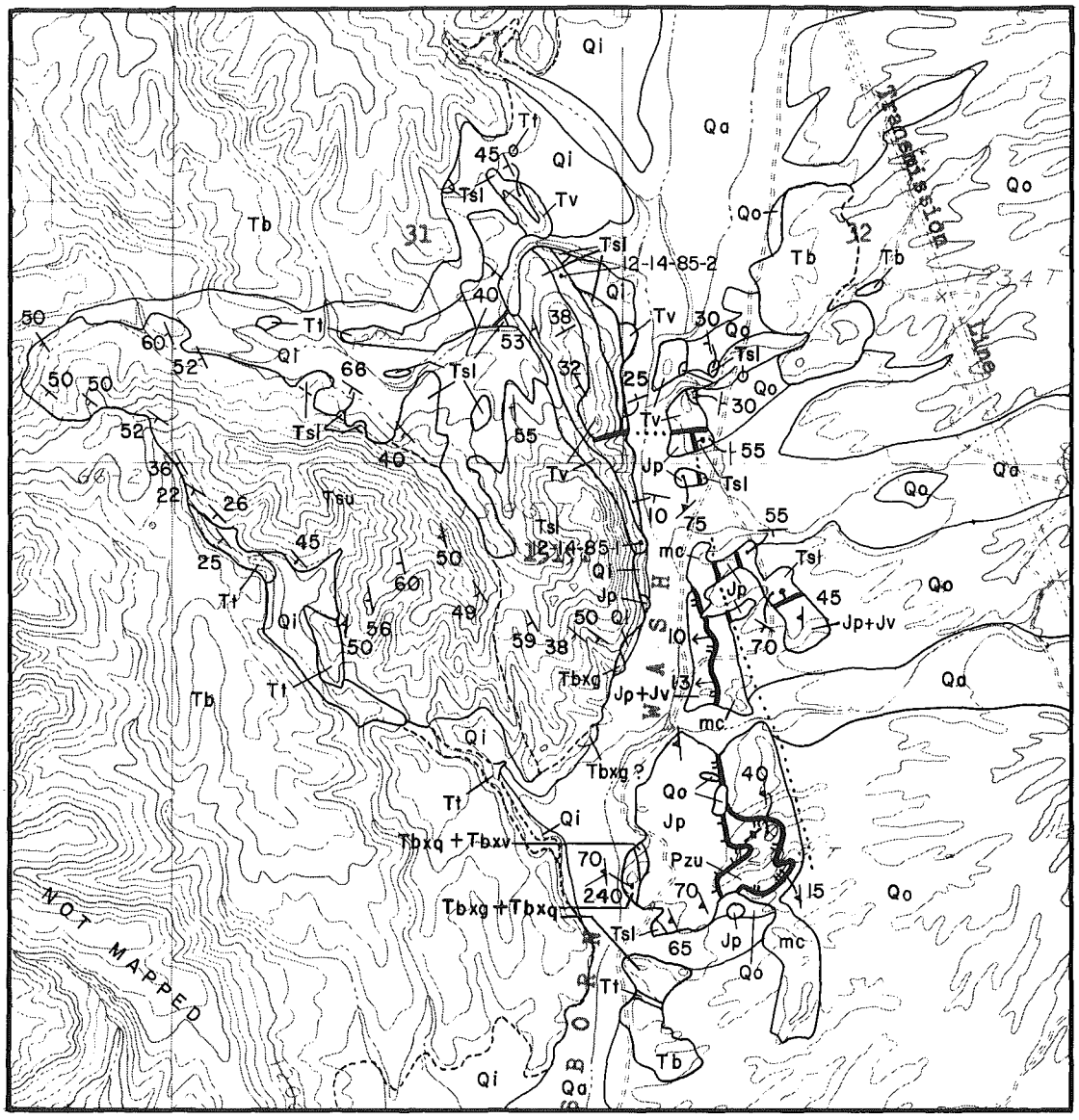

Figure 21 (this and facing pages). Geologic map of upper Osborne Wash near the Pride mine. See Figure 1 for location and Table 2 for map-symbol descriptions.

fault that originally underlay the upper-plate rocks in the Planet and Mineral Hill area was an approximately north- to northwest-dipping fault.

Pride Mine Area

Southwest of Mineral Wash in the Pride mine area, a moderately west- to southwest-dipping sequence of Miocene volcanic and sedimentary rocks and small fault blocks of metamorphosed Mesozoic and Paleozoic volcanic and sedimentary rocks are juxtaposed with lower-plate chloritic breccia and mylonitic crystalline rocks along the gently west-dipping detachment fault (Fig. 21). Upper-plate rocks at the Pride mine consist of dark-brown calcite(?) marble and tan-weathering, white, medium-grained dolomite marble of probable Paleozoic age. In the canyon 0.5 km south of Pride mine, the detachment-fault zone contains little or no gouge and is an unusually tight contact. In this area, siliceous metasedimentary rocks containing recess-forming calcareous layers are tectonically interleaved with lower-plate crystalline rocks over a 2- to 4-m-wide shear zone that represents the detachment fault. Pods of pegmatitic granite form boudins within metasedimentary tectonites in the shear zone.

Upper-plate rocks exposed west of Pride mine along upper Osborne Wash consist of small fault blocks of Mesozoic and Paleozoic rocks overlain by a thick sequence of west- to southwest-dipping Miocene volcanic and sedimentary rocks. The detachment fault is exposed at the base of this sequence and is offset by a north-trending, postdetachment high-angle fault. Jurassic Planet Volcanics are depositionally overlain by Tertiary sedimentary breccia and the lower sandstone unit. The lower sandstone unit is composed of fine- to coarse-

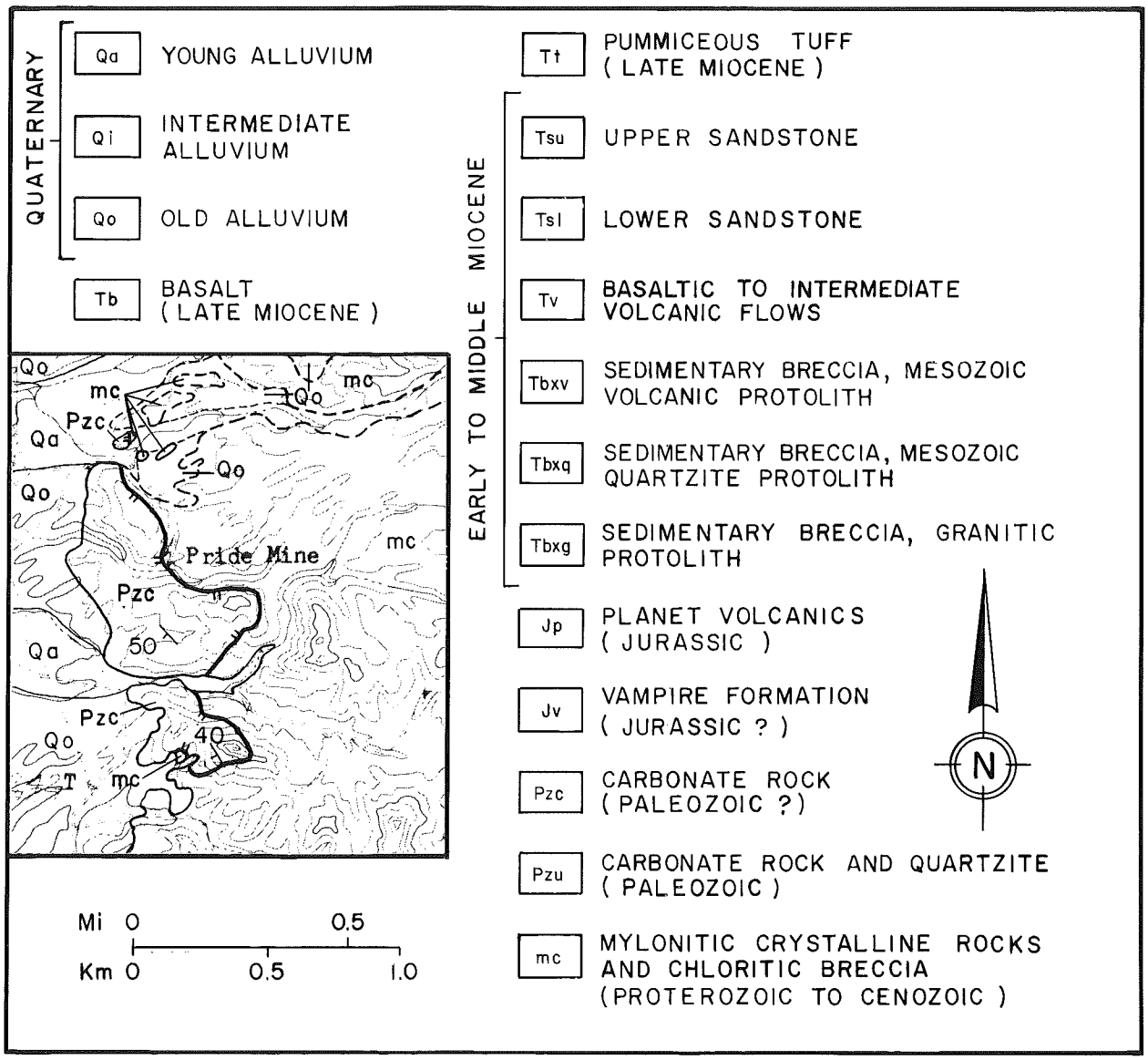

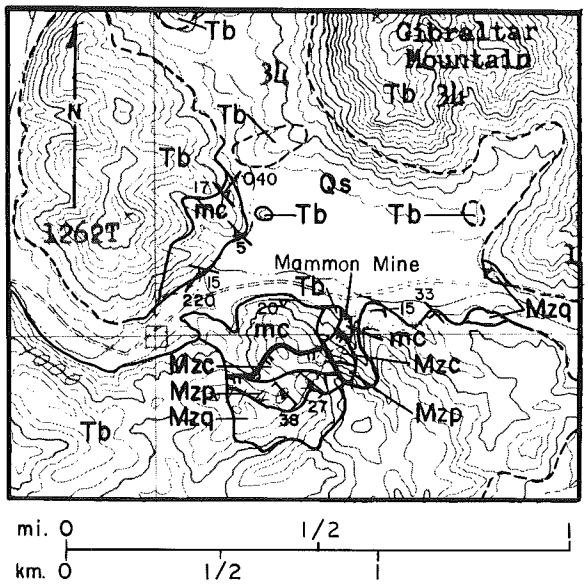

Qs Surficial deposits (Quaternary)
Tb Basalt and local basal volcaniclastic rocks (Miocene)
Mzq Quartzite, medium to fine grained, medium gray, brown weathering (Mesozoic)
Mzp Phyllite, silvery gray to dark gray (Mesozoic)
Mzc Calcareous metasiltstone and metasandstone, green, schistose (Mesozoic)
mc Mylonitic crystalline rocks

Figure 22. Geologic map of the Mammon mine area. See Figure 1 for location and Table 2 for map-symbol descriptions.

grained sandstone with local thinly bedded siltstone and sparse pebbles of quartzite and leucocratic granite. It is so impregnated with secondary calcite that it weathers like massive limestone. The lower sandstone unit is interbedded with vesicular mafic flows that are strongly K metasomatized (Spencer, Shafiqullah, and others, this vol.) and contains calcite in vesicles, in fractures, and as small local replacements. The lower sandstone unit is overlain by the upper sandstone unit, which is composed of conglomeratic sandstone and, in western exposures, conglomerate. Clasts in this unit primarily consist of granitoid rocks. Generally sparse clasts of Mesozoic and Tertiary volcanic rocks are more common in the lower part of the unit. Sparse clasts of reworked Tertiary sandstone, limestone, and mylonite of probable lower-plate derivation are also present.

Mammon Mine Area and Northern Cactus Plain

A well-exposed detachment fault in the Mammon mine area of the southwestern Buckskin Mountains places Mesozoic metasedimentary rocks over variably chloritically altered, lower-plate mylonitic gneiss (Fig. 22). The Buckskin detachment fault is exposed 6 km to the east in upper Osborne Wash, where it juxtaposes similar rock types (Fig. 21). It is virtually certain that the detachment fault at Mammon mine is an exposed segment of the Buckskin detachment fault. A bimodal suite of post-detachment volcanic rocks that yielded K-Ar dates of approximately 10 Ma rest depositionally on both upper- and lower-plate rocks in the Mammon mine area (Fig. 22; Grubensky, this vol.).

Paleozoic, Mesozoic, and Tertiary rocks similar to upper-plate rocks elsewhere in the western Buckskin Mountains compose several small hills south of Black Peak in Cactus Plain (Fig. 23). Tilted Tertiary and Mesozoic rocks are exposed beneath gently dipping basalts at Black Peak along the northwestern margin of Cactus Plain (Grubensky, this vol.). The southwestern continuation of the Buckskin detachment fault probably underlies these rocks as well as much or all of the rest of Cactus Plain.

Lower Bill Williams River

The upper-plate Tertiary stratigraphic sequence along the south side of the lower Bill Williams River (Fig. 24) consists, in ascending order, of the following four units: (1) sedimentary breccia primarily derived from quartzite of the Jurassic(?) Vampire Formation, (2) sandstone and conglomerate containing clasts of various Mesozoic supracrustal rock types, such as those in the Planet and Mineral Hill area, (3) K-metasomatized, mafic to intermediate flows, and (4) a thick sequence of tan sandstone and conglomerate. The entire sequence is lithologically similar to the Miocene stratigraphic sequences in the Planet and Mineral Hill area and in the Pride mine area and is inferred to be correlative.

The upper sandstone and conglomerate unit, which is by far the most widely exposed upper-plate Tertiary

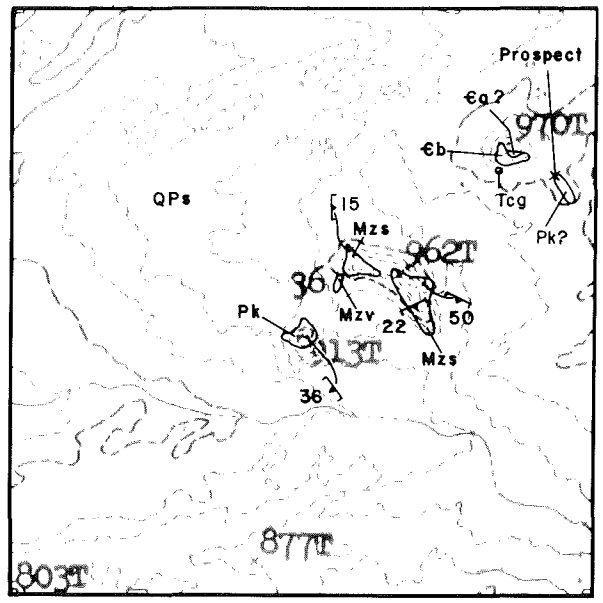

QPs	Surficial deposits (Quaternary and Pliocene)
Tcg	Conglomerate (Miocene)
Mzv	Metavolcanic rocks (Mesozoic)
Mzs	Metasedimentary rocks (Mesozoic)
Pk	Kaibab Limestone (Permian)
Ꞓa	Abrigo Formation (Cambrian)
Ꞓb	Bolsa Quartzite (Cambrian)

Figure 23. Geologic map of outcropping bedrock south of Black Peak in northwestern Cactus Plain. Area shown is 1 mi^2 (sec. 36). See Figure 1 for location and Table 2 for map-symbol descriptions.

unit, was deposited directly on Proterozoic crystalline rocks in sec. 13 and rests on the Tertiary volcanic flows in the adjacent area to the east. The basal beds do not dip as steeply as the underlying Tertiary strata; thus, the upper sandstone and conglomerate unit probably rests unconformably on the underlying Tertiary units. Bedding dips decrease upsection in the upper part of the unit and markedly flatten directly beneath overlying, flat-lying basalt (especially in SW$^1/_4$ sec. 19). This upper unit was thus deposited during the final phase of tilting.

The composition of cobbles and local boulders in the sandstone and conglomerate unit changes significantly with stratigraphic position. The percentage of granitoid clasts increases upsection, from approximately 30% near the base to 80% near the top, and is associated with a corresponding decrease in the abundance of clasts derived from Mesozoic metavolcanic and metasedimentary rocks and Tertiary volcanic and sedimentary rocks (Fig. 3; Table 1). Erosional destruction of Mesozoic and Tertiary strata and corresponding uncovering of underlying Proterozoic crystalline rocks in the clast-source area possibly account for these changes in clast populations. Alternatively, changes in sediment-dispersal patterns resulted in derivation of different types of clasts from different source areas. More than a few percent of the clasts

were derived from the lower plate of the detachment fault during deposition of this unit.

Tertiary strata along the lower Bill Williams River occupy the down-tilted side of a single southwest-tilted fault block. The fault that bounds this fault block to the southwest, referred to as the Havasu Spring fault by G.A. Davis and others (1980), is exposed in the excavated cuts at the Central Arizona Project (CAP) intake station on Lake Havasu (Fig. 24). The fault extends northwestward through Havasu Spring in the northwesternmost Buckskin Mountains (Plate 3) and projects farther northwest along the southwest side of Lake Havasu for at least 15 to 20 km (see Fig. 5 in Davis, G.A., and others, 1980). Pre-Tertiary rocks in this fault block are entirely composed of crystalline rocks of probable Proterozoic age in western exposures flanking the mouth of the Bill Williams River, and of metamorphosed Mesozoic rocks in the Planet and Mineral Hill area just east of the area of Figure 24 (Plates 2 and 3). The contact between these contrasting pre-Tertiary rock types is not exposed, but is inferred to be a thrust fault (see also Reynolds and Spencer, this vol.).

North-trending basaltic dikes in the area around the easternmost exposures of the Havasu Spring fault (northwestern part of Fig. 24) were interpreted to be displaced by this fault (Davis, G.A., and others, 1980). However, we did not recognize any exposures where the fault and dikes were in contact, and two exposed dike segments are aligned across the fault on the west flank of the CAP intake station. We interpret the dikes to be younger than movement on the Havasu Spring fault.

Parker Dam Area

Proterozoic(?) crystalline rocks and depositionally overlying Tertiary strata (Fig. 25) form the southeastern part of one of several northwest-trending, southwest-tilted fault blocks that compose the imbricately normal-faulted upper plate in the eastern Whipple Mountains (Davis, G.A., and others, 1980; Plate 3). Tertiary strata in the Parker Dam area consist, in ascending order but with some interbedding, of the following: (1) tan, reddish-brown, and brownish-red, poorly sorted sandstone and conglomeratic sandstone, and local conglomerate and tuff beds. Clasts were derived from various metamorphosed Paleozoic and Mesozoic sedimentary and volcanic rocks; (2) sedimentary breccia primarily derived from quartzite of the Jurassic(?) Vampire Formation with less abundant foliated Jurassic Planet Volcanics; (3) intermediate to mafic volcanic flows and flow breccias; and (4) red arkosic sandstone and conglomerate containing a very high proportion of subrounded cobbles and local boulders derived from plutonic and high-grade metamorphic rocks. The lower and upper sandstone and conglomerate units were not divided on Figure 25 because of their local similarity and interbedding within the two intervening units. This tilted sequence is unconformably overlain by flat-lying tan sandstone and conglomerate and overlying basalt.

Segments of the basal depositional contact are preserved between crosscutting, east-side-down normal faults in the northern part of the area of Figure 25. Tuff beds approximately 50 to 150 m stratigraphically above the base of the section are not offset, suggesting that fault movement had ended by the time the tuffs were deposited. The dip of bedding gradationally decreases upsection above the tuff beds and below the breccia, indicating that approximately 20° to 30° of tilting occurred during deposition of the basal unit.

Giers Mountain - Billy Mack Mountain Area

Several southwest-tilted fault blocks in the eastern Whipple Mountains extend southeastward into the western Buckskin Mountains, where they are truncated at a high angle by a northeast-striking fault in the area north and west of Giers Mountain (Davis, G.A., and others, 1980; Frost, 1983; Figs. 26 and 27). This fault, referred to herein as the Giers Mountain fault, dips between 20° and 30° to the north or northwest and has probably accommodated displacement on all of the northwest-striking normal faults that project toward it. It is thus kinematically analogous to a detachment fault, but does not have nearly as much displacement as the Whipple or Buckskin-Rawhide detachment faults. We do not consider the fault to be a segment of the Whipple detachment fault (Fig. 5 in Davis, G.A., and others, 1980; Frost, 1983) for three reasons: (1) crystalline rocks above and below the Giers Mountain fault are not appreciably different in degree of deformation or metamorphism; (2) footwall rocks bear little resemblance to the chloritically altered, mylonitic crystalline rocks below the Whipple and Buckskin-Rawhide detachment faults; and (3) footwall rocks appear to be structurally continuous with steeply dipping Tertiary strata at the south edge of Figure 27. We interpret the Giers Mountain fault as a tear fault within the upper plate of the Whipple-Buckskin detachment fault.

The footwall block of the Giers Mountain fault (referred to herein as the Giers Mountain footwall block) extends for almost 10 km in a northeast-southwest direction parallel to the direction of extension. In contrast, the largest tilt blocks in the eastern Whipple Mountains are about half the width of the Giers Mountain footwall block. Steeply dipping Tertiary clastic rocks (southwestern corner of Fig. 27) strike westward toward the middle of the Giers Mountain footwall block and are separated from the Paleozoic and Mesozoic rocks in the Billy Mack Mountain area (Fig. 27) by southeast- and northeast-dipping, low- to high-angle faults. These faults possibly cut across the Giers Mountain footwall block and divide it into two fault blocks with widths similar to other tilt blocks in the Whipple Mountains. However, mapping by Frost (1983) did not reveal any faults cutting across the Giers Mountain footwall block, indicating that if such faults are present, they must be older than, and truncated by, the Giers Mountain fault. It thus appears that extensional faulting did not attenuate the footwall block of the Giers Mountain fault as much as elsewhere in upper-plate rocks of the eastern Whipple and western

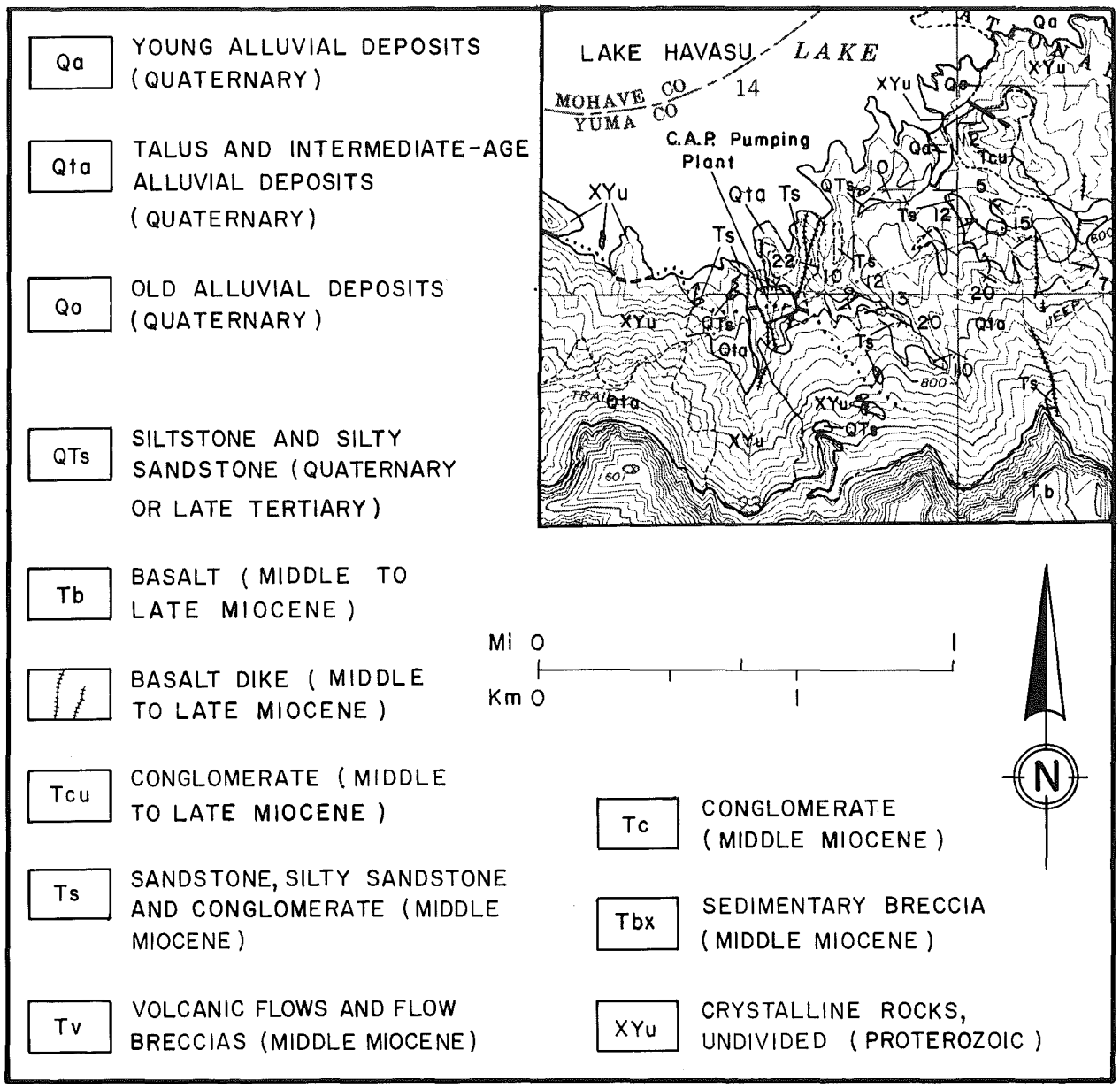

Buckskin Mountains, although it is possible that unmapped faults break the Giers Mountain footwall block.

Complex Tertiary faulting in the area of the Rio Vista and Sue mines has juxtaposed Tertiary clastic and volcanic rocks with pre-Tertiary rocks; no depositional contacts are preserved at the base of the Tertiary section. The high-angle fault near the Sue mine (northwest corner of Fig. 28) does not have large displacement because a Mesozoic fault contact between Proterozoic and Phanerozoic rocks is not significantly offset. Steeply southwest-dipping Tertiary clastic rocks rest depositionally on pre-Tertiary rocks in the area shown at the southwestern corner of Figure 28.

POSTDETACHMENT ROCKS AND STRUCTURES

Moderately to steeply tilted Tertiary clastic and volcanic rocks are unconformably overlain by gently dipping to flat-lying fanglomerate and interbedded basalt west of the Rio Vista mine (Fig. 29). Three of four K-Ar dates on the basalt are between 14 and 16 Ma; the age of the basalt is probably within this range. Tilting and related faulting thus ended in the southeastern Whipple and westernmost Buckskin Mountains before approximately 15 Ma (see also Davis, G.A., and others, 1980, 1982).

Postdetachment, pre-Quaternary sedimentary rocks, designated *basin fill* on many of the geologic maps in this article, vary from immediately postdetachment sedimentary breccias to alluvial-fan deposits that probably range in age from middle Miocene to upper Pliocene. The term *basin fill* is commonly used in Arizona to designate strata deposited during and after formation of late Cenozoic basins. Most of the exposed basin-fill strata in

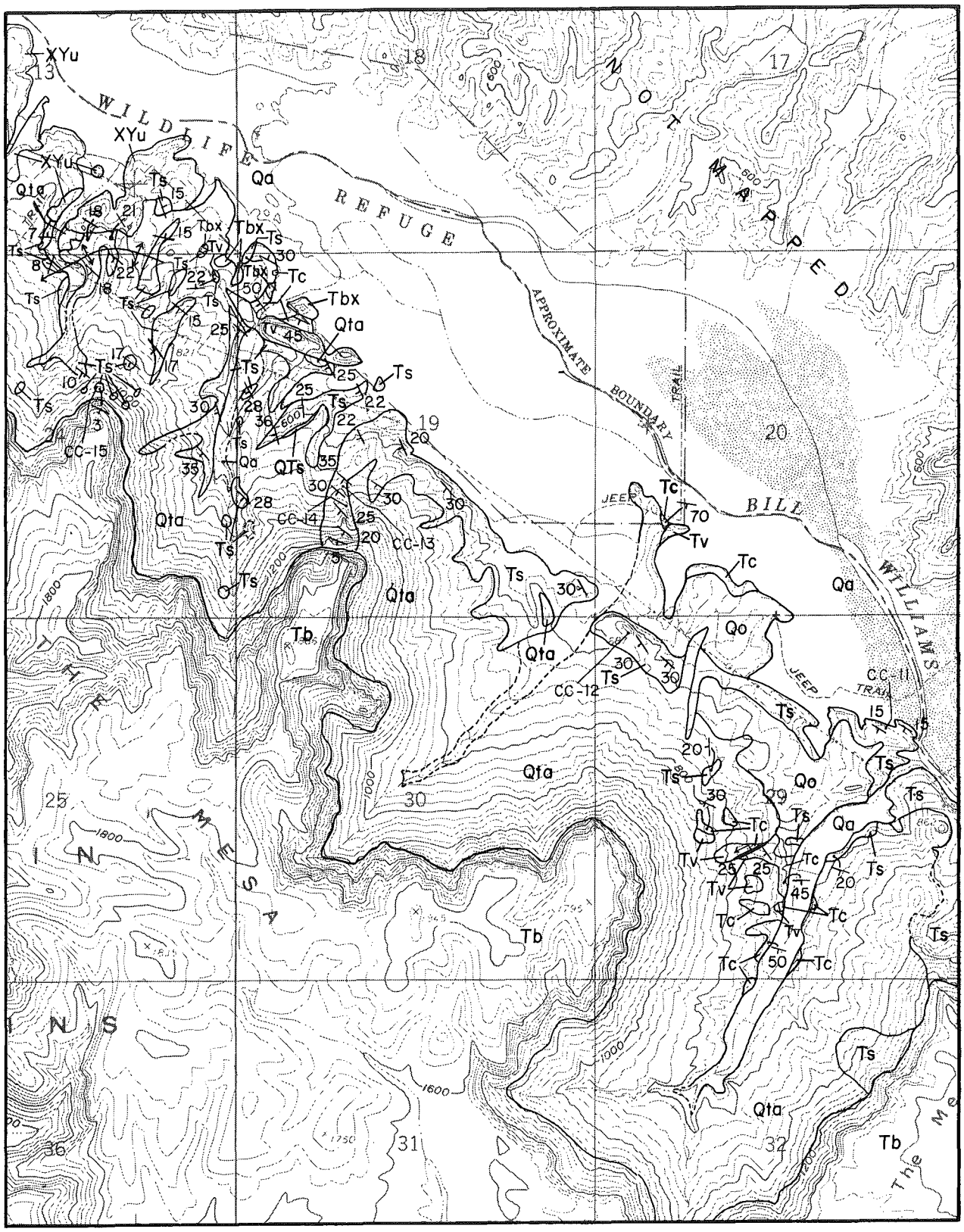

Figure 24. Geologic map of the south flank of the lower Bill Williams River near the east end of Lake Havasu. See Figure 1 for location and Table 2 for map-symbol descriptions.

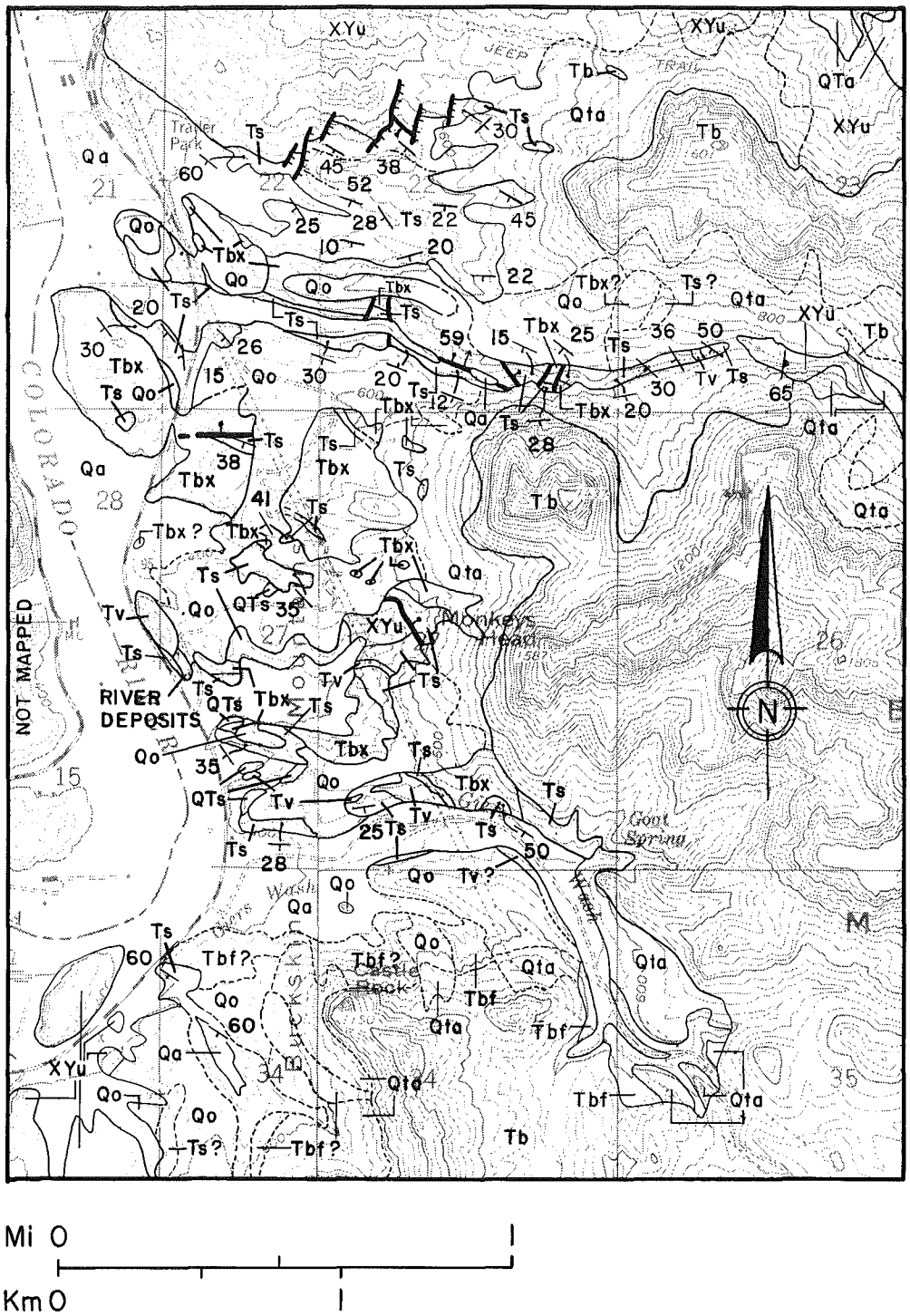

Figure 25. Geologic map of the northwestern Buckskin Mountains in the Parker Dam area, with brief unit descriptions (facing page). See Figure 1 for location and Table 2 for map-symbol descriptions. Small outcrop of Tv in northeast part of map area is composed of tuff.

the Buckskin Mountains are flat-lying to gently dipping, poorly sorted, stratified gravels that locally include moderately sorted conglomerate. Basin fill underlies much of the flat-lying basalt in the western Buckskin Mountains and is preserved along the downdropped northeast side of the Mineral Wash fault. Tilted, variably conglomeratic strata in the southern Bill Williams Mountains (Sherrod, 1988), southern flank of the lower Bill Williams River (Fig. 24), and eastern Rawhide Mountains (Spencer, Grubensky, and others, this vol.) grade upward into very gently dipping to flat-lying strata that are included in the basin-fill unit. Sedimentary breccia

Qa — YOUNG ALLUVIAL DEPOSITS (QUATERNARY)

Qta — TALUS AND INTERMEDIATE-AGE ALLUVIAL DEPOSITS (QUATERNARY)

Qo — OLD ALLUVIAL DEPOSITS (QUATERNARY)

QTs — SILTSTONE AND SILTY SANDSTONE (QUATERNARY OR LATE TERTIARY)

Tb — BASALT (MIDDLE TO LATE MIOCENE)

Tbf — BASIN-FILL CONGLOMERATE AND SANDSTONE (MIDDLE TO LATE MIOCENE)

Ts — SANDSTONE, SILTY SANDSTONE AND CONGLOMERATE (OLIGOCENE(?) TO MIDDLE MIOCENE)

TUFF BED (OLIGOCENE (?) TO MIDDLE MIOCENE)

Tv — VOLCANIC FLOWS AND FLOW BRECCIAS (OLIGOCENE(?) TO MIDDLE MIOCENE)

Tbx — SEDIMENTARY BRECCIA (OLIGOCENE(?) TO MIDDLE MIOCENE)

XYu — CRYSTALINE ROCKS UNDIVIDED (PROTEROZOIC)

deposited near Clara Peak (discussed above in section on upper-plate rocks in the Clara Peak area) is also included in the basin- fill unit.

Areally extensive, flat-lying to very gently dipping basalts and local silicic extrusives in the western Buckskin Mountains and northeastern Bill Williams Mountains postdate tilting of underlying lower-plate rocks (Suneson and Lucchitta, 1983; Grubensky, this vol.; Plate 3) and have yielded K-Ar dates between 9 and 13 Ma (Suneson and Lucchitta, 1979; Reynolds and others, 1986a; Spencer, Shafiqullah, and others, this vol.). The basal contact of the basalts is consistently at an elevation of between 200 and 500 m in the area covered by Figure 1, which is lower than the crests of ENE-trending, lower-plate antiforms and is generally higher than the Colorado and Bill Williams Rivers in this area. The flatness of the landscape over which the basalts were deposited suggests that the structural level of exposure at the time of basalt eruption was not significantly different from the level of exposure at the time detachment faulting ended. Furthermore, the present-day level of exposure is not appreciably different than the level of exposure at the time of basalt eruption. It thus appears that the present level of exposure in the northwestern Buckskin Moun-

Qa — YOUNG ALLUVIAL DEPOSITS (QUATERNARY)

Qta — TALUS AND INTERMEDIATE-AGE ALLUVIAL DEPOSITS (QUATERNARY)

Qo — OLD ALLUVIAL DEPOSITS (QUATERNARY)

Tbo — BOUSE FORMATION (LATE MIOCENE TO PLIOCENE)

Tb — BASALT (MIDDLE TO LATE MIOCENE)

Tbf — BASIN-FILL CONGLOMERATE AND SANDSTONE (MIDDLE TO LATE MIOCENE)

Ts — SANDSTONE, SILTY SANDSTONE AND CONGLOMERATE (OLIGOCENE (?) TO MIDDLE MIOCENE)

Tsx — SEDIMENTARY BRECCIA AND MASSIVE CONGLOMERATE (OLIGOCENE (?) TO MIDDLE MIOCENE)

Tsvx — SEDIMENTARY AND VOLCANIC ROCKS INCLUDING SEDIMENTARY BRECCIA (OLIGOCENE (?) TO MIDDLE MIOCENE)

Tsa — BASAL ARKOSIC SANDSTONE (OLIGOCENE (?) TO MIDDLE MIOCENE)

Jp — PLANET VOLCANICS (JURASSIC)

Mzu — SEDIMENTARY ROCKS, UNDIVIDED (MESOZOIC)

Pzu — SEDIMENTARY ROCKS, UNDIVIDED (PALEOZOIC)

MzXYg — GRANITIC ROCKS, UNDIVIDED (MESOZOIC TO PROTEROZOIC)

XYu — CRYSTALINE ROCKS, UNDIVIDED (PROTEROZOIC)

Figure 26. Map units for Figures 27, 28, and 29.

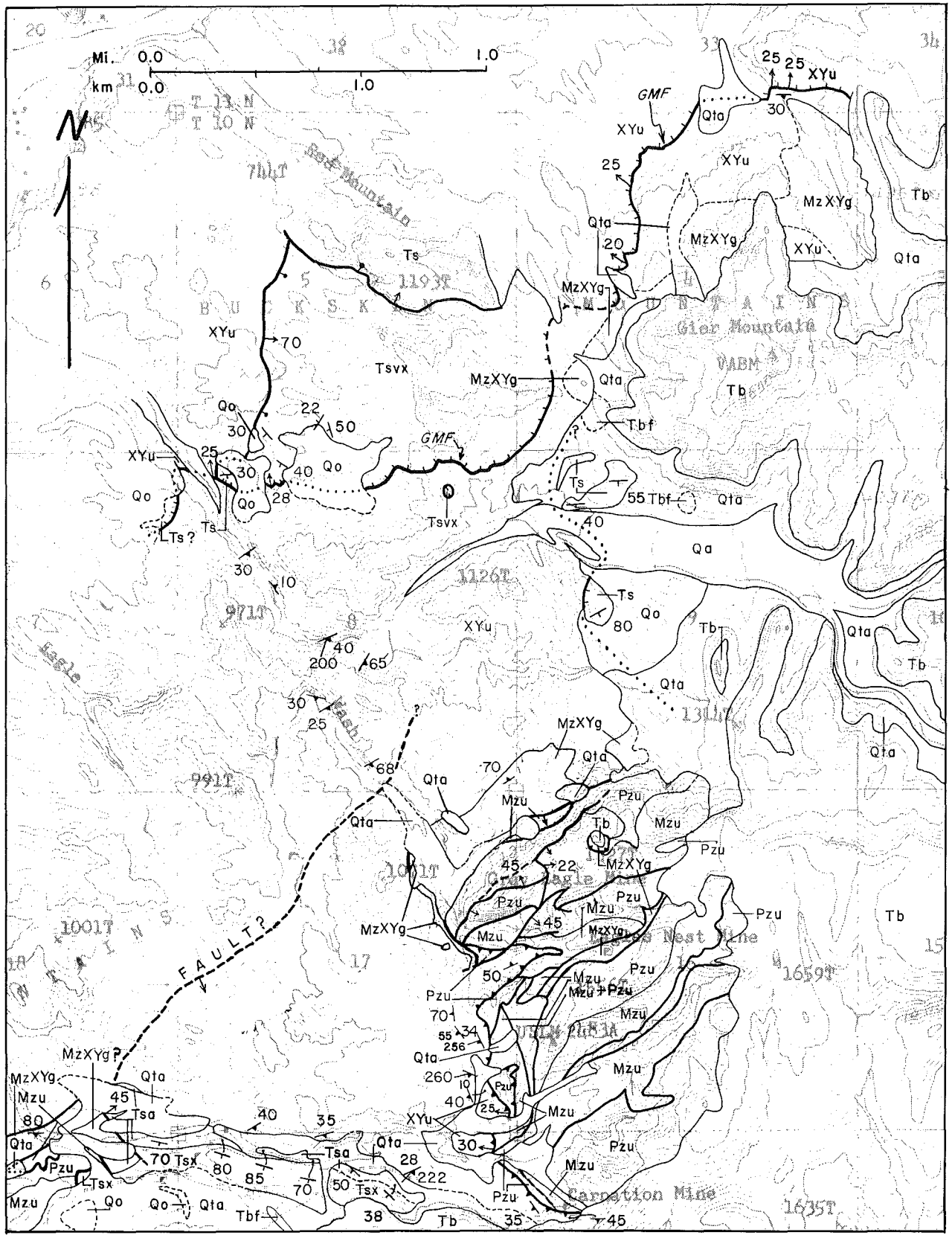

Figure 27. Geologic map of the Giers Mountain - Carnation mine area. See Figure 1 for location, Table 2 for map-symbol descriptions, and Figure 26 for map units. Mylonitic foliation symbol indicates semi-mylonitic, semicrystalloblastic fabric with variably developed, spaced cleavage. Foliation is dominantly Mesozoic in age near thrust faults and is probably Proterozoic elsewhere. GMF = Giers Mountain fault.

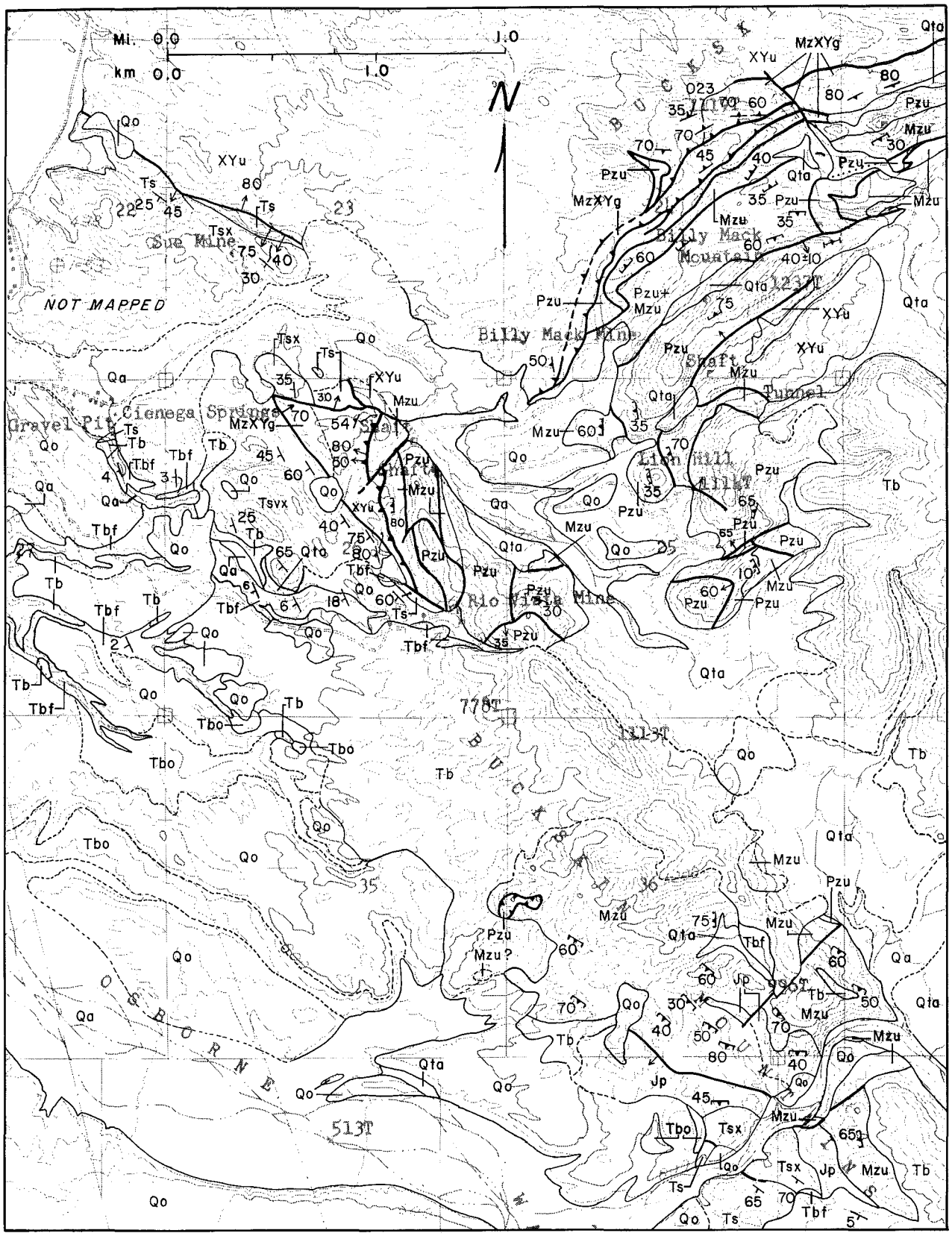

Figure 28. Geologic map of the Rio Vista - Billy Mack area. See Figure 1 for location, Table 2 for map-symbol descriptions, and Figure 26 for map units. Mylonitic foliation symbol indicates semimylonitic, semicrystalloblastic fabric with variably developed, spaced cleavage.

tains, eastern Whipple Mountains, and adjacent areas north of the Bill Williams River is approximately the level of exposure at the time detachment faulting ended, a conclusion reached previously by G.A. Davis and others (1980).

Three sets of northwest-trending, high-angle faults offset the detachment fault in the Buckskin and Rawhide Mountains. The easternmost fault set, with apparent reverse displacements, includes the Lincoln Ranch fault (discussed above in section on Lincoln Ranch basin) and subparallel faults along the gasline road south of Lincoln Ranch basin, along the west side of Lincoln Ranch basin, and on both sides of the Bill Williams River west of Rankin Ranch (Plates 1 and 3). Reverse displacement caused drag folding of the detachment fault and of mylonitic foliation in hanging-wall blocks adjacent to these high-angle faults. Subhorizontal striations along the Lincoln Ranch fault indicate that latest fault movement was strike slip. It is not known if reverse and horizontal displacements were separated by a substantial period of time or were part of a single period of displacement during which movement directions changed. The 2- to 3-km- wide, northwest-trending Swansea fault zone in the central Buckskin Mountains, which includes the Swansea fault, consists of many short fault segments separated by wide areas of unfaulted rock (Fig. 3 in Introduction, this vol.). Displacements in the fault zone are northeast side down and right lateral and range from a few tens to a few hundred meters. Displacement is locally southwest side down (Fig. 10).

The Mineral Wash fault, the westernmost of the three fault sets, is a single, locally bifurcating fault that extends from the lower Bill Williams River southeastward across the Planet Peak and Clara Peak antiforms (Figs. 1 and 19; Plate 2). The fault has approximately 200 m of northeast-side-down displacement where it offsets flat-lying basalt just south of the Bill Williams River. Displacement must be younger than the 10 Ma age of the

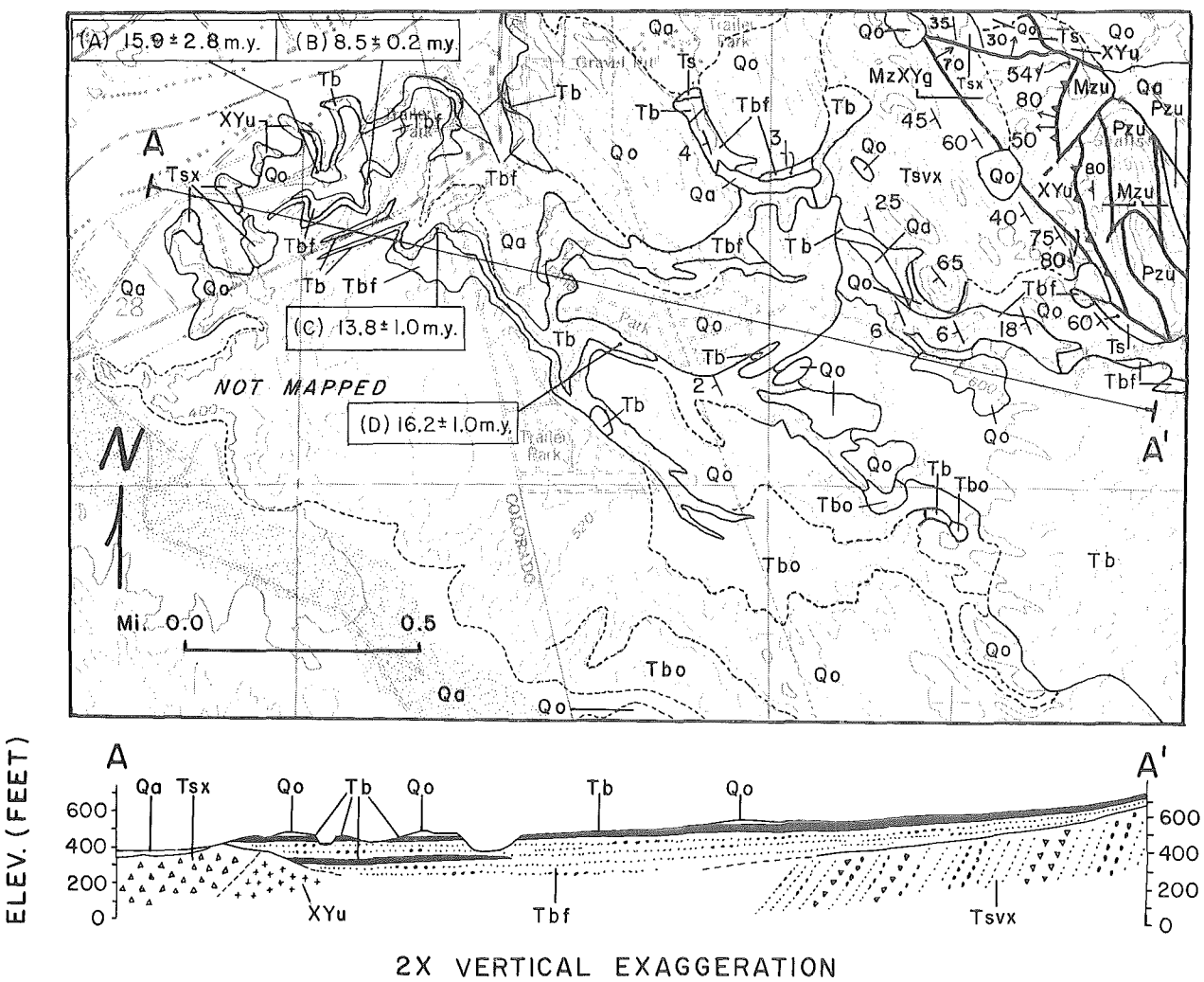

Figure 29. Geologic map and cross section of the area west of the Rio Vista mine. See Figure 1 for location, Table 2 for map-symbol descriptions, and Figure 26 for map units. K-Ar dates of the basalt are from (A) G.A. Davis and others (1982), (B) Marvin and Dobson (1979), (C) Calzia and Morton (1980), and (D) Shafiqullah and others (1980).

basalt (Armstrong and others, 1976; Calzia and Morton, 1980). The crest of the Planet Peak antiform appears to be offset by approximately 1 km of right-lateral displacement and 300 m of northeast-side-down vertical displacement on the Mineral Wash fault. In most areas the fault dips to the northeast, although in one area along Mineral Wash, the fault dips to the southwest (Plate 2). Striations on the fault surface are horizontal and indicate that the latest phase of displacement was strike slip (right lateral). Earlier vertical displacement may have occurred during a separate and distinct period of faulting, or it may have been an earlier part of a single period of faulting during which motion progressively changed from predominantly dip slip to predominantly strike slip.

SYNTHESIS OF TERTIARY STRUCTURAL AND STRATIGRAPHIC RELATIONSHIPS

Stratigraphic Correlations

Stratigraphic correlations among Miocene stratigraphic sequences in the Buckskin Mountains and adjacent areas are difficult to establish because of major lateral facies changes over short distances and difficulties in K-Ar dating due to pervasive K metasomatism. Lithology, cobble composition, and to a lesser degree, K-Ar dates are the main criteria used in our correlations. Stratigraphic correlations, in combination with knowledge of the structural evolution of the area, reveal generalities about evolution of basin geometry. Important paleogeographic features that influenced basin geometry and sediment-dispersal patterns include one or more normal-fault scarps that were the source of sedimentary breccia sheets, and denuded and uplifted lower-plate rocks that were the source of clasts of mylonitic and chloritically altered rocks. Basaltic flows, which erupted during a brief period, are present in many sequences and are probably broadly correlative.

Tertiary strata in the Planet and Mineral Hill area, lower Bill Williams River, and Parker Dam area all contain a four-part sequence of, in ascending order, sedimentary breccia, a lower sandstone and conglomerate unit, mafic flows, and an upper sandstone and conglomerate unit. The Tertiary sequence in upper Osborne Wash is also similar to this four-part sequence; we consider units in each of these areas to be correlative (Fig. 30). The upper three units are correlative with similar rocks in the Whipple Mountains that were assigned to the Copper Basin Formation by G.A. Davis and others (1980). The breccia unit and, at Parker Dam, underlying clastic rocks are correlative with rocks assigned to the Gene Canyon Formation by G.A. Davis and others (1980, following Ransome, 1931, and Kemnitzer, 1937).

The complex stratigraphic sequence in the Swansea area is less easily correlated with other sequences in the Buckskin Mountains. Sedimentary breccias in the lower half of the Swansea sequence were derived from the Jurassic Planet Volcanics, as was much of the breccia in the Planet and Mineral Hill area and areas farther west. K-metasomatized mafic(?) flows are stratigraphically above the breccias in all of these areas as well, suggesting that the breccias and volcanic flows are broadly correlative throughout the western half of the Buckskin Mountains (Fig. 30). Clastic rocks, limestone, and tuff that underlie the breccias at Swansea are not present in the western Buckskin Mountains, except in the far western Parker Dam area where sandstone and minor tuff underlie the breccia. Intermediate volcanic rocks and heterolithologic sedimentary breccia and debris flows are present in the upper part of the Swansea sequence, but are absent at equivalent stratigraphic levels farther to the west. The sedimentary breccias and volcanic flows in the middle part of the Swansea sequence may have been derived from the same source areas as breccias and volcanic flows farther west. The lack of similarity at stratigraphically lower and higher levels, however, suggests that the Swansea sequence was either deposited in another part of the same sedimentary basin or in a different basin altogether.

The Swansea sequence is generally similar to the Artillery Formation in the Artillery Mountains, although it is difficult to match individual units. In ascending order, the two sequences contain the following correlated groups of units (Fig. 30): (1) A basal arkose that grades upward into interbedded sandstone, siltstone, limestone, and tuff. Biotite from a tuff in this part of the Swansea sequence yielded a K-Ar date of 21.8 $\pm$ 0.5 Ma (Spencer, Shafiqullah, and others, this vol.), which is similar to a K-Ar biotite date of 23.0 Ma from a tuff in the lower Artillery Formation (J. Otton and R. Miller, oral commun., 1987); (2) Sedimentary breccia sheets (derived from Planet Volcanics and associated metasedimentary rocks) with interbedded limestone and, in the Artillery Mountains, siltstone, sandstone, and conglomerate; (3) Interbedded mafic(?) volcanic flows, conglomerate, sandstone, and in the Artillery Mountains, siltstone; and (4) A heterolithologic breccia known as the Artillery megabreccia in the Artillery Mountains and including debris flows in the Swansea area. Interbedded, intermediate volcanic rocks, sandstone, and local limestone and conglomerate overlying the heterolithologic breccia in the Swansea area are lithologically dissimilar to, and probably not correlative with, the red sandstone of the Chapin Wash Formation that overlies the Artillery megabreccia and is widely exposed in the eastern Buckskin Mountains. Similarly, the stratigraphically highest tilted unit in the Swansea sequence, which is composed of sandstone and conglomeratic sandstone and does not contain clasts derived from the lower plate, is probably not correlative with the Sandtrap Conglomerate, which contains abundant clasts derived from the lower plate. We interpret the Swansea and Artillery sequences to have been deposited side-by-side in the same sedimentary basin until after deposition of the Artillery megabreccia and equivalent heterolithologic breccia and debris flows in the Swansea area. Most likely, normal faulting disrupted the sedimentary basin and separated the two sequences, resulting in deposition of different noncorrelative sequences above the megabreccia.

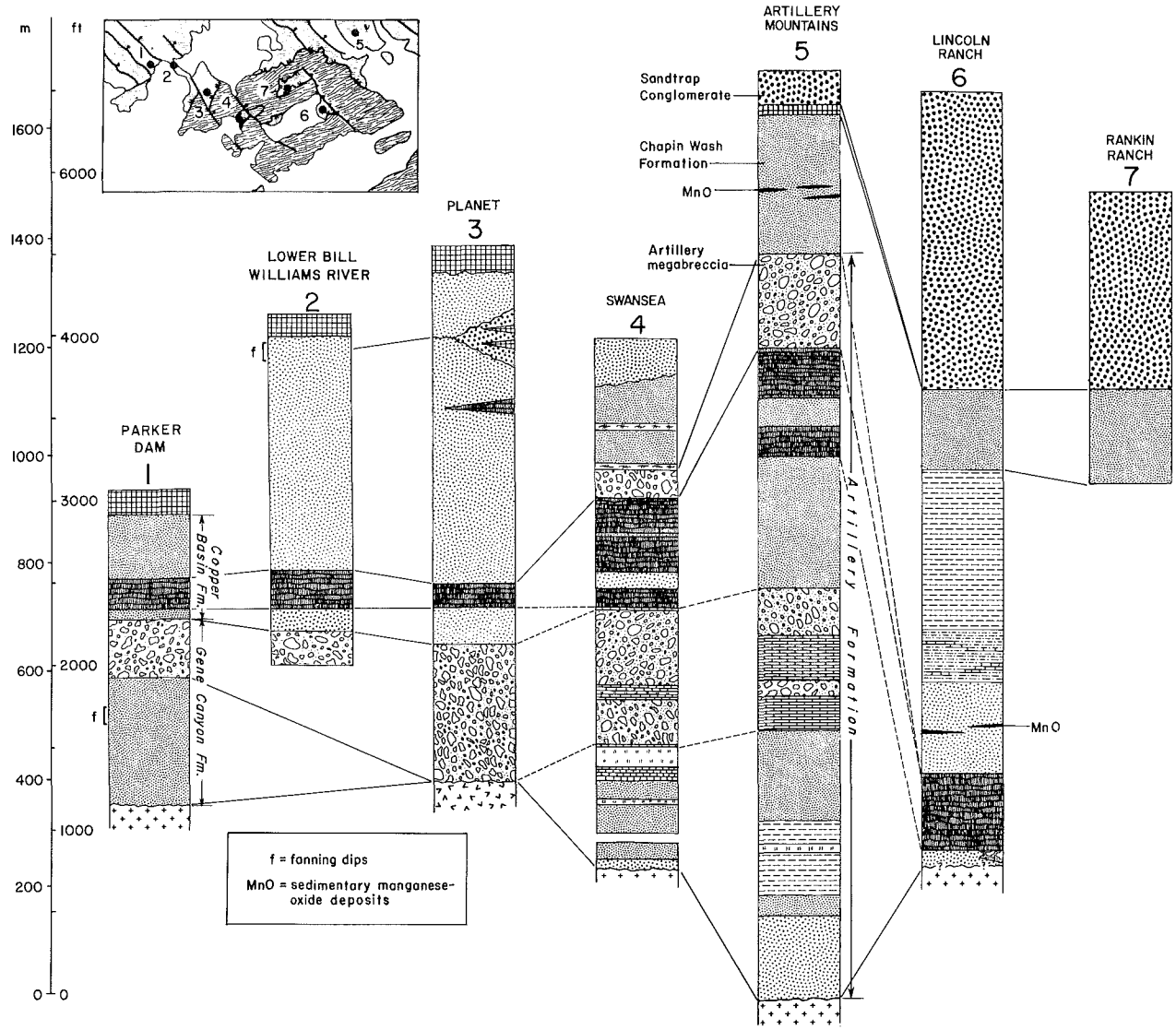

Figure 30. Stratigraphic columns and correlations of upper-plate Tertiary strata in the Artillery (column 5) and Buckskin Mountains. Stratigraphic column of Artillery Mountains from Spencer, Grubensky, and others (this vol.), with formation names from Lasky and Webber (1949). Designation of Copper Basin and Gene Canyon Formations in column 1 is based on descriptions of these formations in G.A. Davis and others (1980) and Frost (1983).

The Sandtrap Conglomerate (Lasky and Webber, 1949), a distinctive, generally tan-colored, poorly sorted, massive to poorly bedded conglomerate in the Artillery and eastern Rawhide Mountains, is identical in appearance to the stratigraphically highest tilted unit in the Lincoln Ranch synform and in the Swansea synform east of Swansea. In the Artillery and eastern Rawhide Mountains, the lower part of the Sandtrap Conglomerate is moderately tilted, whereas the upper part is gently tilted to flat lying and is interbedded with basalt (Lasky and Webber, 1949; Spencer, Grubensky, and others, this vol.) that is part of a regionally extensive, postdetachment suite of bimodal, basalt-dominated volcanic rocks (Suneson and Lucchitta, 1983). The Sandtrap Conglomerate was thus deposited over the time interval during which tilting, and presumably detachment faulting, ceased. Two cobble counts from Rawhide Wash indicate that the Sandtrap Conglomerate contains approximately 10% to 20% clasts derived from the lower plate of the detachment fault, and thus falls in the range of lower-plate-derived clast abundances established for similar conglomerates in the eastern Buckskin Mountains (Fig. 3). On the basis of lithology, clast populations, and stratigraphic position, we correlate the stratigraphically highest, tilted conglomerate units in the Lincoln Ranch basin, Clara Peak area, and Swansea synform east of Swansea with the lower tilted part of the Sandtrap Conglomerate (Fig. 30).

The Sandtrap Conglomerate overlies red sandstone of the Chapin Wash Formation in the Artillery Mountains. Based on lithologic similarity and stratigraphic position, we correlate the red sandstone that underlies the Sandtrap Conglomerate elsewhere in the Rawhide and eastern

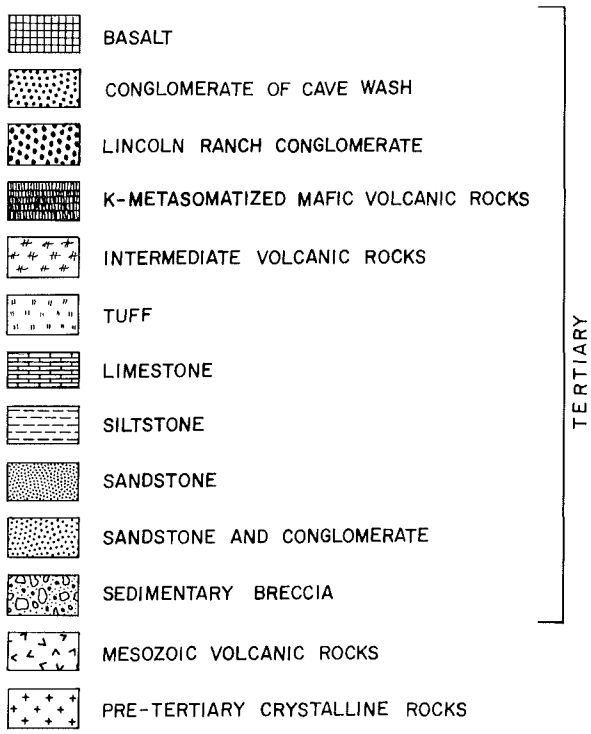

Buckskin Mountains with the Chapin Wash Formation. This correlation is supported by the presence of sparse lower-plate-derived clasts in the Chapin Wash Formation in the Artillery Mountains, (Spencer, Grubensky, and others, this vol.), Rawhide Mountains (Shackelford, this vol.), and Lincoln Ranch basin.

The lower part of the stratigraphic sequence in Lincoln Ranch basin (all units below the top two units on Fig. 30) is difficult to correlate with the other sequences. If basalt near the base of the Lincoln Ranch sequence is correlative with similar volcanic flows in the Swansea and Artillery sequences, then volcanism in the Lincoln Ranch area was preceded by unusually little sedimentation and was followed by a different sedimentary history than in the other areas. The thin sequence of sedimentary breccia, arkosic sandstone, mudstone, siliceous limestone, and tuff below the basalt in Lincoln Ranch basin is probably broadly correlative with lithologically similar strata in the Artillery Formation. A few percent of the clasts in the conglomeratic rocks that overlie the basalt in Lincoln Ranch basin were derived from the lower plate, suggesting that the strata overlying the basalt are correlative with the Chapin Wash Formation and not with the Artillery Formation. This correlation is supported by the presence of sedimentary Mn deposits in strata that overlie the basalt in Lincoln Ranch basin and the Chapin Wash Formation in the Artillery Mountains. The great thickness of siltstone and lacustrine rocks overlying the basalt suggests that this part of the Lincoln Ranch sequence was deposited in a more distal, basin-interior environment than equivalent sandstone-dominated strata that make up the Chapin Wash Formation in other areas.

Sandstone and conglomerate at the top of the sequence of tilted rocks in the Planet and lower Bill Williams River areas contain sparse clasts derived from the lower plate (Fig. 3; Table 1). It is not known if these clasts were derived from the same source as the lower-plate-derived clasts in the Chapin Wash Formation and Sandtrap Conglomerate (probably in the south-central Buckskin Mountains) or from a different source (most likely the Whipple Mountains). It is thus uncertain if the upper Copper Basin Formation and the Chapin Wash Formation were deposited in the same sedimentary basin and received lower-plate-derived clasts from the same source, or were deposited in different basins, possibly at different times, and received clasts from different sources. Lithologic similarity between sandstones in the upper Copper Basin Formation and Chapin Wash Formation suggests, along with cobble compositions, that the two are correlative or that they were deposited, possibly diachronously, in different basins but in similar tectonic and sedimentary environments.

Cross-Sectional Evolution

The Miocene structural and stratigraphic evolution of the Buckskin Mountains and adjacent areas is best understood in the context of general models of the tectonic evolution of metamorphic core complexes. As mentioned earlier, progressive ductile to brittle deformation of the lower plate is accounted for by models in which the lower plate is laterally displaced from beneath the upper plate and cools as it rises isostatically in response to tectonic denudation (e.g., Wernicke, 1981; Davis, G.A., and others, 1986; Fig. 31). The final warped form of detachment faults in metamorphic core complexes, as shown in cross sections parallel to extension direction, primarily reflects laterally varying isostatic rebound that, in turn, reflects lateral variations in tectonic denudation (Spencer, 1984b) and in density heterogeneities in the lithosphere (Holt and others, 1986). The relative significance of these two factors in determining the final geometry of detachment faults is generally not known and probably varies both within metamorphic core complexes and from complex to complex. Observed geometries of low-angle extensional systems vary between (1) a simple, slightly to moderately distended, wedge-shaped upper plate that was displaced laterally away from a gently dipping breakaway fault, and (2) a highly distended upper plate that is separated into a wedge and synformal keel by an arched, uplifted lower plate (Spencer, 1984b, Fig. 1). The former geometry is exemplified by the Harcuvar Mountains (Reynolds and Spencer, 1985), whereas the latter is well established for a transect through the Chemehuevi Mountains (Frost and Okaya, 1986; John, 1987).

It is difficult to place the Buckskin and Rawhide Mountains on this spectrum of geometries because the area to the southwest of the Buckskin Mountains is almost entirely buried by post-Miocene deposits beneath Cactus Plain. In addition, it is not known if the alluvium-surrounded Bouse Hills are structurally part of the upper or lower plate of the Buckskin detachment

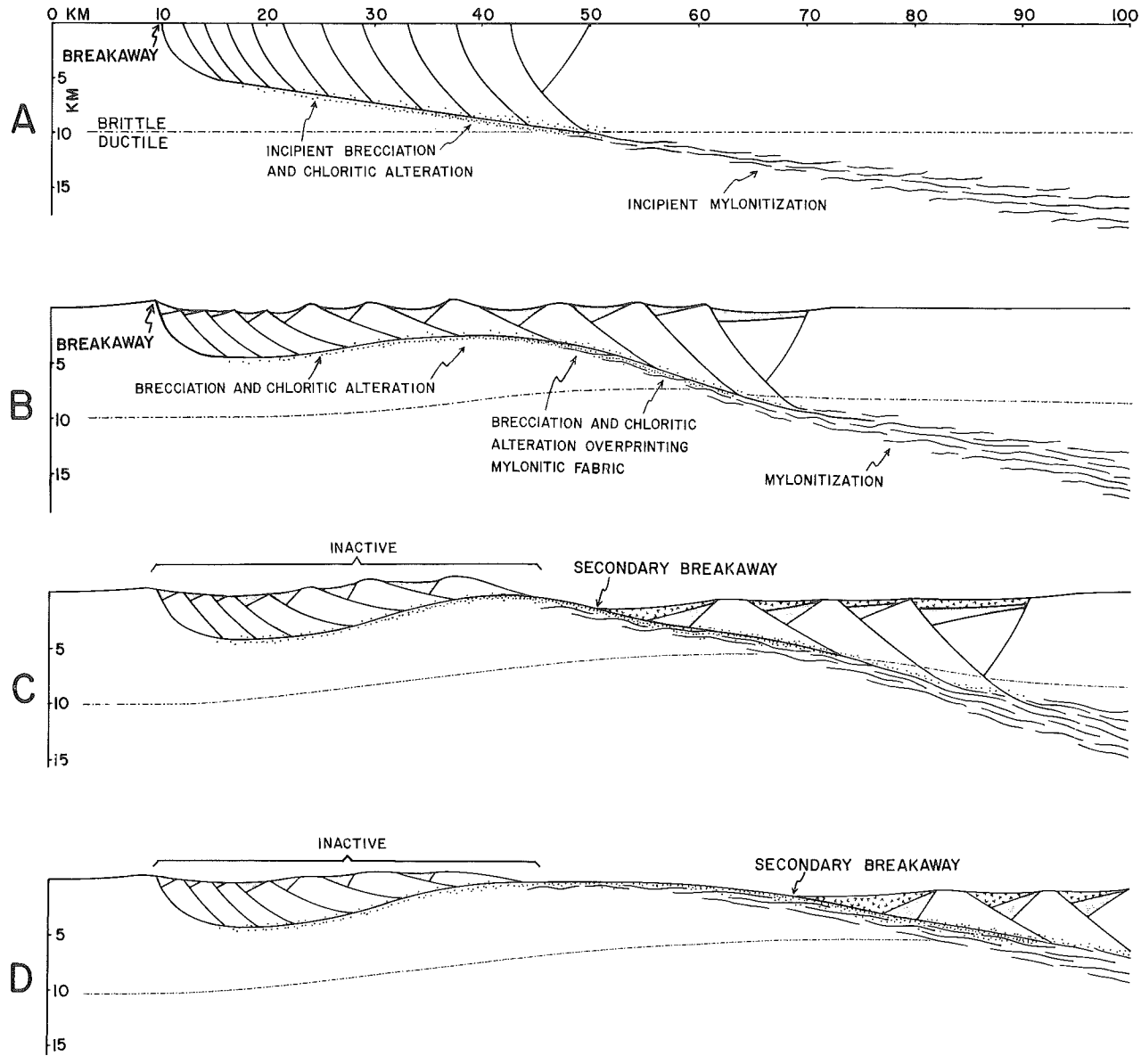

Figure 31. Schematic, cross-sectional evolution diagram for Cordilleran metamorphic core complexes. Geometries vary considerably among complexes and most complexes, unlike the Buckskin-Rawhide Mountains area, have not evolved beyond section C. Diagram is based on concepts and models from Wernicke (1981, 1985), Howard and others (1982b), Reynolds (1982, 1985), Spencer (1984b), and G.A. Davis and others (1986). A mylonitic front is not exposed in the Buckskin and Rawhide Mountains and is not illustrated, but concepts regarding the origin of a mylonitic front (Davis, G.A., 1988; Davis, G.A., and Lister, 1988) are possibly relevant to the tectonic evolution of this area.

fault, although several lines of evidence suggest that they are part of the lower plate. Exposures of lower-plate rocks in the Mammon mine area (Fig. 22) and at Mesquite Mountain (Knapp, 1988) suggest that the detachment fault is at a shallow depth (less than 1 or 2 km) beneath Cactus Plain, and that a thick synformal keel (5 km or more) like that west of the Chemehuevi Mountains is not present west of the Buckskin Mountains. It seems most likely that a thin synformal upper plate, perhaps not more than 1 or 2 km thick, is present beneath Cactus Plain and is represented by exposures of upper-plate rocks in the Mammon mine area (Fig. 22), Black Peak area (Grubensky, this vol.), and within Cactus Plain (Fig. 23). Lower-plate rocks at the east and northeast edge of Cactus Plain are thus interpreted to be part of a thin, synformal upper plate.

Tectonic Aspects of Sedimentation

Syntectonic sedimentary rocks, associated with a metamorphic core complex in which a synformal upper plate was produced before the end of detachment fault-

ing, should record subareal exposure of the arched lower plate if the lower plate is sufficiently uplifted (Spencer, 1984b; Miller and John, 1988). In this scenario, upper-plate rocks originally moving toward the rising lower-plate arch were warped into a broad synform and rendered tectonically inactive as movement ceased on their underlying segment of the detachment fault (Fig. 31C). Subareal exposure of the lower plate marks the approximate time of division of the upper plate into active and inactive parts and the beginning of one-sided denudation of the lower-plate arch (Spencer, 1984b).

Syntectonic sediments are shown as two distinct units in Figure 31. An earlier unit was deposited during tilting of fault blocks within the entire faulted upper plate (section B), and a later unit was deposited only to the right of the uplifted footwall arch (sections C and D). The older unit is represented by the Artillery Formation and correlative strata, and the younger unit is represented by the Chapin Wash Formation and the lower tilted part of the Sandtrap Conglomerate. The transition to one-sided denudation was possibly marked by development of substantial vertical relief (2 km shown on section C between km 40 and km 55) adjacent to the secondary breakaway, and collapse of part of the secondary-breakaway fault scarp to form the Artillery megabreccia (Spencer, Grubensky, and others, this vol.) and correlative strata in the Swansea area.

The Sandtrap Conglomerate, with its abundant clasts derived from lower-plate rocks, is interpreted as having been deposited during one-sided denudation and major subareal exposure of the arched lower plate. The commonly poorly sorted and poorly bedded character of the conglomerate and eastward decrease in clast size in the area east of the Rawhide Mountains (Spencer, Grubensky, and others, this vol.) support the interpretation that the Sandtrap Conglomerate was deposited as alluvial fans shed eastward from the partially denuded lower plate. Continued detachment faulting and associated upper-plate normal faulting dismembered and tilted the Sandtrap Conglomerate and further uncovered the lower plate. Sparse clasts of mylonitic rock and chloritic breccia in the Chapin Wash Formation indicate that the lower plate was initially exposed prior to deposition of the overlying Sandtrap Conglomerate.

The coarse breccia deposited on both lower- and upper-plate rocks east of Swansea and south of Clara Peak provides another key to understanding the Miocene tectonic evolution of the Buckskin Mountains. This breccia, which contains clasts up to 3 m across of Tertiary sandstone and conglomerate and, in some areas, smaller clasts derived from the lower plate, was deposited on both upper and lower plates and is not displaced by the detachment fault. The breccia is restricted to the western margin of the area over which Sandtrap Conglomerate was deposited. The coarseness of the breccia suggests that it was derived from a nearby area of high relief, possibly a fault scarp, and its relationship to the Sandtrap Conglomerate suggests that it was deposited at the margin of the basin in which the Sandtrap Conglomerate was deposited. Our interpretation of the origin of the breccia is that it was either (1) shed eastward off a fault scarp that initially formed as a secondary breakaway fault separating the active eastern part of the upper plate from the inactive western part, or (2) shed westward off an oversteepened dip slope of tilted upper-plate strata. At the time the breccia was deposited, however, all detachment faulting near the breccia must have ceased because it is not displaced where it rests across the detachment fault or on the lower plate. An alternative explanation might be that the breccia was shed off the uplifted west side of the Swansea fault, presumably well after detachment faulting had ended. The Swansea fault, however, does not have more than about 200 m of vertical displacement, yet coarse breccias are present 6 km away from the fault (east edge of Fig. 13).

Breakaway Migration, Incisement, and Excisement

Upper-plate rocks east of the Rawhide Mountains that now compose the Artillery and Poachie Mountains are slightly to moderately broken and distended by normal faults (Lasky and Webber, 1949; Otton, 1982; Bryant, 1988). It thus appears that, following the transition to one-sided denudation, the lower plate of the Buckskin and Rawhide Mountains was displaced toward the WSW out from beneath a structurally coherent, upper-plate wedge that now comprises the Artillery and Poachie Mountains. The northeast-facing monoclinal flexure on the northeast side of the Buckskin and Rawhide Mountains must have migrated laterally behind the tapered end of the upper-plate wedge during detachment faulting and after transition to one-sided denudation (cross-section C to D on Fig. 31). The secondary breakaway repeatedly jumped eastward within the upper plate, stranding small pieces (not shown) of the tapered end of the upper plate that are now the fault blocks scattered across the Rawhide and central and eastern Buckskin Mountains. This style of faulting and footwall flexure has also been recognized in the southern Great Basin (Hamilton, 1988; Wernicke and Axen, 1988; Wernicke and others, 1988).

Detailed geologic studies in the nearby Whipple Mountains and ranges farther north have led to recognition of two processes that may have played a major role in the evolution of detachment faults: *incisement* is the process whereby a new splay of the detachment fault cuts downward through the lower plate and results in transference of a slab of lower-plate rocks to the upper plate; *excisement* is the process whereby a new splay of the detachment fault cuts upward through the upper plate and results in transference of a slab of upper-plate rocks to the lower plate (Davis, G.A., and Lister, 1988; see also John, 1987). The abrupt downward truncation of upper-plate normal faults by the subhorizontal detachment fault in the Whipple Mountains is strong evidence that excisement has transferred, from the upper plate to the lower plate, a slab of rock that contains the presumably listric downdip continuations of the normal faults (Davis, G.A., and Lister, 1988). In the broadest use of the term, excisement could be interpreted as including a range of processes, from formation of a new segment of

a detachment fault where no fault had existed previously, to stepwise migration of the breakaway fault to previously active, upper-plate normal faults. In the latter process, which was not discussed by G.A. Davis and Lister (1988), upper-plate fault blocks are left inactive and stranded on a progressively lengthening, inactive segment of the detachment fault (see also Spencer and Reynolds, 1986b; Hamilton, 1988; Wernicke and others, 1988). In some areas of the Buckskin Mountains, upper-plate faults and folds are apparently truncated discordantly by the detachment fault (location C in Fig. 6; Figs. 8 and 16; Plate 2), but in other areas some faults flatten downward and merge with the detachment fault (western part of Fig. 11, as described at field-trip stop C6 in Spencer and others, 1987; Plate 2). Both stepwise breakaway migration and excisement on new low-angle faults probably influenced the geometry of upper-plate structures in the Buckskin Mountains, but the relative significance of each is difficult to determine.

Every increment of extension of the upper plate results in initial juxtaposition of upper-plate rocks with the detachment fault. This process probably occurs primarily at the intersection of the detachment fault and upper-plate listric or low-angle normal faults. Thus, the hanging-wall rocks of upper-plate listric or low-angle normal faults, originally in fault contact with other upper-plate footwall rocks, are displaced down and onto the detachment fault. It is possible that virtually the entire lower surface of the upper plate in the Buckskin Mountains was juxtaposed with the lower plate in this manner, and thus the detachment fault, *with respect to the upper plate*, is a young structural feature in the history of detachment faulting in the Buckskin Mountains. This is similar to the interpretation of the Whipple detachment fault by G.A. Davis and Lister (1988), although they emphasized low-angle excisement, not listric normal faulting, as the primary causative process.

Incisement of the lower plate in the Buckskin Mountains is suggested by the truncation of mesoscopic, northwest-trending lower-plate folds by the detachment fault (Osborne, 1981; Woodward, 1981). Low-angle faults are present in the lower plate in the eastern Buckskin and Rawhide Mountains (Shackelford, 1976b, this vol., Plate 1; Bryant and Wooden, this vol.), but these faults are discontinuous, do not juxtapose highly contrasting rock types, and probably do not have significant displacement compared to the detachment fault. Similar lower-plate faults have been recognized in the Whipple Mountains (Davis, G.A., and Lister, 1988). Because the detachment fault is exposed, albeit discontinuously, for up to 50 km in the direction of detachment-fault displacement in the Buckskin and Rawhide Mountains, one would expect to find slivers of lower-plate rocks above the detachment fault if incisement had been an important process during the later part of detachment-fault movement. In other words, slivers of mylonitic rock derived from the lower plate in the western Buckskin and Rawhide Mountains and areas farther west might be expected to lie above the Buckskin-Rawhide detachment fault. Such slivers, however, have not been recognized. Available data thus suggest that incisement was not an important process during detachment faulting in the Buckskin and Rawhide Mountains. In contrast with G.A. Davis and Lister's (1988) interpretation for the Whipple Mountains, the detachment fault, *with respect to the lower plate*, could be a long-lived feature in the Buckskin and Rawhide Mountains.

Direction of Extension and Displacement

Primary criteria for determination of displacement and extension direction on detachment faults are the orientation of mylonitic lineations in lower-plate rocks and the dip direction (perpendicular to strike) of upper-plate tilt blocks. The trend of mylonitic lineation averages N40°E to N50°E in the Buckskin, Rawhide, and Whipple Mountains (Shackelford, 1976b, this vol.; Osborne, 1981; Woodward, 1981; Davis, G.A., 1988; Plate 2; Fig. 38 in Appendix 1) and N56°E $\pm$ 7° in the Harcuvar Mountains. Lineation is perpendicular to the northwest strike of tilted, upper-plate fault blocks in the Whipple Mountains (Davis, G.A., and others, 1980), which suggests that faulting and mylonitization are kinematically related. The more westerly strike of upper-plate fault blocks in the Planet area and Artillery Mountains is inferred to be due to the oblique geometry of the breakaway fault, and therefore does not reflect displacement and distension direction. Other areas of upper-plate rocks in the Buckskin and Rawhide Mountains are too folded or complexly faulted to reveal extension and displacement direction accurately without more detailed structural study. A net displacement and extension direction of N50°E $\pm$ 10° encompasses directions indicated in all areas by both criteria. Furthermore, top-to-the-northeast shear is indicated by both asymmetric mylonitic petrofabrics in lower-plate rocks and the dominant southwest tilt of upper-plate fault blocks.

Displacement direction during detachment faulting is suggested by the N55°E to N60°E orientation of axes of lower-plate synforms and antiforms and overlying corrugations of the detachment fault. If folding of lower-plate rocks and extension were synchronous, then the orientations of principle stresses during constrictional extensional strain of footwall rocks (a possible cause of folding) were quite likely the same as the orientations of principle stresses during extensional strain of upper-plate rocks. During later detachment faulting, the antiforms and synforms may have guided the direction of displacement of upper-plate rocks, especially when overlying upper-plate rocks composed a thin and weak sheet, but such guiding would only be a local effect and would be more effective where corrugations are more pronounced, such as in the Harcuvar Mountains. Because of uncertainties in the age and origin of the lower-plate folds, fold-axis orientations only suggest displacement direction.

Magnitude of Extension and Displacement

Tectonic reconstruction of Tertiary extension must place all of the exposed lower-plate rocks in the Buck-

skin and Rawhide Mountains at depths great enough to exceed the approximately 300°C temperature required for mylonitization. If typical geothermal gradients for tectonically active areas were present, the 300°C isotherm would be at a depth of 10 to 15 km. However, the minimum depth for mylonitization may have been considerably less than 10 to 15 km because of heating from Miocene intrusive rocks in the lower plate (Bryant and Wooden, this vol.; Plate 2); a minimum predetachment depth of 5 km seems reasonable, although the actual depth could have been much greater. An absolute minimum of approximately 45 km of restored displacement is necessary to put crystalline rocks in the Artillery Mountains over mylonitic lower-plate rocks at the west end of the Ives Peak and Clara Peak antiforms. Restoring at least another 10 km of displacement is probably necessary to place all the lower-plate rocks at sufficient depth to be at temperatures of mylonitization. Fifty-five kilometers thus appears to be a reasonable estimate for minimum displacement. Restoration of approximately 60

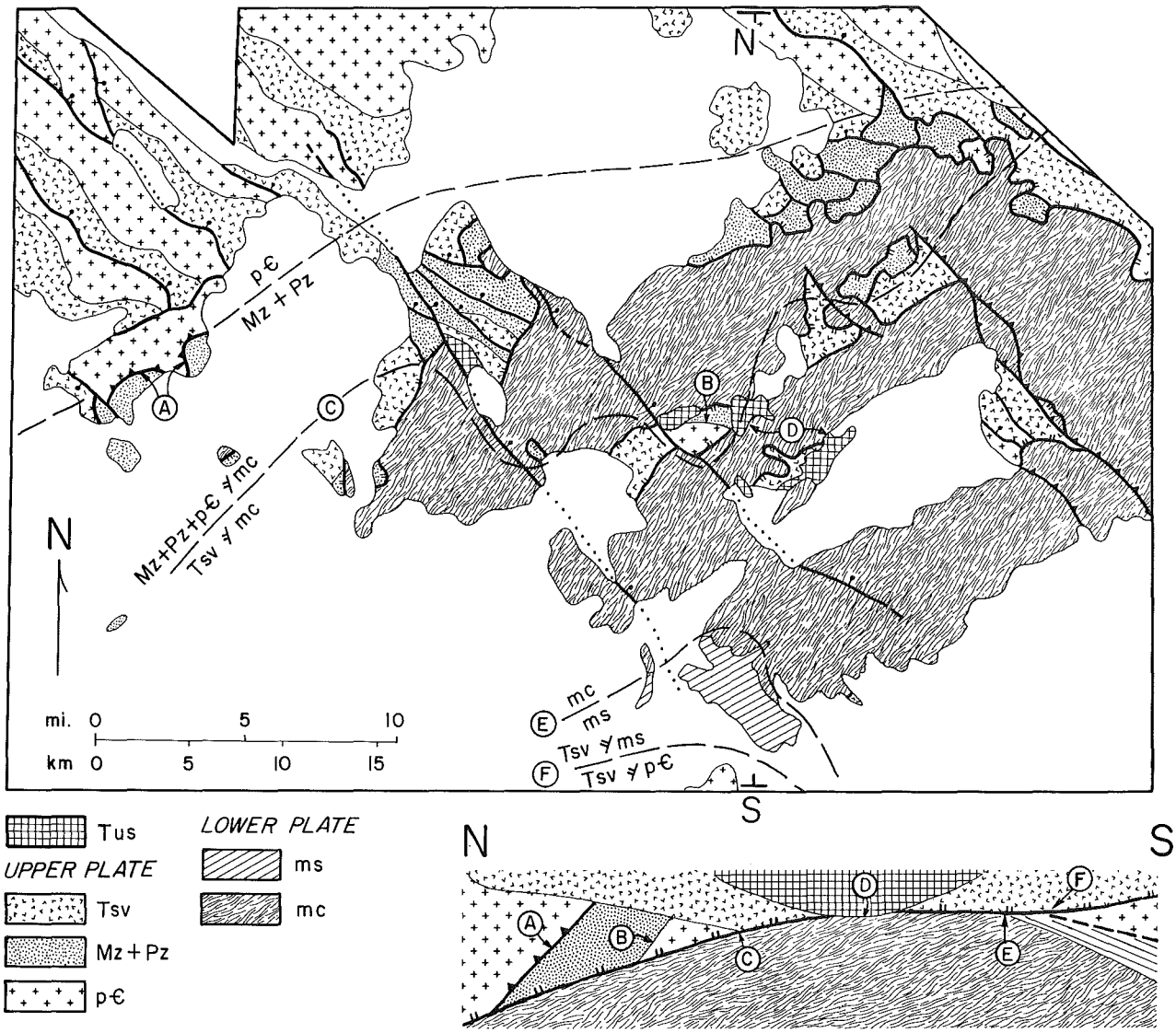

Figure 32. Simplified geologic map and symbolic cross section of lower- and upper-plate rocks in the Buckskin and Rawhide Mountains and some adjacent areas,and postdetachment breccia and conglomerate in the Swansea - Clara Peak area of the Buckskin Mountains. Tus = postdetachment, upper sedimentary unit (breccia and conglomerate); Tsv = upper-plate sedimentary and volcanic strata; Mz = upper-plate Mesozoic strata; Pz = upper-plate Paleozoic strata; p€ = upper-plate Proterozoic crystalline rocks (includes Tertiary granite in Bouse Hills at south edge of map); ms = variably mylonitic to nonmylonitic, lower-plate metasedimentary rocks; mc = variably mylonitic to nonmylonitic, lower-plate crystalline rocks. Circled letters represent tectonic boundaries that are depicted in the symbolic cross section. Boundary A is the dismembered, structurally highest thrust of the Maria fold-and-thrust belt. Boundary F in the lower plate possibly represents a fault within the lower plate, a mylonitic front, or an intrusive contact.

km of displacement would be required to place crystalline rocks in the southeastern Poachie Mountains over mylonitic lower-plate rocks in the Battleship Peak area. Displacement could be approximately 10 km less if a substantial thickness of upper-plate crystalline rock lies beneath Date Creek basin, but this seems unlikely, considering the gentle dip (approximately 10°) of the detachment fault at the west margin of the basin and the great thickness of Tertiary strata in the basin (Lease, 1981). Restoration of 70 km of N60°E displacement would place an early Miocene, silicic volcanic center (McClendon volcano of Brooks, 1985) over a granodiorite pluton in the eastern Bouse Hills that is probably Miocene in age (Shafiqullah and others, 1980).

Restoration of 60 km of displacement of the Artillery and Poachie Mountains places these ranges over the western Buckskin Mountains and Cactus Plain. Restoration of 60 to 75 km of displacement, depending on displacement direction (N45°E to N60°E), would place a substantial thickness of crystalline rocks now in the McCracken, Artillery, and western Poachie Mountains over the Tertiary mylonitic rocks of Mesquite Mountain (Knapp, 1988). This magnitude of displacement is not necessarily required, however, because denudation of Mesquite Mountain could have been due to displacement on normal faults that project beneath the lower-plate rocks in the Buckskin and Rawhide Mountains. Restoration of 75 to 95 km of displacement in the same direction would place these upper-plate rocks adjacent to the unextended Big Maria Mountains. The steep northeast face of the Big Maria Mountains is possibly a geomorphic relict of the Miocene breakaway zone, as is the east side of the Old Woman Mountains (Frost and Okaya, 1986; Howard and John, 1987). If so, 75 to 95 km represents the maximum possible displacement. Based on these various lines of evidence for net offset, we propose that the Artillery and Poachie Mountains have been displaced 75 ± 20 km to the ENE relative to the lower plate of the Buckskin-Rawhide detachment fault.

This estimate of extension is consistent with previous estimates of displacement in adjacent areas. At least 50 km of displacement is estimated to have occurred on the Bullard detachment fault at the east end of the Harcuvar Mountains (Reynolds and Spencer, 1985). An additional 10 to 15 km of displacement could have occurred on the Bullard fault where it projects beneath the Date Creek Mountains. This increased displacement would have been accommodated by extension of upper-plate rocks beneath eastern Date Creek basin and is represented, in part, by a low-angle normal fault that separates upper-plate Tertiary strata from upper-plate crystalline rocks at the northwestern end of Aguila Ridge (Reynolds and Spencer, 1984). A dike swarm in the Mohave Mountains northwest of the Buckskin Mountains is probably offset 40 km from its lower-plate equivalent in the western Whipple Mountains (Howard and others, 1982a; Nakata, 1982; Davis, G.A., and Lister, 1988), although displacement could be greater if dike emplacement occurred after initial fault displacement. The offset dike swarm represents only part of the total displacement because additional displacement occurred on the Crossman Peak low-angle normal fault, which is structurally higher than the Mohave Mountains (Howard and others, 1982a). Displacement on the Crossman Peak fault and possible structurally higher faults between the Mohave and Hualapai Mountains is estimated at 15 to 30 km. Bedrock between the Mohave and Hualapai Mountains is concealed by Quaternary alluvial deposits, but is moderately to highly extended where it is exposed along strike to the southeast between the Bill Williams and McCracken Mountains (Suneson, 1980) and on the north flank of the Buckskin and Rawhide Mountains. Estimated total extension along three extension-parallel transects is, therefore, as follows: (1) 55 to 70 km of displacement of rocks in the Hualapai Mountains with respect to the lower plate of the Whipple detachment fault, (2) 75 ± 20 km of displacement of the Artillery and Poachie Mountains relative to the lower plate of the Buckskin and Rawhide detachment fault, and (3) 60 to 65 km of displacement of crystalline rocks on the north side of the eastern Date Creek basin relative to the Bullard detachment fault.

The Hualapai, Artillery, Poachie, and Date Creek Mountains are not separated from each other by major faults and can be considered the trailing edge of a largely unextended, upper-plate wedge. Similarly, no faults are known to separate the lower-plate rocks of the Whipple, Buckskin, Rawhide, Harcuvar, and Harquahala Mountains; these rocks are probably part of a single footwall block. Similar estimates of extension in the three transects discussed above support the inference of structural continuity within these upper-plate and lower-plate blocks and suggest that total extension along an extension-parallel transect through the Buckskin Mountains is on the lower side of the 75 ± 20-km estimate.

Oblique Breakaway

Structural and stratigraphic variations at high angles to the direction of extension add complexity to the schematic tectonic evolution depicted on Figure 31. Tertiary sedimentary and volcanic rocks rest on the detachment fault in Butler Valley and are the primary rock type above the detachment fault in the Lincoln Ranch synform and in most of the Swansea synform. Pre-Tertiary rocks rest on the detachment fault in most areas north of the Planet Peak antiform (Fig. 32). The large tilt blocks that compose the upper plate in the eastern Whipple, southern Bill Williams, and southwestern McCracken Mountains must thin southeastward along strike toward the flank of the Planet Peak antiform. Southeastward tapering of upper-plate fault blocks reflects the geometry of the upper plate at the time of either breakaway or secondary breakaway formation.

Reconstruction of extension within the upper plate reveals a preextension geometry in which a gently north- to northwest-dipping breakaway or secondary breakaway fault strikes subparallel to the ENE direction of extension. The footwall location of this oblique segment of the breakaway or secondary breakaway fault is unknown, but it may extend eastward from the area between the

Riverside and Big Maria Mountains to the area near the Bouse Hills (see also Howard and John, 1987). If a secondary breakaway fault substantially modified the upper plate in the Buckskin Mountains, it was probably near the Riverside Mountains, Mesquite Mountain, and Cactus Plain. The presence of exclusively lower-plate rocks at Mesquite Mountain, and the thinness of the upper plate beneath postdetachment volcanic rocks in the Mammon mine area near the north edge of Cactus Plain, indicate that a substantial amount of upper-plate rock was not left stranded by formation of an oblique secondary breakaway fault. Therefore, the reconstructed geometry of the upper plate in the Buckskin Mountains and areas to the north and east is interpreted as primarily reflecting the geometry of an oblique breakaway fault, not an oblique secondary breakaway fault.

Irregularities in the breakaway fault, perhaps involving short oblique and normal breakaway-fault segments, could have been present. In addition, the geometry of the breakaway fault is complicated by the Moon Mountains and Plomosa detachment faults and by normal faults in the central Plomosa Mountains (see Fig. 4 in Introduction, this vol.) that almost certainly extend beneath the lower-plate rocks in the Buckskin Mountains. The influence of these factors on the detailed geometry of the breakaway zone is poorly understood, but the general oblique form of the breakaway fault is required by the geometry and distribution of upper-plate rocks.

We interpret the broadly arcuate, east-west-trending form of the belt of south-dipping Tertiary strata in the Artillery Mountains and on the south flank of the Poachie Range (see Fig. 4 in Introduction, this vol.) as reflecting the form of the original breakaway fault. The south-facing margin of these ranges reflects the east-west trend of a segment of the original oblique breakaway fault that was located approximately along the south flank of Cactus Plain.

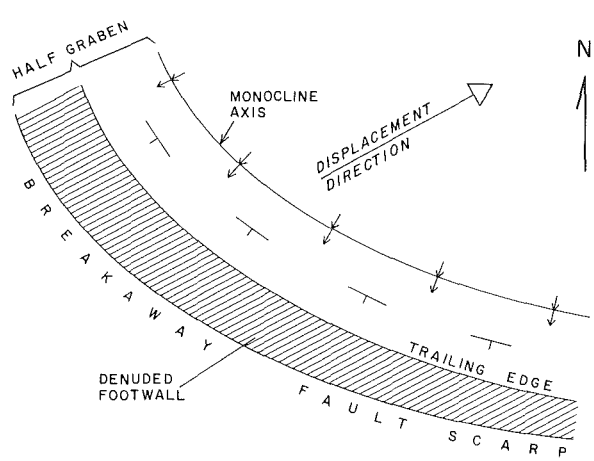

Figure 33. Schematic diagram of structural relationships along an oblique breakaway zone. Illustrated case is for listric fault with the same curvature for any cross section taken perpendicular to the top of the breakaway fault scarp. Modified from Figure 16 in Dokka (1986).

Geometric considerations indicate that, near an oblique listric breakaway, reverse drag should cause the strike of upper-plate strata to curve into approximate parallelism with the breakaway (Fig. 33). Areas where reverse-drag tilting of upper-plate strata may have occurred adjacent to a breakaway fault include the Artillery Mountains (Lasky and Webber, 1949; Spencer, Grubensky, and others, this vol.), north flank of Date Creek basin (Otton, 1982), easternmost Harcuvar Mountains (Reynolds and Spencer, 1985), and Swansea mine area (Fig. 14). The more westerly strike of upper-plate fault blocks in these areas, compared to areas farther north that were not originally adjacent to the oblique breakaway, is interpreted as a consequence of northeast to ENE displacement away from a breakaway fault striking west to WNW. The WNW strike of Tertiary strata in the southern Riverside Mountains (Hamilton, 1964) and northern Plomosa Mountains (Scarborough and Meader, 1982) is possibly due to NNE displacement above structurally deeper normal faults.

Age of Faulting

The timing of detachment faulting is primarily constrained by the ages of tilted and untilted upper-plate strata. Tilted volcanic rocks near the base of the Artillery Formation yielded biotite K-Ar dates of 21.8 Ma near the Swansea mine (Spencer, Shafiqullah, and others, this vol.) and 23.0 Ma in the Artillery Mountains (J. Otton and R. Miller, oral commun., 1987). These dates record the time of early Miocene extensional-basin formation and initial tilting, which probably began at about 24 Ma. Non-K-metasomatized basalt in Lincoln Ranch basin that yielded a 20 Ma plagioclase K-Ar date (Spencer, Shafiqullah, and others, this vol.) directly underlies conglomerate that contains sparse mylonitic clasts probably derived from the lower plate (Fig. 7). It thus appears that extension and denudation of sufficient magnitude to uncover rocks with Tertiary mylonitic fabrics had occurred by this time. Flat-lying basalts in the westernmost Buckskin Mountains overlie moderately to steeply tilted Tertiary strata and are dated at 14 to 16 Ma (Fig. 29). Basalts dated at about 15.5 to 16 Ma along lower Cave Wash in the southeastern Bill Williams Mountains (Spencer, Shafiqullah, and others, this vol.) are tilted (Plate 2), raising the possibility that detachment faulting had ended in the westernmost Buckskin Mountains but not in the central, northern, and eastern Buckskin Mountains. Unfaulted, gently dipping basalt in the western Rawhide Mountains dated at 12 to 13 Ma (Suneson and Lucchitta, 1979; Spencer, Shafiqullah, and others, this vol.) overlies moderately to steeply tilted upper-plate rocks (Plate 3). Detachment faulting in this area ended between approximately 16 and 13 to 12 Ma. The time that detachment faulting ended in the eastern Rawhide and Buckskin Mountains is not well constrained, but could have continued up to perhaps 12 to 10 Ma, as suggested by young fission-track cooling dates from lower-plate rocks in this area (Bryant and Naeser, 1987). If extension occurred in the Rawhide and central and

eastern Buckskin Mountains from 15 to 13 Ma, then this area may have been part of an active extensional belt that continued northward along the east side of the Bill Williams, Mohave, Sacramento, Dead, and Newberry Mountains to the Eldorado, central Black Mountains, and areas farther north, where extension of this age has been documented (Anderson, R.E., and others, 1971; Bohannon, 1984).

Relationship Between Tertiary and Mesozoic Tectonic Features

A fundamental tectonic boundary in the northern Buckskin and Rawhide Mountains separates upper-plate, metamorphosed, Mesozoic and Paleozoic volcanic and sedimentary rocks to the south from upper-plate, dominantly Proterozoic crystalline rocks to the north. Mesozoic and Paleozoic supracrustal rocks are completely absent from this boundary for more than 200 km northward to the Lake Mead area, but are widely preserved to the south within the east-west-trending Maria fold-and-thrust belt (Fig. 34). Mesozoic and Paleozoic supracrustal rocks in the Maria fold-and-thrust belt are preserved beneath thrust sheets of crystalline rock or are suspected to have been tectonically buried because they are pervasively metamorphosed and ductilely deformed (Reynolds and others, 1986b). Late Cretaceous and early Tertiary erosional denudation removed several kilometers of crust in much of the Basin and Range and Transition Zone provinces of the Southwest and accounts for the absence of Mesozoic and Paleozoic supracrustal rocks, except where such rocks had undergone at least several kilometers of tectonic burial. Thrust faulting is therefore inferred not to have significantly affected the upper crust in the area between the Maria fold-and-thrust belt and Lake Mead.

This fundamental tectonic boundary in the northern Buckskin and Rawhide Mountains is the structurally highest fault zone of generally south-vergent thrusts in the Maria fold-and-thrust belt. Mesozoic thrust faults have

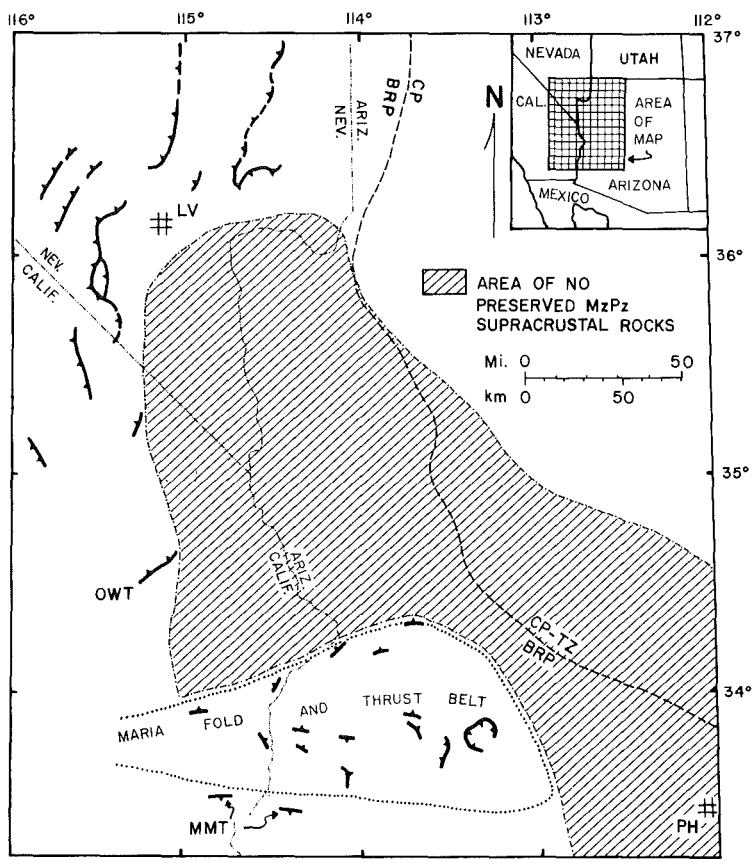

Figure 34. Schematic map showing locations of major thrust faults in western Arizona and adjacent parts of California and Nevada. Ruled area contains no preserved Paleozoic or early to middle Mesozoic strata, which were apparently removed by erosion in Late Cretaceous and early Tertiary time. Paleozoic and Mesozoic strata are preserved beneath thrust faults in west-central Arizona and southeastern California. The distribution of Paleozoic and Mesozoic strata reveals that the structurally highest thrust of the Maria fold-and-thrust belt, which is variably dismembered but locally preserved in the Buckskin Mountains, is a major tectonic feature in the Cordilleran fold-and-thrust belt. BRP = Basin and Range Province; CP = Colorado Plateau; LV = Las Vegas; MMT = Mule Mountains thrust; OWT = Old Woman thrust; PH = Phoenix; TZ = Transition Zone.

been completely dismembered by Tertiary normal faulting in the northern Rawhide Mountains (Plate 1), but are well preserved in the western Buckskin Mountains (Frost, 1983; Reynolds and Spencer, this vol.; Figs. 27 and 28). This tectonic boundary is also preserved in the Riverside Mountains in California, where it places amphibolite-grade gneiss over Mesozoic metasedimentary and plutonic rocks (contact between units Mzf and Mzv of Carr and Dickey, 1980; Lyle, 1982) along a mylonite zone that contains excellent top-to-the-south sense-of-shear indicators (J.E. Spencer, unpublished data). Restoration of displacement on the Whipple-Buckskin-Rawhide detachment fault brings the variably dismembered, structurally highest thrust faults of the northern Buckskin and Rawhide Mountains approximately over the structurally highest thrust fault in the Riverside Mountains; the thrust faults may be correlative.

The belt of uplifted, arched, lower-plate rocks below detachment faults in the lower Colorado River trough extends 130 km from the Newberry Mountains southward along the west side of the Colorado River through the Sacramento and Chemehuevi Mountains to the Whipple Mountains. At the Whipple Mountains, the belt turns abruptly eastward to include the Buckskin and Rawhide Mountains and the mylonitic rocks in the eastern Harcuvar and Harquahala Mountains (Fig. 35). Following restoration of displacement on the Buckskin-Rawhide detachment fault, all of the thrust faults in the Maria fold-and-thrust belt are restricted to an east-west-trending belt approximately 50 km wide and located directly south of the east-west-trending belt of Tertiary mylonitic fabrics below the Whipple-Buckskin-Rawhide-Bullard detachment fault. Thrust faults of the Maria fold-and-thrust belt that are now in the lower plate of the Whipple-Buckskin-Rawhide-Bullard detachment fault dip northward beneath the mylonitic rocks of the Whipple and Harcuvar metamorphic core complexes. The parallelism of these two belts and the spatial coincidence of the root zone of the thrusts with the east-west-trending belt of denuded Tertiary mylonitic fabrics suggest that there is a genetic relationship between Mesozoic and mid-Tertiary tectonism. The root zone of the Maria fold-and-thrust belt is also coincident with the abrupt eastward bend in the belt of arched, uplifted rocks below detachment faults. A genetic relationship is further suggested by the geometry of the breakaway fault or fault zone that marks the west and southwest boundary of the lower Colorado River detachment system. The breakaway trends southward for 160 km from the area near Searchlight, Nevada to the area south of the Arica Mountains, where it turns abruptly east and continues toward the ESE within the Maria fold-and-thrust belt for more than 100 km (Fig. 35).

Early Tertiary erosional denudation in the Maria fold-and-thrust belt was greater than in adjacent areas in the Basin and Range Province, as indicated by widespread, early Tertiary, K-Ar cooling dates (Rehrig and Reynolds, 1980; Martin and others, 1982; Knapp and Heizler, 1988) and widespread exposure of rocks that had undergone greenschist-grade metamorphism during the Cretaceous (Reynolds and others, 1988). Greater erosional denudation was presumably due to greater relief, which, in turn, was due to Cretaceous crustal thickening. Isostatic uplift of the Maria fold-and-thrust belt due to erosional denudation that was of greater magnitude than in adjacent areas would have produced flexural stresses in the crust. These stresses may have controlled the geometry of later-formed detachment faults and may account for (1) the abrupt bend in the trend of Tertiary extensional tectonic features and (2) the spatial coincidence of the root zone of the Maria fold-and-thrust belt with the approximately east-west-trending belt of exposed Tertiary mylonitic fabrics in the Whipple and Harcuvar metamorphic core complexes (Spencer and Reynolds, 1986c; Spencer and Chase, in press).

In an alternative scenario, detachment faults formed along weak zones within the strong brittle-ductile transition zone, which is located at a depth of approximately 8 to 15 km in the upper crust (Brace and Kohlstedt, 1980; Sibson, 1982). Carbonate rocks are weak and highly ductile at typical temperatures within the brittle-ductile transition zone; where they are surrounded by quartzofeldspathic crystalline rocks, they would be especially likely to localize deformation. Lower-plate rocks in the Buckskin and Rawhide Mountains contain sparse but widely scattered carbonate sheets and slivers that are typically a few meters thick and concordant to mylonitic and gneissic layering (Bryant and Wooden, this vol.; Spencer and Welty, this vol.). The carbonate slivers may have originally been intercollated with lower-plate crystalline rocks during shearing along Mesozoic thrust faults (Bryant and Naeser, 1988). If so, the eastward deflection of the breakaway fault and of the belt of arched lower-plate rocks could have been due to initiation of mid-Tertiary detachment faults along north-dipping sheets and slivers of carbonate rock (Fig. 36).

At Mesquite Mountain west of the Buckskin Mountains, carbonate slivers like those in the Buckskin and Rawhide Mountains are present within mylonitic shear zones of probable mid-Tertiary age that cut discordantly across an older, probably mid-Tertiary, mylonitic fabric (Knapp, 1988, and oral commun., 1988). This relationship indicates that such slivering and intercollation occurred in the mid-Tertiary and suggests that intercollation of metasedimentary slivers was a mid-Tertiary event in the Buckskin and Rawhide Mountains as well (Fig. 37). Relationships at Mesquite Mountain thus argue against the thrust-zone reactivation model and support the flexural-stress model.

Strike-Parallel Variations in Structural Styles of Extension

Tertiary extensional faulting along a transect from the Big Maria Mountains through Mesquite Mountain and the central Buckskin and Rawhide Mountains to the Artillery Mountains was characterized by displacement and uplift of the lower plate up and out from beneath an upper plate that largely retained its original wedge-shaped form and was not highly distended by normal

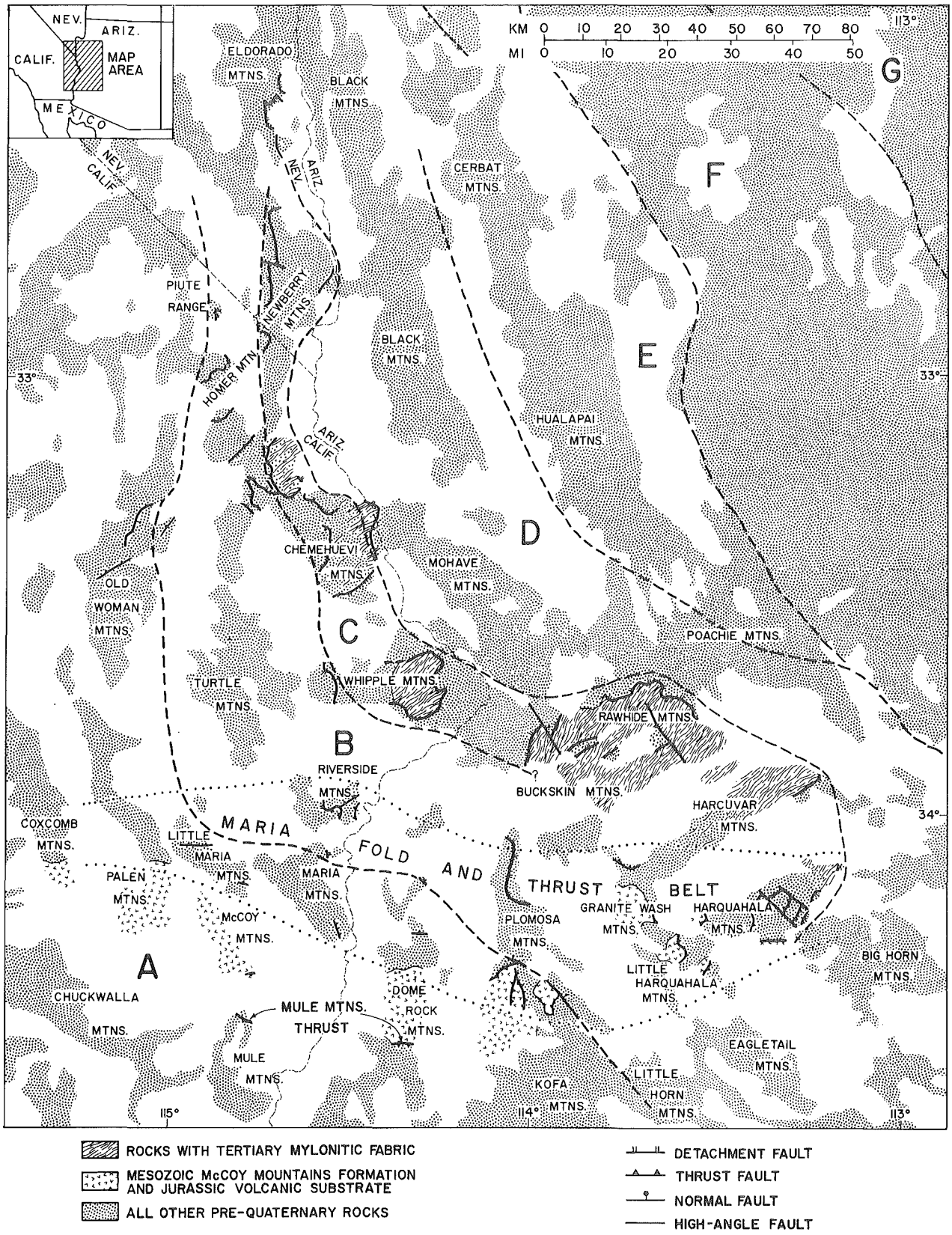

faulting. In contrast, extension within the upper plate in areas to the north, exemplified by the Turtle, Mopah, Whipple, Bill Williams, and Mohave Mountains, was characterized by moderate to extreme structural dismemberment and extension of the upper plate and by preservation of a substantial synformal keel (Davis, G.A., and

Figure 35 (previous page). Generalized tectonic-domain map for mid-Tertiary structures in the northern lower Colorado River region. Displaced, upper-plate fault blocks containing segments of the Maria fold-and-thrust belt, now in the Buckskin and Rawhide Mountains, are not included here in the belt. The outline of the belt is thus restricted to rocks in the lower plate of the Whipple-Buckskin-Rawhide-Bullard detachment fault. The spatial relationship of the fold-and-thrust belt to Tertiary mylonitic rocks is thus largely unaffected by extensional faulting. Note that Tertiary mylonitic rocks parallel, and lie north of, the Maria fold-and-thrust belt. Mid-Tertiary tectonic domains are as follows: (A) area of minor extension at exposed surface levels; (B) synformal keel of distended upper-plate rocks above warped detachment-fault system; (C) belt of uplifted, commonly arched, mylonitic crystalline rocks below detachment faults; (D) wedge-shaped (in cross section) extensional allochthon of moderately to highly extended upper-plate rocks; (E) area of slight to moderate extension characterized by large fault blocks generally with minor tilts; (F) Transition Zone; and (G) Colorado Plateau. Note that the breakaway fault that separates domains A and B abruptly changes trend at the intersection with the Maria fold-and-thrust belt and mirrors the change in trend of domain C.

others, 1980; Frost and Okaya, 1986; Howard and John, 1987). Similarly, south of the Buckskin transect, the Plomosa Mountains are composed of a large tilt-block array (Miller, 1970; Scarborough and Meader, 1982; Stoneman, 1985); south of the Harquahala Mountains, large detachment faults are not exposed and extensional faulting is represented by numerous, highly tilted fault blocks (Capps and others, 1985; Fryxell and others, 1987b; Richard and others, 1988).

Only very minor faulting affected all of these areas after major Miocene extension, and present elevations are similar throughout the area. A greater magnitude of isostatic uplift of the lower plate must have occurred near the Buckskin Mountains where lower-plate mylonitic rocks are widely exposed and where denudation was virtually complete. Large-magnitude uplift of the lower plate of the Buckskin-Rawhide detachment fault, possibly driven in part by a downward-protruding Moho bulge inherited from earlier crustal thickening, may have been necessary for complete tectonic denudation and maintenance of a structurally coherent upper-plate wedge. We speculate that in the absence of a flexurally suppressed Moho bulge or crustal-density heterogeneity to help drive isostatic uplift (e.g., Holt and others, 1986), the upper plate will form a distended tilt-block array and little or no lower-plate mylonitic rock will be exposed (unless perhaps mylonitization occurred at shallow crustal levels because of heating from magmatism). If so, first-order changes in structural style along strike are governed by lateral variations in magnitudes of isostatic uplift, which are, in turn, governed by preexisting lateral variations in crustal thickness and density.

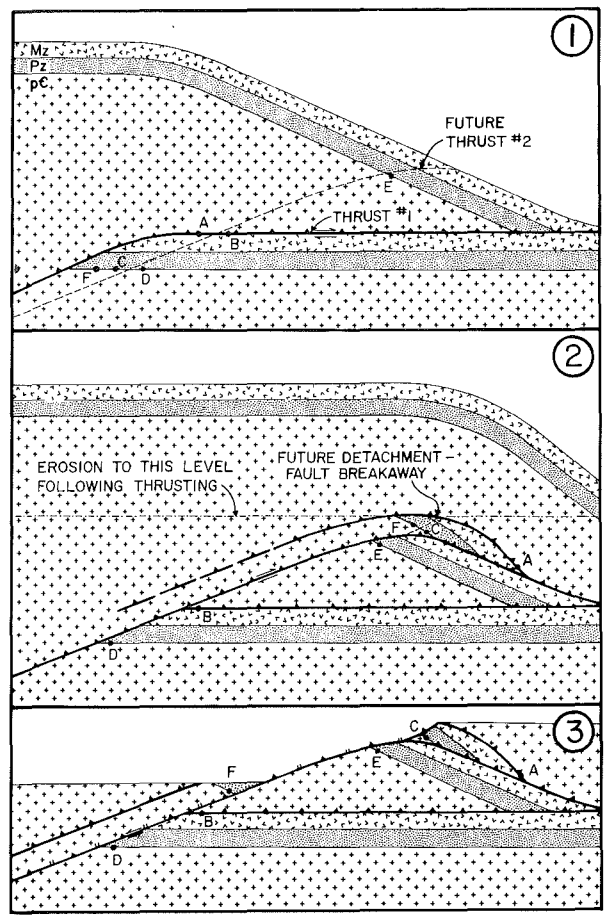

Figure 36. Hypothetical, cross-sectional evolution diagram of thrust and detachment faulting leading to interleaving of slivers of metasedimentary rocks with crystalline rocks now exposed in the lower plate of the Buckskin-Rawhide detachment fault. (1) Thrust burial of Paleozoic and Mesozoic strata and resultant metamorphism. (2) Second thrust cuts through buried and metamorphosed strata. Metamorphosed strata in the hanging wall of thrust #2 and footwall of thrust #1 are dragged across crystalline rocks in the footwall of thrust #2 and hanging wall of thrust #1, resulting in ductile to semi-ductile interleaving of Paleozoic and Mesozoic strata with crystalline rocks along thrust #2 between points "B" and "E." (3) Approximate reactivation of the older thrust zone by the Tertiary Buckskin-Rawhide detachment fault uncovers previously interleaved slivers of metamorphosed Paleozoic and Mesozoic strata within lower-plate crystalline rocks. Point E is possibly represented by contact at base of metasedimentary sequence in Battleship Peak area (see Marshak and Vander Muelen, this vol.).

CONCLUSION

The Miocene structural and stratigraphic evolution of the Buckskin and Rawhide Mountains was dominated by many tens of kilometers of displacement on the Buckskin and Rawhide detachment fault and by resultant sedimentary-basin formation and juxtaposition of dissimilar rock types. Mylonitization of lower-plate rocks was

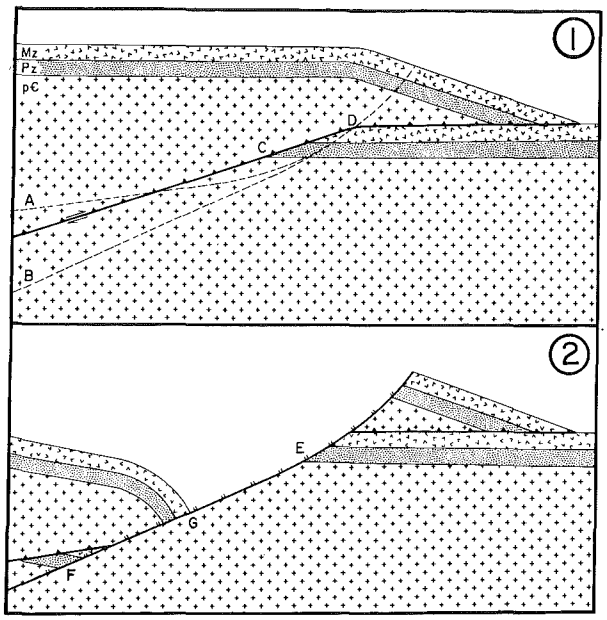

Figure 37. Alternative, hypothetical, cross-sectional evolution diagram of thrust and detachment faulting leading to interleaving of slivers of metasedimentary rocks with crystalline rocks now exposed in the lower plate of the Buckskin-Rawhide detachment fault. (1) Thrust burial of Paleozoic and Mesozoic strata and resultant metamorphism. (2) Buckskin-Rawhide detachment fault cuts across buried metasedimentary strata along one of two paths, designated by dashed lines A and B in cross-section 1. Metamorphosed strata in the upper plate of the detachment fault and footwall of the thrust are dragged across the lower plate and interleaved with crystalline rocks under ductile or semiductile conditions. Metamorphic rocks at F are now exposed along the north flank of the Buckskin and Rawhide Mountains. Point E is possibly represented by contact at base of metasedimentary sequence in Battleship Peak area (see Marshak and Vander Muelen, this vol.).

related to low-angle extensional tectonism in Oligocene(?) and early to middle Miocene time. The progressive ductile to brittle deformation of the lower plate and juxtaposition of contrasting rock types across the detachment fault are accounted for by the shear-zone model for the origin of metamorphic core complexes (e.g., Wernicke, 1981, 1985; Davis, G.A., and others, 1986). A mylonitic front has not been recognized in the Buckskin and Rawhide Mountains; therefore, modification of the shear-zone model to account for a mylonitic front (e.g., Davis, G.A., 1988; Davis, G.A., and Lister, 1988) appears to be unnecessary to explain geologic relationships in these ranges.

Tertiary sedimentary breccia in the western and central Buckskin Mountains is correlative with the sedimentary breccia that forms the upper part of the Gene Canyon Formation in the eastern Whipple Mountains. Sedimentary breccia in the western Buckskin Mountains is overlain by widespread Tertiary sedimentary and volcanic strata correlative with the Copper Basin Formation in the eastern Whipple Mountains. In the Planet and Mineral Hill area (Plate 2) and in upper Osborne Wash (Fig. 21), the breccia rests directly on pre-Tertiary bedrock, whereas to the west and east Tertiary sedimentary rocks are present below the breccia. Pre-breccia sedimentary deposits were areally restricted at the time of deposition or were eroded from much of what is now the western Buckskin Mountains before deposition of the widespread sedimentary breccia unit. The sedimentary breccia thus appears to mark the initial formation of a large sedimentary basin through linkage of previously separate basins. An alternative explanation is that basins remained separate, but had similar tectonic and sedimentary histories.

The lower and middle parts of a thick, lithologically diverse sequence of sedimentary and volcanic strata west of Swansea mine in the central Buckskin Mountains appear to be correlative with the Artillery Formation, as suggested previously by Woodward (1981) and Wilkins and Heidrick (1982). Lithologic similarity between sedimentary breccias in the Artillery and Gene Canyon Formations suggests that both were near the same topographic edifice that provided the dominantly metasedimentary and metavolcanic debris. The lack of similarity in other parts of the sequences, however, suggests that the formations were deposited in different sedimentary basins or in different parts of the same basin that had different successions of sedimentary environments. The breccias may have been derived from a breakaway scarp near the Big Maria Mountains. The stratigraphically higher, heterolithologic Artillery megabreccia at the top of the Artillery Formation in the Artillery Mountains and possibly correlative breccia and debris flows in the Swansea mine area mark the top of correlative sedimentary units in the two areas.

The Chapin Wash Formation and overlying Sandtrap Conglomerate in the Artillery, Rawhide, and eastern Buckskin Mountains do not resemble strata overlying the heterolithologic sedimentary breccia west of Swansea mine. Units above the megabreccias in the two sequences are inferred to have been deposited in separate sedimentary basins that were previously joined before dismemberment by extensional faulting. Dismemberment was followed by the widespread initial appearance of mylonitic debris derived from the lower plate of the detachment fault. The Chapin Wash Formation and overlying Sandtrap Conglomerate are thus interpreted as having been deposited during one-sided denudation of the lower plate. It is not known if mylonitic debris in the stratigraphically highest tilted rocks in the lower Bill Williams River and Planet and Mineral Hill area was derived from lower-plate rocks in the Buckskin or Whipple Mountains, or some other, now concealed area. If derived from the same source as mylonitic debris in the Chapin Wash Formation, mylonite-clast-bearing strata in the northwestern Buckskin Mountains could be correlative with the Chapin Wash Formation.

The stratigraphy of Tertiary sedimentary rocks in the Buckskin Mountains sequentially records (1) sedimentary-basin formation during initial extensional faulting; (2) increased basin-margin relief leading to megabreccia deposition; (3) basin widening leading to widespread,

dominantly sandstone deposition in the Copper Basin Formation; and (4) successive west-to-east termination of extensional faulting, during which the lower plate was extensively exposed and provided clastic debris to the Chapin Wash Formation and Sandtrap Conglomerate. This last phase of tectonism was associated with tilting and possibly widening of a large sedimentary basin east of an exposed, northeast-migrating lower-plate monocline.

The direction of extension can be inferred from several criteria. Mylonitic lineations in lower-plate rocks are oriented N40°E to N50°E in the Whipple, Buckskin, and Rawhide Mountains and N55°E to N60°E in the Harcuvar Mountains; they reveal the direction of extension during early displacement, when lower-plate rocks were still hot enough for ductile deformation. Mylonitic petrofabrics indicate top-to-the-northeast shear. Tilt directions of upper-plate rocks in the Buckskin Mountains are generally complex and are not clear indicators of extension direction, but suggest a general northeast direction of extension and displacement. Tilt directions and offset markers in nearby ranges indicate a northeast direction of displacement of upper-plate rocks relative to the lower plate (Reynolds and Spencer, 1985; Howard and John, 1987; Davis, G.A., and Lister, 1988).

The total crustal extension accommodated by the Buckskin-Rawhide detachment fault is estimated to be 75 $\pm$ 20 km in the direction N50°E $\pm$ 10°. Restoration of such displacement places many kilometers of rock above lower-plate mylonitic rocks and presumably places lower-plate rocks at sufficient depth to be at temperatures needed for mylonitization. Estimates of net extension along transects in areas north and south of the Buckskin and Rawhide Mountains are consistent with, but on the low side of, this estimate.

Variations in the nature of lithologic juxtapositions across the detachment fault and oblique to displacement direction indicate that the detachment fault cuts structurally downward to the north or northwest in the upper plate. This relationship could be interpreted as largely reflecting the geometry of the detachment fault near its oblique breakaway zone or the oblique geometry of a secondary breakaway or excisement zone. An oblique breakaway zone is considered the primary cause of this upper-plate geometry because of (1) the large areal extent of the southward-thinning upper plate (from the eastern Whipple Mountains to the McCracken Mountains and possibly the Poachie Mountains), and (2) the absence of a significant volume of upper-plate rock near Mesquite Mountain and the Riverside Mountains that would have been left stranded behind a secondary breakaway or below an excisement fault.

Sedimentary-basin formation, and by inference extensional faulting, began before deposition of a 23 Ma tuff in the Artillery Mountains. Flat-lying basalt that overlies tilted upper-plate rocks in the western Buckskin Mountains yielded three K-Ar dates between 14 and 16 Ma. Tilted basalts in the southeastern Bill Williams Mountains yielded K-Ar plagioclase dates of 15.5 to 16 Ma and could have been erupted after extensional faulting ended in areas farther southwest. Extensional faulting ended in the western Rawhide Mountains by 13 to 12 Ma, but could have continued after this time in the eastern Rawhide and Buckskin Mountains. This chronology of extension is consistent with available data on the thermochronology of the lower plate (Bryant and Naeser, 1987; Fryxell and others, 1987a; Spencer, Shafiqullah, and others, this vol.).

The regional geometry of Tertiary structures in the northern Colorado River extensional corridor appears to be influenced by the presence of an east-west-trending segment of the Cordilleran fold-and-thrust belt. Stresses inherited from an isostatically suppressed crustal welt may have influenced the geometry of detachment faults and caused the formation of a regional oblique breakaway zone. We speculate that the remarkably widespread exposures of lower-plate mylonitic rocks, in contrast to other areas of highly extended, upper-plate tilt-block arrays with no exposures of lower-plate rocks, are the result of uplift of an isostatically suppressed crustal welt (Spencer and Reynolds, 1986c; see also Holt and others, 1986).

ACKNOWLEDGMENTS

We thank Bruce Bryant, Greg Davis, J. Lawford Anderson, Steve Richard, Jim Otton, Ivo Lucchitta, Steve Marshak, and Eric Frost for stimulating discussions on the Cenozoic geology of the Buckskin Mountains and surrounding areas. We also thank Eric Frost for a copy of his unpublished geologic map of the westernmost Buckskin Mountains, which resulted in reexamination of some field relationships and refinement of interpretations.

APPENDIX 1

DESCRIPTION OF MAP UNITS: LINCOLN RANCH BASIN (FIGS. 38 AND 39)

Postdetachment Units

Qa ALLUVIAL DEPOSITS (QUATERNARY) -- Unconsolidated gravel, sand, and silt in washes and along the Bill Williams River, and soil deposits in Reid Valley.

Qt TALUS DEPOSITS (QUATERNARY) -- Unconsolidated angular clasts that form steep talus slopes.

Qo OLD ALLUVIAL DEPOSITS (QUATERNARY) -- Light-gray to light-tan, unconsolidated to very poorly consolidated, poorly sorted conglomeratic sandstone and conglomerate. Typically forms perched terraces and flats above modern washes.

Qvo VERY OLD ALLUVIAL DEPOSITS (QUATERNARY) -- Very light gray, unconsolidated to poorly consolidated, poorly sorted conglomeratic sandstone and conglomerate. Forms perched ridges and hills topographically higher than nearby map-unit Qo and typically rests on pre-Quaternary rock units. Clearly distinguishable on aerial photos from map-unit Qo by its lighter color, more rounded ridge form, and relative elevation.

Qovo OLD AND VERY OLD ALLUVIAL DEPOSITS, UNDIVIDED (QUATERNARY) -- Includes units Qo and Qvo. In southwestern part of map area, within about 1 to 2 km of exposed crystalline lower-plate rocks, this unit contains sparse cobbles and boulders of intermediate to silicic volcanic flow breccia, presumably derived from upper-plate rocks that were exposed to the south of this area but have since been eroded away.

Tbf BASIN-FILL DEPOSITS (UPPER TERTIARY) -- Stratified, poorly sorted, light-brown, semiconsolidated pebbly sandstone and cobble conglomerate. Clasts locally as large as 50 cm. Consists of clasts representative of both upper- and lower-plate lithologies, but ratio of upper- to lower-plate lithologies is much higher in clasts of this unit than in younger alluvial deposits in the same area, suggesting that upper-plate rocks were more widespread during deposition of this unit.

Upper-Plate Units

Tuc UPPER CONGLOMERATE (TERTIARY) -- Massive to poorly bedded cobble conglomerate. Forms resistant rounded outcrops. Base is marked by upward transition from dominantly sandstone beds to dominantly or entirely conglomerate beds. Locally graded. Thickness approximately 500 m.

Tus UPPER SANDSTONE (TERTIARY) -- Red to reddish-brown bedded sandstone. Locally includes silty sandstone and graded sandstone beds with silty tops and well-preserved mud cracks. Some beds have basal gravel layers or pebbly channel fill. Beds typically 5 to 50 cm thick. Very local cobble to boulder conglomerate beds. Ripples 2 to 4 cm high, asymmetric, and 20 cm apart mark top of some sandstone beds. In SE $^1/_4$ SW $^1/_4$ SW $^1/_4$ sec. 19, near Lincoln Ranch fault, sandstone is interbedded with limestone and brown calcareous sandstone and siltstone. Base of unit is gradational, with underlying siltstone unit grading upward through interbedded sandstone and siltstone to dominantly sandstone. Transition zone varies from perhaps 5 to 50 m in thickness. Total thickness varies from approximately 150 to 300 m.

Tslt SILTSTONE (TERTIARY) -- Total thickness varies from 0 to approximately 300 m.

Tl LACUSTRINE ROCKS (TERTIARY) -- Total thickness varies from approximately 100 to 200 m.

Tll LACUSTRINE LIMESTONE (TERTIARY) -- Medium- to dark-gray to dark-brown limestone, locally silty, with silicic stringers and laminations. Bedding defined by variations in color and resistance to weathering. Thickness difficult to determine due to deformation, but ranges from 0 to approximately 100 m.

Tls LOWER SANDSTONE (TERTIARY) -- Dark-red to dark-red-brown sandstone with very sparse, 5- to 50-cm-thick, silty limestone beds. Thickness approximately 100 m.

Tlc LOWER CONGLOMERATE (TERTIARY) -- Thickness varies from approximately 50 to 100 m.

Tlsc LOWER SANDSTONE AND CONGLOMERATE, UNDIVIDED (TERTIARY) -- Interbedded sandstone and conglomerate.

Tv INTERMEDIATE VOLCANICS (TERTIARY) -- Flow breccias of dark- and light-gray, brown, and reddish-brown intermediate volcanics containing

plagioclase and quartz ± biotite ± hornblende phenocrysts. Clasts in flow breccias are 1 to 10 cm in diameter.

Tbs BASAL SEDIMENTARY UNIT (TERTIARY) -- Dark-brown siliceous limestone; brown mudstone; tan, brown, and purple-brown arkosic sandstone; and sparse white to gray volcanic ash. Sandstone beds are commonly graded. Sandstone is composed of 2 to 4 mm quartz and feldspar grains and sparse detrital muscovite and tuff fragments in a purple-brown matrix. Basal contact with underlying shattered granite is not highly sheared and could be a slightly sheared depositional contact.

Tbx SEDIMENTARY BRECCIA, GRANITIC PROTOLITH (TERTIARY)

Tbxt TECTONIC BRECCIA (TERTIARY) -- Variably shattered blocks and slivers of Tertiary volcanic rocks, Tertiary conglomerate and sandstone, mylonitic metasedimentary tectonite, and chloritic breccia derived from mylonitic tectonite. Forms fault-bounded slivers along the Lincoln Ranch fault.

Tbxtg TECTONIC BRECCIA, GRANITIC PROTOLITH (TERTIARY) -- Medium-grained biotite granite of unknown age intruded by mafic dikes of probable Tertiary age. Variably fractured, faulted, and disrupted.

Pk KAIBAB LIMESTONE (PERMIAN)

Pc COCONINO SANDSTONE (PERMIAN)

Pzc CARBONATE, UNDIVIDED (PALEOZOIC) -- Brown-, tan-, or gray-weathering, tectonized, variably siliceous carbonate. Layering, defined by variations in color and resistance to weathering and by irregular, elongate siliceous stringers and blebs (recrystallized chert?), may represent transposed bedding.

MzXc INTRUSIVE ROCKS, UNDIVIDED (TERTIARY [?], MESOZOIC [?], AND PROTEROZOIC [?]) -- Includes biotite granite with feldspar phenocrysts as large as 3 cm, medium-grained biotite granite with 0.5- to 2-m-thick mafic dikes, and local foliated plutonic and gneissic rocks. Typically strongly shattered.

Lower-Plate Units

ms METASEDIMENTARY ROCKS (CENOZOIC TO PROTEROZOIC) -- Highly tectonized, variably mylonitic metasedimentary rocks. Composed of interlayered, banded to thinly laminated, white, pale-yellow, tan, pale-red, and gray, variably siliceous carbonate tectonite; very fine grained quartzite; green to tan calc-silicate containing epidote and chlorite; gray phyllite; and greenish-gray sandstone. Protolith of carbonates is probably Paleozoic in age; protolith of sandstone is probably Mesozoic in age. All rocks are tectonized and contain intrafolial folds. Boudinlike pods of pegmatite are mylonitized and contain quartz ribbons. Fractures of variable density are coated or filled with hematite, chlorite, epidote, and quartz.

mc MYLONITIC CRYSTALLINE ROCKS (CENOZOIC TO PROTEROZOIC) -- Mylonitic granitic and high-grade metamorphic rocks. Includes foliated megacrystic granite with K-feldspar augen up to 3 cm in diameter. Top-to-the-northeast shear during mylonitization is indicated by S-C fabrics. A variety of foliated granitic rocks have probable protolith ages of Proterozoic or Mesozoic, and possibly Tertiary. Amphibolitic gneissic rocks have probable Proterozoic protoliths.

cmu MYLONITIC CRYSTALLINE ROCKS AND METASEDIMENTARY ROCKS, UNDIVIDED (CENOZOIC TO PROTEROZOIC) -- Includes mylonitic plutonic rocks and high-grade metamorphic rocks, and tectonized metasedimentary rocks.

Figure 38 (next two pages). Geologic map of Lincoln Ranch basin. See Figure 1 for location, Table 2 for map-symbol descriptions, and Figure 8 for cross section. Coordinates of upper left and lower right corners of map are 34°12.60' N., 113°42.40' W. and 34°09.40' N., 113°37.50' W., respectively.

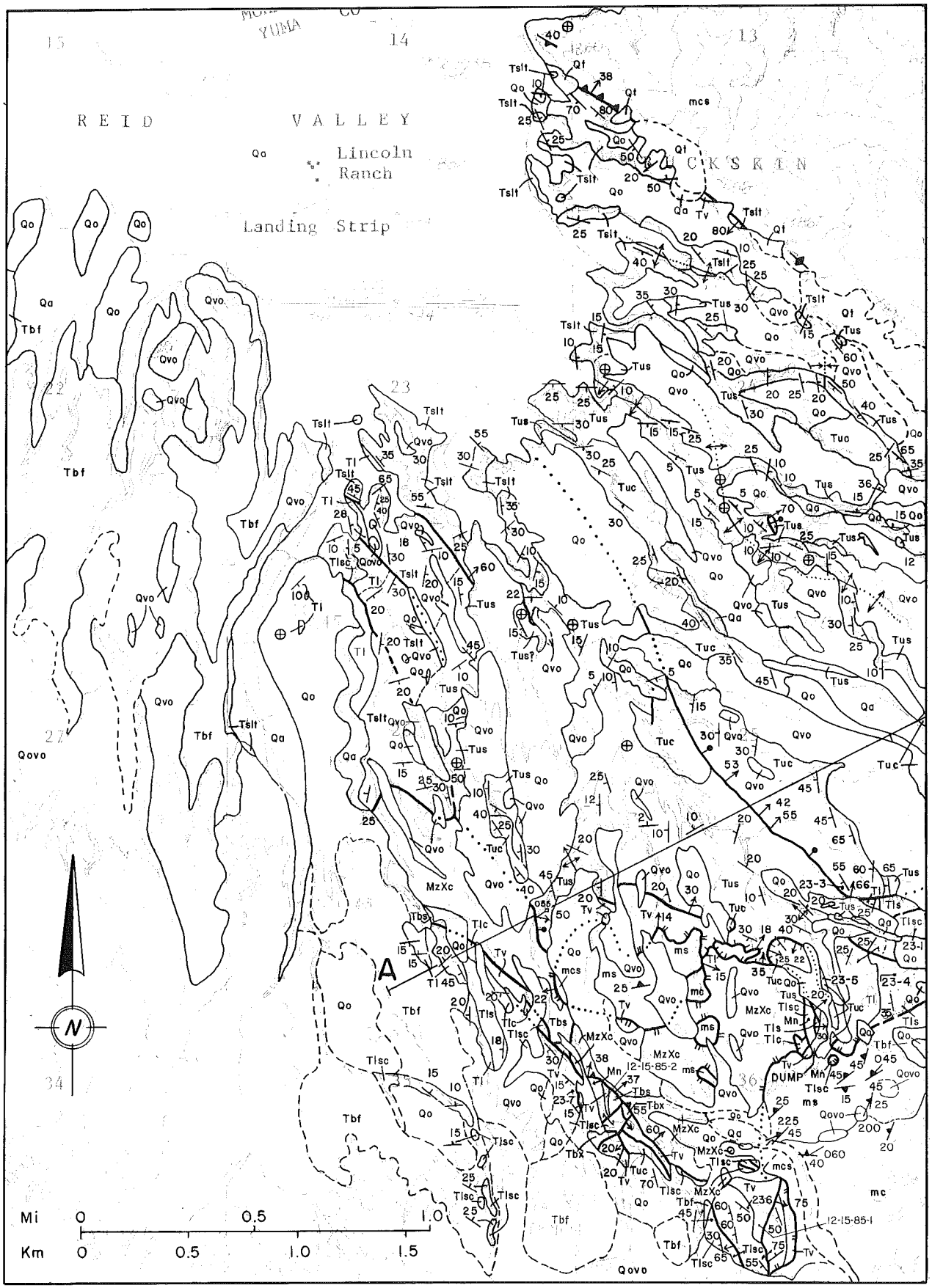
YUMA
REID
VALLEY
Lincoln
Ranch
Landing Strip
A
N
Mi 0 0.5 1.0
Km 0 0.5 1.0 1.5

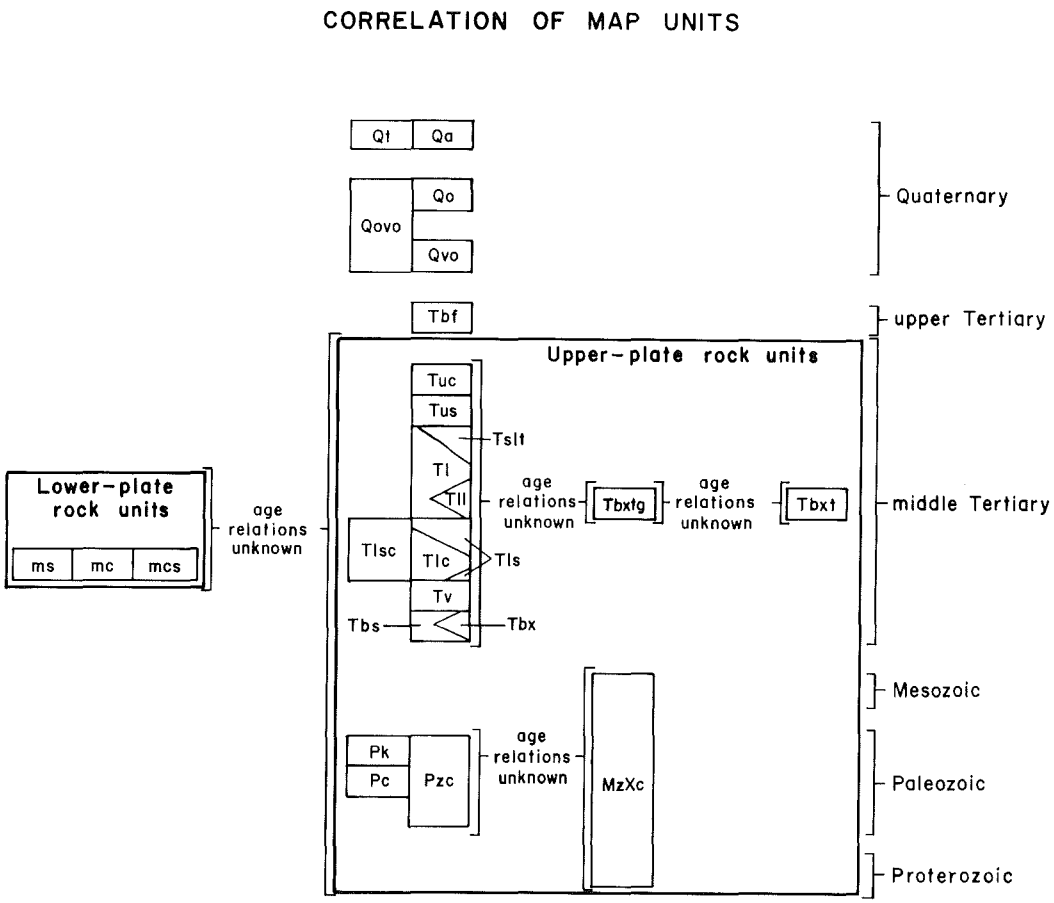

Figure 39. Stratigraphic-correlation diagram for geologic map of Lincoln Ranch basin (Fig. 38).

APPENDIX 2

DESCRIPTION OF MAP UNITS: SWANSEA - COPPER PENNY AREA (FIGS. 40 AND 41)

Postdetachment Units

Qa YOUNG ALLUVIAL DEPOSITS (QUATERNARY) -- Unconsolidated gravel, sand, and silt in washes.

Qo OLD ALLUVIAL DEPOSITS (QUATERNARY) -- Light-gray to light-tan, unconsolidated to very poorly consolidated, poorly sorted conglomeratic sandstone and conglomerate. Typically forms perched terraces and flats topographically above washes.

QTo VERY OLD ALLUVIAL DEPOSITS (QUATERNARY TO LATE TERTIARY) -- Deeply weathered, calcite-cemented, light-tan to medium-brown alluvial deposits.

Tbf BASIN-FILL DEPOSITS (LATE TERTIARY) -- Massive to crudely unsorted to poorly sorted, unconsolidated to weakly consolidated, tan to medium-brown conglomerate, conglomeratic sandstone, and sedimentary breccia.

Tbfx BASIN-FILL BRECCIA DEPOSITS (LATE TERTIARY) -- Resistant cobbles and boulders up to 2 m in diameter of Tertiary volcanic rocks, Paleozoic metasedimentary rocks, and other lithologies in an unconsolidated, unsorted to poorly sorted matrix of cobbles, sand, and silt.

Tbfv BASIN-FILL VOLCANICLASTIC DEPOSITS (LATE TERTIARY) -- Light-yellow lapilli tuff and tuffaceous sandstone. Exposed only in the

Arizona-Montana Mine
Blue Bell Mine
MOUNTAINS
A'
13
18
17
19
20
29
30
31
36

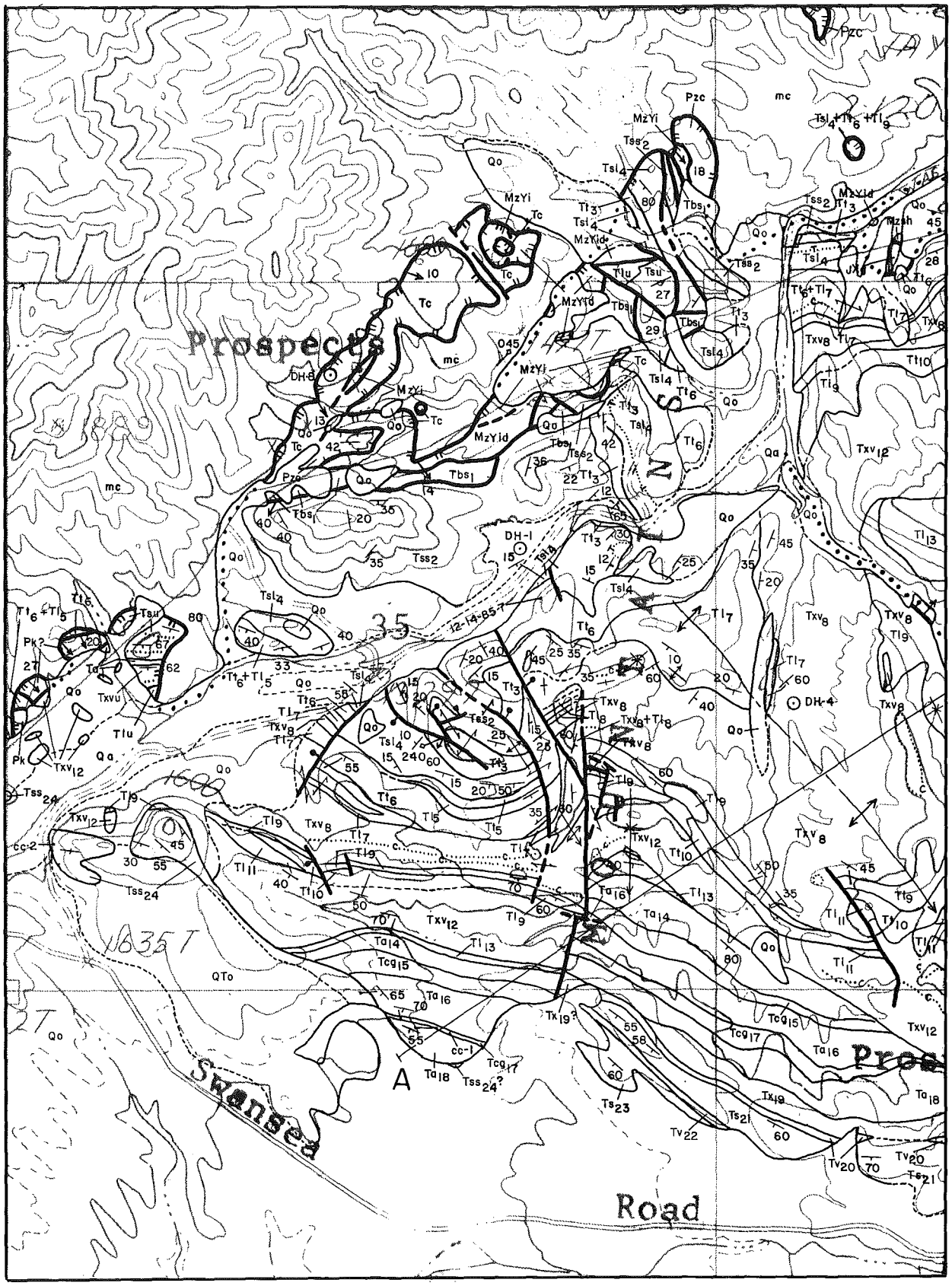

Figure 40. Geologic map of western part of Swansea - Copper Penny area. See Figure 1 for location, Table 2 for map-symbol descriptions, and Figure 16 for cross section. Coordinates of upper left and lower right corners of map are 34°10.69' N., 113°54.23' W. and 34°09.15' N., 113°51.38' W., respectively.

center of sec. 25 where it dips approximately 10° to the east.

Upper-Plate Units

Copper Penny Section. Numbers associated with each unit indicate stratigraphic position in Copper Penny section.

Tss_{24} SANDSTONE (MIOCENE) -- Brown, medium-grained sandstone and conglomeratic sandstone. Locally contains conglomerate with clasts up to 10 cm in diameter and thin, sedimentary breccia(?) layers. Clasts are composed of carbonate rocks, Tertiary sandstone, and Tertiary volcanics. Volcanic-clast layers are possibly volcanic agglomerate. Sandstone has been variably but generally strongly impregnated and probably replaced with secondary carbonate, resulting in weathered surfaces with the roughness and texture of weathered limestone.

Ts_{23} SEDIMENTARY ROCKS (MIOCENE) -- Tan to reddish-brown, medium-grained calcareous sandstone and tan, buff, and gray limestone. Unit is medium to thin bedded.

Tv_{22} VOLCANIC FLOWS AND FLOW BRECCIAS (MIOCENE) -- Pinkish-brown, reddish-brown, or gray breccia composed of 1- to 10-cm-diameter angular fragments of fine-grained volcanic rock with less than 5% partially altered feldspar phenocrysts. Alteration is due to K metasomatism. Unit is generally monolithologic, but locally contains clasts of other Tertiary and pre-Tertiary rock types. Bedding in breccia is locally defined by variations in average clast size and ratio of matrix to clasts. Matrix commonly includes broken rock fragments, and outcrops variably resemble volcanic flow breccia, monolithologic megabreccia, and sedimentary breccia.

Ts_{21} SEDIMENTARY ROCKS (MIOCENE) -- Calcareous sandstone and limestone similar to unit Ts_{23}.

Tv_{20} VOLCANIC FLOWS AND FLOW BRECCIAS (MIOCENE) -- Maroonish-gray to medium-gray volcanic breccia similar to unit Tv_{22}, but less altered. Alteration is due to K metasomatism. Unit contains 1 to 2% phenocrysts of sanidine, altered plagioclase, and trace amounts of biotite. Rims of secondary adularia(?) on some plagioclase phenocrysts are visible in hand sample, and feldspar microlites are almost entirely converted to adularia(?) as seen in thin section. Sample of unit yielded a K-Ar feldspar date of 20.1 $\pm$ 0.5 Ma, which is interpreted as the time of K metasomatism and a minimum age of the rock.

Tx_{19} SEDIMENTARY BRECCIA (MIOCENE) -- Coarse sedimentary breccia containing large blocks of phyllitic, Jurassic metavolcanic rocks; nonphyllitic, quartz-feldspar-phyric, Jurassic volcanic rocks; foliated but unlineated, coarse-grained porphyritic granite; and Paleozoic(?) carbonate rocks. Matrix is reddish, poorly sorted quartzose sandstone.

Ta_{18} ANDESITIC VOLCANIC FLOWS (MIOCENE) -- Dark-weathering, massive to thickly layered andesite to basalt flows and local flow breccias. Rock is commonly vesicular, dark gray on fresh surfaces, and extensively altered. Brownish carbonate material is common in vesicles and in patchy to pervasive replacements, especially near the detachment fault.

Tcg_{17} CONGLOMERATE (MIOCENE) -- Reddish-brown, poorly sorted conglomerate and conglomeratic sandstone. Clasts are dominantly of quartz-feldspar-phyric, Jurassic volcanic and metavolcanic rocks; medium- to coarse-grained granite; and Mesozoic chloritic schist; with lesser amounts of high-grade, Proterozoic(?) metamorphic rocks and reworked, Tertiary clastic rocks. Clasts of Jurassic volcanic rocks are variably rounded to angular, but granitic clasts are generally rounded to subrounded. Unit is 1 to 10 m thick.

Ta_{16} ANDESITIC VOLCANIC FLOWS (MIOCENE) -- Similar to unit Ta_{18}.

Tcg_{15} CONGLOMERATE (MIOCENE) -- Reddish-brown conglomerate and sedimentary breccia composed of clasts up to 1 m in diameter of Jurassic, light-colored, massive, weakly metamorphosed and schistose, metamorphosed volcanic rocks. Unit is locally as thick as 25 m.

Ta_{14} ANDESITIC VOLCANIC FLOWS (MIOCENE) -- Similar to unit Ta_{18}.

Tl_{13} LIMESTONE (MIOCENE) -- Brownish-gray, brownish-tan, and gray limestone with dark-brown, locally shattered siliceous layers. Limestone is generally thin to medium bedded and locally forms resistant ledges and ridge crests. Limestone is 1 to 5 m thick.

Txv_{12} SEDIMENTARY BRECCIA (MIOCENE) -- Massive, unbedded, generally monolithologic sedimentary breccia composed of angular clasts of light-colored, phyllitic, Jurassic metavolcanic rocks (quartz-feldspar-sericite-magnetite schist).

Tl_{11} LIMESTONE (MIOCENE) -- Brown and gray, thin- to medium-bedded limestone. Unit is closely associated with, and not everywhere mapped separately from, the underlying tuff (unit Tt_{10}). Unit is laterally discontinuous but generally several meters thick.

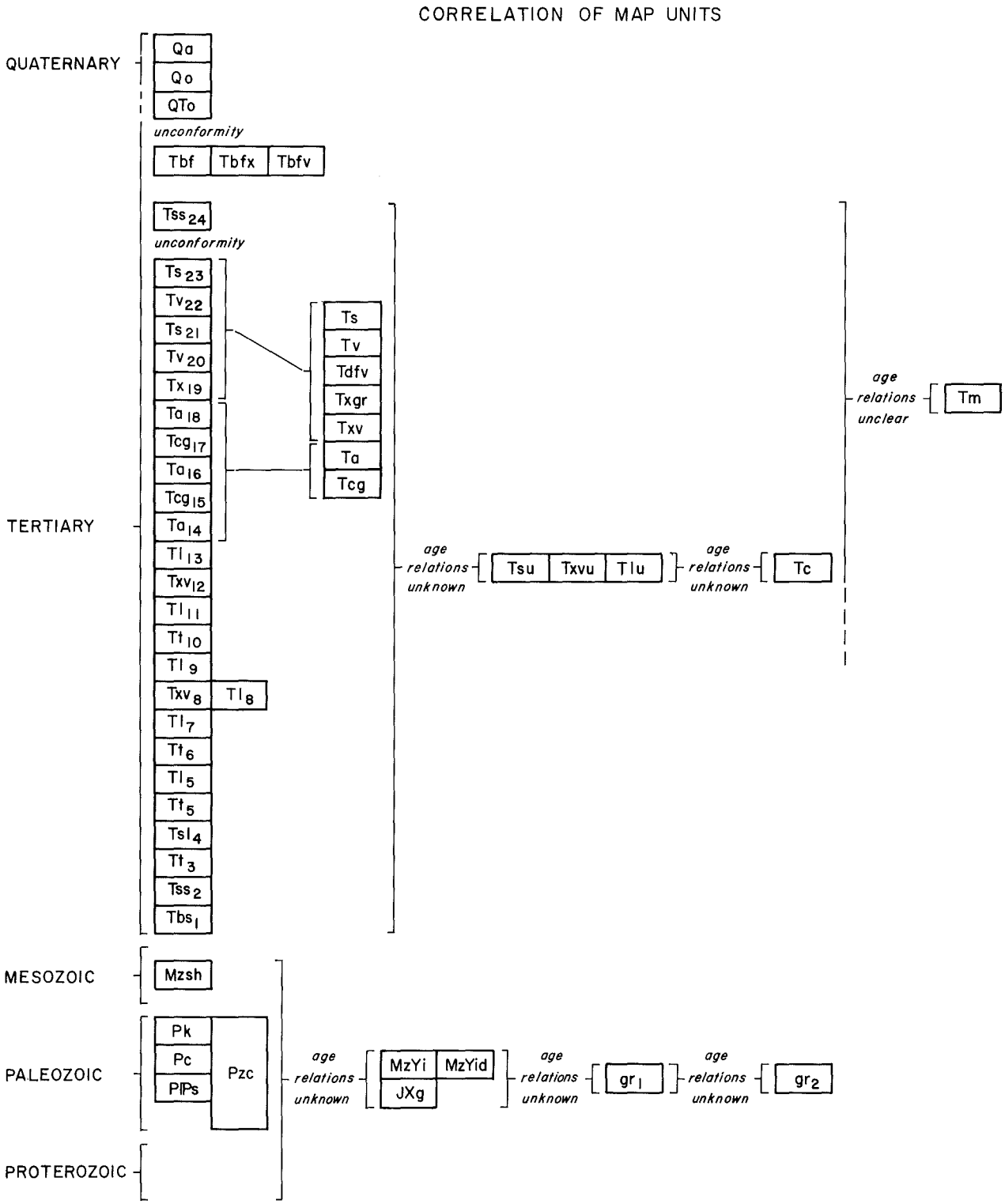

Figure 41. Stratigraphic-correlation diagram for geologic map of western part of Swansea - Copper Penny area (Fig. 40).

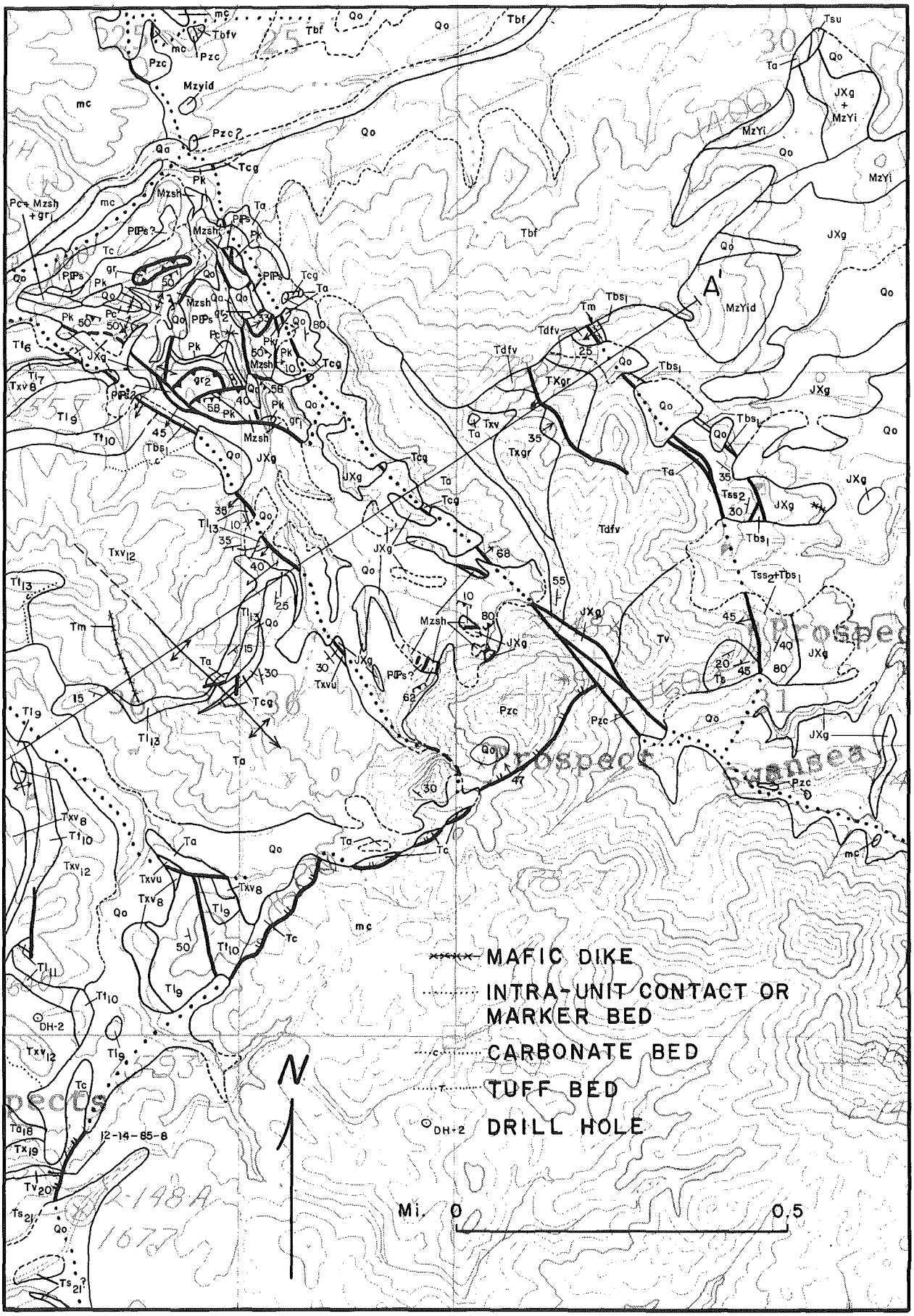
MAFIC DIKE
INTRA-UNIT CONTACT OR MARKER BED
CARBONATE BED
TUFF BED
DRILL HOLE
N
Mi. 0
0.5
A
A'
DH-2
12-14-85-8

composed of maroonish- to purplish-gray volcanic rock with 1 to 8% phenocrysts of feldspar (plagioclase?), trace amounts of biotite, and vugs less than 0.5 mm in diameter. Unit weathers to maroon, tan, and brown and is probably in part flow breccia.

Tdfv DEBRIS FLOWS (MIOCENE) -- Massive, clast- or matrix-supported, unsorted conglomerate and sedimentary breccia. Matrix is dark-brown to reddish-brown sandstone and mudstone, with blocks and cobbles of Jurassic volcanic rocks, vesicular Tertiary andesite, granite, Tertiary sandstone, carbonate rocks, and Mesozoic phyllite. Some matrix material contains coarse-grained quartz and feldspar, probably derived from granitic rock. Some blocks of granite are more than 6 m in diameter.

Txgr SEDIMENTARY BRECCIA, GRANITIC PROTOLITH (MIOCENE) -- Coarse, massive sedimentary breccia, including megabreccia interpreted as catastrophic debris-avalanche deposits, derived from coarse-grained granite with a well-defined mylonitic to gneissic foliation, but no lineation. Granite clasts contain biotite and some bluish quartz. Sedimentary breccia at top of unit contains blocks of Paleozoic rocks, including gray, foliated calcite marble, Coconino Sandstone, brownish carbonate rocks, and at least one block of banded gneiss 10 m in diameter.

Txv SEDIMENTARY BRECCIA, VOLCANIC PROTOLITH (MIOCENE) -- Coarse, massive sedimentary breccia, including megabreccia interpreted as catastrophic debris-avalanche deposits, composed of large angular clasts of light-gray, foliated, Jurassic metavolcanic rocks and more rounded clasts of medium-gray, unfoliated, quartz-feldspar-phyric, Jurassic volcanic rocks. Unit is locally capped by 1 to 4 m of reddish-brown sedimentary breccia with a muddy matrix and large Paleozoic carbonate blocks.

Ta ANDESITIC VOLCANIC FLOWS (MIOCENE) -- Dark-gray, locally vesicular andesite to basalt flows and local flow breccias.

Tcg CONGLOMERATE (MIOCENE) -- Massive to poorly bedded, reddish-brown indurated conglomerate, with subangular clasts, 1 to 30 cm in diameter, of Mesozoic volcanic rocks. Locally includes sandstone.

Other Upper-Plate Units.

Tsu SEDIMENTARY ROCKS, UNDIVIDED (MIOCENE) -- In the west-central part of sec. 35, this unit consists of thinly bedded (2- to 20-mm layers), light- to medium-gray, tan, or pale-red, silty, platy-weathering limestone and calcareous siltstone. Locally includes 2- to 20-cm-thick gray limestone beds. In the northeastern corner of sec. 29, this unit is composed of conglomerate with cobbles up to 30 cm in diameter of primarily reworked Tertiary sandstone and less abundant porphyritic granite, limestone, Tertiary volcanic rocks, and sparse mylonite clasts probably derived from the lower plate.

Txvu SEDIMENTARY BRECCIA, UNDIVIDED (MIOCENE) -- Massive, clast-supported sedimentary breccia with clasts of Mesozoic volcanic rocks. Located in west-central part of sec. 35.

Tlu LIMESTONE, UNDIVIDED (MIOCENE) -- Located in west-central part of sec. 35.

Tc HYDROTHERMAL CARBONATE (MIOCENE) -- Generally dark-chocolate-brown to medium-brown, hydrothermal carbonate rock that replaces various host rocks. Typically located above and along the basal detachment fault. In SE $^1/_4$ sec. 36, carbonate forms invasive veins into Tertiary andesite that has undergone progressively greater replacement toward the carbonate.

Tm MAFIC DIKE (MIOCENE) -- Fine-grained, dark- to medium-gray, northwest-trending mafic dikes. Youngest intruded unit is Txv_{12}.

Mzb BUCKSKIN FORMATION (MESOZOIC) -- Dark-orangish-brown- and brown-weathering, ledge- and cliff-forming, massive to moderately bedded quartzite; calcareous quartzite; and greenish calc-silicate rocks. Siliciclastic rocks are generally fine to medium grained and well sorted, but are locally only moderately sorted, coarse grained, and probably slightly feldspathic. Unit contains gray, greenish-gray, and purplish-gray phyllite and cream-colored gritty sandstone.

Mzp PHYLLITE (MESOZOIC) -- Gray, greenish-gray, and purplish-gray phyllite and calcareous phyllite interpreted as stratigraphically overlying unit Mzsc.

Mzsc SANDSTONE AND CONGLOMERATE (MESOZOIC) -- Gritty quartzose to quartzofeldspathic sandstone, fine-grained conglomerate, quartzite, and calcareous quartzite. Conglomerate contains clasts of quartz and probable decomposed granite. Unit is interpreted to be in overturned depositional contact with granite of unit MzYi and is most conglomeratic adjacent to this contact.

Mzsh SCHIST (MESOZOIC) -- Includes quartz-sericite-chlorite schist, phyllite, calc-silicate and carbonate rocks, and local slivers of Mesozoic

Tt_{10} TUFF (MIOCENE) -- Brownish-tan, lithic-poor welded tuff with 0.5 to 2% phenocrysts. Unit locally includes lithic tuff, flow breccia, and laharic(?) breccia with clasts of Tertiary limestone and Jurassic volcanics. Unit is 6 m thick.

Tl_9 LIMESTONE (MIOCENE) -- Similar to unit Tl_{11}, but is more commonly gray than brown and includes some pinkish-gray silty limestone and calcareous siltstone. Also includes local, chaotic flexural-flow (penecontemporaneous) folds, probably formed during emplacement of overlying monolithologic sedimentary breccia. Limestone is 2 to 12 m thick.

Txv_8 SEDIMENTARY BRECCIA (MIOCENE) -- Massive, monolithologic sedimentary breccia composed of angular to subrounded clasts of brown-weathering, unfoliated to weakly foliated, quartz-feldspar-phyric, Jurassic volcanic rocks. Some clasts contain trace amounts of biotite; some others are derived from volcaniclastic rocks. Top of unit is dominated by clasts of light-colored, strongly foliated and phyllitic, Jurassic metavolcanic rocks. Unit is approximately 30 m thick.

Tl_7 LIMESTONE (MIOCENE) -- Gray to brown, thin- to medium-bedded limestone, generally 1 to 5 m thick.

Tt_6 TUFF (MIOCENE) -- Tan to buff-colored, massive, welded ash-flow tuff. Varies from approximately 5 to 20 m thick, with 1 to 2% phenocrysts of biotite, quartz, and feldspar up to 1 mm in diameter. Unit locally consists of two tuffs, separated by several meters of altered (tuffaceous?) fine-grained sandstone. One tuff unit yielded K-Ar dates of 20.3 $\pm$ 0.4 Ma (feldspar) and 21.8 $\pm$ 0.5 Ma (biotite). This unit is closely associated with, and not everywhere mapped separately from, underlying and overlying limestones (units Tl_5 and Tl_7). Combined thickness of tuff and limestones varies from 5 to 30 m.

Tl_5 LIMESTONE (MIOCENE) -- Tan, brown, and gray, thinly bedded limestone and silty limestone, associated with pinkish-gray, buff, and pale-tan siltstone and moderately sorted lithic sandstone. Interbedded with unit Tt_6 in the SE $^1/_4$ sec. 35.

Tt_5 TUFF (MIOCENE) -- Ash-flow tuff similar to unit Tt_6.

Tsl_4 SANDSTONE, SILTSTONE, AND LIMESTONE (MIOCENE) -- Pinkish-gray- to purplish-gray- or pale-orange- to brown-weathering, thin- to medium-bedded calcareous siltstone and mudstone; poorly sorted, locally pebbly, brown arkosic sandstone and gritty sandstone; medium- to dark-gray or greenish-gray, poorly sorted volcaniclastic sandstone; medium-brown fine-grained sandstone; brown silty limestone; brown to gray, laminated to thinly bedded, variably siliceous limestone; and rare tuff.

Tt_3 TUFF (MIOCENE) -- Slope- and ledge-forming tuff, including the following varieties: (1) light-cream-colored tuff with 2 to 5% quartz phenocrysts 0.5 to 2 mm in diameter; (2) slightly purplish-gray tuff with 1 to 2% altered feldspar (plagioclase) phenocrysts; and (3) pinkish- to purplish-gray tuff with approximately 1% dark, volcanic lithic fragments and 1% fine-grained phenocrysts, including trace amounts of biotite.

Tss_2 SANDSTONE (MIOCENE TO UPPER OLIGOCENE[?]) -- Dark-weathering, fine-grained, variably calcareous sandstone that is pale green, greenish brown, or medium to light brown. Contains interbedded gray to dark-greenish-gray siltstone and mudstone, and gray and brown limestone beds 0.5 to 1 m thick containing siliceous layers 2 to 5 cm thick. Unit contains a thin, locally mappable marker tuff similar in character to unit Tt_3.

Tbs_1 BASAL SANDSTONE (MIOCENE TO UPPER OLIGOCENE[?]) -- Maroon, pale-red, pale-gray, purplish-gray, or light-cream-colored, medium- to fine-grained arkosic sandstone and conglomerate. Clasts are subrounded to rounded pebbles and cobbles up to 15 cm in diameter of massive, foliated, feldspar-biotite-phyric, Mesozoic volcanic rocks; white quartzite with some quartz grains 1 mm in diameter; granite; alaskite; granodiorite; altered andesite; Jurassic volcaniclastic rocks; and slightly feldspathic, Mesozoic quartzose sandstone. Unit is locally interbedded with pale-gray to tan, dark-brown-weathering, thinly bedded to laminated, variably calcareous siltstone. Basal conglomerate is 2 to several meters thick along north edge of NW $^1/_4$ sec. 31, where it contains cobbles to boulders of primarily foliated, Mesozoic metasedimentary and metavolcanic rocks with sparse clasts of Tertiary volcanic rocks and megacrystic granite.

Section East of Swansea Fault.

Ts SEDIMENTARY ROCKS (MIOCENE) -- Thin- to medium-bedded, tan to brown conglomerate largely composed of clasts of the underlying volcanic breccia. Stratigraphically higher part of unit contains tan, buff, and brownish-gray, thin-bedded calcareous sandstone and limestone.

Tv VOLCANIC ROCKS (MIOCENE) -- Breccia

Geology and mineral deposits of the central Artillery Mountains

JON E. SPENCER
MICHAEL J. GRUBENSKY
JOHN T. DUNCAN
JONATHAN D. SHENK
Arizona Geological Survey, 845 N. Park Ave., #100, Tucson, Arizona 85719

JOHN C. YARNOLD
JAMES P. LOMBARD
Department of Geosciences, University of Arizona, Tucson, Arizona 85721

ABSTRACT

Miocene strata in the central Artillery Mountains record tectonic processes that occurred at the boundary between the slightly extended Transition Zone in central Arizona and a highly distended part of the Basin and Range Province that encompasses the Harcuvar metamorphic core complex of west-central Arizona. Strata in the study area were deposited within a southwest-tilted half graben during graben tilting. The lower to middle Miocene Artillery Formation, a lithologically diverse sequence of sedimentary and volcanic rocks that includes siltstone, sandstone, conglomerate, limestone, sedimentary breccia, and volcanic flows and tuffs, rests on Proterozoic crystalline rocks and forms most of the Tertiary stratigraphic sequence in the Artillery Mountains. Clastic sedimentary rocks in the lower Artillery Formation record the initial stages of basin formation and were derived primarily from the north or east. In contrast, a significant amount of detritus in the upper Artillery Formation was derived from the south or west and probably records emergence of a major graben-bounding normal-fault scarp to the southwest. The overlying Chapin Wash Formation and Sandtrap Conglomerate record formation of a broad sedimentary basin dominated by fluvial sedimentation. These two units were deposited largely or entirely after the transition to one-sided denudation of the Harcuvar metamorphic core complex and contain clasts derived from the emerging mylonitic footwall.

The Artillery Mountains contain the largest known Mn reserves in the United States. Most of the Mn deposits are sedimentary in origin and are hosted by the Chapin Wash Formation. Fracture-filling Mn deposits at the Shannon and Priceless mines are younger than the Chapin Wash Formation. Quartz, calcite, and barite gangue minerals within these two Mn deposits contain fluid inclusions having less than 3 wt. % NaCl equivalent. Fluids in these inclusions are significantly less saline than those in nearby detachment-fault-related Cu-Fe deposits, which indicates that the two deposit types are not closely related.

in Spencer, J.E., and Reynolds, S.J., eds., 1989, Geology and mineral resources of the Buckskin and Rawhide Mountains, west-central Arizona: Arizona Geological Survey Bulletin 198, p. 168-183.

INTRODUCTION

The study area in the central Artillery Mountains (Fig. 1) is within a WNW-striking belt of SSW-dipping Miocene strata that rest depositionally on Proterozoic crystalline rocks. Proterozoic rocks are exposed almost continuously from the northern margin of the study area northeast through the Transition Zone of central Arizona to the edge of the Colorado Plateau. The Buckskin and Rawhide Mountains southwest of the Artillery Mountains (Fig. 1) are primarily composed of mylonitic crystalline rocks that are bounded above by the Buckskin-Rawhide detachment fault. The study area thus encompasses the boundary between an area of minor extensional faulting, the Transition Zone, and an area of large-magnitude extension, the Harcuvar metamorphic core complex within the Basin and Range Province. The thick, well-exposed section of Miocene strata in the study area records processes associated with large-magnitude extension and sedimentary-basin formation at this important tectonic boundary.

Miocene strata in the central Artillery Mountains consist of a sequence of interbedded conglomerate, sandstone, mudstone, limestone, sedimentary breccia, and volcanic flows and tuffs (Figs. 2, 3, 4, and 5; Appendix 1; Lasky and Webber, 1949; Otton, 1982). Sandstone in the upper part of the sequence contains strata-bound, fracture-filling, and open-space-filling Mn deposits that make up the largest known Mn reserves in the United States (Lasky and Webber, 1949). The youngest conglomerate in the Miocene sequence contains clasts of mylonite derived from the Buckskin and Rawhide Mountains and records tectonic unroofing of the detachment-fault footwall (see also Spencer and Reynolds, this vol.).

Previous studies in the central Artillery Mountains focused on the modes of occurrence and mineralogy of the Mn deposits (Lasky and Webber, 1949; Mouat, 1962). In this article, we present the results of new geologic mapping, describe the stratigraphy of Miocene sedimentary and volcanic rocks, outline evidence regarding sediment-dispersal patterns, and present a tectonic model

volcanic rocks, quartzite, and variably mylonitic crystalline rocks, including coarse-grained, porphyritic biotite granite, banded gneiss, and alaskite. Chloritic schist is locally calcareous and associated with gypsiferous soil, probably derived from bedded gypsum. Many of the various lithologies have gradational contacts and are widely interlayered. Carbonate is orange, brown, or gray. Well-developed foliation and cleavage and complex interleaving of diverse lithologies suggest that Mesozoic thrust faults, possibly with large displacement, are contained within this unit. Rocks included in this unit probably range in age from Proterozoic to Mesozoic.

Pk KAIBAB LIMESTONE (PERMIAN) -- Light- to medium-gray, tan, light-brown, and yellowish-cream-colored limestone and dolomitic marble, locally with abundant dark-weathering, resistant siliceous layers, stringers, blobs, and irregular knots, typically 0.5 to 10 cm thick. Lithologic layering (bedding?) is defined by the orientation of siliceous layers and by color banding in the carbonate rocks.

Pc COCONINO SANDSTONE (PERMIAN) -- Pinkish-tan-weathering, vitreous quartzite.

Ps SUPAI GROUP (PERMIAN AND PENNSYLVANIAN) -- Dark-brown- to orangish-tan-weathering, ledge- and cliff-forming, thin-bedded to laminated quartzite and calcareous quartzite. Quartzite is well sorted and generally fine grained. Unit locally includes thin marbles.

Pzc CARBONATE ROCKS, UNDIVIDED (PALEOZOIC) -- Tan, gray, and tannish-brown calcite and dolomite marble, massive to well bedded with local siliceous layers and stringers.

Pzcc CALCITE MARBLE (PALEOZOIC) -- Generally gray, thick-bedded to moderately bedded calcite marble with or without siliceous layers and stringers.

Pzcd DOLOMITE MARBLE (PALEOZOIC) -- Generally tan, thick-bedded dolomite marble with or without siliceous layers and stringers.

MzYi MAFIC INTRUSIVE ROCKS (MESOZOIC OR PROTEROZOIC) -- Foliated and locally lineated, medium- to dark-green, aphanitic metavolcanic(?) to fine-grained, locally medium-grained, dioritic intrusive rock. Probably primarily represents shallow-level mafic intrusions of Mesozoic age.

MzYid DIORITIC INTRUSIVE ROCKS (MESOZOIC OR PROTEROZOIC) -- Fine- to medium-grained dioritic granitoids. Gradational with unit MzYi.

JXg GRANITIC ROCKS (JURASSIC OR PROTEROZOIC) -- Primarily megacrystic biotite granite, but locally includes fine-grained equivalents. Medium- to fine-grained leucocratic granite in S $^1/_2$ sec. 29 could be Mesozoic. The megacrystic granite was considered to be Mesozoic by Wicklein (1980) based on Rb-Sr data from a pegmatite, but a genetic relationship between the pegmatite and the granite has not been established. We consider the granite to be Proterozoic in age based on lithologic similarity to Proterozoic granitic rocks elsewhere in west-central Arizona.

gr_1 GRANITOID (MESOZOIC[?]) -- Foliated medium-grained granite(?). Forms fault-bounded blocks in NE $^1/_4$ sec. 36 and in S $^1/_2$ sec. 25. Could be Proterozoic, but is probably Mesozoic.

gr_2 GRANITOID (MESOZOIC[?]) -- Leucocratic, fine-grained granite(?) or granodiorite(?) with weak to moderate mylonitic foliation and local lineation.

Lower-Plate Unit

mc MYLONITIC CRYSTALLINE ROCKS (CENOZOIC TO PROTEROZOIC) -- Mylonitic granitic and high-grade metamorphic rocks. Includes foliated megacrystic granite with K-feldspar augen up to 3 cm long. Moderate- to well-developed, ENE-trending lineation is present on mylonitic foliation. Top-to-the-northeast shear during Tertiary mylonitization is indicated by S-C fabrics. Near the Buckskin-Rawhide detachment fault, these rocks have been converted to chloritic breccia and, directly below the fault, to microbreccia.

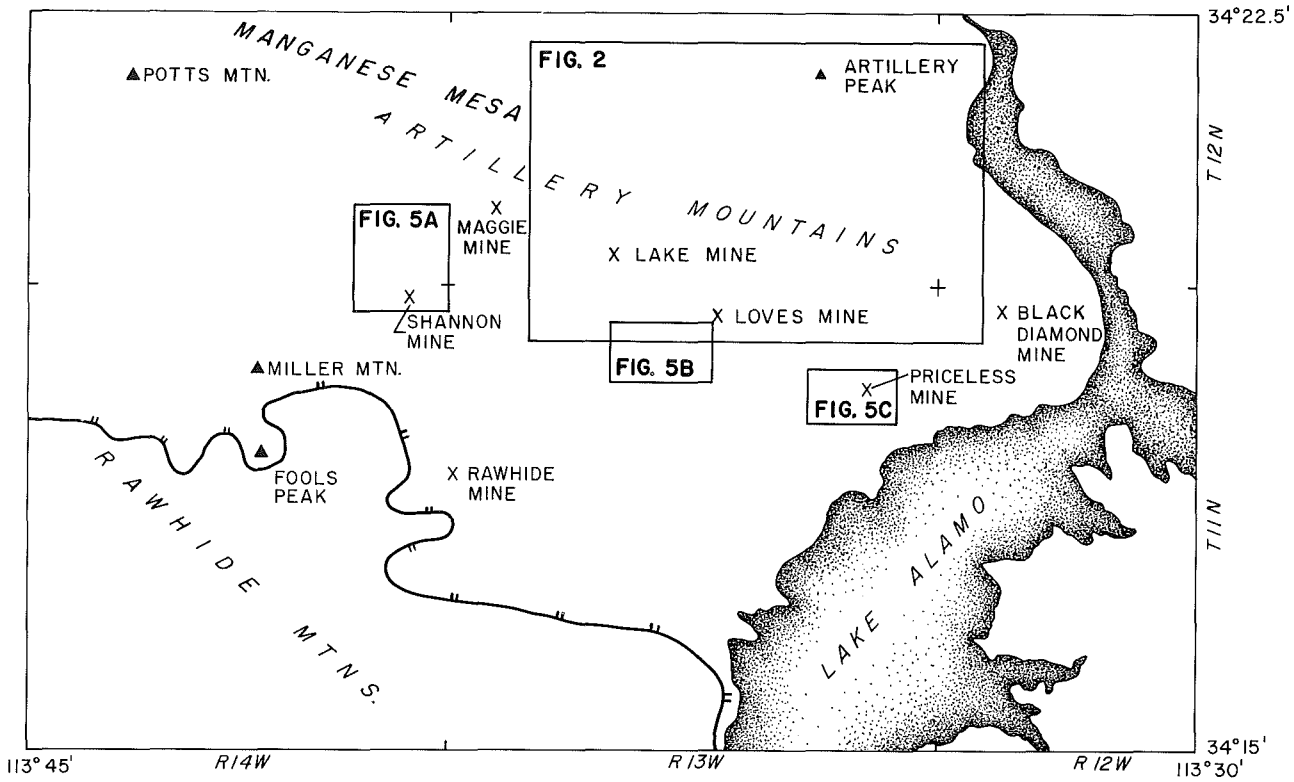

Figure 1. Location map of the Artillery Mountains showing locations of Figures 2 and 5. Buckskin-Rawhide detachment fault is shown by thick line with double hatchures on hanging-wall block.

for basin formation and evolution. In addition, we describe some of the numerous Mn deposits in the Artillery Mountains and present results of fluid-inclusion studies of minerals associated with Mn deposits and barite veins.

STRATIGRAPHY AND PROVENANCE

Miocene sedimentary and volcanic rocks form a 2- to 3-km-thick, SSW-dipping sequence in the central Artillery Mountains. This sequence has been divided, in ascending order, into five formations (Lasky and Webber, 1949): (1) Artillery Formation, (2) Chapin Wash Formation, (3) Cobwebb Basalt, (4) Sandtrap Conglomerate, and (5) Manganese Mesa basalt (new name). We maintain usage of these divisions and divide the Artillery Formation into lower, middle, and upper members on the basis of rock type and clast lithology.

The lower member of the Artillery Formation, as defined here, encompasses the four stratigraphically lowest units (basal arkose unit up section through the limestone unit in Fig. 2) and forms a broadly fining-upward sequence (Fig. 4). The basal unit of the Artillery Formation consists of arkosic sandstone, conglomeratic sandstone, and conglomerate derived largely or entirely from Proterozoic crystalline rocks, such as those directly beneath the arkose. The arkose grades upward into a unit of interbedded mudstone, sandstone, and limestone that contains two beds of biotite-feldspar-phyric tuff. A thin section of one of the tuff beds revealed devitrified undeformed glass shards that indicate an air-fall or unwelded ash-flow origin for the now-altered and lithified tuffs. A sample from a probably correlative tuff 1 to 2 km east of the study area (Jim Otton, oral commun., 1987) yielded a biotite K-Ar date of 23.0 Ma (Bob Miller, oral commun., 1987). The mudstone, sandstone, and limestone unit is overlain successively by a unit of sandstone, with subordinate siltstone and limestone, and a unit of limestone. The limestone unit is commonly folded and contains sparse lenses and sheets of sedimentary breccia derived from Mesozoic metavolcanic and metasedimentary rocks.

The overlying middle member of the Artillery Formation is lithologically diverse and is characterized by marked lateral facies and thickness changes (Figs. 2 and 4). Sedimentary breccia sheets derived from metamorphosed Jurassic volcanic rocks first appear in the underlying limestone unit and are widespread in the middle member. These sedimentary breccias are significant because they were probably derived from the west, where metavolcanic rocks are exposed in the Rawhide and Buckskin Mountains. In contrast, clasts in the basal arkose consist entirely of crystalline rocks that were probably derived from the north or east. Quartzite pebbles within clastic rocks in the middle member also reflect a change in provenance. Basalt flows are common in the middle member and may reflect the change in basin geometry that was responsible for the influx of metamorphic-rock debris.

The upper member of the Artillery Formation consists of the Artillery megabreccia and locally over-

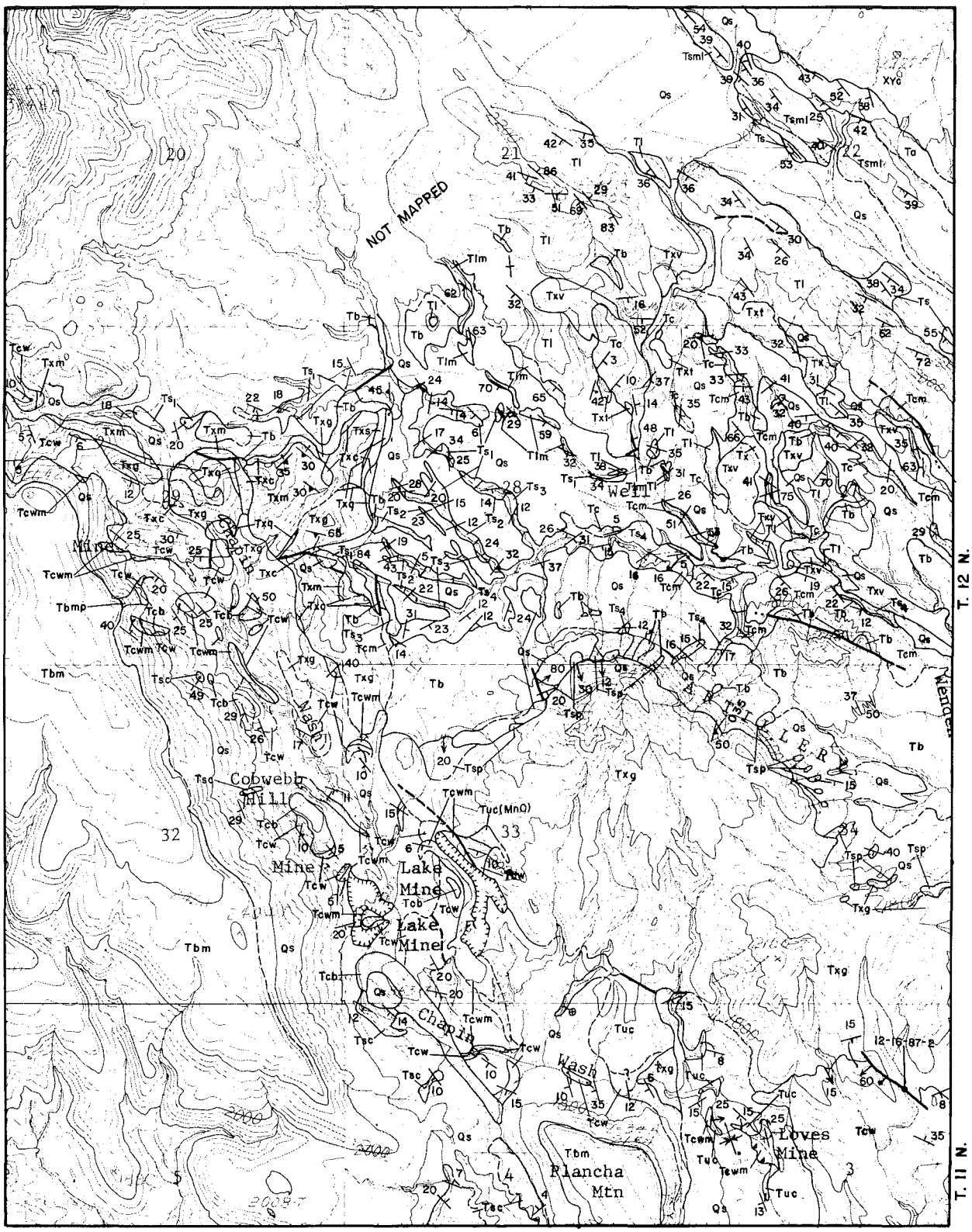
NOT MAPPED
Cobweb Hill
Mine
Lake Mine
Lake Miner
Chapin Wash
Well
Loves Mine
Plancha Mtn
T. 12 N.
T. 11 N.
R. 13 W.

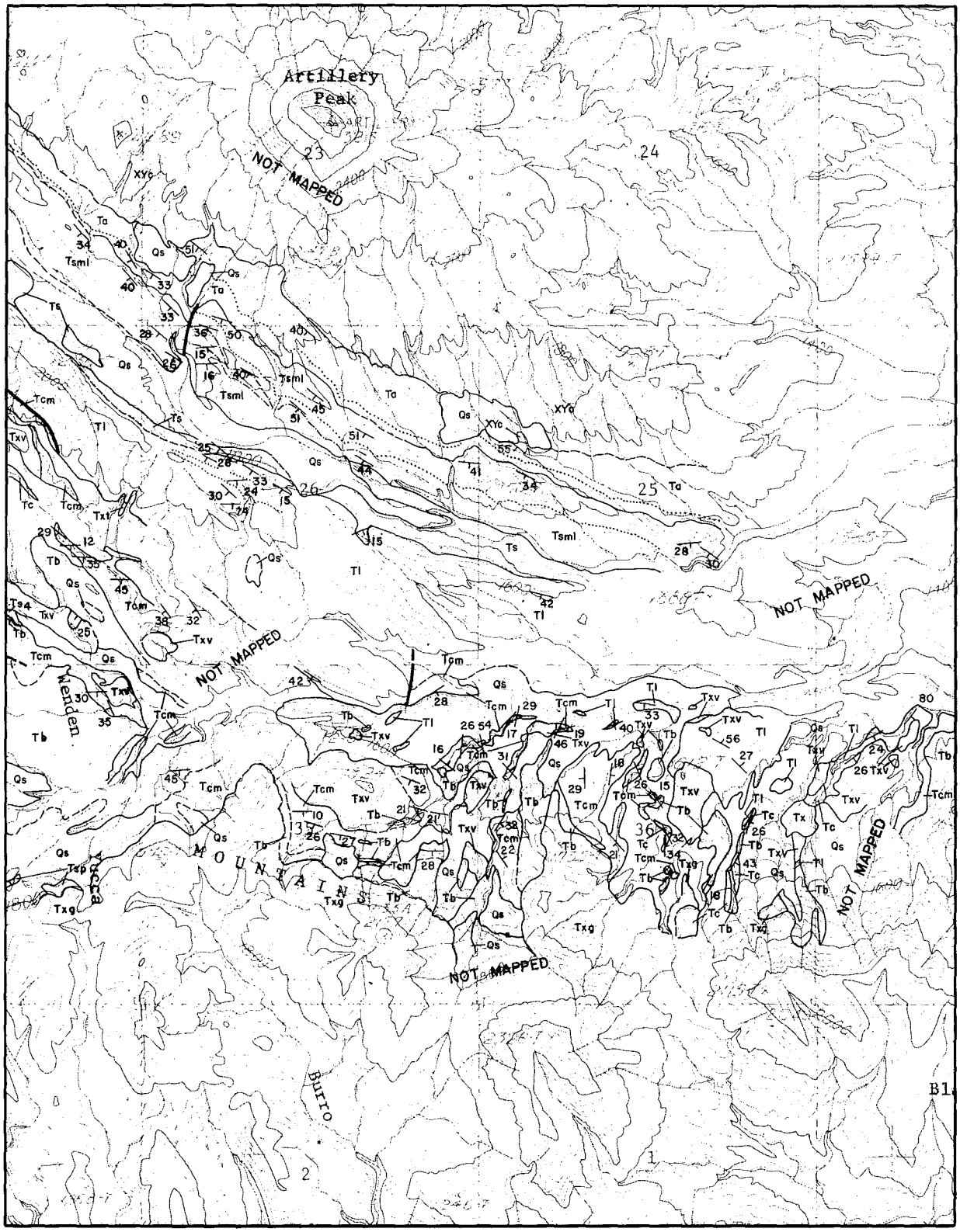

Figure 2. Geologic map of the central Artillery Mountains. See Table 1 for map units and symbols. Coordinates of upper left and lower right corners of map are 34°22.50' N., 113°38.60' W. and 34°19.37' N., 113°32.90' W., respectively.

Table 1. Map units and symbols for Figures 2 and 5.

MAP UNITS AND SYMBOLS

QUATERNARY UNITS

Qs	SURFICIAL DEPOSITS

MIOCENE UNITS

Tbm	BLACK MESA BASALT
Tbmp	PYROCLASTIC ROCKS BENEATH BLACK MESA BASALT
Tsc	SANDTRAP CONGLOMERATE
Tcb	COBWEBB BASALT
Tcw	CHAPIN WASH FORMATION
Tcwm	MANGANIFEROUS CHAPIN WASH FORMATION
Tuc	UPPER CONGLOMERATE
Txg	ARTILLERY MEGABRECCIA, GRANITIC PROTOLITH
Txm	ARTILLERY MEGABRECCIA, METAMORPHOSED JURASSIC VOLCANIC PROTOLITH
Txs	ARTILLERY MEGABRECCIA, MESOZOIC SCHIST PROTOLITH
Txq	ARTILLERY MEGABRECCIA, QUARTZITE PROTOLITH
Txc	ARTILLERY MEGABRECCIA, PALEOZOIC(?) CARBONATE PROTOLITH
Tsp	SANDSTONE AND PEBBLY SANDSTONE
Tb	BASALT FLOWS
Ts_4	SANDSTONE AND MUDSTONE UNIT, UPPER MUDSTONE MEMBER
Ts_3	SANDSTONE AND MUDSTONE UNIT, UPPER SANDSTONE MEMBER
Ts_2	SANDSTONE AND MUDSTONE UNIT, LOWER MUDSTONE MEMBER
Ts_1	SANDSTONE AND MUDSTONE UNIT, LOWER SANDSTONE MEMBER
Txv	MEGABRECCIA, METAMORPHOSED JURASSIC VOLCANIC PROTOLITH
Txt	MEGABRECCIA, METAMORPHOSED JURASSIC ASH-FLOW TUFF PROTOLITH
Tx	MIXED BRECCIA OF METAMORPHOSED ROCKS AND TERTIARY LIMESTONE
Tcm	CONGLOMERATE AND MUDSTONE
Tc	CONGLOMERATE
Tlm	LIMESTONE AND MUDSTONE
Tl	LIMESTONE
Ts	SANDSTONE
Tsml	MUDSTONE, SANDSTONE, AND LIMESTONE
Ta	BASAL ARKOSE

PROTEROZOIC UNITS

XYc	QUARTZO-FELDSPATHIC CRYSTALLINE ROCKS

MAP SYMBOLS

47	CONTACT, SHOWING DIP -- Depositional, dashed where approximately located.
60	HIGH-ANGLE FAULT, SHOWING DIP -- Dashed where inferred.
40	HIGH-ANGLE NORMAL FAULT, SHOWING DIP -- Dashed where inferred.
35	REVERSE FAULT, SHOWING DIP -- Dashed where inferred.
25	STRIKE AND DIP OF BEDDING
80	STRIKE AND DIP OF METAMORPHIC FOLIATION

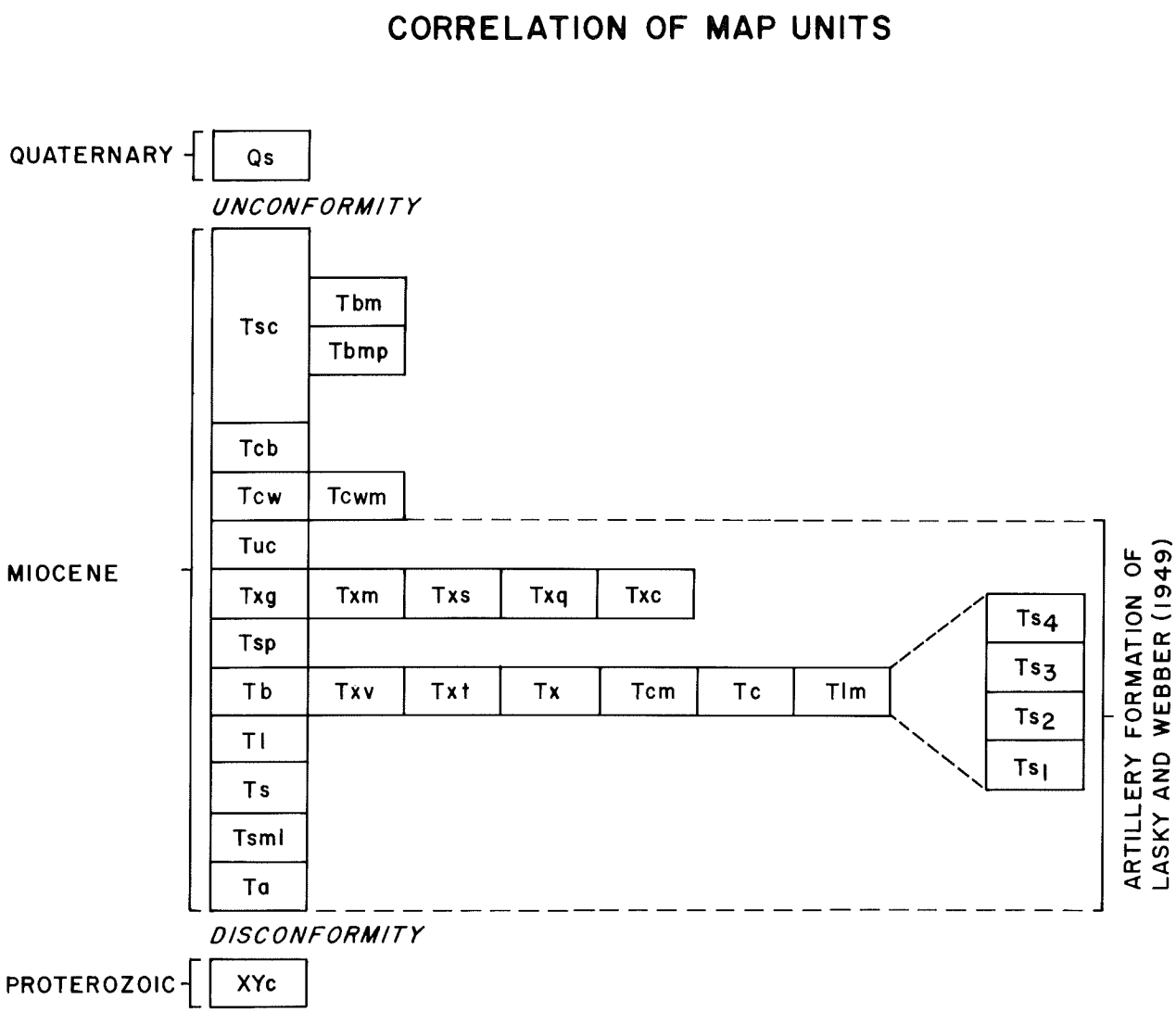

Figure 3. Stratigraphic-correlation diagram for map units in Figures 2 and 5.

lying conglomerate derived from the megabreccia. Most of the megabreccia is composed of megacrystic biotite granite and pink, fine-grained leucocratic granite, both of which are probably Proterozoic in age. In some areas the megacrystic granite has a nonlineated to weakly lineated, moderately to strongly mylonitic fabric that does *not* resemble the strongly lineated, Tertiary mylonitic fabric in the Harcuvar metamorphic core complex. The megabreccia varies from highly shattered and disaggregated rocks to massive, slightly fractured rocks exposed laterally for hundreds of meters. Sedimentary breccia and structurally coherent rock masses derived from metamorphosed Paleozoic and Mesozoic sedimentary and volcanic rocks form the northwest end of the Artillery megabreccia outcrop belt. The presence of these metamorphic rocks in the Artillery megabreccia indicates that it was derived from the west (or possibly south) where such rock types are widespread, and not from the north or east where they are completely absent.

Miocene strata overlying the Artillery Formation include, in ascending order, the Chapin Wash Formation, Cobwebb Basalt, Sandtrap Conglomerate, and Manganese Mesa basalt. The Chapin Wash Formation consists of 200 to 300 m of sandstone with minor interbedded siltstone and conglomerate. Local crossbedding, ripple marks, mudcracks, mudflakes, and scours indicate a fluvial sedimentary environment (Lasky and Webber, 1949). Manganiferous sandstone forms a zone several meters to several tens of meters thick generally near the middle of the Chapin Wash Formation. The stratigraphically overlying Cobwebb Basalt marks an abrupt upward transition from sandstone of the Chapin Wash Formation to fanglomerate of the Sandtrap Conglomerate. The Sandtrap Conglomerate commonly forms distinctive, massive, rounded outcrops with little internal variation in grain size or resistance to weathering and is more poorly sorted than conglomerates in the Artillery Formation. Mylonitic clasts derived from the footwall of the Buckskin-Rawhide detachment fault are a clearly recognizable component of clast populations (see also Spencer

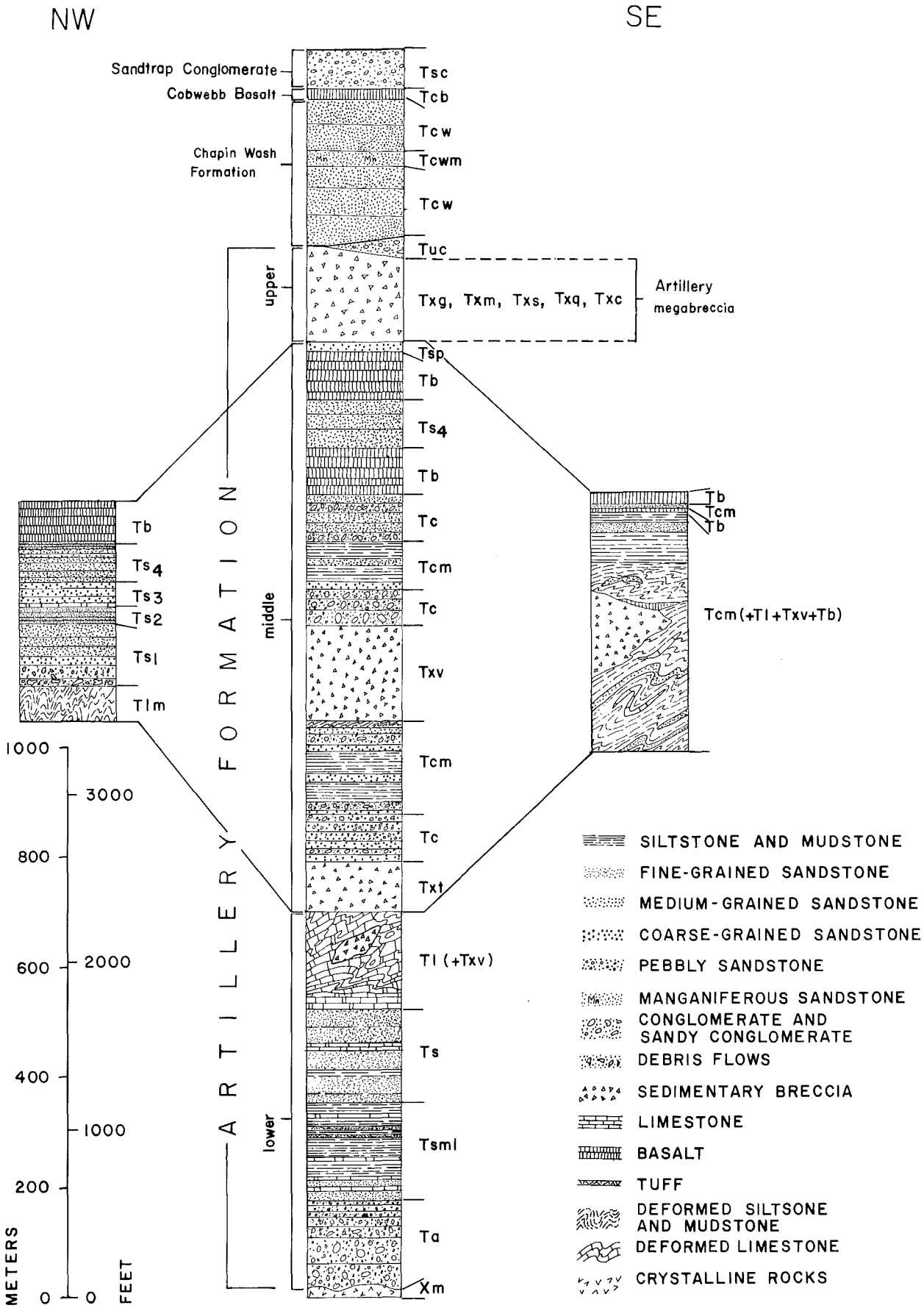
NW
SE
Sandtrap Conglomerate
Cobwebb Basalt
Chapin Wash Formation
Tsc
Tcb
Tcw
Tcwm
Tcw
Tuc
Txg, Txm, Txs, Txq, Txc
Artillery megabreccia
Tsp
Tb
Ts4
Tb
Tc
Tcm
Tc
Txv
Tcm
Tc
Txt
Tl (+Txv)
Ts
Tsml
Ta
Xm
upper
middle
lower
ARTILLERY FORMATION
Tb
Ts4
Ts3
Ts2
Ts1
Tlm
Tb
Tcm
Tb
Tcm(+Tl+Txv+Tb)
1000
3000
800
600
2000
400
1000
200
0
0
METERS
FEET
SILTSTONE AND MUDSTONE
FINE-GRAINED SANDSTONE
MEDIUM-GRAINED SANDSTONE
COARSE-GRAINED SANDSTONE
PEBBLY SANDSTONE
MANGANIFEROUS SANDSTONE
CONGLOMERATE AND SANDY CONGLOMERATE
DEBRIS FLOWS
SEDIMENTARY BRECCIA
LIMESTONE
BASALT
TUFF
DEFORMED SILTSONE AND MUDSTONE
DEFORMED LIMESTONE
CRYSTALLINE ROCKS

Figure 4 (previous page). Stratigraphic column for Miocene rocks of the central Artillery Mountains showing lateral variations of the middle member of the Artillery Formation.

and Reynolds, this vol.). Cobble imbrication and eastward decrease in clast size indicate a general sediment-transport direction to the east or northeast.

Northwest of the Shannon mine, basalt mapped as Sandtrap basalt by Lasky and Webber (1949) is continuous with basalt mapped by them as Quaternary basalt; the two units are thus the same and are herein named the Manganese Mesa basalt. The Manganese Mesa basalt rests conformably on Sandtrap Conglomerate and is, in turn, overlain by conglomerate and conglomeratic sandstone essentially identical to that which underlies the basalt (Fig. 5A). The basalt pinches out in this area; there is no mappable contact within the Sandtrap Conglomerate at the horizon of the basalt flow where the basalt is absent. Some of the Sandtrap Conglomerate is therefore younger than the Manganese Mesa basalt.

TECTONICS OF BASIN EVOLUTION

Middle Tertiary sedimentation associated with extensional faulting in the Basin and Range Province of the southwestern United States was preceded in many areas by a period of regional uplift and erosion during Late Cretaceous and early Tertiary time. Paleozoic and lower Mesozoic strata were completely removed from the Basin and Range Province in northwestern Arizona and from much of the Transition Zone prior to the middle Tertiary. In west-central Arizona, Paleozoic and lower Mesozoic strata underwent Cretaceous tectonic burial and metamorphism due to generally south-directed thrust faulting (Reynolds and others, 1986b). These metamorphic rocks were partially uncovered during early Tertiary erosional denudation. North and east of the Buckskin and Rawhide Mountains, middle Tertiary stratigraphic sequences rest on Proterozoic crystalline rocks. Within and to the south and west of the Buckskin and Rawhide Mountains, middle Tertiary sequences rest on a variety of rock types, including metamorphosed Mesozoic and Paleozoic sedimentary and volcanic rocks. The restricted distribution of these metamorphic rocks is thus an important mid-Tertiary paleogeographic feature that is helpful in determining mid-Tertiary sediment-dispersal patterns.

Mid-Tertiary normal faulting and sedimentary-basin formation in much of west-central Arizona occurred as a result of ENE-WSW extension within the hanging wall of the Buckskin-Rawhide-Bullard detachment fault (Reynolds and Spencer, 1985; Spencer and Reynolds, this vol.). Within the central Artillery Mountains, mid-Tertiary strata underwent approximately continuous tilting during sediment deposition (Fig. 6) because of synsedimentary, rotational normal faulting. Deposition of the lower member of the Artillery Formation probably occurred in a half graben within the hanging wall of the detachment fault and was a consequence of gentle southwestward tilting of the underlying fault block of Proterozoic crystalline rocks (Fig. 7). Cobbles, pebbles, and arkosic sand derived from Proterozoic crystalline rocks were probably shed down the southwest-sloping top of the underlying fault block. As faulting and tilting continued,

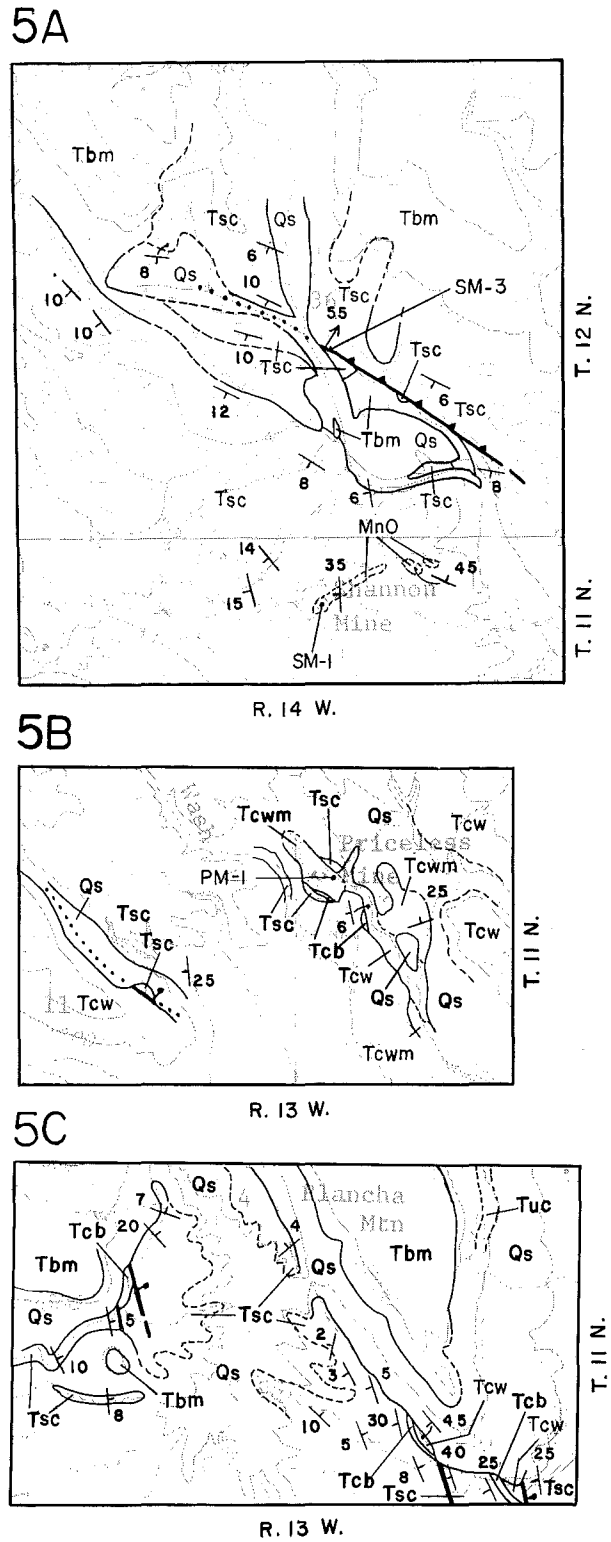

Figure 5. Geologic maps of the Shannon mine area (A), Priceless mine area (B), and Plancha Mountain area (C). See Figure 1 for locations and Figure 2 for map symbols.

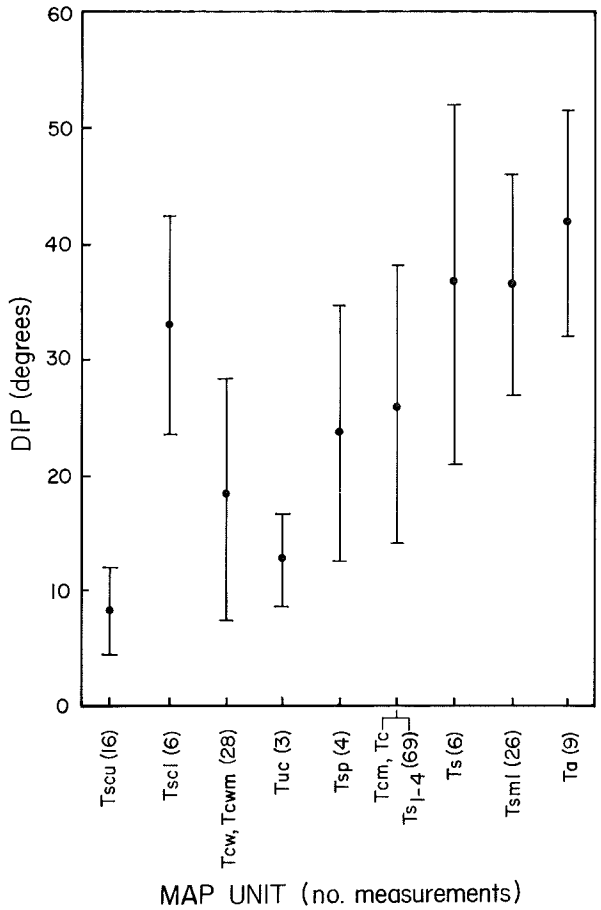

Figure 6. Graph of dip versus stratigraphic position. Attitudes were taken from Figures 2 and 5 and are represented as mean (point) and one standard deviation (error bars). Units Tl and Tlm were not incorporated into this diagram because of internal deformation of these units, including isoclinal folding. Attitudes from the Sandtrap Conglomerate (unit Tsc) are divided into two groups in this diagram and are shown as Tscl and Tscu. The points define a strong correlation between dip and stratigraphic position. This correlation is strengthened if data from units Tuc and Tscl are ignored. Attitudes for these two units are from areally restricted areas (Figs. 2 and 5C) and are interpreted as products of local anomalous tilting or lack of tilting.

megabreccias, probably shed off an adjacent fault block to the west or south, became a major component of the clastic sediments in the middle and upper members of the Artillery Formation. Thus, the transition from northward- or eastward-derived to southward- or westward-derived clastic sedimentation is a major aspect of basin evolution during deposition of the Artillery Formation. The limestone unit at the top of the lower member of the Artillery Formation possibly represents the depositional axis of the basin.

The lower member of the Artillery Formation in the central Artillery Mountains forms a broadly fining-upward sedimentary sequence that probably represents some combination of the following: (1) northeastward migration of the basin axis; the basal arkose represents fluvial basin-margin deposits and the limestone represents lacustrine basin-interior deposits; and (2) basin enlargement; the basal arkose represents initial sedimentary deposits near the axis of a narrow sedimentary basin and the limestone represents lacustrine deposits within the interior of a much larger basin. The succession of northward- or eastward-derived clastic sedimentation, basin-axis limestone, and westward- or southward-derived clastic sedimentation indicates northeastward migration of sedimentary environments within the basin (Fig. 7). Artillery Formation sedimentation culminated with the deposition of the Artillery megabreccia, which contains metamorphosed Paleozoic and Mesozoic rocks and was almost certainly derived from a high-relief, basin-bounding fault block to the west or south.

In the central Artillery Mountains, the contrast between the lithologically diverse conglomerate, sandstone, mudstone, limestone, and sedimentary breccia of the Artillery Formation and the relatively homogeneous sandstone of the Chapin Wash Formation reflects a change in depositional environment and possibly in tectonic setting. This change may have occurred because of increased basin size or integration of drainages from several isolated basins to a single basin with through-going drainage. In either case, an areally extensive, fluvial sedimentary environment, represented by the Chapin Wash Formation, superseded much more localized, laterally variable sedimentary environments, represented by the middle and upper members of the Artillery Formation. The presence of the Chapin Wash Formation in the Rawhide and eastern Buckskin Mountains (Spencer and Reynolds, this vol.) supports the interpretation of a regionally extensive, fluvial depositional environment. In addition, the absence of megabreccia in strata above the Artillery Formation indicates that topographic relief at basin margins was reduced or that extensional faulting increased basin width and areas of high relief were farther away. In the Chapin Wash Formation, the presence of local mylonitic clasts derived from the footwall of the Buckskin-Rawhide detachment fault and the great abundance of such clasts in the overlying Sandtrap Conglomerate indicate that the Chapin Wash Formation was

Figure 7 (next page). Evolutionary cross-section diagram for the central Artillery Mountains. Section line A-A' in cross-section D is an idealized cross section through the study area and is based on data in Figures 2, 4, 5, and 6. Underlying fault geometries are interpretive and are based in part on regional tectonic considerations (Spencer and Reynolds, this vol.). Interfingering facies boundaries and lateral facies changes are shown schematically. Rotation of A-A' results from untilting the sequence to model the setting of progressively older strata. Diagrams represent the following: (1) end of deposition of lower member of Artillery Formation, (2) end of deposition of Artillery megabreccia, (3) end of deposition of Sandtrap Conglomerate, and (4) the present. See text for details.

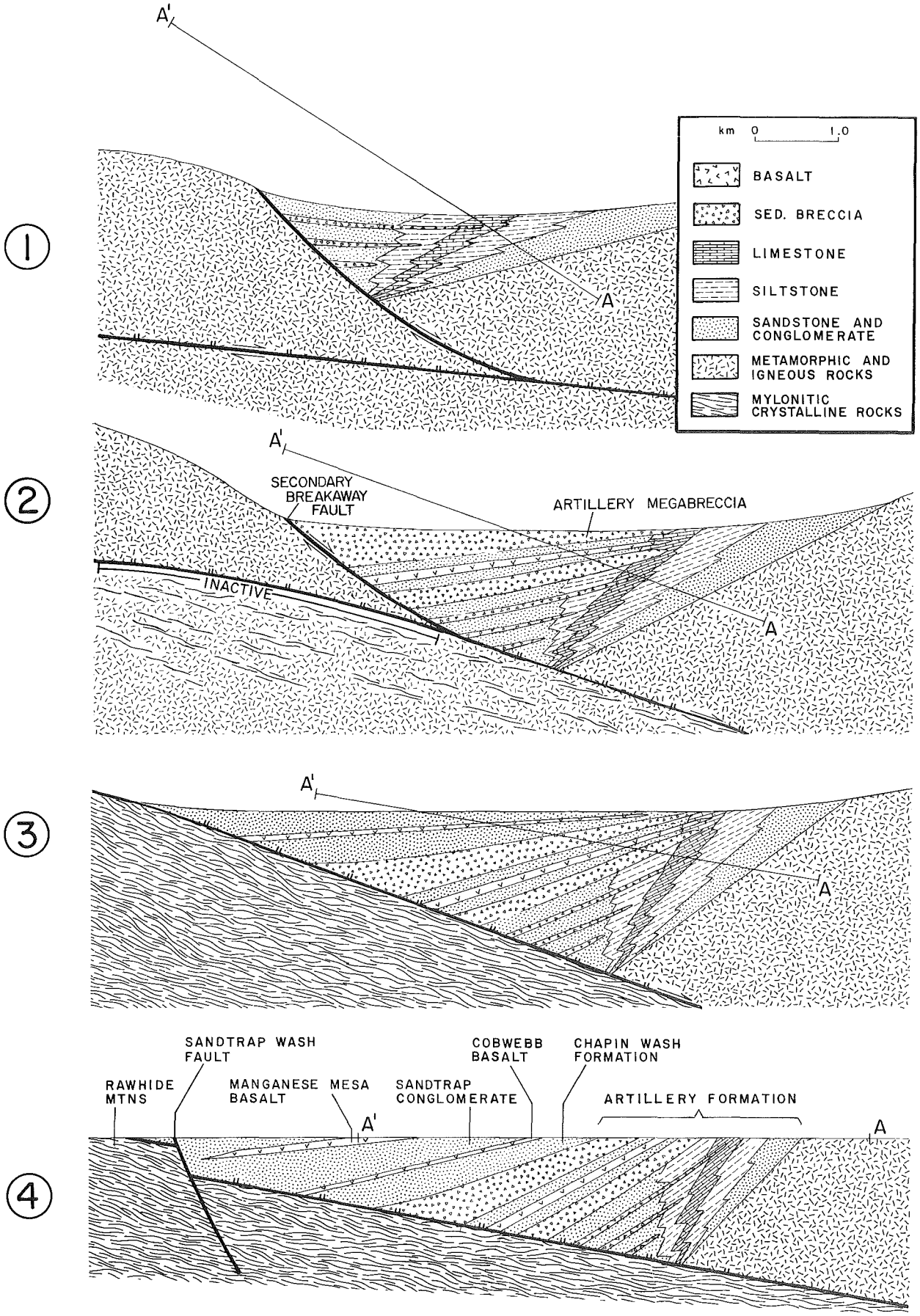
1
A'
A
km 0 1.0
BASALT
SED. BRECCIA
LIMESTONE
SILTSTONE
SANDSTONE AND CONGLOMERATE
METAMORPHIC AND IGNEOUS ROCKS
MYLONITIC CRYSTALLINE ROCKS
2
A'
SECONDARY BREAKAWAY FAULT
ARTILLERY MEGABRECCIA
INACTIVE
A
3
A'
A
4
SANDTRAP WASH FAULT
COBWEBB BASALT
CHAPIN WASH FORMATION
RAWHIDE MTNS
MANGANESE MESA BASALT
SANDTRAP CONGLOMERATE
ARTILLERY FORMATION
A'
A

deposited during exhumation and subaerial exposure of the footwall mylonites.

Miocene basin evolution in the central Artillery Mountains occurred within a broader framework of detachment faulting, tectonic denudation, and isostatic uplift of the mylonitic footwall rocks of the Buckskin and Rawhide Mountains. Stratigraphy in the study area fits within this broader framework in the following evolutionary sequence (see also Fig. 7):

(1) Strata of the lower and middle members of the Artillery Formation were deposited within a half graben formed by rotational normal faulting in the hanging wall of the regionally northeast-dipping Buckskin-Rawhide detachment fault.

(2) Deposition of the Artillery megabreccia occurred in response to accelerated fault movement on the southwest flank of the basin as the adjacent fault block to the southwest slowed or ceased movement above the Buckskin-Rawhide detachment fault. The graben-bounding fault became the *secondary breakaway fault* at approximately this time (see also Spencer, 1984b; Spencer and Reynolds, this vol.). The increased rate of movement and the development of a large, unstable fault scarp occurred as extensional strain, formerly distributed among two or more faults to the southwest, was transferred largely or entirely to this single normal fault.

(3) Rapid widening of the half-graben basin resulted in regionally extensive fluvial sedimentation that formed the Chapin Wash Formation and, as the detachment-fault footwall was uncovered, the Sandtrap Conglomerate.

MINERAL DEPOSITS

Introduction

Lasky and Webber's (1949) study of Mn deposits in the Artillery Mountains outlined the characteristics and geologic setting of many of the individual deposits in the area, most of which are hosted by the Chapin Wash Formation. Lasky and Webber recognized that most of the Mn deposits are sedimentary in origin. This evidence included friable flakes of manganiferous clay within sandstone beds and intimately interlaminated, manganiferous and nonmanganiferous clastic sedimentary rocks. Bedded manganiferous sandstone within the Chapin Wash Formation is not any more or less resistant to weathering than adjacent nonmanganiferous sandstone, supporting the inference that the Mn is detrital and not hydrothermal in this setting. The bedded Mn is discontinuously exposed in the study area in a belt extending from the east flank of Manganese Mesa (also known as Black Mesa) southeastward through Lake mine and Loves mine (Figs. 1 and 2) to the Priceless mine (Fig. 5B; Lasky and Webber, 1949). Near Lake mine, close to the center of section 33, breccia and conglomerate at the top of the Artillery megabreccia contain a hard, manganiferous matrix that is probably the "supergene enriched ore" of Lasky and Webber (1949).

Priceless and Shannon Mines

Our field observations are largely consistent with those of Lasky and Webber, but mining activity at the Priceless mine (Fig. 5B) since their study has revealed features not described by them. Within the Priceless mine pit, abundant, fracture-filling, colloform, Mn-oxide encrustations up to 1 cm thick fill northwest-striking, subvertical fractures in the Chapin Wash Formation. X-ray diffraction analysis indicates that the manganese-oxide encrustations are composed of ramsdellite and cryptomelane (see also Mouat, 1962). Cobwebb Basalt exposed at the southern edge of the pit and just southeast of the pit (Fig. 5B) is similarly mineralized, indicating that major Mn mineralization occurred after eruption of the basalt.

At the Shannon mine, the Sandtrap Conglomerate hosts fracture-filling and disseminated Mn oxides along an east-northeast-trending zone that is possibly a shear zone (Fig. 5A). Unlike Mn deposits at the Priceless mine, the Shannon deposit contains abundant black and white calcite that form crystals up to 2 cm in diameter. Approximately 1 km north of the Shannon mine, a northwest-trending, northeast-dipping reverse fault that cuts Sandtrap Conglomerate and interbedded Manganese Mesa basalt contains Mn oxides and sparse barite (Fig. 5A).

Fluid-Inclusion Data

Fluid inclusions in gangue minerals and nonmanganiferous veins were studied to determine the temperatures and salinities of mineralizing aqueous solutions. An effort was made to use only primary fluid inclusions for salinity and temperature determinations; however, the well-developed cleavage and later Mn mineralization in barite and calcite made it difficult to distinguish primary from secondary fluid inclusions under the microscope. If more than one generation of inclusions are present, it is not apparent in salinity data, which are not bimodal for any of the samples. The homogenization temperatures have not been corrected for pressure. Such a correction would be small because of the inferred shallow depths of mineralization. Evidence of boiling was not seen in any of the samples.

At the Priceless mine, very sparse chalcedonic quartz is associated with fracture-filling Mn oxides. In one polished thick section, microcrystalline quartz and chalcedony are gradational into younger, euhedral, finely crystalline quartz. Exposed faces of euhedral, open-space-filling quartz crystals are coated with amorphous, opaque Mn oxides, and some quartz crystals appear to be surrounded by Mn oxides. The quartz contains sparse primary two-phase fluid inclusions, which contain 1 to 2 wt. % NaCl equivalent and have homogenization temperatures of approximately 165°C to 170°C. A several-meter-thick barite vein exposed along the road several hundred meters northwest of the Priceless mine strikes toward the mine and has the same orientation as Mn-filled fractures at the mine. A genetic relationship between the barite vein and the Mn deposit at the Priceless mine is

supported by the similarity of fluid-inclusion salinities at both deposits (Fig. 8, samples PM-1 and 12-15-87-4).

Calcite and barite are associated with Mn deposits in the Shannon mine area (Fig. 5A). Calcite from the Shannon mine (sample SM-1) and barite from a mineralized fault north of the Shannon mine (sample SM-3) formed earlier than the Mn oxides that fill interstices and cleavage-plane fractures. Fine sprays of acicular pyrolusite are identifiable in some cleavage-plane fractures. Fluid-inclusion salinities vary from approximately 0 to 3 wt. % NaCl equivalent (Fig. 8).

A barite vein not associated with a Mn deposit is present along a fault that juxtaposes the Chapin Wash Formation with Artillery megabreccia. Polished thick sections from a sample of this vein (sample 12-16-87-2 in Figs. 2 and 8) reveal blocky barite crystals that are broken or shattered and fluid inclusions in younger fluorite crystals that contain 7 to 11 wt. % NaCl equivalent (Fig. 8). Homogenization temperatures from fluid inclusions in the fluorite fall within two ranges: 140°C to 170°C and 280°C to 315°C (Fig. 9). The contrast in salinities between this barite vein and Mn-calcite-barite deposits elsewhere suggests that the two are not related.

Relationship to Detachment Faults

Numerous Cu-Fe mineral deposits in the Buckskin and Rawhide Mountains are present along and adjacent to the Buckskin-Rawhide detachment fault (Wilkins and Heidrick, 1982; Wilkins and others, 1986; Spencer and Welty, 1986, this vol.). Spencer and Welty (1986)

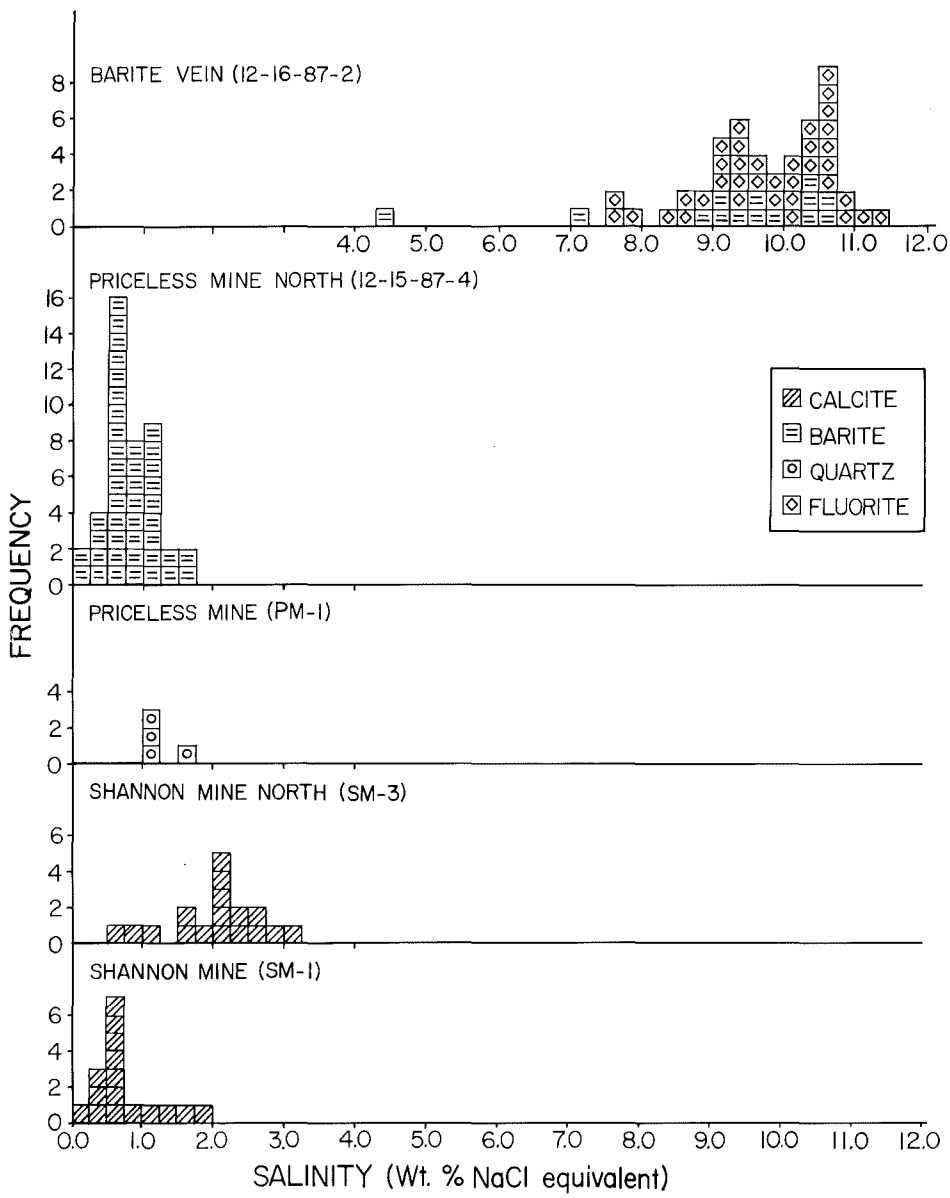

Figure 8. Salinity versus frequency histogram for fluid inclusions from selected Mn deposits and barite veins in the central Artillery Mountains.

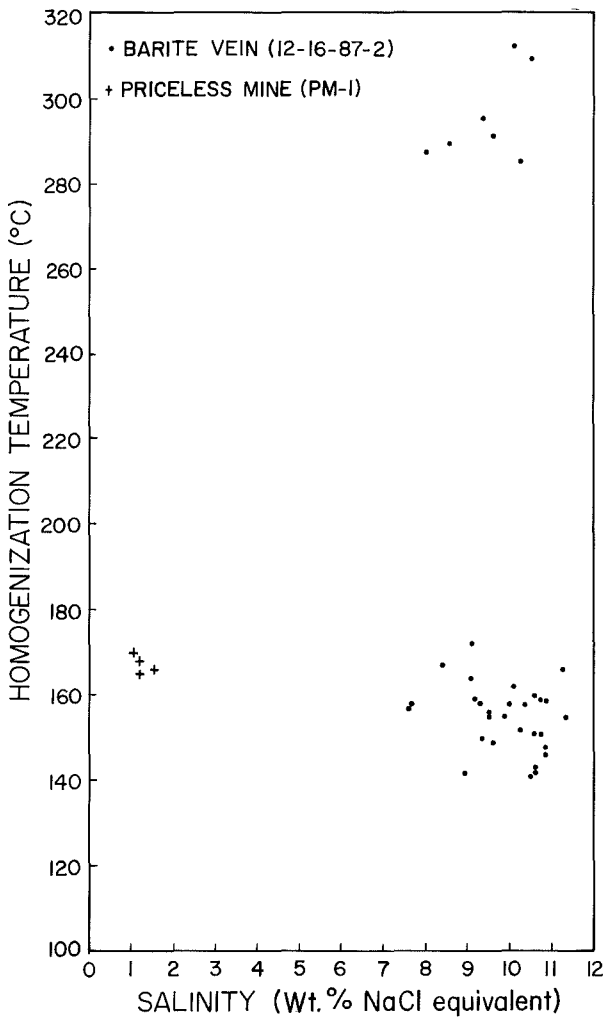

Figure 9. Salinity versus homogenization-temperature diagram for fluid inclusions in fluorite from barite-vein sample no. 12-16-87-2 and in quartz from the Priceless mine.

proposed that hydrothermal solutions, ascending along detachment faults and causing Cu-Fe mineralization, eventually reached surface or near-surface levels with greatly increased Mn:Fe ratios. Mn deposits, such as those in the Artillery Mountains, were thought to have formed from hydrothermal fluids that originally contained both Fe and Mn, subsequently lost most of the Fe in detachment-fault-related deposits, and carried Mn-rich solutions to sites of Mn mineralization in the hanging walls of detachment faults. Fluid inclusions from detachment-fault-related deposits contain approximately 12 to 22 wt. % NaCl equivalent (Wilkins and others, 1986; Roddy and others, 1988). Fluid-inclusion data from the Shannon and Priceless deposits indicate that Mn and associated calcite, barite, fluorite, and quartz formed from fluids that had salinities of less than 3 wt. % NaCl equivalent. Thus, Mn mineralization in the young fracture-filling deposits was not related in any simple manner to detachment-fault-related mineralization; in fact, the two may not have been related at all.

Mineralization at the Shannon and Priceless mines is younger than the Cobwebb Basalt and thus is younger than the volumetrically more significant sedimentary Mn deposits within the Chapin Wash Formation. It is not known if the sedimentary Mn deposits in the Chapin Wash Formation were also derived from low-salinity fluids or from high-salinity fluids that caused Cu-Fe mineralization at depth along the Buckskin-Rawhide detachment fault.

ACKNOWLEDGMENTS

We thank Jim Otton and Bob Miller of the USGS for unpublished data on the geology of the Artillery Mountains and Randy Koski of the USGS for informative discussions concerning the manganese deposits.

APPENDIX 1. MAP UNIT DESCRIPTIONS

Qs **SURFICIAL DEPOSITS (Quaternary)** -- Unconsolidated to weakly consolidated sandstone, conglomeratic sandstone, and conglomerate. Includes talus and unconsolidated sand in modern washes.

Tbm **MANGANESE MESA BASALT (Miocene)** -- Gently southwest-dipping basalt flows that form the top of Manganese Mesa (also known as Black Mesa). Includes Sandtrap basalt of Lasky and Webber (1949).

Tbmp **PYROCLASTIC ROCKS BENEATH BLACK MESA BASALT (Miocene)** -- Tan volcaniclastic sandstone composed of planar and planar cross-bedded beds greater than 1 m thick. Possibly a pyroclastic surge deposit.

Tsc **SANDTRAP CONGLOMERATE (Miocene)** -- Tan to locally reddish-tan consolidated conglomerate, conglomeratic sandstone, and local sandstone and siltstone, named Sandtrap Conglomerate by Lasky and Webber (1949). Unit forms rounded outcrops, in some areas with massive appearance, and varies from matrix-supported conglomerate to stratified, clast-supported gravel that resembles Quaternary fanglomerates. Clasts include a variety of Proterozoic(?) crystalline rocks, Paleozoic(?) carbonates,

Jurassic(?) metavolcanics, quartzite, Tertiary volcanics, Tertiary sandstone, and mylonitic crystalline rocks. Mylonitic, crystalline rock fragments are variably overprinted by chloritic alteration and fracture-filling chlorite and epidote and were almost certainly derived from the footwall of the Buckskin-Rawhide detachment fault. A siltstone facies south of Lake mine is interpreted as having been deposited in a small playa between northeast-prograding alluvial fans that form the bulk of the Sandtrap Conglomerate and a southwest-tilted dipslope at the top of the underlying Cobwebb Basalt.

Tcb **COBWEBB BASALT (Miocene)** -- Generally aphanitic, nonvesicular to slightly vesicular, discontinuous basalt flows named Cobwebb Basalt by Lasky and Webber (1949).

Tcw **CHAPIN WASH FORMATION (Miocene)** -- Tan, brown, red, and brick-red sandstone and local conglomerate, conglomeratic sandstone, and siltstone. Sandstone is locally calcareous and silicified. Manganiferous sandstone near middle of unit northwest of Cobwebb Hill (section 29) marks an upward color transition from red to tan sandstone. Zone of manganiferous sandstone thickens southeastward from section 29 toward Lake mine (section 33). Mylonitic clasts at Cobwebb Hill were possibly derived from the detachment-fault footwall in the Rawhide Mountains. This unit was named the Chapin Wash Formation by Lasky and Webber (1949).

Tcwm **MANGANIFEROUS CHAPIN WASH FORMATION (Miocene)** -- Black to brownish- or reddish-black, manganiferous sandstone beds that form a manganiferous zone up to several tens of meters thick.

Tuc **UPPER CONGLOMERATE (Miocene)** -- Brown, brownish-red, to brick-red conglomerate at top of Artillery Formation of Lasky and Webber (1949). Composed of mixed, angular, subrounded, and locally well-rounded clasts, typically 5 to 50 cm in diameter but locally up to 100 cm in diameter, of coarse-grained megacrystic granite, foliated granite, and sparse migmatitic gneiss in a poorly sorted arkosic matrix. Many angular clasts of crystalline rock resemble most of the underlying Artillery megabreccia and were probably derived from it.

Txg **ARTILLERY MEGABRECCIA, GRANITIC PROTOLITH (Miocene)** -- Megacrystic biotite granite of probable Proterozoic age, sparse mylonitic megacrystic biotite granite, and pink, fine-grained leucocratic granite. Grades from highly shattered, clast-supported megabreccia to slightly fractured, resistant, cliff-forming outcrops that are no more fractured than typical outcrops of structurally coherent bedrock crystalline rock. Basal contact is well exposed at south edge of SE$^1/_4$ sec. 28, where an approximately 50-m-thick ledge of massive, structurally coherent, fine-grained granite is juxtaposed with underlying conglomeratic sandstone along a cryptic, several-millimeter-thick planar contact. Pebbles directly below the thin contact zone are unbroken, and there are no lineations along the contact. Beds in the underlying unit are truncated at the contact.

Txm **ARTILLERY MEGABRECCIA, JURASSIC METAVOLCANIC PROTOLITH (Miocene)** -- Foliated to massive, gray to greenish-gray to brown, metavolcanic rocks virtually identical to the Jurassic Planet Volcanics in the Buckskin Mountains (Plate 2). Varies from structurally coherent and unshattered (east edge of section 28) to highly shattered, clast-supported breccia.

Txs **ARTILLERY MEGABRECCIA, MESOZOIC SCHIST PROTOLITH (Miocene)**--Quartz-sericite-chlorite schist in structurally coherent mass at west side of section 28.

Txq **ARTILLERY MEGABRECCIA, QUARTZITE PROTOLITH (Miocene)** -- Pure, white, highly shattered quartzite with red, silicified matrix.

Txc **ARTILLERY MEGABRECCIA, PALEOZOIC(?) CARBONATE PROTOLITH (Miocene)** -- Medium- to light-gray to dusty white, medium-grained calcite marble with no chert nodules or siliceous stringers.

Tsp **SANDSTONE AND PEBBLY SANDSTONE (Miocene)** -- Nonresistant, light-red or buff-colored, thick-bedded to massive, generally medium-grained, well-sorted arkosic sandstone with subordinate lenses of pebbly sandstone.

Tb **BASALT FLOWS (Miocene)** -- Dark-gray, weakly resistant, amygdaloidal flows of two-pyroxene-olivine-phyric, plagioclase-microphyric basalt. Poorly sorted tuff breccia with clasts of basaltic rocks is exposed around the periphery of the oldest flow in NW$^1/_4$ SW$^1/_4$ sec. 27. This same flow is associated with a 40-m-wide zone of locally

intense folding of adjacent siltstones and mudstones (map unit Tcm) on its northern contact. A 2- to 3-m-thick younger flow is interbedded with the bedded sandstones of map unit Ts_4. Phenocrysts of olivine (up to 10% of the rock) are completely replaced by iddingsite, whereas the less abundant pyroxene phenocrysts are only slightly altered. In SE$^1/_4$ sec. 27, the unit is a dark-colored, moderately resistant, aphyric to quartz-plagioclase-pyroxene-phyric, mafic to intermediate flow with a basal flow breccia. Thickness is as great as 80 m.

SANDSTONE AND MUDSTONE UNIT (Miocene) -- A sequence of sandstone and mudstone in the northwestern part of the map area (primarily section 28) is divisible into four map units. Each of two fining-upward sequences (Ts_1-Ts_2 and Ts_3-Ts_4) consists of a coarse-grained, thickly bedded to massive lower portion and a finer grained, silty, more thinly bedded upper portion locally including calcareous muds. The lower sequence is underlain by or includes a basal section of matrix-supported conglomerates that are interpreted as debris flows and are spectacularly exposed in NW$^1/_4$ sec. 28. This unit is as much as 300 m thick and is composed of the following members:

Ts_4 **SANDSTONE AND MUDSTONE UNIT, UPPER MUDSTONE MEMBER** -- Thinly bedded to medium-bedded, well-sorted siltstone and fine-grained sandstone.

Ts_3 **SANDSTONE AND MUDSTONE UNIT, UPPER SANDSTONE MEMBER** -- Thickly bedded to massive, well-sorted, coarse- to medium-grained sandstone with local pebble stringers. Plane beds are the dominant bedform. Rip-up clasts of underlying calcareous mudstone and other pebble-sized clasts are present in the basal bed of the member.

Ts_2 **SANDSTONE AND MUDSTONE UNIT, LOWER MUDSTONE MEMBER** -- Thinly bedded to medium-bedded, well-sorted, variably and locally calcareous siltstone and fine-grained sandstone. Ripple cross-laminations are present near the top of the member. Micaceous sandstone is more abundant than in the underlying member.

Ts_1 **SANDSTONE AND MUDSTONE UNIT, LOWER SANDSTONE MEMBER** -- Thickly bedded to massive, poorly sorted to well-sorted, coarse-grained sandstone, and matrix-supported sandy conglomerate. Locally clast-supported with a weakly developed imbrication. Bed thickness and grain size decrease up section.

Txv **MEGABRECCIA, JURASSIC METAVOLCANIC PROTOLITH (Miocene)** -- Dark-green-weathering, moderately resistant, tabular bodies of massive, brecciated metavolcanic rocks of Jurassic age. These sheets of monolithologic breccia apparently have a scoop-shaped lower contact, and steep, sharp marginal contacts with intensely folded limestones (map unit Tl and Tlm) and pebbly conglomerates and mudstones (map units Tc and Tcm) within a few tens of meters of the contact. It is not clear how much of the folding occurred during megabreccia emplacement and how much occurred later because of tectonic activity. This clast-supported breccia contains little or no matrix and clasts fit tightly together. Clasts contain medium-sized, subhedral phenocrysts of quartz and two(?) feldspars in an aphanitic groundmass. Unit may locally include debris flows.

Txt **MEGABRECCIA, JURASSIC ASH-FLOW TUFF PROTOLITH (Miocene)** -- Light-gray, moderately resistant, tabular bodies of Jurassic quartz-feldspar-phyric, ash-flow tuff, metamorphosed to lower greenschist grade. Conspicuous quartz phenocrysts, up to 5 mm in diameter, and color distinguish this map unit from the otherwise similar unit Txv. This unit is associated with a mixed zone along its southeastern periphery exposed in NE$^1/_4$ sec. 27 (map unit Tx). Fiamme and flattened lithic fragments distinguishable in some clasts are indicative of the ash-flow origin of the protolith. Unit may locally include debris flows.

Tx **MIXED BRECCIA OF METAMORPHOSED ROCKS AND TERTIARY LIMESTONE (Miocene)** -- Nonresistant, mixed zones consisting of clasts of metamorphosed ash-flow tuff in a matrix of limy mud derived from map unit Tl. Clasts of the Jurassic(?) rocks range from 2 to 10 mm in diameter. The mixed zone locally includes intensely deformed, thinly bedded mudstones similar to those in nearby exposures of map unit Tl. Unit may locally include debris flows.

Tcm **CONGLOMERATE AND MUDSTONE (Miocene)** -- Weakly resistant, interbedded limestone, calcareous mudstone, and brown pebbly sandstone. Limestone beds are mesoscopically similar to those of map unit Tl and are typically 1 m or less thick, whereas the brown pebbly sandstone beds form packages on the order of 3 to 4 m thick. Contacts between different types of beds are sharp.

Tc **CONGLOMERATE (Miocene)** -- Dark-brown, weakly resistant, interbedded pebbly sandstone and sparse sandstone and siltstone. The unit is typically poorly bedded, with individual beds defined by gradational variations in grain size. Most clasts are angular to subangular and consist of quartzite of uncertain affinity.

Tlm **LIMESTONE AND MUDSTONE (Miocene)**-- Light-gray and green, weakly resistant, thinly bedded to laminated mudstone, calcareous mudstone, and siltstone. Unit is strongly folded in exposures in $N^1/_2$ sec. 28, where some folds have wavelengths of as little as a few centimeters.

Tl **LIMESTONE (Miocene)** -- Light-tan to gray, resistant, thickly bedded to massive limestone that is commonly folded, with fold wavelengths larger than 10 m. Translucent, lens-shaped, siliceous zones and nodules form replacements of calcareous algal mats and contain well-preserved gastropod fossils. Lower portion of this unit is silty and thinly bedded. Large blocks or tongue-shaped bodies of brecciated Mesozoic schist and metavolcanic rock are present at several, widely separated locations. Stratigraphic thickness is estimated at approximately 180 m. Folding has resulted in structural thickening of the unit to more than 350 m in the northwest portion of the map area.

Ts **SANDSTONE (Miocene)** -- Tan, fine-grained, thinly bedded to laminated sandstone and subordinate siltstone and calcareous siltstone. Rocks of this unit are interbedded with limestone within a few meters of the contact with unit Tl.

Tmsl **MUDSTONE, SANDSTONE, AND LIMESTONE (Miocene)** -- Green, thin-bedded to laminated, well-sorted sandstone, mudstone, and limestone. Mudstones are rhythmically interbedded with the fine-grained sandstones; each bedset is between 30 cm and 120 cm thick. Beds locally contain mudcracks. Unit contains two beds of pink, moderately resistant, biotite-feldspar-phyric tuff containing less than 3% phenocrysts. Both beds are interpreted as lithified and altered air-fall tuffs based on thin-section examination that reveals devitrified, undeformed glass shards.

Ta **BASAL ARKOSE (Miocene)** -- Conglomerate, conglomeratic sandstone, and sandstone. Dotted line within map unit divides an upper assemblage of dark-brown, weakly resistant, bedded, moderately sorted, arkose and pebbly arkose containing clasts of Proterozoic crystalline rocks from an underlying assemblage of medium-brown, weakly resistant, massive to poorly bedded arkose, conglomeratic arkose, conglomerate, and debris flows(?) derived from Proterozoic crystalline rocks. Both upper and lower assemblages thicken to the southeast; within the map area, they reach maximum thicknesses of approximately 70 m and 180 m, respectively. This map unit forms a broadly fining-upward package that rests disconformably on Proterozoic crystalline rocks.

XYc **QUARTZO - FELDSPATHIC CRYSTALLINE ROCKS (Proterozoic X and Y[?])** -- Schist, gneiss, and foliated and unfoliated granitic rocks.

K-Ar geochronology of Miocene extension, volcanism, and potassium metasomatism in the Buckskin and Rawhide Mountains*

JON E. SPENCER *Arizona Geological Survey, 845 N. Park Ave., #100, Tucson, Arizona 85719*
M. SHAFIQULLAH *Laboratory of Isotope Geochemistry, Department of Geosciences, University of Arizona, Tucson, Arizona 85721*

ROBERT J. MILLER
LEDABETH G. PICKTHORN
U.S. Geological Survey, 345 Middlefield Rd., Menlo Park, California 94025

ABSTRACT

Nineteen conventional K-Ar dates from the Buckskin and Rawhide Mountains clarify the timing of Miocene extension, volcanism, and K metasomatism. Two samples of mylonitic crystalline rock from the lower plate of the Buckskin-Rawhide detachment fault yielded biotite K-Ar dates of approximately 15 Ma. These dates are interpreted as a record of the time when the temperature of lower-plate rocks decreased to below approximately 310° to 345° C. This cooling was probably due to tectonic denudation and isostatic uplift. Feldspar concentrates from nine samples of K-metasomatized mafic flows and flow breccias, interbedded with upper-plate Tertiary sedimentary rocks, yielded K-Ar dates between 15.5 and 20.5 Ma, which is broadly interpreted as the time of K metasomatism and a minimum age for the mafic flows. A biotite-feldspar pair from a tuff stratigraphically below the K-metasomatized mafic flows yielded dates of 22 and 20 Ma, respectively. The biotite date of 22 Ma is interpreted as the approximate age of the tuff and provides an older limit to the age of the mafic flows. Plagioclase K-Ar dates of 16.2 and 15.5 Ma from a tilted, nonmetasomatized basalt on the north side of the Bill Williams River near the northwestern Buckskin Mountains indicate that tilting occurred after this time. Two K-Ar dates from a flat-lying basalt in the western Rawhide Mountains indicate that tilting associated with detachment faulting in this area ended by 12 Ma.

INTRODUCTION

The nature and age of tectonic, magmatic, thermal, and geochemical phenomena that affected rocks exposed in the Buckskin and Rawhide Mountains can be clarified by application of conventional K-Ar geochronologic techniques. Large-magnitude displacement on the Buckskin-Rawhide detachment fault resulted in pervasive faulting and tilting of upper-plate rocks and in isostatic uplift and rapid cooling of lower-plate crystalline rocks. Magmatism during this time produced intrusions in the lower plate and widely distributed, upper-plate volcanic flows and tuffs. Basin formation during extension resulted in sediment accumulation and development of conditions favorable for K metasomatism. K-Ar data reported here indicate that these phenomena were broadly synchronous and occurred over a several-million-year period in Miocene time.

This K-Ar study is restricted to the Buckskin Mountains and directly adjacent areas. The locations of all samples, except postdetachment basalt sample no. 11-4-86-8, are plotted in figures in Spencer and Reynolds (this vol.), Grubensky (this vol.), and on Plate 2. Analytical data are presented in Tables 1 and 2.

LOWER-PLATE ROCKS

Variably mylonitic, lower-plate crystalline rocks in the Buckskin and Rawhide Mountains contain little biotite because of the pervasive retrograde metamorphism at high structural levels and the biotite-poor composition of mainly felsic protolith rocks. Rocks that contain unaltered biotite are locally present in areas deeply cut by erosion.

Two samples, which were collected from the deeply eroded parts of the lower plate, yielded K-Ar biotite dates of 15.1 ± 0.2 and 14.8 ± 0.2 Ma (Table 1). Sample no. 2-7-85-1 was collected from a canyon in the incised hanging-wall block of the Lincoln Ranch reverse fault in the eastern Buckskin Mountains (Fig. 38, Spencer and Reynolds, this vol.), approximately 200 m structurally below the projection of the Buckskin-Rawhide detachment fault. Sample no. 12-5-84-1 was collected from a canyon that cuts across the Clara Peak antiform in the central Buckskin Mountains (Fig. 9, Spencer and Reynolds, this vol.), approximately 150 m structurally below the projection of the Buckskin-Rawhide detachment fault. Rocks at both sampling localities are weakly to moderately

* This report has not been reviewed for conformity with U.S. Geological Survey editorial standards or stratigraphic nomenclature.

in Spencer, J.E., and Reynolds, S.J., eds., 1989, Geology and mineral resources of the Buckskin and Rawhide Mountains, west-central Arizona: Arizona Geological Survey Bulletin 198, p. 184-189.

Table 1. K-Ar geochronologic data from non-K-metasomatized rocks in the Buckskin and Rawhide Mountains. Date calculation is based on decay and abundance constants from Steiger and Jaeger (1977). Error in calculated date is determined by method of Cox and Dalrymple (1967), which assumes standard deviation of 0.3% for tracer calibration. K was measured by flame photometry with a lithium internal standard. Error in K analysis is either sample standard deviation of K analyses or 0.5%, whichever is greater. Multiple laboratory sample numbers indicate multiple Ar extractions. Single laboratory sample numbers with multiple $^{40}Ar_{rad}$ indicate multiple analyses of Ar from a single Ar extraction.

Field Sample Number	Date(m.y.)	Material Dated	Rock Type	%K	$^{40}Ar_{rad}$ mol/gm($\times 10^{-11}$)	$\%Ar_{rad}$	Lat.(N)	Lon.(W)	Lab Sample Number(Ar)	Lab(Ar)	Lab(K)	Argon Analyst
LOWER-PLATE ROCKS												
LINCOLN RANCH BASIN												
2-7-85-1	15.1±0.2	biotite	mylonitic	6.4275	16.8076	46.8	34°10.75'	113°37.92'	851485	USGS	UA	JES
			gneiss	6.3652	16.8538	49.0			851497	"	"	"
				6.3718								
CLARA PEAK - SWANSEA MINE AREA												
12-5-84-1A	15.1±0.2	biotite	mylonitic	4.8765	12.8455	40.2	34°09.55'	113°49.82'	851489	USGS	UA	JES
	14.6±0.2	with 10%	gneiss	4.8853	12.4294	39.8			851498	"	"	"
		chlorite		4.8782								
12-5-84-1B	14.5±0.3	biotite	mylonitic	3.7804	9.73808	43.0	"	"	851492	"	"	"
	14.4±0.3	with 20-25%	gneiss	3.8853	9.69160	32.3			851499	"	"	"
		chlorite		3.8955							"	
UPPER-PLATE ROCKS												
SWANSEA-COPPER PENNY AREA												
12-14-85-7	20.3±0.4	feldspar	Tertiary	3.245	11.59	86.5	34°09.99'	113°53.45'	UAKA86-06	UA	UA	MS
			tuff	3.256	11.48	86.2			"	"	"	"
				3.262	11.47	86.0			"	"	"	"
				3.228							"	
12-14-85-7	21.8±0.5	biotite	Tertiary	5.578	2.108	70.1	"	"	UAKA86-06	"	"	"
			tuff	5.552	2.098	70.7			"	"	"	"
				5.491	2.107	69.7			"	"	"	"
				5.550	2.104	70.2					"	
SOUTHEASTERN BILL WILLIAMS MOUNTAINS												
12-2-86-4	16.2±0.5	plagioclase	basalt(?)	.8468	2.3834	38.4	34°16.01'	114°00.37'	871173	USGS	USGS	RJM
			flow	.8385					"		"	
12-2-86-5	15.5±0.7	plagioclase	basalt(?)	.8717	2.31153	28.5	34°16.01'	114°00.48'	871174	USGS	USGS	RJM
			flow	.8385					"		"	
POST-DETACHMENT ROCKS												
SOUTHWESTERN BUCKSKIN MOUNTAINS (SOUTH FLANK OF THE MESA)												
BPG-106	10.5±0.2	sanidine	Tertiary	5.247	9.559	93.9	34°07.60'	114°06.45'	UAKA87-10	UA	UA	MS
			rhyolite	5.251	9.556	94.0			"	"	"	"
				5.247	9.525	94.0			"	"	"	"
					9.555	94.1			"	"		"
BPG-106	10.5±0.3	feldspar	Tertiary	3.740	7.016	75.8	34°07.60'	114°06.45'	UAKA87-10	UA	UA	MS
		concentrate	rhyolite	3.785	6.756	72.6			"	"	"	"
				3.722	6.908	76.5			"	"	"	"
				3.758	6.809	76.9			"	"	"	"
				3.774	6.912	74.7			"	"	"	"
					6.989	74.4			"	"		"
					6.710	75.3			"	"		"
WESTERN RAWHIDE MOUNTAINS												
11-4-86-8	11.6±0.3	feldspar	basalt	1.060	2.128	47.7	34°16.94'	113°50.14'	UAK87-282	UA	UA	MS
		concentrate		1.066	2.158	47.1			"	"	"	"
				1.067	2.148	48.4			"	"	"	"

Table 2. K-Ar geochronologic data from K-metasomatized rocks in the Buckskin Mountains. Geochronologic calculations and lab procedures are the same as reported in caption for Table 1. Sample no. 12-15-85-2 from the Lincoln Ranch basin was analyzed by two laboratories; the weighted average of both dates is 20.2 ± 0.9 Ma.

Field Sample Number	Date(m.y.)	Material Dated	Rock Type	%K	$^{40}Ar_{rad}$ mol/gm($\times 10^{-11}$)	$\%Ar_{rad}$	Lat.(N)	Lon.(W)	Lab Sample Number(Ar)	Lab(Ar)	Lab(K)	Argon Analyst
LINCOLN RANCH BASIN												
12-15-85-1	15.8±0.5	feldspar	Tertiary	12.41	34.64	62.1	34°09.54'	113°40.06'	861529	USGS	USGS	LBGP
		concentrate	volcanic	12.36	33.61	61.4			861442	"	"	"
			flow									
12-15-85-2	20.7±0.5	feldspar	Tertiary	2.712	9.811	88.8	34°09.88'	113°40.60'	UAKA86-09	UA	UA	MS
		concentrate	volcanic	2.674	9.729	88.1			"	"	"	"
			flow	2.719	9.706	88.3			"	"	"	"
				2.704	9.754	88.4			"	"	"	"
12-15-85-2	19.4±0.6	feldspar	Tertiary	2.79	9.535	69.0	34°09.88'	113°40.60'	861530	USGS	USGS	LBGP
		concentrate	volcanic	2.77	9.271	67.1			861443	"	"	"
			flow									
12-19-86-3	16.1±0.4	feldspar	Tertiary	10.01	28.42	84.9	34°11.19'	113°39.08'	UAKA87-9	UA	UA	MS
		concentrate	volcanic	10.21	28.51	85.4			"	"	"	"
			flow	10.17	28.38	85.3			"	"	"	"
				9.98	28.19	84.8			"	"	"	"
				10.12							"	
SWANSEA-COPPER PENNY AREA												
12-14-85-8	20.1±0.5	feldspar	Tertiary	9.574	33.58	80.7	34°09.31'	113°52.81'	UAKA86-07	UA	UA	MS
		concentrate	volcanic	9.734	34.16	81.0			"	"	"	"
			flow	9.638	34.01	81.4			"	"	"	"
				9.654	34.13	80.9			"	"	"	"
				9.649							"	
PLANET-MINERAL HILL AREA												
12-13-85-4	17.6±0.4	feldspar	Tertiary	4.568	13.98	88.1	34°13.44'	113°58.82'	UAKA86-04	UA	UA	MS
		concentrate	volcanic	4.504	13.77	88.6			"	"	"	"
			flow	4.640	13.94	88.1			"	"	"	"
				4.491							"	
				4.500							"	
12-13-85-5	18.5±0.4	feldspar	Tertiary	9.890	31.88	93.6	34°13.52'	113°58.92'	UAKA86-05	UA	UA	MS
		concentrate	volcanic	9.948	31.97	91.5			"	"	"	"
			flow	9.949	32.40	91.7			"	"	"	"
12-4-86-2	16.8±0.3	feldspar	Tertiary	9.397	27.51	76.4	34°14.98'	114°00.39'	871187	USGS	USGS	RJM
		concentrate	volcanic	9.414							"	
			flow									
UPPER OSBORNE WASH												
12-14-85-1	16.1±0.3	feldspar	Tertiary	4.733	13.22	80.6	34°09.35'	114°03.66'	861477	USGS	UA	RJM
		concentrate	volcanic	4.730							"	
			flow	4.698							"	
				4.720							USGS	
12-14-85-2	15.8±0.3	feldspar	Tertiary	11.03	30.29	77.8	34°09.83'	114°03.76'	861477	USGS	UA	RJM
		concentrate	volcanic	11.00							"	
			flow	11.04							"	
				11.02							USGS	

mylonitic, biotite-bearing, foliated gneiss (2-7-85-1) and granite (12-5-84-1).

Biotite in sample no. 12-5-84-1 was intergrown with chlorite; the two minerals could not be completely separated. To evaluate the effect of the chlorite on the K-Ar systematics of the sample, the biotite-chlorite mineral separate was split into low- and high-chlorite fractions of approximately 10% and 20 to 25% chlorite, respectively. Two Ar extractions were done on each fraction. The fractions yielded approximately identical ages; thus chlorite contamination of biotite did not significantly affect biotite K-Ar systematics in this sample. The weighted-average date, calculated by the method of Long and Rippeteau (1974), for the four Ar extractions is 14.8 ± 0.3 Ma.

Based on lithology, protolith rock types at both sampling localities are interpreted as pre-middle Tertiary in age. These rocks are lithologically dissimilar to lower-plate rocks of known or suspected middle Tertiary age and lithologically similar to pre-middle Tertiary rocks elsewhere in west-central Arizona. Bryant and Wooden (this vol.), however, suggest that rocks in the area of

sample no. 12-5-84-1 are of Tertiary age, based on preliminary geochronologic data. If the Tertiary intrusions are substantially older than 15 Ma, or if they do not compose a significant volume of the footwall rocks near the sampling localities, then the two K-Ar dates from lower-plate rocks discussed herein reflect cooling unrelated to an immediately postmagmatic cooling event.

Mylonitization of lower-plate rocks in metamorphic core complexes was due to ductile shearing along the downdip projection of detachment faults (Wernicke, 1981; Davis, G.H., 1983; Reynolds, 1985; Davis, G.A., and others, 1986). Low-angle extensional deformation of this type resulted in progressive tectonic denudation and isostatic uplift of the lower plate (Howard and others, 1982; Spencer, 1984). If the initial temperature was hot enough, the lower plate would have cooled through the closure-temperature isotherm for Ar in biotite during uplift. The two middle Miocene biotite K-Ar dates discussed above are thought to represent the time of cooling through the approximate 310° to 345° C closure-temperature isotherm for Ar in biotite (closure temperatures are for cooling rates of 10 °C/Ma to 100 °C/Ma, respectively; Harrison and others, 1985). Other fission-track (Bryant and Naeser, 1987) and $^{40}Ar/^{39}Ar$ (Fryxell and others, 1987a) geochronologic data are generally consistent with this interpretation.

UPPER-PLATE ROCKS

Most of the Tertiary volcanic rocks that were faulted and tilted by movement along and above the Buckskin-Rawhide detachment fault have undergone K metasomatism. Conventional K-Ar dating generally cannot determine the age of protolith volcanic rocks when large secondary additions of K have occurred, but in rocks that have been severely K metasomatized, such dating can determine the approximate age of K metasomatism. The age of Tertiary volcanic rocks in the Buckskin Mountains that were not K metasomatized can be approximately determined by the K-Ar method.

Volcanic Rocks Not Significantly Affected by K Metasomatism

A sample of ash-flow tuff from the lower part of the Tertiary stratigraphic section in the Copper Penny mine area of the central Buckskin Mountains yielded K-Ar dates of 20.3 ± 0.4 Ma (feldspar) and 21.8 ± 0.5 Ma (biotite; Table 1). A biotite K-Ar date of 27.3 ± 1.1 Ma (Wilkins and Heidrick, 1982) was derived from the same unit; however, the agreement of dates yielded by the biotite-feldspar pair supports the interpretation that the age of the tuff is closer to 22 Ma.

Mafic flows are interbedded with conglomerate along Cave Wash in the southeastern Bill Williams Mountains. The moderately tilted conglomerate, referred to informally as the conglomerate of Cave Wash (Plate 2), contains abundant well-rounded cobbles and boulders of Proterozoic crystalline rock. A similar conglomerate near Tunnel Peak (Plate 2) rests unconformably on the widely exposed tilted section of sandstone, conglomerate, mafic flows, and sedimentary breccia in the Tunnel Peak area. Plagioclase from two samples of basalt yielded K-Ar dates of 16.2 ± 0.5 Ma and 15.5 ± 0.7 Ma. This basalt did not undergo K metasomatism. These K-Ar dates are interpreted as the age of basalt eruption and as a minimum age for the widely exposed, tilted Tertiary rocks in the Planet/Mineral-Hill area.

K-Metasomatized Volcanic Rocks

K metasomatism has affected Tertiary sedimentary and volcanic rocks in many areas of the southwestern United States (Chapin and Glazner, 1983). It typically enriches the rocks in K, Ba, and Rb and depletes them of Na, Ca, Mg, Sr, and Mn. The replacement of groundmass and plagioclase by microcrystalline adularia is typical, as is an increase in $^{18}O/^{16}O$. In the Basin and Range Province, this type of alteration is the apparent result of low-temperature diagenesis in alkaline, saline lake environments within closed hydrographic basins (Chapin and Lindley, 1986).

Mafic flows and flow breccias are common in tilted Tertiary sequences in the Buckskin Mountains. The stratigraphic position of these volcanic rocks is well known in four areas: Lincoln Ranch basin, Copper Penny mine area, Planet/Mineral-Hill area, and upper Osborne Wash near the Pride mine (Spencer and Reynolds, this vol.). In each of these areas, the volcanic rocks are present in one stratigraphic interval and are related to a brief period of mafic volcanism. One to three K-Ar dates were obtained from each of these areas to determine the ages of volcanism and K metasomatism.

All nine dated samples were weakly to severely K metasomatized, as indicated by high K content and petrographic evidence. In thin sections of strongly K-metasomatized samples, plagioclase has been converted to a cryptocrystalline to finely microcrystalline aggregate of a high-K (as indicated in thin sections stained for K) mineral or mineraloid that is possibly adularia. Thin sections of moderately K-metasomatized samples reveal fuzzy plagioclase with relict albite twins that are mantled by a K-rich mineral. Fresh albite-twinned cores are present in the one weakly K-metasomatized sample (no. 12-15-85-2). An abundant, anhedral opaque mineral in K-metasomatized rocks is probably hematite, which is common in other areas of K metasomatism (Chapin and Lindley, 1986; Roddy and others, 1988). In three of the four areas studied, several samples were collected from the same volcanic unit and possibly from the same flow. Wide variation in K content of individual units is interpreted to indicate large lateral variations in degree of K metasomatism.

Pure plagioclase mineral separates could not be obtained from these K-metasomatized rocks because of the altered state of the plagioclase in most samples. Feldspar concentrates from the volcanic rock samples were weak to nonmagnetic and were within the density range of feldspar. Calcite and clay minerals were removed by acid treatment (diluted HNO_3 and HF) and

ultrasonic vibration.

Three samples from the same volcanic unit in the Lincoln Ranch basin yielded K-Ar dates that range from 20.2 ± 0.9 Ma (weighted average of two dates) to 15.8 ± 0.5 Ma (Table 1). The amount of K in these samples ranged from 2.7 to 12.4 wt. %. A correlation exists between K-Ar date and K content: a higher K content corresponds to a younger date (Fig. 1). This relationship is consistent with the hypotheses that K metasomatism occurred at temperatures below the Ar-closure temperature for plagioclase and that K-Ar dates reflect the combined contributions of K and Ar from a primary igneous feldspar and a secondary K-rich mineral, each of a different age.

A relationship between K content and K-Ar date was not, however, apparent in the other dated samples. Three samples from the Planet area do not define a trend, and two samples from upper Osborne Wash, whose K content varies by a factor of two, are approximately the same age (Fig. 1). Evidence for a relationship between K content and K-Ar date is thus inconsistent, possibly because K metasomatism occurred over several million years and at different times in different areas.

The mafic flows are inferred to be approximately the same age throughout the Buckskin Mountains, based on lithologic similarity and the absence of similar volcanic rocks elsewhere within Tertiary stratigraphic sections (Spencer and Reynolds, this vol.). If this inference is correct, the following K-Ar dates constrain the age of these flows between 18 and 21 Ma: (1) 20.2 ± 0.9 Ma from a weakly metasomatized sample in the Lincoln Ranch basin, (2) 18.6 ± 1.5 Ma (hornblende) from the Copper Penny mine area (Wilkins and Heidrick, 1982), and (3) 20.3 ± 0.4 Ma (feldspar) and 21.8 ± 0.5 Ma (biotite) from a stratigraphically lower tuff in the Copper Penny mine area. K metasomatism occurred between approximately 20.5 and 15.8 Ma, as indicated by K-Ar dates yielded by all nine K-metasomatized samples. A secondary K-rich mineral produced by K metasomatism is probably the primary source of K and Ar in most of the dated mineral concentrates. K metasomatism in the Planet area ended before the 16 Ma conglomerate of

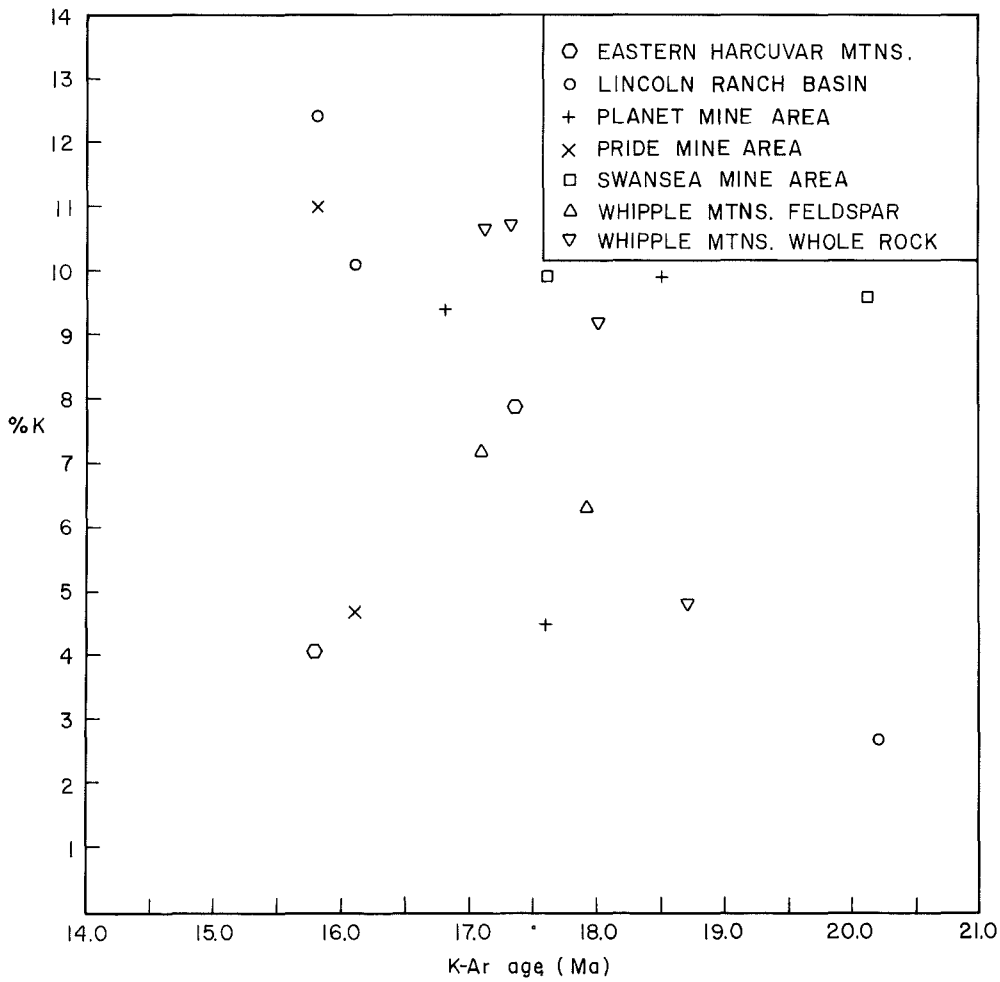

Figure 1. Graph of K-Ar date versus percent-K content for samples from the Buckskin, Whipple, and eastern Harcuvar Mountains. Data from the Whipple Mountains are from G.A. Davis and others (1982). Data from the eastern Harcuvar Mountains are from Scarborough and Wilt (1979). The sample from the Swansea mine area is from Wilkins and Heidrick (1982). All other data are from Table 2.

Cave Wash and interbedded basalt were deposited.

K metasomatism has affected Miocene volcanic rocks across a wide area in western and southern Arizona. Because of its typically subtle nature in hand specimen, however, it was not recognized until the early 1980's; therefore, many K-Ar dates of whole-rock and feldspar samples, previously reported as reflecting the true age of the rock, actually reflect the age of K metasomatism. For example, six dates obtained from volcanic rocks in the Copper Basin Formation of the Whipple Mountains, two of "plagioclase" and four of whole rock, fall within the range of 17 to 19 Ma (Davis, G.A., and others, 1982). The amount of K reported for these samples ranges from 5% to 11%, which is too high for plagioclase. A secondary K-rich mineral produced by K metasomatism is probably the primary source of K and Ar in these samples; thus, K-Ar data indicate that K metasomatism occurred at approximately the same time in the Whipple and Buckskin Mountains. Volcanic rocks at the east end of the Harcuvar Mountains, which are east of the Buckskin Mountains, have yielded similar whole-rock K-Ar data (Scarborough and Wilt, 1979) and are K metasomatized (Brooks, 1988; Roddy and others, 1988). K metasomatism, therefore, strongly affected mid-Tertiary volcanic rocks across a large area between approximately 21 and 15 Ma. K-Ar data from such rocks partially or entirely reflect the age of K metasomatism and represent a younger age limit for volcanic rocks (Brooks, 1986).

POSTDETACHMENT ROCKS

K-Ar dates of flat-lying, generally basaltic volcanic rocks in the Buckskin and Rawhide Mountains place a younger age limit on termination of low-angle extensional faulting and related tilting. In the western Rawhide Mountains, a very gently west-dipping sequence of basalt flows rests unconformably on more steeply tilted rocks and has yielded a whole-rock date of 13.0 $\pm$ 0.5 Ma (Suneson and Lucchitta, 1979) and a plagioclase-concentrate date of 11.6 $\pm$ 0.3 Ma (Table 1). The weighted mean average of these dates, 12.0 $\pm$ 1.1 Ma, is considered to represent the age of the basalt and constrains the time that tilting related to detachment faulting ended.

Flat-lying basalt and locally interbedded intermediate to silicic flows, tuffs, and volcaniclastic sediments rest with gentle to steep angular unconformity on tilted Tertiary and older rocks across a large area in the western Buckskin Mountains and southeastern Bill Williams Mountains. The flat-lying basalt that forms The Mesa in the western Buckskin Mountains has yielded K-Ar dates of 10.3 $\pm$ 0.3 Ma (Armstrong and others, 1976) and 9.6 $\pm$ 0.6 Ma (Fugro, 1975, as reported by Calzia and Morton, 1980). Correlative basalt in the southeastern Bill Williams Mountains yielded a K-Ar date of 9.2 $\pm$ 0.2 Ma (Suneson and Lucchitta, 1979). A sequence of intermediate to silicic tuffs and flows that underlies the flat-lying basalt along the southern flank of The Mesa (Grubensky, this vol.) yielded plagioclase-concentrate and sanidine K-Ar dates of 10.5 $\pm$ 0.3 Ma and 10.5 $\pm$ 0.2 Ma, respectively (Table 1). Widespread, posttilting, predominantly basaltic volcanism, therefore, occurred between approximately 12 and 9 Ma.

CONCLUSION

Both magmatism and cooling due to uplift influenced the Cenozoic thermal history of lower-plate rocks in the Buckskin and Rawhide Mountains. Geochronologic data presented herein (Table 1) and elsewhere (Bryant and Naeser, 1987; Fryxell and others, 1987a) record a major Miocene cooling event that affected the entire lower plate. The regional nature of this event, which also affected lower-plate mylonitic rocks in adjacent ranges (Rehrig and Reynolds, 1980; Davis, G.A., and others, 1987), supports the hypotheses that isostatic uplift of footwall rocks during tectonic denudation resulted in the cooling event and that magmatism was of secondary importance.

An upper-plate tuff in the lower part of the Tertiary stratigraphic section in the Copper Penny mine area yielded a biotite K-Ar date of 21.8 $\pm$ 0.5 Ma, which is interpreted as the approximate age of the tuff. Stratigraphically higher mafic volcanic flows in several areas of the Buckskin Mountains yielded a K-Ar hornblende date of 18.6 $\pm$ 1.5 Ma (Wilkins and Heidrick, 1982) and a weakly K-metasomatized plagioclase-concentrate date of 20.2 $\pm$ 0.9 Ma (Table 1). These dates support the inference that mafic flows were erupted between approximately 21 and 18 Ma. Tilted basalts in the southeastern Bill Williams Mountains yielded two plagioclase K-Ar dates of approximately 16 Ma, which indicates that tilting related to extensional faulting continued until after this time.

Widespread K metasomatism of mafic volcanic rocks caused alteration and K enrichment of plagioclase and formation of encrustations of a K-rich mineral. K-Ar dates of feldspar concentrates from these rocks reflect the time of K metasomatism. All nine K-Ar dates from K-metasomatized volcanic rocks in the Buckskin Mountains and several dates from adjacent ranges are within the range of 15.5 to 20.5 Ma. This is interpreted to be the time of K metasomatism.

Uplift and cooling of lower-plate rocks, eruption of mafic volcanic rocks in syntectonic extensional basins, and K metasomatism all occurred between approximately 22 and 15 Ma, a remarkably active time in the geologic history of the Buckskin Mountains. This was followed by posttectonic, basaltic, and locally rhyolitic volcanism in the western Buckskin, southeastern Bill Williams, and northern Rawhide Mountains between approximately 12 and 9 Ma.

Fluid regimes and geochemical mass transport in the development of mylonites and chloritic breccias at Copper Penny, Buckskin Mountains

R. DAVID HALFKENNY, JR.* *Department of Geology, University of Western Ontario, London, Ontario, Canada N6A 5B7*
ROBERT KERRICH *Department of Geological Sciences, University of Saskatchewan, Saskatoon, Saskatchewan, Canada S7N OWO*
WILLIAM A. REHRIG *Applied Geologic Studies, 2875 W. Oxford #3, Englewood, Colorado 80110*

ABSTRACT

The Copper Penny mine area in the Buckskin Mountains of the Harcuvar metamorphic core complex is characterized by three tectonic plates with two intervening detachment faults. The lower plate is composed of amphibolite-facies granitic gneiss, which grades upward into protomylonite and mylonite near the lower detachment fault. Mylonites have developed by dynamic recrystallization of quartz, and by recrystallization of K-feldspar and plagioclase porphyroblasts to trails of ultra-fine-grained aggregates of secondary feldspar that define high-strain domains. Partial retrograde alteration of biotite to chlorite signifies lower-amphibolite- to greenschist-facies conditions. Mylonitization was an essentially isochemical and isovolumetric process, except for minor trends toward enhanced Fe, Mg, and LOI near the lower detachment fault.

The lower detachment fault is marked by the conversion of mylonites to chloritic breccias and cataclasites, owing to superimposed brittle transgranular fracturing accompanied by intense metasomatism. Ratios of the alteration-insensitive elements signify that the chloritic breccias may locally be tectonic mixtures of a compositionally distinct precursor lithology with cataclastically deformed granitic mylonites of the lower plate. Metasomatism involved massive additions of Fe, Mn, and Mg and is reflected in the modal abundance of chlorite. Concomitant losses of Si, Na, and K correspond to the hydrolysis of plagioclase and K-feldspar during chloritization. Chloritic breccias display locally augmented amounts of S, Cu, and Zn, reflecting disseminated base-metal sulfides and late calcite veins.

$\delta^{18}O$ values of calcite veinlets vary widely and nonsystematically throughout the tectonic section, with a total range of 9 to 20.8 per mil. $\delta^{13}C$ values are relatively constrained and are consistent with hydrothermal redistribution of middle-plate limestones. O- and C-isotopic compositions of calcite veins in lower- and middle-plate rocks are similar to compositions of calcites in upper-plate rocks, and the carbonates probably formed from a common reservoir that contained a component of meteoric or evolved meteoric water.

The tectonic section records a transition from ductile creep to brittle deformation, high to low temperatures, low to high water/rock ratios, and isochemical to open-system conditions. A two-fluid regime is indicated: a deeper, hotter, reduced, and crust-equilibrated reservoir focused along the detachment fault and involved in Fe, Mn, and Mg metasomatism; and a higher-level, cooler, oxidized reservoir from the upper plate, implicated in late overprinting by calcite Fe-Mn-oxide veins.

INTRODUCTION AND SCOPE OF STUDY

Metamorphic core complexes constitute a distinctive structural-lithological entity in the tectonic architecture of the North American Cordillera. They are geologically characterized by a core of intensely deformed metamorphic and/or plutonic rocks grading upward through gently dipping mylonites to a low-angle detachment fault. This metamorphic infrastructure, or lower plate, is overlain by a suprastructure, or upper plate, of attenuated, listrically faulted, allochthonous and unmetamorphosed Tertiary rocks. Core-complex development postdated Mesozoic thrusting, preceded basin-range faulting, and was generally contemporaneous with Tertiary ignimbritic activity. Twenty-five such core complexes have been identified to date, discontinuously arrayed in a belt along the axis of the North American Cordillera from northwest Mexico to British Columbia (Coney, 1980).

Metamorphic core complexes are interesting from the standpoint of fluid regimes that accompany crustal-scale deformation. Evidence of fluid flow, represented by minor but pervasive mineralogic changes in the mylonites, includes the development of metasomatic chloritic breccias beneath detachment faults and oxidative alteration of allochthonous upper-plate volcanic rocks to a K-feldspar, calcite, Fe-Mn-oxide assemblage, with spo-

*Present address: HMCS Iroquois, FMO Halifax, Halifax, Nova Scotia, Canada B3K 2XO.

in Spencer, J.E., and Reynolds, S.J., eds., 1989, Geology and mineral resources of the Buckskin and Rawhide Mountains, west-central Arizona: Arizona Geological Survey Bulletin 198, p. 190-202.

radic Cu-Au and base-metal mineralization (Crittenden and others, 1980; Wilkins and Heidrick, 1982).

To assess fluid and thermal regimes, light-stable-isotope studies have been conducted on three metamorphic core complexes: the Picacho complex of central Arizona (Kerrich and others, 1984, 1986; Rehrig and others, 1986; Kerrich and Rehrig, 1987), the South Mountain complex of south-central Arizona (Smith and Reynolds, 1985), and the Bitterroot detachment zone of western Montana (Kerrich and Hyndman, 1986). This study addresses the processes involved in chloritic-breccia development in the Buckskin Mountains of the Harcuvar metamorphic core complex in west-central Arizona. Drill cores from upper- and lower-plate rocks in the Copper Penny mine area of the Buckskin Mountains provide exceptional control for semicontinuous sampling of the transitions in lithology, deformation style, and metasomatism. The first sections of this paper describe the geologic setting, petrography, and deformational characteristics of the various tectonic units. Geochemical data from the drill cores are used to discriminate protolith types and quantify the geochemical mass transport involved in development of chloritic breccias. This paper is largely based on a B.Sc. thesis conducted by the senior author at the University of Western Ontario, London, Canada.

The geologic characteristics of metamorphic core complexes in Arizona and western California have been comprehensively described by Davis (1980), Davis and others (1980), Rehrig and Reynolds (1980), Reynolds and Rehrig (1980), and Rehrig (1986); accordingly, the reader is referred to those papers for details of the regional geology.

GEOLOGIC SETTING OF THE COPPER PENNY MINING PROSPECT

The Copper Penny mining prospect is in the central Buckskin Mountains approximately 40 km due east of Parker, Arizona. This mining prospect is located along an east-northeast-trending synform on the Buckskin detachment fault. A detailed geologic map of the Copper Penny prospect was prepared by Wilkins and Heidrick (1982), a simplified version of which is presented as Figure 1. The geology of this specific area, and of the Buckskin Mountains as a whole, is typical of southwestern metamorphic core complexes: lower, middle, and upper plates are present and are separated by detachment faults with associated chloritic breccias (Fig. 2).

Lower-Plate Rocks

The lower-plate rocks are quartzofeldspathic granitic gneiss and include coarse-grained augen to fine-grained banded varieties. The gneiss contains a gently dipping foliation and a mineral lineation defined by elongate quartz rods, trails of recrystallized micas, and flattened K-feldspar porphyroclasts. The foliation in the gneiss intensifies up structural section, where a diagnostic mylonitic fabric is prevalent. This mylonitic fabric is truncated up section by a zone of chloritic breccia that underlies the detachment surface. Within the breccia zone, there is a marked upward transition in intensity and style of deformation from an incipient breccia at the base, through various combinations of cataclastic and hydraulic breccias, to a microbreccia that marks the subhorizontal detachment fault. The term *cataclastic breccia* is used here to denote a rock formed by coarse- and fine-scale transgranular fracturing along the detachment fault, whereas *hydraulic breccia* signifies a rock in the subjacent chloritic breccia that was disrupted by brittle tensile fractures that contain secondary hydrothermal minerals. Chloritic-breccia zones extend discontinuously to depths that exceed 365 m (Wilkins and Heidrick, 1982).

The Buckskin detachment fault is a relatively planar surface composed of a microbreccia, which caps the lower-plate succession. The detachment fault is overlain by a diverse sequence of lithologies, which include limestone, intermediate to mafic volcanic rocks, middle Tertiary clastic rocks, Mesozoic and Paleozoic metasedimentary and metavolcanic rocks, and Proterozoic plutonic and metamorphic rocks. Wilkins and Heidrick (1982) report that the composition of the detachment-zone microbreccia is not related to the hanging-wall rocks. They concluded that the detachment surface acted like a conveyor belt with little interaction between the microbreccia and the rock being transported.

Middle-Plate Rocks

An unusual feature of the Copper Penny area is a sequence of rocks that separates the detachment surface and upper plate. These middle-plate rocks are present in a wedge-shaped lens that occupies the synform between foliation arches (Wilkins and Heidrick, 1982). The lithologies of the middle plate as encountered in drill holes (DH) 2 and 8 (Fig. 2) include granitic breccia, dolomitic to calcite-marble breccia, and cataclastic schists. These units do not exist in DH-4; instead, a sequence of brecciated, bleached, and slightly chloritized arkosic mudstone, siltstone, and shale is present (Fig. 2). The middle plates show the effects of chloritic brecciation and cataclastic deformation, but do not possess the mylonitic fabric characteristic of the lower plate.

Upper-Plate Rocks

Delineating the precise stratigraphy of the sedimentary and volcanic rocks in the upper plate, or suprastructure, is complicated because some contacts are structural in character and units are locally repeated and/or truncated along normal faults. The upper-plate section consists of basal arkosic sandstone overlain by a sequence of megabreccias, volcanic flows and tuffs, conglomerate, sandstone, siltstone, and limestone (Spencer and Reynolds, this vol.). The upper-plate lithologies strike N20°W to N40°W and are only slightly metamorphosed and propylitized.

Structural Sequence

The structural sequence at Copper Penny records a vertical transition in deformation mechanism from ductile intracrystalline creep in the lower-plate mylonites to brittle transgranular fracturing in the upper and middle plates. The microbreccia marking the sole of the Buckskin detachment fault reflects intense cataclasis at the tectonic break; the intensity of brecciation diminishes down section. Extreme distension is the net effect of movement on the primary structural features, which include normal faults, detachment faults, chloritic breccias, and mylonites.

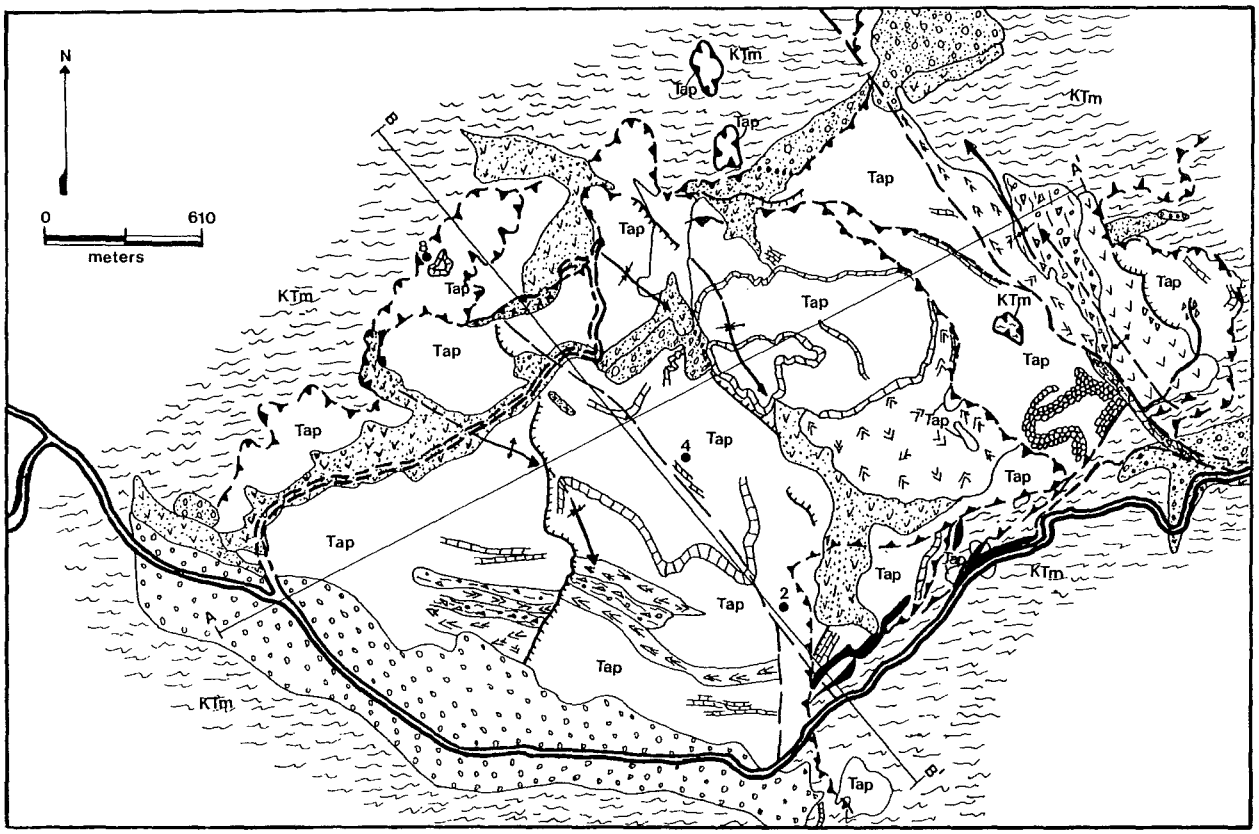

Legend:

Lithology

Quarternary

- Alluvium, showing boulder accumulation
- Terrace gravel
- Pediment gravel

Oligocene(?)-Miocene

Artillery Formation (Tap)

- Laharic basalt
- Vesicular basalt
- Marble breccia
- Lacustrine limestone beds
- Fanglomerate (top) and conglomerate (bottom)
- Tuffaceous (top) and porphyritic felsitic igneous rocks (bottom)

Cretaceous-Tertiary

- Mylonite (KTm)

Structure

- Low-angle detachment surface
- Basin-range fault
- High-angle fault
- Anticline
- Syncline

Miscellaneous

- Hematitic jasper cataclasite
- Drillhole location

Figure 1. Geologic map of the Copper Penny mining prospect, Swansea mineral district, Yuma County, Arizona, showing locations of drill holes (DH) 2, 4, and 8 (simplified from Wilkins and Heidrick, 1982).

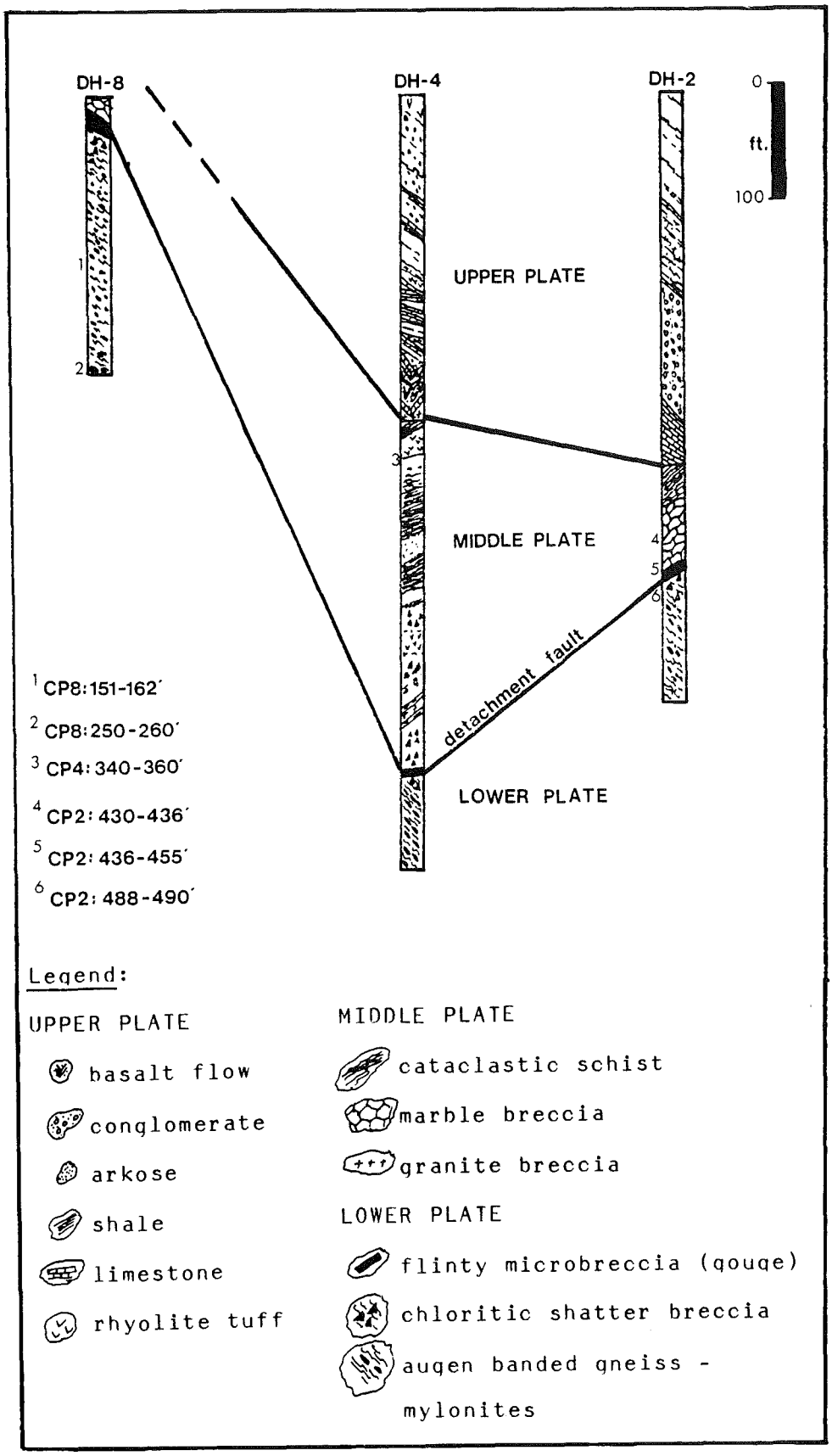

Figure 2. Cross section detailing the lithological and structural divisions in DH-2, DH-4, and DH-8, as well as the sample-depth locations (modified from Wilkins and Heidrick, 1982).

Metamorphism and Alteration

There is a pronounced trend toward increased metamorphic grade down structural section to the core of the lower plate. Upper-plate rocks have not experienced a regional metamorphic event, whereas hematized arkosic siltstones and limestones of the middle plate are metamorphosed to lower greenschist grade. Wilkins and Heidrick (1982) conclude that the middle plate displays the effects of a weak to moderate dynamothermal metamorphism with an intensity intermediate between that of the unmetamorphosed upper plate and the intensely deformed lower plate. The lower plate grades from lower-amphibolite facies in granitic gneiss to mid-greenschist facies in mylonitic rocks, as indicated by the assemblage quartz, biotite, orthoclase, epidote, and retrograde chlorite after biotite.

An envelope of propylitic alteration is manifested by the ubiquitous presence of chlorite and, to a lesser degree, calcite and epidote in the lower plate and by gypsum, calcite, and minor chlorite in the middle plate. An asymmetrical distribution of chlorite about the detachment-fault zone and a volumetric increase in calcite above the detachment are apparent. Calcite abundance diminishes as chlorite increases, as reflected in the petrology of the chloritic breccia and the middle-plate marbles and clastic rocks. In the breccia, chlorite accounts for as much as 20% of the rock volume, whereas the volume of calcite, which is confined to fine hydrothermal veinlets, is insignificant. In contrast, up structural section into the marbles and arkosic siltstones, chlorite abundance ranges from 5% to 10% and the volume of vein calcite ranges from 10% in the marbles to 30% in the arkosic siltstone. Epidote, intergrown with chlorite, is confined to veinlets in the chloritic breccia and mylonites of the lower plate. Gypsum mineralization, present only in middle-plate clastic rocks recovered from DH-4, forms veins, microveinlets, and selvages that coexist with pervasive calcite veins.

PETROGRAPHIC DESCRIPTIONS OF THE MIDDLE-PLATE DETACHMENT-FAULT ZONE AND LOWER-PLATE LITHOLOGIES

Lower-Plate Rocks

The lithologies of the lower plate include mylonitic dioritic dikes, protomylonite, mylonite, incipient chloritic breccia, and variably altered chloritic breccia. The lower-plate samples examined in this study were obtained from DH-2 and DH-8.

Diorite. A holocrystalline porphyritic rock recovered from the base of DH-8 is composed of coarse-grained, flattened K-feldspar augen set in a green-black aphanitic matrix and is considered to be dioritic in composition. Microscopically, this diorite is composed of K-feldspar, quartz, biotite, and chlorite, minor amounts of epidote and sericite, and trace amounts of sphene and ilmenite. A crude mylonitic fabric and mineral lineation are defined by elongate rods of recrystallized quartz, recrystallized fine-grained feldspar, and fractured biotite altered to chlorite. These mylonitic ribbons are deflected around and between the flattened porphyroclasts of K-feldspar and define the microscopic deformational fabric.

Protomylonite. The base of the ductile mylonitic zone is represented by the transition from a quartzo-feldspathic, coarse-grained, granitic augen gneiss to fine-grained, compositionally banded mylonitic gneiss. These rocks, termed *protomylonite,* are characterized by relict lenticular megacrysts predominantly composed of K-feldspar, with an intervening fine-grained matrix of alternating light- and dark-colored quartz ribbons and other minerals.

Protomylonite is composed of K-feldspar, quartz, biotite, chlorite, and sericite, minor amounts of epidote, and trace amounts of sphene, allanite, and magnetite. The mylonitic fabric is more fully developed in the protomylonite than it is in the diorite. A strong mineral lineation is defined by quartz ribbons, bands of fractured biotite, and hypidiomorphic accumulations of mortar-textured, recrystallized quartz and feldspar. This compositionally banded matrix is deflected around the porphyroclasts and contains discontinuous trains of fine opaque phases.

The coarse-grained, poikilitic feldspar augen of plagioclase, orthoclase, and microperthite constitute about half of the rock volume. These augen locally have relict igneous cores. Recrystallization at grain boundaries has produced fine-grained secondary feldspar aggregates, which extend in trails from the margins of the porphyroclasts. Coarser grained feldspars exhibit transgranular microfracturing, microfaulting, undulose extinction, and deformation twinning.

Quartz composes approximately 30% of the protomylonite. It generally forms a recrystallized fine-grained matrix that appears to have flowed around the feldspar augen. Chlorite and biotite together account for 10% of the rock volume. Biotite forms finely fractured grains that are partially altered to chlorite and have a preferred dimensional and crystallographic orientation.

Sericite is a common alteration product in the cores and on the grain boundaries of K-feldspar, as well as in association with biotite. Opaques, specifically magnetite, ilmenite, minor pyrite, and trace hematite, are present in short trains and as disseminated grains throughout the matrix. Medium- to coarse-grained, euhedral sphene is present in the finely comminuted matrix and is commonly associated with opaques. Sphene was apparently unaffected by the mylonitization event, displaying no evidence of inter- or intracrystalline grain-size reduction.

Mylonite. A thick zone of mylonite structurally overlies the zone of protomylonite. Although mylonite has the same low-angle foliation and east-northeast-trending lineation, there are striking dissimilarities between mylonite and protomylonite in color, grain size, texture, and mineralogy. Mylonite has a bimodal grain-size distribution, with relict augen of feldspar supported by a crudely foliated, ultra-fine-grained quartz-feldspar matrix. The porphyroclasts of feldspar are of considerably finer grain size than in protomylonite, and biotite

has been completely retrograded to chlorite plus muscovite.

Microscopically, mylonite is composed of relict porphyroclasts of orthoclase and plagioclase, fine-grained recrystallized ribbons of quartz and feldspar, major veins of chlorite and epidote, minor veinlets of chlorite, calcite, and hematite, and trace amounts of disseminated sphene, allanite, pyrite, and ilmenite. A crude compositional layering has developed, consisting of alternating bands of recrystallized quartz and mortar-textured quartz and feldspar. Ultrafine, secondary feldspar aggregates are present at grain boundaries, drawn into trails extending away from the parent grains. Chlorite is present at grain boundaries, and centers of feldspar porphyroclasts are extensively altered to sericite. Undulose extinction and deformation twins penetrate into grains from the grain boundaries. Orthoclase and plagioclase exhibit both linear fractures that terminate at grain boundaries and irregular fractures that terminate within crystals. Fractures are occupied by secondary products compositionally similar to the parent grain.

Fine-grained euhedral ilmenite and pyrite are present throughout the matrix as short "veinlets" parallel to the foliation. Disseminated rhombohedral sphene and sharply defined cores of dark-brown, pleochroic allanite (the LREE-enriched epidote) are also present within the matrix. As in protomylonite, these two minerals appear unstrained and have not undergone the comminution by transgranular fracturing or dynamic recrystallization that is evident in all other matrix minerals.

Chloritic Breccia. The chloritic breccia caps the lower-plate sequence at the detachment fault and represents the culmination of the transition from granitic gneisses through mylonitic equivalents to brecciated and hydrothermally altered products. Remnants of the original gneisses and mylonites exist in rotated clasts and as relict subangular augen of orthoclase and plagioclase, supported by a propylitized and hematized matrix. The trend of the mylonitic foliation in these remnants differs from clast to clast because of varied degrees of internal deformation and rotation. Brecciation is marked by a network of chlorite and epidote veins at the base of the section. Up structural section, brecciation intensifies and both the augen and fragments become correspondingly finer within a hematized matrix.

The chloritic breccia is mineralogically similar to the subjacent mylonitic zone. In the upper part of the unit, however, there is a marked increase in the modal abundance of the alteration minerals chlorite, epidote, hematite, and sulfides with respect to increasing intensities of brecciation. At initial stages, chlorite and epidote are the dominant fracture-infilling minerals between remnant mylonitic fragments. Proximal to the detachment fault, however, the mylonitic remnants are supported in a matrix almost exclusively composed of hematite plus chlorite. Although the bulk dimensional alignment intrinsic to the mylonitic fabric has been lost because of disaggregation, shearing, and physical rotation, relict rock fragments still retain many textural features of mylonite and protomylonite, attesting to the nature of the protolith.

Epidote, chlorite, hematite, calcite, and sulfides form irregularly distributed veinlet networks. Epidote veinlets, generally associated with chlorite as disseminated prismatic grains in a chloritic groundmass, are present between and within mylonitic blocks. Chlorite is also present in breccia pipes and in a stockwork of finer, interconnected veinlets. Hematite replaces chlorite in breccia pipes and is also present in veinlets; it is generally spatially related to chlorite and fine calcite veins. Isolated hematite veinlets are common in the cap of the chloritic breccia and are continuous through veins of chlorite. Microfaults displace both chlorite veinlets and the mylonitic fabric, and the fracture traces have been filled with hematite. Several veinlets of fine-grained sulfides, chalcopyrite, and pyrite are present in the breccia. Aggregates of fine-grained euhedral pyrite partially pseudomorphed by hematite are also present in the matrix of the breccia.

Detachment-Fault Rocks

The Buckskin detachment fault is marked along much of its surface by a microbreccia, which can be subdivided into nonmineralized and mineralized units. The nonmineralized microbreccia is a fine-grained cataclasite, with coarse-grained remnants of recrystallized quartz, alkali feldspar, and relict mylonitic fragments. Resting structurally above and in sharp contact with the nonmineralized microbreccia is the mineralized counterpart. Mineralogically and texturally these two are similar, but the latter is distinguished by variably abundant pyrite, chalcopyrite, specular hematite, and calcite.

Middle-Plate Rocks

A sequence of moderately metamorphosed, variably foliated but nonlineated rocks is present above the detachment fault and below the upper-plate rocks. The lithologies encountered in DH-2 and DH-8 include granitic breccia, intensely brecciated dolomitic marble, and cataclastic schists. DH-4 contains a sequence of arkosic mudstone, siltstone, and shale that is variably brecciated, bleached, slightly chloritized, and iron-manganese stained. In this study, the carbonate unit from DH-2 and the clastic lithologies from DH-4 were examined in detail.

Carbonate Rocks. In DH-2, a metamorphic carapace directly overlying the microbreccia and detachment fault is composed of three distinct carbonate units: (1) white, holocrystalline granular marble cut by veinlets of hematite, sulfides, and minor chlorite; (2) chloritic brecciated marble with extensive chlorite and carbonate veining; and (3) holocrystalline gray-black marble pervaded by numerous white veinlets of calcite.

Microscopically, the white marble is a fine- to medium-grained aggregate of dolomite and calcite. Several generations of coarse-grained carbonate veins crosscut the unit. Minor quantities of chlorite, hematite, pyrite, and sphene are present. The marble contains deformation features, such as stylolites, which themselves appear slightly deformed, and microfaults and shear zones that

cut carbonate veins.

The chloritic brecciated marble is a holocrystalline fine-grained rock essentially composed of calcite, dolomite, and chlorite, with minor amounts of quartz, sphene, and pyrite. The groundmass is cut by a network of coarser grained carbonate veins with chloritic margins and by chlorite microveinlets.

The dark marble is an aphanitic, gray-black rock

Table 1. Abundances of major-element oxides and selected trace elements in lower-plate rocks at Copper Penny in the Buckskin Mountains.

Rock Type	Cataclasites		Chloritic Breccia				Brecciated Mylonite				Protomylonite			Diorite Dike	Average Protomylonite
Sample* Number	1	2	3	4	5	6	7	8	9	10	11	12	13	14	15
SiO_2	21.10	39.30	60.50	66.60	68.10	64.20	71.00	70.70	72.00	65.70	72.60	74.50	71.20	67.70	72.77
TiO_2	0.38	0.52	0.70	0.69	0.84	0.80	0.20	0.23	0.20	0.68	0.17	0.06	0.23	0.36	0.15
Al_2O_3	7.25	8.69	13.50	13.40	12.30	13.90	14.20	14.40	13.80	15.10	14.10	13.60	14.70	16.10	14.13
Fe_2O_3	52.20	12.20	7.05	5.98	4.88	6.62	1.96	1.98	1.74	3.65	1.30	0.86	1.78	2.58	1.28
MnO	0.17	0.45	0.12	0.05	0.04	0.05	0.01	0.01	0.01	0.02	0.01	0.01	0.01	0.03	0.01
MgO	6.78	7.10	2.61	2.27	1.08	2.45	0.49	0.57	0.40	0.83	0.35	0.12	0.61	1.11	0.36
CaO	1.99	14.50	4.97	2.99	3.42	3.55	1.27	1.22	1.09	2.04	1.24	1.14	1.83	2.85	1.40
Na_2O	<0.01	<0.01	1.53	3.25	3.37	3.49	3.34	3.44	3.53	3.31	3.97	3.68	4.32	4.88	3.99
K_2O	0.56	1.21	3.36	1.74	3.05	1.77	5.56	5.70	5.25	5.66	4.91	5.20	3.87	2.85	4.66
P_2O_5	0.10	0.19	0.21	0.20	0.31	0.27	0.06	0.07	0.06	0.16	0.05	0.02	0.07	0.11	0.05
LOI	6.47	14.30	5.39	2.54	2.08	2.47	1.23	1.00	1.08	1.62	0.77	0.77	0.77	1.31	0.77
Total	97.00	98.50	100.10	99.90	99.60	99.70	99.40	99.40	99.20	98.90	99.60	100.00	99.50	100.00	99.70
S	10001	1559	58	56	309	226	46	47	42	55	39	46	41	67	42
V	144	79	52	44	34	51	18	23	16	43	10	10	16	26	12
Sc	9	9	14	12	16	15	2	3	2	13	3	1	2	5	2
Cr	36	30	31	44	51	46	58	45	48	71	62	98	62	53	74
Ni	23	15	12	9	7	10	3	3	3	6	4	3	4	6	4
Co	-	45	23	20	20	27	6	6	6	7	7	80	8	11	32
Cu	4293	196	10	11	20	10	8	8	8	9	9	9	9	10	9
Pb	25	16	34	27	32	23	27	20	24	29	40	38	34	38	37
Zn	476	241	88	60	23	44	7	4	6	15	7	5	19	37	10
Rb	-	35	100	50	70	45	112	96	99	121	140	124	109	96	124
Sr	-	117	504	585	439	623	406	419	365	484	301	316	497	734	371
Y	-	38	83	52	80	61	-	-	-	16	2	-	-	9	2
Zr	78	195	384	382	448	365	105	104	102	168	101	49	94	140	81
Hf	<1	5	10	10	10	11	3	4	3	6	3	2	3	4	3
Nb	9	24	18	13	14	10	8	1	7	15	12	1	10	17	8
Ba	-	109	966	736	1191	761	1906	2325	1527	2914	965	1046	1266	1025	1092
Ga	29	18	14	12	11	11	10	7	10	13	11	11	12	16	11
U	5	4	1	1	1	1	3	3	4	9	5	2	2	7	3
Th	9	10	2	3	2	3	7	9	10	9	16	5	6	8	9
Ti/Zr	29	16	11	11	11	13	11	13	12	24	10	7	15	15	
Al_2O_3/TiO_2	19	16	19	19	15	17	71	63	69	22	83	227	64	45	
Zr/Y	-	5.1	4.6	7.3	5.6	6.0	-	-	-	10	51	-	-	16	
Zr/Sc	8.7	21	27	32	28	24	53	35	51	13	34	49	47	28	
Zr/Th	8.7	20	192	127	224	122	15	12	10	19	6.3	9.8	16	18	
Th/U	1.8	2.5	2.0	3.0	2.0	3.0	2.3	3.0	2.5	1.0	3.2	3.5	3.0	1.1	

Major-element oxides expressed in weight percent, trace elements in ppm.
Dash (-) represents abundances below detection level.
Sample Identification:

1. 2 445-455 b
2. 2 445-455 c
3. 2 488-490 d
4. 2 488-490 c
5. 2 488-490 a
6. 2 488-490 b
7. 8 152-161 b
8. 8 152-161 a
9. 8 152-161 c
10. 8 152-161 d
11. 8 250-260 b
12. 8 250-260 d
13. 8 250-260 c
14. 8 250-260 a
15. 8 250-260 b,c,d average

* Samples arranged in stratigraphic order.

with a random stockwork of white veinlets and vugs of carbonate. Microscopically, this dark marble is composed of calcite and dolomite, with minor chlorite, quartz, pyrite, and plagioclase. Isolated vugs are filled by coarse-grained subhedral grains of carbonate rimmed by chlorite. Concentrations of quartz create a decussate fabric. Stylolites range in length from a few millimeters to several centimeters.

All three carbonate units show pervasive microfracturing. Microfractures were sequentially filled with (1) calcite with chloritic selvages, (2) chlorite, and (3) fine-grained sulfide minerals.

Clastic Rocks. In DH-4, the structural position of the metamorphic carapace in DH-2 is occupied by a clastic unit that overlies the flinty microbreccia of the detachment-fault surface. This unit is composed of two distinct lithologies: (1) arkosic siltstone pervaded by calcite and gypsum veining; and (2) fine-grained laminated siltstone with compositional banding reflected in the alternating brown- and green-colored shale partings.

The arkosic siltstone unit of the middle plate consists of albite, quartz, chlorite, sericite, disseminated hematite and pyrite aggregates, opaque oxides, and calcite. Disseminated hematite and Mn oxides impart a characteristic red-brown color, which is preferentially concentrated near the veins.

The laminated siltstone is essentially composed of albite, quartz, chlorite, and minor amounts of biotite and muscovite; hematite has stained the rock. In thin section, the lamination is defined by alternating light bands of alkali feldspar, quartz, muscovite, and sericite and darker bands of biotite, chlorite, and hematite-goethite.

Both clastic units are extensively brecciated and cut by calcite-gypsum veins, veinlets of chlorite, and local pyrite veins. The gypsum typically has a fibrous habit: orthogonal and oblique fiber orientations are present, signifying complex incremental dilation. Sedimentary laminae and veins are offset by microfaults.

GEOCHEMISTRY

Analytical Methods

Major-element oxides, together with S, Cr, Co, Ni, Cu, Zn, Pb, Rb, Sr, Y, Zr, Nb, and Ba, were determined by X-ray fluorescence spectrometry. Sc, Hf, U, and Th were analyzed by means of instrumental neutron-activation analysis (INAA). CO_2 was extracted from carbonate minerals using 100% H_3PO_4 (McCrea, 1950). Isotopic data for O are reported as $\delta^{18}O$ values in per mil relative to Standard Mean Ocean Water (SMOW) and for C as $\delta^{13}C$ values referenced to PDB.

Chemical Mass Balance

In order to evaluate chemical changes involved in the progressive transformation of a protolith into chloritic breccia, it is necessary first to establish that all samples originally belonged to a single, compositionally uniform protolith. To a first approximation, this can be resolved by inspection of the abundances and mutual ratios of the alteration-insensitive elements. For example, if a group of elements, such as Al, Hf, Sc, and Zr, maintains uniform interelement ratios in a suite of samples representing progressive intensities of metasomatism, then it is likely that they all originally belonged to a compositionally homogeneous protolith. Because this criterion is not satisfied in the suite of lower-plate rocks, it is invalid to conduct rigorous two-way chemical mass balance; hence, only qualitative estimates of chemical transport are possible.

Protoliths

Bulk-rock compositions vary greatly throughout the structural sequence, as anticipated from the pronounced spatial differences in modal mineralogy. For instance, SiO_2 ranges from 21 to 74 wt. % and Fe_2O_3 ranges from 0.9 to 52.5 wt. %. Consequently, it is critical to separate compositional variations that arise from the presence of different protoliths from those induced by superimposed metasomatism.

The abundances and mutual ratios of the alteration-insensitive elements define two basic populations of samples that correlate in a simple manner with rock types in the structural section (Table 1). Protomylonites and brecciated mylonites constitute one population, and are characterized by intermediate abundances of TiO_2 (0.25 wt. % $\pm$ 0.20 1σ), Zr (103 $\pm$ 35 ppm) and Th (8 $\pm$ 2 ppm), and low abundances of P_2O_5 (0.09 $\pm$ 0.04 wt. %) and Sc (3.72 $\pm$ 4.1 ppm). In contrast, the second population, which comprises chloritic breccias, possesses enhanced abundances of TiO_2 (0.76 $\pm$ 0.07 wt. %), Zr (395 $\pm$ 36 ppm), P_2O_5 (0.25 $\pm$ 0.05 wt. %), and Sc (14 $\pm$ 2 ppm), but relatively low levels of Th (2.5 $\pm$ 0.6 ppm). The two populations, as shown in Figure 3, have systematically different interelement ratios of Al_2O_3/TiO_2 (85 $\pm$ 65 vs. 17 $\pm$ 2), Zr/Sc (40 $\pm$ 14 vs. 28 $\pm$ 3), and Zr/Th (12 $\pm$ 4 vs. 166 $\pm$ 50). These results suggest that the protomy-

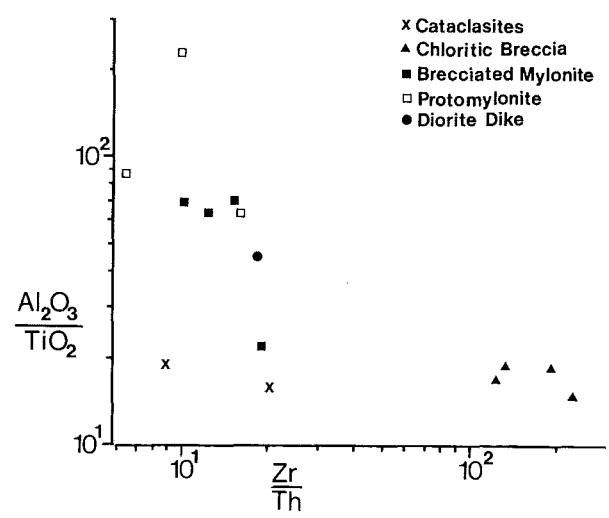

Figure 3. Interelement-variation diagram of alteration-insensitive elements for the principal lithological types. Source of data: Table 1.

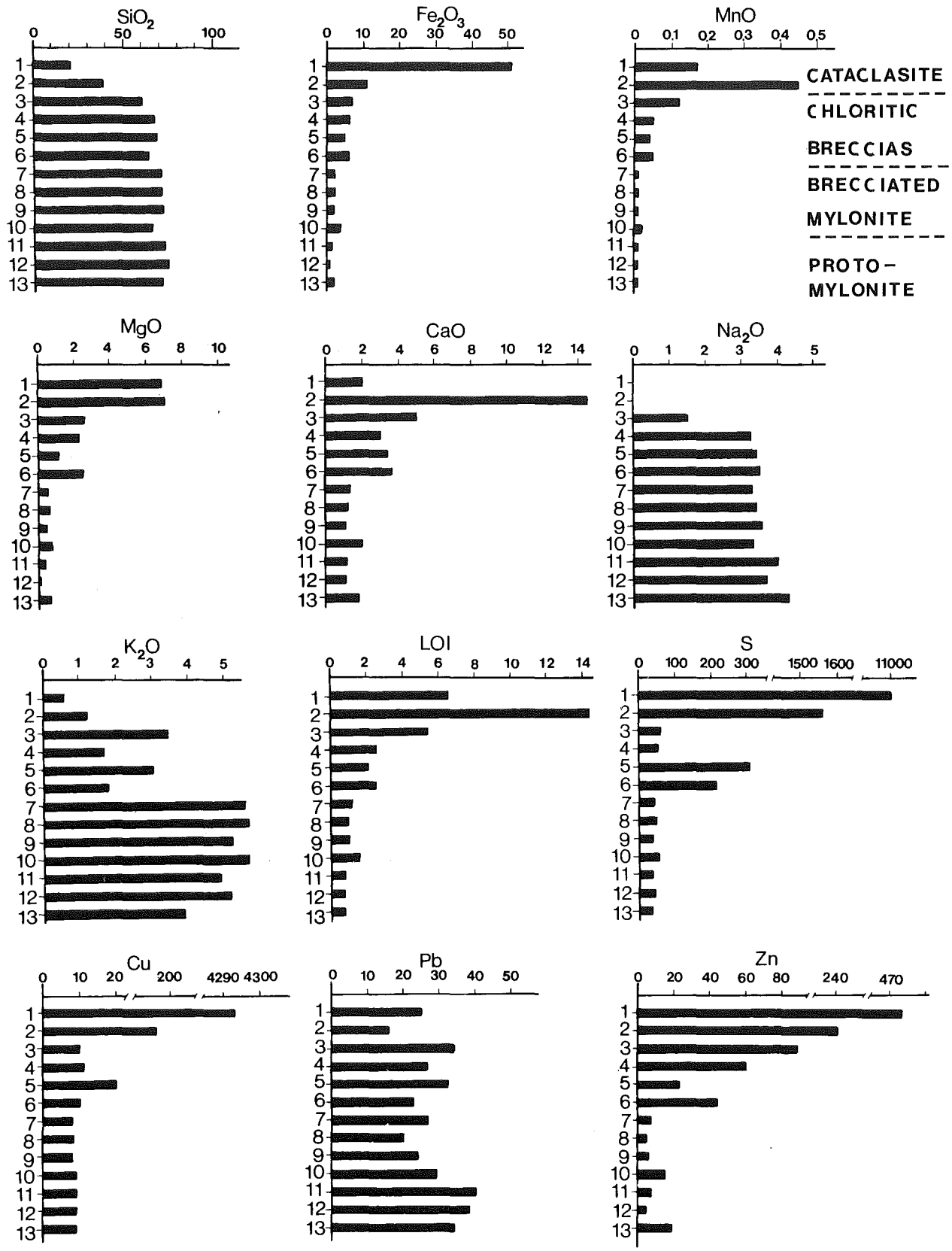

Figure 4. Abundances of selected major-element oxides and trace elements, as a function of tectonic position at Copper Penny. Source of data: Table 1. Samples corresponding to numbers 1 through 13 are listed in Table 1.

lonites and brecciated equivalents developed from a common granitoid protolith in the lower plate, whereas the chloritic breccias represent metasomatism of a distinct protolith, or alternatively, mixed protoliths.

Chloritic breccias possess high levels of TiO_2, P_2O_5, Zr, and Hf relative to the protomylonites and mylonites (Table 1; Kerrich and others, this vol.). This is illustrated in Figure 3 where the chloritic breccias plot in a field distinct from that of the mylonites. These relations raise the possibility that the specific chloritic breccias analyzed in this study developed by deformation and metasomatism of a tectonic mixture of lower-plate lithologies with another protolith. Fault-zone cataclasites are compositionally heterogeneous with respect to the alteration-insensitive elements; accordingly, they are interpreted to represent tectonic mixtures of distinct lithotypes.

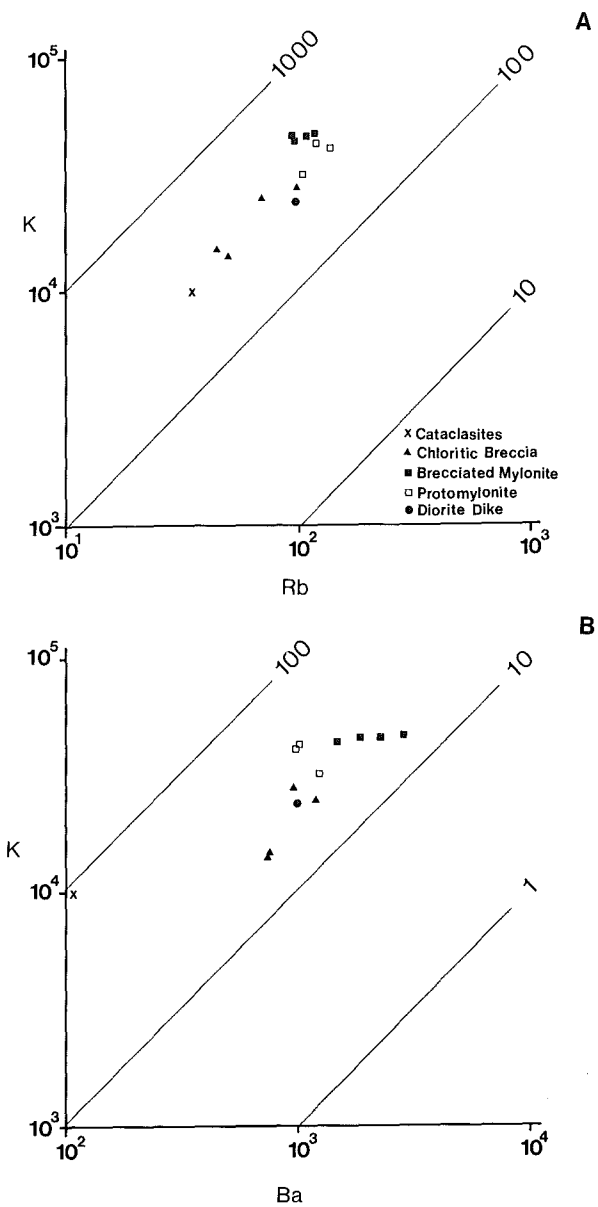

Figure 5. Plots of K vs. Rb and K vs. Ba.

Geochemical Trends

Profiles of the absolute abundance of selected major-element oxides and trace elements are plotted in structural sequence in Figure 4. The most notable trends in the transition from mylonites to chloritic breccias and cataclasites are increasing contents of Fe, Mn, and Mg, variable percentages of Ca and LOI, and systematically diminished levels of Si, Na, and especially K. These trends reflect the increasing abundance of chlorite, epidote, and Fe and Mn oxides, variable proportions of calcite (correlated trends in LOI and Ca), and the disappearance of plagioclase and K-feldspar relative to the mylonites. The cataclasites are also characterized by relatively abundant S, Cu, and Zn corresponding to the presence of disseminated chalcopyrite and sphalerite, whereas Pb content remains stable throughout the metasomatic sequence. As discussed above, these trends do not take into account either compositional variations intrinsic to differences in protolith or possible volume changes, and consequently cannot *a priori* be interpreted as real gains or losses of chemical components. Excursions in composition and mass-balance trends for sample no. 11 are probably due to its more mafic protolith, as signified by the conjunction of enhanced abundances of Ti, Fe, Mg, Ca, and Sc and a diminished level of Si.

Development of the chloritic breccia is marked by massive additions of Fe, Mn, and Mg relative to a hypothetical fresh, or least altered, precursor. Sympathetic gains of these elements are even more pronounced in the cataclasites and reflect the abundance of chlorite and Fe and Mn oxides. Levels of Si, K, and Na diminish up section through the chloritic breccias and cataclasites, and Na is quantitatively removed from the cataclasites where no plagioclase remains.

Levels of K, Rb, and Ba generally correlate well throughout the sequence of rocks and vary by a factor of more than 10 in absolute abundance (Fig. 5). In the mylonites, K/Rb averages 380, a value somewhat higher than the average for igneous rocks (250). Chloritic breccias and cataclasites trend toward somewhat lower ratios (K/Rb 315), possibly because of selective incorporation of Rb in secondary or hydrothermal phases. K/Ba ratios are remarkably uniform, though lower than in igneous rocks where K/Ba averages 40. Covariation of K and Ba is evident in lower-plate rocks; in upper-plate rocks, however, K/Ba ratios are scattered and extend to lower values because of the precipitation of barite (Kerrich and others, this vol.).

Stable-Isotope Relationships

Eight carbonate-bearing samples were analyzed for C- and O-isotopic compositions (Fig 6). These include four marbles and brecciated equivalents in the middle plate above the Buckskin detachment fault, two microbreccias from the detachment fault, and two lower-plate chloritic breccias from areas where calcite is present in syntectonic veins. Dolomite was identified in four of the eight samples, but only in minor quantities (Table 2).

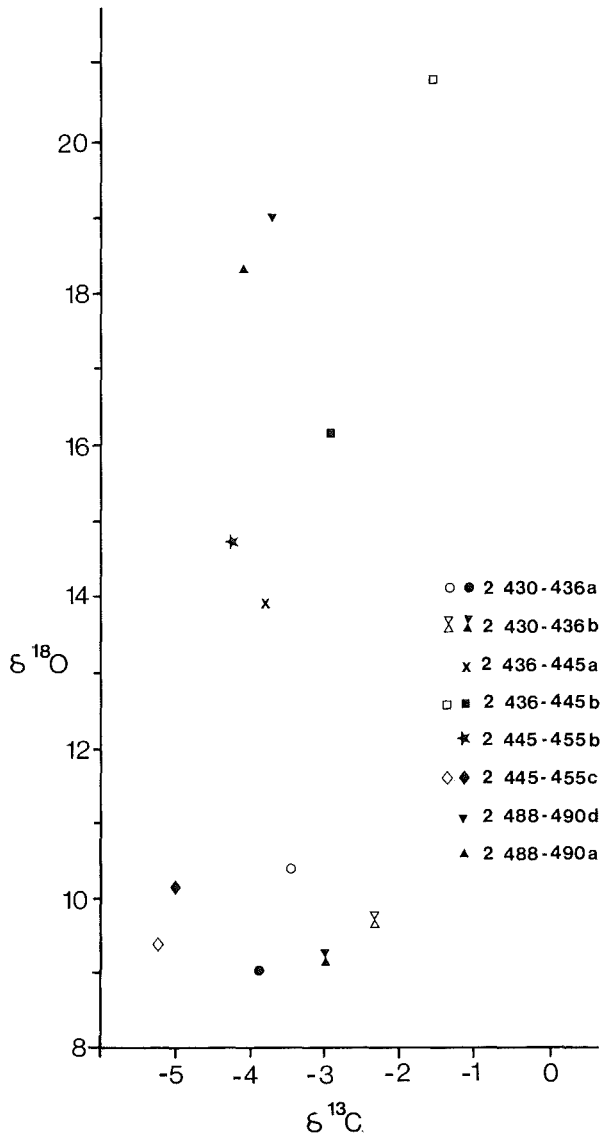

Figure 6. Plot of $\delta^{13}C$ vs. $\delta^{18}O$ for carbonates. Source of data: Table 2. Calcite is plotted with solid symbols; dolomite is plotted with open symbols. Prefix 2 indicates drill hole. Six-figure numbers are sample depths of core.

The total range of $\delta^{18}O$ values spans 9.0 to 20.8 per mil. Where dolomite is present, its $\delta^{18}O$ value positively correlates with that of coexisting calcite, but is variably displaced by -0.7 to +4.7 per mil (Fig. 7). There are too few data to define isotopic trends with any degree of confidence. However, $\delta^{18}O$ values appear to be more closely related to structural position than to primary lithology. In the middle-plate marbles, $\delta^{18}O$ values increase from 9 per mil to 14 to 16 per mil with increasing proximity to the detachment fault. A sharp downturn to 10 per mil has been recorded for one sample of unmineralized microbreccia, with a return to high $\delta^{18}O$ values in calcite veins within structurally subjacent chloritic breccia.

Carbonate minerals possess a relatively narrow range of $\delta^{13}C$ values from -5.2 to -1.6 per mil (the average $\delta^{13}C$ value of calcite is -3.8 $\pm$ 0.6 per mil, 1σ). In general, the dolomites are isotopically concordant with coexisting calcites. According to Ohmoto and Rye (1979), C-isotope fractionations are small between coexisting carbonate species under hydrothermal conditions.

Wilkins and Heidrick (1982) suggest that marbles of the middle plate are lacustrine in origin. Spencer and Reynolds (1987), however, proposed that Paleozoic marine carbonates are present in the section. C-isotopic compositions of freshwater carbonates ($\delta^{13}C$ = -9 to -2) are, on average, slightly depleted relative to marine carbonates ($\delta^{13}C$ = -3 to +4; Ohmoto and Rye, 1979). The $\delta^{13}C$ values of marbles (-2.9 to -3.9) do not discriminate between these alternatives (Table 2), particularly because all of the marbles have undergone pervasive isotopic exchange. The $\delta^{18}O$ values are substantially too low for primary limestones of either freshwater or marine origin. This indicates that either pervasive exchange occurred at moderate temperatures with a low $\delta^{18}O$ aqueous reservoir of probable meteoric or evolved meteoric origin or that some carbonates are hydrothermal deposits. Without temperature constraints, it is difficult to interpret the trends in $\delta^{18}O$ values of carbonates within the tectonic section. Such trends could represent either the tectonic juxtaposition of domains with different fluid-rock histories or, alternatively, hydrologically and/or temporally separated fluid regimes. Resolution of these questions awaits results of more comprehensive analyses of silicate and carbonate minerals. We note, however, that the total range of $\delta^{18}O$ values is comparable to that recorded for calcite in upper-plate volcanic rocks (see Kerrich and others, this vol.).

The source of C in the carbonate veins is also problematic. C-isotopic compositions of hydrothermal carbonates depend on the temperature, Eh, and pH at the site of precipitation, as well as the total C-isotopic composition of the hydrothermal fluid. Ohmoto and Rye (1979) have emphasized the difficulties in interpreting the source of C in hydrothermal carbonates where $\delta^{13}C$ values are approximately -5 per mil because the average $\delta^{13}C$ values for igneous, metamorphic, and sedimentary rocks are all about -5 per mil. The source reservoir for the hydrothermal carbonates may have been the middle-plate limestones, dissolved and redistributed by hydrothermal systems in the core complex.

SUMMARY AND CONCLUSIONS

The transition from ductile mylonites through brittlely deformed equivalents to chloritic breccias at the detachment fault is a characteristic feature of metamorphic core complexes. At Copper Penny, mylonites developed in the lower plate from a granitic precursor under amphibolite-facies conditions, as signified by the dominantly biotite-stable mineral assemblage. Sporadic overprinting under greenschist-facies conditions is indicated by the development of chlorite and brittle fracturing of feldspar in mylonites.

Development of the mylonites involved ductile deformation under greenschist-facies conditions. This

Table 2. $\delta^{18}O$ and $\delta^{13}C$ values of carbonates in the middle plate, detachment zone, and lower plate in the Buckskin Mountains.

Sample Number	Depth	Rock Type	1 hr $\delta^{13}C$	1 hr $\delta^{18}O$	24 hr $\delta^{13}C$	24 hr $\delta^{18}O$
2 430-436a	430-436	marble with calcite veins	-3.9	+9.0	-3.4	+10.4
2 430-436b	430-436	brecciated marble	-3.0	+9.2	-2.3	+9.7
2 436-445a	436-445	brecciated marble	-3.8	+13.9	-	-
2 436-445b	436-445	marble	-2.9	+16.1	-1.6	+20.8
2 445-455b	445-455	mineralized flinty micro-breccia	-4.3	+14.7	-	-
2 445-455c	445-455	unmineralized flinty micro-breccia	-4.9	+10.2	-5.2	+9.4
2 488-490d	488-490	hematized chloritic breccia	-3.7	+18.9	-	-
2 488-490a	488-490	chloritic breccia	-4.1	+18.3	-	-

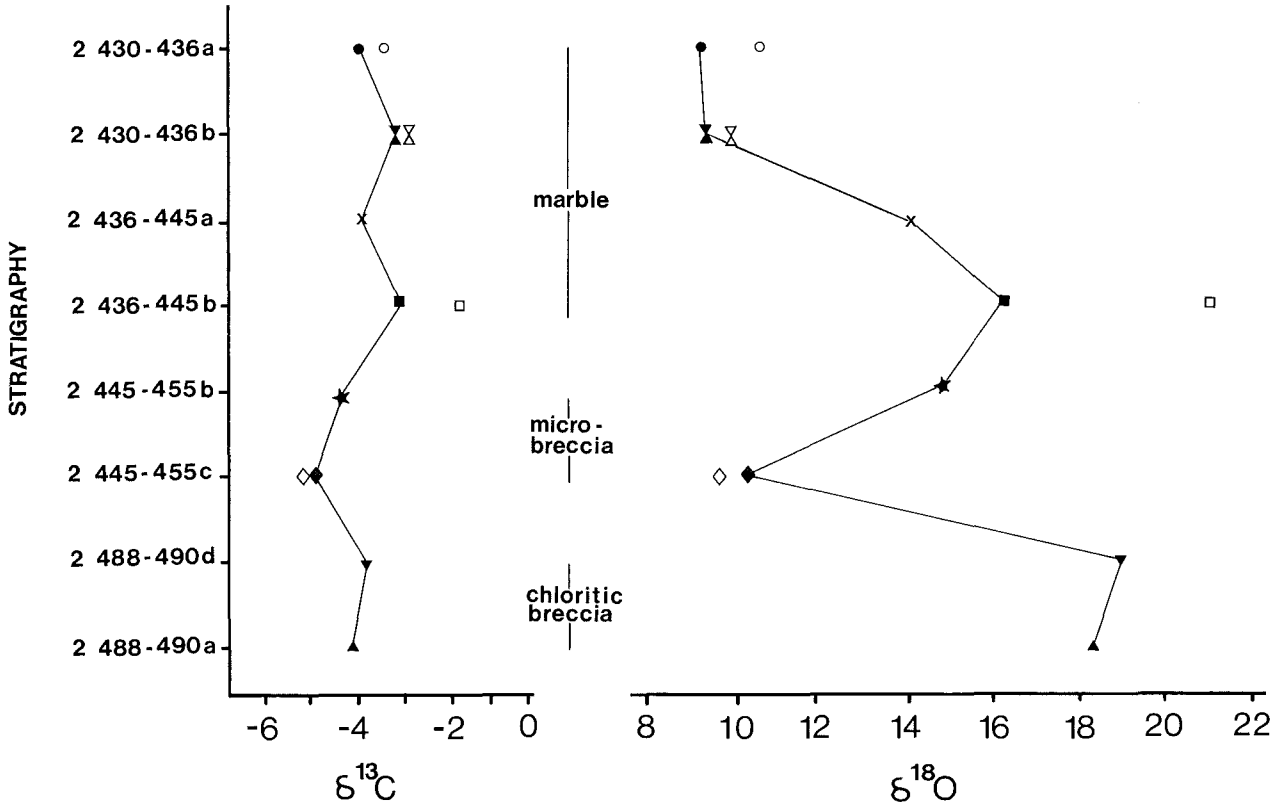

Figure 7. Plot of $\delta^{18}O$ and $\delta^{13}C$ of carbonates against stratigraphic position. Source of data: Table 2. Calcite is plotted with solid symbols; dolomite is plotted with open symbols. Prefix 2 indicates drill hole. Six-figure numbers are sample depths of core.

process was essentially isovolumetric and isochemical, except for subtle additions of Fe, Mg, and LOI near the detachment fault, reflecting the incipient chloritization of plagioclase.

Chloritic breccias at the detachment fault developed from a protolith different from the underlying mylonites, and cataclasites represent a heterogeneous tectonic mix of several different lithotypes. Both the chloritic breccias and cataclasites record massive additions of Fe, Mn, and Mg, corresponding to abundant chlorite and Fe and Mn oxides. Concomitant losses of Na and K reflect the hydrolysis of plagioclase and K-feldspar during chloritization.

O-isotopic compositions of calcites vary greatly, and $\delta^{18}O$ values are erratically distributed through the tectonic section. The magnitude of the range is attributed to variations in both temperature of deposition and $\delta^{18}O$ values of hydrothermal fluids, which included a component of low-^{18}O meteoric or evolved meteoric water. Because the ranges of $\delta^{18}O$ and $\delta^{13}C$ values of calcite in the middle and lower plates at Copper Penny are similar to the isotopic ranges of calcites in upper-plate volcanic rocks (Kerrich and others, this vol.), we infer that the carbonates formed from a common fluid reservoir(s) and under similar ambient conditions. The source of C in the carbonates remains obscure, but dissolution of middle-plate limestones is a plausible source.

Differences between processes that caused chloritic alteration in lower-plate breccias, and alteration of upper-plate rocks, as reflected in mineralogy, composition, and oxidation state of Fe, can be explained by a two-fluid reservoir system. A deeper level, higher temperature, more reduced and crust-equilibrated hydrothermal fluid produced the chloritic breccias, whereas at higher structural levels, a cooler, more oxidized, and less isotopically evolved reservoir was involved in alteration of the upper plate. The latter reservoir locally penetrated downward to overprint earlier and higher-temperature assemblages with calcite, Fe and Mn oxides, and sulfates.

More detailed work is required to define geochemical trends in the development of mylonites and chloritic breccias. In addition, comparative studies are required to establish the nature and magnitude of differences between chloritic breccias at Copper Penny and counterparts in detachment faults where Cu, Zn, and Mn mineralization is absent.

ACKNOWLEDGMENTS

The authors express their appreciation to J. Spencer and S. Reynolds for the invitation to submit this contribution. Special thanks are extended to S. Reynolds for an incisive critique of an earlier draft, for insightful discussions on metamorphic core complexes, and for clarifying many of their geologic relationships. We thank E. McLarty for skillful assistance in preparing the text and drafting many of the diagrams, R. Daddar for help with the isotopic analyses, and A. Heppner for typing the manuscript. R. Kerrich acknowledges support from an operating grant from the Natural Science and Engineering Research Council of Canada.

Volcanic rocks in the suprastructure of metamorphic core complexes, southwest Arizona: Geochemical and isotopic evidence for primary magma types and secondary hydrothermal regimes

ROBERT KERRICH *Department of Geological Sciences, University of Saskatchewan, Saskatoon, Saskatchewan, Canada S7N OWO*
WILLIAM A. REHRIG *Applied Geologic Studies, 2875 W. Oxford #3, Englewood, Colorado 80110*
ELISABETH McLARTY *Department of Geology, University of Western Ontario, London, Ontario, Canada N6A 5B7*

ABSTRACT

A compositionally distinct facies of Oligocene-Miocene volcanic rocks form part of the suprastructure of metamorphic core complexes (MCC) in southwestern Arizona and southeastern California. The volcanic rocks were extended by movement on listric normal faults in the upper plate of detachment faults of the MCC. The volcanic rocks were metasomatized and altered to an assemblage of K-feldspar, calcite, and Fe and Mn oxides; most replacement occurred near the detachment faults.

These volcanic rocks were formerly thought to be andesites, dacites, or, based on whole-rock chemical analyses, ultrapotassic trachytes; however, the high abundances of alteration-insensitive incompatible elements (Th, LREE, P_2O_5, and fractionated REE distributions [$La_{cn}/Yb_{cn} \approx 18$]) and the elevated levels of mafic-affiliated trace elements (Cr, Co, Ni, and Sc) indicate that these volcanics were originally alkali basalts and intermediate rocks. In addition, primary K_2O contents are estimated at 3 to 6 wt. % and troughs are consistently present at Ta, Nb, and Ti on chondrite-normalized diagrams. Collectively, these characteristics are similar to those of alkali basalts that form during late stages of extension, in association with convergent plate boundaries.

Hydrothermal alteration in the volcanics involved introduction of massive quantities of K, Fe, Ca, and CO_2, which is evident by the abundance of secondary K-feldspar, hematite, and calcite. Na was systematically depleted. Whole-rock $\delta^{18}O$ values span 4 to 18 per mil, which confirms the extent of isotopic exchange with an aqueous reservoir. Alteration occurred at temperatures of 100° to 250° C, where fluid $\delta^{18}O$ is estimated at limiting values of -11 to +11 per mil.

The sources of K, Fe, Ca, and CO_2 remain unknown, but may have involved extensive internal redistribution of these components within the surficial upper-plate setting and/or fluid expulsion from the ductilely deformed lower plates. The latter may be due to dehydration triggered by isothermal decompression during extension.

in Spencer, J.E., and Reynolds, S.J., eds., 1989, Geology and mineral resources of the Buckskin and Rawhide Mountains, west-central Arizona: Arizona Geological Survey Bulletin 198, p. 203-214.

INTRODUCTION AND SCOPE OF STUDY

Volcanic rocks of Oligocene-Miocene age are widely distributed in western Arizona and adjacent areas of southeastern California. A compositionally distinct facies of these rocks is near the metamorphic core complexes (MCC) of this region, in upper-plate or suprastructure positions. The volcanics largely consist of flows intercalated between chaotic sedimentary breccias and fanglomerates and in some critical respects are distinct from coeval volcanic-sedimentary counterparts distal to the MCC. Listric normal faulting in these volcanic rocks reflects extension above the detachment faults of the MCC (e.g., Coney, 1980). The upper-plate volcanic rocks display variable degrees of metasomatism and alteration, with the most intense development generally associated with detachment faults (Brooks, 1985, 1986). Alteration is manifest as secondary K-feldspar, carbonate, and Fe and Mn oxides and hydroxides.

This paper reports the results of a preliminary geochemical and isotopic study of these volcanic rocks, to clarify their primary magmatic character, and to quantify the geochemical mass transport involved in their alteration. Because of the limited sample population, conclusions regarding the timing, nature, and conditions of K-concentration processes should be considered preliminary and general.

SAMPLES AND PETROGRAPHIC CHARACTERISTICS

Representative samples of upper-plate volcanic rocks were collected from Savahia Peak, the southern Riverside, Whipple, Buckskin, and Harquahala Mountains (Fig. 1), and the Picacho area (Fig. 2); all areas correspond to or are associated with Cordilleran MCC. Given the reconnaissance nature of this study, the number of samples that had complete geochemical analyses is limited. A

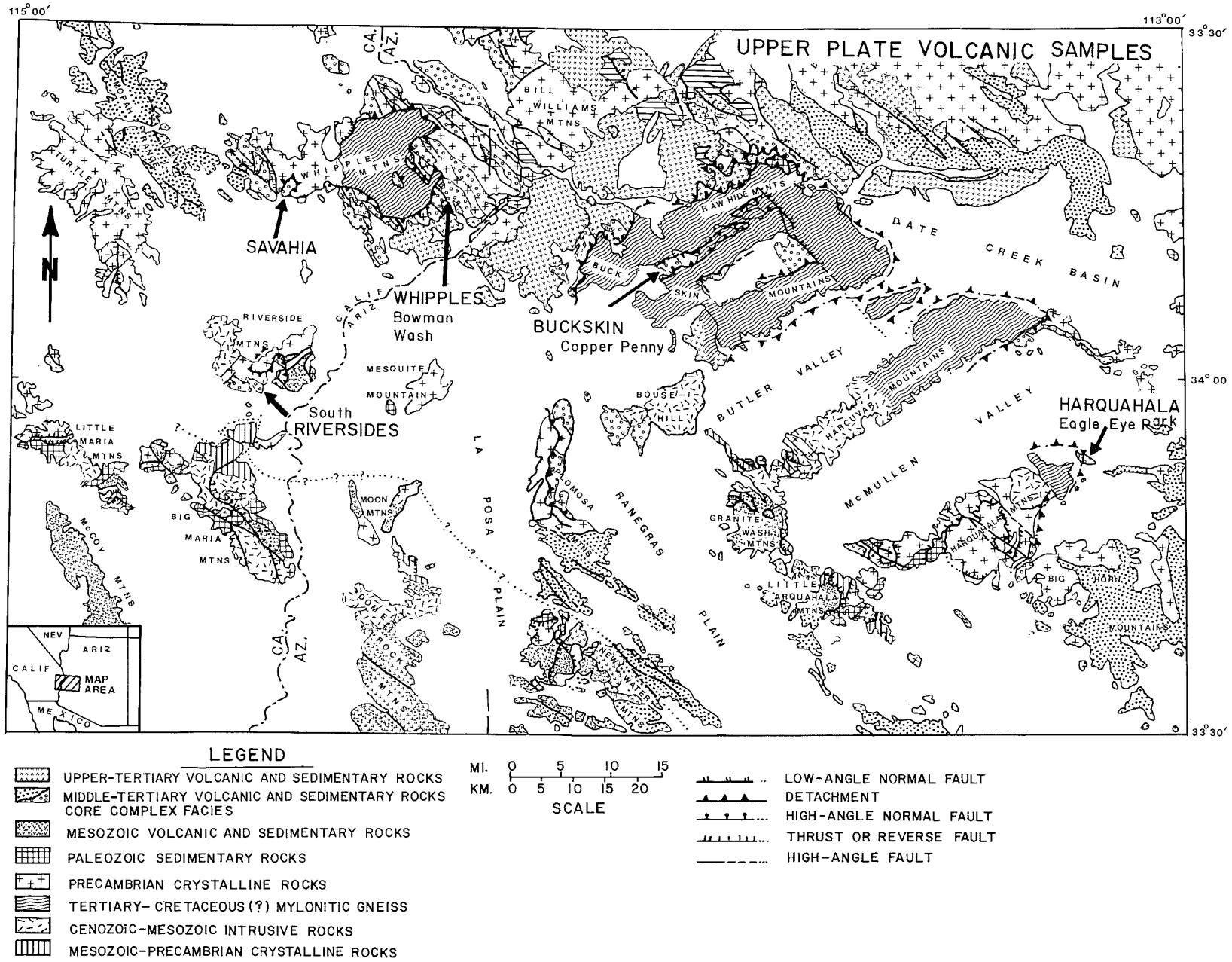

Figure 1. Simplified geologic map of western Arizona and neighboring areas of eastern California (Fig. 1 of Spencer, 1984a) showing the sample locations of upper-plate volcanic rocks.

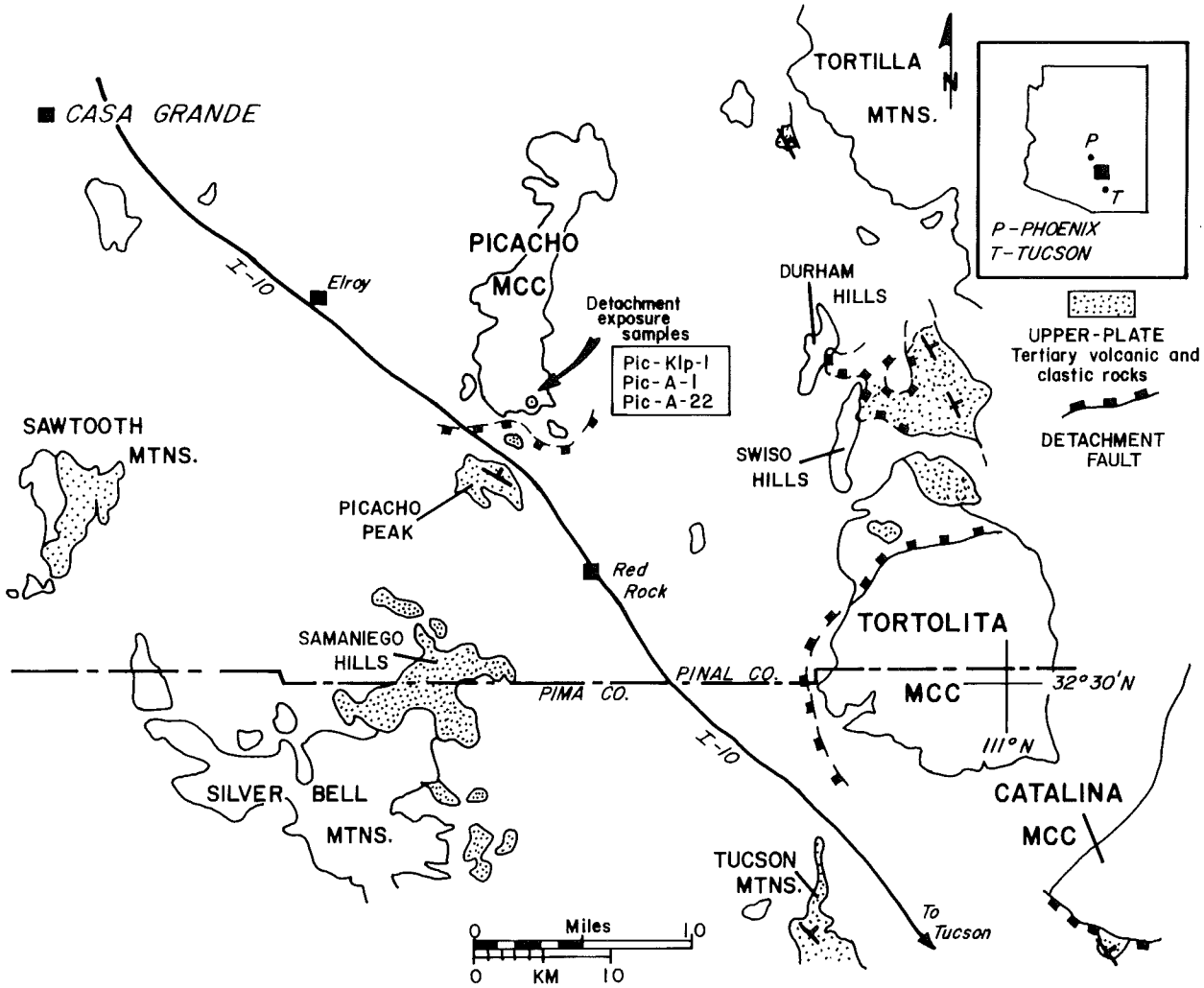

Figure 2. Simplified geologic map of the Picacho area of south-central Arizona showing sample locations of upper-plate volcanic rocks.

more comprehensive suite of rocks was collected and data for some of these rocks have been plotted in the variation diagrams.

The majority of the upper-plate volcanic rocks are autobrecciated flow units that have experienced intense hydrothermal alteration. Plagioclase phenocrysts, albeit altered, are sporadically preserved, as are trachytic textures. Most of the plagioclase phenocrysts and matrix have been converted to secondary K-feldspar, although some relict laths are anorthoclase or labradorite. In many samples, the high-K rocks appear unaltered: they appear to consist of fresh phenocrystic and interstitial K-feldspar and are devoid of primary quartz. Thus, initial analysis of petrographic and analytical data suggests that the rocks formed from lava flows composed almost exclusively of K-feldspar. Representative microprobe analyses of feldspars are presented in Figure 3. Variably abundant secondary carbonate, which is mostly calcite, and minor secondary quartz are present in the rocks. Hematite is disseminated throughout the volcanic rocks, but is concentrated in late microfractures as are Mn-oxides. Deposition of anhydrite in tensile microfractures appears to reflect the last stage of fluid infiltration. The geometry of these fractures indicates dilation in three orthogonal directions. Further details of the petrographic characteristics are given in Halfkenny (1985) and Kerrich and others (1986).

ANALYTICAL METHODS

X-ray fluorescence spectrometry was used to identify major-element oxides and S, Cr, Co, Ni, Cu, Zn, Pb, Rb, Sr, Y, Zr, Nb, and Ba. Instrumental neutron activation analysis (INAA) was used to analyze Au, As, Sb, Sc, Ta, and the REE. Ag was analyzed by conventional atomic absorption photospectrometry.

Oxygen was extracted from minerals and whole-rock powders with BrF_5 and converted to CO_2 prior to mass spectrometric analysis according to the technique of Clayton and Mayeda (1963). CO_2 was extracted from carbonate minerals using 100% H_3PO_4 (McCrea, 1950). Isotopic data for oxygen are reported as $\delta^{18}O$ values in per mil relative to Standard Mean Ocean Water (SMOW), and for carbon as $\delta^{13}C$ values referenced to PDP. Analysis of NBS-28 gave 9.6 per mil (cf. Coplen and others, 1983).

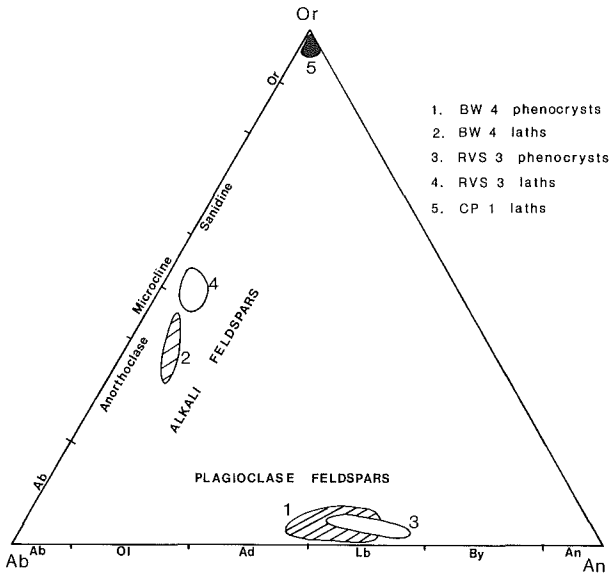

Figure 3. Representative feldspar analyses from volcanic rocks.

GEOCHEMISTRY

Introduction

In attempting to deduce the original geochemical characteristics of volcanic rocks in the upper plate, we found it difficult to separate primary compositional features intrinsic to the magmas from secondary effects induced by superimposed chemical exchange during ensuing alteration. Accordingly, emphasis was placed on elements such as Ti, Al, Sc, Th, Hf, Cr, Ni, and the REE, which are less sensitive to alteration during most hydrothermal metasomatism, but whose abundances and mutual interelement ratios may be diagnostic of primary magmatic parentage, even in altered products (Pearce and Cann, 1973; Floyd and Winchester, 1978; Jahn and others, 1980; Costa and others, 1983; Kerrich, 1983).

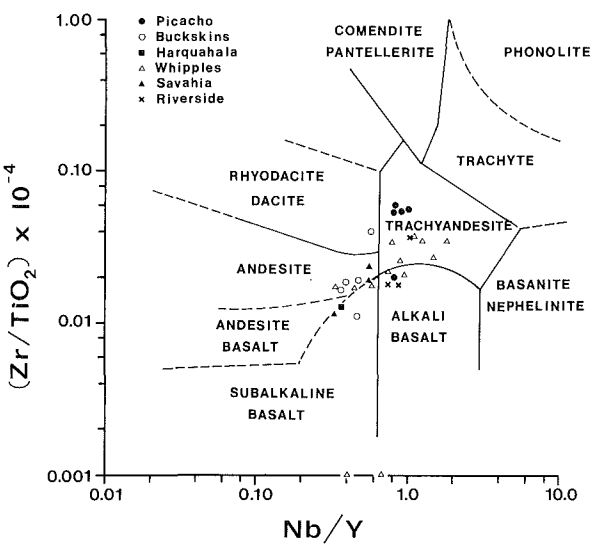

Figure 4. Discrimination diagram, modified from Floyd and Winchester (1978). Data for upper-plate volcanic rocks cluster within mafic to intermediate alkaline fields.

For the suite of volcanic rocks under study, the problem of separating primary from secondary geochemical characteristics is compounded by the fact that many of the samples appear to be compositionally related to mafic alkaline rocks, but at the same time K addition is the single most diagnostic feature of secondary hydrothermal processes. Keeping this factor in mind, we plotted the data on diagrams cast in coordinates of incompatible to compatible element ratios, or normalized abundances. On such diagrams the rocks separate into data clusters or groups of elements commensurate with independent field, textural, and petrographic criteria (Fig. 4).

Picacho Peak

Fragmental volcanic rocks in the upper plate of the southern Picacho Range (Fig. 2) are intensely altered to an assemblage of K-feldspar, carbonate, and hematite, specifically in domains superjacent to the Picacho detachment fault (Brooks, 1985; Rehrig, 1986). Hydraulic carbonate breccias sporadically developed at the base of the upper plate attest to hydrothermal activity (Kerrich and Rehrig, 1987). These altered flow units have formerly been referred to as dacites or andesites (Briscoe, 1967) and ultrapotassic trachyte flows (Shafiqullah and others, 1976).

The volcanic rocks are compositionally uniform with respect to many of the major-element oxides and trace elements (Table 1). A characteristic feature is the spectacularly enhanced abundance of K_2O (1.3 to 10.9 wt. %). CaO (7.9 to 11.0 wt. %), volatiles (7.5 to 8.8 wt. %), Fe_2O_3 (5.9 to 6.6 wt. %), and P_2O_5 (0.6 to 1.0 wt. %) are also present at uniformly high levels relative to typical dacites or andesites. Bulk-rock compositions are controlled by the relative modal proportions of K-feldspar, calcite, hematite, and apatite. The volcanic rocks contain systematically low levels of SiO_2 (47.2 to 48.9 wt. %) and Na_2O (0.45 to 0.52 wt. %).

In terms of trace-element distribution, the volcanic rocks are characterized by relatively enhanced levels of Cr (81 $\pm$ 21 ppm, 1δ), Ni (33 $\pm$ 4.5 ppm), Th (10 $\pm$ 0.1 ppm), Zr (472 $\pm$ 44 ppm), Rb (407 $\pm$ 26 ppm), and Ba (1,403 $\pm$ 289 ppm; Table 1). REE patterns show systematic enrichments of the LREE ($La_{cn} \approx 200$), followed by a smooth monotonic decrease to Dy, and a flat HREE profile. Overall, the REE are moderately fractionated, where La_{cn}/Yb_{cn} equals approximately 18 (Fig. 5). On the discrimination diagram of Floyd and Winchester (1978), cast in Zr/TiO_2 versus Nb/Y coordinates, the data cluster in the fields of trachyandesite and alkali basalt (Fig. 4).

Whipple Mountains and Savahia Peak

Upper-plate volcanic rocks in the Whipple Mountains and Savahia Peak have many of the compositional features of similar rocks in the Picacho area. K is

systematically but variably enriched from 2.4 to 13.4 wt. % K_2O. Similarly, Fe_2O_3, CaO, and LOI contents are variably but systematically high. SiO_2 and Na_2O are present at low absolute levels. Bulk chemical compositions are controlled by the relative modal proportion of K-feldspar, hematite, and calcite. Concentrations of P_2O_5 are consistently lower than in their volcanic counterparts in the Picacho area. Some of the variability in abundance of major-element oxides is controlled by the extent of secondary-calcite deposition. For example, levels of SiO_2 are highest in samples containing the lowest CaO and LOI, and the converse also holds true (Table 1).

Similarities in major-element oxide compositions of the Picacho and Whipple Mountain volcanic rocks extend to trace-element distributions. The suite of samples from the Whipple Mountains are characterized by variably enhanced abundances of Cr (179 $\pm$ 81 wt. %), Ni (79 $\pm$ 61 wt. %), Zr (248 $\pm$ 81 wt. %), Rb (262 $\pm$ 163 wt. %), and Ba (1,408 $\pm$ 735 wt. %). REE patterns display systematic enrichments in the LREE (La_{cn} = 90), a smooth monotonic decrease to Dy, and flat HREE profiles (Fig. 5). Lower absolute abundances of the REE and Th, with correspondingly less-fractionated patterns, correlate with diminished levels of P_2O_5 in the Whipple Mountain volcanics compared to equivalents at Picacho Peak (Table 1; Figs. 5 to 8). These relationships may signify that a trace phosphorous phase, such as apatite, controls REE distributions. Data from the Whipple Mountain volcanic rocks cluster around the apex of the trachyandesite, alkali basalt, and andesite fields on the discrimination diagram (Fig. 4).

Harquahala, Buckskin, and Riverside Mountains

There are fewer data available for Tertiary volcanic rocks from the Harquahala, Buckskin, and Riverside Mountains (Table 1). Within constraints imposed by limited data, these volcanic rocks share mineralogic and compositional characteristics with their counterparts in the Picacho and Whipple Mountain areas. As discussed above, the prominent geochemical features are variably enhanced levels of K_2O, Fe_2O_3, CaO, LOI, and P_2O_5, in conjunction with elevated abundances of incompatible (Th and Zr) and mafic-affiliated (Sc, Cr, and Ni) trace elements.

LIGHT STABLE-ISOTOPE SYSTEMATICS

Results of oxygen-isotope analyses on volcanic rocks pretreated for the removal of carbonate are reported in Table 2. The table also lists determinations of $\delta^{18}O$ and $\delta^{13}C$ values for carbonate minerals from the upper-plate rocks expressed in 1-hour and 24-hour extractions; the former corresponds to calcite and the latter to dolomitic carbonate.

Whole-rock $\delta^{18}O$ values of the silicate fraction are extremely erratic; values range from 3.8 to 18.1 per mil (Table 2; Fig. 9). Fresh tholeiitic rocks from the oceanic environment are characterized by a restricted range of $\delta^{18}O$ values of 5.7 $\pm$ 0.3 per mil. Alkaline volcanic rocks are systematically enriched in $\delta^{18}O$ relative to tholeiitic basalts, extending up to a maximum of about 7.5 per mil (Kyser and others, 1982; Fig. 9). On this basis it is evident that upper-plate volcanic rocks throughout western Arizona and neighboring areas of eastern California have undergone pervasive oxygen-isotope exchange with an external aqueous reservoir. The pronounced disturbance from primary magmatic $\delta^{18}O$ values corroborates the altered nature of these volcanic rocks as independently deduced from geochemical and petrographic criteria.

In the absence of constraints on the ambient temperatures of exchange, it is difficult to calculate the oxygen-isotope composition of the hydrothermal fluids. For example, a temperature range of 100° to 250° C would yield limiting values for $^{18}OH_2O$ of -11 to +11 per mil ($\delta^{18}O$ ksp = 6; 100° C and $\delta^{18}O$ ksp = 18; 250° C). These estimates are based on a linear extrapolation of the alkali-feldspar/water equation of O'Neil and Taylor (1967). Fluids with this isotopic composition could represent evolved meteoric water or mixtures of various independent fluid reservoirs. Additional data would be required to resolve this issue.

Oxygen-isotope compositions of carbonate minerals are also erratically distributed, spanning a total interval of 10.1 to 24.9 per mil (Table 2). In general, the 1-hour and 24-hour extractions agree to within 0.6 per mil; contamination from oxygen in sulfates might be responsible for some of the disparity. Carbonate $\delta^{13}C$ values range from -6.6 to 0.2 per mil.

Textural observations reveal that the precipitation of carbonate minerals occurred during and after the development of secondary K-feldspar. The $\delta^{18}O$ values for silicate and carbonate minerals are positively correlated, albeit they are highly scattered (Fig. 10). These isotopic relationships are consistent with the generation of K-feldspar and carbonate in the same hydrothermal regime, where the coupled trend for high values of $\delta^{18}O$ is a function of diminishing temperatures.

A covariant relationship exists between the $\delta^{18}O$ and $\delta^{13}C$ values of the carbonate minerals (Fig. 11). Most of the scatter in the isotopic data can be explained by variable temperatures of equilibration, given that $\delta^{18}O$ and $\delta^{13}C$ values of hydrothermal carbonates undergo positive shifts with diminishing temperatures when all other variables are held constant.

Carbon-isotope compositions of hydrothermal carbonates depend on the T, Eh, and pH at the site of precipitation, as well as the total carbon-isotope composition of the hydrothermal fluid. Ohmoto and Rye (1979) emphasized the difficulties inherent to interpreting the source of carbon in hydrothermal carbonates when $\delta^{13}C$ values are approximately -5 per mil, given that the average $\delta^{13}C$ values for igneous, sedimentary, and metamorphic rocks are also about -5 per mil.

DISCUSSION

Primary Versus Secondary K-Enrichment

Mafic volcanic rocks characterized by extremely

Table 1. Abundances of major-element oxides and selected trace elements in volcanic rocks. Major-element oxides are given in weight percent, trace elements in ppm, and Au in ppb.

Location Sample	PICACHO			HARQUAHALA			BUCKSKINS	WHIPPLES		
Number	1	2	3	4	5	6	7	8	9	10
SiO_2	47.70	47.20	48.90	43.20	32.60	43.20	43.3	47.10	56.40	44.60
TiO_2	0.90	0.83	0.79	0.99	0.75	1.07	0.75	1.18	0.93	1.07
Al_2O_3	14.10	13.70	13.40	12.80	10.70	14.30	13.00	15.90	16.10	14.50
Fe_2O_3	6.58	5.88	6.15	7.48	0.92	10.10	5.65	9.49	6.44	8.86
MnO	0.10	0.13	0.11	0.31	0.93	0.39	0.30	0.17	0.10	0.26
MgO	0.36	0.29	0.74	0.50	3.42	5.68	0.0	4.57	0.83	2.07
CaO	9.69	11.00	9.86	12.10	19.10	7.13	13.10	9.09	2.67	8.46
K_2O	11.10	11.30	10.90	10.80	6.23	6.71	11.26	2.39	12.50	9.64
Na_2O	0.45	0.46	0.52	0.15	0.27	0.79	0.04	1.58	0.54	0.41
P_2O_5	0.70	0.60	1.04	0.35	0.25	0.32	0.18	0.25	0.27	0.34
LOI	7.93	8.77	7.47	10.40	18.20	10.50	11.30	8.23	3.16	9.00
Total	99.90	100.40	100.10	99.30	100.40	100.40	100.10	100.10	100.20	99.50
* S	<4	<4	309	<4	<4	<4	<1	<4	820	79
Au	6	4	<5	<2				<3	<3	<3
Ag			<2							
Sc	11.2	11.1	10.5	17.8	23	29	15	33.5	15.5	21.2
Cr	69	63	111	130	334	376	194	202	106	327
Co	72	48	4	<3	42	44	15	70	17	62
Ni	309	28	33	37	120	131	18	91	46	206
Cu	66	142	35	41	57	33	146	20	21	26
Zn	77	132	38	61	828	758	88	165	67	165
Pb	405	365	334	138	93	40	73	36	60	59
Th	9.9	10	10	1.1	2.7	3.6	1.7	2.8	7	4.9
U	2.5	1.6	2.2	1.7	1.9	1.6	5.3	1.1	1.8	1.4
Rb	442	401	379	463	255	315	316	65	488	328
Sr	314	262	247	1469	179	342	276	472	186	211
Y	35	29	30	31	27	30	17	31	26	25
Zr	533	455	429	131	125	199	83	193	373	227
Hf	11	9	7.6	2.7	2.3	2.9	2.1	3.6	7.2	4.4
Nb	29	28	25	10	10	12	8	14	27	24
Ta	2	2	0.8	<1	<1	<1	<0.5	<1	2	1
Ba	1727	1457	1026	1859	552	727	1630	811	1690	1216

enhanced abundances of K may be the result of either specialized lithophile-element enrichment processes in the mantle source regions, or alternatively from secondary enrichment of magmas that were not necessarily intrinsically potassic. Inasmuch as primary alkaline mafic rocks (*sensu stricto*) convey information regarding tectonic setting, and secondary K-enrichment provides constraints on hydrothermal regimes, it is clearly of paramount importance to address the timing and context of K-enrichment processes.

Discrimination of primary magmatic characteristics from secondary effects is generally resolvable on the basis of petrography, the abundances and mutual ratios of alteration-insensitive elements, and light stable-isotope systematics. Mafic igneous rocks with primary K-enrichment generally contain enriched proportions of the associated large-ion-lithophile (LIL) elements, such as Ba, Rb, Th, and the LREE, as well as elevated amounts of Zr, P_2O_5, Sc, Cr, and Ni. Of these LIL elements, Th and, to a lesser extent, the LREE are relatively immobile compared to Ba, Rb, and K. Accordingly, a signature of primary alkaline mafic rocks may be retained even in samples in which the latter three elements have been severely disturbed by hydrothermal processes. On the other hand, secondary concentration of K may be accompanied by enrichment of Ba and Rb (Fig. 8), but the behavior of these alkali and alkaline earth metals is decoupled from Th and the LREE, as well as from P_2O_5, Zr, Cr, Ni, and Sc.

Igneous rocks characterized by pronounced second-

Table 1 (continued)

Location Sample	WHIPPLES			SAVAHIA			RIVERSIDES		
Number	11	12	13	14	15	16	17	18	19
SiO_2	57.26	46.40	56.40	41.40	35.30	49.40	51.80	45.70	42.50
TiO_2	0.93	1.42	0.92	0.72	0.76	0.81	1.27	1.02	1.39
Al_2O_3	16.16	16.40	16.80	11.90	10.70	15.00	15.20	13.00	16.70
Fe_2O_3	6.54	10.50	6.31	5.51	6.31	3.54	8.28	6.05	8.90
MnO	0.03	0.29	0.17	0.53	0.24	0.40	0.44	0.30	0.19
MgO	0.24	3.85	0.36	0.47	0.58	0.68	0.53	0.74	1.39
CaO	2.81	11.90	1.94	15.10	19.60	8.38	4.25	11.10	12.40
K_2O	13.40	1.30	12.70	9.87	9.01	11.70	12.10	10.90	3.29
Na_2O	0.38	2.57	0.59	0.26	0.09	0.04	0.44	0.10	2.40
P_2O_5	0.25	0.26	0.22	0.47	0.11	0.23	0.31	0.49	0.67
LOI	2.31	5.39	2.23	12.50	16.80	7.85	3.85	9.62	9.00
Total	100.50	100.40	99.20	99.10	99.70	99.00	98.90	99.30	99.10
* S		<1	112		13	781	635	549	421
Au		<5			<3	<3	<3		<5
Ag		<2							
Sc	15	32.4	15.1	16.1	23.2	22.6	22.9	17	16.8
Cr	105	219	113		214	347	116	357	90
Co	<3	38	17		8	26	9	20	27
Ni	23	68	40		48	33	25	54	83
Cu	31	22	9		46	41	85	54	46
Zn	38	258	83		170	102	66	56	890
Pb	103	45	44		119	251	784	57	187
Th	7	1.2	7.8	8.3	0.6	4.9	4.1	5.7	9.1
U	2.3	0.5	2.0	2.5	1.2	1.6	1.4	17	2.4
Rb	320	27	347		353	393	407	257	110
Sr	90	552	210		55	1060	1619	114	1194
Y	20	27	12		21	26	32	31	27
Zr	250	123	319		87	192	239	183	249
Hf	6.6	2.8	7.2	6.1	1.4	3.8	4.5	4.2	6.2
Nb	30	11	22		7	15	18	23	24
Ta	1	0.6	1.0	1	<1	<1	<1	0.7	<0.6
Ba	1890	294	2549		1317	2899	2011	1964	1102

ary K-enrichment have been described for a variety of geologic environments, including spilitized ocean-floor rhyolites, gold deposits, porphyry Cu and Mo deposits, and MCC. Munha and others (1980) described how primary rhyolites from the Iberian pyrite belt have been converted to adularia-bearing products with the addition of approximately 8 wt. % K_2O. This process involved the ion-exchange reaction of K in seawater with Na and Ca in igneous plagioclase during low-temperature spilitization. The adularia is characterized by shifts of about +10 per mil in $\delta^{18}O$ relative to the plagioclase reactant, with corresponding negative quartz/K-feldspar fractionations. Munha and others (1980) concluded that, whereas Na-metasomatism of submarine volcanic rocks was the predominant style of alteration in the oceanic environment (Na/K seawater = 28), potassic alteration was thermodynamically favored at temperatures of $\leq 150^{\circ}$ C. Extreme potassic alteration and similar $\delta^{18}O$ enrichment have also been reported in volcanic rocks of primary trondhjemitic composition from the Malartic area of the Archean Abitibi greenstone belt (Kerrich, 1983).

A distinct style of K-feldspar-dominated alteration

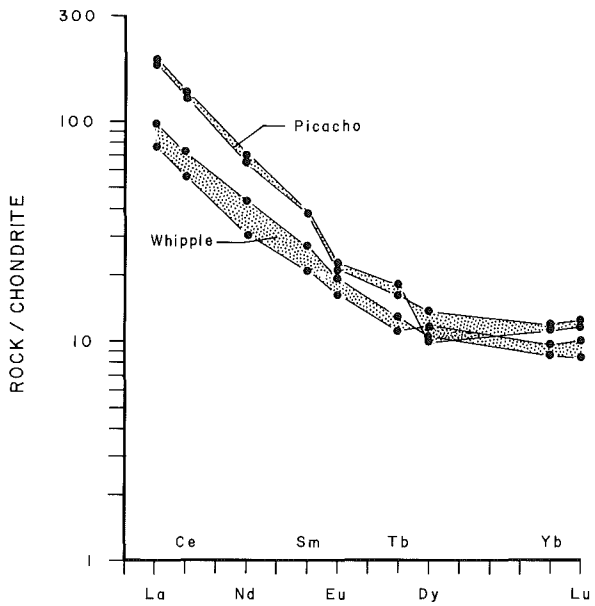

Figure 5. Envelopes of chondrite-normalized rare-earth-element distributions for representative volcanic rocks from Picacho Peak and the Whipple Mountains.

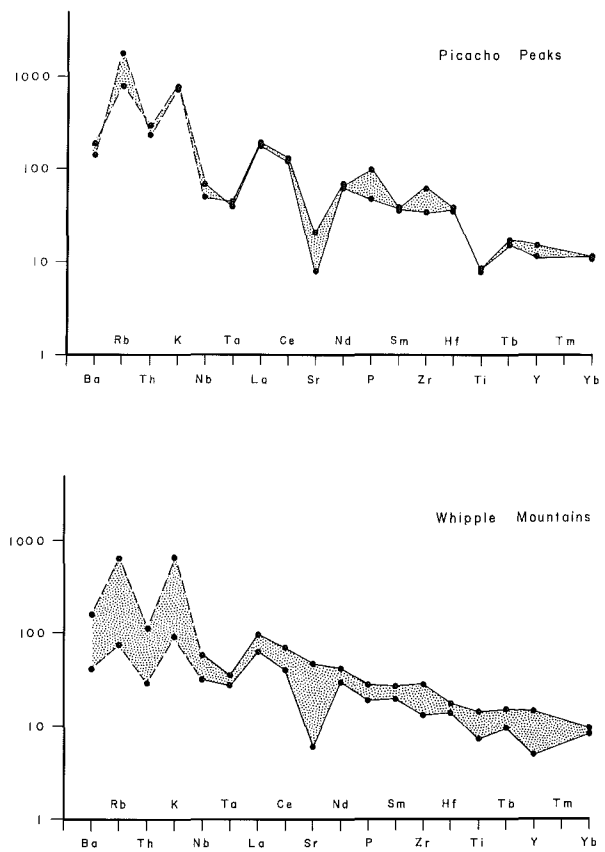

Figure 6. Extended chondrite-normalized element distributions for volcanic rocks from Picacho Peak and the Whipple Mountains. Normalizing factors after Thompson and others (1984).

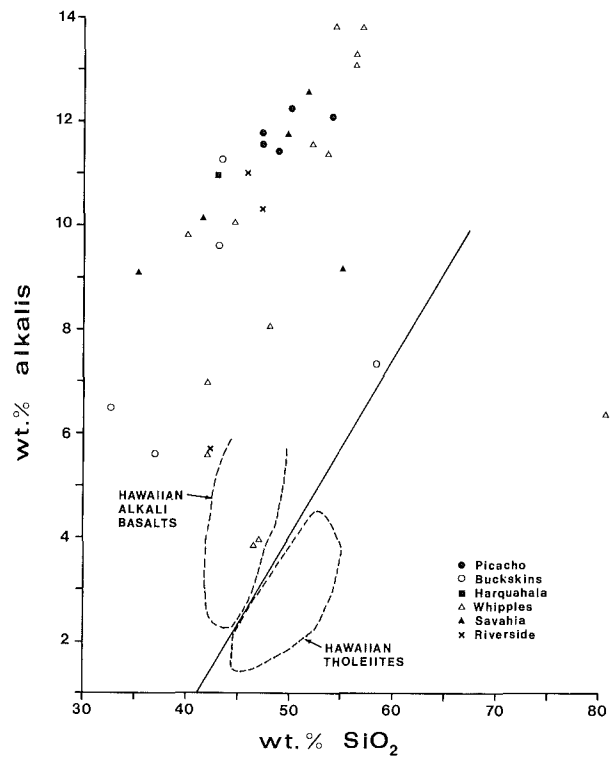

Figure 7. Plot of alkalis (Na_2O + K_2O) versus SiO_2 for upper-plate volcanic rocks. Hawaiian-tholeiite and alkali-basalt fields are superimposed.

is associated with certain Archean vein-type gold deposits (Kerrich, 1983; Kerrich and Watson, 1984; McNeil and Kerrich, 1986). Primary lithotypes include trondhjemites and alkali gabbros. Notwithstanding these intrinsic differences in lithotypes, the alteration is characterized by coenrichments of K, Rb, and Ba, while at the same time the alteration-insensitive elements Ti, Zr, Hf, Sc, and Th behave essentially isochemically. The characteristic potassic alteration related to porphyry Cu and Mo deposits was reviewed by Rose and Burt (1979). Kerrich and Rehrig (1987) briefly described the mineralogic and isotopic features of potassic rocks in the upper plates of certain MCC.

Interpretation of Data

The data indicate that the upper-plate volcanic rocks sampled in this study were the product of intrinsically mafic to intermediate quartz-deficient magmas with a variably alkaline (K-rich) character. The primary mafic nature is evident from the systematically elevated levels of the mafic-affiliated (and alteration-insensitive) trace elements, Cr, Ni, and Sc. At the same time, enhanced abundances of Th and the LREE, in conjunction with P_2O_5 and Zr, are consistently too high compared to most volcanic rocks of andesitic or dacitic composition. Accordingly, the upper-plate volcanic rocks are hereafter

Figure 8 (next page). Plots of K vs. Ba and K vs. Rb.

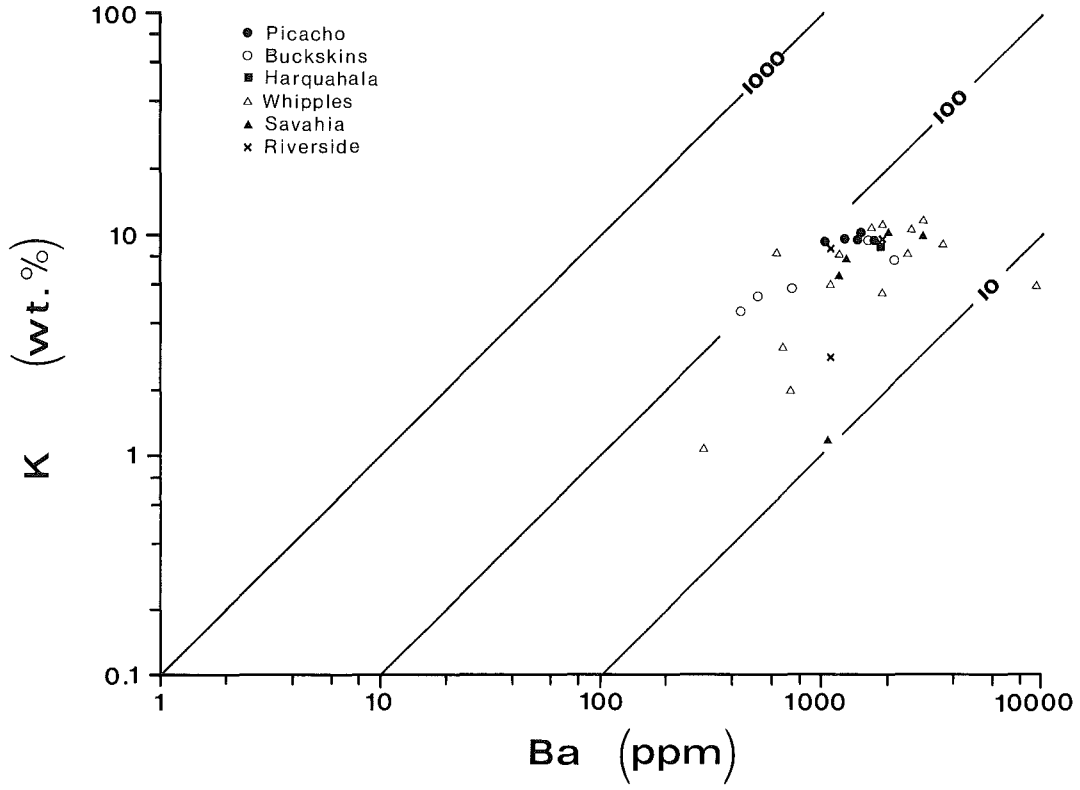
Picacho
Buckskins
Harquahala
Whipples
Savahia
Riverside
1000
100
10
K (wt. %)
Ba (ppm)
100
10
1
0.1
1
10
100
1000
10000

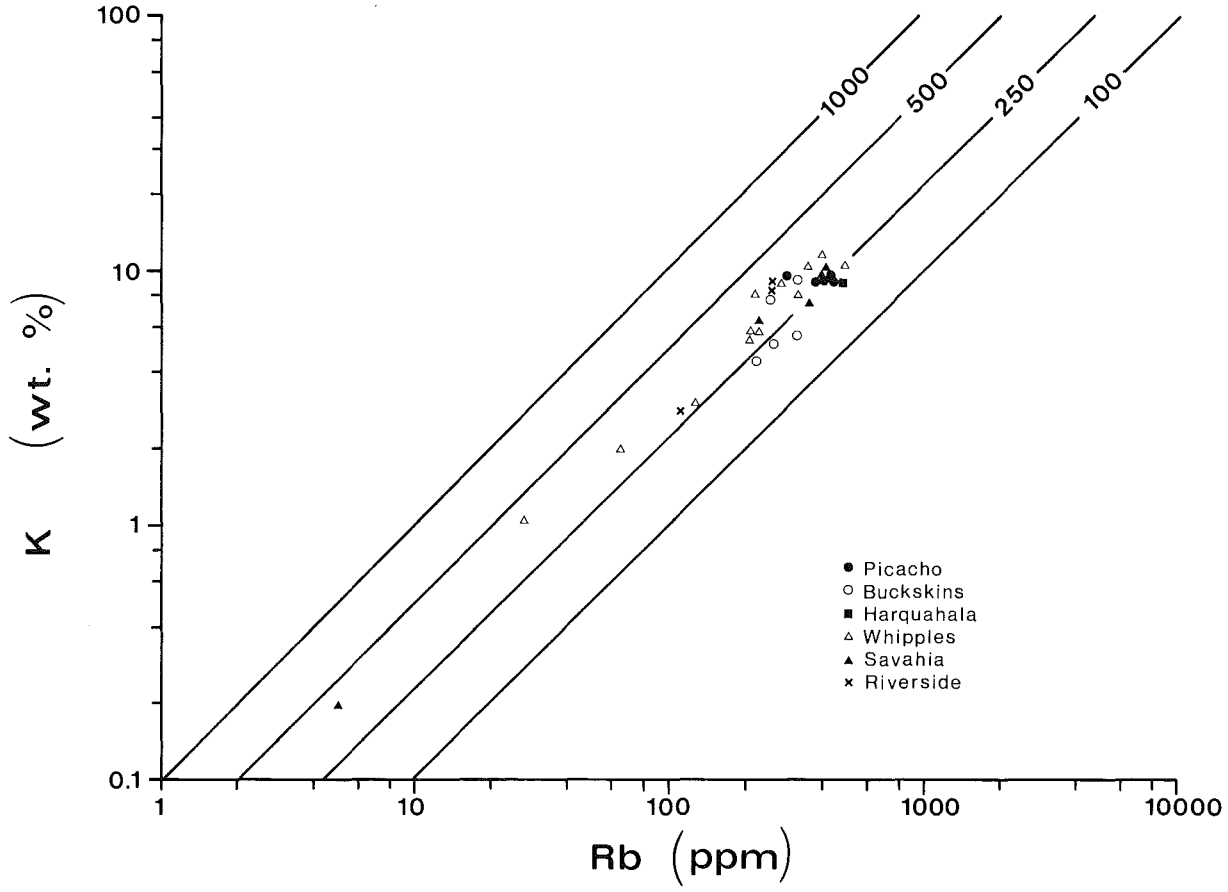
1000
500
250
100
Picacho
Buckskins
Harquahala
Whipples
Savahia
Riverside
K (wt. %)
Rb (ppm)
100
10
1
0.1
1
10
100
1000
10000

Table 2. Isotopic compositions of whole rocks and carbonates from upper-plate volcanic rocks.

	δ^{18} Whole Rock	$\delta^{18}O$		$\delta^{13}C$	
		1	24	1	24
Picacho					
Picklp 1A	12.7	20.6	21.4	-5.6	-3.6
Picklp 1B	12.7	21.0	21.4	-2.5	-2.8
Picklp 1C	17.5	21.2	20.1	-3.2	-4.4
Pic A1	16.5	24.8	24.9	-1.5	-1.8
Pic A22	9.5	22.3	21.4	-1.1	-1.7
Harquahala					
HQ-7	9.8	18.6	20.0	-3.8	-3.5
Buckskins					
WAZ-4		20.5	22.0	-6.6	-6.5
CP-4	9.9	19.6	20.2	-3.1	-3.3
Whipples					
WAZ-5A	9.3	14.6	15.2	-4.7	-4.5
WAZ-5B	12.6	17.5	19.4	-3.1	-3.0
WAZ-6A	15.0	-	-	-	-
WAZ-6B	11.0	19.3	18.3	-3.7	-4.6
WAZ-6C	16.9	21.8	21.2	-3.6	-3.9
BW-1					
BW-2					
BW-3		20.7		-3.0	
BW-4	7.1	13.1	12.4	-4.6	-4.4
BW-4af		10.1	10.0	-4.2	-4.1
BW-5f		16.5		-4.3	
BW-6f		16.5	14.8	-3.4	-3.5
BW-7f		15.3		-4.8	
BW-8f		15.0		-3.0	
Savahia					
WAZ-7		12.5	12.2	-1.6	-1.6
WAZ-8	18.1	-	-	-	-
WAZ-9A	10.3	12.6		-1.8	
WAZ-9B	3.8	12.8	12.3	-1.6	-1.6
WAZ-10	6.5	18.4	17.8	-1.8	-1.8
WAZ-11	6.2	22.7	20.0	-0.5	-1.5
Riverside					
RVS-1		19.1	18.2	-3.4	-4.6
RVS-2		20.2	18.0	-2.8	-4.6
RVS-3	9.2	18.5	17.5	-2.4	-2.1

* $\delta^{18}O$ whole rock is for carbonate free fraction.
$\delta^{18}O$ referenced to SMOW, $\delta^{13}C$ referenced to PDB.

referred to as alkali basalts or intermediate volcanics.

There is a consensus that alkali basalts may be generated in the mantle by low degrees of partial melting that preferentially enrich the liquid phase in LIL elements. An alternative hypothesis infers that an LIL-enriched metasomatizing fluid was added to the mantle source region before melting occurred (Thompson and others, 1984).

The troughs at Ta-Nb and Ti on chondrite normalized diagrams (Fig. 6) are a consistent geochemical feature of the volcanic rocks. Depletion of Ta and Nb relative to the neighboring (alteration-insensitive) lithophile elements, Th and La, is generally attributed to one of two possible processes: the incorporation of sediments that carry a signature of Ta, Nb, and Ti depletion into the source region, or the stabilization of a Ti phase in the source region that preferentially retains Ta and Nb relative to Th and La. The latter hypothesis relies not only on the concurrence of troughs at Ta, Nb, and Ti, but also on crystal chemical considerations.

Irrespective of the causal mechanism, magmas characterized by Ta-Nb troughs are uniquely associated with destructive plate-margin environments (Thompson and others, 1984). In contrast, alkaline magmatic counterparts from continental rifts or ocean islands generally display smooth chondrite-normalized profiles (Fitton and James, 1986). These geochemical features of upper-plate volcanic rocks may then signify that the extensional environment of MCC was related in some way to subduction-related magmatic processes. Finally, we note that

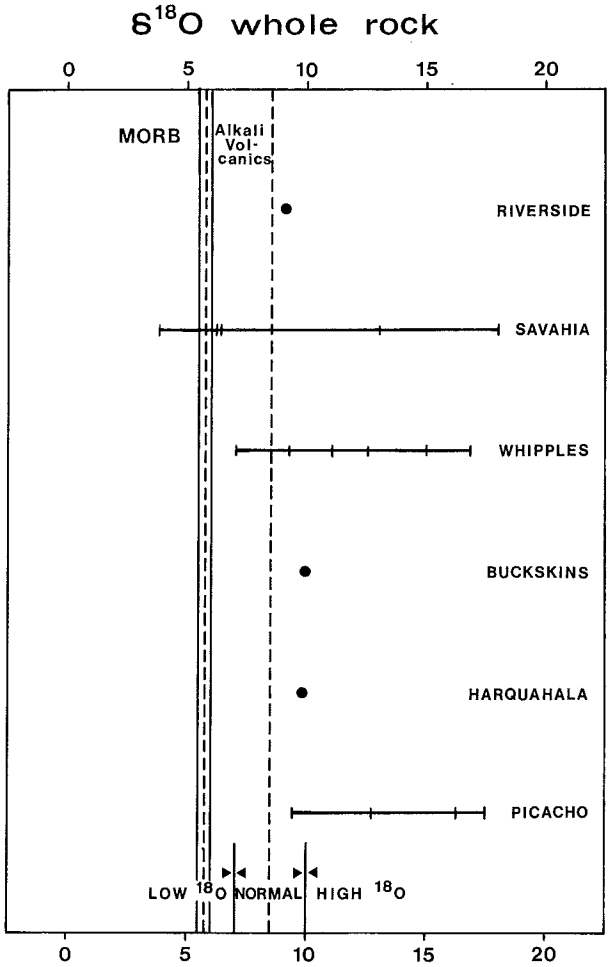

Figure 9. Compilation of oxygen-isotope data for carbonate-free whole rocks from specified localities. The solid vertical lines indicate the range of fresh mid-ocean ridge basalts ($\delta^{18}O$ = 5.7 ± 0.3) and the dashed vertical line corresponds to the upper limit of $\delta^{18}O$ values for fresh alkaline volcanic rocks (after Kyser, 1986). Low, normal, and high $\delta^{18}O$ categories of felsic plutonic rocks are based on whole-rock $\delta^{18}O$ values, given by Taylor (1978).

the Ta and Nb depletion shifts data points to the left on the discrimination diagram (Fig. 4) relative to alkaline counterparts with smooth chondrite-normalized distributions. Accordingly, reference to fresh volcanic rocks that plot in the same region would result in underestimation of the primary K_2O contents of the altered volcanic rocks considered in this study.

It is difficult to assess the magnitude of primary K_2O contents, given the extent of secondary hydrothermal alteration and the apparent absence of pristine volcanic members. A consistent feature of the chondrite-normalized plots is the trough at Th relative to Rb and K (Fig. 6), which provides a more rigorous means to estimate primary K_2O contents. Based on the assumption that the magma had a relatively smooth, normalized distribution through these LIL-elements, excepting Ta and Nb (cf. Fitton, 1986), and on projection from La to Th,

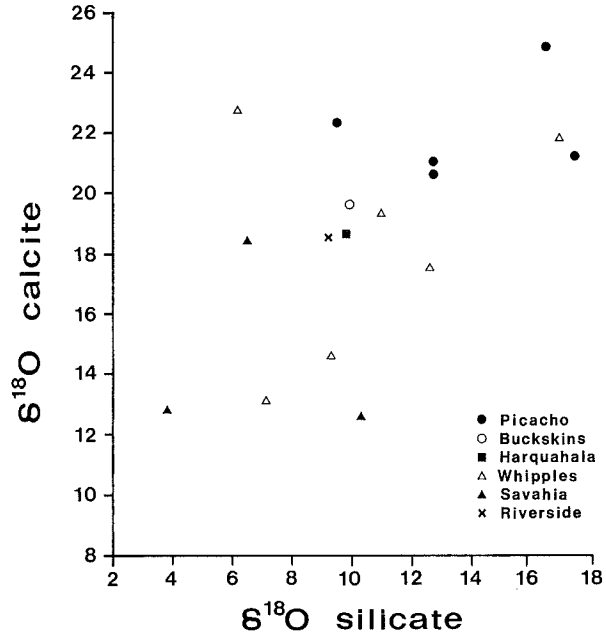

Figure 10. Plot of $\delta^{18}O$ calcite versus $\delta^{18}O$ whole-rock silicate (carbonate-free).

primary levels of K would have been in the range of 3 to 6 wt. % K_2O. If this approach has validity, many of the volcanic rocks have had additions of K_2O (increments of up to 7 wt. %) beyond their intrinsically potassic character. Rb and Ba were coenriched with K (Fig. 8).

Quantitative estimates of the gain and loss of chemical components during hydrothermal alteration can-

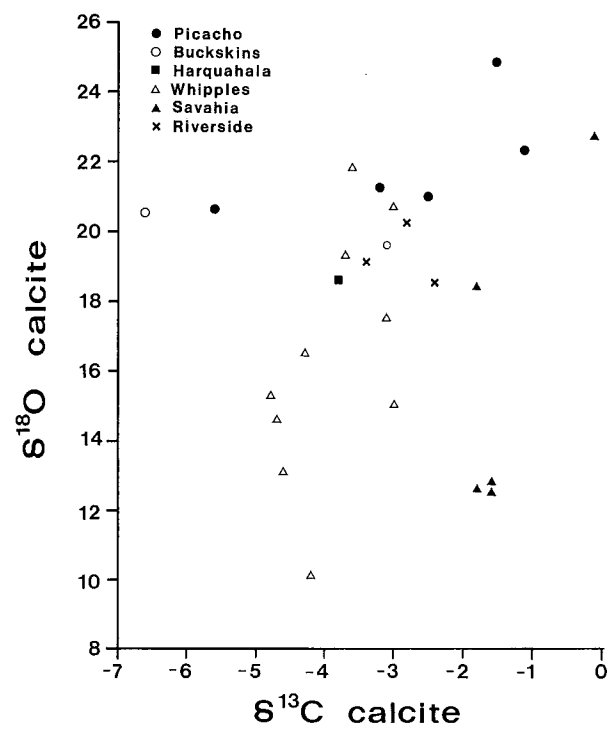

Figure 11. Plot of $\delta^{18}O$ calcite versus $\delta^{13}C$ calcite.

not be made in the absence of a perfectly fresh precursor. In qualitative terms, however, additions of K_2O were accompanied by an increase of Fe_2O_3, CaO, and LOI and a concomitant depletion in MgO and Na_2O. As discussed above, Th, LREE, Zr, Hf, Sc, Cr, and Ni behaved isochemically during hydrothermal metasomatism.

There are many compositional and tectonic characteristics of the volcanic rocks that remain poorly understood or are completely enigmatic. Prominent among these unknowns is the source of K. We tentatively suggest two possible processes that might account for the observed K enrichment. First, K was possibly released during decompressional dehydration and penetrative deformation of lower-plate rocks that accompanied extensional tectonics and detachment faulting. This scheme is based on the fact that the trajectories of metamorphic dehydration reactions have a relatively shallow slope at low pressure; therefore isothermal decompression could have induced dehydration. Decompression would also drive decarbonation reactions. Thermal doming, the tectonic superposition of younger and cooler units on older and hotter crust, as well as volatiles released from magmas generated by decompression, are other plausible mechanisms for generating K-bearing fluids in an extensional environment. A second possibility is that low-temperature hydrothermal alteration of upper-plate volcanic rocks caused redistribution of K within the volcanic sequence. The fluid reservoir donating K may have been independent from surficial fluids (brines) in aquifers within or above the upper plate.

SUMMARY AND CONCLUSIONS

Several questions regarding the genesis of MCC remain unanswered, such as what process drives extension, what is the fundamental nature of this extension, and how much displacement has been accommodated between upper and lower plates. The results of this preliminary research provide insight to these questions, but no definitive answers. The distinctive primary magmatic and superimposed metasomatic characteristics of the volcanic rocks in upper plates of MCC suggest that special magmatic and fluid processes were associated with extension within the complexes. The apparent absence of these characteristics in coeval volcanic sequences surrounding the complexes implies that the special geochemical processes associated with extension were not operative in marginal areas (e.g., eastern Bighorn and Belmont Mountains, Vulture Mountains, and Kofa Mountains). If these relationships are valid, it is possible that some or all of the metasomatized alkali basalts of the MCC upper plates are parautochthonous, rather than being fortuitously displaced upon the mylonitic lower plates from great distances.

There is a consensus that such alkali volcanics form at late stages of extensional regimes in settings of plate convergence and subduction, with the site of magma production substantially inboard of the plate margin. Certainly the general setting of the MCC is back-arc extension in such a subduction regime; however, in the southwestern United States, a transform boundary was evolving during the time of the volcanism in question.

The potassic nature of the upper-plate volcanic rocks has a dual origin: primary magmas were intrinsically potassic, in the range 3-6 wt. % K_2O, but local pseudomorphic metasomatism and hydrothermal alteration increased K content up to 13 wt. % K_2O, with concomitant additions of Fe, Ca, and CO_2. The sources of K, Fe, Ca, and CO_2 remain enigmatic, and could have evolved either by redistribution of elements entirely within the upper plate, or by introduction from the lower plate. Realistically, both processes are possible. For example, ascending fluids from below the detachment fault could mix and exchange with higher-level fluids in the upper plate, with subsequent downward hydrologic collapse to the detachment faults. Calcite-cemented hydraulic breccias found just above detachment faults are suggestive of such hydraulic advection.

Pervasive ductile extensional deformation and uplift in the MCC must involve decompression and evolution of hydrous phases. The slope of dehydration reactions in PT coordinates is such that dehydration could be driven by isothermal decompression. These processes may have been significant in generating fluid reservoirs within the MCC, and such reservoirs may have been responsible for some of the observed metasomatism.

ACKNOWLEDGMENTS

The authors express their appreciation to J. Spencer and S. Reynolds for their invitation to submit this contribution. We also thank S. Reynolds and J. Spencer for incisive editing and helpful suggestions. We are grateful to R. Daddar for assistance with conducting the isotopic analyses, S. Sparkes for drafting some of the diagrams, and D. Irwin for typing the manuscript. R. Kerrich acknowledges provision of an operating grant from the Natural Science and Engineering Research Council of Canada.

Mineralization in the central part of the Planet mineral district, northwestern Buckskin Mountains

NORMAN E. LEHMAN *1650 N. Indigo Dr., Tucson, Arizona 85745*
JON E. SPENCER *Arizona Geological Survey, 845 N. Park Ave., #100, Tucson, Arizona 85719*

ABSTRACT

The Buckskin-Rawhide detachment fault places primarily Mesozoic metasedimentary and metavolcanic rocks over mylonitic crystalline rocks in the Planet mineral district in the northwestern Buckskin Mountains. Most mineral deposits are located along and directly above the detachment fault and adjacent to upper-plate normal and tear faults. Fault zones were conduits for movement of mineralizing fluids. Calcareous sandstone and siltstone of the lower Mesozoic Buckskin Formation host massive, fracture-filling, disseminated specular hematite and younger fracture-filling chrysocolla. Quartzites of the stratigraphically overlying Vampire Formation host fewer and smaller Fe and Cu deposits, but contain greater concentrations of Au. Au is associated with earthy hematite, chrysocolla, and chlorite. Most of the mineralization is located along a 1,000-m-wide, northeast-trending belt that overlies a synformal groove in the underlying detachment fault.

INTRODUCTION

The Planet mineral district (Keith and others, 1983) contains two of the largest known Cu deposits associated with Tertiary detachment faults in the southwestern United States. The larger deposit is at the Mineral Hill mine just west of the study area; the smaller Planet mine is in the northeastern part of the study area. (See Fig. 1 for location of study area.) Mineral deposits at both mines lie almost entirely within upper-plate Mesozoic metasedimentary rocks of the Buckskin Formation and are adjacent to the Buckskin-Rawhide detachment fault. The deposits are typically characterized by massive specular hematite with fracture-filling chrysocolla. Numerous smaller deposits are present at significant distances (greater than 50 m) above the detachment fault.

The Vampire Formation of Late Triassic or Early to Middle Jurassic age is the primary host to Au mineralization in the study area. The Vampire Formation is composed of quartzose to moderately feldspathic sandstone with sparse conglomeratic sandstone and fine-grained silty sandstone. These greenschist-facies rocks are indurated and, relative to other Mesozoic units in the area, chemically inert. Pervasive fracturing of quartzose units in the Vampire Formation greatly increased permeability, thereby allowing movement of mineralizing fluids during mid-Tertiary extensional faulting.

Au is concentrated in the quartzites of the Vampire Formation, whereas Cu and Fe are more significant in reactive calcareous host rocks of the Buckskin Formation. Both deposits are common above a northeast-trending groove in the underlying Buckskin-Rawhide detachment fault.

Data and many of the conclusions presented here regarding mineralization and alteration are the results of a study conducted by the lead author during 1983-84 for AMAX, Inc.

STRATIGRAPHY

Upper-plate rocks in the Planet mineral district consist of a sequence of Mesozoic sedimentary and volcanic rocks metamorphosed to lower greenschist facies, and an unconformably overlying sequence of Miocene sedimentary and volcanic rocks (Reynolds and Spencer, this vol.; Plate 2). These rocks are well exposed in several northwest-striking, southwest-tilted fault blocks. Tertiary sedimentary rocks were deposited during Miocene extensional faulting above the Buckskin-Rawhide detachment fault (Fig. 2).

The Mesozoic rocks are composed of the Buckskin Formation, the Vampire Formation, and the Planet Volcanics, in ascending order. The Buckskin Formation consists of four members, in ascending order: (1) variably calcareous quartzite, silty quartzite, and phyllite; (2) quartzite; (3) phyllite; and (4) calc-silicate and variably calcareous quartzite and quartz-sericite schist. The overlying Vampire Formation consists of quartzite, schistose quartz-feldspar-sericite metasandstone, and local conglomeratic quartzite and conglomerate; it rests with gentle angular unconformity on all members of the Buckskin Formation. The Vampire Formation is overlain by the Planet Volcanics, which consist of variably cleaved and schistose silicic to intermediate metavolcanic rocks. The Buckskin Formation probably correlates with the Triassic Moenkopi Formation; the Vampire Formation probably correlates with the Upper Triassic Chinle Formation, Lower Jurassic Navajo Sandstone, or Middle Jurassic Carmel Formation and Entrada Sandstone (Reynolds and others, 1987). The Planet Volcanics are part of a regional suite of middle Jurassic volcanic rocks

in Spencer, J.E., and Reynolds, S.J., eds., 1989, Geology and mineral resources of the Buckskin and Rawhide Mountains, west-central Arizona: Arizona Geological Survey Bulletin 198, p. 215-222.

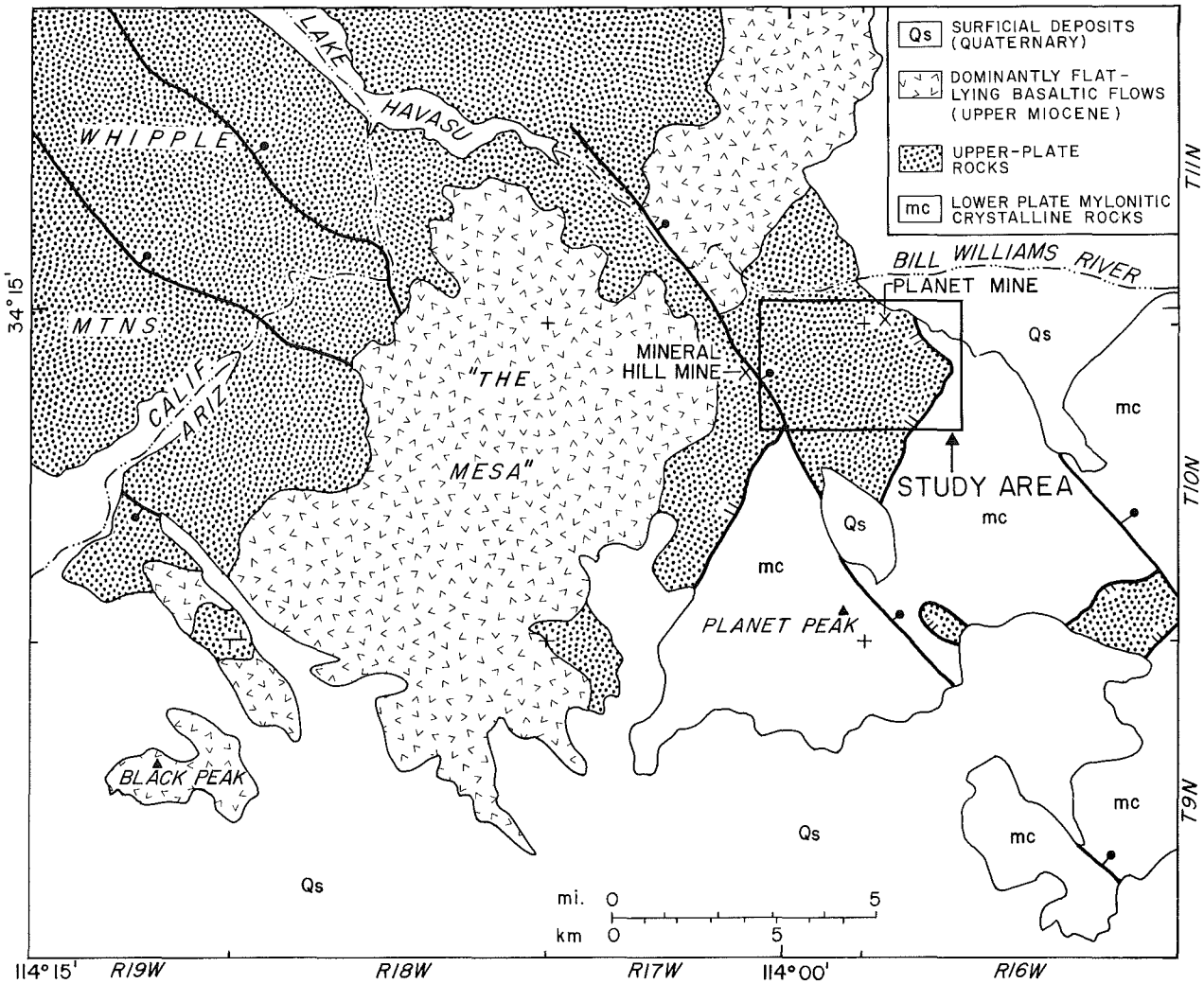

Figure 1. Map showing location of study area within the western Buckskin Mountains.

that are present in many ranges in southern and west-central Arizona.

Tertiary rocks that unconformably overlie the Mesozoic rocks consist of, in ascending order, sedimentary breccias, a lower clastic sedimentary unit, mafic flows, and an upper clastic sedimentary unit. The basal breccia unit is the thickest unit and the dominant Tertiary rock type in the study area. It is generally composed of unsorted, angular clasts of the Planet Volcanics, which depositionally underlie it. These breccias are thought to be landslide and debris-avalanche deposits shed from fault blocks during Miocene normal faulting (Spencer and Reynolds, this vol.). The overlying sandstone, conglomerate, and volcanic flows are not widely exposed in the study area, nor are they significant hosts to mineral deposits.

STRUCTURE

Three structural events affected upper-plate rocks in the study area: (1) Mesozoic formation of cleavage and foliation; (2) Oligocene(?) to middle Miocene detachment faulting and high-angle extensional faulting and tilting; and (3) upper Miocene or Pliocene high-angle faulting. The first deformation event affected Mesozoic rocks. It produced a cleavage or metamorphic foliation that is the result of Mesozoic thrusting and related deformation and metamorphism. The second deformation event was associated with large-magnitude (tens of kilometers of) displacement of upper-plate rocks to the east-northeast above the Buckskin-Rawhide detachment fault and juxtaposition of these rocks with lower-plate mylonitic crystalline rocks. Upper-plate normal faulting accompanied by detachment faulting resulted in southwestward tilting of northwest-striking fault blocks. The entire study area lies within three of these tilt blocks. Numerous northeast-striking faults with minor displacement probably accommodated differential rotation along strike within each northwest-striking tilt block. The postdetachment Mineral Wash fault, a high-angle, northwest-trending, northeast-side-down fault, has 100 to 150 m of vertical displacement and an unknown amount of strike-slip displacement. It cuts the Mineral Hill orebody; the offset downthrown continuation of the

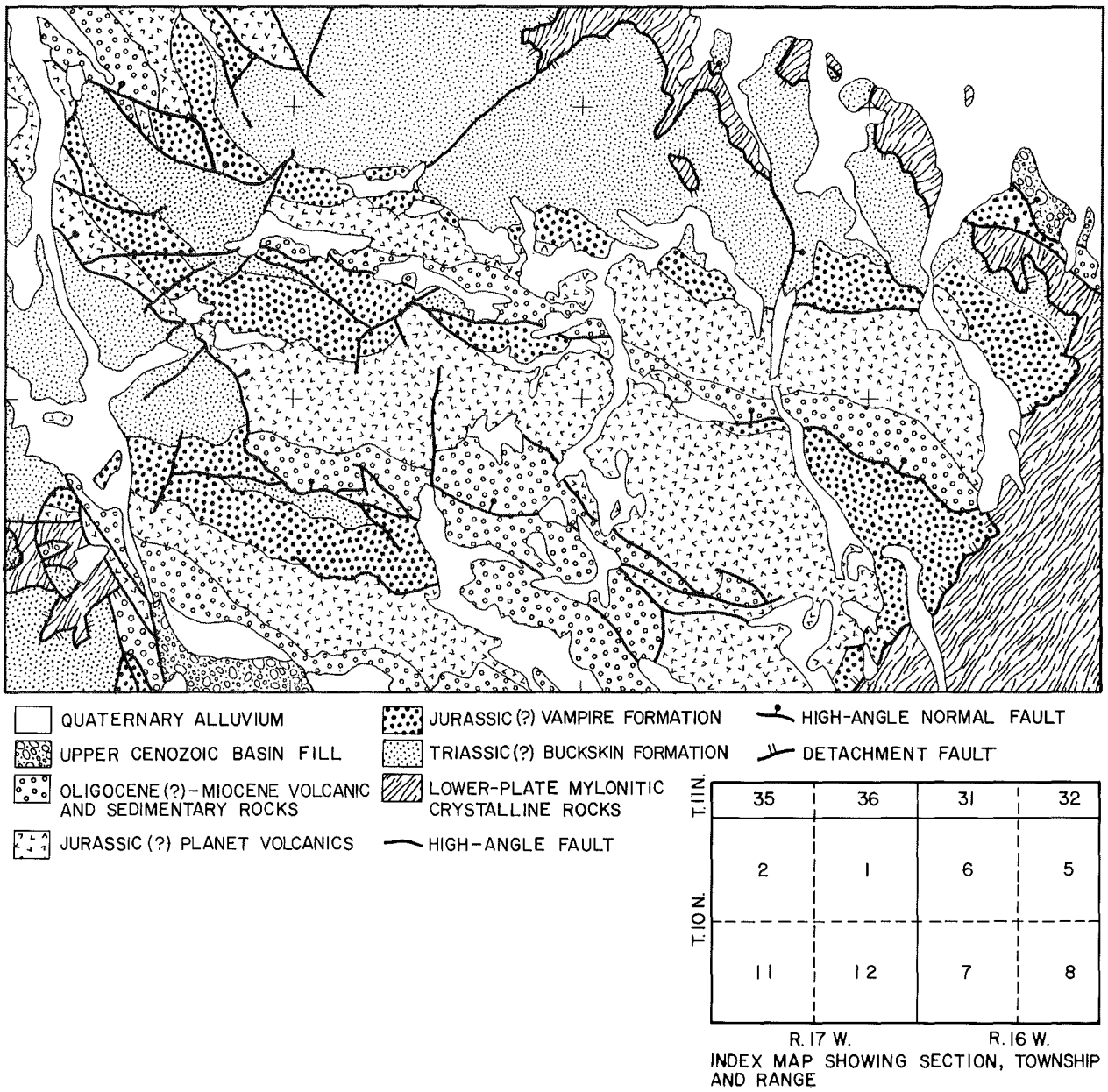

Figure 2. Simplified geologic map of study area (modified from Plate 2).

orebody has not been located.

Lower-plate rocks underwent pre-Tertiary deformation and metamorphism that resulted in gneissic layering. The age and significance of the deformation that produced these structures are unclear because of overprinting by Tertiary deformation. Tertiary mylonitization was followed by brecciation and chloritic alteration near (typically within 10 to 100 m of) the detachment fault. Microbrecciation and cataclasis overprinted these fabrics within a few centimeters to 1 m of the detachment fault (Davis, G.A., and others, 1980; Rehrig and Reynolds, 1980). These sequential lower-plate deformations were the result of ductile shearing (mylonitization) along the downdip projection of the Buckskin-Rawhide detachment fault, followed by brittle deformation (brecciation and cataclasis) as the lower plate cooled during uplift and tectonic denudation (Davis, G.A., and others, 1986).

The detachment fault itself is an undulating irregular surface, as indicated by outcrop pattern and drill-hole data. A synformal keel or groove has a southwest-plunging, northeast-trending axis (N50°E) that transects the study area, passes through the Planet mine to the northeast, and projects toward the Mineral Hill mine to the southwest (Fig. 3). It is not known if this groove is an original feature of the fault or if it was produced by folding.

Extensive fracturing and brecciation that accompanied detachment faulting and associated upper-plate normal faulting formed conduits for movement of mineralizing fluids. Structural disruption of rocks along the

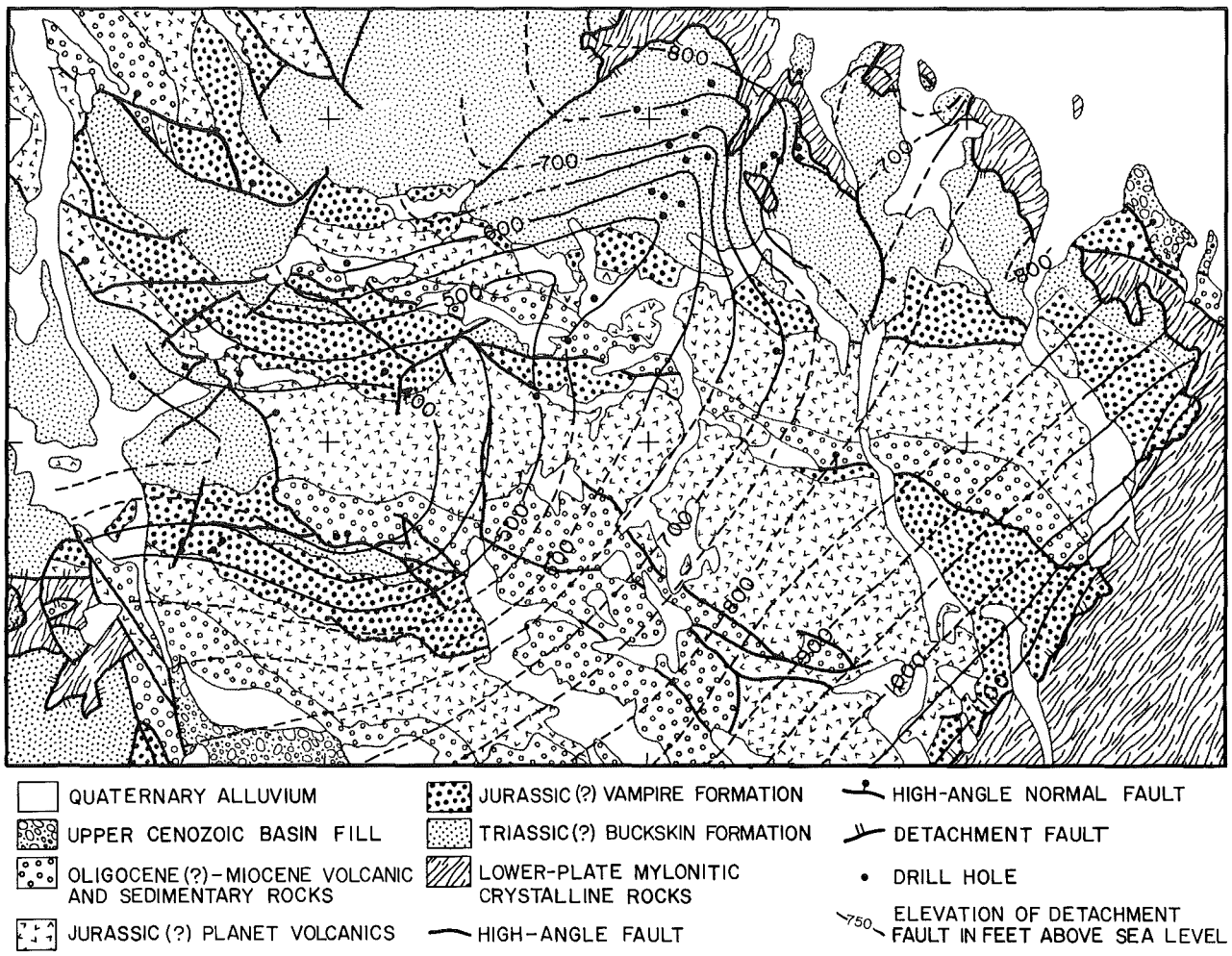

Figure 3. Contour map of elevation of detachment fault within study area, superimposed on geologic map. Elevation is determined from drill-hole data and fault trace.

detachment fault was severe; this zone of highly fractured rocks was the most important conduit for movement of mineralizing fluids. Chloritic alteration of lower-plate rocks near the detachment fault was a consequence of initial fracturing and formation of permeable pathways for fluid movement, but was not necessarily related to mineralizing solutions.

ALTERATION

Introduction

Obvious alteration in the Planet mineral district is controlled by structure and lithology. On a district-wide scale, alteration is most prevalent within a N50°E-trending zone that is approximately 1,000 m wide and crosscuts all stratigraphic units. This belt extends east of Mineral Wash (NE^1/4 sec. 11, T. 10 N., R. 18 E.) to the Planet mine area (Fig. 4). Alteration studies were not conducted west of Mineral Wash, but a brief reconnaissance of the area suggests that the zone is offset to the north by the Mineral Wash fault and continues to the southwest beneath basalts that form The Mesa.

Alteration above the detachment fault was the result of highly oxidized and/or CO_2-dominated fluids that contained very little sulfur. Alteration at and immediately below the detachment surface was caused by reduced sulfur-bearing fluids.

The lack of evidence for intrusive activity in upper-plate rocks in the study area indicates a nonmagmatic fluid source. The distribution of alteration assemblages suggests that fluids migrated along the detachment zone and reached the upper plate through permeable zones formed by brecciated rocks and faults. Because the strongest alteration is above the axis of the northeast-trending groove in the detachment surface, rocks along the detachment fault and within the groove must have been exceptionally effective conduits for movement of mineralizing fluids.

Quartz-Sericite-Hematite Alteration

Quartzite in the Vampire Formation commonly shows preferential quartz-sericite-hematite alteration (Fig. 4). Where alteration is strongest, the interbedded metamorphosed quartz wacke and local sandy shale in the Vam-

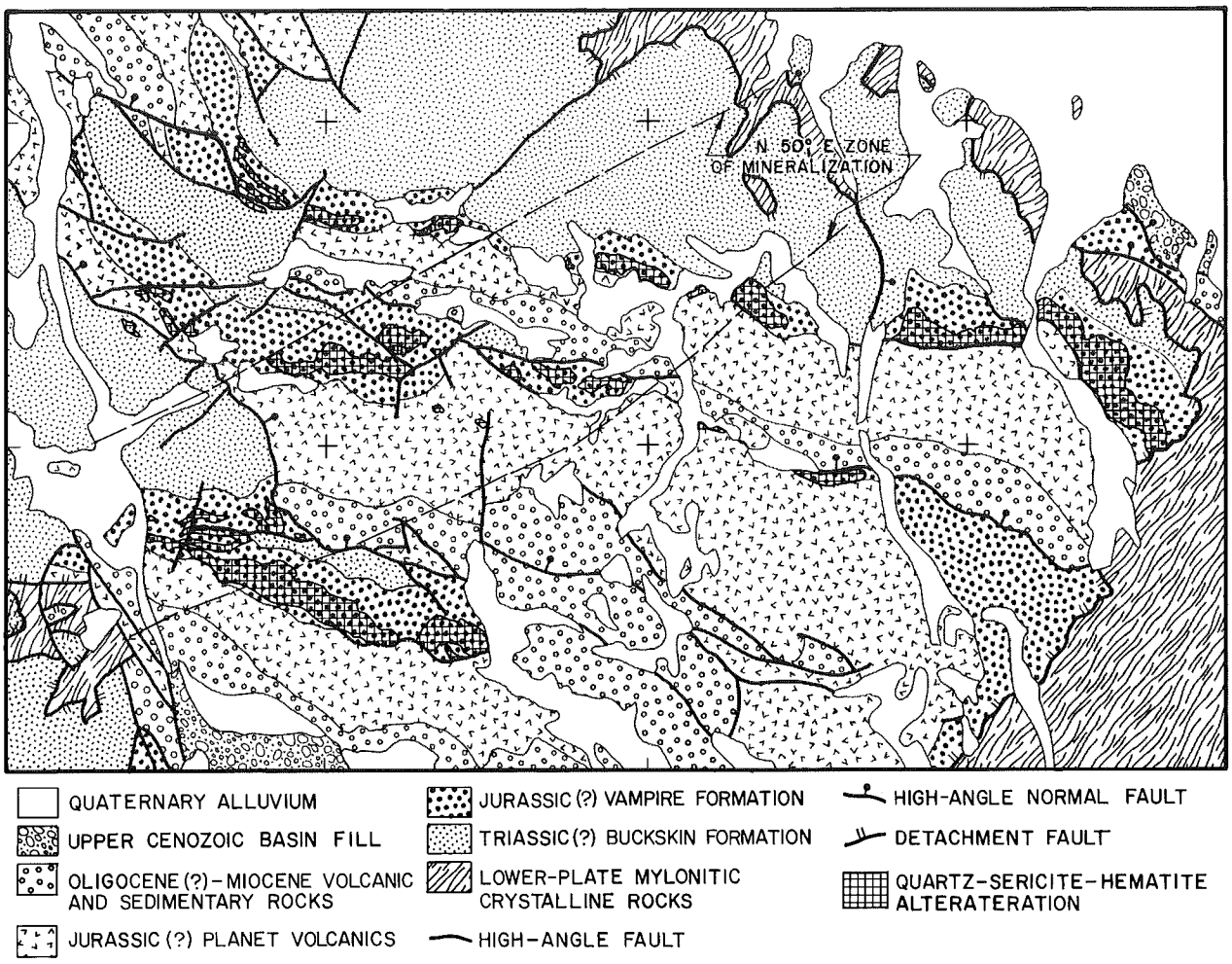

Figure 4. Areas of quartz-sericite alteration superimposed on geologic map.

pire Formation were also altered. Outside the areas of greatest alteration, the quartzites are slightly to moderately bleached and weakly to strongly silicified and typically contain trace to minor amounts of hematite. Hematite mineralization in these areas is pervasive in quartzite units that are adjacent to listric normal faults, such as those that crop out near the northern edge of sec. 7, T. 10 N., R. 16 W. Locally intense quartz-sericite-hematite alteration is also present in footwall blocks adjacent to northeast-trending, high-angle faults near the center of section 2 and in the northwest quarter of section 1.

The most intense area of quartz-sericite-hematite alteration in the Vampire Formation is immediately east of Mineral Wash (NE$^1/4$ sec. 11, T. 10 N., R. 16 W.). Most of the quartzite in this area contains 5% to more than 10% hematite, is intensely silicified, and commonly contains coarse-grained and fine-grained sericite; veinlets of specular hematite are common. Weak alteration is present in the Vampire Formation in the north-central part of section 11. Other areas of moderate to intense quartz-sericite-hematite alteration in quartzite are present in the southwest, southeast, and east-central portions of section 1.

Chlorite-Quartz-Hematite Alteration

Less brittle units in the Vampire Formation, such as those composed of impure sandstones and of pebbly quartz wacke, generally were not as strongly affected by hydrothermal alteration as the quartzite units. The alteration assemblage in these rocks is chlorite-quartz-hematite.

It is difficult to distinguish hydrothermal from metamorphic chlorite in the Planet mineral district because most of the chlorite is disseminated and fine grained. Veinlets of chlorite-quartz-hematite are primarily located in small areas or within mineralized fault-vein structures. The hydrothermal chlorite is usually greenish black, although some suspected hydrothermal chlorite is an apple-green color. Hematite is locally pervasive.

Alteration of this type is best developed in metamorphosed quartz wacke of the Vampire Formation in the northeast quarter of section 11 and in S$^1/2$ sec. 1, T. 10 N., R. 17 W.

Alteration of Calc-Silicate Rocks

Calcareous clastic rocks form the upper and lower

members of the Buckskin Formation. These rocks were metamorphosed to hornfels siltstones and calc-silicate rocks and contain epidote, diopside, garnet, tremolite, magnetite, and calcite. Directly above the detachment fault, these rocks were replaced by massive calcite and specular hematite with minor amounts of fine-grained and cryptocrystalline quartz, chlorite, and manganese oxides. Elsewhere in the Planet mineral district, veinlets of chlorite, chlorite-specular hematite, quartz-chlorite-specular hematite, and actinolite are present.

Alteration At or Below the Detachment Surface

Epidote and chlorite alteration has affected lower-plate rocks in a 150- to 300-m-thick zone below the fault. Epidote is mainly present on the outer (lower) fringe of this alteration zone, where it has replaced 10% to 15% of the crystalline rocks. Closer to the detachment surface, epidote decreases and chlorite increases in abundance. Chlorite replaces feldspar and mafic minerals and forms microveinlets with epidote, calcite, pyrite, or specular hematite.

Alteration minerals at or below the detachment fault are, in decreasing order of abundance, chlorite, pyrite, specular hematite, epidote, quartz, calcite, sericite, and fluorite. These minerals form disseminated to massive replacements of cataclastic and mylonitic rocks, and are also present as crosscutting veinlets of various combinations of these minerals. Fluorite is present in veinlets at the Mineral Hill mine and as disseminated grains in the Swansea mineral district (Wilkins and Heidrick, 1982). Greenish-black chlorite is locally massive and common in veinlets with quartz, epidote, and pyrite. Up to 15% disseminated pyrite was present at the detachment surface in core from one drill hole. Two to five percent pyrite was typically present below the fault in drill samples.

MINERALIZATION

History and Production

High-grade Cu mineralization was discovered at the Planet mine in the early 1850's. Production from this and other mines in the Planet mineral district mainly occurred between 1872 and 1923 (Keith, 1978). From 1964 to 1970, open-pit operations at the Mineral Hill mine produced most of the ores of the district. More than 23-million lb of Cu, 400 oz of Au, and 100 oz of Ag were recovered from a total district production of slightly more than 1-million tons of ore (Keith and others, 1983). Underground ores from the Planet mine averaged 10% Cu, which was primarily derived from chrysocolla with minor amounts of malachite, azurite, chalcopyrite, and bornite. Smaller mines produced ores containing 0.4 to 1.0 oz of Au per ton of ore.

Cu-Fe Mineralization Associated With the Detachment Fault

Small, high-grade, upper-plate deposits of copper oxides and minor sulfides form discontinuous, tabular ore bodies that are paraconformable with the detachment surface in the Planet mine area. A sharp contact does not exist between mineralization and barren upper-plate wall rocks. Mineralization peripheral to the high-grade (5% to 10% Cu) deposits consists of scattered veinlets and pods of copper-oxide minerals. The Mineral Hill mine contained sufficient Cu mineralization to yield nearly 1-million tons of ore that averaged 0.68% Cu.

The high-grade Cu deposits ranged in size from a few cubic meters to deposits more than 200 m long, 80 m wide, and 5 to 15 m thick (Cummings, 1946). Ore minerals are dominated by chrysocolla with minor amounts of malachite, azurite, chalcopyrite, and bornite, all of which are present in a gangue of earthy and specular hematite with calcite, chlorite, and quartz.

Massive, tabular, and lenticular bodies of specular hematite directly above the detachment fault are associated with the high-grade Cu deposits. Individual zones up to 300 m long, more than 100 m wide, and 15 m thick contain 50% to 68% Fe and trace amounts of Cu. The U.S. Bureau of Mines drilled several churn and diamond drill holes in the Planet and Mineral Hill mine areas and estimated that 1.25-million tons of iron ore, averaging 60% Fe, are present (Harrer, 1964). Lower-grade Cu and Fe are also present in mylonitic gneiss as much as 80 m below the detachment fault.

Copper-sulfide mineral deposits, which consist of chalcopyrite and bornite, are mainly present immediately adjacent to the detachment fault in the Planet district. The sulfides are intensely brecciated, which suggests that they were deposited before final movement occurred along the detachment fault.

Mineralization in Upper-Plate Normal Faults

Cu and Au mineral deposits are present in or adjacent to high-angle and listric normal faults that are above the detachment surface. Individual deposits are continuous along northeast-trending faults for approximately 100 m. Several deposits form adjacent tabular bodies along individual faults. The northeast trend is clearly a preferred direction of mineralization; this is indicated by gash veins perpendicular to the listric normal faults. Another preferred orientation is northwest, parallel to the listric normal faults. The highest Au values for dump samples from the district were measured in rocks along or adjacent to the northeast- and northwest-trending faults. Other favorable zones include the upper and lower contacts of quartzite units where the quartzites are commonly brecciated, possibly in response to bedding-plane slip between rocks of different competencies.

Mineral deposits in prospect pits are commonly not confined to distinct fault and shear zones, but may be present as discontinuous gash veins perpendicular to listric normal faults, as gently dipping veinlets parallel to those faults, or as stockwork veins in which a dominant structural direction is absent.

Ore minerals consist of veinlets and pods of

chrysocolla with rare malachite and azurite. Au forms medium- to coarse-grained flakes, which were not seen in discrete vein structures. Earthy hematite is the most common gangue mineral, followed by chlorite, sericite, quartz, specular hematite, calcite, manganese oxides, limonite, and clay. Pyrite is notably absent, although rare casts of limonite after pyrite are present.

Prospects that contain Au consistently contain chrysocolla and earthy hematite and commonly contain chlorite. A greasy, olive- to apple-green mineral, commonly associated with Au, was X-rayed and identified as duftite, a Cu-Pb arsenate. Autunite may be present, but positive identification of the mineral was not made.

In the district, manganese deposits are present in tilted Tertiary sedimentary units near Tunnel Peak. Ore minerals consist of psilomelane and other manganese oxides. Barite veins are common in all Tertiary units and some are present in the Mesozoic metamorphic rocks. These veins are generally less than 2 to 3 cm thick, commonly strike north, and are nearly vertical. Seams of barite, up to 0.5 m thick, parallel bedding in the Tertiary sedimentary units.

Geochemical Surveys

The following geochemical surveys aided in the evaluation of Au mineralization in the district: 1) samples of high-grade deposits from mine and prospect dumps; 2) chip samples of quartzite units in the Vampire Formation taken perpendicular to strike of bedding; and 3) stream sediment samples from major drainages and tributaries in the area. These surveys were conducted to determine areas of anomalous Au and associated mineralization.

Dump Samples. The AMAX Metallurgical Laboratory in Denver, Colorado analyzed 304 dump samples, which weighed 1 to 3 kg each, for Au, Ag, Cu, Pb, Zn, and Mo. Samples were analyzed for Au and Ag with a fire-assay/AA technique; the remaining elements were analyzed by ICP methods. Assay results were computerized and statistically processed to obtain anomalous threshold values.

Dump samples that contained more than 1 ppm Au are considered anomalous for the sample population of dumps in the Buckskin project area; these constitute the upper 30th percentile of the distribution range. Samples with between 5 and 9 ppm and those with more than 9 ppm Au are considered moderately and strongly anomalous, respectively, and fall above the upper 17th and 12th percentiles, respectively, of the distribution range. The ranges of values for elements in these dumps are as follows: Au = 0.01 to 62 ppm, Ag = 0.1 to 39 ppm, Cu = 1.0 ppm to 33.7%, Pb = 1 to 7,200 ppm, Zn = 14 ppm to 3.4%, and Mo = 1 to 1,140 ppm. Nearly 60% of the dump samples contain more than 1% Cu.

Dump samples anomalous in Au were mainly from quartzite and adjacent units in the Vampire Formation, but were not strictly confined to those units. A small percentage of samples from each lithology of the upper plate, with the exception of the Tertiary sedimentary and volcanic rocks, yielded anomalous values. A group of dump samples from a volcaniclastic unit in the Planet Volcanics also yielded anomalous values. Samples taken from dumps and workings in calcareous clastic rocks of the Buckskin Formation, at or immediately above the detachment surface in the northeast part of the study area, contained little or no Au.

Average metal ratios for areas with anomalous Au vary greatly, but distinct patterns indicative of mineralization zoning are not obvious. Dumps in the Planet Volcanics contain the highest average values for Ag, Pb, and Zn and the lowest average value for Mo. The Au:Ag ratio for all anomalous areas ranges from 3 to 7.

Rock-Chip Samples. Nearly 600 samples were collected from quartzite units in the Vampire Formation. These samples were analyzed for Au, Ag, Cu, Pb, Zn, and Mo by the same methods used on the dump samples. Samples were collected from altered and unaltered quartzite, as well as interbedded units of quartz wacke and chloritic schist. The chip and grab samples, which weighed approximately 1 kg each, were taken on traverses perpendicular to the strike of quartzite outcrops. The sample intervals along each traverse were designed to represent about 8 m of stratigraphic thickness.

The background level for Au is 0.005 ppm. A log-normal cumulative-frequency plot for the rock-chip data does not show distinct populations indicative of anomalous values. Au values for cumulative percentages of 73, 80, and 90 are 0.016 ppm, 0.028 ppm, and 0.066 ppm, respectively.

Twenty percent of the samples contain more than 0.28 ppm Au. Nearly 75% of these anomalous samples are present in the 1,000-m-wide, northeast-trending belt that hosts the bulk of the mineral deposits and alteration zones in the district. Only four quartzite rock-chip samples that contain more than 0.28 ppm Au were taken from more than 300 m outside that belt. Quartzites in all areas of relatively high Au values are altered and brecciated and contain quartz and/or specular hematite veins.

Stream-Sediment Samples. Nearly 100 stream-sediment samples were collected within and adjacent to the Buckskin study area. Each sample contained 6 kg of material taken from a 130- to 160-m traverse within a drainage. About 300 g were collected at 7-m intervals. Where the drainage exceeded 2 m in width, samples were collected from both sides of the drainage at 7-m intervals. The 6-kg samples were sieved in the field to -20 mesh and shipped to the AMAX Metallurgical Laboratory in Golden, Colorado for analysis.

In the lab, each sample was sieved to -48 mesh and up to 300 g were analyzed for Au. Au analysis was performed by the AMAX cyanide leach procedure. The samples contained from 0 to 0.7 ppm Au. All samples that contained detectable Au are considered anomalous.

The stream-sediment sampling program was conducted in two phases. Samples from phase one were collected at 400- to 800-m spacing across the major drainage basins of the area. After the phase-one assay data were received, the drainages that contained detectable Au were subdivided into smaller areas defined by tributaries

feeding the major drainages, and a second sample set was collected. Sample spacing for this second set ranged from 100 m to many hundreds of meters.

Assay data from these samples indicated that several large areas are anomalous in Au. Most of the samples that contained the highest Au concentration were from areas within the northeast-trending belt of mineralization and alteration (Fig. 4). Streams that drain areas that are anomalous in Au, as detected in rock-chip and/or dump samples, also yielded stream-sediment samples that are anomalous in Au.

SUMMARY AND CONCLUSION

Mineral deposits in the Planet mineral district are present along and adjacent to the Buckskin-Rawhide detachment fault and the upper-plate normal and tear faults. Sheared rocks along faults served as conduits for ascending fluids that were not related to local magmatism. Quartz, hematite, sericite, and chlorite are common alteration minerals in silicic upper-plate rocks, whereas calcareous siliceous rocks contain a greater proportion of epidote, calcite, and specular hematite. Alteration below the Buckskin-Rawhide detachment fault produced abundant chlorite and epidote with less abundant quartz, calcite, sericite, fluorite, pyrite, and specular hematite.

Massive, disseminated, and fracture-filling specular hematite and younger fracture-filling chrysocolla form tabular masses within upper-plate calc-silicate rocks, whereas upper-plate quartzites host Au mineralization. Au is concentrated along and adjacent to upper-plate normal and tear faults.

Nearly 80% of the mineral deposits east of Mineral Wash are within a 1,000-m-wide, N50°E-trending zone that contains the best-developed alteration in the district (Figs. 3 and 4). Most of the remaining mineral deposits are within 300 m on either side of that zone. This strongly suggests a structural control for mineralization that coincides with the synformal axis in the detachment surface.

ACKNOWLEDGMENTS

We gratefully acknowledge permission from AMAX Exploration and U.S. Borax to present these data and interpretations.

Geology of mineral deposits in the Buckskin and Rawhide Mountains

JON E. SPENCER
JOHN W. WELTY
Arizona Geological Survey, 845 N. Park Ave., #100, Tucson, Arizona 85719

ABSTRACT

Numerous Miocene mineral deposits are located close to the subhorizontal Buckskin-Rawhide detachment fault in the Buckskin and Rawhide Mountains of west-central Arizona. These deposits are characterized by massive and fracture-filling specular hematite, with local earlier-formed sulfides, and abundant, younger fracture-filling chrysocolla. The detachment-fault zone and high-angle faults within the hanging wall and footwall are the most common sites of mineralization. Less numerous but volumetrically significant replacement deposits are present within calcareous rocks directly above the detachment fault. The consistent association of this type of Cu-Fe mineral deposit with the detachment fault and the general absence of associated Miocene igneous rocks supports the previously proposed hypothesis that these deposits were derived from aqueous fluids ascending along the gently dipping detachment-fault zone. Miocene sedimentary Mn deposits are also locally present within syntectonic sedimentary sequences.

INTRODUCTION

Metamorphic core complexes of western North America are distinctive assemblages of diverse rock types and associated structures. Typical features are a subhorizontal fault, commonly referred to as a *detachment fault,* that separates a footwall of variably mylonitic crystalline rocks from a structurally distended hanging-wall sheet. Hanging-wall rocks are compositionally diverse and usually include Tertiary sedimentary and volcanic rocks. The dissimilar character of hanging-wall and footwall rock types across large areas indicates that displacement on detachment faults has generally been at least several tens of kilometers. Detachment faulting, uplift, and mylonitization of footwall rocks and distension of hanging-wall rocks are all inferred products of large-magnitude, normal displacement on gently dipping shear zones (Wernicke, 1981; Davis, G.H., 1983; Reynolds, 1985; Davis, G.A., and others, 1986). Mineral deposits are locally associated with detachment faults in some metamorphic core complexes and are remarkably common and widespread in and around the Buckskin and Rawhide Mountains.

Almost all of the mineral deposits in the Buckskin and Rawhide Mountains are known or strongly suspected to be Miocene in age and to be associated with the Buckskin-Rawhide detachment fault. Virtually all deposits have similar mineral assemblages: massive or fracture-filling specular hematite with younger fracture-filling (and locally massive) chrysocolla and malachite or brochantite. Some deposits contain early-formed Cu and Fe sulfides that are now largely oxidized. The larger deposits form replacements in variably calcareous upper-plate rocks directly above the detachment fault. Numerous smaller replacement and fracture-filling deposits are present along the fault or are within a few tens of meters to perhaps 100 m above or below the fault. The consistent mineralogy, structural style, and association with the Tertiary detachment fault indicate that these deposits are genetically related to the fault (see also Reynolds, 1980a; Wilkins and Heidrick, 1982; Spencer and Welty, 1986; Wilkins and others, 1986). Cu has been the primary commodity recovered from these deposits, with additional recovery of minor Au, Ag, Pb, and Zn (Table 1). Sedimentary and fracture- or open-space-filling Mn deposits of Miocene age are also present in upper-plate sandstones and sedimentary breccias. Mn deposits and deposits related to detachment faults are probably not directly related to each other; however, they may both be related to broadly synchronous geochemical phenomena.

This article is the product of a systematic field examination of almost all of the mines and prospects in the Buckskin and Rawhide Mountains and some deposits in the Burnt Well mineral district in the nearby northeastern Harcuvar Mountains. Appendix 1, which includes Figures 7 through 18, gives locations and descriptions of mines and prospects in the study area and forms the basis for many of our conclusions. Many mines and prospects in the Buckskin Mountains were also described in detail by Keith (1978). Deposits are grouped into mineral districts and subdistricts based on geologic and geographic criteria (Fig. 1). District boundaries vary slightly from those previously proposed by Keith and others (1983). Similar deposits are present in the Whipple Mountains (Ridenour and others, 1982), easternmost Harcuvar Mountains (Roddy and others, 1988), northern Plomosa Mountains (Jemmett, 1966; Keith, 1978), and northern Moon Mountains (Spencer and others, 1988).

in Spencer, J.E., and Reynolds, S.J., eds., 1989, Geology and mineral resources of the Buckskin and Rawhide Mountains, west-central Arizona: Arizona Geological Survey Bulletin 198, p. 223-254.

Table 1. Deposit type and recorded production for mineral districts and subdistricts in the Buckskin and Rawhide Mountains. Production data are from the U.S. Bureau of Mines. Deposit types are indicated on Figure 2.

MINERAL DISTRICT AND SUBDISTRICT	DEPOSIT TYPES	TONS ORE PRODUCED	lbs. Cu (% Cu)	lbs. Pb (% Pb)	lbs. Zn (% Zn)	oz. Ag (oz/T Ag)	oz. Au (oz/T Au)	lbs. Mn (% Mn)
BUCKSKIN MOUNTAINS								
ALAMO	B	692	38,295	15,593	-	326	81	-
			(2.77)	(1.27)	-	(0.471)	(0.117)	-
Alamo West	B	unknown	-	-	-	-	-	-
Bluebell	B	692	38,295	15,593	-	326	81	-
			(2.77)	(1.27)	-	(0.471)	(0.117)	-
Ives Peak	B	unknown	-	-	-	-	-	-
CIENEGA	G,H,I	19,092	1,713,533	-	-	1,596	12,011	-
			(4.49)	-	-	(0.084)	(0.629)	-
CLARA	F,J	49,728	4,668,908	-	-	1,738	35	-
			(4.69)	-	-	(0.035)	(<0.001)	-
LINCOLN RANCH	K	68,700	-	-	-	-	-	24,000,000
			-	-	-	-	-	(17.5)
MAMMON	B	841	86,993	-	-	142	60	-
			(5.17)	-	-	(0.169)	(0.071)	-
MIDWAY	B,F	214	9,410	-	-	35	45	-
			(2.20)	-	-	(0.164)	(0.210)	-
Battleship	B	15	1,200	-	-	1	-	-
			(4.00)	-	-	(0.067)	-	-
Green Streak	B	189	4,800	-	-	21	37	-
			(1.31)	-	-	(0.111)	(0.196)	-
Mammoth	B,F	10	3264	-	-	13	8	-
			(16.32)	-	-	(1.300)	(0.800)	-
Midway Northeast	B	unknown	-	-	-	-	-	-
PLANET	C,E,H	1,009,771	19,503,012	-	-	268	317	-
			(0.97)	-	-	(0.026)	(<0.001)	-
Mineral Hill	C,E,H	970,756	13,222,300	-	-	49	2	-
			(0.17)	-	-	(<0.001)	(<0.001)	-
Planet	C,E,H	39,015	6,280,712	-	-	219	315	-
			(8.05)	-	-	(0.006)	(0.008)	-
PRIDE	B,F	38	21	-	-	6	78	-
			(0.28)	-	-	(0.158)	(2.052)	-
SWANSEA	A,B,D,F	544,918	26,457,302	-	-	33,112	507	-
			(2.43)	-	-	(0.061)	(<0.001)	-
Copper Penny	F	unknown	-	-	-	-	-	-
Squaw Peak	A,B	unknown	-	-	-	-	-	-

MINERAL DISTRICT AND SUBDISTRICT	DEPOSIT TYPES	TONS ORE PRODUCED	lbs. Cu (% Cu)	lbs. Pb (% Pb)	lbs. Zn (% Zn)	oz. Ag (oz/T Ag)	oz. Au (oz/T Au)	lbs. Mn (% Mn)
Swansea	D	544,918	26,457,302	-	-	33,112	507	-
			(2.43)	-	-	(0.061)	(<0.001)	-
HARCUVAR MOUNTAINS								
BURNT WELL	F	unknown	-	-	-	-	-	-
RAWHIDE MOUNTAINS								
BLACK BURRO	K	820	-	-	-	-	-	331,000
			-	-	-	-	-	(20.0)
CLEOPATRA	A,B,C,F,G,H,J	20,089	476,962	462	-	11,669	1,730	-
			(1.19)	(<0.01)	-	(0.581)	(0.086)	-
Cleopatra	G,H	14,744	430,879	-	-	3,339	1,624	-
			(1.46)	-	-	(0.226)	(0.110)	-
Kimble	A,B,C,F,H	4,482	30,783	-	-	124	52	-
			(0.34)	-	-	(0.028)	(0.012)	-
Lola	H,J	unknown	-	-	-	-	-	-
Silverfield	B,F,H	863	15,300	462	-	8,206	54	-
			(0.89)	(0.27)	-	(9.509)	(0.063)	-
LEAD PILL	H,K	1,451	27,973	404,986	-	2,227	530	-
			(0.96)	(14.00)	-	(1.535)	(0.365)	-
MESA	K	300	-	-	-	-	-	60,000
			-	-	-	-	-	(10.0)
OWEN	A,B	792	1,692	62,617	110	10,326	105	-
			(0.11)	(3.95)	(0.00631)	(13.038)	(0.132)	-
RAWHIDE	F,H	708	10,548	260,145	22,900	8,124	38	-
			(0.74)	(18.37)	(1.617)	(11.474)	(0.054)	-
TOTAL		1,718,183	52,994,649	743,803	23,010	69,569	15,537	24,391,000
			(1.54)	(0.02)	(0.00067)	(0.041)	(0.009)	(0.709)

Although similar deposits are present in other areas of the Basin and Range Province, they are nowhere as well developed and widespread as in west-central Arizona and adjacent southeastern California.

MINERALOGY AND SETTING OF DEPOSITS

Specular hematite (specularite) is by far the most volumetrically significant mineral in mineral deposits of the Buckskin and Rawhide Mountains. Areas of specularite mineralization commonly contain younger fracture-filling (and locally massive) chrysocolla and less abundant malachite, brochantite, quartz, calcite, barite, fluorite, chlorite, and Mn oxides. Brochantite and malachite from these deposits are megascopically similar; as a result, the relative abundance of each is not presently known. In some lower-plate deposits, such as in the Squaw Peak subdistrict of the Swansea mineral district and the New Standard subdistrict of the Pride mineral district, quartz and chlorite are intimately intergrown with 1- to 10-mm-diameter crystals of unusually hard specularite. Upper-plate deposits hosted by variably calcareous Mesozoic metasandstone and metasiltstone at the Mineral Hill and Planet mines contain much fine-grained (1 mm or less) specularite and earthy hematite. In these deposits, abundant earthy hematite and fracture-filling specularite are common at the margins of the zone of massive specularite mineralization.

Cu and Fe sulfides formed early during the genesis of many deposits, although their original abundance is difficult to assess because of extensive oxidation and overprinting by younger specularite-chrysocolla mineralization. Pyrite is rare to nonexistent in most deposits, but relict, limonite-stained cubes or cubic pits are locally common. Veins and disseminations of chalcopyrite within massive and disseminated specular hematite were the target of underground mining at the Swansea mine, and chalcopyrite is locally present in other deposits.

Common settings of Cu-Fe mineral deposits (Fig. 2) are as follows: (1) massive replacement deposits in metasedimentary carbonate slivers within lower-plate crystalline rocks (A in Fig. 2); (2) fracture-filling and local massive replacement(?) deposits in northwest-trending, steeply to moderately dipping shear zones within lower-plate crystalline rocks (B in Fig. 2); (3) massive replacement deposits in upper-plate hydrothermal carbonate replacements, marble, and variably calcareous metasandstone and metasiltstone that directly overlie the detachment fault (C, D, and E, respectively, in Fig. 2); deposits of this type are the largest known mineral deposits in the Buckskin and Rawhide Mountains; (4) fracture-filling and massive replacement(?) deposits in commonly silicified, Fe-stained, and brecciated lower- and upper-plate rocks adjacent to the detachment fault (F in Fig. 2); and (5) fracture-filling and local massive replacement deposits in high-angle shear zones within upper-plate rocks (G, H, and I in Fig. 2). In addition to Cu-Fe deposits, calcite-barite-Mn-oxide veins are common in upper-plate rocks (J in Fig. 2) and are probably related to the other deposit types.

Several Mn deposits form stratabound layers and beds within middle Tertiary sandstone, siltstone, and conglomerate (K in Fig. 2). Mn-oxide deposits consist of black, variably indurated aggregates of microcrystalline to cryptocrystalline Mn oxides, referred to as *wad*. Mn deposits in the Artillery mineral district east of the Rawhide Mountains, which are much larger but otherwise similar to deposits in the Buckskin and Rawhide Mountains, are present as wad composed at least in part of cryptomelane, hollandite, psilomelane, and pyrolusite (Lasky and Webber, 1949; Mouat, 1962).

MAJOR DEPOSITS AND DEPOSIT TYPES

Lower-Plate Deposits

Mineral deposits within lower-plate crystalline rocks are present in numerous steeply dipping shear zones and sparse subhorizontal carbonate slivers. Deposits of this type include virtually all those of the Alamo, Midway, Pride, and Owen mineral districts and the Squaw Peak subdistrict of the Swansea mineral district, and many of those in the Silverfield and Kimble subdistricts of the Cleopatra mineral district. Mineralized shear zones typically strike northwest-southeast (Fig. 3) and contain fracture-filling specularite and chrysocolla. In some lower-plate deposits, especially in the Squaw Peak subdistrict of the Swansea district, massive specularite is present in shear zones and probably represents replacement of crushed quartzo-feldspathic crystalline rocks. Relict pyrite cubes as large as 3 cm and euhedral fluorite cubes as large as 2 cm are present in the Owen mineral district and the Silverfield subdistrict of the Cleopatra district. Specularite forms unusually hard and coarse-grained crystals in these deposits and is commonly associated with chlorite.

Thin subhorizontal slivers of Paleozoic(?) carbonates are locally present within lower-plate crystalline rocks and were probably interleaved with them by Mesozoic thrust faulting or Tertiary detachment faulting (Spencer and Reynolds, this vol.). Massive replacement and fracture-filling deposits within these carbonate slivers are present in the Owen mineral district, the Bluebell subdistrict of the Alamo mineral district, and the Squaw Peak subdistrict of the Swansea mineral district. Some of the carbonate-replacement deposits are cut by high-angle shear zones; such zones were probably pathways for mineralizing fluids that moved from the detachment fault down through lower-plate crystalline rocks to sites of mineralization.

Detachment-Fault-Zone Deposits

Fracture-filling deposits within the detachment-fault zone characterize the deposits of the Clara mineral district and the Copper Penny subdistrict of the Swansea district, as well as some mines in the Midway, Planet, Pride, and Rawhide districts and the Kimble subdistrict of the Cleopatra district. In some of these deposits, fault movement continued after mineralization ceased, as indicated by the abrupt downward or upward termination of mineral deposits at what appears to be the youngest slip surface within the fault zone. At other deposits, mineralization affected rocks throughout the fault zone, which suggests that mineralization outlasted faulting.

Swansea Mine (Swansea Mineral District)

Massive specularite replacement deposits at the Swansea mine are present within an ENE-trending, approximately 1.5-km-long sliver of dominantly Paleozoic carbonate rocks along the southeast flank of the Swansea synform (Spencer and Reynolds, this vol.). The Paleozoic rocks are tectonically interlayered with Proterozoic crystalline rocks and schists derived from Mesozoic sedimentary rocks. Underground mining was directed at chalcopyrite veins and disseminations within the specularite. Much of the ore was localized near the contact between schists and carbonates, which implies that ore-forming solutions reached reactive carbonates by traveling through permeable, highly fractured schists (L.E. Reber, Jr., unpub. manuscript, undated). Chalcocite, bornite, minor cuprite, and native Cu were observed in underground ores (Kislingbury, 1916).

Replacement deposits at the Swansea mine are primarily within a 3- to 30-m-thick zone near the detachment fault, but smaller yet significant deposits are also present farther from the fault. From 1911 to 1947, the gently northeast-plunging, 600-m-long orebody

yielded approximately 545,000 tons of ore averaging 3.5% to 4% Cu.

Planet Mineral District

Two groups of mines and prospects, known as the Planet and Mineral Hill mines, make up most of the mines of the Planet mineral district (Figs. 4 and 5; Table 2). At both groups of mines, numerous tabular masses of brown hydrothermal carbonate are present directly above the detachment fault. The hydrothermal carbonate forms replacements, typically 1- to 10-m-thick, of the lower calc-silicate member of the Triassic Buckskin Formation (Plate 2). These replacement carbonates were first recognized by Wicklein (1980).

Massive specularite has replaced hydrothermal carbonate and variably calcareous metasandstone and metasiltstone of the Buckskin Formation. Halos of fracture-filling specularite and earthy red hematite are present above and adjacent to zones of massive specularite. Chrysocolla and malachite commonly fill fractures in areas of hematite mineralization. At two localities, one each in the Planet and Mineral Hill mine groups, chrysocolla is concentrated along the interface between veins of specular hematite and hydrothermal carbonate. Mineralization affected some of the lower-plate rocks at the Mineral Hill mine, which suggests that mineralization outlasted faulting at this locality.

Cienega Mineral District

The Cienega mineral district has yielded an amount of Au (12,000 oz; Table 1) greater than the total Au production from all other deposits in the Buckskin and Rawhide Mountains. These other deposits are all within 50 to 100 m of the Buckskin-Rawhide detachment fault, whereas the deposits of the Cienega district are an unknown, but probably substantial (several hundred meters) distance above the fault. Most deposits of the Cienega district are along or near a Mesozoic thrust fault that places Proterozoic crystalline rocks over multiply deformed Paleozoic and Mesozoic metasedimentary and metavolcanic rocks (Reynolds and Spencer, this vol.). Deposits form either fracture fillings within shear zones or replacements within carbonates (see also Zambrano, 1965; Keith, 1978). Two of the deposits are near or on contacts between Proterozoic crystalline rocks and Tertiary conglomerate and volcanic rocks. One of these deposits, at the Sue mine, is the only deposit in the Cienega district where preserved sulfides have been recognized (Zambrano, 1965; Keith, 1978). At the Sue mine, chalcopyrite is variably replaced by bornite, covellite, and chalcocite, and zones containing these minerals are cut by veinlets of hematite followed by malachite, azurite, and chrysocolla (Zambrano, 1965).

Mn Deposits

Upper-plate Miocene sandstone and local conglomerate host sedimentary Mn deposits in the Black Burro and Lincoln Ranch mineral districts. In addition, Mn oxides form fracture and open-space fillings at one location each in the Planet and Mesa mineral districts. These deposits are similar to some of the much larger deposits in the adjacent Artillery Mountains (Lasky and Webber, 1949; Spencer, Grubensky, and others, this vol.).

ORIGIN OF MINERAL DEPOSITS

Miocene extensional tectonism in the study area and surrounding areas was associated with several alteration and mineralization phenomena (Fig. 6): (1) K metasomatism of upper-plate sedimentary and volcanic rocks, (2) chloritic alteration of brecciated rocks directly below detachment faults, (3) Cu-Fe mineralization along and near detachment faults, (4) replacement of rocks directly above detachment faults by hydrothermal carbonate, and (5) sedimentary and fracture- and open-space-filling Mn mineralization. Establishing the existence or nonexistence of genetic relationships among these different phenomena has been one goal of past research. Except for chloritic alteration, which occurred at deep structural levels and may not have involved significant fluid movement (Smith and Reynolds, 1985; Reynolds and Lister, 1987), the other phenomena are probably related.

Most of the basic features of detachment-fault-related mineral deposits were first recognized by Wilkins and Heidrick (1982) and Ridenour and others (1982), who proposed that mineralization was broadly synchronous with detachment faulting and that the detachment-fault zone was the primary conduit for migration of mineralizing fluids. Reynolds (1980a) had earlier recognized the importance of detachment faults as fluid conduits during syndetachment mineralization and proposed that elevated geothermal gradients produced by footwall uplift were the cause of the hydrothermal circulation that led to mineralization. Fluid-inclusion studies indicate that mineralizing fluids were saline (12-24 wt. % NaCl equiv.) and were between 175°C and 300°C (Wilkins and others, 1986; Roddy and others, 1988). The high salinities, presence of petroleum daughter products in fluid inclusions (Wilkins and others, 1986), and oxygen isotopic composition of hydrothermal quartz and calcite (Roddy and others, 1988) are consistent with a basinal-brine source for mineralizing fluids. Spencer and Welty (1986) proposed that

Figure 1 (next two pages). Simplified geologic map of the Buckskin and Rawhide Mountains (area of Plate 3) showing locations of mineral districts and subdistricts and of Figures 7 through 18 in Appendix 1. Areas where Paleozoic and Mesozoic upper-plate metasedimentary rocks are present, but largely buried beneath Quaternary and Pliocene sediments, are considered to have a moderate probability of containing concealed deposits similar to those at the Copperstone mine (500,000 oz Au), and a high probability of containing deposits similar to those in the Cienega mineral district (12,000 oz Au) and at the Swansea mine (25 million lbs Cu). Such deposits, if present, may be shallow enough to be profitably mined.

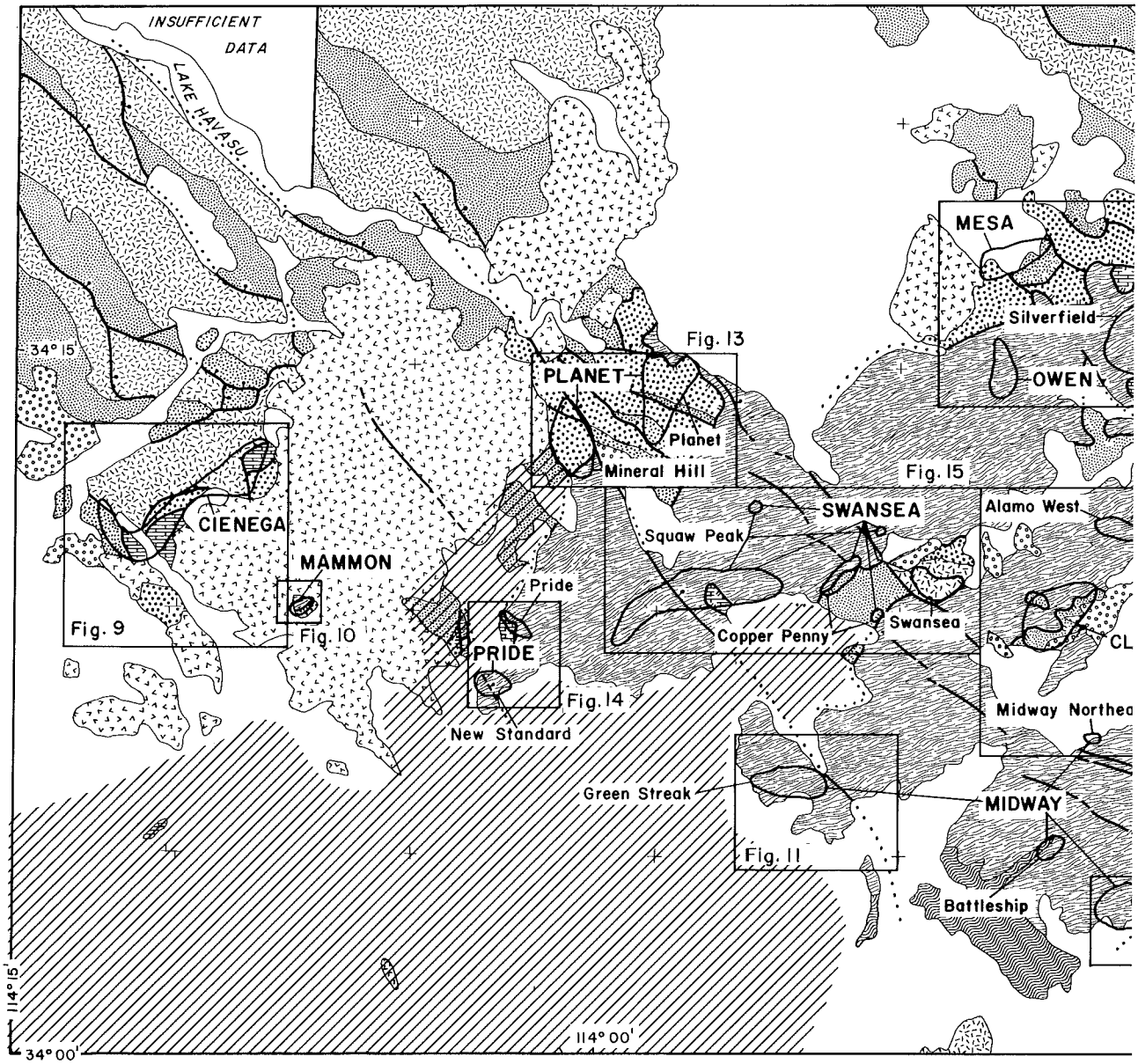

POST-DETACHMENT UNITS

- SURFICIAL DEPOSITS (QUATERNARY TO LATEST TERTIARY)
- BASALT AND LOCAL INTERMEDIATE TO SILICIC VOLCANIC ROCKS AND SEDIMENTARY ROCKS, FLAT LYING TO GENTLY TILTED (MIDDLE TO LATE MIOCENE)
- SEDIMENTARY ROCKS (MIDDLE TO LATE MIOCENE)

UPPER-PLATE UNITS

- SEDIMENTARY AND VOLCANIC ROCKS, GENERALLY MODERATELY TO STEEPLY DIPPING (LATE OLIGOCENE TO MIDDLE MIOCENE)
- METAVOLCANIC AND METASEDIMENTARY ROCKS (MESOZOIC)
- METASEDIMENTARY ROCKS (PALEOZOIC)
- CRYSTALLINE ROCKS (LARGELY PROTEROZOIC, LOCALLY TERTIARY AND MESOZOIC)

LOWER-PLATE UNITS

- MYLONITIC CRYSTALLINE ROCKS (TERTIARY TO PROTEROZOIC)
- MYLONITIC METASEDIMENTARY ROCKS (MESOZOIC AND PALEOZOIC)

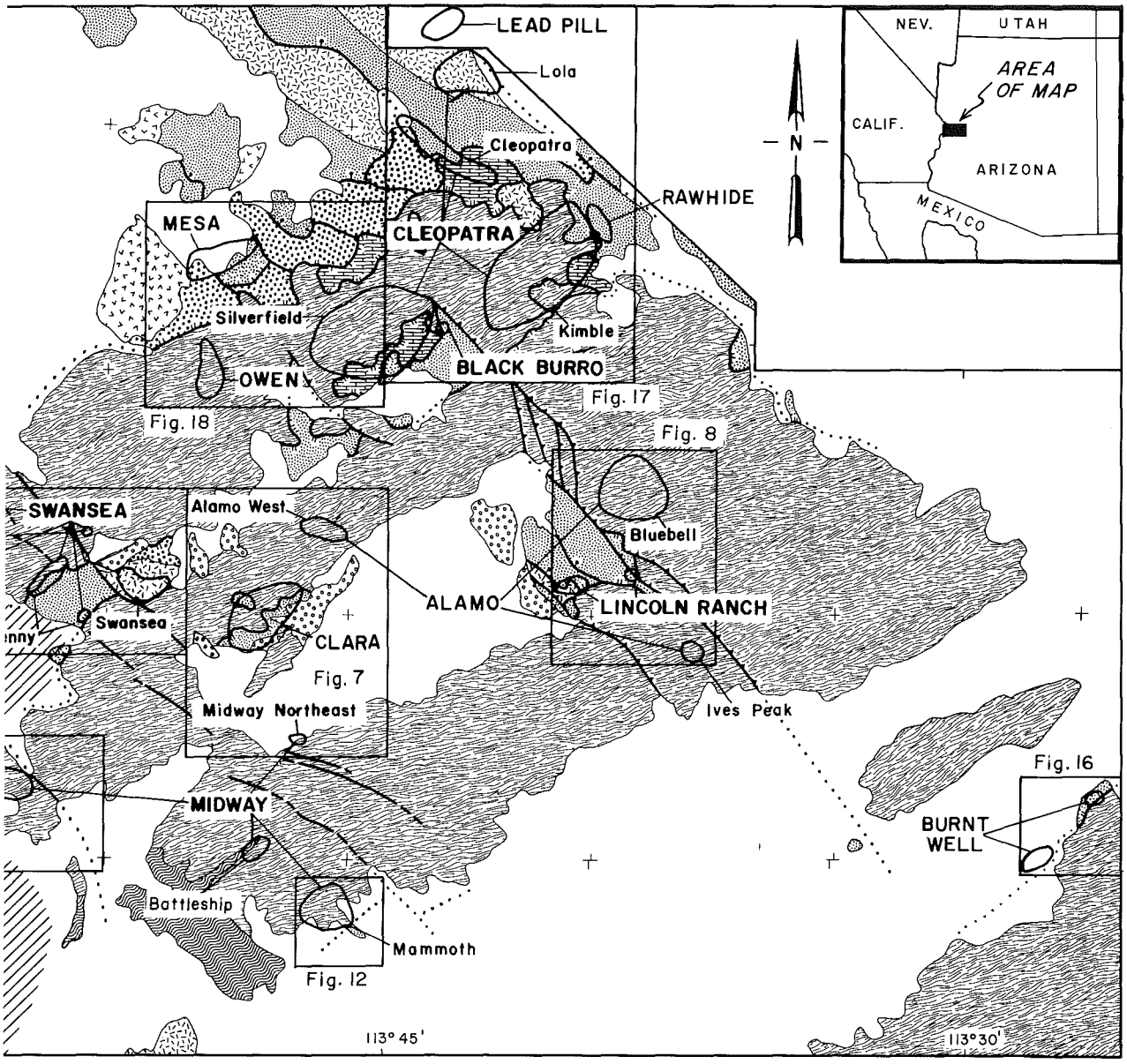

SYMBOLS

BUCKSKIN-RAWHIDE DETACHMENT FAULT

LOW-ANGLE NORMAL FAULT

HIGH-ANGLE NORMAL FAULT

HIGH-ANGLE FAULT

THRUST OR REVERSE FAULT

ALL FAULTS DASHED WHERE APPROXIMATELY LOCATED OR INFERRED, DOTTED WHERE CONCEALED.

DISTRICT

Subdistrict

AREA OF HIGH MINERAL-RESOURCE POTENTIAL

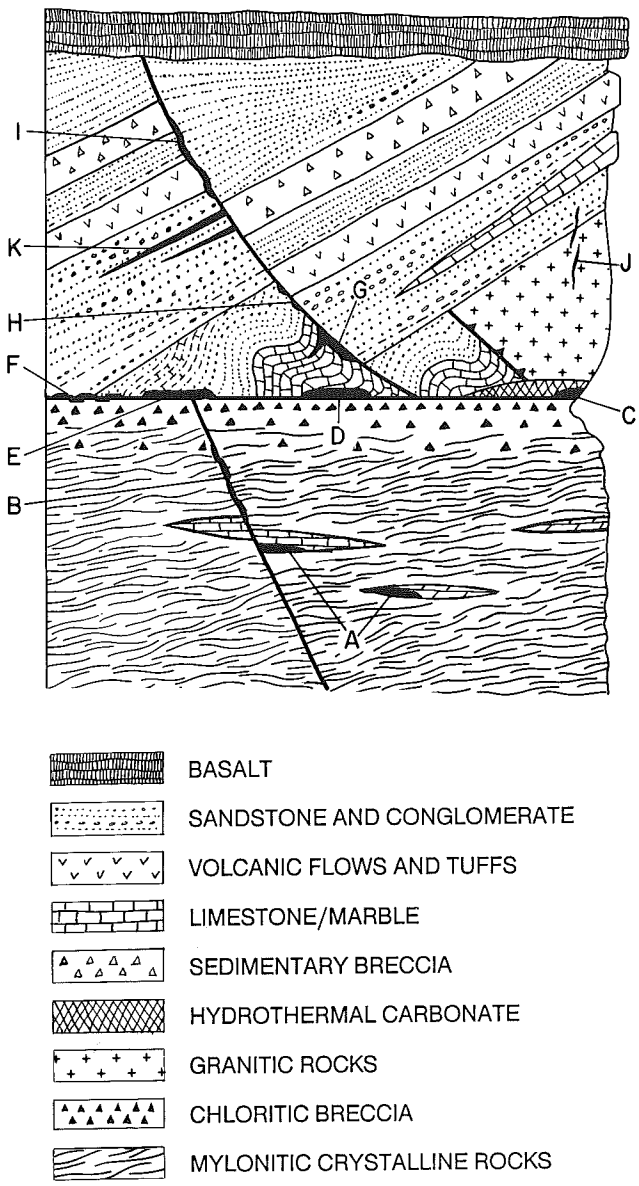

Figure 2. Sites of mineralization in Buckskin and Rawhide Mountains (Cu-Fe mineralization except for K): (A) replacement deposits in carbonate slivers within mylonitic footwall rocks; (B) fracture-filling and local replacement deposits within high-angle fault zones in mylonitic footwall rocks; (C) replacement deposits within hydrothermal replacement carbonate; (D) replacement deposits within Paleozoic carbonate rocks; (E) replacement deposits within calcareous Mesozoic clastic rocks of the Buckskin Formation; (F) fracture-filling deposits along the detachment-fault zone; (G) replacement deposits within Paleozoic carbonate rocks adjacent to upper-plate, high-angle normal faults; (H) fracture-filling deposits along faults that cut Mesozoic metasedimentary rocks; (I) fracture-filling deposits within high-angle fault zones in Miocene sedimentary rocks; (J) vein deposits, possibly along fractures or minor shear zones, within a variety of upper-plate rock types; and (K) sedimentary Mn deposits within Tertiary sandstone and conglomerate.

fluids that yielded Fe and Cu at depth along detachment faults reached low-temperature surface or near-surface levels with high Mn:Fe ratios, and that Mn deposits in areas of detachment faulting were derived from such fluids (see also Krauskopf, 1957; Hewett, 1966). Widespread K metasomatism approximately synchronous with detachment faulting (Brooks and Marvin, 1985; Brooks, 1986; Chapin and Lindley, 1986; Spencer, Shafiqullah, and others, this vol.) supports the hypothesis that K metasomatism by low-temperature saline fluids in extensional sedimentary basins liberated elements that were carried to detachment-fault-related Fe-Cu and Mn deposits by originally K-metasomatizing fluids (Roddy and others, 1988).

Wilkins and Heidrick (1982) and Wilkins and others (1986) proposed that the axes of synformal warps of the detachment-fault surface were the primary conduits for mineralizing fluids and that, as a result, mineralization occurred primarily in the synforms (see also Lehman and Spencer, this vol.). However, the greater abundance of mineral deposits in synforms could be an artifact of preservation, and many deposits could have formed along or above the detachment fault near the axes of antiforms, but these deposits have been eroded away.

We consider three mechanisms for precipitation of metallic minerals in detachment-fault-related deposits: (1) increase in oxygen activity of mineralizing fluids due to mixing of ascending, reducing, metal-bearing fluids with oxidizing, presumably shallow-level aqueous fluids (Spencer and Welty, 1986); (2) decrease in temperature of ascending mineralizing fluids (Roddy and others, 1988); and (3) increase in pH of mildly acidic fluids due to reaction with calcareous rocks. The numerous and volumetrically significant replacement deposits almost certainly formed by reaction of mildly acidic fluids with

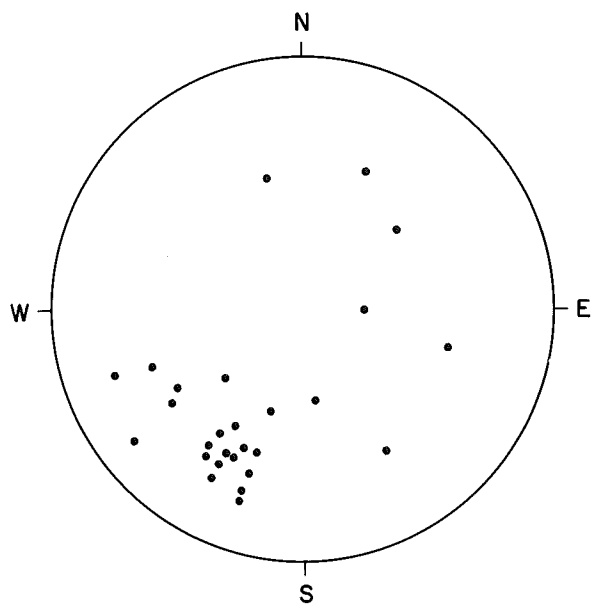

Figure 3. Lower-hemisphere stereonet diagram of poles to mineralized, lower-plate shear zones.

certainly of similar age and genesis (Spencer and others, 1988).

The Cactus Plain area southwest of the Buckskin Mountains is underlain, at least in part, by upper-plate rocks similar to those that are mineralized in the Buckskin and Rawhide Mountains and at the Copperstone mine. We consider it likely that Cu deposits comparable to those at the Swansea, Planet, and Mineral Hill mines and Au deposits comparable to those in the Cienega and Cleopatra districts are present beneath Cactus Plain (Fig. 1). Au deposits comparable to Copperstone may also be present. Such deposits, if they exist, are concealed by Quaternary and Pliocene surficial deposits and would have to be delineated using geophysical techniques.

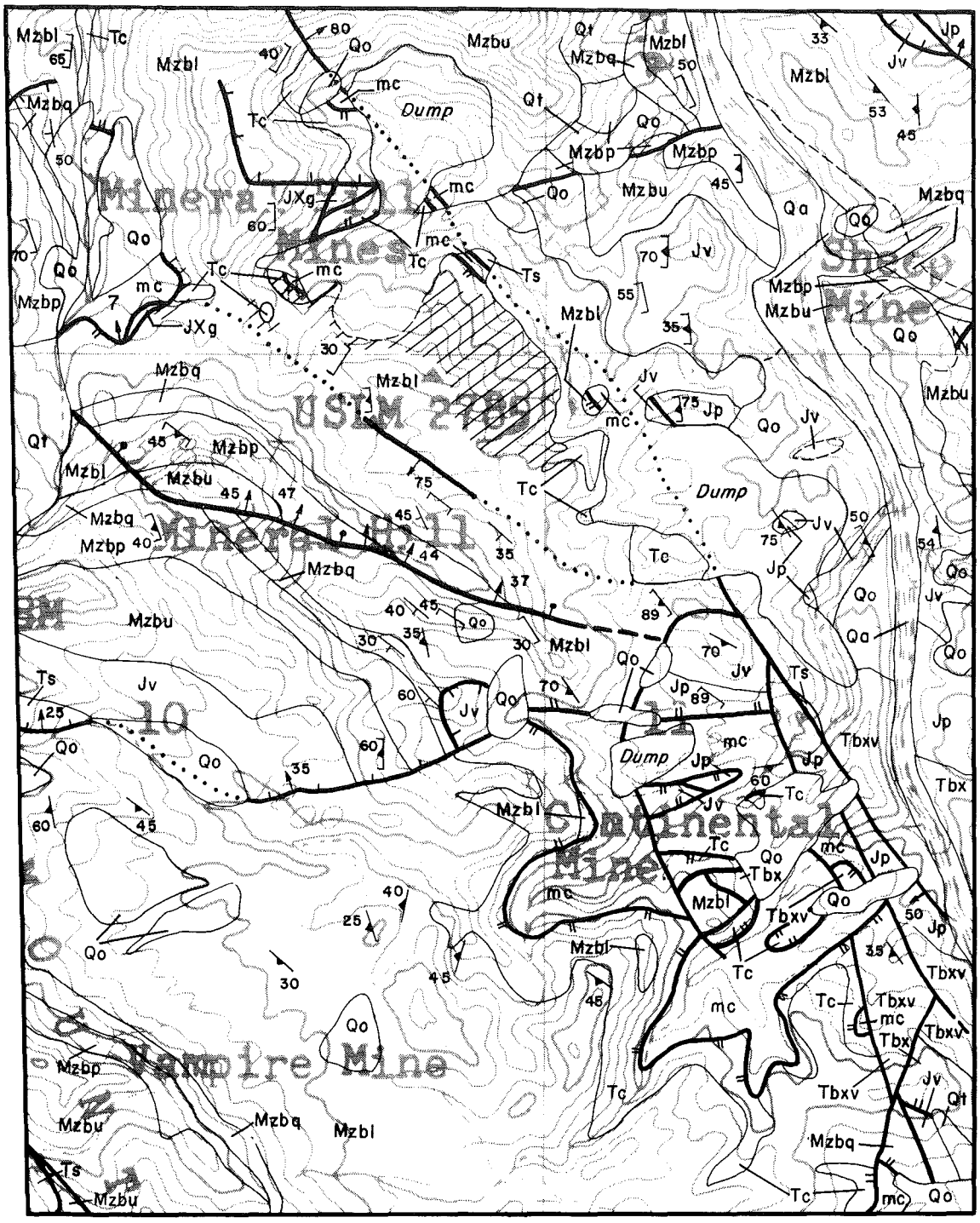

Figure 5. Geologic map of the Mineral Hill mineral district (adapted from Plate 2, with additions by S. J. Reynolds). See Table 2 for explanation of map symbols.

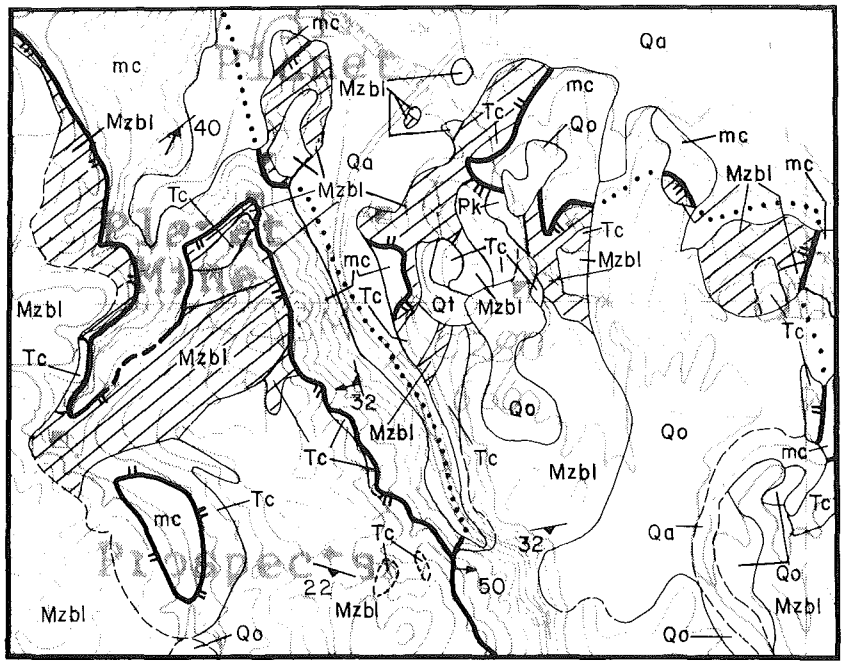

Figure 4. Geologic map of the Planet mineral district (adapted from Plate 2, with additions by J.E. Spencer). See Table 2 for explanation of map symbols.

calcareous rocks, resulting in an increase in the pH of fluids and precipitation of hematite (e.g., Garrels and Dreyer, 1952). The consistent absence of significant wall-rock alteration suggests that the pH was not far from neutral. Less volumetrically significant fracture-filling mineralization could have resulted from cooling of ascending fluids and/or mixing of metal-bearing aqueous fluids with more oxidizing, near-surface aqueous fluids.

The consistent loci, mineralogy, and fluid-inclusion chemistry of widely distributed detachment mineral deposits, as well as the consistent absence of associations between these deposits and Tertiary igneous rocks, strongly support the hypothesis that such deposits are not products of magmatic activity, but are related to large-scale movement of saline fluids along regional, gently dipping detachment-fault zones (Reynolds, 1980a; Wilkins and Heidrick, 1982; Beane and others, 1986; Spencer and Welty, 1986; Wilkins and others, 1986; Roddy and others, 1988). The scattered presence of sedimentary Mn deposits and calcite-barite-Mn-oxide veins of Miocene age in upper-plate rocks in areas of detachment faulting and K metasomatism supports the inference that Mn mineralization was related to detachment faulting and K metasomatism (e.g., Spencer and Welty, 1986; Roddy and others, 1988). However, radically different fluid-inclusion salinities (1 to 3 wt. % NaCl equiv.) from Mn deposits in the Artillery Mountains (Spencer, Grubensky, and others, this vol.) indicate that some Mn deposits did not precipitate directly from fluids that had caused detachment-fault-related mineralization.

MINERAL-RESOURCE POTENTIAL

Of the total Au production from all mines in the Buckskin and Rawhide Mountains (15,635 oz), 83.7% was produced from just four mines: three in the Cienega district (Billy Mack, Carnation, and Lion Hill mines) and one in the Cleopatra district (Cleopatra mine). All of these deposits are hosted by Paleozoic marble or Mesozoic schist and all are at least several tens of meters structurally above the Buckskin-Rawhide detachment fault (Appendix 1; Spencer and Reynolds, this vol.; Plate 1). The Cleopatra and Carnation deposits contain more hydrothermal quartz than is typical for detachment-fault-related deposits. (It was not possible to examine the Billy Mack deposit in detail.) It is perhaps significant that the Copperstone Au deposit in the Moon Mountains is at least several hundred meters above the Moon Mountains detachment fault and contains numerous quartz veins (Spencer and others, 1988). It thus appears that deposits with significant Au that are related to detachment faults are unusually quartz rich and are primarily present in Paleozoic and Mesozoic metasedimentary rocks at least many tens of meters above detachment faults.

The existence of the Copperstone Au deposit approximately 30 km south of the westernmost Buckskin Mountains has implications for mineral-resource potential in the area within and around the Buckskin and Rawhide Mountains. The Copperstone mine is above the Moon Mountains detachment fault (Durning and Hillemeyer, 1986; Spencer and others, 1988), which is possibly correlative with the Buckskin-Rawhide detachment fault (Spencer and Reynolds, this vol.). Except for the presence of amethystine quartz veins and a large amount of Au (6 million tons of ore at average grade of 0.085 oz/ton Au), the Copperstone deposit is very similar to other detachment-fault-related deposits and is almost

Table 2. Legend for Figures 4 and 5.

MAP UNITS AND SYMBOLS

POST-DETACHMENT UNITS

Qa	YOUNG ALLUVIAL DEPOSITS (QUATERNARY)
Qt	TALUS DEPOSITS (QUATERNARY)
Qo	OLD ALLUVIAL DEPOSITS (QUATERNARY)

UPPER-PLATE UNITS

Tc	REPLACEMENT CARBONATE (LOWER TO MIDDLE MIOCENE?)
Ts	SEDIMENTARY ROCKS, UNDIVIDED (LOWER TO MIDDLE MIOCENE?)
Tbx	SEDIMENTARY BRECCIA, UNDIVIDED (UPPER OLIGOCENE? TO MIDDLE MIOCENE?)
Tbxg	SEDIMENTARY BRECCIA, GRANITIC PROTOLITH (UPPER OLIGOCENE? TO MIDDLE MIOCENE?)
Tbxv	SEDIMENTARY BRECCIA, MESOZOIC VOLCANIC PROTOLITH (UPPER OLIGOCENE? TO MIDDLE MIOCENE?)
Jp	PLANET VOLCANICS (JURASSIC)
Jv	VAMPIRE FORMATION (JURASSIC?)
Mzbu	BUCKSKIN FORMATION, UPPER MEMBER (TRIASSIC OR JURASSIC)
Mzbp	BUCKSKIN FORMATION, PHYLLITE MEMBER (TRIASSIC OR JURASSIC)
Mzbq	BUCKSKIN FORMATION, QUARTZITE MEMBER (TRIASSIC OR JURASSIC)
Mzbl	BUCKSKIN FORMATION, LOWER MEMBER (TRIASSIC OR JURASSIC)
JXg	GRANITIC ROCKS (PROTEROZOIC OR JURASSIC)

LOWER-PLATE UNITS

mc	MYLONITIC CRYSTALLINE ROCKS (PROTEROZOIC TO CENOZOIC)

MAP SYMBOLS

	CONTACT – Depositional or intrusive, dashed where approximately located.
10	BUCKSKIN-RAWHIDE DETACHMENT FAULT, SHOWING DIP -- Dashed where inferred, dotted where concealed. Double hatchures on upper plate.
16	LOW-ANGLE (LESS THAN 35 DEGREES) NORMAL FAULT, SHOWING DIP -- Dashed where inferred, dotted where concealed. Single hatchures on upper plate.
45	HIGH-ANGLE (GREATER THAN 35 DEGREES) NORMAL FAULT, SHOWING DIP -- dashed where inferred, dotted where concealed. Bar and ball on hangingwall block.
60	HIGH-ANGLE (GREATER THAN 35 DEGREES) FAULT, SHOWING DIP -- Dashed where inferred, dotted where concealed.
40	STRIKE AND DIP OF BEDDING
32	STRIKE AND DIP OF METAMORPHIC FOLIATION -- Locally includes mylonitic foliation and cleavage.
17	STRIKE AND DIP OF CLEAVAGE
19 / 45	STRIKE AND DIP OF MULTIPLE, PARALLEL, PLANAR COMPOSITIONAL AND/OR FABRIC ELEMENTS -- Shown for example: metamorphic foliation and cleavage, bedding and cleavage.
	LEADER CONNECTING AREAS OF SAME ROCK UNIT
	HEMATITE MINERALIZATION

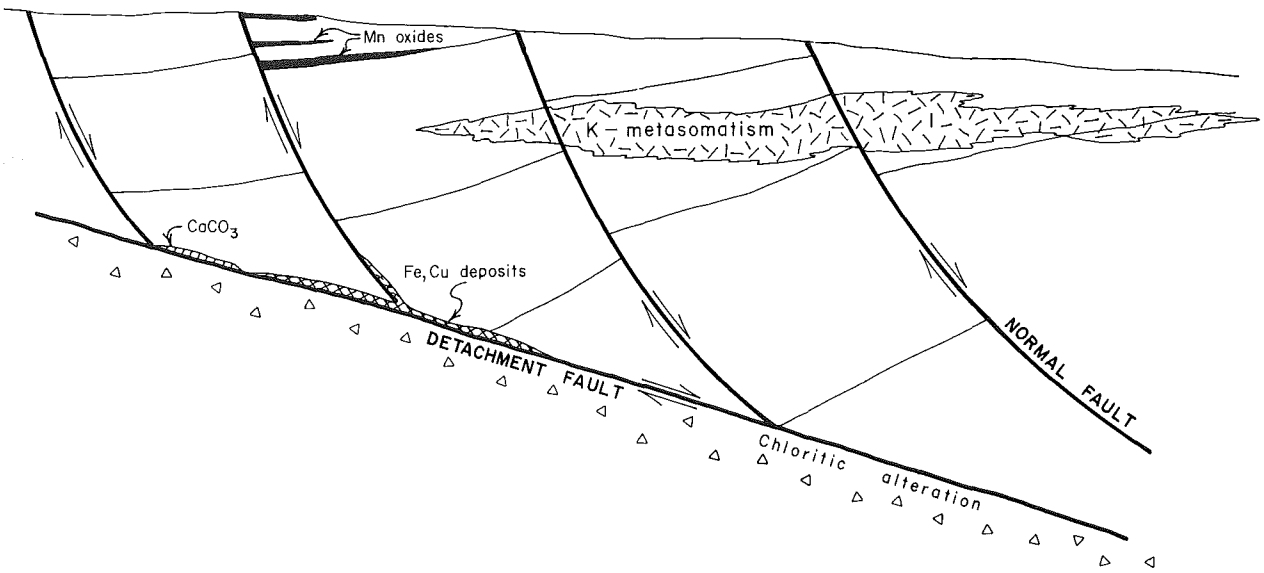

Figure 6. Diagram showing the settings of the five hydrothermal and alteration phenomena that occurred during Miocene detachment faulting in the Buckskin and Rawhide Mountains and surrounding areas.

CONCLUSION

Documentation of mineral-deposit characteristics at virtually all of the numerous mines and prospects in the Buckskin and Rawhide Mountains supports the hypothesis that the deposits are related to the Buckskin-Rawhide detachment fault and originated from aqueous fluids that circulated along the fault. Most deposits formed by precipitation of Cu and Fe minerals in fractures and open spaces. Less abundant but volumetrically more significant deposits formed by replacement of calcareous Mesozoic and Paleozoic metasedimentary rocks. Four deposits that yielded most of the Au in the Buckskin and Rawhide Mountains are hosted by Paleozoic and Mesozoic metasedimentary rocks and are well above the detachment fault. Four other deposits that together yielded approximately 50 million pounds of Cu are in upper-plate Paleozoic, Mesozoic, and Tertiary metasedimentary and sedimentary rocks directly above (and in contact with) the detachment fault. Au and Cu deposits similar to those in the Buckskin and Rawhide Mountains are almost certainly present beneath alluvial cover in Cactus Plain, and a Copperstone-size deposit could be present as well.

ACKNOWLEDGMENTS

We thank Steve Reynolds and Norm Lehman for many informative discussions in the field and elsewhere concerning the nature and origin of mineral deposits in the Buckskin and Rawhide Mountains. We also thank Joe Wilkins, Jr. for chemical analyses of the Clara Peak vein samples.

APPENDIX 1

BUCKSKIN MOUNTAINS

ALAMO DISTRICT (Alamo West subdistrict; Fig. 7)

LOCATION NUMBER: 4-11-86-8
DESCRIPTION: Slightly to moderately fractured, chloritically altered, lower-plate crystalline rocks contain fracture-filling hematite, siliceous hematite, and very sparse chrysocolla and malachite(?). Fracturing is more significant in area of mineralization. Moderately abundant to sparse quartz veins in mine dump next to shaft formed as open-space fillings along fractures. Unfoliated diorite-amphibolite body (not dike) adjacent to shaft is suspected to be middle Tertiary in age.

LOCATION NUMBER: 4-11-86-9
DESCRIPTION: Shear zone exposed in prospect pit strikes north-south and dips 30°E. Hematite staining is pervasive in fractures in coarse-grained Proterozoic(?) granite.

LOCATION NUMBER: 4-12-86-1
DESCRIPTION: Planar fault surface (attitude N68°W, 45°NE) forms hanging wall of decline that is at least 20 m deep. On fracture surfaces in fault zone that is 2 to

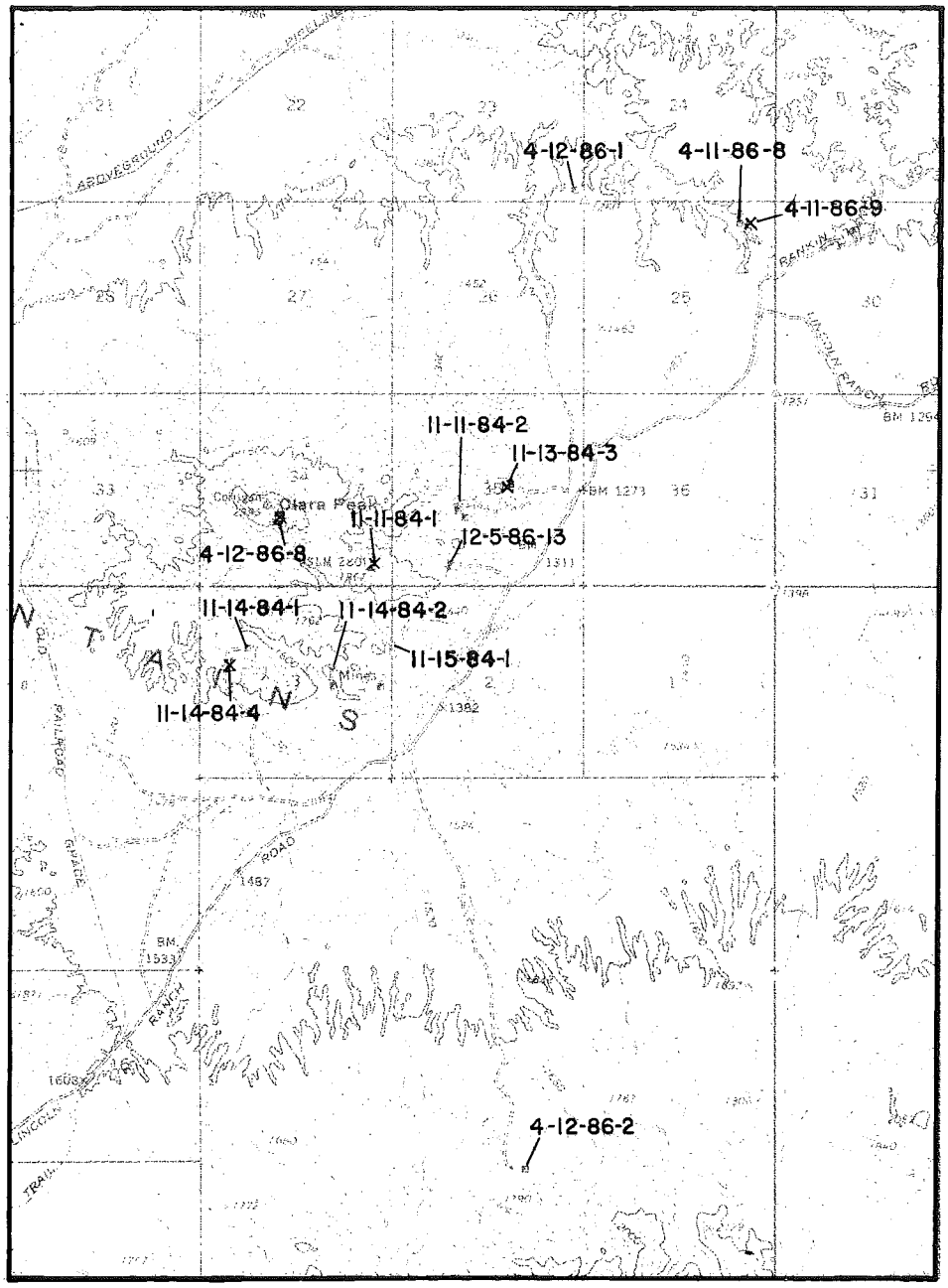

Figure 7. Location map of mines and prospects in the Clara mineral district, the Alamo West subdistrict of the Alamo mineral district, and the Midway northeast subdistrict of the Midway mineral district. See Figure 1 for location of map.

3 m wide, hematite staining is pervasive. Quartz veins and open-space fillings are common. Sparse to moderately abundant chrysocolla is present in mine dump. Megacrystic augen-gneiss host with gneissic layering is discontinuously overprinted on foliation surfaces by mylonitic fabric with ENE-trending lineation.

ALAMO DISTRICT (Bluebell subdistrict; Fig. 8)

LOCATION NUMBER: 2-6-85-2
DESCRIPTION: Decline in mineralized shear zone that dips 50°NE. Hematite, chrysocolla, malachite, and vuggy quartz along fractures in metasedimentary tectonite host. Feldspars in host are locally altered to clay near mineralized areas.

LOCATION NUMBER: 2-6-85-3
DESCRIPTION: Iron oxides, chrysocolla, quartz, and fluorite along fractures in steeply dipping, brittle shear zone that cuts metasedimentary tectonite. Prospect is located in carbonate lens in metasedimentary tectonite. Quartz forms overgrowths on iron and copper minerals. Fluorite crystals are clear and up to 1 cm in diameter.

LOCATION NUMBER: 2-6-85-5 (Bluebell mine)
DESCRIPTION: Chrysocolla, hematite, quartz, and fluorite with sparse specular hematite in shear zone that dips 50°NE. Mine is decline in shear zone; adits to northwest are on same shear zone. Host is mixed metasedimentary and metaigneous gneiss.

LOCATION NUMBER: 2-6-85-6
DESCRIPTION: Chrysocolla and iron oxides on fracture surfaces along brittle shear zone that strikes N55°W and dips 50°NE. Host rocks are metasedimentary tectonite with subhorizontal foliation.

LOCATION NUMBER: 2-6-85-7
DESCRIPTION: Malachite, fluorite, and quartz along fractures in shear zone that dips 65°NE. This is the same shear zone as at location 2-6-85-6.

LOCATION NUMBER: 2-6-85-8
DESCRIPTION: Shaft estimated to be 50 to 60 m deep in metasedimentary tectonite. Mine dump contains fresh metaigneous gneiss and sparse specular hematite, malachite, and chrysocolla.

LOCATION NUMBER: 2-6-85-9 (Arizona-Montana mine)
DESCRIPTION: Iron oxides, chrysocolla, quartz, and calcite in shear zone that strikes N70°W and dips 65°NE. Host is mylonitic gneiss with igneous protolith and subhorizontal foliation.

LOCATION NUMBER: 2-6-85-10
DESCRIPTION: Shear zone (attitude N70°W, 58°NE) with adit hosts fracture-filling chrysocolla and iron oxides. Host rocks are mylonitic gneiss.

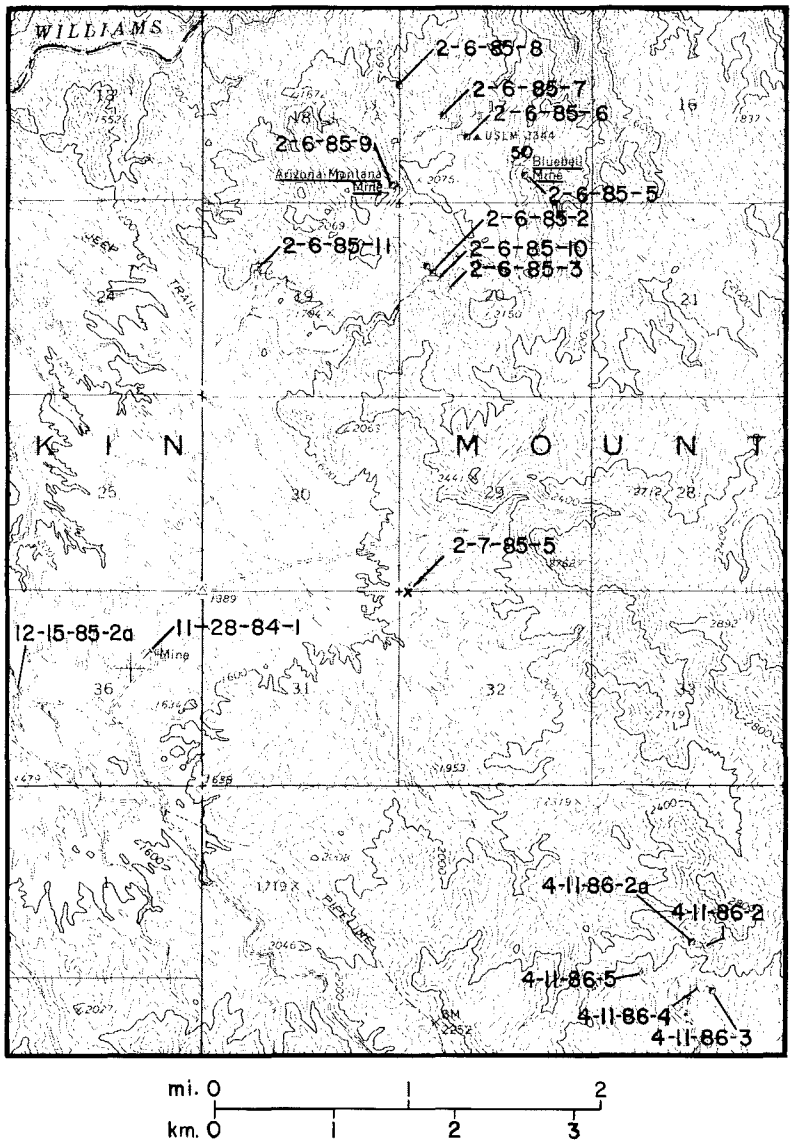

Figure 8. Location map of mines and prospects in the Lincoln Ranch mineral district and the Bluebell and Ives Peak subdistricts of the Alamo mineral district. See Figure 1 for location of map.

LOCATION NUMBER: 2-6-85-11
DESCRIPTION: Adits and declines along shear zone (attitude N60°W, 55°NE) that contains fracture-filling chrysocolla and iron oxides. Host rock is mylonitic gneiss with subhorizontal foliation.

ALAMO DISTRICT (Ives Peak subdistrict; Fig. 8)

LOCATION NUMBER: 4-11-86-2
DESCRIPTION: Shear zone (attitude N70°W, 50°NE) in lower-plate mylonitic crystalline rocks is characterized by fracture-filling chrysocolla and drusy quartz, with minor amounts of epidote, specular hematite, and malachite. Hard, dark-brown silicified(?) hematite is common along shear zone.

LOCATION NUMBER: 4-11-86-2a
DESCRIPTION: Same shear zone and style of mineralization as at location 4-11-86-2. Decline shown as shaft on map plunges 35°N, 50°E along shear zone that strikes N40°W and dips 35°NE. Slickenside lineations on fault surface trend N11°E in fault plane. Mylonitic foliation strikes N56°E and dips 22°SE, with N55°E-trending lineation.

LOCATION NUMBER: 4-11-86-3
DESCRIPTION: Shear zone (attitude N70° ± 10°W, 35° ± 5°NE) contains open-space- and fracture-filling quartz, hematite, and chrysocolla. Quartz crystals are up to 2 cm long. Shaft plunges more steeply than dip of shear zone, and the mine dump contains much fresh amphibolite gneiss.

LOCATION NUMBER: 4-11-86-4
DESCRIPTION: Decline along shear zone (attitude N83°E, 30°N) that contains fracture-filling quartz, hematite, and chrysocolla.

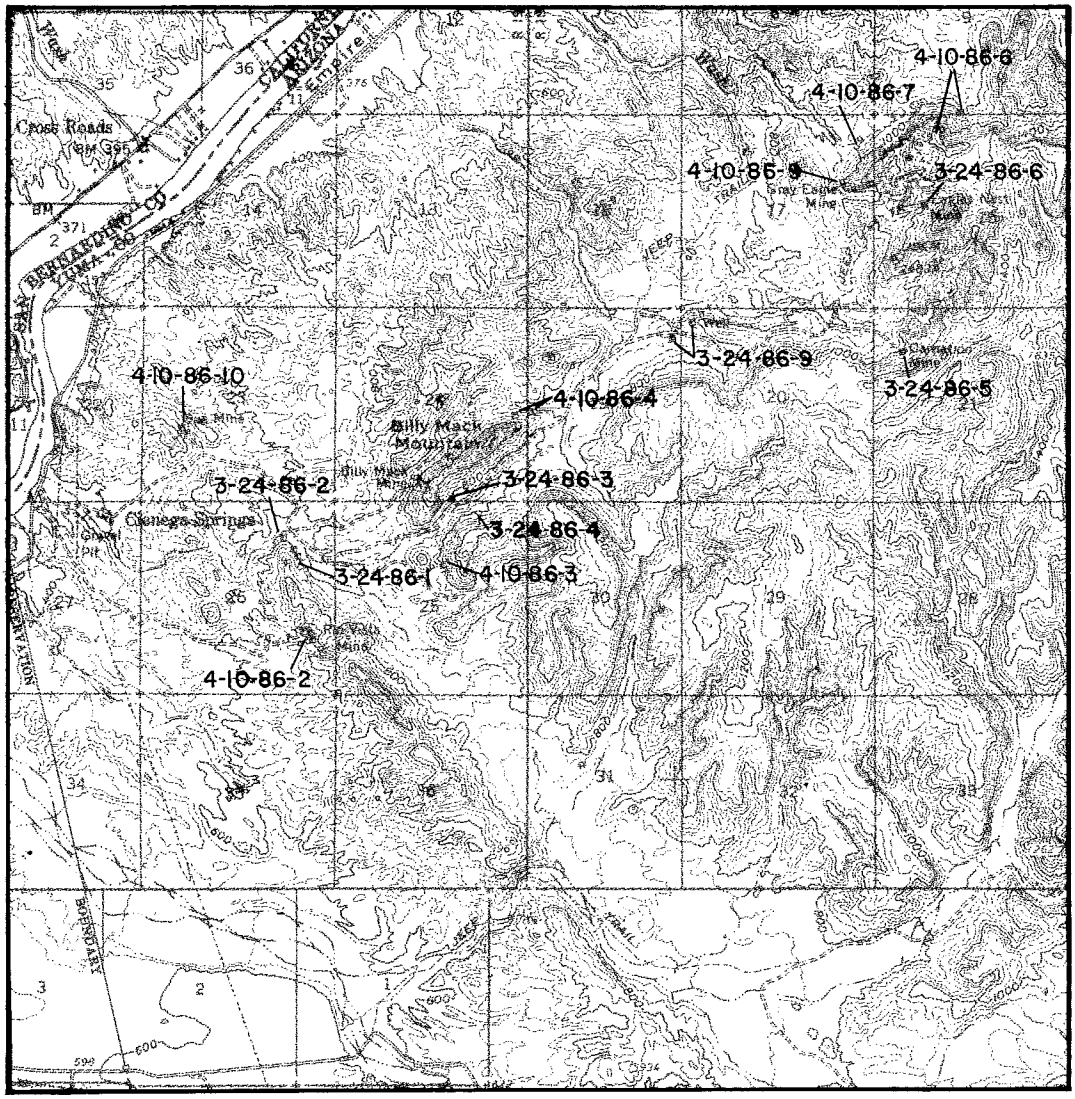

Figure 9. Location map of mines and prospects in the Cienega mineral district. See Figure 1 for location of map.

LOCATION NUMBER: 4-11-86-5
DESCRIPTION: Quartz, hematite, and chrysocolla form fracture and open-space fillings along 0.5-m-wide shear zone that strikes N54°W and dips 56°NE. Some quartz is chalcedonic.

CIENEGA DISTRICT (Fig. 9)

LOCATION NUMBER: 3-24-86-1
DESCRIPTION: Adit in 2- to 3-m-wide shear zone (attitude N30°W, 60°NE) that contains massive and honeycomb-texture calcite veins and less abundant quartz, chrysocolla, malachite(?), earthy hematite, and manganese oxides. Fractures in host rocks contain both earthy hematite and specular hematite. Host rocks include Mesozoic quartz-sericite-chlorite schist and white quartzite.

LOCATION NUMBER: 3-24-86-2
DESCRIPTION: One- to 5-cm-thick, milky quartz veins and fracture-filling chrysocolla and calcite in Paleozoic marble.

LOCATION NUMBER: 3-24-86-3
DESCRIPTION: Fractures in foliated porphyritic granite and alaskitic granite are coated with hematite, specular hematite, and sparse chrysocolla and quartz.

LOCATION NUMBER: 3-24-86-4
DESCRIPTION: Fault contact between Mesozoic quartz-sericite-chlorite schist and Paleozoic marble is mineralized and has three adits along it. Hematite-limonite staining and sparse fracture-filling chrysocolla, quartz, calcite, and specular hematite are hosted primarily by schist along fault contact. Limonite staining is apparent in areas where relict pyrite cubes are present.

LOCATION NUMBER: 3-24-86-5 (Carnation mine)
DESCRIPTION: Decline (plunging 45°, S30°W) in quartz-sericite schist derived from lower Mesozoic sedimentary rocks. Vuggy quartz, fracture-filling chrysocolla, hematite, specular hematite, relict sulfides (mainly chalcopyrite), sparse siderite, and manganese(?) oxides are hosted by schist in a zone parallel to an adjacent shear zone. The abundance of quartz and relict sulfides and absence of specular hematite and chrysocolla, characteristic of this mine, are atypical.

LOCATION NUMBER: 3-24-86-6 (Eagle's Nest mine)
DESCRIPTION: At workings on hillside south of mine shaft, Paleozoic marble hosts massive specular-hematite replacements with fracture-filling chrysocolla, goethite, quartz, calcite, earthy hematite, and dioptase. Pervasive fractures trend east-west and dip 60°N. Shaft is in foliated granite with fracture-filling specular hematite, hematite, and chrysocolla. Two other adits in vicinity are along faults that juxtapose granite and Paleozoic units.

LOCATION NUMBER: 3-24-86-9
DESCRIPTION: Barite/manganese-oxide veins up to 5 cm across with sparse specular hematite and chrysocolla in steeply tilted Tertiary conglomerate.

LOCATION NUMBER: 4-10-86-2
DESCRIPTION: High-angle shear zones that form contacts between quartzite and schist contain fracture-filling specular hematite, chrysocolla, quartz, and manganese oxide. Specular-hematite replacement deposits are present in two adits to southeast in Kaibab Limestone.

LOCATION NUMBER: 4-10-86-3 (Lion Hill mine group)
DESCRIPTION: Planar shear zone (attitude N76°E, 45°NW) in Paleozoic marble at lower adit contains specular hematite and chrysocolla that extends up to 10 m into footwall of fault. Upper adit is on shear zone (attitude N70°W, 55°SW) with same mineral assemblage and style of mineralization as at lower adit.

LOCATION NUMBER: 4-10-86-4
DESCRIPTION: At adit, sparse, milky vein quartz, specular hematite, and hematite form fracture fillings directly below fault contact that juxtaposes Paleozoic marble over quartz-sericite-chlorite schist. Two shafts are shown as one shaft on topographic map. Lower shaft contains fracture-filling chrysocolla, specular hematite, and quartz in Mesozoic schist and Paleozoic marble. Upper shaft is located along high-angle shear zone (attitude N20°E, 70°SE) in Paleozoic marble containing specular hematite and sparse chrysocolla as fracture fillings and possibly as replacements.

LOCATION NUMBER: 4-10-86-6
DESCRIPTION: Massive specular-hematite replacements and fracture-filling specular hematite, a minor amount of chrysocolla, manganese oxides, and calcite in Paleozoic marble.

LOCATION NUMBER: 4-10-86-7
DESCRIPTION: High-angle shear zone in Mesozoic quartz-feldspar-sericite-chlorite schist hosts fracture-filling specular hematite, chrysocolla, and calcite. At nearby adit to southwest, Paleozoic carbonates and structurally underlying quartz-feldspar-sericite-chlorite schist host fracture-filling specular hematite and chrysocolla along shear zone oriented N40°E, 25°SE.

LOCATION NUMBER: 4-10-86-9 (Gray Eagle mine)
DESCRIPTION: Massive specular-hematite replacements and fracture-filling specular hematite and chrysocolla in Paleozoic marble.

LOCATION NUMBER: 4-10-86-10 (Sue mine)
DESCRIPTION: Chrysocolla, manganese oxides, hematite, and barite are present within a high-angle shear zone (attitude N48°W, 60°SW) that juxtaposes Tertiary volcanic and conglomeratic rocks, and within fractures in volcanic rocks.

CLARA DISTRICT (Fig. 7)

LOCATION NUMBER: 11-11-84-1
DESCRIPTION: Brecciated volcanic rocks above 1- to 2-m-thick gouge zone along the Buckskin-Rawhide detachment fault contain chalcopyrite, bornite, and relict pyrite cubes. Chrysocolla, malachite, and selenite are present in fractures. Rocks below the detachment fault are composed of shattered, silicified mylonitic gneiss with fractures that contain drusy quartz (1- to 2-mm crystals), chrysocolla, and specular hematite. Irregular veins of chrysocolla and quartz-hematite-chrysocolla, up to 1 cm thick, are present in brecciated lower-plate rocks. Drusy quartz fills fractures in and along actual fault zone and apparently postdates fault movement. Hematite below fault in breccia is slightly fractured to unfractured.

LOCATION NUMBER: 11-11-84-2
DESCRIPTION: Shattered chloritic breccia directly below Buckskin-Rawhide detachment fault contains malachite, chrysocolla, hematite, and drusy quartz in fractures. Late-stage selenite fills fractures in upper plate.

LOCATION NUMBER: 11-13-84-3
DESCRIPTION: Adits and prospects along and just above Buckskin-Rawhide detachment fault. Highly fractured upper-plate rocks contain chrysocolla on fracture surfaces. Zones up to 50 cm thick contain quartz, calcite, hematite, and manganese oxides. Hematite staining is pervasive. Mineralized zones typically follow northeast-striking, southeast-dipping, upper-plate shear zones. Host is silicified and shattered Tertiary sandstone and Tertiary volcanic or hypabyssal rocks.

LOCATION NUMBER: 11-14-84-1
DESCRIPTION: Chrysocolla, malachite, quartz, calcite, botryoidal hematite, and silicified hematite along gently dipping fractures in Tertiary volcanic(?) breccia directly above the Buckskin-Rawhide detachment fault.

LOCATION NUMBER: 11-14-84-2
DESCRIPTION: Brecciated conglomerate with silica-hematite matrix located directly above the Buckskin-Rawhide detachment fault. Gently dipping fractures are pervasively limonite stained and contain much red to black hematite. Sparse selenite is also present.

LOCATION NUMBER: 11-14-84-4
DESCRIPTION: Underground workings in crushed rocks along the Buckskin-Rawhide detachment fault. Fractures in upper-plate, silicic, Tertiary volcanic or hypabyssal rocks contain hematite, chrysocolla, and malachite.

LOCATION NUMBER: 11-15-84-1
DESCRIPTION: Chrysocolla, malachite, hematite, and barite are present in fractures along the Buckskin-Rawhide detachment fault zone. Adit 60 m to northwest is along upper-plate shear zone that contains chrysocolla, malachite, quartz, and hematite with quartz primarily present as fine-grained colloform overgrowths on other minerals.

LOCATION NUMBER: 4-12-86-8
DESCRIPTION: The Clara Peak klippe is composed of variably but typically strongly silicified or calcified, brown to reddish-brown Miocene conglomerate. One- to 3-cm-thick, quartz-barite-calcite-hematite veins, with or without manganese oxides, are locally numerous within the klippe and may be as much as 1 m thick. Some irregular veins are probably replacements and contain conglomerate clasts. Veins and replacements are typically banded with dark-red silicified hematite, gray calcite, and white bladed barite. Calcite-barite-hematite veins, 1 to 2 cm thick, locally form stockworks. Vein orientation is variable, but NNW strikes and vertical to steep northeast dips are common. Six 8- to 16-in. chip-channel samples collected from six different barite veins contain less than 0.02 ppm Au and less than 20 ppm Ag (Table 3).

LOCATION NUMBER: 12-5-86-13
DESCRIPTION: Detachment-fault surface forms roof of adit. Microbreccia below fault contains fracture-filling chrysocolla. One-meter-thick fault-gouge zone between microbreccia and upper plate is not mineralized. Gouge zone contains clasts of Mesozoic metavolcanic rocks.

LINCOLN RANCH DISTRICT (Fig. 8)

LOCATION NUMBER: 11-28-84-1
DESCRIPTION: Miocene conglomerate and a minor amount of sandstone with pervasive, black manganese oxides that fill pore spaces and coat cobbles along 20-

Table 3. Chemical analyses for calcite-barite-Mn-oxide veins at Clara Peak.

CLARA PEAK Ba-Mn VEIN SAMPLES
(analyses in ppm)

Sample no.	Au	Ag	Cu	Mo	Pb	Zn	As	Sb	Ba	Mn	Mg
CPB-1	0.005	2.4	35	6	170	45	40	4	260,000	4,300	1,300
CPB-2	0.007	2.1	75	6	390	30	110	4	250,000	4,200	900
CPB-3	0.003	0.5	15	2	35	35	30	2	220,000	5,700	870
CPB-4	0.014	14.0	35	8	125	30	125	4	27,000	21,000	2,000
CPB-5	<0.002	8.9	10	2	10	15	20	2	420,000	330	410
CPB-6	0.015	13.0	10	2	20	25	40	6	300,000	3,800	680

to 50-m-wide shear zone between clastic sedimentary rocks and unmineralized granitic breccia. Shear zone is oriented N20°W, 55°NE at one location where planar wall of shear zone is mineralized. Mineralization thus occurred after faulting started, but before it ended, because adjacent granitic breccia is not mineralized. Faults within mineralized shear zone are complex, moderately irregular, and multiple. Mineralization has not affected adjacent lower-plate rocks and is older than final detachment-fault movement that juxtaposed upper- and lower-plate rocks.

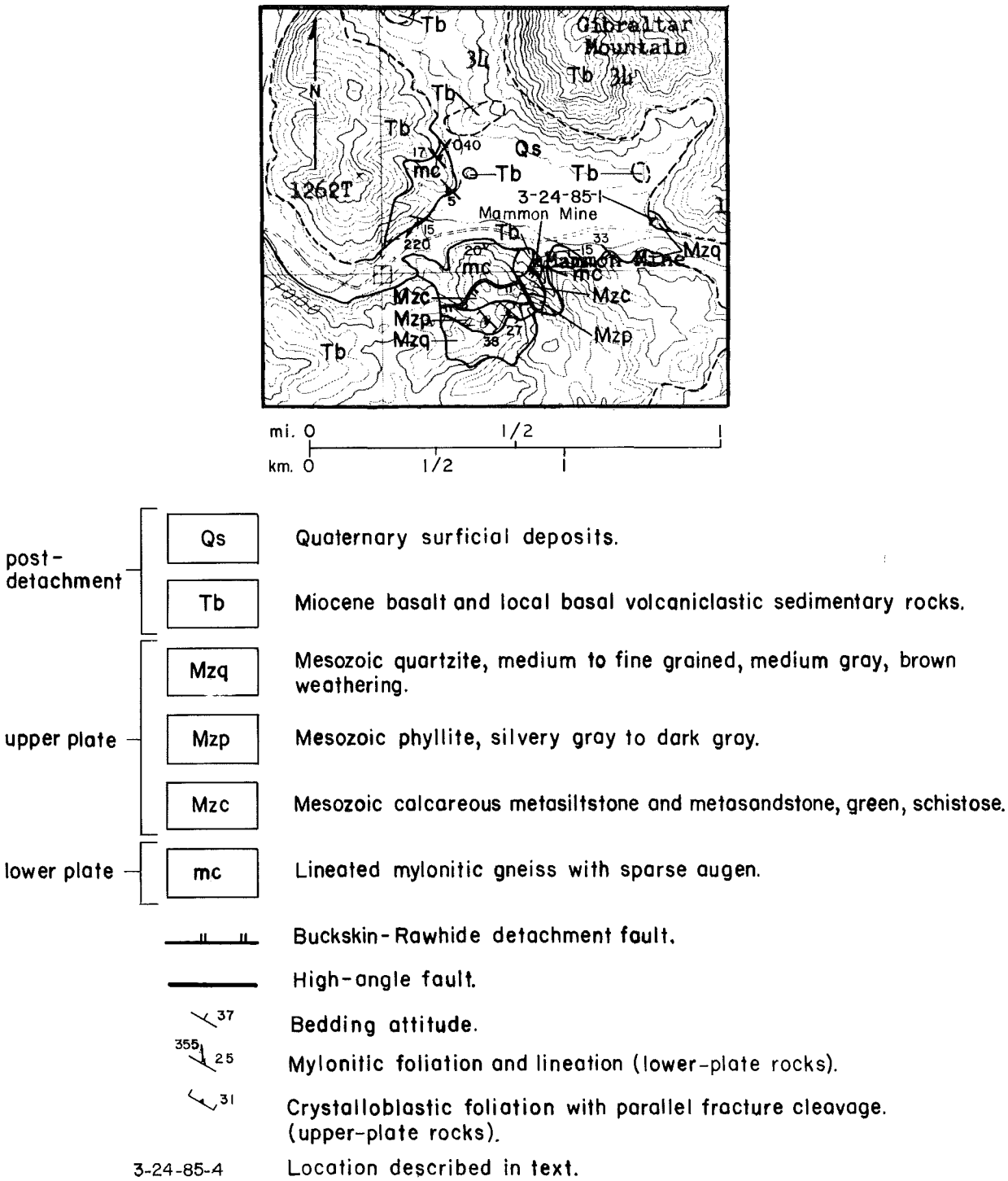

Figure 10. Location map of mines and prospects in the Mammon mineral district. See Figure 1 for location of map.

LOCATION NUMBER: 2-7-85-5
DESCRIPTION: Black manganiferous sandstone and siltstone within reddish-brown, unmineralized middle Tertiary sandstone and siltstone. Manganese is strata-bound and probably sedimentary.

LOCATION NUMBER: 12-15-85-2a
DESCRIPTION: Black manganese oxides hosted by brown sandstone. Interpreted as a primary sedimentary deposit.

MAMMON DISTRICT (Fig. 10)

LOCATION: Mammon mine
DESCRIPTION: Decline in shear zone (attitude N40°W, 40°SW) in lower-plate mylonitic gneiss. Shear zone is parallel to foliation. Brittlely sheared rocks in walls of decline are strongly stained with iron oxides and contain fracture-filling chrysocolla and malachite. Nearby exposures of massive specularite contain fracture-filling malachite and chrysocolla, and late calcite on some fracture surfaces. Mineralized areas around Mammon mine are within 50 m of structurally overlying Buckskin-Rawhide detachment fault.

LOCATION NUMBER: 3-24-85-1

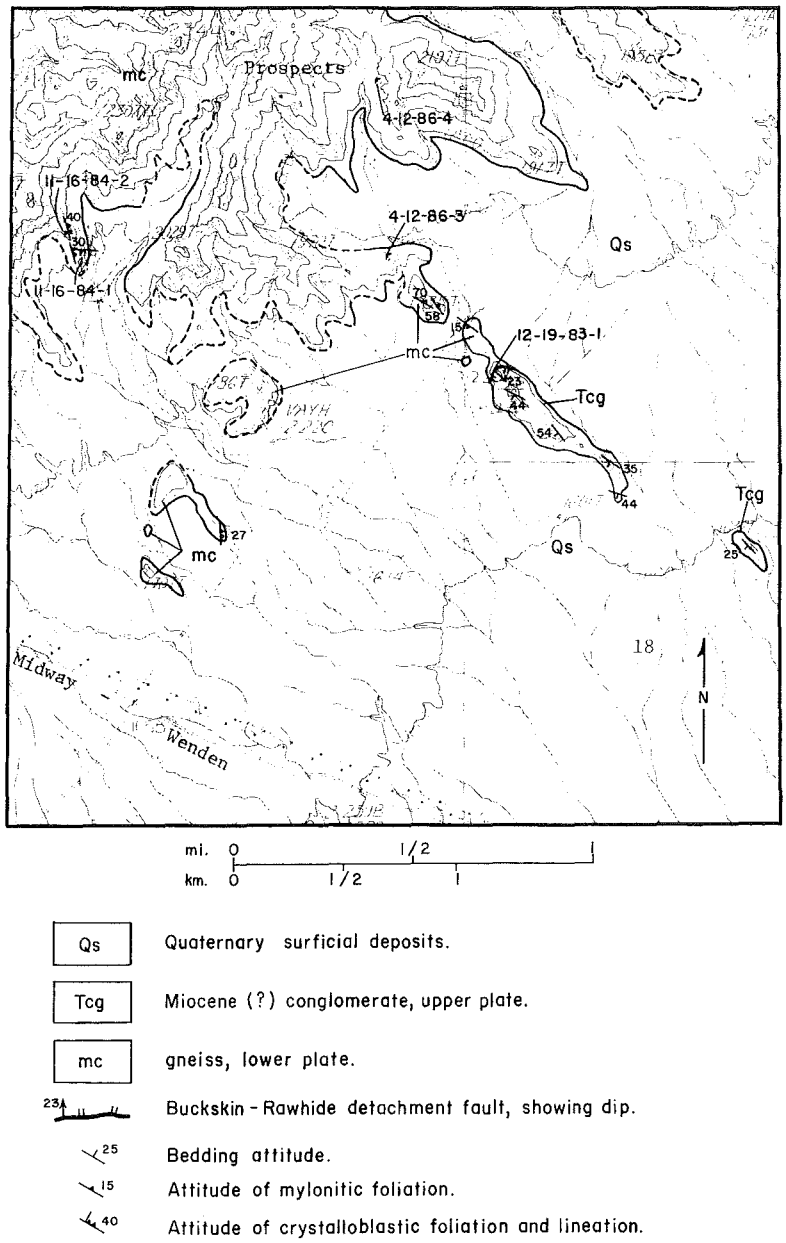

Figure 11. Location map of mines and prospects in the Green Streak subdistrict of the Midway mineral district. See Figure 1 for location of map.

DESCRIPTION: Mesozoic quartzite hosts fracture-filling and replacement(?) specular hematite and very sparse chrysocolla.

MIDWAY DISTRICT (Battleship Peak subdistrict; Fig. 1)

LOCATION: South flank of Battleship Peak
DESCRIPTION: Prospects on south flank of Battleship Peak are located in quartzite, calc-silicate, and carbonate tectonite. Mineralization is characterized by fracture-filling chrysocolla, malachite(?), goethite, hematite, and manganese oxides.

LOCATION: Summit of Battleship Peak
DESCRIPTION: Summit of Battleship Peak is 2-m-thick, subhorizontal microbreccia zone with local quartz-chrysocolla-malachite(?)-hematite-pyrite mineralization on fracture surfaces, in vugs, and as scattered grains within microbreccia.

MIDWAY DISTRICT (Green Streak subdistrict; Fig. 11)

LOCATION NUMBER: 4-13-86-1 (Green Streak mine)
DESCRIPTION: Shear zone (attitude N35°W, 55°NE) in lower-plate crystalline rocks hosts fracture-filling chrysocolla and quartz. Mine dump includes shattered hematite-silica rock. Mine dump is large for this type of deposit.

LOCATION NUMBER: 4-13-86-2
DESCRIPTION: Sparse hematite-stained fractures at small prospect in augen gneiss with inferred megacrystic granite protolith.

LOCATION NUMBER: 4-13-86-3
DESCRIPTION: Shear zone (attitude N70°W, 70°NE) in lower-plate crystalline rocks hosts hematite, chrysocolla, quartz, and rare specular hematite. Quartz is abundant and locally fills voids between host-rock clasts that are surrounded by radial, cavity-filling quartz crystals up to 5 mm long. Decline is approximately 15 m deep and adit is of unknown (but not great) length.

LOCATION NUMBER: 4-13-86-4
DESCRIPTION: Moderately northeast-dipping shear zone, 1 m wide, with fracture-coating limonite and/or hematite. Adit here is approximately 3 m in length.

LOCATION NUMBER: 4-13-86-5
DESCRIPTION: Moderately northeast-dipping shear zone, 1 m wide, with fracture-coating limonite-hematite. Adit here is approximately 3 m in length.

MIDWAY DISTRICT (Mammoth subdistrict; Fig. 12)

LOCATION NUMBER: 12-19-83-1
DESCRIPTION: Decline dipping approximately 20° within microbreccia, chloritic breccia, and generally shattered gneiss directly below the Buckskin-Rawhide detachment fault. The roof of the decline is the smooth, polished fault surface that forms the base of the brown, upper-plate Tertiary conglomerate. Striations on fault surface trend N50°E. Numerous fractures in upper-plate conglom-

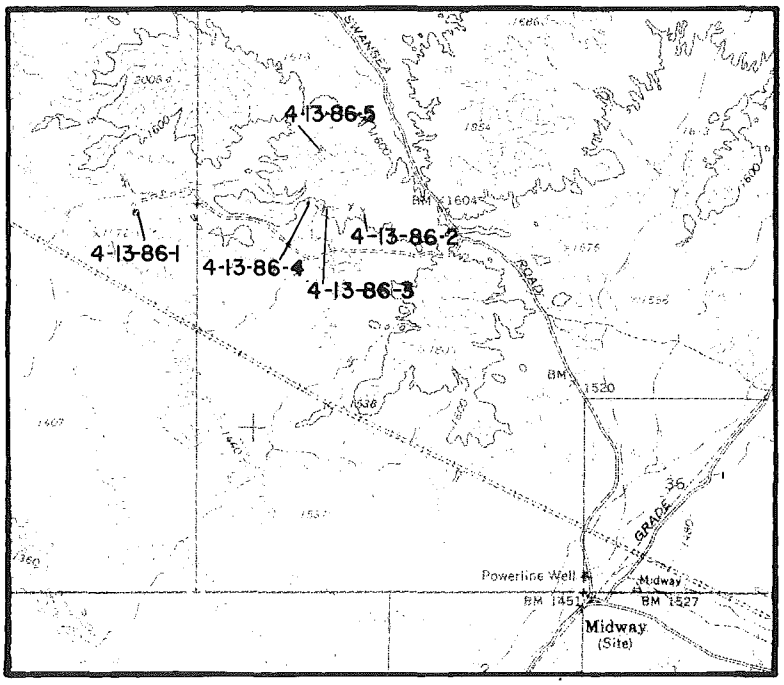

Figure 12. Location map of mines and prospects in the Mammoth subdistrict of the Midway mineral district. See Figure 1 for location of map.

erate within several meters of fault are both parallel and at a high angle to fault and are typically filled with chrysocolla. Pervasively shattered rocks in lower plate adjacent to fault contain chrysocolla and hematite and are altered to deep-red color, apparently because of pervasive iron-oxide staining. Chrysocolla is present only within 1 to 5 m of fault. Up to 1-cm-thick fracture-filling veins of hematite and specular hematite are present in lower-plate gneiss for several tens to perhaps more than 100 m structurally below fault. Hematite veins strike approximately N35°W and dip 75°NE.

LOCATION NUMBER: 11-16-84-1
DESCRIPTION: Malachite, chrysocolla, barite, calcite, quartz, hematite, and manganese oxides form open-space fillings in brecciated gneiss. Mine shaft is in steeply dipping shears and fractures. Host rock is quartz-feldspar-biotite gneiss with gently to moderately dipping crystalloblastic foliation.

LOCATION NUMBER: 11-16-84-2
DESCRIPTION: Same type of mineralization as at 11-16-84-1. Shaft is in 50-cm-wide, mineralized shear zone that strikes N60°W and dips 66°NE. Host gneiss has local, weak mylonitic foliation with local weak lineation. Compositionally banded gneiss includes augen gneiss.

LOCATION NUMBER: 4-12-86-3
DESCRIPTION: Mineralized shear zone (attitude N20°W, 55°NE) in lower-plate crystalline rocks contains hematite, specular hematite, chrysocolla, malachite(?), and sparse calcite on fracture surfaces. Decline that plunges 55° is at least 20 m deep.

LOCATION NUMBER: 4-12-86-4
DESCRIPTION: Mineralized shear zone (attitude N20°W, 55°NE) in lower-plate crystalline rocks contains hematite, specular hematite, chrysocolla, malachite(?), and quartz on fracture surfaces.

MIDWAY DISTRICT (Midway Northeast subdistrict; Fig. 7)

LOCATION NUMBER: 4-12-86-2
DESCRIPTION: Shear zone (attitude N60°E, 55°NW) in lower-plate, variably mylonitic crystalline rocks with specular hematite, hematite, drusy quartz, and chrysocolla along fracture surfaces. Decline on shear zone is 5 to 8 m deep. Metasedimentary rocks are locally present within crystalline rocks.

PLANET DISTRICT (Mineral Hill subdistrict; Fig. 13)

LOCATION: Mineral Hill mines
DESCRIPTION: Host rocks are shattered greenschist-grade quartzite, schist, and calc-silicates of the lower

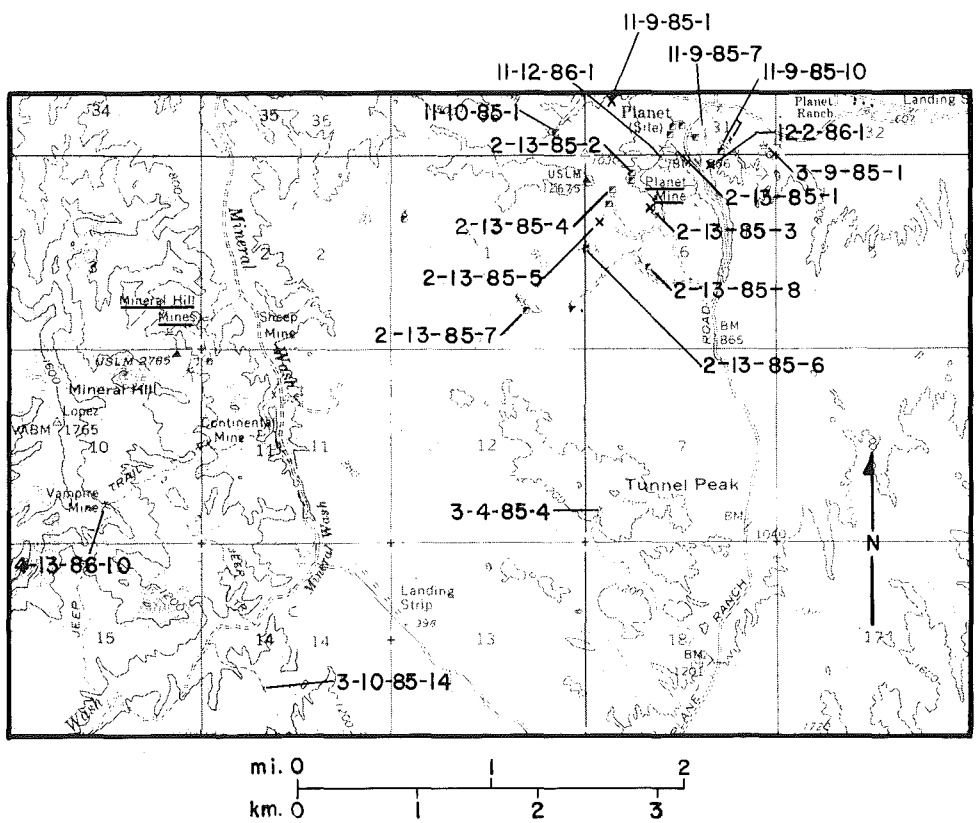

Figure 13. Location map of mines and prospects in the Planet mineral district. See Figure 1 for location of map.

member of the Triassic Buckskin Formation and massive hydrothermal carbonate that forms replacements within the Buckskin Formation. Mineral deposits are directly above the Buckskin-Rawhide detachment fault and are characterized by disseminated, massive, and fracture-filling specular hematite with later thin fractures filled with chrysocolla and malachite. Main part of deposit is composed of massive or disseminated specular hematite and is surrounded by a peripheral zone of sparse, fracture-filling specular hematite.

Massive replacement carbonate is replaced by specular hematite; chrysocolla is present along contacts between the two. At one location, a pod of massive specular hematite in layered fault gouge grades upward into earthy hematite with chrysocolla, which in turn is bounded upward by a 1-cm-thick chrysocolla vein that in turn is bounded above by replacement carbonate. Chrysocolla zone seems to have formed at interface between carbonates and specular hematite (S.J. Reynolds, written commun., 1987).

Locally occurring, black, soft powdery mineral gives off sulfuric smell when treated with HCl and contains mixed oxides of copper, iron, manganese, and zinc (Robert O'Haire, oral commun., 1985). Bull quartz is only locally present in mineralized rocks and could be related to older Mesozoic metamorphism. Local iron oxides and chrysocolla are present in lower-plate, chloritically altered mylonitic gneiss, which suggests that mineralization in this area continued after termination of fault movement. Unidentified, white, soft fibrous mineral locally forms veins in upper-plate rocks. Mineralization abruptly terminates to northeast at northwest-striking, postmineralization, high-angle, Mineral Wash fault with northeast-side-down displacement.

LOCATION NUMBER: 3-10-85-14
DESCRIPTION: Specular hematite is present in prospects in upper-plate carbonate-replacement rocks along the detachment fault. Lower-plate metasedimentary(?) rocks have locally been mineralized.

LOCATION NUMBER: 4-13-86-10 (Vampire mine)
DESCRIPTION: Shear zone (attitude N35°W, 75°SW) in metasedimentary rocks of the Triassic Buckskin Formation contains fracture-filling chrysocolla, malachite(?), calcite, and specular hematite. Hematite staining is common around mine area.

PLANET DISTRICT (Planet subdistrict; Fig. 13)

LOCATION NUMBER: 2-13-85-1
DESCRIPTION: Small adit in shattered rocks along Buckskin-Rawhide detachment fault. Chrysocolla, malachite, and quartz are present in fractures.

LOCATION NUMBER: 2-13-85-2 (Planet mine)
DESCRIPTION: Silicified, massive specular hematite forms resistant rubble around mine, which is located on the Buckskin-Rawhide detachment fault. Quartz and malachite are present in voids and fractures. Drusy quartz coats malachite, and malachite coats quartz; both relationships are represented.

LOCATION NUMBER: 2-13-85-3
DESCRIPTION: Upper-plate replacement carbonate hosts hematite, chrysocolla, and malachite on fracture surfaces directly above Buckskin-Rawhide detachment fault. Quartz overgrowths are present on copper minerals.

LOCATION NUMBER: 2-13-85-4
DESCRIPTION: Shaft in upper-plate, siliceous metasedimentary rocks is at least 50 to 70 m deep, as indicated by presence of unmineralized mylonitic gneiss in mine dump that came from below the Buckskin-Rawhide detachment fault. Abundant specular hematite is present in dump. One-meter-thick, massive, white quartz vein is present 10 m from shaft.

LOCATION NUMBER: 2-13-85-5
DESCRIPTION: Decline, approximately 10 m deep, in shear zone (attitude N50°E, 40°NW) within upper-plate Mesozoic metasedimentary rocks. Fracture-filling chrysocolla is present in shear zone.

LOCATION NUMBER: 2-13-85-6
DESCRIPTION: Shear zone in white quartzite with hematite and a very minor amount of chrysocolla. Quartz vein in quartzite is of uncertain relationship to mineralization.

LOCATION NUMBER: 2-13-85-7
DESCRIPTION: Fault (attitude N30°W, 25°NE) contains fracture-filling chrysocolla and specular hematite. Shear zone places Mesozoic quartzite over greenish-gray, fine-grained, quartzose, Mesozoic metasedimentary rock.

LOCATION NUMBER: 2-13-85-8
DESCRIPTION: Chrysocolla, hematite, and bull quartz in mine dump.

LOCATION NUMBER: 3-4-85-4
DESCRIPTION: Shear zone that dips 75°NE within Tertiary megabreccia contains abundant black manganese oxides. Hematite staining on fracture surfaces is common. To northwest along strike, this shear zone contains pervasive manganese-oxide minerals with less abundant barite veins along vertical fractures. Local quartz(?)-barite-calcite veins are present to south. Calcite-barite veins and manganese-oxide coatings on fracture surfaces are locally present in this general area.

LOCATION NUMBER: 3-9-85-1
DESCRIPTION: Massive specular hematite with minor amounts of chrysocolla and malachite in Mesozoic metasandstone immediately above Buckskin-Rawhide detachment fault.

LOCATION NUMBER: 11-9-85-1

DESCRIPTION: Lower-plate chloritic breccia adjacent to detachment fault contains fracture-filling chrysocolla and manganese oxides. Both lower- and upper-plate rocks are variably silicified. Upper-plate rocks contain fracture-filling veins of milky quartz and specular hematite up to 2 cm thick.

LOCATION NUMBER: 11-9-85-7
DESCRIPTION: Massive specular hematite forms partial to complete replacements of Triassic Buckskin Formation and contains abundant fracture-filling chrysocolla.

LOCATION NUMBER: 11-9-85-10
DESCRIPTION: Specular-hematite replacements, fracture-filling specular hematite and chrysocolla, and hematite staining within Triassic Buckskin Formation.

LOCATION NUMBER: 11-10-85-1
DESCRIPTION: Rocks above and below(?) the detachment fault are pervasively shattered and variably silicified and contain fracture-filling and replacement hematite, specular hematite, and late fracture-filling chrysocolla. Decline descends from detachment fault into lower plate. Smaller adits are present in upper plate. Upper-plate shear zone (attitude N30°E, 30°SE) is highly fractured and contains much chrysocolla. Replacement carbonate, 10 to 20 m thick, overlies detachment fault adjacent to mine and contains moderately abundant specular hematite.

LOCATION NUMBER: 11-12-86-1
DESCRIPTION: High-angle shear zone contains massive and fracture-filling specular hematite in host Triassic

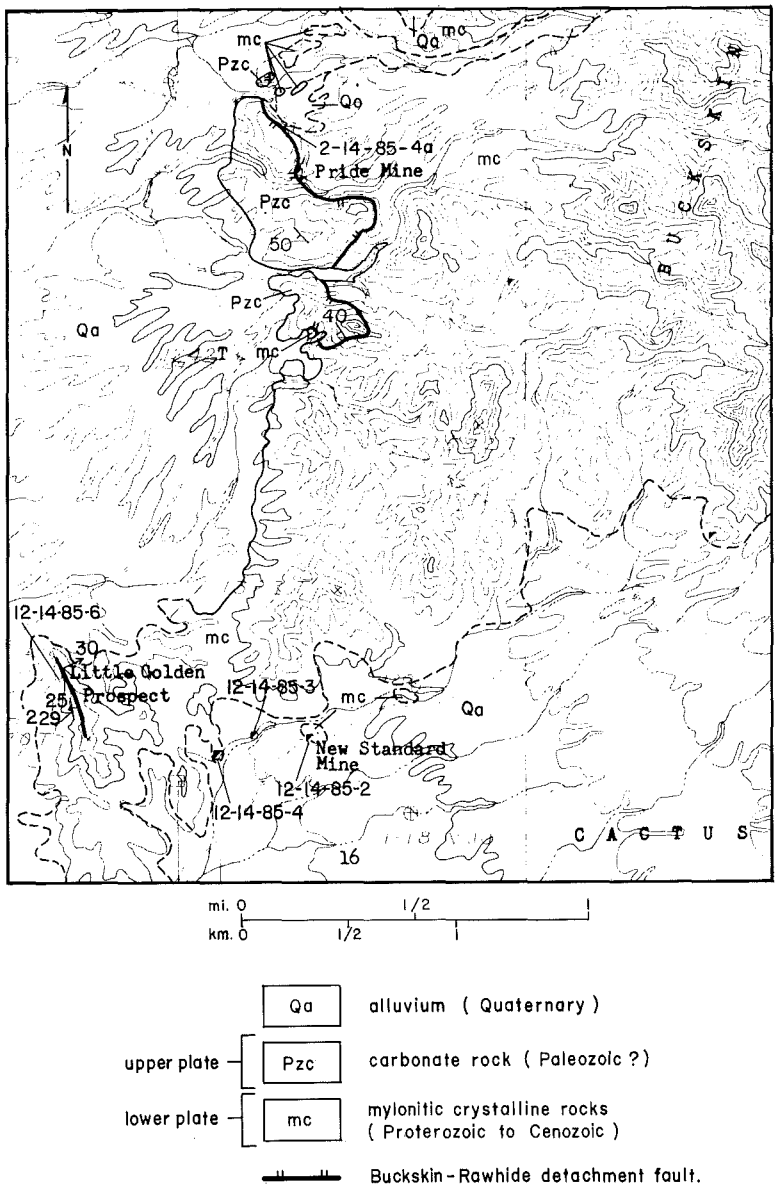

Figure 14. Location map of mines and prospects in the Pride mineral district. See Figure 1 for location of map.

Buckskin Formation. Also present in fractures are calcite, drusy quartz, and malachite(?).

LOCATION NUMBER: 12-2-86-1
DESCRIPTION: Prospect at top of cliff above Planet Wash is within replacement carbonate that hosts 1-m-thick vein of specular hematite and quartz with 1- to 10-cm-thick chrysocolla-rich zone at interface between carbonate and hematite-quartz. Sparse calcite, manganese oxide, and oxidized pyrite cubes up to 1.5 cm in diameter are also present. Detachment-fault surface at base of cliff has N30°E-trending striations in hematite-manganese oxide that coats hanging wall, indicating that latest faulting was younger than mineralization. Footwall also contains earthy hematite in fractures.

PRIDE DISTRICT (New Standard subdistrict; Fig. 14)

LOCATION NUMBER: 12-14-85-2 (New Standard mine)
DESCRIPTION: Chloritically altered, variably shattered and brecciated, lower-plate crystalline rocks host massive, tabular, subhorizontal, specular-hematite replacement masses up to 2 m thick. Chlorite and brown calcite form anastamosing zones 2 to 20 cm thick. Fracture-filling chrysocolla, quartz, and white calcite are common. Specular hematite is unusually hard and coarse grained (up to 1-cm crystals).

LOCATION NUMBER: 12-14-85-3
DESCRIPTION: Three-meter-deep shaft in limonite-stained, lower-plate crystalline rocks with sparse fracture-filling chrysocolla and black manganiferous material that possibly contains other base-metal oxides.

LOCATION NUMBER: 12-14-85-4
DESCRIPTION: Shear zone (attitude N60°W, 60°NE) in lower-plate crystalline rocks hosts veinlets, spotty replacements, and fracture fillings of specular hematite and chrysocolla. Staining by iron oxides is pervasive. A fine-grained mafic dike is present at the shaft.

LOCATION NUMBER: 12-14-85-6 (Little Golden prospect)
DESCRIPTION: Fracture surfaces along moderately northeast-dipping shear zone in lower-plate crystalline rocks contain chrysocolla and are associated with pervasive iron staining. Sparse quartz and specular hematite are present.

PRIDE DISTRICT (Pride subdistrict; Fig. 14)

LOCATION: Pride mine
DESCRIPTION: Chrysocolla and quartz with sparse specular hematite along and near Buckskin-Rawhide detachment fault. Both chrysocolla and drusy quartz are brecciated in some areas, indicating that mineralization occurred before faulting ended. Drusy quartz forms overgrowths on chrysocolla. Mineralized shear zone (attitude N15°E, 50°NW) is significantly steeper than dip of detachment fault, as indicated by trace of detachment fault across topography. A decline is present in this probable, lower-plate, mineralized shear zone.

Upper-plate rocks are mostly massive, tan to brown limestone with sparse 10- to 40-cm-thick layers of microcrystalline quartz (chert?). Along detachment fault, carbonates and siliceous rocks of the upper plate are locally interleaved with lower-plate gneisses over a zone 2 to 4 m wide and contain boudinlike pods of pegmatitic granite. Carbonates in this area include dark-brown calcite marble and tan-weathering, white, medium-grained dolomitic marble. The age of these carbonates is not known, but is suspected to be Paleozoic.

LOCATION NUMBER: 2-14-85-4a
DESCRIPTION: Malachite, chrysocolla, hematite, limonite, and drusy quartz in fractured rocks along Buckskin-Rawhide detachment fault. Drusy quartz forms overgrowths on chrysocolla.

SWANSEA DISTRICT (Copper Penny subdistrict; Fig. 15)

LOCATION NUMBER: 11-17-85-4
DESCRIPTION: Microbreccia directly below detachment fault hosts fracture-filling chrysocolla between 5 and 30 cm below fault. Hematite staining is ubiquitous. Minor amounts of manganese oxides, limonite staining, and fracture-filling pyrite are also present.

LOCATION NUMBER: 11-17-85-7
DESCRIPTION: Rocks in prospect pits in microbreccia below detachment fault contain hematite, limonite, manganese oxides, and sparse malachite(?). Nearby upper-plate quartz-chlorite-sericite schist contains quartz veins, possibly of predetachment age, and younger specular hematite. Upper-plate carbonate rocks in this area also host minor amounts of specular-hematite veinlets and replacements.

LOCATION NUMBER: 11-19-86-7
DESCRIPTION: Microbreccia forms northwest-sloping surface of hillside; trace of northwest-dipping detachment fault is at base of hillside. Microbreccia contains less than 1 to several percent, relict, 0.5- to 2-mm pyrite cubes, which are now pits containing iron oxides. Veinlets of quartz and chalcedony(?) contain a greater abundance of the relict pyrite and are typically strongly stained with hematite.

SWANSEA DISTRICT (Squaw Peak subdistrict; Fig. 15)

LOCATION NUMBER: 2-12-85-6
DESCRIPTION: Specular hematite, chrysocolla, and calcite in brittle shear zone in lower-plate mylonitic orthogneiss. Mild chloritic alteration of host gneiss is probably the result of proximity to the once overlying, but now eroded away, Buckskin-Rawhide detachment fault.

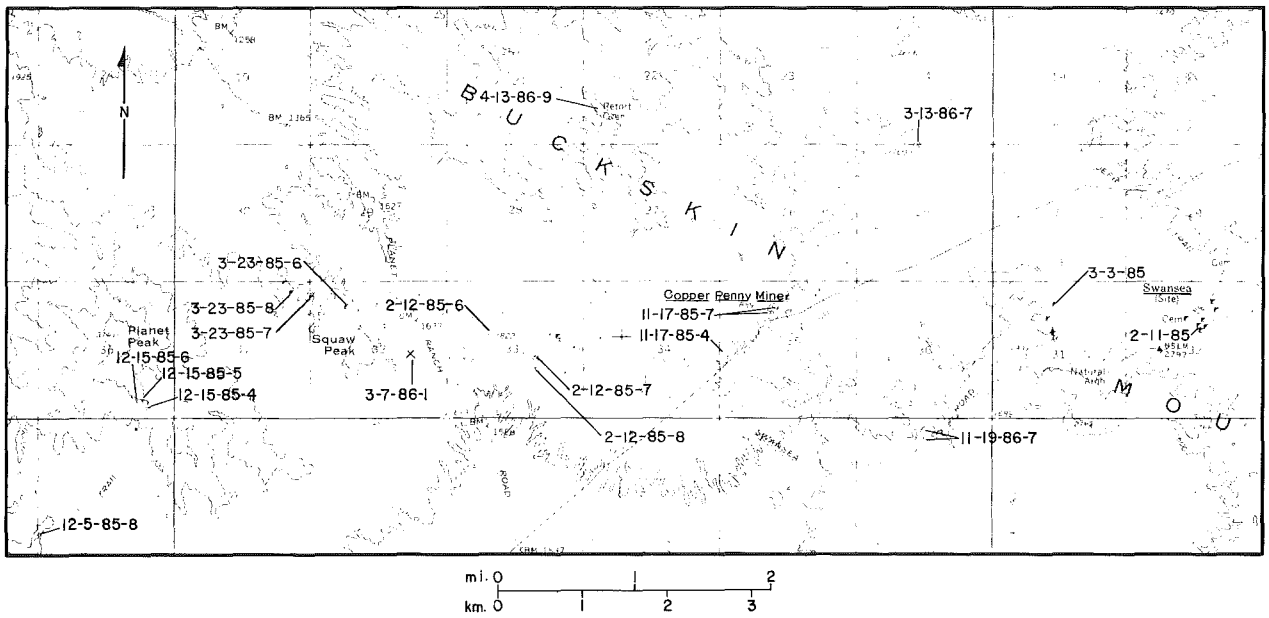

Figure 15. Location map of mines and prospects in the Swansea mineral district. See Figure 1 for location of map.

LOCATION NUMBER: 2-12-85-7
DESCRIPTION: Massive, coarsely crystalline, specular hematite with euhedral quartz crystals lining the walls of fractures. Mylonitic-orthogneiss host.

LOCATION NUMBER: 2-12-85-8
DESCRIPTION: Specularite, chrysocolla, and chlorite in mylonitic-gneiss host.

LOCATION NUMBER: 3-23-85-6
DESCRIPTION: Decline in shear zone (attitude N75°E, 45°SE) that hosts massive specular hematite and fracture--filling chrysocolla and malachite, hematite stain on fracture surfaces, and sparse, thin, fine-grained drusy quartz covering specular hematite and copper minerals on fracture surfaces. Host mylonitic gneiss contains fracture-filling epidote. Adit adjacent to decline has same type of mineralization, with quartz lining fractures and vugs. Prospect shown on USGS topographic map northeast of decline is also same type of mineralization with calcite coating some fracture surfaces in massive specular hematite and gneiss.

LOCATION NUMBER: 3-23-85-7
DESCRIPTION: Brittle shear zone (attitude N65°W, 50°SW) in gneiss contains massive, coarsely crystalline, specular hematite, and sparse malachite and chrysocolla.

LOCATION NUMBER: 3-23-85-8
DESCRIPTION: Massive specularite, chrysocolla, malachite, and quartz in lower-plate gneiss.

LOCATION NUMBER: 12-15-85-4
DESCRIPTION: Adits in subhorizontal lenses and tabular masses of tan dolomitic marble, 1 to several meters thick and several to several tens of meters long. Marble contains sparse, thin siliceous layers that are isoclinally folded and refolded and very sparse, light-gray, 3-cm-thick, discontinuous quartzite layers. Specular hematite forms massive replacements of dolomite. One specular-hematite mass is bounded by a smooth striated surface, indicating that shearing is in part younger than mineralization. Sparse fracture-filling chrysocolla, quartz, calcite, and manganese oxides are also present. Limonitic staining has affected carbonate-enclosing, variably mylonitic, gneissic crystalline rocks.

LOCATION NUMBER: 12-15-85-5
DESCRIPTION: Massive, coarse-grained specular hematite and late fracture-filling chrysocolla form replacement masses in carbonate sliver and form fracture fillings along high-angle shear zone. Carbonate lens is part of a metasedimentary sheet that is structurally higher than those at location 12-15-85-4.

LOCATION NUMBER: 12-15-85-6
DESCRIPTION: Mineralization as at location 12-15-85-5, but concentrated along the base of a carbonate sliver.

LOCATION NUMBER: 12-15-85-8
DESCRIPTION: Several-meter-thick dolomite sliver in gneiss contains pervasive replacement and fracture-filling epidote, local fracture-filling chlorite and manganese oxides, and very sparse chrysocolla.

LOCATION NUMBER: 3-7-86-1
DESCRIPTION: Lower-plate, interleaved crystalline and metasedimentary rocks contain a tan dolomite sliver that is partially replaced by massive specular hematite with fracture-filling chrysocolla and sparse drusy quartz. Chrysocolla is locally cut by specular-hematite-filled fractures.

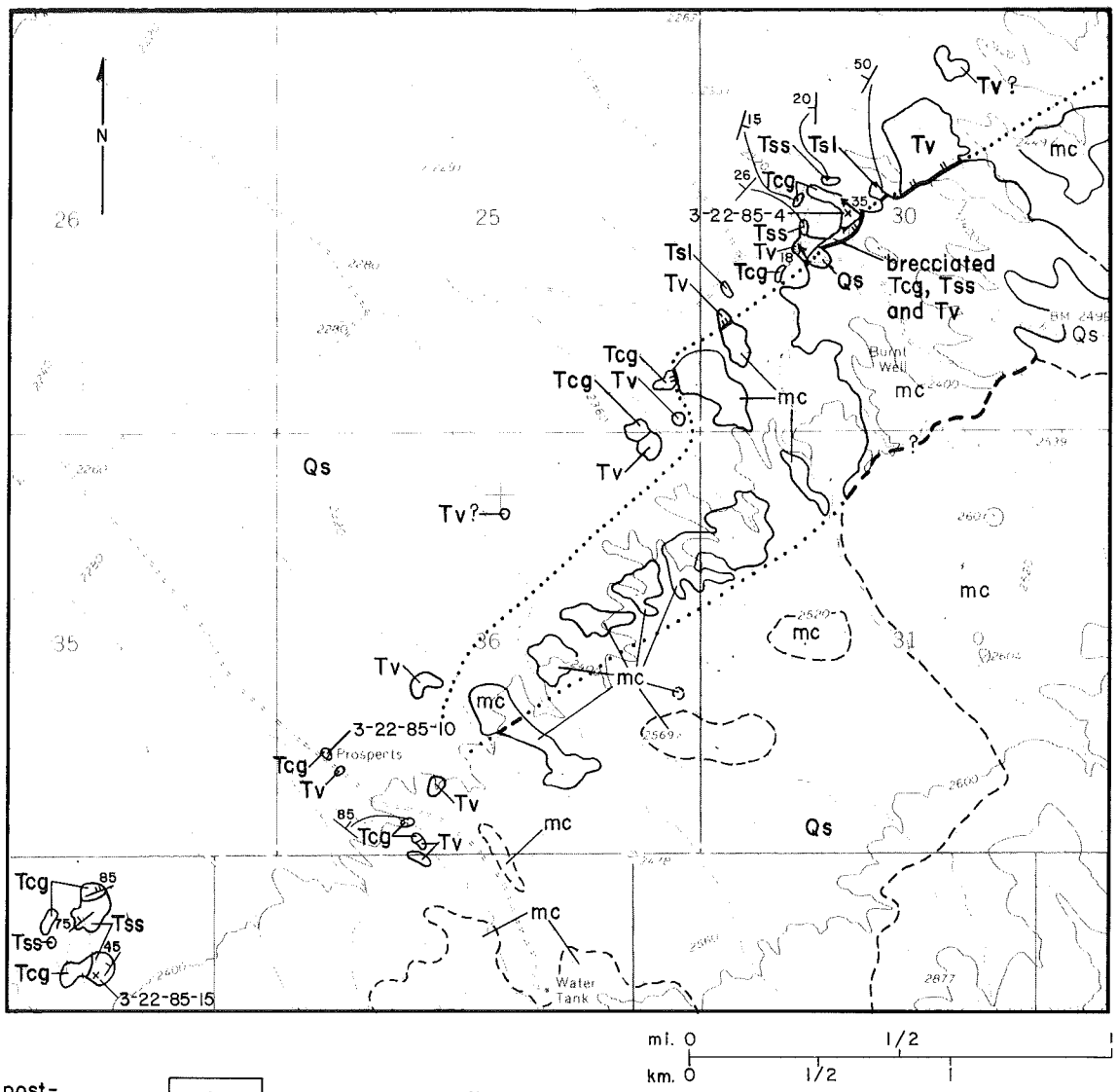

mi. 0 1/2 1

km. 0 1/2 1

post-detachment	Qs	Quaternary surficial deposits.
upper plate	Tcg	Miocene (?) conglomerate, medium brown to medium or dark reddish brown, with locally interbedded sandstone and siltstone.
	Tss	Miocene (?) sandstone, light tan, light brown, or reddish brown, locally tuffaceous or calcareous, with locally interbedded siltstone.
	Tsl	Miocene (?) siltstone, maroon, locally includes dark brown sandstone and thin limestone layers.
	Tv	Miocene (?) volcanics, medium gray to dark reddish brown massive andesite (?) and andesite (?) flow breccia.
lower plate	mc	mylonitic gneiss.

Inferred or approximately located fault, dotted where concealed.

Bullard-Buckskin-Rawhide detachment fault, showing dip. Dotted where concealed.

27 Bedding attitude

85 Bedding attitude, top direction known (upright)

3-22-85-15 × Location described in text

Figure 16 (previous page). Location map of mines and prospects in the Burnt Well mineral district in the Harcuvar Mountains. See Figure 1 for location of map.

LOCATION NUMBER: 3-13-86-7
DESCRIPTION: Highly chloritic, shattered, lower-plate, mylonitic crystalline rocks host fracture-filling chrysocolla, specular hematite, manganese oxides, and quartz.

LOCATION NUMBER: 4-13-86-9
DESCRIPTION: Small pile of massive specular hematite next to retort oven must have come from prospects 1 km to west near ridge crest (center of sec. 21).

SWANSEA DISTRICT (Swansea subdistrict; Fig. 15)

LOCATION NUMBER: 2-11-85 (Swansea mine)
DESCRIPTION: An elongate, WSW-ENE-trending body of dominantly Paleozoic carbonate, approximately 1.5 km long, crops out adjacent to mine shafts of the Swansea mine. The carbonate is present at depth beneath the shafts and was the host to the ore that was mined in the early 1900's. This ore consisted of veins of chalcopyrite surrounded by massive specular hematite (John Challinor, oral commun., 1985).

The nearest surficial exposures of carbonate are highly sheared; they contain numerous fracture fillings and anastomosing podlike zones up to 1 m thick of massive specular hematite and fracture-filling malachite and chrysocolla. The elongate body of exposed carbonate southwest of the Swansea mine is separated from lower-plate mylonitic gneiss by the Buckskin-Rawhide detachment fault, which here dips about 40°NW beneath the carbonate.

LOCATION NUMBER: 3-3-85
DESCRIPTION: High-angle fault zone between Precambrian granite and mid-Tertiary silty carbonate. Fault and adjacent rock units are in upper plate of Buckskin-Rawhide detachment fault. Silty carbonate is mineralized; granite is not. Mineralized shear zones in silty carbonate are parallel to adjacent high-angle fault, indicating that mineralization occurred after faulting started, but ended before faulting ceased, because adjacent granite and fault are not mineralized. Dominantly near-vertical shear zones contain purple fluorite, brown calcite, drusy quartz, hematite, chrysocolla, and malachite. Most if not all mineralization is open-space filling. Fault dips 85°W.

HARCUVAR MOUNTAINS

BURNT WELL DISTRICT (Fig. 16)

LOCATION NUMBER: 3-22-85-4 (Silver Lining mine)
DESCRIPTION: Shaft in upper-plate, tan and maroon Miocene siltstone, within conglomerate map unit, located approximately 40 to 80 m horizontally from detachment fault. Tertiary sedimentary rocks in mine dump contain hematite, chrysocolla, calcite, and sparse manganese oxides.

LOCATION NUMBER: 3-22-85-10
DESCRIPTION: Shaft approximately 10 to 15 m deep in Miocene conglomerate. Sparse chrysocolla and hematite stain are present on rocks in mine dump.

LOCATION NUMBER: 3-22-85-15
DESCRIPTION: Prospect on quartz-barite vein in locally calcareous Miocene sandstone.

RAWHIDE MOUNTAINS

BLACK BURRO DISTRICT (Fig. 17)

LOCATION NUMBER: 11-2-86-1 (Black Burro mine)
DESCRIPTION: Manganiferous, Miocene sandstone and siltstone bed approximately 1 to 3 m thick. Fine-grained red sandstone at base of bed contains elongate nodules and lamination of manganese oxide. Manganiferous bed is exposed for 30 to 50 m and outcrops discontinuously along strike nearby. Structural disruption is significant. Manganiferous bed with declines strikes N80°E and dips 25°S. A 1-m-thick, light-brown tuff bed is exposed next to the manganiferous bed, although relative stratigraphic position is unknown.

CLEOPATRA DISTRICT (Cleopatra subdistrict; Fig. 17)

LOCATION NUMBER: 3-20-85-7
DESCRIPTION: Chalcopyrite and magnetite form replacements in upper-plate, tectonized, and layered calcite marble, fine-grained argillite(?), and quartzite, with sparse pyrophyllite in zones parallel to foliation. One marble lens is several meters thick. Epidote, calcite, manganese oxides, and iron oxides are present on fracture surfaces. Deposit is interpreted as skarn of probable Mesozoic age.

LOCATION NUMBER: 3-20-85-8 (Cleopatra mine)
DESCRIPTION: Quartz, manganese oxides, hematite, malachite, and chrysocolla in fractures within upper-plate marble and siliceous metasedimentary rocks. Moderately abundant, massive quartz probably represents replacements. Quartz is locally vuggy. Massive quartz and absence of specular hematite, as seen here, is atypical and not generally characteristic of other detachment-fault-related deposits in the Buckskin and Rawhide Mountains.

LOCATION: New England mine
DESCRIPTION: Quartz with spotty malachite, hematite, calcite, and manganese oxides along shear zone that trends N55°E and dips 35°SE. Host rocks are gray and

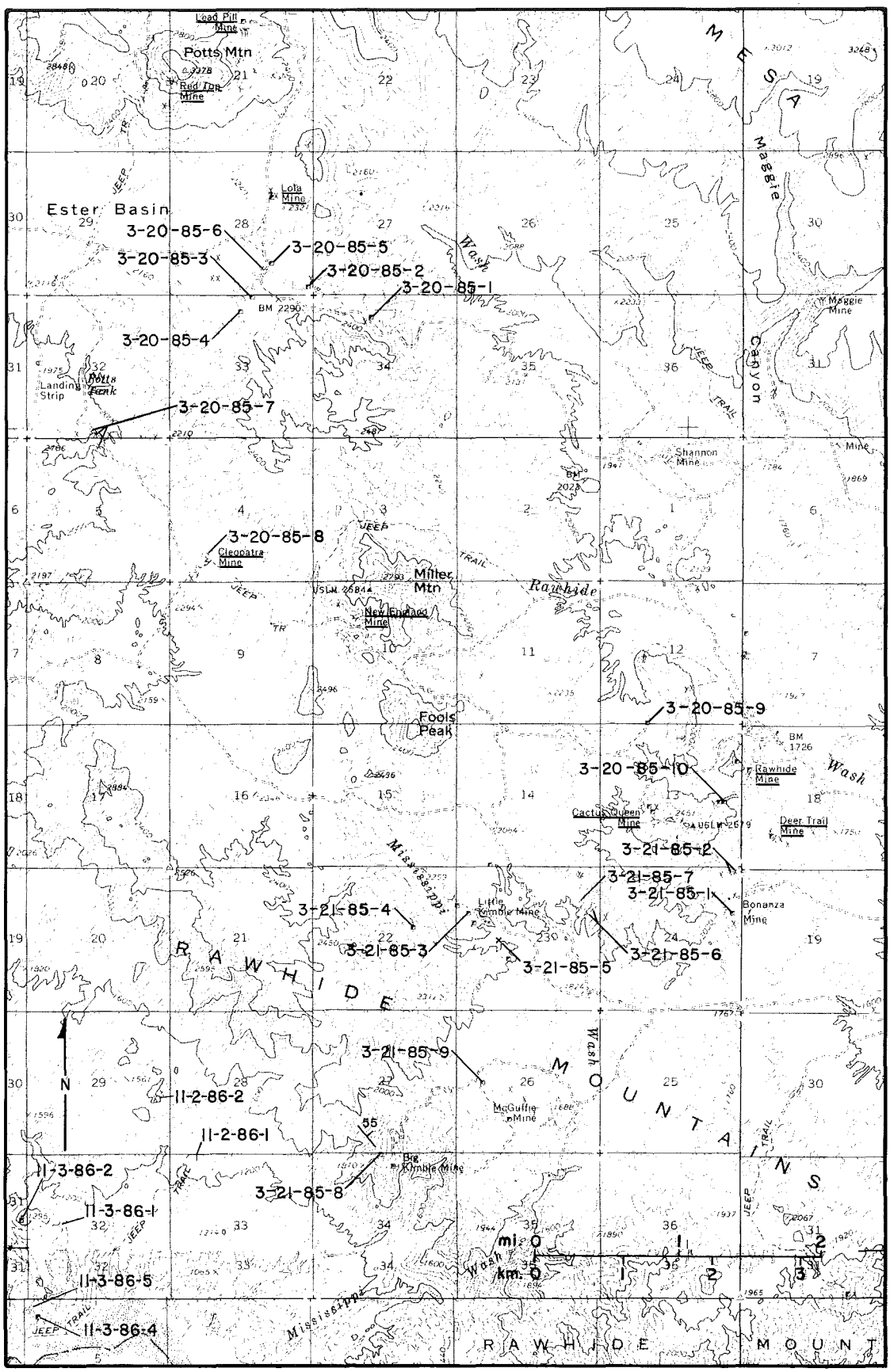
Lead Pill Mine
Potts Mtn
Red Top Mine
Lola Mine
Ester Basin
3-20-85-6
3-20-85-5
3-20-85-3
3-20-85-2
3-20-85-1
BM 2290
3-20-85-4
Potts Landing Strip
Potts Peak
3-20-85-7
Maggie Mine
Shannon Mine
3-20-85-8
Cleopatra Mine
Miller Mtn
New Enfiado Mine
Fools Peak
3-20-85-9
3-20-85-10
Rawhide Mine
Cactus Queen Mine
Deer Trail Mine
3-21-85-2
3-21-85-7
3-21-85-1
Bonanza Mine
3-21-85-4
Little Kimble Mine
3-21-85-3
3-21-85-5
3-21-85-6
RAWHIDE MOUNTAINS
3-21-85-9
McGuffie Mine
11-2-86-2
11-2-86-1
Big Kimble Mine
3-21-85-8
11-3-86-2
11-3-86-1
11-3-86-5
11-3-86-4
Mesa
Maggie Canyon
Rawhide Wash
Mississippi Wash
mi 0 1 2
km 0 1 2 3

Figure 17 (previous page). Location map of mines and prospects in the Black Burro, Lead Pill, and Rawhide mineral districts and in all of the Cleopatra district except the western half of the Silverfield subdistrict. See Figure 1 for location of map.

brown, variably siliceous carbonates. Quartz is locally vuggy.

CLEOPATRA DISTRICT (Kimble subdistrict; Fig. 17)

LOCATION NUMBER: 3-20-85-9
DESCRIPTION: Manganese and iron oxides and chrysocolla in shear zone that trends N65°W and dips 50°NE. Host rocks are silicified and contain 1-cm-thick quartz veins.

LOCATION: Cactus Queen mine
DESCRIPTION: Adit lowest on hillside is approximately 20 m below Buckskin-Rawhide detachment fault and is in chloritic breccia that has no apparent mineralization. Top of northwest shaft is upper-plate Tertiary sandstone and conglomerate hosting chrysocolla, malachite, and sparse calcite in fractures. Top of shaft is approximately 20 m above detachment fault. A brown, carbonate replacement(?) lens is present along the fault. Manganese and iron oxides are locally present in fractures. At southeast shaft, Mesozoic metavolcanic rocks host fluorite, malachite, quartz, hematite, and rare chrysocolla in shear zone that strikes N5°W and dips 50°E.

LOCATION NUMBER: 3-20-85-10
DESCRIPTION: Massive specular hematite with thin fracture-filling chrysocolla, malachite, and sparse quartz. Host rocks are upper-plate granitoids, although chloritic breccia in dump indicates that shaft penetrated lower plate. Lenses of replacement(?) carbonate are present along fault in this area. This is typical detachment-fault mineralization as seen in Buckskin Mountains.

LOCATION NUMBER: 3-21-85-1 (Bonanza mine)
DESCRIPTION: Prospect east of shaft is in alluvium above silicified chloritic breccia with hematite staining and sparse chrysocolla. Similar mineralogy characterizes the shaft and adit, which are located in microbreccia and chloritic breccia directly below Buckskin-Rawhide detachment fault. Prospects and adits to west and northwest are along hematite-stained quartz veins in massive upper-plate carbonates.

LOCATION NUMBER: 3-21-85-2
DESCRIPTION: Shattered, slightly to moderately chloritic, lower-plate gneiss containing massive specular hematite with chrysocolla and drusy quartz-filling fractures.

LOCATION NUMBER: 3-21-85-3
DESCRIPTION: Lower-plate mylonite gneiss hosting chrysocolla, quartz, hematite, and sparse specular hematite in fractures along shear zone that trends N28°W and dips 52°NE.

LOCATION NUMBER: 3-21-85-4
DESCRIPTION: Quartz, chrysocolla, hematite, and manganese oxides with sparse iron-oxide clots surrounding chalcopyrite cores along brittle fracture zone that trends N18°W and dips 70°NE. Host rocks are lower-plate mylonitic gneiss.

LOCATION NUMBER: 3-21-85-5
DESCRIPTION: Small adit in shear zone (attitude N30°W, 50°NE); several prospects aligned along zone (including inconsequential shaft shown on topographic map to southeast). Quartz, hematite, and very sparse chrysocolla characterize deposit.

LOCATION NUMBER: 3-21-85-6
DESCRIPTION: Massive specular hematite with chrysocolla(?), azurite(?), malachite, and quartz in fractures and open-space fillings in chloritic breccia approximately 50 m below Buckskin-Rawhide detachment fault.

LOCATION NUMBER: 3-21-85-7
DESCRIPTION: Adit partially in metasedimentary carbonate lens within weakly to moderately chloritic and brecciated, lower-plate mylonitic gneiss. Massive specular hematite with chrysocolla characterizes deposit. Dump also contains talc, but talc does not host copper-iron minerals.

LOCATION NUMBER: 3-21-85-8 (Big Kimble mine)
DESCRIPTION: At northwest shaft, hematite, chrysocolla, calcite, barite, and manganese oxides are present in 1-m-wide shear zone that trends N35°W to N38°W and dips 65° to 85°NE. Also present in mineralized rocks are dark-brown to black, porous, microcrystalline mixed oxides that give off a sulfurous smell when treated with HCl. Southeast shaft is located on same shear zone, which is 1 to 2 m wide here. Quartz, chrysocolla, and manganese oxides with a minor amount of calcite and abundant hematite stains characterize mineral deposits. Quartz is massive and vuggy. Drag of foliation near shear zone suggests northeast-side-down (normal) displacement.

LOCATION NUMBER: 3-21-85-9 (McGuffie mine area)
DESCRIPTION: Shear zone (attitude N63°W, 55°NE) hosts open-space and fracture-filling quartz with hematite staining on quartz and fracture surfaces, and sparse chrysocolla. At McGuffie mine proper, quartz, chrysocolla, and malachite, with hematite stain on fracture surfaces, are present in shear zone oriented N30°W, 80°NE. Host rocks are lower-plate mylonitic gneiss with local, weak chloritic alteration.

CLEOPATRA DISTRICT (Lola subdistrict; Fig. 17)

LOCATION: Lola mine, eastern Ester Basin
DESCRIPTION: Quartz, chrysocolla, barite, calcite, man-

ganese oxides, hematite, and specular hematite (rare) in numerous small veins (fracture filling?) and replacements. Host is coarse-grained, Precambrian(?) granitic rock.

LOCATION NUMBER: 3-20-85-1
DESCRIPTION: Fluorite, hematite, chrysocolla, malachite, quartz, and relict pyrite (now iron oxides) in 1-m-wide shear zone that trends N70°W and dips 55°NE. Host is Precambrian(?) granite in which feldspars have been altered to sericite(?) and clay minerals. Iron oxides locally form fracture fillings in granite. Hematite, copper oxides, and relict sulfides are sparse. No specular hematite was visible.

LOCATION NUMBER: 3-20-85-2
DESCRIPTION: Calcite, barite, and quartz with minor amounts of chrysocolla. Calcite is white and coarsely crystalline. Vugs are lined with fine-grained quartz that is coated with limonite. Fine-grained dioritic dike that trends N80°W and dips 55°S was mined out. No apparent shearing.

LOCATION NUMBER: 3-20-85-3
DESCRIPTION: Quartz and calcite with subordinate hematite, chrysocolla, manganese oxides, fluorite, and barite within shear zone that trends N30°E and dips 55°SE. Host is Precambrian(?) granite in which feldspars have been altered to white clay(?), and mafic minerals have been altered to unidentified oxides(?). Hematite coats abundant fractures in granite. Nearby small quartz-calcite veins trend N20°W±10°.

LOCATION NUMBER: 3-20-85-4
DESCRIPTION: Quartz, calcite, and chalcedonic quartz, with a minor amount of barite, in fracture zone that trends due north and dips 50°E. Host is locally silicified, middle Tertiary basal arkose.

LOCATION NUMBER: 3-20-85-5
DESCRIPTION: Barite, calcite, chrysocolla, malachite, manganese oxides, hematite, and a minor amount of quartz in fractures in Precambrian(?) granite. Fractures trend N13°E and dip 40°E. Feldspars in host granite are altered to amorphous, gray clay mineral.

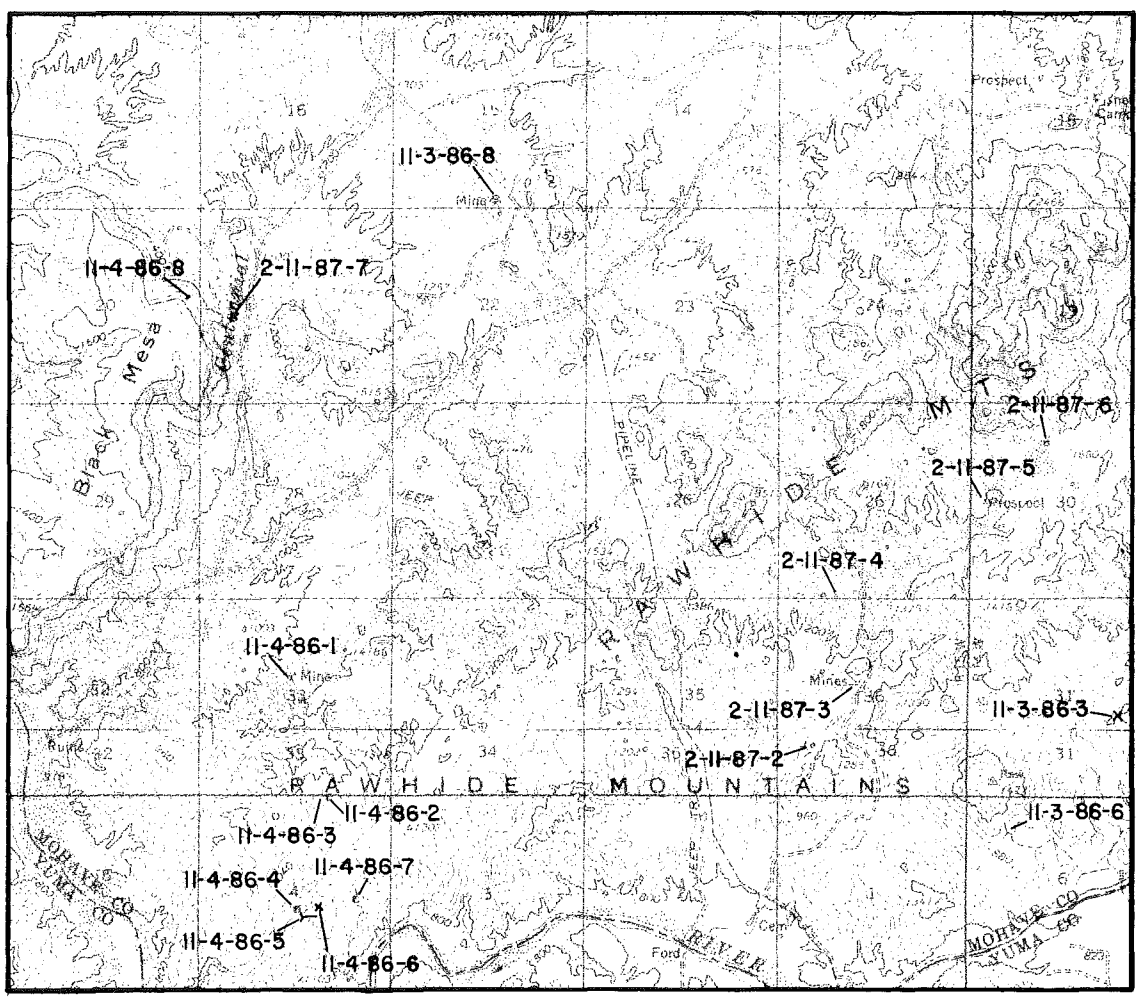

Figure 18. Location map of mines and prospects in the Mesa and Owen mineral districts and the western half of the Silverfield subdistrict of the Cleopatra mineral district. See Figure 1 for location of map.

LOCATION NUMBER: 3-20-85-6
DESCRIPTION: Manganese oxides, calcite, chrysocolla, hematite, and specular hematite in shear zone that trends N10°E and dips 20°SE. Host is Precambrian(?) granite.

CLEOPATRA DISTRICT (Silverfield subdistrict; Figs. 17 and 18)

LOCATION NUMBER: 11-2-86-2
DESCRIPTION: Massive, brecciated Paleozoic carbonate with slivers of extremely shattered quartzite, 10 to 15 m above the detachment fault. Quartzite and carbonate host some vein quartz. Prospects in quartzite reveal fracture-filling chrysocolla, iron-oxide staining, sparse manganese-oxide staining, sparse malachite(?), a minor amount of fluorite, galena(?), and a sparse yellowish-green mineral or mineraloid of unknown composition. Carbonates do not host significant mineralization. Laminations interpreted as relict bedding indicate that at least some quartzite has a sedimentary protolith; however, some of it may actually be vein quartz.

LOCATION NUMBER: 11-3-86-1
DESCRIPTION: Adit in schistose, fine-grained, highly shattered Mesozoic metasedimentary and/or metavolcanic rocks, estimated to be 30 to 50 m above the detachment fault. Rocks in mine dump contain sparse calcite on fracture surfaces and a minor amount of bull quartz, but are largely devoid of evidence of mineralization. Adit could be as much as 100 m long based on size of dump.

LOCATION NUMBER: 11-3-86-2
DESCRIPTION: At approximately 10 m above detachment fault, shattered rocks of the Supai Group contain fracture-filling silica, chrysocolla, a minor amount of malachite(?), black hematite, and manganiferous silica. Shaft may reach fault surface, although no lower-plate fragments were seen in mine dump.

LOCATION NUMBER: 11-3-86-3
DESCRIPTION: Paleozoic(?) carbonate rock and quartzite contain sparse copper, iron, and manganese oxides.

LOCATION NUMBER: 11-3-86-4
DESCRIPTION: Shaft in lower-plate rocks. Top of shaft is at approximate level of detachment fault. No evidence of mineralization was visible.

LOCATION NUMBER: 11-3-86-5
DESCRIPTION: Quartz-feldspar-sericite schist with probable Mesozoic sedimentary protolith is highly sheared and contains sparse chrysocolla along fractures. Schist is overlain by Paleozoic(?) carbonate rock.

LOCATION NUMBER: 11-3-86-6
DESCRIPTION: Quartzite and quartz-sericite-chlorite schist with sparse manganese oxides and calcite on fracture surfaces. A minor amount of milky-white vein quartz is present in mine dump. No evidence of copper mineralization was visible; it is uncertain if mineralization was related to detachment faulting.

LOCATION NUMBER: 2-11-87-2
DESCRIPTION: Shear zone in lower-plate crystalline rocks strikes north-south and dips 20°W. Chrysocolla, epidote, and fluorite crystals are up to 2 cm in diameter; clear and brown calcite and oxidized iron sulfides(?) are present. Adit is on shear zone.

LOCATION NUMBER: 2-11-87-3
DESCRIPTION: Sheared, lower-plate crystalline rocks with abundant drusy quartz and chalcedony, and sparse, fracture-filling specular hematite and chrysocolla. Iron- and manganese-oxide staining is common.

LOCATION NUMBER: 2-11-87-4
DESCRIPTION: Small adit in subhorizontal mineralized zone in lower-plate crystalline rocks. Center of mineralized zone is 5 to 50 cm thick, soft, white powdery material that is probably clay-rich residue from alteration. Above and below this zone, sequentially outward, are hematite, chrysocolla, and epidote, with hematite and chrysocolla locally in reverse sequence. Mine dump contains massive, unusually soft, specular hematite in crystals up to 2 cm in diameter; abundant chrysocolla; and moderate to abundant iron-oxide pits, 1 to 4 mm in diameter, representing relict pyrite.

LOCATION NUMBER: 2-11-87-5
DESCRIPTION: Low-angle shear(?) zone in lower-plate crystalline rocks with massive, fine-grained specular hematite, earthy hematite, manganese oxide, chrysocolla, and epidote.

LOCATION NUMBER: 2-11-87-6
DESCRIPTION: Lower-plate crystalline rocks within carbonate sliver at collar of shaft. Abundant earthy hematite and epidote, and sparse specular hematite and chrysocolla in small mine dump.

LEAD PILL DISTRICT (Fig. 17)

LOCATION: Lead Pill mine and nearby adits
DESCRIPTION: Blue-green and purple, 0.5- to 2-cm, subhedral to euhedral fluorite with subordinate manganese oxides filling randomly(?) oriental fractures and open spaces. Hematite stains and sparse calcite are youngest minerals, with a very minor amount of chrysocolla. Host is moderately to highly fractured, Precambrian(?), medium-grained biotite granite with sparse, 3- to 4-cm, K-feldspar megacrysts. Chloritic alteration of granite is moderate to strong.

LOCATION: Red Top mine
DESCRIPTION: Quartz, fluorite, manganese oxides, chrysocolla, and barite along shear zones in silicic, quartz-bearing hypabyssal intrusive or thick ash-flow tuff of middle to upper Tertiary age. In order of de-

creasing abundance, manganese, fluorite, copper, and barite characterize mineralization. A major, mineralized shear zone at the Red Top mine trends N60°W and dips 5°NE. Quartz-barite-calcite veins and open-space fillings are present in brecciated, silicic volcanic or hypabyssal rocks within 200 m of Red Top mine.

MESA DISTRICT (Fig. 18)

LOCATION NUMBER: 11-3-86-8
DESCRIPTION: Manganiferous, gently dipping, red Miocene sandstone. Manganese mineralization is minor.

LOCATION NUMBER: 11-4-86-8
DESCRIPTION: Location of K-Ar sample of postmineralization basalt (see Spencer, Shafiqullah, and others, this vol.).

LOCATION NUMBER: 2-11-87-7
DESCRIPTION: Megabreccia of Paleozoic carbonates and quartzite hosts pervasive manganese oxides as amorphous wad. Also includes sparse, fracture-filling manganese-oxide crystals up to 1 mm in diameter and white and black calcite crystals up to 8 mm in diameter. Preservation of fracture-filling and open-space-filling minerals indicates that mineralization occurred after deposition of the host sedimentary breccia.

OWEN DISTRICT (Fig. 18)

LOCATION NUMBER: 11-4-86-1
DESCRIPTION: Prospect pit and adit. Prospect is in sliver of micaceous, highly cleaved, tan dolomite with massive specular-hematite replacements and younger fracture-filling chrysocolla and sparse malachite(?). Very little mineralization occurred at small adit below prospect pit on hillside, where host rocks are lower-plate, mylonitic crystalline rocks.

LOCATION NUMBER: 11-4-86-2
DESCRIPTION: Adit, not shaft as shown on topographic map, is located in crushed, chloritic, lower-plate crystalline rocks with spotty hematitic stains and a minor amount of epidote on fracture surfaces.

LOCATION NUMBER: 11-4-86-3
DESCRIPTION: Small prospect in shattered, silicified, lower-plate crystalline rocks with minor amounts of open-space- and fracture-filling specular hematite, chrysocolla, and quartz. Also present is a green serpentinelike mineral. Tan dolomite slivers, 1 to 3 m long and 0.5 to 1 m thick, are present in lower-plate crystalline rock in this general area.

LOCATION NUMBER: 11-4-86-4
DESCRIPTION: Shaft in shattered, lower-plate, mylonitic crystalline rocks that host massive specular hematite; oxidized, euhedral pyrite cubes up to 3 cm in diameter; euhedral, purple and white, locally zoned fluorite cubes up to 1 cm in diameter; and late fracture-filling quartz, calcite, and chrysocolla. High-angle shear zone on one side of shaft could have been an important control of mineralization. Scattered small slivers of dolomite are present in this general area.

LOCATION NUMBER: 11-4-86-5
DESCRIPTION: Adit in tan dolomite sliver approximately 20 m long that hosts massive specular-hematite replacements and younger fracture-filling chrysocolla.

LOCATION NUMBER: 11-4-86-6
DESCRIPTION: Mylonitic crystalline rocks host massive specular hematite with fracture-filling chrysocolla.

LOCATION NUMBER: 11-4-86-7
DESCRIPTION: Volume of mine dumps adjacent to shaft indicates that shaft could be more than 100 m deep. Dump contains sparse, massive and fracture-filling specular hematite with minor amounts of chrysocolla, fluorite, and green serpentinelike mineral. Adit at northeast foot of hill, adjacent to shaft, is in high-angle shear zone with broken, tan carbonate slivers along shear zone and massive specular-hematite replacements and fracture-filling chrysocolla in carbonate slivers. Carbonate slivers are common in this general area.

RAWHIDE DISTRICT (Fig. 17)

LOCATION: Rawhide mine
DESCRIPTION: Hematite, chrysocolla, manganese oxides, and sparse calcite in brecciated and silicified granite host. Main adit is caved. Mine dump below shaft northwest of Rawhide mine contains moderate amounts of black calcite and sparse fluorite within Tertiary, conglomerate host rocks. Scattered quartz veins and locally abundant, black calcite veins formed as open-space fillings in steeply east-dipping fractures. Host rocks include Tertiary sandstone and mudstone. Adit highest on hillside northwest of Rawhide mine is located on a subvertical quartz-calcite vein with sparse chrysocolla, hosted in silicified Tertiary breccia containing clasts of Mesozoic volcanic rocks and silicified granite.

LOCATION: Deer Trail mine
DESCRIPTION: Prospect east of shaft located in shattered lower-plate mylonite with hematite-stained fracture surfaces and local alteration of host rocks to clay minerals. Hematite staining affects wall rocks adjacent to fractures, giving rock a red-and-white mottled appearance. Adit and shaft shown on topographic map are same mine and are located in chloritic breccia 5 to 15 m below Buckskin-Rawhide detachment fault. Host breccia has pervasive, red hematite stain with black, microcrystalline specular hematite on some fracture surfaces. Prospect just west of shaft is located in strongly brecciated and silicified chloritic breccia grading upward into microbreccia at base of Buckskin-Rawhide detachment fault. Mineralization characterized by hematite, jarosite(?), and pyrite.

Geology of postdetachment, Miocene volcanic rocks in the southwestern Buckskin Mountains

MICHAEL J. GRUBENSKY *Arizona Geological Survey, 845 N. Park Ave., #100, Tucson, Arizona 85719*

ABSTRACT

The Osborne Wash Formation in the western Buckskin Mountains consists primarily of flat-lying to gently tilted, middle to upper Miocene basalt flows. Southeast of the Mammon mine, trachyte flows and related pyroclastic rocks are interbedded with these basalts. The vent areas for the trachytes are also exposed in the study area. Several lines of evidence suggest that the trachytes evolved from the associated basalts. All of these volcanic rocks postdate detachment faulting in the western Buckskin Mountains, but are considered to be broadly related to extension.

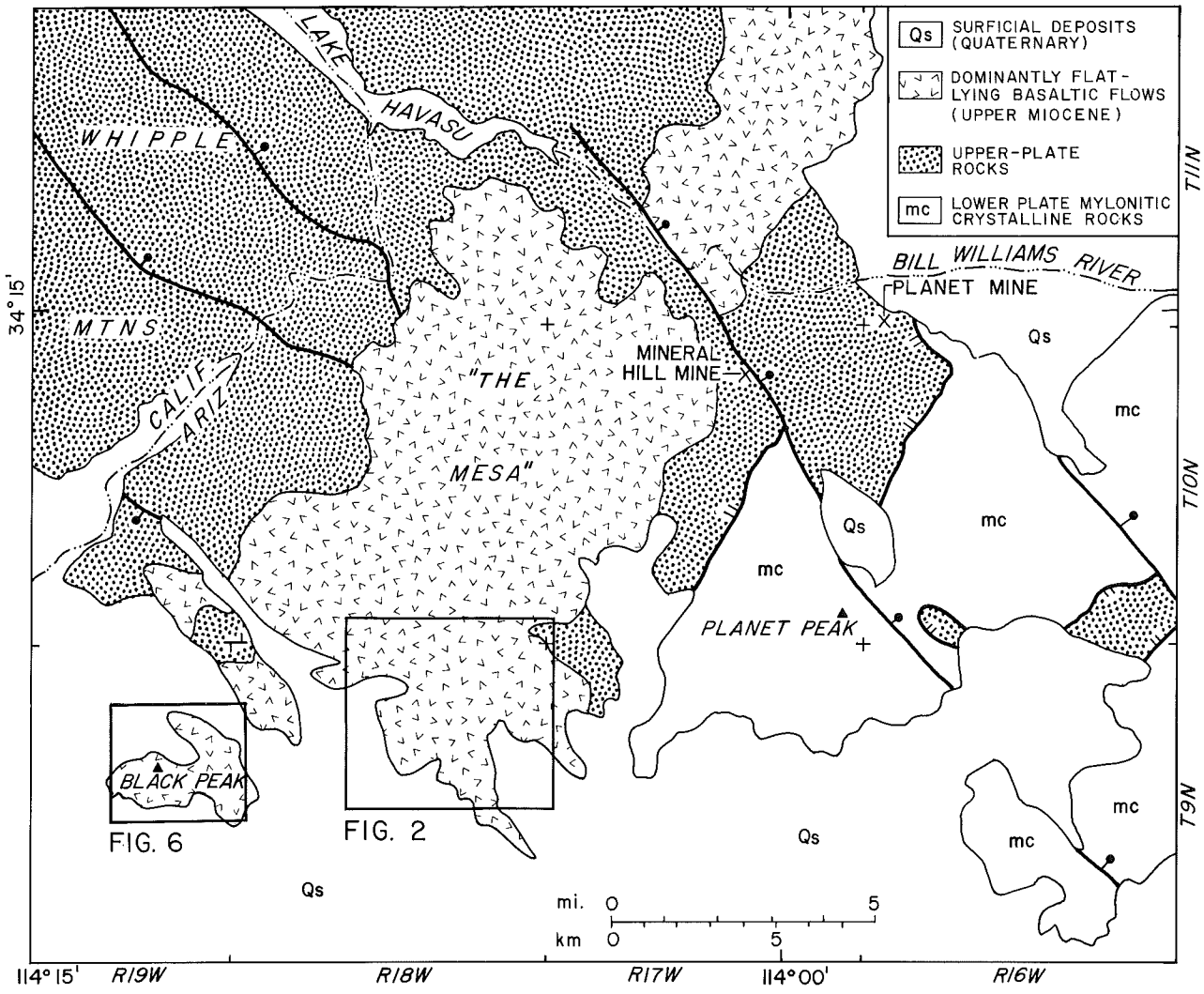

Figure 1. Map showing locations of study areas (Figures 2 and 6).

in Spencer, J.E., and Reynolds, S.J., eds., 1989, Geology and mineral resources of the Buckskin and Rawhide Mountains, west-central Arizona: Arizona Geological Survey Bulletin 198, p. 255-262.

INTRODUCTION

Flat-lying to gently dipping, middle to upper Miocene, olivine-bearing basalts, trachyte lava flows, and subordinate pyroclastic rocks are the primary rock types in the southwestern Buckskin Mountains (Fig. 1). These rocks have not been previously mapped or described in detail. Broadly correlative rocks to the west are named the Osborne Wash Formation (Davis, G.A., and others, 1980). Frost (1983) correlated all flat-lying basalts and sediments in the western Buckskin Mountains that are older than the Pliocene Bouse Formation, including almost all of the rocks in the study area, with the Osborne Wash Formation. The underlying sedimentary, volcanic, and metamorphic rocks have been affected by rotational normal faulting above a regional low-angle normal (detachment) fault (Spencer and Reynolds, this vol.). Volcanic rocks in the study area were erupted within a few million years after large-magnitude crustal extension and displacement occurred along the detachment fault. Most K-Ar dates on flat-lying basalts from the Osborne Wash area fall in the range from 13 to 16 Ma. Tilting and normal faulting in the study area thus ended by this time.

Dominantly basaltic rocks in similar structural and stratigraphic position that have yielded middle to late Miocene K-Ar dates are present in several ranges adjacent to the Buckskin Mountains (Suneson and Lucchitta, 1979, 1983). Rhyolitic rocks are associated with basalts in the Castaneda Hills, which are north of the Buckskin Mountains, in contrast with the basalt-trachyte association in Osborne Wash. Both areas were volcanic centers that developed shortly after major extensional faulting ended.

A MIDDLE MIOCENE TRACHYTIC VOLCANIC CENTER IN OSBORNE WASH

An assemblage of four trachyte lava flows and their associated pyroclastic deposits were erupted from a small, Miocene volcanic field in the southwestern Buckskin Mountains. Vents for all but one of the flows were probably clustered in the eastern portion of the map area (Figs. 2 and 3). Erosion has removed the vent rocks, exposing autobrecciated, intrusive plugs. Each trachyte flow was preceded by explosive eruption of pyroclastic material, including air falls, surges, and in some cases, ash flows. Surge-related tuffs are most abundant in

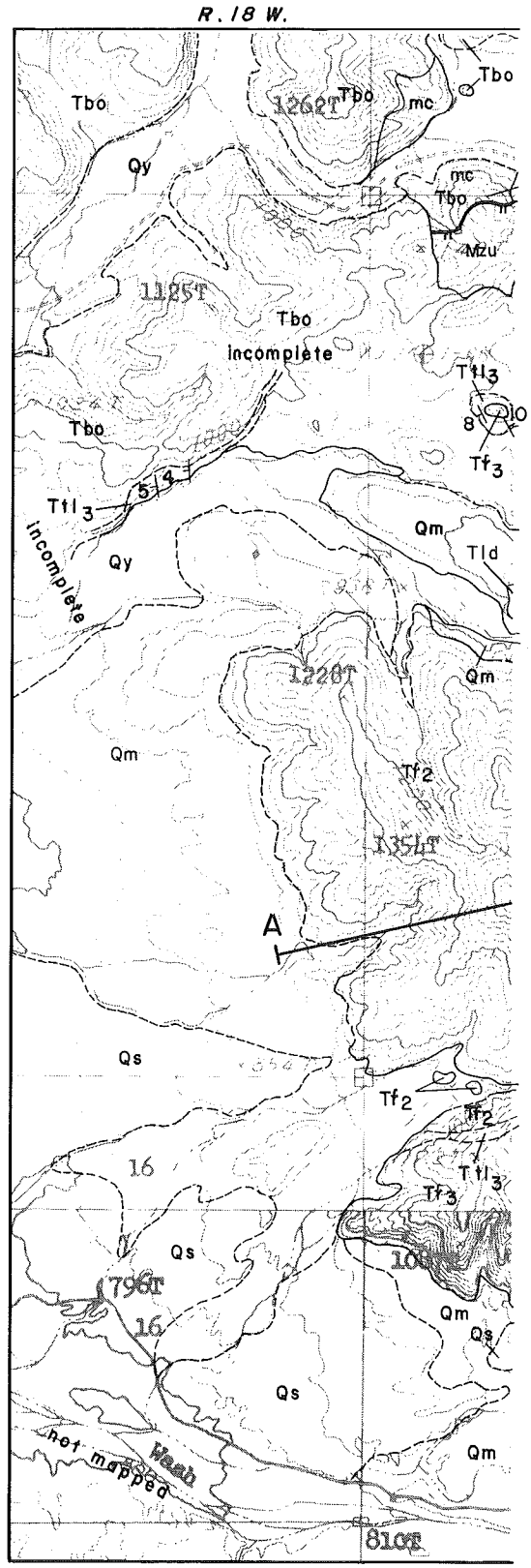

Figure 2 (right). Geologic map of small, Miocene volcanic field in southwestern Buckskin Mountains. Unit Tld is a lava dome. Trachytic lava flows of units Tf_1, Tf_2, and Tf_3 are preserved as a "layer-cake" sequence in the southwestern portion of the map area. Each trachyte flow is associated with an intrusive plug exposed in either the southern part of section 2 or the unsurveyed area south of section 2. Contacts between trachyte flows in this region are steep, as evident from their map pattern. Cross section A-A' is shown in Figure 3; descriptions of units are given in Figure 4. The location for a K-Ar-dated sample from unit Tf_1 (Spencer and others, this vol.) is also shown. The Rawhide-Whipple-Buckskin detachment fault is shown as a heavy barbed line.

exposures adjacent to intrusive rocks. Surge deposits, recognized by long-wavelength crossbeds, are less common north and west of the intrusive rocks. Minor intrusive mafic and intermediate dikes are present only in the eastern portion of the map area. The oldest trachyte flow is preserved solely as a dome-shaped hill, depositionally overlain by younger outward-dipping flows and pyroclastic rocks, in the western map area. A fairly

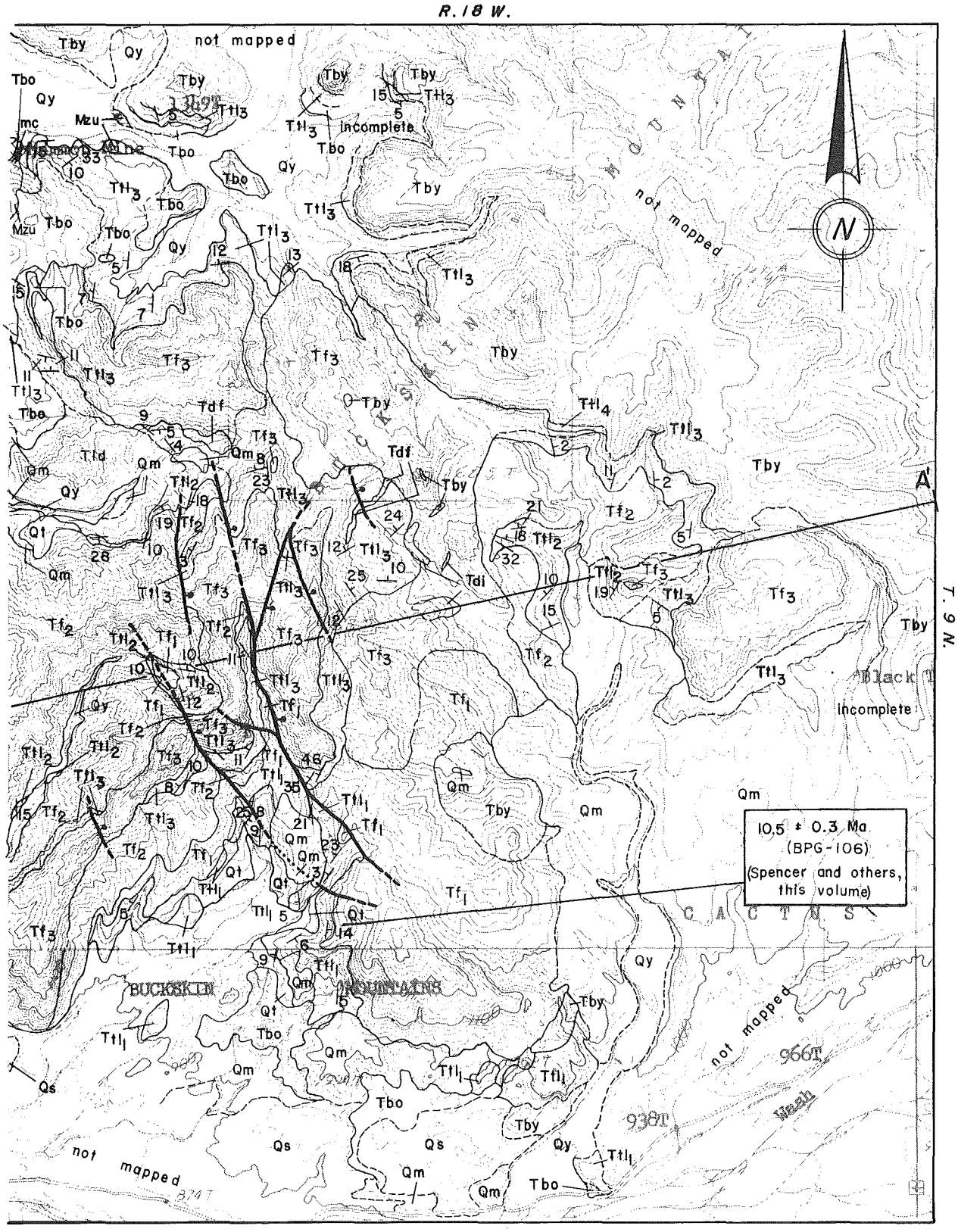

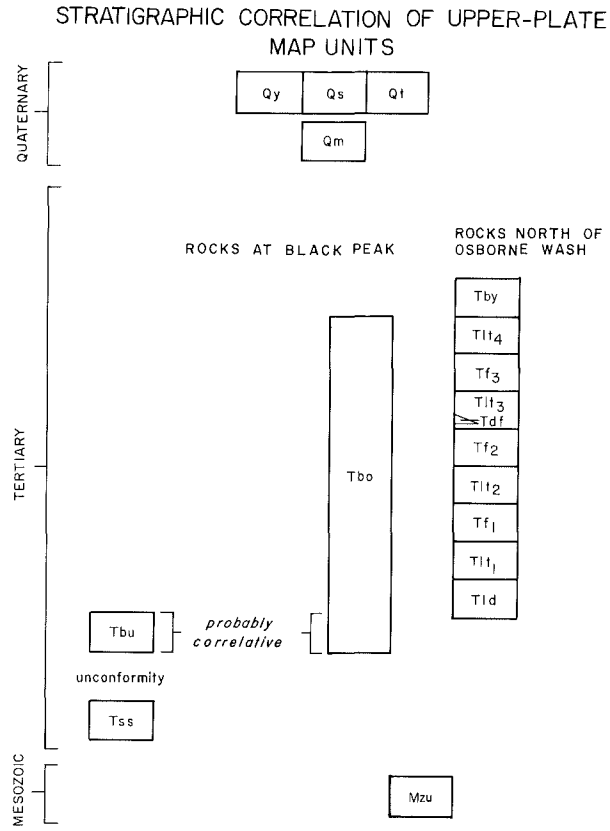

Figure 3. Stratigraphic correlation diagram for rocks in Figures 1 and 2. Quaternary sediments include younger alluvium (Qy), windblown sand (Qs), talus (Qt), and older alluvium (Qm). All Tertiary volcanic and sedimentary rocks are described in Figure 5, except for intrusive dikes of unit Tdi.

complete record of the volcanic history of this field is preserved in a gently west-dipping homocline in the southwestern map area, where the assemblage is 300 m thick.

The volume of trachyte flows and plugs is greater than that of associated pyroclastic rocks. About 0.75 km^3 of trachyte is exposed. The exposed volume of each flow and associated plug, from oldest to youngest, is 0.028 km^3, 0.14 km^3, 0.31 km^3, and 0.28 km^3. The volume of pyroclastic rocks erupted from this volcanic center was not estimated, partly because their full extent is unknown.

Because chemical data were not available, all four lavas have been classified as trachyte (rocks that are slightly alkaline to alkaline in composition) based on thin-section observation and the guidelines of Williams and others (1982, p. 145). The mineralogy, size, and approximate mode of phenocrysts vary among flows, but broad generalizations about petrography can be made: (1) phenocryst mineralogy includes one or two feldspars and fine-grained clinopyroxene and olivine; and (2) clinopyroxene is almost always slightly pleochroic green and olivine is typically yellow. Feldspar phenocrysts are absent in the oldest lava and consist of only sanidine in unit Tf_1, plagioclase feldspar in unit Tf_2, and anorthoclase in unit Tf_3. The groundmass feldspar is sanidine in all lavas, which is recognizable in thin section by Carlsbad twinning and a low refractive index. Where plagioclase phenocrysts are present, they have coronas of radially oriented microlites of sanidine and an opaque phase. Accessory phases are zircon and apatite. Quartz and aenigmatite, mineral phases associated with strongly alkaline rocks such as pantellerite and pantelleritic trachyte, are not present (Sutherland, 1974).

Although all trachyte flows are broadly similar in character, there is an apparent trend toward features characteristic of rocks of lower alkalinity with each successive eruption: (1) there is a consistent increase in phenocryst size and approximate mode from the oldest microphyric lava to the youngest porphyritic lava; and (2) conspicuous sanidine phenocrysts in lavas formed during earlier eruptions are rare relative to plagioclase and anorthoclase, which were formed during later events. The younger lavas were probably quite viscous; flow foliation is more apparent and on a finer scale in older trachytes, which are also thinner relative to later flows (Fig. 4). The last lava flow is especially noteworthy because it has not only the coarsest phenocrysts, but also inclusions of a darker lava with abundant, still coarser (up to 1 cm) phenocrysts of plagioclase feldspar. The inclusions have petrologic implications for the origin of the lavas; these are discussed in more detail later in this report.

Intrusive plugs, which presumably fed vents for three of the four lavas, are clustered in the eastern portion of the map area (Fig. 2). The westward dip of the flows in the western map area and the westward- and northward-thinning of pyroclastic deposits between flows suggest that all were emplaced onto the flanks of a small, cone-shaped stratovolcano (Fig. 5). The eastern and southern flanks of the stratovolcano were eroded away, but basalt flows buried the erosional scarp on the east. Pyroclastic rocks, which underlie each trachyte flow, are similar throughout the section, but their composition is uncertain. They have a lower color index than the flows and are probably more evolved (less mafic and more alkaline). All units are essentially aphanitic, exhibit the same low degree of welding, have similar bedding and total thicknesses, and include cross-beds and planar beds. Pyroclastic units are locally juxtaposed on one another along angular unconformities with up to 40° of discordance. These remarkable unconformities do not extend beyond the trachyte flows, which suggests that relief and slope decrease as distance from the vent increases.

Pyroclastic rocks of unit Tlt_3 extend to the north and west of the Mammon mine, beyond both the flows and the map area. Because pyroclastic rocks throughout the assemblage are mesoscopically similar, unit Tlt_3 may include pyroclastic rocks of other units that are juxtaposed with it. Pyroclastic rocks mapped as unit Tlt_3 are intercalated with two basalt flows, one of which may be the lower basalt (unit Tbo) along the western periphery of the volcanic center. Basaltic volcanism was intermit-

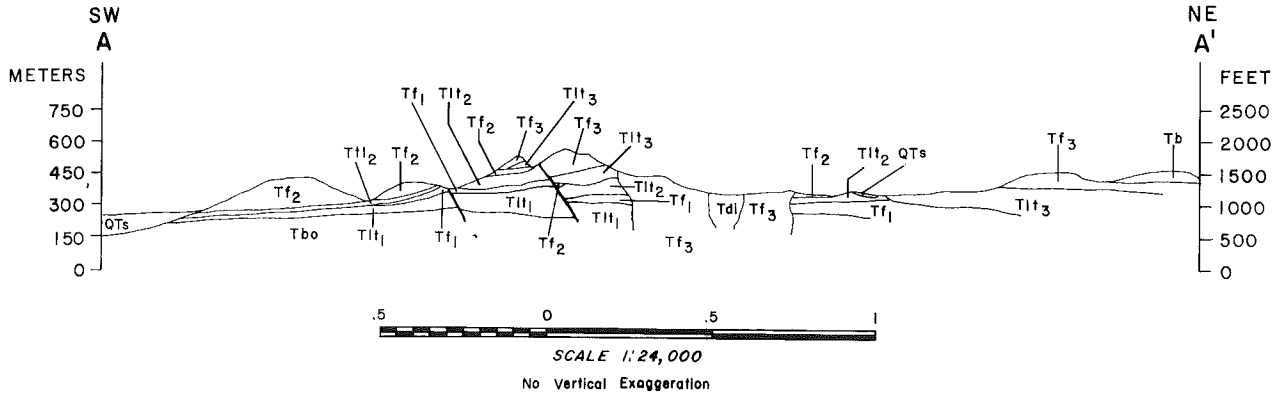

Figure 4. Cross section A-A' through the volcanic field shown in Figure 2.

tent not only before and after trachytic volcanism, but also during the eruption of the more evolved lavas. North of the Mammon mine, pyroclastic rocks mapped as unit Tlt_3 lie conformably between basalt flows, all of which extend at least 1 km northwest of the map area (Figs. 2 and 3). Air-fall tuff near the base of the Osborne Wash Formation (Davis, G.A., and others, 1980) may have erupted from this volcanic center.

TIMING OF BASALTIC-TRACHYTIC VOLCANISM AND EXTENSION

Rocks of the Osborne Wash Formation unconformably overlie moderately to steeply tilted, older Tertiary volcanic and sedimentary rocks, including arkose and conglomeratic arkose near Black Peak, that probably correlate with the Copper Basin Formation of G.A. Davis and others (1980). Five K-Ar dates on volcanic rocks from the Copper Basin Formation in the eastern Whipple Mountains range from 17.1 $\pm$ 0.8 Ma to 18.7 $\pm$ 0.8 Ma (Davis, G.A., and others, 1982). Three K-Ar dates were obtained on the basalt flows of Black Peak: 14.1 $\pm$ 0.7 Ma (Fugro, 1975); 16.1 $\pm$ 0.8 Ma (Shafiqullah and others, 1980); and 20.3 $\pm$ 3.1 Ma (Eberley and Stanley, 1978; see also Fig. 6 and Spencer and Reynolds, this vol.). The first two dates are similar to those of basalts of the Osborne Wash Formation (Martin and others, 1980; Shafiqullah and others, 1980). The 20.3 Ma date is comparatively old and associated with a large uncertainty. Thus, the oldest rocks of the Osborne Wash Formation in the southwestern Buckskin Mountains are probably 14 to 16 Ma; however, a K-Ar date of 10.5 $\pm$ 0.3 Ma (Spencer and others, this vol.) on a feldspar concentrate from the oldest trachyte flow (unit Tf_1 in Fig. 2) suggests that substantial sections of the Osborne Wash Formation are somewhat younger than 14 to 16 Ma (Frost, 1983).

Several northwest-striking normal faults in the trachytic volcanic field (Fig. 2) have dip-slip separations of several meters to several tens of meters. All of these faults dip between 50° and 70° to the northeast, an orientation identical to many detachment-related, upper-plate normal faults in the Buckskin Mountains. At the Mammon mine, however, trachyte flows conformably overlie basalts that, in turn, depositionally overlie the Buckskin-Rawhide-Whipple detachment and lower-plate mylonitic rocks (Frost, 1983; Spencer and Welty, this vol.). Minor normal faulting that occurred after deposition of the Osborne Wash Formation was younger and unrelated to detachment faulting (Frost, 1983).

PETROLOGIC IMPLICATIONS OF MAFIC INCLUSIONS

The presence of mesoscopic, dark-colored, trachytic inclusions in the youngest lava suggests that all lavas at this center are comagmatic and may be, in part, differentiates of the magma erupted as the associated basalt flows (Fig. 5). Wholesale mixing of two, texturally discrete magmas is probably the most common process for producing small volumes of intermediate magmas in eruptive centers with marked basalt-rhyolite associations. The mafic inclusions in lava Tf_1 are vesicular, unlike the host rock, and coarser grained than all the other non-basaltic lavas of this volcanic field. They have a phenocryst assemblage comparable to the trachyte flows (plagioclase, anorthoclase, clinopyroxene, and olivine) in the study area. A groundmass of mostly sanidine microlites and similar phenocryst mineralogy demonstrate that the inclusions, though discrete, are mineralogically intermediate between the trachytes and the more voluminous basalts. Slight differences in the mode and size of phenocrysts and colorless clinopyroxene and olivine in

Figure 5 (next page). Graphic, composite columnar section of Miocene volcanic and sedimentary rocks mapped in the Osborne Wash area (Fig. 2). Thickness of each unit is proportional to maximum exposed thickness; thickest exposed section is 300 m. Line pattern is for pyroclastic rocks, rectangular pattern for basalts, dot pattern for sandstone, and hachured long dashes for trachyte. Dark blobs in unit Tf_3 denote dark inclusions (see text). Quaternary sediments and Precambrian-Mesozoic rocks are not shown for brevity, but the latter are described elsewhere (Frost, 1983; Reynolds and Spencer, this vol.; Spencer and Reynolds, this vol.)

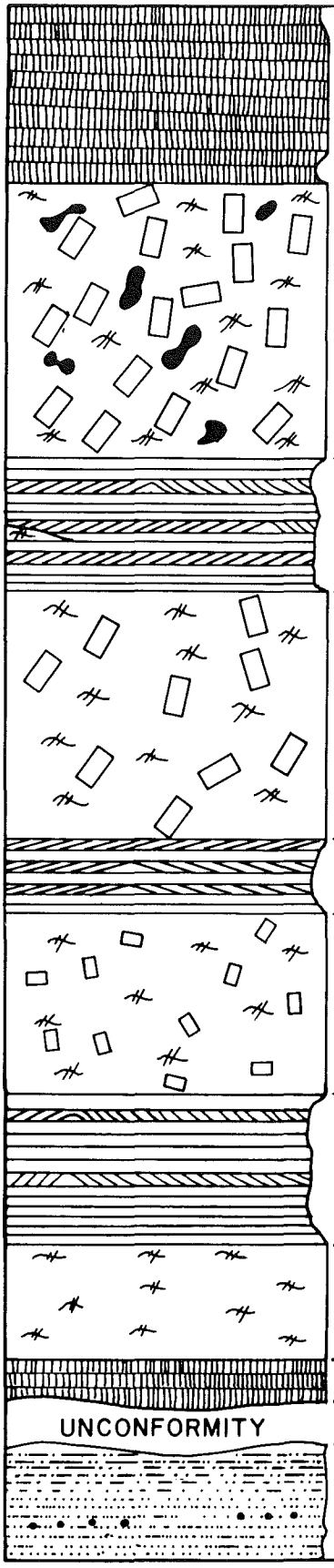

Tby-- Basalt flows with phenocrysts of fine-grained olivine, clinopyroxene, and plagioclase. This unit can be 80 m thick.

Tlt_4-- Unwelded, generally aphyric, ash-flow tuff with lithic fragments no larger than pebbles. Only one small exposure is in the northeastern periphery of the map area (Fig. 1), where it is not more than 10 m thick.

Tf_3-- Trachyte flow (60 m to 100 m thick) with phenocrysts of coarse-grained anorthoclase and fine-grained clinopyroxene* and olivine* in an intergranular-textured groundmass of sanidine microlites, apatite, zircon, and an opaque. Anorthoclase phenocrysts are clear to white-colored in hand specimen and subhedral and locally form 2- to 3-grain aggregates up to 1 cm across. Mesoscopic, spherical inclusions of coarse-grained, darker, vesicular trachyte are present in some exposures. Inclusions range from less than 1 cm to about 25 cm across and contain phenocrysts of coarse-grained plagioclase and anorthoclase and fine-grained, colorless clinopyroxene and olivine. Tridymite(?) is interstitial to sanidine microlites in the groundmass and also coats vesicle walls. Coronas of radially oriented microlites of sanidine and an opaque mineral are present on plagioclase and anorthoclase grains. Vesicles are usually 1 to 2 mm across and spherical to elliptic.

Tlt_3-- As much as 75 m of thin-bedded, lithic-rich air-fall tuff and surge-related tuff. Includes thickly bedded, partly welded ash flows and locally a dark-brown lava flow, which is 10 m thick.

Tf_2-- Coarsely flow-foliated trachyte lava (158 m thick) with 10% to 15% phenocrysts of plagioclase, clinopyroxene*, and olivine*. Plagioclase phenocrysts are 1 to 5 mm across and typically a chalky-white color; an andesine composition was determined optically. Sanidine and opaque microlites can form coronas around plagioclase. The groundmass comprises sanidine microlites, interstitial glass, and accessory apatite and zircon.

Tlt_2-- About 35 m of thin- to medium-bedded tuffs, very similar to layered tuffs of units Tlt_1, Tlt_3, and Tlt_4.

Tf_1-- Trachyte flow exposed primarily in the southeastern map area (Fig. 1) as a dome with abrupt flanks. Contains 5% to 7% phenocrysts of adularescent euhedral sanidine, and subhedral clinopyroxene* and olivine* in a devitrified, aphyric groundmass. Sanidine phenocrysts are 2 to 3 mm across and ferromagnesian minerals are less than 1 mm across. Fine-scale flow foliation is characteristic of this unit. The thickness of this unit varies from 20 m in the west to 100 m in the southeast (Fig. 1).

Tlt_1-- About 75 m of thick-bedded ash-flow tuff, and thin-bedded to laminated air-fall tuff and surge-related tuffs.

Tld-- Trachyte exogenous dome with cryptic, near-horizontal layering on the scale of several meters. A holocrystalline, trachytic texture is defined by fine-grained, 1-mm phenocrysts of sanidine and subordinate (<3%) groundmass clinopyroxene* and olivine* that form crystals less than 0.5 mm across. Zircon and apatite are accessory phases.

Tbo(Tbu)-- At least 20 m of basalt flows with phenocrysts of clinopyroxene, olivine, and plagioclase. Plagioclase phenocrysts up to 1 cm across are resistant relative to the groundmass and weather out to form resistant knobs.

Tss-- At least 60 m of tan, poorly bedded, coarse-grained arkose and conglomeratic arkose. Base is covered.

* Clinopyroxene is slightly pleochroic green and probably a ferroaugite; olivine is yellow and probably a fayalitic olivine.

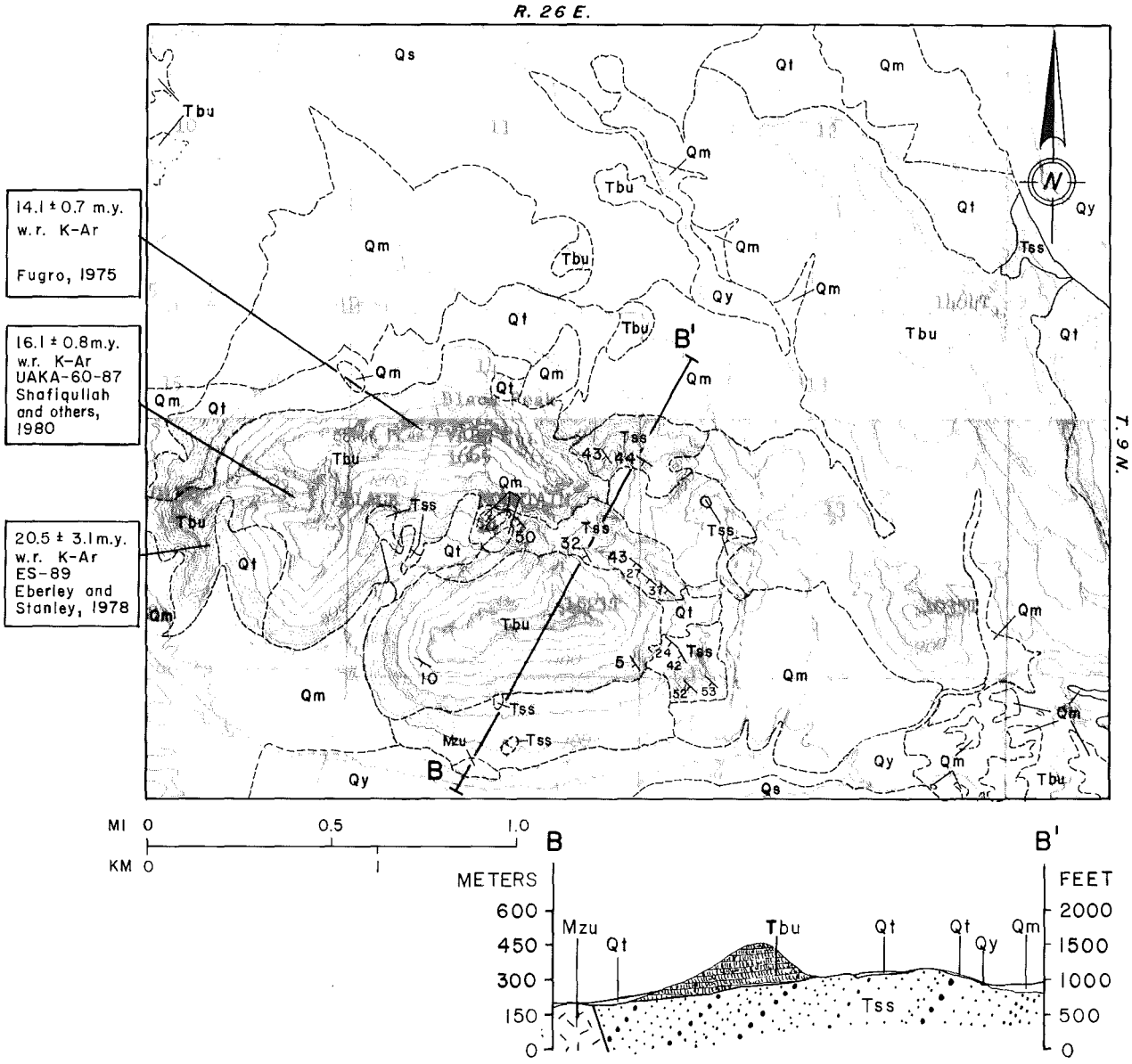

Figure 6. Geologic map of Black Peak area showing locations of published K-Ar dates of basalts of Osborne Wash Formation. Cross section B-B' has no vertical exaggeration.

the inclusions, however, suggest that the host lava flow has a slightly more evolved, less mafic composition. A lack of quench textures in the host rock and the rounded or globular shape and vesicular nature of inclusions indicate that two magmas were mixed in a partially liquid state (Eichelberger, 1980).

The clustered vents and the outward dip of lavas and associated pyroclastic rocks about the vent area were the core of a low-relief stratovolcano. The broadly consistent mineralogy of lavas, the systematic decrease in alkalinity of lavas with decreasing age, and the closeness of their respective vents suggest that the trachyte flows were products of the same magmatic system or chamber. The more mafic, less evolved inclusions in the youngest trachyte flow, which is apparently also the least alkaline, formed at depth by mixing between evolved and less evolved magmas late in the eruptive history of this system. The apparent compositional gap between inclusions and their host rocks denotes the coexistence of discrete magmas of slightly different composition in the chamber. The consistent texture and size of vesicles within inclusions developed in a chamber divided by an abrupt change in composition and temperature (Eichelberger, 1975); the magma chamber was zoned. Mixing and subsequent vesiculation probably occurred before eruption. The apparent decrease in alkalinity from oldest to youngest lavas in this assemblage and the appearance of mafic inclusions late in its eruptive history are features similar to those of more thoroughly studied alkaline or mildly peralkaline volcanic systems (Mahood, 1981, Mahood and Hildreth, 1983). Pyroclastic rocks interbedded between trachyte flows in Osborne Wash could be peralkaline in composition: the tuffs have a lower color index and are compositionally more evolved.

Strontium isotopic data indicate that basalts and rhyolites in the bimodal volcanic field in the Castaneda Hills were derived from different sources. Initial $^{87}Sr/^{86}Sr$ isotopic ratios for these rhyolites suggest that they were not differentiates of associated, mantle-derived, alkali olivine basalts, but partial melts of the lower crust (Suneson and Lucchitta, 1983). However, the trachyte flows of Osborne Wash, which are similar in age to rhyolites in the Castaneda Hills, may have differentiated from olivine-bearing basalts such as those interbedded with them. All the trachytes are at least slightly alkaline and they could lie at the end of a differentiation lineage common to the nepheline-normative, continental, alkali-basalt magma series (Williams and others, 1982, p. 110). This is an especially attractive hypothesis if the basalts of Osborne Wash are also alkaline. The mafic lavas of the Osborne Wash Formation were inferred to be alkali olivine basalts (Frost, 1983) because of their similarity in appearance, phenocryst assemblage, and age to alkali olivine basalts in the Castaneda Hills, as described by Suneson and Lucchitta (1979, 1983). This inference remains to be tested through chemical and petrographic analyses. There is, however, an apparent lack of lavas, such as hawaiite and mugearite, that are intermediate in composition between trachyte and alkali olivine basalt. Late Miocene volcanism in northwestern Arizona included hawaiites, as well as alkali olivine basalt and peralkaline rhyolite (Best and Brimhall, 1974). The bimodal association of trachyte with alkali olivine basalt is common in the East African Rift, which is also an extensional tectonic environment (Weaver and others, 1972).

CONCLUSION

The presence of trachytic volcanic rocks interbedded with olivine-bearing basalts of the Osborne Wash Formation raises the possibility that magmatic differentiates of basaltic melts may be preserved in the western Buckskin Mountains. Further isotopic and geochemical studies are needed to test this hypothesis. Based on petrographic and field studies, the volcanic rocks are tentatively considered to be genetically related and to be broadly associated with regional extension.

Appendix A: Map-unit descriptions and cross sections for Plate 2 (Geologic map of the Planet-Mineral Hill area, northwestern Buckskin Mountains, west-central Arizona)

JON E. SPENCER
STEPHEN J. REYNOLDS — *Arizona Geological Survey, 845 N. Park Ave., #100, Tucson, Arizona 85719*
NORMAN E. LEHMAN *1650 N. Indigo Dr., Tucson, Arizona 85745*

INTRODUCTION

The Planet and Mineral Hill area is in the northwestern Buckskin Mountains, west-central Arizona (Fig 1). Rocks in the area are divided into three groups: (1) generally flat-lying, upper Cenozoic, postdetachment basalt and sedimentary rocks; (2) metamorphosed, Mesozoic sedimentary and volcanic rocks and depositionally overlying, unmetamorphosed, Miocene sedimentary and volcanic rocks that together form the upper plate of the Buckskin detachment fault; and (3) mylonitic crystalline rocks that form the lower plate of the Buckskin detachment fault. The upper-plate rocks were distended and tilted by movement on normal faults that are cut by, or flatten downward to merge with, the Buckskin detachment fault (Fig. 2). The Planet and Mineral Hill mineral deposits directly overlie the detachment fault.

POSTDETACHMENT UNITS

Qa YOUNG ALLUVIAL DEPOSITS (QUATERNARY) -- Unconsolidated gravel, sand, and silt in washes and along the Bill Williams River. Includes all deposits mobilized during periods of heavy rainfall.

Qi INTERMEDIATE ALLUVIAL DEPOSITS (QUATERNARY) -- Unconsolidated gravel, sand, and silt in washes that typically form alluvial surfaces 1 to 2 m higher than adjacent wash floors. Also includes semiconsolidated silt and soil along the flanks of the Bill Williams River, some of which has been modified by farming. Deposits of this map unit were probably mobilized by very large floods and probably represent, in part, flood deposits along present drainages.

Qt TALUS DEPOSITS (QUATERNARY) -- Unconsolidated angular clasts that form steep talus slopes.

Qo OLD ALLUVIAL DEPOSITS (QUATERNARY) -- Light-gray to light-tan, unconsolidated to very poorly consolidated, poorly sorted conglomeratic sandstone and conglomerate. Typically forms perched terraces and flats above modern washes. Includes all deposits older than those of units Qa and Qi and younger than those of unit QTo. Does not generally include talus deposits (unit Qt), although gradational contacts between these two units makes division imprecise.

QTo VERY OLD ALLUVIAL DEPOSITS (QUATERNARY OR UPPER TERTIARY) -- Light-gray, unconsolidated to poorly consolidated, poorly sorted conglomeratic sandstone and conglomerate. Forms perched ridges and hills topographically higher than nearby unit Qo. Clearly distinguishable on aerial photographs from unit Qo by its lighter color, greater degree of dissection, more rounded landforms, and higher relative elevation. Crude stratification and poor sorting indicate deposition as alluvial fans in present topographic basins.

Tb MESA-FORMING BASALT (UPPER MIOCENE) -- Flat-lying basalt flows and flow breccias. Basalt is medium gray, vesicular to nonvesicular, and aphanitic to slightly porphyritic with phenocrysts of plagioclase, clinopyroxene, and partially resorbed quartz eyes. On the northeastern flank of The Mesa, the unit consists of a lower sequence of approximately six thin flows overlain by a thicker flow that caps the mesa. Thin lenses of tan fanglomerate occur directly below the mesa-capping flow in channels eroded into the lower flows.

Tbf BASIN-FILL CONGLOMERATE AND SANDSTONE (UPPER TO MIDDLE MIOCENE) -- Oldest post-detachment-faulting sedimentary rocks that rest unconformably on tilted Tertiary sedimentary and volcanic rocks and older rocks. Generally poorly sorted, matrix-supported cobble to pebble fanglomerate and pebbly sandstone with medium- to light-brown, tan, or local

in Spencer, J.E., and Reynolds, S.J., eds., 1989, Geology and mineral resources of the Buckskin and Rawhide Mountains, west-central Arizona: Arizona Geological Survey Bulletin 198, p. 263-269.

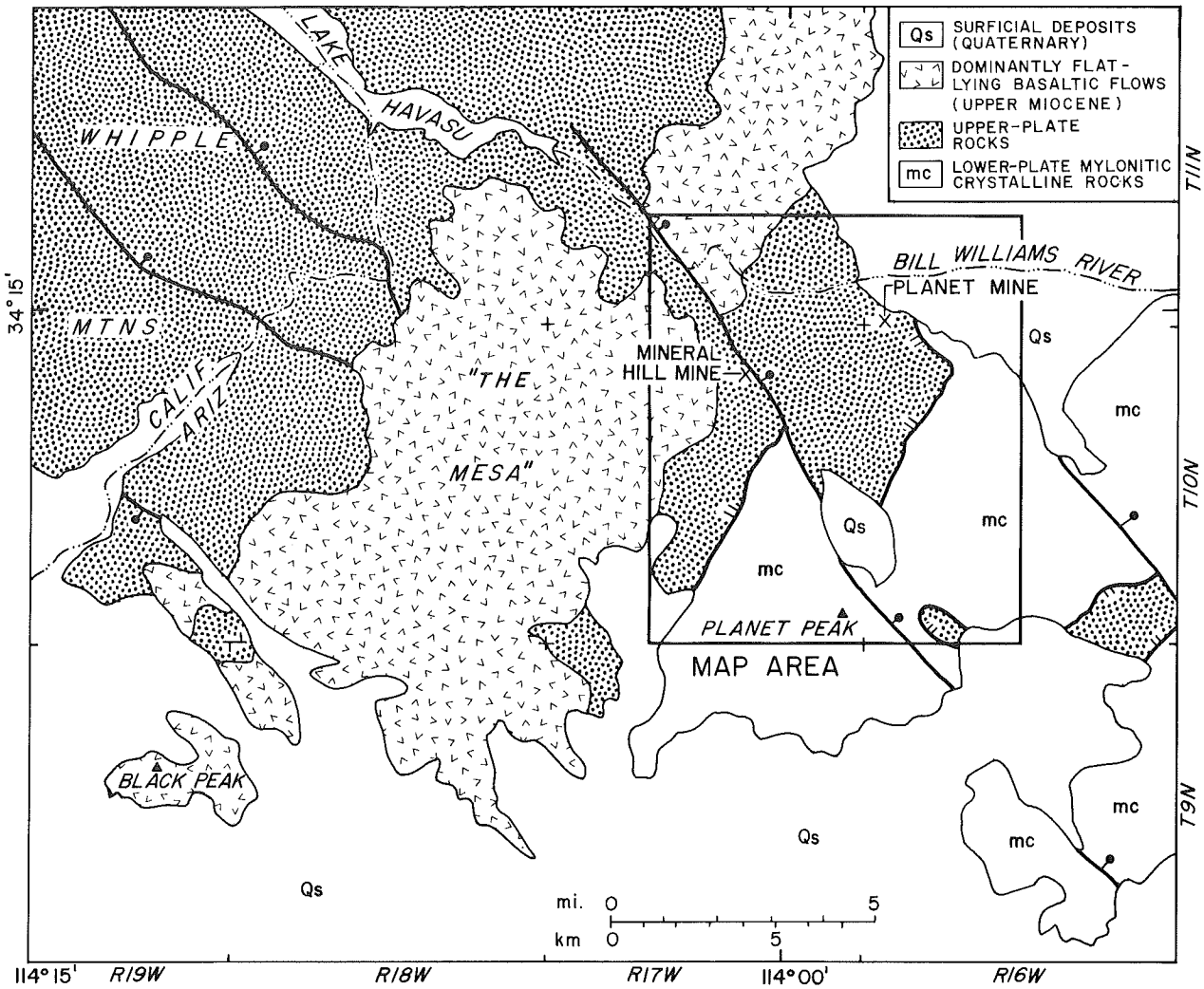

Figure 1. Location map of area of Plate 1.

reddish-brown color. Stratification is moderately well developed on a scale of meters, but poorly developed on a scale of centimeters. Locally includes thin, light-gray, buff, or cream-colored tuff and tuffaceous sandstone. In valley north of Planet Peak, clasts consist of intermediate to mafic Tertiary volcanic rocks, phyllitic Planet Volcanics, Tertiary sedimentary rocks, granite, and sparse replacement carbonate (unit Tc), lower-plate mylonite, and tectonized carbonates. Abundance of clasts of Planet Volcanics and of Tertiary sedimentary breccia derived from the volcanics increases to west toward Continental mine; clast imbrication in this area indicates transport toward the ESE. In northwestern corner of map area, south of Bill Williams River, clasts include Planet Volcanics; Mesozoic quartzite; vesicular Tertiary volcanics; foliated (not obviously mylonitic), medium-grained granitic rocks; fine-grained, leucocratic granitic rocks; reworked, reddish-brown Tertiary sandstone, conglomerate, and sedimentary breccia; and nonfoliated, medium-grained, pink biotite granite with 1- to 2-cm K-feldspar phenocrysts. Many granitic clasts are much more rounded than other clasts, which suggests a second-generation derivation from middle Tertiary conglomerate. Unit is less well bedded and is coarser where deposited near erosionally resistant quartzite of the upper Buckskin Formation. In the northeast corner of the map area, south of the Bill Williams River, clasts include Planet Volcanics, mylonitic granitic rocks, and granitic and gneissic rocks with epidote- and chlorite-filled fractures, which strongly suggests derivation from the lower plate.

UPPER-PLATE UNITS

Tcw CONGLOMERATE OF CAVE WASH (MIDDLE MIOCENE[?] TO UPPER OLIGOCENE[?]) – Massive to moderately bedded, cobble to boulder conglomerate with subrounded to very well rounded clasts, 3 to 30 cm in diameter (locally up to 1 m in diameter), of

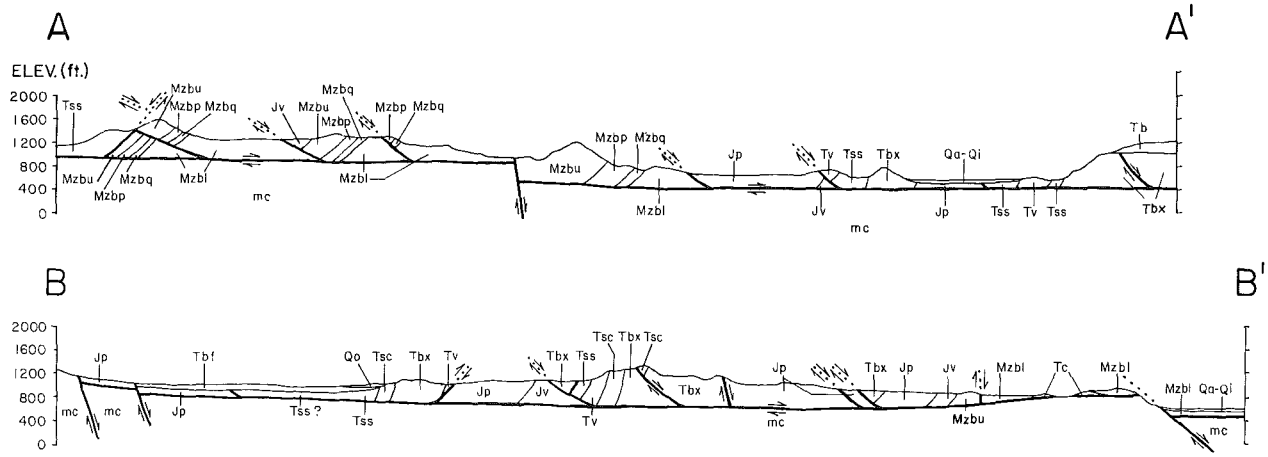

Figure 2. Geologic cross sections of Planet and Mineral Hill area. See Plate 1 for locations of cross sections.

coarse-grained, porphyritic, Proterozoic(?) granitic rocks; medium- to fine-grained, Proterozoic(?) granitic and gneissic rocks; and bull quartz. Exposures south of Tunnel Peak also contain subangular clasts of locally derived Planet Volcanics.

Tcwb BASALT OR BASALTIC ANDESITE OF CAVE WASH (MIDDLE MIOCENE[?] TO UPPER OLIGOCENE[?]) -- Medium- to dark-gray flows and flow breccias interbedded with conglomerate of Cave Wash.

Tc REPLACEMENT CARBONATE (MIDDLE TO LOWER MIOCENE[?]) -- Medium- to dark-brown, massive, hydrothermal carbonate deposits that replace Mesozoic rocks above the detachment fault. Also occurs in unmapped veins along upper-plate faults and as partially fault-bounded lenses directly above detachment fault. Unit locally has a diffuse layering parallel to detachment fault or parallel to foliation in adjacent, unreplaced Mesozoic rocks. Elsewhere, unit is composed of clasts of strongly brecciated brown carbonate in a darker brown carbonate matrix that is not shattered, even though unit directly overlies detachment fault. Near the Continental mine, the carbonate forms a tabular body that directly overlies the detachment fault and underlies and truncates an upper-plate normal fault that separates Tertiary sedimentary breccia and sandstone from Mesozoic Buckskin Formation.

Tcg UPPER CONGLOMERATE (MIDDLE TO LOWER MIOCENE[?]) -- Light-brown and tan conglomerate and conglomeratic sandstone that are poorly sorted and poorly to moderately bedded. Clasts consist of Tertiary sandstone, conglomerate, and intermediate volcanics; Planet Volcanics; fine- and coarse-grained granite; and less abundant carbonate rocks and rocks derived from the lower-plate, including mylonitic quartzofeldspathic gneiss, lineated and laminated mafic schist, and hematitic breccia.

Ts SEDIMENTARY ROCKS, UNDIVIDED (MIDDLE TO LOWER MIOCENE[?]) -- Siltstone, sandstone, and conglomerate in small faulted outcrops in center of map area. Unit is typically moderately consolidated, poorly to moderately sorted, moderately to weakly resistant, and various shades of red and brown. Typically faulted and tilted to gentle to steep dips by movement on normal faults above the detachment fault.

Tss SANDSTONE AND SILTSTONE (MIDDLE TO LOWER MIOCENE[?]) -- Moderately to poorly sorted, variably reddish-brown, brown, yellowish-brown, or tan, weakly to moderately resistant sandstone, locally silty or pebbly sandstone, and siltstone. Sparse pebbly beds contain 1- to 5-cm clasts of medium- to fine-grained, leucocratic granitic rocks and finely vesicular, dark-brown to black, intermediate to mafic volcanic rocks. Sandstone in Cave Wash is thin bedded, well stratified, and pale yellowish green to pale reddish brown or medium red. In the southwestern part of the map area, unit includes siltstone and silty sandstone and contains 1- to 10-cm-thick, light- to dark-gray or light-tan limestone and silty limestone; buff-colored, biotite-bearing air-fall tuff; and medium- to coarse-grained arkosic sandstone that locally contains well-preserved biotite flakes. In this area (sec. 21 and 22, T. 10 N., R. 17 W.), 10- to 30-cm-thick crossbeds indicate paleocurrent directions varying from east to SSE.

Tsc CONGLOMERATE (MIDDLE TO LOWER MIOCENE[?]) -- Moderately to poorly sorted, moderately resistant, massive to moderately well-

bedded, typically matrix-supported conglomerate and fanglomerate. In northeast corner of map area, south of Bill Williams River, reddish-brown, mostly massive conglomerate contains subangular cobbles and boulders of Planet Volcanics and Mesozoic metasedimentary rocks. At north edge of map area in Cave Wash, fanglomerate contains subrounded cobbles and pebbles of granitic rocks, intermediate Tertiary volcanics, and gray carbonate rocks and is interbedded with poorly sorted, poorly stratified sandstone and pebbly sandstone. On northeast side of long ridge east of mouth of Mineral Wash, massive cobble to boulder conglomerate contains clasts of porphyritic biotite granite with distinctive green plagioclase and pink K-feldspar phenocrysts, quartzite, and Planet Volcanics. South of Tunnel Peak, unit is arkosic reddish-brown conglomerate and conglomeratic sandstone that contains subangular clasts of coarse- grained granite with K-feldspar phenocrysts 1 to 4 cm long and a well-developed Mesozoic(?) foliation defined by flattened quartz, oriented biotite, and K-feldspar augen.

Tv INTERMEDIATE VOLCANIC ROCKS (MIDDLE TO LOWER MIOCENE[?]) -- Medium- to dark-gray, variably vesicular volcanic flows and flow breccias. Unit is brown to black weathering and composed of 0 to 15% lathlike plagioclase phenocrysts 1 to 6 mm long in a reddish or greenish, dark-gray matrix. Vesicles are generally filled with light-brown carbonate that preferentially weathers to form pits. High K_2O content of up to 10% on feldspar concentrates indicates that unit is variably K metasomatized.

Tt AIR-FALL TUFF (MIDDLE TO LOWER MIOCENE[?]) -- Grayish-white, poorly consolidated, fine-grained, friable air-fall-tuff bed interbedded with sandstone (unit Tss) in sec. 28, T. 10 N., R. 17 W.

Tbx SEDIMENTARY BRECCIA, UNDIVIDED (MIDDLE MIOCENE[?] TO UPPER OLIGOCENE[?]) -- Generally monolithologic, unsorted, massive to poorly bedded, clast-supported breccia composed of angular rock fragments, typically ranging from a few to a few tens of centimeters in diameter, contained in a matrix of pulverized rock. Unit generally has a reddish or reddish-brown color due to widespread hematite and is commonly very resistant to erosion, forming craggy strike ridges. Breccia was derived from various Mesozoic, Paleozoic, and Proterozoic units, with monolithologic breccia derived from one protolith commonly in abrupt stratigraphic contact with breccia sheets of some other lithology. Locally contains tabular blocks of brecciated, but otherwise intact, rock (megabreccia) as large as several hundred meters in length and several tens of meters thick. Inferred to represent catastrophic debris avalanches.

Tbxg SEDIMENTARY BRECCIA, GRANITIC PROTOLITH (MIDDLE MIOCENE[?] TO UPPER OLIGOCENE[?]) -- In northern part of map area, along Bill Williams River, unit is composed of clasts of granite and minor foliated-granite breccia in a red matrix. Exposures west of Tunnel Peak include mylonitic granitic rocks with 2- to 3-cm-long K-feldspar augen, with foliation crudely aligned from clast to clast. Foliation is not associated with strong lineation and is suspected to be a pre-Tertiary fabric. South of Tunnel Peak, clasts in unit are composed of foliated porphyritic granite, gneissic granite, and granitic gneiss of probable Proterozoic age.

Tbxv SEDIMENTARY BRECCIA, MESOZOIC VOLCANIC PROTOLITH (MIDDLE MIOCENE[?] TO UPPER OLIGOCENE[?]) -- Generally the stratigraphically lowest and most widely exposed of all breccia types. Unit is widely exposed at base of Tertiary section in most large fault blocks and is reddish brown and monolithologic. Composed of unsorted, angular clasts of Planet Volcanics. Typically rests depositionally on Planet Volcanics. Contact between breccia and its volcanic substrate varies from sharp to gradational change in color and degree of brecciation; where contact is gradational, amount of landslide-type transport may have been small. Breccia contains some interbedded, matrix-supported, polylithologic, debris-flow conglomerate and some large blocks of weakly brecciated to unbrecciated Planet Volcanics that have relict foliation cleavage parallel to bedding in nearby Tertiary units. Unit also locally includes clasts of volcaniclastic sandstone and other lithologies typically associated with Planet Volcanics. In the Tunnel Peak area, includes slabs of quartz-feldspar-biotite schist cut by quartz veins, and lenses of variably shattered quartz-feldspar porphyry (Planet Volcanics).

Tbxs SEDIMENTARY BRECCIA, MESOZOIC SEDIMENTARY PROTOLITH (MIDDLE MIOCENE[?] TO UPPER OLIGOCENE[?]) -- Sedimentary breccia derived from Vampire and Buckskin Formations. Occurs along flanks of Bill Williams River in north-central map area where unit includes monolithologic and polylithologic breccia and mudflow-type sedimentary breccia.

Tbxq SEDIMENTARY BRECCIA, QUARTZITE PROTOLITH (MIDDLE MIOCENE[?] TO UPPER OLIGOCENE[?]) -- Protolith consists of Jurassic(?) Vampire Formation at mouth of Mineral Wash or Permian Coconino Sandstone south of Tunnel Peak.

Tbxc SEDIMENTARY BRECCIA, PALEOZOIC

CARBONATE PROTOLITH (MIDDLE MIOCENE[?] TO UPPER OLIGOCENE[?]) -- Protolith consists of light- to medium-brown or gray calcite or dolomite marble, locally with dark-brown siliceous stringers and knots. Locally includes thinly bedded to laminated calcareous siltstone and sandstone. Clast size is highly variable and includes moderately shattered, but well-cemented, blocks as long as several tens of meters.

Tbxp SEDIMENTARY BRECCIA, UNDIVIDED PALEOZOIC PROTOLITH (MIDDLE MIOCENE[?] TO UPPER OLIGOCENE[?]) -- Adjacent to Mineral Wash fault near upper Mineral Wash, where protolith includes Paleozoic carbonate rocks, Coconino Sandstone, and Supai Formation.

Jp PLANET VOLCANICS (JURASSIC) -- Highly cleaved to schistose, quartz-feldspar-muscovite-magnetite-bearing, silicic to intermediate volcanic and metavolcanic rocks. Most outcrops are homogeneous in composition over several tens of meters and are light to medium gray, silvery gray, and greenish gray, with a local slight reddish tint. Some outcrops, especially near base of unit, are strongly mylonitic with ribbon quartz and a well-developed, variably trending lineation. Many outcrops include quartz-feldspar-bearing, metamorphosed volcaniclastic sandstone. Other local lithologies are chloritic schist and weakly foliated, blocky, reddish-weathering variety with quartz and feldspar phenocrysts 1 to 6 mm in diameter. The entire assemblage of rocks represent variably deformed and metamorphosed, rhyodacitic to rhyolitic ash-flow tuffs, volcaniclastic sediments, and possible hypabyssal intrusions. In the northwestern part of the map area, the volcanic and metavolcanic rocks are in tight, unbrecciated, foliation-parallel contact with intercollated quartzite layers and lenses.

Jv VAMPIRE FORMATION (JURASSIC[?]) -- White to light-gray, well- to moderately sorted quartzite; slightly feldspathic quartzite; quartz-feldspar-muscovite schistose metasandstone; pebbly to gritty conglomeratic sandstone; and pebble to cobble conglomerate. Unit weathers light tan to dark brown or gray, with widespread orangish, yellowish, and reddish iron-oxide stain. Quartzite is typically medium grained and moderately sorted, but conglomeratic sandstone and conglomerate are poorly sorted and locally very feldspathic and muscovitic, in part reflecting a volcaniclastic component. Some volcaniclastic sandstones contain several percent opaque minerals (magnetite?). Cobbles are primarily of quartzite and quartzose sandstone with less common clasts of (1) poorly to well-sorted Mesozoic sandstone, siltstone, phyllite, and rare quartz-pebble conglomerate; (2) fine- to medium-grained granite; (3) light-gray to cream-colored, quartz- and feldspar-phenocrystic, foliated silicic volcanic, volcaniclastic, and metavolcanic rocks; and (4) fine-grained, quartz-feldspar phenocrystic felsite. Cobble to pebble conglomerate at base. Well-sorted orthoquartzite locally contains randomly distributed, spheroidal siliceous concretions 4 to 7 mm in diameter. Overlies Buckskin Formation with slight to moderate angular unconformity. This unit is considered to be Jurassic(?) in age based on tentative correlation with Jurassic Navajo Sandstone of the Colorado Plateau.

Mzbu BUCKSKIN FORMATION, UPPER MEMBER (JURASSIC OR TRIASSIC) -- Fine- to locally medium-grained, locally calcareous quartzite. Generally massive to poorly bedded, dark-brown to black weathering. Quartz-sericite schist weathers light or medium gray and was presumably derived from silty, medium- to fine-grained quartzite. Calc-silicate is light to dark green on fresh surfaces and dark-brown to black weathering, and is inferred to have been derived from siltstone, silty sandstone, and fine-grained sandstone, all variably calcareous. Calc-silicate locally forms resistant beds in less resistant quartz-sericite schist. Unit forms resistant, dark-colored ridges and cliffs.

Mzbp BUCKSKIN FORMATION, PHYLLITE MEMBER (JURASSIC OR TRIASSIC) -- Phyllite, phyllitic sandstone, and sandstone. Phyllite is medium to light gray to medium silvery gray. Also occur as beds and laminations in phyllitic sandstone and sandstone. Grades into phyllitic sandstone which is light to medium gray to greenish gray with fine to coarse, dominantly quartz sand. Sandstone is typically micaceous and foliated and in places is calcareous, as indicated by green calc-silicate minerals such as epidote. Rounded quartzite pebbles and cobbles locally occur in basal 1 to 4 m of micaceous quartz sandstone. Unit is slope forming and rests with sharp conformable contact on underlying quartzite member.

Mzbq BUCKSKIN FORMATION, QUARTZITE MEMBER (JURASSIC OR TRIASSIC) -- Medium-brown to chocolate-brown weathering, resistant, massive to very poorly bedded, light-gray fine-grained quartzite.

Mzbl BUCKSKIN FORMATION, LOWER MEMBER (JURASSIC OR TRIASSIC) -- Quartzite, silty quartzite, sandy phyllite, phyllite, variably calcareous sandstone and siltstone, and local calc-silicate. Quartzite is dark gray and medium to fine grained, weathers medium brown to choc-

olate brown, and is more resistant to weathering than adjacent fine-grained silty sandstone and sandy phyllite. Impure sandstone and silty sandstone are commonly medium to light brown to orangish brown or tan, are variably calcareous, and form beds 1 to 100 cm thick. Quartzite and impure sandstone grade through silty quartzite and sandy phyllite to phyllite. More phyllitic varieties are typically gray to dark-gray or brown weathering, more strongly foliated and cleaved, and less resistant to weathering. Local green-weathering calcareous siltstone grades into fine-grained silty sandstone. Unit contains crudely coarsening-upward packages several to several tens of meters thick: phyllite and phyllitic sandstone grade upward into coarser and less phyllitic sandstone; resistant chocolate-brown quartzite or tan to brown, variably calcareous sandstone forms top of package; sharp contact separates latter from phyllite or phyllitic sandstone of overlying package.

Mzu METAVOLCANIC AND METASEDIMENTARY ROCKS, UNDIVIDED, OF THE SQUAW PEAK KLIPPE (MESOZOIC) -- Foliated, gray to greenish-gray phyllite, quartzofeldspathic schist, and quartz-muscovite-chlorite schist derived from siltstone, sandstone, and conglomerate, probably partly of volcaniclastic derivation. Also includes metavolcanic rocks with biotite as large as 4 mm in diameter and feldspar as large as 6 mm in diameter. Conglomerate contains stretched, moderately to well-rounded cobbles and pebbles up to 20 cm in diameter of medium- to coarse-grained quartzite in a matrix of gritty, moderately sorted sandstone with 10% metamorphic muscovite (derived from feldspar?). Schist is kink folded near sharp fault contact with overlying Paleozoic carbonate rocks. Includes local conglomerate with elongate, stretched, subrounded quartzite clasts up to 20 cm in diameter within schist matrix.

Mzg GRANITIC ROCKS, UNDIVIDED (MESOZOIC[?]) -- Porphyritic leucocratic granitoid that intrudes Buckskin Formation west of Planet mine. Fracture foliation within intrusives is parallel to foliation in host metasedimentary rocks, which indicates intrusion prior to deformation. Mafic minerals in this unit have been destroyed by alteration.

Pk KAIBAB FORMATION (PERMIAN) -- Tan and brownish-tan, massive to weakly foliated and bedded, dolomitic marble and dolomitic calcite marble and gray to tan, massive to thinly foliated calcite marble, with local brown-weathering siliceous layers derived from chert. Siliceous layers locally outline isoclinal folds with axial surfaces parallel to foliation, which indicates that bedding has been locally transposed. Foliation is also locally strongly folded. Top of unit includes 2 m of quartzose sandstone.

Pc COCONINO SANDSTONE (PERMIAN) -- Well-sorted, fine-grained vitreous quartzite that weathers tan, pinkish gray, and brown.

ℙs SUPAI GROUP (PERMIAN AND PENNSYLVANIAN) -- Well-sorted, fine- to medium-grained, quartzite and calcareous siliciclastic rocks that are greenish gray on fresh surfaces and tan to brown weathering. Unit is commonly medium bedded to thinly foliated, with ledge-forming quartzite alternating with slope-forming calcareous units.

MDu MARTIN AND REDWALL FORMATIONS, UNDIVIDED (MISSISSIPPIAN AND DEVONIAN) -- Tan and brown dolomite marble and dolomitic calcite marble (mostly Martin Formation) and cream-colored to light-gray, tan, or brownish-gray calcite marble with local chert and pinkish to purplish tints (Redwall Formation).

Pzc CALCAREOUS SEDIMENTARY ROCKS, UNDIVIDED (PALEOZOIC) -- At Squaw Peak, includes light-gray calcite marble grading into irregular areas of tan and brown dolomitic marble. Light- to dark-brown siliceous bands and stringers (chert?) are several centimeters to perhaps 30 cm thick. At other nearby klippen, unit includes brown to gray, massive calcite marble with local, brown, siliceous-carbonate thin beds and laminations and dark-brown siliceous stringers that locally define rootless isoclinal folds. Locally includes calcareous siliciclastic rocks (Supai Group) and vitreous quartzite (Coconino Formation). Along detachment fault, carbonate and quartzite are commonly brecciated with an unbrecciated matrix of darker brown (replacement) carbonate (unit Tc) that is locally vuggy and is veined with a network of siliceous selvages. Contact between this replacement carbonate and foliated Paleozoic marble and quartzite is locally gradational.

Pzu SEDIMENTARY ROCKS, UNDIVIDED (PALEOZOIC) -- Calcareous and dolomitic marble, with or without siliceous stringers, and quartzite and calc-silicate, representative of the Paleozoic units described above.

JXg GRANITIC ROCKS, UNDIVIDED (JURASSIC OR PROTEROZOIC) -- Sheared fault slivers of unit are present on west side of Squaw Peak, west of Mineral Hill, and in northwest corner of map area. At Squaw Peak, unit consists of foliated porphyritic granite with K-feldspar phenocrysts as long as 1.5 cm and local ribbon quartz.

Foliated granite locally contains dikes(?) of finer grained, quartzofeldspathic rock, probably aplitic granite. Foliated granite is commonly shattered, but is locally in tight, tectonized (Mesozoic fault) contact with overlying Paleozoic units; contact is subconcordant with foliation in adjacent rocks.

LOWER-PLATE UNITS

Ti INTERMEDIATE TO MAFIC INTRUSIVE (MIDDLE MIOCENE[?] TO UPPER OLIGOCENE[?]) -- Homogeneous, dark-gray, fine-grained dioritic(?) intrusive. Mylonitic foliation is variably developed, but is generally weaker than in older host crystalline rocks. Foliation and lineation are locally very weak to almost nonexistent. Contains concordant screens of host foliated granitic and gneissic rocks, including strongly mylonitic gneiss. Locally, contact with host rock is low-angle fault marked by chloritic and hematitic breccia and microbreccia(?). Generally has a sill-like form.

mc MYLONITIC CRYSTALLINE ROCKS (CENOZOIC TO PROTEROZOIC) -- Granitic and high-grade metamorphic rocks generally overprinted by a gently dipping mylonitic foliation with an ENE-trending stretching lineation and top-to-the-northeast sense of shear, as indicated by *S-C* fabrics and asymmetric feldspar porphyroclasts. Various foliated granitic rocks have probable protolith ages of Proterozoic or Mesozoic, and possibly Tertiary. Amphibolite-grade gneissic rocks have probable Proterozoic protoliths and locally preserved, nonmylonitic gneissic foliation that is cut by mylonitic fabric. Sheets of calc-silicate rocks, quartzite, and tan-brown-weathering dolomitic marble as thick as 3 m are locally interlayered with pegmatitic high-grade gneiss, but lack such pegmatitic segregations. Dolomitic marble south of Planet Peak contains intrafolial rootless isoclines of fine-grained quartzite(?) or recrystallized chert(?). Directly below detachment fault, lower-plate rocks have been overprinted by brecciation and chlorite-epidote alteration and converted into chloritic breccia and silicified microbreccia.

References Cited

Anderson, C.A., Scholz, E.A., and Strobell, J.D., Jr., 1955, Geology and ore deposits of the Bagdad area, Yavapai County, Arizona: U.S. Geological Survey Professional Paper 278, 103 p.

Anderson, J.L., Barth, A.P., and Young, E.D., 1988, Mid-crustal roots of Cordilleran metamorphic core complexes: Geology, v. 16, p. 366-369.

Anderson, R.E., 1971, Thin skin distension in Tertiary rocks of southeastern Nevada: Geological Society of America Bulletin, v. 82, p. 43-58.

Armstrong, R.L., 1968, Mantled gneiss domes in the Albion Range, southern Idaho: Geological Society of America Bulletin, v. 79, p. 1295-1314.

____ 1972, Low-angle (denudation) faults, hinterland of the Sevier orogenic belt, eastern Nevada and western Utah: Geological Society of America Bulletin, v. 83, p. 1729-1754.

Armstrong, R.L., and Hansen, Edward, 1966, Cordilleran infrastructure in the eastern Great Basin: American Journal of Science, v. 264, p. 112-127.

Armstrong, R.L., Speed, R.C., Graustein, W.C., and Young, A.Y., 1976, K-Ar dates from Arizona, Montana, Nevada, Utah, and Wyoming: Isochron/West, no. 16, p. 1-6.

Bancroft, Howland, 1911, Reconnaissance of the ore deposits in northern Yuma County, Arizona: U.S. Geological Survey Bulletin 451, 130 p.

Beane, R.E., Wilkins, Joe, Jr., and Heidrick, T.L., 1986, A geochemical model for gold mineralization in the detachment fault environment, *in* Beatty, Barbara, and Wilkinson, P.A.K., eds., Frontiers in geology and ore deposits of Arizona and the Southwest: Arizona Geological Society Digest, v. 16, p. 222.

Bell, T.H., 1978, Progressive deformation and reorientation of fold axes in a ductile mylonite zone: The Woodroffe thrust: Tectonophysics, v. 44, p. 285-320.

Best, M.G., and Brimhall, W.H., 1974, Late Cenozoic alkalic basaltic magmas in the western Colorado Plateaus and the Basin and Range transition zone, U.S.A., and their bearing on mantle dynamics: Geological Society of America Bulletin, v. 85, p. 1677-1690.

Blacet, P.M., 1972, Massive Miocene gravity(?) faults in Arizona: U.S. Geological Survey Progress Report for 1972, p. A43-A44.

Blanchard, R.C., 1913, The geology of the western Buckskin Mountains, Yuma County, Arizona: New York, Columbia University, unpublished Ph.D. dissertation, 80 p.

Bohannon, R.G., 1984, Nonmarine sedimentary rocks of Tertiary age in the Lake Mead region, southeastern Nevada and northwestern Arizona: U.S. Geological Survey Professional Paper 1259, 72 p.

Brace, W.F., and Kohlstedt, D.L., 1980, Limits on lithospheric stress imposed by laboratory experiments: Journal of Geophysical Research, v. 85, p. 6248-6252.

Briscoe, J.A., 1967, General geology of the Picacho Peak area: Tucson, University of Arizona, unpublished M.S. thesis, 52 p.

Brooks, W.E., 1985, Analyses of upper-plate volcanic rocks at Picacho Peak, Pinal County, Arizona: U.S. Geological Survey Open-File Report 85-740, 5 p.

____ 1986, Distribution of anomalously high K_2O volcanic rocks in Arizona: Metasomatism at the Picacho Peak detachment fault: Geology, v. 14, p. 339-342.

____ 1988, Recognition and geologic implications of potassium metasomatism in upper-plate volcanic rocks at the detachment fault at the Harcuvar Mountains, Yavapai County, Arizona: U.S. Geological Survey Open-File Report 88-17, 9 p.

Brooks, W.E., and Marvin, R.F., 1985, Discordant isotopic ages and potassium metasomatism in volcanic rocks from Yavapai County, Arizona [abs.]: Geological Society of America Abstracts with Programs, v. 17, p. 344.

Bryant, Bruce, 1988, Geologic map of the Poachie Range, Yavapai and Mohave Counties, Arizona: U.S. Geological Survey Open-File Report 88-390, scale 1:50,000.

Bryant, Bruce, and Naeser, C.W., 1987, Fission-track dating across the transition between the Basin and Range Province and the Colorado Plateau, west-central Arizona [abs.]: Geological Society of America Abstracts with Programs, v. 19, p. 604.

____ 1988, Laramide events in the Colorado Plateau transition zone and the adjacent part of the Basin and Range, west-central Arizona [abs.]: Geological Society of America Abstracts with Programs, v. 20, no. 3, p. 146.

Burchfiel, B.C., 1966, Tin Mountain landslide, southeastern California, and the origin of megabreccia: Geological Society of America Bulletin, v. 77, p. 95-100.

Burchfiel, B.C., and Davis, G.A., 1971, Clark Mountain thrust complex in the Cordillera of southeastern California: Geologic summary and field trip guide: University of California at Riverside Museum Contributions, v. 1, Field Trip no. 1, p. 1-28.

____ 1972, Structural framework and evolution of the southern part of the Cordilleran orogen, western United States: American Journal of Science, v. 272, p. 97-118.

____ 1975, Nature and controls of Cordilleran orogenesis, western United States: Extensions of an earlier synthesis: American Journal of Science, v. 275-A, p. 363-396.

Calzia, J.P., and Morton, J.L., 1980, Compilation of

in Spencer, J.E., and Reynolds, S.J., eds., 1989, Geology and mineral resources of the Buckskin and Rawhide Mountains, west-central Arizona: Arizona Geological Survey Bulletin 198, p. 270-279.

isotopic ages within the Needles 1° by 2° quadrangle, California and Arizona: U.S. Geological Survey Open-File Report 80-1303, scale 1:250,000.

Cameron, T.E., and Frost, E.G., 1981, Regional development of major antiforms and synforms coincident with detachment faulting in California, Arizona, Nevada, and Sonora [abs.]: Geological Society of America Abstracts with Programs, v. 13, p. 421-422.

Capps, R.C., Reynolds, S.J., Kortemeier, C.P., Stimac, J.A., Scott, E.A., and Allen, G.B., 1985, Preliminary geologic maps of the eastern Bighorn and Belmont Mountains, west-central Arizona: Arizona Bureau of Geology and Mineral Technology Open-File Report 85-14, 25 p., scale 1:24,000, 2 sheets.

Carr, W.J., and Dickey, D.D., 1977, Cenozoic tectonics of eastern Mojave Desert, *in* U.S. Geological Survey Research 1976: U.S. Geological Survey Professional Paper 1000, p. 75.

____ 1980, Geologic map of the Vidal, California, and Parker SW, California-Arizona quadrangles: U.S. Geological Survey Miscellaneous Investigations Series Map I-1125, scale 1:24,000.

Carter, N.L., Christie, J.M., and Griggs, D.T., 1964, Experimental deformation and recrystallization of quartz: Journal of Geology, v. 72, p. 687-733.

Cebull, S.E., 1970, Bedrock geology and orogenic succession in southern Grant Range, Nye County, Nevada: American Association of Petroleum Geologists Bulletin, v. 54, p. 1828-1842.

Chapin, C.E., and Glazner, A.F., 1983, Widespread K_2O metasomatism of Cenozoic volcanic and sedimentary rocks in the southwestern United States [abs.]: Geological Society of America Abstracts with Programs, v. 15, p. 282.

Chapin, C.E., and Lindley, J.I., 1986, Potassium metasomatism of igneous and sedimentary rocks in detachment terranes and other sedimentary basins: Economic implications, *in* Beatty, Barbara, and Wilkinson, P.A.K., eds., Frontiers in geology and ore deposits of Arizona and the Southwest: Arizona Geological Society Digest, v. 16, p. 118-126.

Christie, J.M., 1960, Mylonitic rocks of the Moine thrust zone in the Assynt region, northwest Scotland: Geological Society of Edinburgh Transactions, v. 18, p. 79-93.

Clayton, R.N., and Mayeda, T.K., 1963, The use of bromine pentafluoride in the extraction of oxygen from oxides and silicates for isotopic analysis: Geochimica et Cosmochimica Acta, v. 27, p. 43-52.

Coney, P.J., 1974, Structural analysis of the Snake Range "decollement," east-central Nevada: Geological Society of America Bulletin, v. 85, p. 973-978.

____ 1980, Cordilleran metamorphic core complexes: An overview, *in* Crittenden, M.D., Jr., and others, eds., Cordilleran metamorphic core complexes: Geological Society of America Memoir 153, p. 7-31.

Conway, C.M., Connelly, T.J., and Robison, L.C., 1986, An early Proterozoic volcanic-hydrothermal-exhalative system at Bagdad, Arizona, *in* Beatty, Barbara, and Wilkinson, P.A.K., eds., Frontiers in geology and ore deposits of Arizona and the Southwest: Arizona Geological Society Digest, v. 16, p. 24-34.

Cooper, J.R., 1960, Some geologic features of the Pima mining district, Pima County, Arizona: U.S. Geological Survey Bulletin 1112-C, 103 p.

Cooper, J.R., and Silver, L.T., 1964, Geology and ore deposits of the Dragoon quadrangle, Cochise County, Arizona: U.S. Geological Survey Professional Paper 416, 196 p.

Coplen, T.B., Kendall, C., and Hopple, J., 1983, Comparison of stable isotope reference samples: Nature, v. 360, p. 236-238.

Corbitt, L.L., and Woodward, L.A., 1973, Tectonic framework of Cordilleran foldbelt in southwestern New Mexico: American Association of Petroleum Geologists Bulletin, v. 57, p. 2207-2216.

Costa, U.R., Barnett, R.L., and Kerrich, R., 1983, The Mattagami Lake mine Archean Zn-Cu sulphide deposit, Quebec: Hydrothermal coprecipitation of talc and sulphides in a sea floor brine pool--Evidence from geochemistry, $^{18}O/^{16}O$, and mineral chemistry: Economic Geology, v. 78, p. 1144-1203.

Cox, Allan, and Dalrymple, G.B., 1967, Statistical analysis of geomagnetic reversal data and the precision of potassium-argon dating: Journal of Geophysical Research, v. 72, p. 2603-2614.

Crittenden, M.D., Jr., Coney, P.J., and Davis, G.H., eds., 1980, Cordilleran metamorphic core complexes: Geological Society of America Memoir 153, 490 p.

Cummings, J.B., 1946, Exploration of New Planet iron deposit, Yuma County, Ariz.: U.S. Bureau of Mines Report of Investigations 3982, 37 p.

Darton, N.H., 1925, A resume of Arizona geology: Arizona Bureau of Mines Bulletin 119, 298 p.

Davis, G.A., 1988, Rapid upward transport of mid-crustal mylonitic gneisses in the footwall of a Miocene detachment fault, Whipple Mountains, southeastern California: Geologische Rundschau, v. 77/1, p. 191-209.

Davis, G.A., Anderson, J.L., and DeWitt, Ed, 1987, Rapid Miocene tectonic uplift of mid-crustal mylonitic rocks, Whipple Mountains, southeastern California [abs.]: Geological Society of America Abstracts with Programs, v. 19, p. 636.

Davis, G.A., Anderson, J.L., Frost, E.G., and Shackelford, T.J., 1980, Mylonitization and detachment faulting in the Whipple-Buckskin-Rawhide Mountains terrane, southeastern California and western Arizona, *in* Crittenden, M.D., Jr., and others, eds., Cordilleran metamorphic core complexes: Geological Society of America Memoir 153, p. 79-129.

Davis, G.A., Anderson, J.L., Martin, D.L., Krummenacher, Daniel, Frost, E.G., and Armstrong, R.L., 1982, Geologic and geochronologic relations in the lower plate of the Whipple detachment fault, Whipple Mountains, southeastern California: A progress report, *in* Frost, E.G., and Martin, D.L., eds., Mesozoic-Cenozoic tectonic evolution of the Colorado River region, California, Arizona, and Nevada: San Diego, Cordilleran Publishers, p. 408-432.

Davis, G.A., and Lister, G.S., 1988, Detachment faulting in continental extension: Perspectives from the southwestern U.S. Cordillera, *in* Clark, S.P., Jr., and others, eds., Processes in continental lithospheric deformation: Geological Society of America Special Paper 218, p. 133-160.

Davis, G.A., Lister, G.S., and Reynolds, S.J., 1986, Structural evolution of the Whipple and South Mountains shear zones, southwestern United States: Geology, v. 14, p. 7-10.

Davis, G.H., 1975, Gravity-induced folding off a gneiss dome complex, Rincon Mountains, Arizona: Geological Society of America Bulletin, v. 86, p. 979-990.

_____ 1980, Structural characteristics of metamorphic core complexes, southern Arizona, *in* Crittenden, M.D., Jr., and others, eds., Cordilleran metamorphic core complexes: Geological Society of America Memoir 153, p. 35-77.

_____ 1983, Shear-zone model for the origin of metamorphic core complexes: Geology, v. 11, p. 342-347.

Davis, G.H., Anderson, P., Budden, R.T., Keith, S.B., and Kiven, C.W., 1975, Origin of lineation in the Catalina-Rincon-Tortolita gneiss complex, Arizona [abs.]: Geological Society of America Abstracts with Programs, v. 7, p. 602.

Davis, G.H., and Coney, P.J., 1979, Geological development of the Cordilleran metamorphic core complexes: Geology, v. 7, p. 120-124.

DeWitt, Ed, Sutter, J.F., Davis, G.A., and Anderson, J.L., 1986, $^{40}Ar/^{39}Ar$ age-spectrum dating of Miocene mylonitic rocks, Whipple Mountains, southeastern California [abs.]: Geological Society of America Abstracts with Programs, v. 18, p. 584.

Dokka, R.K., 1986, Patterns and modes of early Miocene crustal extension, central Mojave Desert, California, *in* Mayer, Larry, ed., Extensional tectonics of the southwestern United States: A perspective on processes and kinematics: Geological Society of America Special Paper 208, p. 75-96.

Dokka, R.K., McCurry, Michael, Woodburne, M.O., Frost, E.G., and Okaya, D.A., 1988, A field guide to the Cenozoic crustal structure of the Mojave Desert, *in* Weide, D.L., and Faber, M.L., eds., This extended land, geological journeys in the southern Basin and Range: Geological Society of America Annual Meeting, Cordilleran Section, 84th, Las Vegas, Nev., 1988, Field Trip Guidebook, p. 21-44.

Donath, F.A., and Parker, D.B., 1964, Folds and folding: Geological Society of America Bulletin, v. 75, p. 45-62.

Drewes, Harald, 1971, Mesozoic stratigraphy of the Santa Rita Mountains, southeast of Tucson, Arizona: U.S. Geological Survey Professional Paper 658-C, 81 p.

Durning, W.P., and Hillemeyer, F.L., 1986, Colosseum-Morning Star-Roadside-Copperstone: Precious metal deposits of southern California and western Arizona, *in* Beatty, Barbara, and Wilkinson, P.A.K., eds., Frontiers in geology and ore deposits of Arizona and the Southwest: Arizona Geological Society Digest, v. 16, p. 248-266.

Eberly, L.D., and Stanley, T.B., Jr., 1978, Cenozoic stratigraphy and geologic history of southwestern Arizona: Geological Society of America Bulletin, v. 89, p. 921-940.

Eichelberger, J.C., 1975, Origin of andesite and dacite: Evidence of mixing at Glass Mountain in California and at other circum-Pacific volcanoes: Geological Society of America Bulletin, v. 86, p. 1381-1391.

_____ 1980, Vesiculation of mafic magma during replenishment of silicic magma reservoirs: Nature, v. 288, p. 446-450.

Ellis, M.J., 1982, Structural analysis of the Big Maria Mountains, Riverside County, California, *in* Frost, E.G., and Martin, D.L., Mesozoic-Cenozoic tectonic evolution of the Colorado River region, California, Arizona, and Nevada: San Diego, Cordilleran Publishers, p. 222-234.

Fernandez, H.E., 1965, Geology of Pride and New Standard mine area, northwestern Yuma County, Arizona: Rolla, University of Missouri, unpublished M.S. thesis, 88 p.

Fitton, J.G., and James, D., 1986, Basic volcanism associated with intraplate linear features: Philosophical Transactions of the Royal Society of London, v. A 317, 253-266.

Fleck, R.J., 1970, Age and tectonic significance of volcanic rocks, Death Valley area, California: Geological Society of America Bulletin, v. 81, p. 2807-2815.

Floyd, P.A., and Winchester, J.A., 1978, Identification and discrimination of altered and metamorphosed rocks using immobile elements: Chemical Geology, v. 21, p. 291-306.

Frost, E.G., 1981a, Mid-Tertiary detachment faulting in the Whipple Mtns., Calif., and Buckskin Mtns., Ariz., and its relationship to the development of major antiforms and synforms [abs.]: Geological Society of America Abstracts with Programs, v. 13, p. 57.

_____ 1981b, Structural style of detachment faulting in the Whipple Mountains, California and Buckskin Mountains, Arizona: Arizona Geological Society Digest, v. 13, p. 25-29.

_____ 1983, Structural geology of a portion of the Whipple-Buckskin detachment terrane, southeastern California and western Arizona: Los Angeles, University of Southern California, unpublished Ph.D. dissertation, 333 p.

Frost, E.G., and Martin, D.L., 1982, Comparison of Mesozoic compressional tectonics with mid-Tertiary detachment faulting in the Colorado River area, California, Arizona, and Nevada, *in* Cooper, J.D., comp., Geologic excursions in the California desert: Geological Society of America Annual Meeting, Cordilleran Section, 78th, Anaheim, Calif., 1982, Field Trip Guidebook, p. 113-159.

Frost, E.G., and nine others, 1987, Crustal transect: Colorado Plateau -- detachment terrane -- Salton trough: Arizona Bureau of Geology and Mineral Technology Special Paper 5, p. 398-422.

Frost, E.G., and Okaya, D.A., 1986, Application of seismic reflection profiles to tectonic analysis in mineral

exploration, *in* Beatty, Barbara, and Wilkinson, P.A.K., eds., Frontiers in geology and ore deposits of Arizona and the Southwest: Arizona Geological Society Digest, v. 16, p. 137-152.

Fryxell, J.E., Richard, S.M., Sutter, J.F., and Lucchitta, I., 1987a, Contrasting $^{40}Ar/^{39}Ar$ thermochronology of minerals from lower plate rocks of the Buckskin-Bullard-Eagle Eye detachment fault system, west-central Arizona [abs.]: Geological Society of America Abstracts with Programs, v. 19, p. 670.

Fryxell, J.E., Stimac, J.A., and Reynolds, S.J., 1987b, Superimposed domino-style normal faults in a Tertiary bi-modal volcanic complex, Wickenburg Mountains and vicinity, central Arizona [abs.]: Geological Society of America Abstracts with Programs, v. 19, p. 670.

Fugro, Inc., 1975, Geotechnical investigations, Parker Valley alternate site, Sun Desert Nuclear Project: San Diego Gas and Electric Company, Section 2.5, p. 53-63.

Garrels, R.M., and Dreyer, R.M., 1952, Mechanism of limestone replacement at low temperature: Geological Society of America Bulletin, v. 63, p. 325-380.

Gassaway, J.S., 1972, Geology of the Lincoln Ranch basin, Buckskin Mountains, Yuma County, Arizona: San Diego, San Diego State University, unpublished undergraduate thesis, 64 p.

_____ 1973, Late Tertiary sediments in the Lincoln Ranch basin, Buckskin Mountains, Yuma County, Arizona [abs.]: Geological Society of America Abstracts with Programs, v. 5, p. 47.

Gibbs, A., 1987, Hangingwall geometry of normal faults, *in* Extended abstracts - Applied extension tectonics: Bureau of Mineral Resources Research Symposium, 16th, Canberra, Australia, 1987, p. 80-86.

Halfkenny, R.D., Jr., 1985, Thermal, mechanical, chemical and fluid regimes associated with detachment zones in the Buckskin Mountain metamorphic core complex, Arizona: Petrographic, chemical and isotopic considerations: London, Ontario, University of Western Ontario, unpublished HBSc thesis, 430 p.

Hamblin, W.K., 1965, Origin of "reverse drag" on the downthrown side of normal faults: Geological Society of America Bulletin, v. 76, p. 1145- 1163.

Hamilton, Warren, 1964, Geologic map of the Big Maria Mountains NE quadrangle, Riverside County, California, and Yuma County, Arizona: U.S. Geological Survey Geologic Quadrangle Map GQ-350, scale 1:24,000.

_____ 1971, Tectonic framework of southeastern California [abs.]: Geological Society of America Abstracts with Programs, v. 3, p. 130-131.

_____ 1982, Structural evolution of the Big Maria Mountains, northeastern Riverside County, southeastern California, *in* Frost, E.G., and Martin, D.L., eds., Mesozoic-Cenozoic tectonic evolution of the Colorado River region, California, Arizona, and Nevada: San Diego, Cordilleran Publishers, p. 1-27.

_____ 1987, Mesozoic geology and tectonics of the Big Maria Mountains region, southeastern California, *in* Dickinson, W.R., and Klute, M.A., eds., Mesozoic rocks of southern Arizona and adjacent areas: Arizona Geological Society Digest, v. 18, p. 33-47.

_____ 1988, Extensional faulting in the Death Valley region [abs.]: Geological Society of America Abstracts with Programs, v. 20, p. 165-166.

Hansen, Edward, 1971, Strain facies: New York, Springer-Verlag, New York, 207 p.

Harding, L.E., and Coney, P.J., 1985, The geology of the McCoy Mountains Formation, southeastern California and southwestern Arizona: Geological Society of America Bulletin, v. 96, p. 755-769.

Harrer, C.M., 1964, Reconnaissance of iron resources in Arizona: U.S. Bureau of Mines Information Circular 8236, 204 p.

Harrison, T.M., Duncan, Ian, and McDougall, Ian, 1985, Diffusion of ^{40}Ar in biotite: Temperature, pressure, and compositional effects: Geochimica et Cosmochimica Acta, v. 49, p. 2461-2468.

Hauser, E.C., Gephart, J., Latham, T., Oliver, J., Kaufman, S., Brown, L., and Lucchitta, I., 1987, COCORP Arizona transect: Strong crustal reflections and offset Moho beneath the transition zone: Geology, v. 15, p. 1103-1106.

Heard, H.C., and Carter, N.L., 1968, Experimentally induced "natural" intragranular flow in quartz and quartzite: American Journal of Science, v. 266, p. 1-42.

Hewett, D.F., 1956, Geology and mineral resources of the Ivanpah quadrangle, California and Nevada: U.S. Geological Survey Professional Paper 275, 172 p.

_____ 1966, Stratified deposits of the oxides and carbonates of manganese: Economic Geology, v. 61, p. 431-461.

Higgins, M.W., 1971, Cataclastic rocks: U.S. Geological Survey Professional Paper 687, 97 p.

Holt, W.E., Chase, C.G., and Wallace, T.C., 1986, Crustal structure from three-dimensional gravity modeling of a metamorphic core complex: A model for uplift, Santa Catalina-Rincon Mountains, Arizona: Geology, v. 14, p. 927-930.

Howard, K.A., 1986, PACE - the Pacific to Arizona crustal experiment [abs.]: Geological Society of America Abstracts with Programs, v. 18, p. 362.

Howard, K.A., Goodge, J.W., and John, B.E., 1982a, Detached crystalline rocks in the Mohave, Buck, and Bill Williams Mountains, western Arizona, *in* Frost, E.G., and Martin, D.L., eds., Mesozoic-Cenozoic tectonic evolution of the Colorado River region, California, Arizona, and Nevada: San Diego, Cordilleran Publishers, p. 377-392.

Howard, K.A., and John, B.E., 1987, Crustal extension along a rooted system of imbricate low-angle faults: Colorado River extensional corridor, California and Arizona, *in* Coward, M.P., and others, eds., Continental extensional tectonics: Geological Society of London Special Publication 28, p. 299-311.

Howard, K.A., Stone, Paul, Pernokas, M.A., and Marvin, R.F., 1982b, Geologic and geochronologic reconnaissance of the Turtle Mountains area, California, west

border of the Whipple Mountains detachment terrane, *in* Frost, E.G., and Martin, D.L., eds., Mesozoic-Cenozoic tectonic evolution of the Colorado River region, California, Arizona, and Nevada: San Diego, Cordilleran Publishers, p. 341-354.

Hunt, C.B., and Mabey, D.R., 1966, Stratigraphy and structure, Death Valley, California: U.S. Geological Survey Professional Paper 494-A, 162 p.

Jahn, B.M., Auvray, B., Blais, S., Capdevila, R., Vidal, F., and Hameurt, J., 1980, Trace element geochemistry and petrogenesis of Finnish greenstone belts: Journal of Petrology, v. 21, p. 201-244.

Jemmet, J.P., 1966, Geology of the northern Plomosa Mountain range, Yuma County, Arizona: Tucson, University of Arizona, unpublished Ph.D. dissertation, 128 p.

John, B.E., 1987, Geometry and evolution of a mid-crustal extensional fault system: Chemehuevi Mountains, southeastern California, *in* Coward, M.P., and others, eds., Continental extensional tectonics: Geological Society of London Special Publication 28, p. 313-335.

Johnson, M.R.W., 1967, Mylonite zones and mylonite banding: Nature, v. 213, p. 246-247.

Keith, Stanley B., Gest, D.E., DeWitt, Ed, Woode Toll, Netta, and Everson, B.A., 1983, Metallic mineral districts and production in Arizona: Arizona Bureau of Geology and Mineral Technology Bulletin 194, 58 p.

Keith, Stanton B., 1978, Index of mining properties in Yuma County, Arizona: Arizona Bureau of Geology and Mineral Technology Bulletin 192, 185 p.

Kemnitzer, L.E., 1937, Structural studies in the Whipple Mountains, southeastern California: Pasadena, California Institute of Technology, unpublished Ph.D. dissertation, 150 p.

Kerrich, R., 1983, Geochemistry of gold deposits in the Abitibi greenstone belt: Canadian Institute of Mining and Metallurgy Special Paper 27, 75 p.

Kerrich, R., and Hyndman, D., 1986, Thermal and fluid regimes in the Bitterroot lobe-Sapphire block detachment zone, Montana: Evidence from $^{18}O/^{16}O$ and geologic relations: Geological Society of America Bulletin, v. 97, p. 147-155.

Kerrich, R., and Rehrig, W., 1987, Fluid motion associated with Tertiary mylonitization and detachment faulting: $^{18}O/^{16}O$ evidence from the Picacho metamorphic core complex, Arizona: Geology, v. 15, p. 58-62.

Kerrich, Robert, Rehrig, W., Arima, M., and McLarty, E., 1986, Southwest metamorphic core complexes - upper plate Tertiary potassic mafic volcanics and their hydrothermal metasomatism [abs.]: Geological Society of America Abstracts with Programs, v. 18, p. 124.

Kerrich, R., Rehrig, W.A., and Willmore, L.M., 1984, Deformation and hydrothermal regimes in the Picacho metamorphic core complex detachment--Arizona: Oxygen isotope evidence [abs.]: Eos (American Geophysical Union, Transactions), v. 65, p. 1124.

Kerrich, R., and Watson, G.P., 1984, The Macassa mine Archean lode gold deposit, Kirkland Lake, Ontario: Geology, patterns of alteration, and hydrothermal regimes: Economic Geology, v. 79, p. 1104-1130.

King, P.B., 1969, The tectonics of North America - A discussion to accompany the tectonic map of North America: U.S. Geological Survey Professional Paper 467, 127 p., scale 1:5,000,000.

Kislingbury, George, 1916, Unpublished report on the Swansea mine, Yuma County, Arizona: Arizona Geological Survey mine-file data, 7 p.

Knapp, J.H., 1988, Ductile to brittle structural evolution at Mesquite Mountain, west-central Arizona [abs.]: Geological Society of America Abstracts with Programs, v. 20, p. 173.

Knapp, J.H., and Heizler, M.T., 1988, $^{40}Ar/^{39}Ar$ geochronology of crystalline thrust nappes of the Late Cretaceous Maria fold and thrust belt, west-central Arizona [abs.]: Geological Society of America Abstracts with Programs, v. 20, no. 3, p. 173.

Knipe, R.J., 1982, Interaction of footwall geometry and folds developed during detachment faulting, *in* Frost, E.G., and Martin, D.L., eds., Mesozoic-Cenozoic tectonic evolution of the Colorado River region, California, Arizona, and Nevada: San Diego, Cordilleran Publishers, p. 608.

Krauskopf, K.B., 1957, Separation of manganese from iron in sedimentary processes: Geochimica et Cosmochimica Acta, v. 12, p. 61-84.

Krieger, M.H., 1974, Generalized geology and structure of the Winkelman 15-minute quadrangle and vicinity, Pinal and Gila Counties, Arizona: U.S. Geological Survey Journal of Research, v. 2, p. 311-321.

Kyser, T.K., O'Neil, J.R., and Carmichael, I.S.E., 1982, Genetic relations among basic lavas and ultramafic nodules: Evidence from oxygen isotope compositions: Contributions to Mineralogy and Petrology, v. 81, p. 88-102.

Lanphere, M.A., Wasserburg, G.J.F., Albee, A.L., and Tilton, G.R., 1964, Redistribution of strontium and rubidium isotopes during metamorphism, World Beater complex, Panamint Range, California, *in* Craig, H., and others, eds., Isotopic and cosmic chemistry: Amsterdam, North Holland Publishing Company, p. 269-320.

Lasky, S.G., and Webber, B.N., 1944, Manganese deposits in the Artillery Mountains region, Mohave County, Arizona: U.S. Geological Survey Bulletin 936-R, p. 417-448.

_____ 1949, Manganese resources of the Artillery Mountains region, Mohave County, Arizona: U.S. Geological Survey Bulletin 961, 86 p.

Laubach, S.E., 1986, Polyphase deformation, thrust-induced strain and metamorphism, and Mesozoic stratigraphy of the Granite Wash Mountains, west-central Arizona: Urbana-Champaign, University of Illinois, unpublished Ph.D. dissertation, 191 p.

Lease, L.W., 1981, Summary geologic report on drilling in western Prescott and Williams quadrangles, Mohave, Yavapai, and Yuma Counties, Arizona: U.S. Department of Energy Open-File Report GJBX-293(81),

82 p.
Lee, W.T., 1908, Geologic reconnaissance of a part of western Arizona: U.S. Geological Survey Bulletin 352, 96 p.
Lingrey, S.H., Evans, K.V., and Davis, G.A., 1977, Tertiary denudational faulting, Whipple Mountains, southeastern San Bernardino County, California [abs.]: Geological Society of America Abstracts with Programs, v. 9, p. 454-455.
Lister, G.S., and Snoke, A.W., 1984, *S-C* mylonites: Journal of Structural Geology, v. 6, p. 617-638.
Long, Austin, and Rippeteau, Bruce, 1974, Testing contemporaneity and averaging radiocarbon dates: American Antiquity, v. 39, p. 205-215.
Longwell, C.R., 1945, Low-angle normal faults in the Basin-and-Range province: American Geophysical Union Transactions, v. 26, p. 107-118.
_____ 1951, Megabreccia developed downslope from large faults: American Journal of Science, v. 249, p. 343-355.
Lucchitta, Ivo, and Suneson, Neil, 1981a, Comment *on* Tertiary tectonic denudation of a Mesozoic-early Tertiary(?) gneiss complex, Rawhide Mountains, western Arizona: Geology, v. 9, p. 50-51.
_____ 1981b, On autochthonous upper plates and allochthonous lower plates: Core-complex underthrusting in west-central Arizona [abs.]: Geological Society of America Abstracts with Programs, v. 13, p. 68.
Lyle, J.H., 1982, Interrelationships of late Mesozoic thrust faulting and mid-Tertiary detachment faulting in the Riverside Mountains, southeastern California, *in* Frost, E.G., and Martin, D.L., eds., Mesozoic-Cenozoic tectonic evolution of the Colorado River region, California, Arizona, and Nevada: San Diego, Cordilleran Publishers, p. 470-491.
McCarthy, J., Fuis, G.S., and Wilson, J., 1987, Crustal structure in the region of the Whipple Mountains metamorphic core complex, from seismic refraction results [abs.]: Geological Society of America Abstracts with Programs, v. 19, p. 763.
McCarthy, Jill, and Thompson, G.A., 1988, Seismic imaging of extended crust with emphasis on the western United States: Geological Society of America Bulletin, v. 100, p. 1361-1374.
McCrea, J.M., 1950, The isotopic chemistry of carbonates and a paleotemperature scale: Journal of Chemistry and Physics, v. 18, p. 849.
McNeil, A.M., and Kerrich, R., 1986, Archean lamprophyric dykes and gold mineralization, Matheson, Ontario: The conjunction of LIL-enriched mafic magmas, deep crustal structures and Au concentration: Canadian Journal of Earth Science, v. 23, p. 324-343.
Mahood, G.A., 1981, Chemical evolution of a Pleistocene rhyolitic center: Sierra La Primavera, Jalisco, Mexico: Contributions to Mineralogy and Petrology, v. 77, p. 129-149.
Mahood, Gail, and Hildreth, Wes, 1983, Nested calderas and trapdoor uplift at Pantelleria, Strait of Sicily: Geology, v. 11, p. 722-726.
Marshak, R.S., 1979, A reconnaissance of Mesozoic strata in northern Yuma County, southwestern Arizona: Tucson, University of Arizona, unpublished M.S. thesis, 110 p.
Marshak, Stephen, Vander Muelen, Marc, and Bhagat, Snehal, 1987, Geology of the Battleship Peak area, Buckskin Mountians, La Paz County, Arizona: Arizona Bureau of Geology and Mineral Technology Miscellaneous Map MM-87-B, scale 1:8,000.
Martin, D.L., Krummenacher, Daniel, and Frost, E.G., 1982, K-Ar geochronologic record of Mesozoic and Tertiary tectonics of the Big Maria- Little Maria-Riverside Mountains terrane, *in* Frost, E.G., and Martin, D.L., eds., Mesozoic-Cenozoic tectonic evolution of the Colorado River region, California, Arizona, and Nevada: San Diego, Cordilleran Publishers, p. 518-549.
Marvin, R.F., and Dobson, S.W., 1979, Radiometric ages: Compilation B, U.S. Geological Survey: Isochron/West, no. 26, p. 3-32.
Mauger, R.L., Damon, P.E., and Livingston, D.E., 1968, Cenozoic argon ages on metamorphic rocks from the Basin and Range Province: American Journal of Science, v. 266, p. 579-589.
Miller, F.K., 1970, Geologic map of the Quartzsite quadrangle, Yuma County, Arizona: U.S. Geological Survey Geologic Quadrangle Map GQ-841, 3 p., scale 1:62,500.
Miller, J.M.G., and John, B.E., 1988, Detached strata in a Tertiary low- angle normal fault terrane, southeastern California: A sedimentary record of unroofing, breaching, and continued slip: Geology, v. 16, p. 645-648.
Misch, Peter, 1960, Regional structural reconnaissance in central-northeast Nevada and some adjacent areas: Observations and interpretations, *in* Boettcher, J.W., and Sloan, W.W., Jr., eds., Guidebook to the geology of east-central Nevada: Intermountain Association of Petroleum Geologists, 11th Annual Field Conference Guidebook, p. 17-42.
Misch, P., and Hazzard, J.C., 1962, Stratigraphy and metamorphism of late Precambrian rocks in central northeastern Nevada and adjacent Utah: American Association of Petroleum Geologists Bulletin, v. 46, p. 289-343.
Miyashiro, A., 1972, Metamorphism and metamorphic belts: New York, Halsted Press, 492 p.
Moores, E.M., 1968, Plio-Pleistocene sediments, gravity slides, and their tectonic significance, east-central Nevada: Journal of Geology, v. 76, p. 88-98.
Mouat, M.M., 1962, Manganese oxides from the Artillery Mountains area, Arizona: American Mineralogist, v. 47, p. 744-757.
Munha, J., Fyfe, W.S., and Kerrich, R., 1980, Adularia, the characteristic mineral of felsic spilites: Contributions to Mineralogy and Petrology, v. 75, p. 15-19.
Nakata, J.K., 1982, Preliminary report on diking events in the Mohave Mountains, Arizona, *in* Frost, E.G., and Martin, D.L., eds., Mesozoic- Cenozoic tectonic evolution of the Colorado River region, California,

Arizona, and Nevada: San Diego, Cordilleran Publishers, p. 85-89.

Nelson, R.B., 1966, Structural development of northernmost Snake Range, Kern Mountains, and Deep Creek Range, Nevada-Utah: American Association of Petroleum Geologists Bulletin, v. 50, p. 921-951.

Noble, L.F., 1941, Structural features of the Virgin Spring area, Death Valley, California: Geological Society of America Bulletin, v. 52, p. 941-1000.

Ohmoto, Hiroshi, and Rye, R.O., 1979, Isotopes of sulphur and carbon, *in* Barnes, H.L., ed., Geochemistry of hydrothermal ore deposits (2nd ed.): New York, John Wiley and Sons, p. 509-562.

O'Neil, J.R., and Taylor, H.P., 1967, The oxygen isotope and cation exchange chemistry of feldspars: American Mineralogist, v. 52, p. 1414-1437.

Osborne, G.M., 1981, The structural geology of the Squaw Peak area of the Buckskin Mountains, Yuma County, Arizona: Los Angeles, University of Southern California, unpublished M.S. thesis, 164 p.

Otton, J.K., 1982, Tertiary extensional tectonics and associated volcanism in west-central Arizona, *in* Frost, E.G., and Martin, D.L., eds., Mesozoic-Cenozoic tectonic evolution of the Colorado River region, California, Arizona, and Nevada: San Diego, Cordilleran Publishers, p. 143-157.

Pain, C.F., 1985, Cordilleran metamorphic core complexes in Arizona: A contribution from geomorphology: Geology, v. 13, p. 871-874.

Pearce, J.A., and Cann, J.R., 1973, Tectonic setting of basic volcanic rocks determined using trace element analysis: Earth and Planetary Science Letters, v. 19, p. 290-300.

Ransome, F.L., 1931, Geological reconnaissance of the revised Parker route through the Whipple Mountains: Consulting report to the Metropolitan Water District of Southern California, 10 p.

Rehrig, W.A., 1986, Processes of regional Tertiary extension in the western Cordillera: Insights from the metamorphic core complexes: Geological Society of America Special Paper 208, p. 97-122.

Rehrig, William, Halfkenny, R.D., Jr., and Kerrich, Robert, 1986, Tectonic-economic significance of isotopic and geochemical data from detachment zones of metamorphic core complexes (MCC), southwestern United States [abs.]: Geological Society of America Abstracts with Programs, v. 18, p. 174-175.

Rehrig, W.A., and Reynolds, S.J., 1980, Geologic and geochronologic reconnaissance of a northwest-trending zone of metamorphic core complexes in southern and western Arizona, *in* Crittenden, M.D., Jr., and others, eds., Cordilleran metamorphic core complexes: Geological Society of America Memoir 153, p. 131-157.

Reynolds, M.W., 1974, Geology of the Grapevine Mountains, Death Valley, California: A summary, *in* Guidebook: Death Valley region, California and Nevada: Shoshone, Calif., Death Valley Publishing Company, p. 91-97.

Reynolds, S.J., 1980a, A conceptual basis for the occurrence of uranium in Cordilleran metamorphic core complexes, *in* Coney, P.J., and Reynolds, S.J., eds., Cordilleran metamorphic core complexes and their uranium favorability, *with contributions by* G.H. Davis and others: U.S. Department of Energy Open-File Report GJBX-258(80), p. 187-245.

_____ 1980b, Geologic framework of west-central Arizona, *in* Jenney, J.P., and Stone, Claudia, eds., Studies in western Arizona: Arizona Geological Society Digest, v. 12, p. 1-16.

_____ 1982a, Geology and geochronology of the South Mountains, central Arizona: Tucson, University of Arizona, unpublished Ph.D. dissertation, 220 p.

_____ 1982b, Multiple deformation in the Harcuvar and Harquahala Mountains, west-central Arizona, *in* Frost, E.G., and Martin, D.L., eds., Mesozoic-Cenozoic tectonic evolution of the Colorado River region, California, Arizona, and Nevada: San Diego, Cordilleran Publishers, p. 137-142.

_____ 1985, Geology of the South Mountains, central Arizona: Arizona Bureau of Geology and Mineral Technology Bulletin 195, 61 p.

Reynolds, S.J., Florence, F.P., Welty, J.W., Roddy, M.S., Currier, D.A., Anderson, A.V., and Keith, S.B., 1986a, Compilation of radiometric age determinations in Arizona: Arizona Bureau of Geology and Mineral Technology Bulletin 197, 258 p.

Reynolds, S.J., Keith, S.B., and Coney, P.J., 1980, Stacked overthrusts of Precambrian crystalline basement and inverted Paleozoic sections emplaced over Mesozoic strata, west-central Arizona, *in* Jenney, J.P., and Stone, Claudia, eds., Studies in western Arizona: Arizona Geological Society Digest, v. 12, p. 45-51.

Reynolds, S.J., and Lister, G.S., 1987, Structural aspects of fluid-rock interactions in detachment zones: Geology, v. 15, p. 362-366.

Reynolds, S.J., and Rehrig, W.A., 1980, Mid-Tertiary plutonism and mylonitization, South Mountains, central Arizona, *in* Crittenden, M.D., Jr., and others, eds., Cordilleran metamorphic core complexes: Geological Society of America Memoir 153, p. 159-175.

Reynolds, S.J., Richard, S.M., Haxel, G.M., Tosdal, R.M., and Laubach, S.E., 1988, Geologic setting of Mesozoic and Cenozoic metamorphism in Arizona, *in* Ernst, W.G., ed., Metamorphism and crustal evolution of the conterminous western United States: Englewood Cliffs, N.J., Prentice-Hall, p. 467-501.

Reynolds, S.J., and Spencer, J.E., 1984, Geologic map of the Aguila Ridge- Bullard Peak area, eastern Harcuvar Mountains, west-central Arizona: Arizona Bureau of Geology and Mineral Technology Open-File Report 84-4, 2 p., scale 1:24,000.

_____ 1985, Evidence for large-scale transport on the Bullard detachment fault, west-central Arizona: Geology, v. 13, p. 353-356.

Reynolds, S.J., Spencer, J.E., Asmerom, Yemane, DeWitt, Ed, and Laubach, S.E., 1989, Early Mesozoic uplift in west-central Arizona and southeastern California: Geology, v. 17 (in press).

Reynolds, S.J., Spencer, J.E., and DeWitt, Ed, 1987, Stra-

tigraphy and U-Th-Pb geochronology of Triassic and Jurassic rocks in west-central Arizona, *in* Dickinson, W.R., and Klute, M.A., eds., Mesozoic rocks of southern Arizona and adjacent areas: Arizona Geological Society Digest, v. 18, p. 65-80.

Reynolds, S.J., Spencer, J.E., Richard, S.M., and Laubach, S.E., 1986b, Mesozoic structures in west-central Arizona, *in* Beatty, Barbara, and Wilkinson, P.A.K., eds., Frontiers in geology and ore deposits of Arizona and the Southwest: Arizona Geological Society Digest, v. 16, p. 35-51.

Richard, S.M., 1982, Preliminary report on the structure and stratigraphy of the southern Harquahala Mountains, Yuma County, Arizona, *in* Frost, E.G., and Martin, D.L., eds., Mesozoic-Cenozoic tectonic evolution of the Colorado River region, California, Arizona, and Nevada: San Diego, Cordilleran Publishers, p. 235-242.

Richard, S.M., Fryxell, J.E., Reynolds, S.J., and Grubensky, M.J., 1988, Southeast termination of the Buckskin-Bullard detachment fault, west-central Arizona: One versus many normal faults [abs.]: Geological Society of America Abstracts with Programs, v. 20, p. A382.

Ridenour, James, Moyle, P.R., and Willett, S.L., 1982, Mineral occurrences in the Whipple Mountains Wilderness Study Area, San Bernardino County, California, *in* Frost, E.G., and Martin, D.L., eds., Mesozoic-Cenozoic tectonic evolution of the Colorado River region, California, Arizona, and Nevada: San Diego, Cordilleran Publishers, p. 69-75.

Roddy, M.S., Reynolds, S.J., Smith, B.M., and Ruiz, Joaquin, 1988, K-metasomatism and detachment-related mineralization, Harcuvar Mountains, Arizona: Geological Society of America Bulletin, v. 100, p. 1627-1639.

Rose, A.W., and Burt, D.M., 1979, Hydrothermal alteration, *in* Barnes, H.L., ed., Geochemistry of hydrothermal ore deposits (2nd ed.): New York, John Wiley and Sons, 173-235.

Ross, C.P., 1922, Geology of the lower Gila region, Ariz., *in* Shorter contributions to general geology: U.S. Geological Survey Professional Paper 129, p. 183-198.

Ross, J.V., 1971, Mylonitic rocks and flattened garnets in the southern Okanogan of British Columbia: Canadian Journal of Earth Science, v. 10, p. 1-17.

Scarborough, Robert, and Meader, Norman, 1982, Reconnaissance geology of the northern Plomosa Mountains, Arizona: Arizona Bureau of Geology and Mineral Technology Open-File Report 83-24, 35 p.

Scarborough, Robert, and Wilt, J.C., 1979, A study of uranium favorability of Cenozoic sedimentary rocks, Basin and Range Province, Arizona; Part I, General geology and chronology of pre-late Miocene Cenozoic sedimentary rocks: Arizona Bureau of Geology and Mineral Technology Open-File Report 79-1, 101 p.

Shackelford, T.J., 1975, Late Tertiary gravity sliding in the Rawhide Mountains, western Arizona: Geological Society of America Abstracts with Programs, v. 7, p. 372-373.

____ 1976a, Juxtaposition of contrasting structural and lithologic terranes along a major Miocene gravity detachment surface, Rawhide Mtns., Arizona [abs.]: Geological Society of America Abstracts with Programs, v. 8, p. 1099.

____ 1976b, Structural geology of the Rawhide Mountains, Mohave County, Arizona: Los Angeles, University of Southern California, unpublished Ph.D. dissertation, 176 p.

____ 1980, Tertiary tectonic denudation of a Mesozoic-early Tertiary(?) gneiss complex, Rawhide Mountains, western Arizona: Geology, v. 8, p. 190-194.

____ 1981, Reply *to* Comment *on* Tertiary tectonic denudation of a Mesozoic-early Tertiary(?) gneiss complex, Rawhide Mountains, western Arizona: Geology, v. 9, p. 51-52.

Shafiqullah, M., Damon, P.E., Lynch, D.J., Reynolds, S.J., Rehrig, W.A., and Raymond, R.H., 1980, K-Ar geochronology and geologic history of southwestern Arizona and adjacent areas, *in* Jenney, J.P., and Stone, Claudia, eds., Studies in western Arizona: Arizona Geological Society Digest, v. 12, p. 201-260.

Shafiqullah, M., Lynch, D.J., Damon, P.E., and Peirce, H.W., 1976, Geology, geochronology and geochemistry of the Picacho Peak area, Pinal County, Arizona: Arizona Geological Society Digest, v. 10, p. 305-324.

Sherrod, D.R., 1988, Preliminary geologic map of the Monkeys Head quadrangle, Mohave and La Paz Counties, Arizona: U.S. Geological Survey Open-File Report 88-597, scale 1:24,000.

Sibson, R.H., 1982, Fault zone models, heat flow, and the depth distribution of earthquakes in the continental crust of the United States: Bulletin of the Seismological Society of America, v. 72, p. 151-163.

Simpson, Carol, and Schmid, S.M., 1983, An evaluation of criteria to deduce the sense of movement in sheared rocks: Geological Society of America Bulletin, v. 94, p. 1281-1288.

Smith, B.M., and Reynolds, S.J., 1985, Oxygen and hydrogen isotope study of mylonitization and detachment faulting, South Mountains, central Arizona [abs.]: Eos (American Geophysical Union, Transactions), v. 66, p. 1138.

Spencer, J.E., 1982, Origin of folds of Tertiary low-angle fault surfaces, southeastern California and western Arizona, *in* Frost, E.G., and Martin, D.L., eds., Mesozoic-Cenozoic tectonic evolution of the Colorado River region, California, Arizona, and Nevada: San Diego, Cordilleran Publishers, p. 123-134.

____ 1984a, Geometry of low-angle normal faults in west-central Arizona: Arizona Bureau of Geology and Mineral Technology Fieldnotes, v. 14, no. 3, p. 6-8.

____ 1984b, Role of tectonic denudation in warping and uplift of low-angle normal faults: Geology, v. 12, p. 95-98.

____ 1987, Reduction of crustal flexural rigidity during

folding of crystalline rocks in the Harcuvar and Whipple metamorphic core complexes, west-central Arizona and southeastern California [abs.]: Geological Society of America Abstracts with Programs, v. 19, p. 853.

Spencer, J.E., and Chase, C.G., 1989, Role of crustal flexure in initiation of low-angle normal faults and implications for structural evolution of the Basin and Range Province: Journal of Geophysical Research, v. 94, p. 1765-1775.

Spencer, J.E., Duncan, J.T., and Burton, W.D., 1988, The Copperstone mine: Arizona's new gold producer: Arizona Bureau of Geology and Mineral Technology Fieldnotes, v. 18, no. 2, p. 1-3.

Spencer, J.E., and Reynolds, S.J., 1986a, Geologic map of the Lincoln Ranch Basin, eastern Buckskin Mountains, western Arizona: Arizona Bureau of Geology and Mineral Technology Open-File Report 86-2, 6 p., scale 1:24,000.

_____ 1986b, Relationship of the Transition Zone to Mesozoic and Cenozoic tectonism in the Basin and Range Province, Ariz. [abs.]: Geological Society of America Abstracts with Programs, v. 18, p. 415.

_____ 1986c, Some aspects of the middle Tertiary tectonics of Arizona and southeastern California, *in* Beatty, Barbara, and Wilkinson, P.A.K., eds., Frontiers in the geology and ore deposits of Arizona and the Southwest: Arizona Geological Society Digest, v. 16, p. 102-107.

_____ 1987, Geologic map of the Swansea-Copper Penny area, central Buckskin Mountains, west-central Arizona: Arizona Bureau of Geology and Mineral Technology Open-File Report 87-2, scale 1:12,000.

_____ 1988, Middle Tertiary tectonics of Arizona and adjacent areas, *in* Jenney, J.P., and Reynolds, S.J., eds., Geologic evolution of Arizona: Arizona Geological Society Digest, v. 17 (in press).

Spencer, J.E., Reynolds, S.J., Anderson, J.L., Davis, G.A., Laubach, S.E., Richard, S.M., and Marshak, Stephen, 1987, Field-trip guide to parts of the Harquahala, Granite Wash, Whipple, and Buckskin Mountains, west-central Arizona and southeastern California, *in* Davis, G.H., and VandenDolder, E.M., eds., Geologic diversity of Arizona and its margins: Excursions to choice areas: Arizona Bureau of Geology and Mineral Technology Special Paper 5, p. 351-364.

Spencer, J.E., Reynolds, S.J., and Lehman, N.E., 1986, Geologic map of the Planet-Mineral Hill area, northwestern Buckskin Mountains, west-central Arizona: Arizona Bureau of Geology and Mineral Technology Open-File Report 86-9, 13 p., scale 1:24,000.

Spencer, J.E., and Welty, J.W., 1985, Reconnaissance geology of mineralized areas in parts of the Buckskin, Rawhide, McCracken, and northeastern Harcuvar Mountains, western Arizona: Arizona Bureau of Geology and Mineral Technology Open-File Report 85-6, 31 p.

_____ 1986, Possible controls of base- and precious-metal mineralization associated with Tertiary detachment faults in the lower Colorado River trough, Arizona and California: Geology, v. 14, p. 195-198.

Steiger, R.H., and Jager, E., 1977, Subcommission on geochronology: Convention on the use of decay constants in geo- and cosmochronology: Earth and Planetary Science Letters, v. 36, p. 359-362.

Stone, Paul, Howard, K.A., and Hamilton, Warren, 1983, Correlation of metamorphosed Paleozoic strata of the southeastern Mojave Desert region, California and Arizona: Geological Society of America Bulletin, v. 94, p. 1135-1147.

Stone, Paul, and Kelly, M.M., 1988, Preliminary geologic map of the Palen Pass quadrangle, Riverside County, California: U.S. Geological Survey Open-File Report 88-503, scale 1:24,000.

Stone, Paul, Page, V.M., Hamilton, Warren, and Howard, K.A., 1987, Cretaceous age of the upper part of the McCoy Mountains Formation, southeastern California and southwestern Arizona, and its tectonic significance: Reconciliation of paleobotanical and paleomagnetic evidence: Geology, v. 15, p. 561-564.

Stoneman, D.A., 1985, Structural geology of the Plomosa Pass area, northern Plomosa Mountains, La Paz County, Arizona: Tucson, University of Arizona, unpublished M.S. thesis, 99 p.

Streckeisen, A.L., 1967, Classification and nomenclature of igneous rocks: Neues Jahrbuch fur Mineralogie Monatschefte, v. 107, p. 144-240.

Suneson, N.H., 1980, The origin of bimodal volcanism, west-central Arizona: Santa Barbara, University of California, unpublished Ph.D. thesis, 293 p.

Suneson, Neil, and Lucchitta, Ivo, 1979, K/Ar ages of Cenozoic volcanic rocks, west-central Arizona: Isochron/West, no. 24, p. 25-29.

_____ 1983, Origin of bimodal volcanism, southern Basin and Range province, west-central Arizona: Geological Society of America Bulletin, v. 94, p. 1005-1019.

Sutherland, D.S., 1974, Petrography and mineralogy of the peralkaline silicic rocks: Bulletin Volcanologique, v. 38, p. 517-547.

Sylvester, A.G., and Christie, J.M., 1968, The origin of crossed-girdle orientation of optic axes in deformed quartzites: Journal of Geology, v. 76, p. 571-580.

Taylor, H.P., Jr., 1978, Oxygen and hydrogen isotope studies of plutonic granitic rocks: Earth and Planetary Science Letters, v. 38, p. 177-210.

Terry, A.H., 1972, The geology of the Whipple Mountains thrust fault, southeastern California: San Diego, San Diego State University, unpublished M.S. thesis, 90 p.

Theodore, T.G., 1967, Structure and petrology of the gneisses and mylonites at Coyote Mountain, Borrego Springs, California: Los Angeles, University of California, unpublished Ph.D. dissertation, 268 p.

Thompson, R.N., Morrison, M.A., Hendry, G.L., and Parry, S.J., 1984, An assessment of the relative roles of crust and magma genesis: An elemental approach: Philosophical Transactions of the Royal Society of London, v. A310, p. 549-590.

Todd, V.R., 1975, Late Tertiary low-angle faulting and folding in Matlin Mountains, northwestern Utah

[abs.]: Geological Society of America Abstracts with Programs, v. 7, p. 381-382.

Tosdal, R.M., 1988, Mesozoic rock units along the Late Cretaceous Mule Mountains thrust system, southeastern California and southwestern Arizona: Santa Barbara, University of California, unpublished Ph.D. dissertation, 365 p.

Tosdal, R.M., Haxel, G.B., and Wright, J.E., 1988, Jurassic geology of the Sonoran Desert region, southern Arizona, southeast California, and northernmost Sonora: Construction of a continental-margin magmatic arc, *in* Jenney, J.P., and Reynolds, S.J., eds., Geologic evolution of Arizona: Arizona Geological Society Digest, v. 17 (in press).

Turner, F.J., 1968, Metamorphic petrology: Mineralogical and field aspects: New York, McGraw-Hill, 403 p.

Turner, F.J., and Verhoogen, J., 1960, Igneous and metamorphic petrology: New York, McGraw-Hill, 694 p.

Walker, J.D., 1988, Permian and Triassic rocks of the Mojave Desert and their implications for timing and mechanisms of continental truncation: Tectonics, v. 7, p. 685-709.

Weaver, S.D., Sceal, J.S.C., and Gibson, I.L., 1972, Trace-element data relevant to the origin of trachytic and pantelleritic lavas in the East African rift system: Contributions to Mineralogy and Petrology, v. 36, p. 181-194.

Wernicke, Brian, 1981, Low-angle normal faults in the Basin and Range Province: Nappe tectonics in an extending orogen: Nature, v. 291, p. 645-648.

_____ 1985, Uniform-sense normal simple shear of the continental lithosphere: Canadian Journal of Earth Sciences, v. 22, p. 108-125.

Wernicke, Brian, and Axen, G.J., 1988, On the role of isostasy in the evolution of normal fault systems: Geology, v. 16, p. 848-851.

Wernicke, Brian, Walker, J.D., and Hodges, K.V., 1988, Hanging wall structural evolution of the Tucki Mountain detachment system, Death Valley region, southeastern California [abs.]: Geological Society of America Abstracts with Programs, v. 20, p. 242.

Wicklein, P.C., 1980, Geologic map of the Bill Williams district, Yuma County, Arizona: Arizona Bureau of Geology and Mineral Technology Open- File Report 80-2, scale 1:24,000, 2 sheets.

Wilkins, Joe, Jr., Beane, R.E., and Heidrick, T.L., 1986, Mineralization related to detachment faults: A model, *in* Beatty, Barbara, and Wilkinson, P.A.K., eds., Frontiers in geology and ore deposits of Arizona and the Southwest: Arizona Geological Society Digest, v. 16, p. 108-117.

Wilkins, Joe, Jr., and Heidrick, T.L., 1982, Base and precious metal mineralization related to low-angle tectonic features in the Whipple Mountains, California and Buckskin Mountains, Arizona, *in* Frost, E.G., and Martin, D.L., eds., Mesozoic-Cenozoic tectonic evolution of the Colorado River region, California, Arizona, and Nevada: San Diego, Cordilleran Publishers, p. 182-203.

Willden, Ronald, Thomas, H.H., and Stearn, T.W., 1967, Oligocene or younger thrust faulting in the Ruby Mountains, northeastern Nevada: Geological Society of America Bulletin, v. 78, p. 1345-1358.

Williams, Howell, Turner, F.J., and Gilbert, C.M., 1982, Petrography: An introduction to the study of rocks in thin sections (2d ed.): San Francisco, W.H. Freeman, 626 p.

Wilson, E.D., 1960, Geologic map of Yuma County, Arizona: Arizona Bureau of Mines, scale 1:375,000.

Wilson, E.D., and Moore, R.T., 1959, Geologic map of Mohave County, Arizona: Arizona Bureau of Mines, scale 1:375,000.

Wilson, E.D., Moore, R.T., and Cooper, J.R., 1969, Geologic map of Arizona: Arizona Bureau of Mines and U.S. Geological Survey, scale 1:500,000.

Woodward, R.J., 1981, The structural geology of the Swansea area, east-central Buckskin Mountains, Yuma County, Arizona: Los Angeles, University of Southern California, unpublished M.S. thesis, 106 p.

Woodward, R.J., and Osborne, G.M., 1980, Low-angle detachment faulting and multiple deformation of the central Buckskin Mountains, Yuma County, Arizona [abs.]: Geological Society of America Abstracts with Programs, v. 12, p. 160.

Wright, J.E., Anderson, J.L., and Davis, G.A., 1986, Timing of plutonism, mylonitization, and decompression in a metamorphic core complex, Whipple Mountains, CA [abs.]: Geological Society of America Abstracts with Programs, v. 18, p. 201.

Wright, L.A., Otton, J.K., and Troxel, B.W., 1974, Turtleback surfaces of Death Valley viewed as phenomena of extensional tectonics: Geology, v. 2, p. 53-54.

Wright, L.A., and Troxel, B.W., 1969, Chaos structure and Basin and Range normal faults: Evidence for a genetic relationship [abs.]: Geological Society of America Abstracts with Programs, part 7, p. 242.

Zambrano, Elias, 1965, Geology of the Cienega mining district, northwestern Yuma County, Arizona: Rolla, University of Missouri, unpublished M.S. thesis, 64 p.